From STM to LEECs: Syntheses and Applications of Multifunctional Bipyridine Ligands and their Iridium(III) Complexes

Stefan Graber

Cuvillier Verlag Göttingen
Internationaler wissenschaftlicher Fachverlag

From STM to LEECs: Syntheses and Applications of Multifunctional Bipyridine Ligands and their Iridium(III) Complexes

Inauguraldissertation

zur
Erlangung der Würde eines Doktors der Philosophie
vorgelegt der
Philosophisch-Naturwissenschaftlichen Fakultät
der Universität Basel

von
Stefan Graber
aus Basel

Basel, 2009

Bibliografische Information der Deutschen Nationalbibliothek
Die Deutsche Nationalbibliothek verzeichnet diese Publikation in der Deutschen Nationalbibliografie; detaillierte bibliografische Daten sind im Internet über http://dnb.ddb.de abrufbar.
1. Aufl. - Göttingen : Cuvillier, 2009
Zugl.: Basel, Univ. Diss., 2009

978-3-86955-113-5

Genehmigt von der Philosophisch-Naturwissenschaftlichen Fakultät
auf Antrag von

Prof. Dr. Edwin C. Constable
Prof. Dr. Wolfgang Meier

Basel, den 26.05.2009

Prof. Dr. Eberhard Parlow
Dekan

Nonnenstieg 8, 37075 Göttingen
Telefon: 0551-54724-0
Telefax: 0551-54724-21
www.cuvillier.de

1. Auflage, 2009
Gedruckt auf säurefreiem Papier

978-3-86955-113-5

Acknowledgments

In acknowledging my debts, I must begin with *Ed Constable*. He allowed me to work in his group and I enjoyed the benefit of his advice and experience. It has been a great honour for me to work for him in an environment of scientific freedom which was very beneficial for the creativity of such an interdisciplinary project.

To have *Catherine Housecroft* as the second supervisor has made the working environment even more attractive. Her profound knowledge of the principles of chemistry has always been very helpful. This thesis was corrected and revised by her for which I am exceedingly thankful. Furthermore, I enjoyed talking with her about more than just science.

I would like to thank the people from Valencia (Spain), namely *Henk Bolink*, *Rubén Costa*, *Michele Sessolo*, and *Enrique Ortí*, for the splendid collaboration we shared. It has been a great pleasure to discuss further steps in the LEEC project and to reflect together on all the amazing results they provided. Furthermore, they allowed the publication of their results in this thesis. Without the last chapter of this thesis, which essentially is their work, the scope of the preceding chapters would not have made much sense.

I am indebted to *Markus Neuburger* and *Silvia Schaffner* for being able to obtain crystal structures of even the smallest single crystals. I also enjoyed the discussion with *Markus Neuburger* about many aspects of crystallography, and especially for his help in plane group considerations for the STM images.

Next, I have to name *Beatrice Erismann*, *Markus Hauri*, *Alois Schäuble*, *Franz Stehlin*, and *Bernhard Jung* for their outstanding help in all administrative matters including IT support. It was a great pleasure to work with all of them and I enjoyed the numerous conversations with them. I am especially thankful for *Beatrice* and *Bernhard* for their deeper friendship.

I am very thankful for the collaboration with *Roman Kovàsy*, *Christian Markert*, and *Thomas Belser* regarding HPLC analysis and separation, and *Axel Franzke* for his help with the polarimeter. I am indebted to *Dieter Seebach* for granting samples of TADDOL, and *Klaus Kulicke* and *Daniel Häussinger* for their help with NMR measurements. *Peter Nadig* and *Werner Kirsch* performed the FAB-/EI-mass spectra measurements and elemental analyses, respectively, for which I am very thankful.

Special thanks go to *Dominik Frank* and *Ludmila Sachno* who worked for me during their Wahlpraktikum. It was a great pleasure to guide them as they showed high motivation and outstanding work ethics. Their work is not presented in this thesis. I would like to thank *Zeynep Aksoy* for the synthesis of some bipyridine precursors.

I am deeply indebted to *Lukas Scherer* and *Kevin Doyle* who coached me in all aspects of chemistry. Indeed, I am truly amazed by their deep knowledge and experience in theoretical and synthetical chemistry and by their vision of science in a grander perspective. They proved to be undoubtedly the best chemists I have ever met during my career and I consider myself lucky to be friends of

them for which I am very thankful. Moreover, I am enormously grateful to *Kevin* for handing over the LEEC project which he started. Without his work and brilliant ideas, LEECs would still suffer low stability. With his first compounds revealing the intramolecular π-π stacking, the doors to real-world applications of these devices were opened. Likewise, I want to thank *Lukas* for his instructions regarding STM and for sharing all his hints and tricks with this technique.

I would like to thank *Ralf Schmitt* and *Pirmin Rösel* not only for performing ESI mass spectra, but also for the great discussions and the humour we shared during the work in the lab. It was great fun to work with them and I also appreciated their profound knowledge of synthetic chemistry. Speaking of humour, I must thank the *Malarek brothers* for making the day such fun; it was "awesome" having worked with them.

Next, it is a pleasure for me to thank *Liselotte Siegfried* for her help with the synthesis of iridium(III) complexes. I have really enjoyed working with her, as she did a wonderful job and the compounds she prepared were always of the purest grade. Furthermore, she perfectly managed many administrative affairs, *e.g.* ordering of chemicals, which eased my work in the lab.

For 500 MHz NMR measurements I want to thank *Ana Hernández*, *Kate Harris* (she also corrected these acknowledgments for which I am very grateful), *Jonathon Beves*, and *Valérie Jullien*. I am also thankful to *William Kylberg* for his help and advice for electrochemical measurements. Special thanks go to *Emma Dunphy*, who helped me with basically every other machine or apparatus not mentioned before.

I would like to thank the whole Constable/Housecroft group for the great time we shared, especially (in alphabetical order) *Lumni Ademi*, *Jonathon Beves*, *Amar Boudebous*, *Biljana Bozic Weber*, *Conor Brennan*, *Barbara Brisig*, *Valérie Chaurin*, *Hoi Shan Chow*, *Paulina Chwalisz*, *Kevin Doyle*, *Emma Dunphy*, *Deborah Gusmeroli*, *Kate Harris*, *Marc Häusler*, *Ana Hernández*, *Valérie Jullien*, *Marzena Kocik*, *Swarna Kokatam*, *William Kylberg*, *Azad Mahmood*, *Dan Malarek*, *Michael Malarek*, *Elaine Medlycott*, *Jason Price*, *Sébastien Reymann*, *Pirmin Rösel*, *David Scanu*, *Frank Schaper*, *Lukas Scherer*, *Ralf Schmitt*, *Alexandra Senger*, *Ellie Shardlow*, *Liselotte Siegfried*, *Yaqiu Tao*, *Jennifer Zampese*, and *Guoqi Zhang*.

Next, I want to thank *Roman Hofer* and *Christoph Hefti* for being my flat mates during the time of my PhD. I had a wonderful time with them and I have appreciated their unconditional friendship.

I want to close my acknowledgments with my deepest expressions of gratitude to my family. They have supported me in every aspect and without their help I would not be where I am now. On this occasion, I would also like to thank my brother *Michael* for having lunch together every day. I had a marvellous time with him and I miss our conversations, which only rarely dealt with aspects of chemistry, for which I am actually glad.

Liebsti *Angelika*, ich möcht Dir an dere Stell vo tiefstem Härze dangge für Dini Fründschaft und Beziehig. Dangge für Dis Verständnis und s'Verzichte uf mi bsunders während de letschde Wuche bim Zämmeschribe. I freu mi riisig uf alles wo no kunnt und mir zämme dörfe erläbe.

I want to express my deepest thanks to the creator of this world.

And God said: “Let there be light”;
And there was light.
And God saw that the light was good.

Genesis 1, 3–4

Contents

Acknowledgments iii

Contents vi

Abbreviations ix

Abstract xiii

Chapter 1 Background 1

1.1 Supramolecular chemistry 2
1.1.1 History and terminology 2
1.1.2 Weak chemical bonds 3
1.1.2.1 Hydrogen bonding 3
1.1.2.2 π-π Interactions 4
1.1.3 Self-assembly 6
1.2 Dendrimers 7
1.2.1 History and terminology 7
1.2.2 Construction of dendrimers 7
1.2.3 Fréchet-type dendrimers 10
1.3 Coordination chemistry 11
1.3.1 History and concepts 11
1.3.2 Oligopyridines 13
1.3.3 Iridium and its complexes 13
1.4 Scanning tunnelling microscopy 15
1.4.1 History 15
1.4.2 Concept 16
1.5 Solid state lighting 18
1.5.1 History and terminology 18
1.5.2 General principles of electroluminescence 19
1.5.3 OLEDs and LEECs 20

Chapter 2 Instruments and Methods 25

2.1 General experimental 26
2.2 Analytical equipment 27

2.3 Scanning tunnelling microscopy....29
2.3.1 Setup....29
2.3.2 Processing images....33
2.3.3 Assigning and overlaying molecules....34
2.4 LEEC devices....35

Chapter 3 Synthesis and STM Imaging of Achiral and Chiral Dendrons....37

3.1 Introduction and aims....38
3.2 Synthesis and discussion....39
3.2.1 Achiral dendrons....39
3.2.2 Chiral dendrons....40
3.2.3 Second generation dendrons....42
3.2.4 Dendrons with different chain lengths....43
3.3 STM imaging and discussion....44
3.4 Experimental part....52

Chapter 4 Synthesis and STM Imaging of Achiral and Chiral Bipyridine Ligands....59

4.1 Introduction and aims....60
4.2 Synthesis and discussion....62
4.2.1 Achiral ligands....62
4.2.2 Chiral ligands....63
4.2.3 Second generation ligands....68
4.2.4 Ligands with different chain lengths....69
4.3 STM imaging and discussion....70
4.3.1 Air/solid-interface....71
4.3.2 Liquid/solid-interface....74
4.4 Experimental part....79

Chapter 5 Synthesis and STM Imaging of Perfluorinated Dendrons and Ligands....87

5.1 Introduction and aims....88
5.2 Synthesis and discussion....88
5.2.1 Dendron synthesis....88
5.2.2 Ligand synthesis....92
5.3 STM imaging and discussion....94
5.4 Experimental part....96

Chapter 6 Synthesis and STM Imaging of Ligands for Iridium(III) Complexes....101

6.1 Introduction and aims....102
6.2 Synthesis and discussion....103
6.2.1 Simple ligands....103

6.2.2 Dendronised ligands....110
6.3 STM imaging and discussion....114
6.4 Experimental part....116

Chapter 7 Synthesis and STM Imaging of Cyclometallated Iridium(III) Complexes....123

7.1 Introduction and aims....124
7.2 Synthesis and discussion....125
7.2.1 Cyclometallated Ir(III) dimers....125
7.2.2 Cyclometallated Ir(III) complexes....128
7.2.2.1 Ir(III) complexes with different *N*,*N*′-ligands....129
7.2.2.2 Ir(III) complexes with different *C*,*N*-ligands....132
7.3 Characterisation of the Cyclometallated Ir(III) complexes....134
7.3.1 General characterisation....134
7.3.2 UV-Vis absorption....135
7.3.3 Photoluminescence and lifetime....140
7.3.4 Cyclic voltammetry....144
7.3.5 Crystal structures....146
7.4 STM imaging of the cyclometallated Ir(III) complexes and discussion....160
7.5 Experimental part....163

Chapter 8 Light-Emitting Electrochemical Cells....175

8.1 Introduction and aims....176
8.2 Device performance and discussion....179
8.2.1 Phenanthroline based complexes....179
8.2.2 Simple bipyridine based complexes....180
8.2.3 Archetype and dendronised based complexes....181
8.2.4 Modified phenyl-pyridine based complexes....183
8.2.5 Pyrazole based complexes....184
8.3 Conclusions....185

Appendix A: References....187

Appendix B: Crystal structure data....196

Abbreviations

General

2D	two-dimensional
3D	three-dimensional
HOMO	highest occupied molecular orbital
LC	ligand centred
LUMO	lowest unoccupied molecular orbital
MC	metal centred
MLCT	metal-to-ligand charge transfer
MO	molecular orbital
S_0	ground state

Chemical

Aliquat 336	NR_4Cl; R = mixture of $-C_8H_{17}$ and $-C_{10}H_{21}$
aq.	aqueous
Ar	aryl / aromate
bpy	2,2'-bipyridine
Bu	butyl
de	diastereomeric excess
DEAD	diethyl azodicarboxylate
DMF	N,N-dimethylformide
dpbpy	6,6'-diphenyl-2,2'-bipyridine (**32**)
ee	enantiomeric excess
fac	facial
Hbzq	7,8-benzoquinoline
Hdfppy	2-(2,4-difluorophenyl)pyridine
Hdmppz	3,5-dimethyl-1-phenylpyrazole
Hpiq	1-phenylisoquinoline
Hppy	2-phenylpyridine
Hppz	1-phenylpyrazole
L	ligand
M	metal
mer	meridional
n	unspecified number
n-alkyl	normal alkyl, *i.e.* unbranched alkyl
pbpy	6-phenyl-2,2'-bipyridine (**31**)
PCC	pyridinium chlorochromate
PEG-300	polyethylene glycol (average molecular weight of 300 g mol^{-1})

Ph	phenyl
Py	pyridine
phen	1,10-phenanthroline
ppbpy	4,6-diphenyl-2,2'-bipyridine
$(HO)_2$ppbpy	4-(3,5-dihydroxyphenyl)-6-phenyl-2,2'-bipyridine (**37**)
$(H_3CO)_2$ppbpy	4-(3,5-dimethoxyphenyl)-6-phenyl-2,2'-bipyridine (**35**)
$(H_{21}C_{10}O)_2$ppbpy	4-(3,5-bis(decyloxy)phenyl)-6-phenyl-2,2'-bipyridine (**38**)
$(G1–O)_2$ppbpy	4-(3,5-bis(3,5-bis(dodecyloxy)benzyloxy)phenyl)-6-phenyl-2,2'-bipyridine (**39**)
$(G2–O)_2$ppbpy	4-(3,5-bis(3,5-bis(3,5-bis(dodecyloxy)benzyloxy)benzyloxy)phenyl)-6-phenyl-2,2'-bipyridine (**40**)
pphen	2-phenyl-1,10-phenanthroline (**30**)
qtpy	2,2':6',2'':6'',2'''-quaterpyridine
R	(organic) rest
r.t.	room temperature
sat.	saturated
(+)-TADDOL	(4*S*,5*S*)-2,2-dimethyl-α,α,α',α'-tetraphenyldioxolane-4,5-dimethanol
(–)-TADDOL	(4*R*,5*R*)-2,2-dimethyl-α,α,α',α'-tetraphenyldioxolane-4,5-dimethanol
THF	tetrahydrofuran
tpy	2,2':6',2''-terpyridine

Chemical analysis

a.u.	arbitrary units
br	broad (NMR, IR)
calcd.	calculated
COSY	correlated spectroscopy (NMR)
CV	cyclic voltammetry
d	doublet (NMR)
δ	chemical shift (NMR)
DEPT	distortionless enhancement by polarisation transfer
ε	extinction coefficient
EI	electron impact
ESI	electrospray ionisation
FAB	fast-atom bombardment
Fc	Ferrocene
HMBC	heteronuclear multiple bond correlation (NMR)
HMQC	heteronuclear multiple quantum correlation (NMR)
HPLC	high performance liquid chromatography
IR	infrared spectroscopy
J	coupling constant (NMR)
λ	wavelength

λ_{em}	emission wavelength
λ_{ex}	excitation wavelength
m	multiplet (NMR); medium strong (IR); mass (MS)
MALDI	matrix assisted laser desorption ionisation
mp	melting point
MS	mass spectrometry
$\tilde{\nu}$	wavenumber (IR)
NMR	nuclear magnetic resonance spectroscopy
NOESY	nuclear overhauser effect (NMR)
ppm	parts per million (NMR)
q	quartet (NMR)
R_f	retention factor (TLC)
s	singlet (NMR); strong (IR)
t	triplet (NMR)
TLC	thin layer chromatography
TMS	tetramethylsilane
TOF	time of flight
UV-Vis	ultra-violet visible spectroscopy
w	weak (IR)
z	charge (MS)

Scanning probe microscopy

AFM	atomic force microscopy / microscope
HOPG	highly oriented pyrolytic graphite
SAM	self-assembled monolayer
SPM	scanning probe microscopy / microscope
STM	scanning tunnelling microscopy / microscope

Solid state lighting

DFT	density functional theory
EL	electroluminescence
IL	ionic liquid
ITO	indium tin oxide
LCD	liquid crystal display
LEC	see LEEC
LED	light-emitting diode
LEEC	light-emitting electrochemical cell
OLED	organic light-emitting diode

PEDOT:PSS	poly(3,4-ethylenedioxythiophene) : poly-styrenesulfonate
PL	photoluminescence
RGB	red, green, blue
SSL	solid state lighting
$t_{1/2}$	time from voltage turn-on to the time where the luminance is half of the maximum value
$t_{1/5}$	time from voltage turn-on to the time where the luminance is one fifth of the maximum value
t_{on}	time to reach the maximum luminance

Abstract

The theoretical background for this thesis is given in **Chapter 1**. It covers the field of supramolecular chemistry including the phenomena of self-assembly, the history and synthesis of dendrimers, the concept of coordination chemistry and the chemistry of iridium, the history and principles of the scanning tunnelling microscope (STM), and the theory and applications of solid state lighting, especially of the light-emitting electrochemical cells (LEECs).

The background chapter is followed by a short introduction to the materials, methods, and instruments used in this thesis (**Chapter 2**).

In the following two chapters, the syntheses of achiral and chiral Fréchet dendrimers (**Chapter 3**) and the subsequent reactions to the achiral and chiral Fréchet dendronised 2,2'-bipyridine ligands (**Chapter 4**) are described. Additionally, for most of the compounds presented in these chapters, the monolayer behaviour on graphite was studied with STM. For example, for 3,5-bis(dodecyloxy)-phenylmethanol, a very highly resolved image could be detected and detailed considerations of the adopted monolayer could be performed. Chirality was introduced into the molecules for the purpose of altering the preference for a particular conformation, as it has been shown before by *L. Scherer*[1] that these type of ligands tend to adopt different conformations when adsorbed on graphite. Unfortunately, the measurements of the chiral ligands did not reveal any significant information. Therefore, no detailed discussion of the conformations in the monolayer could be given. Nevertheless, in a monolayer of the diastereomeric mixture of 4,4'-bis(1-(3,5-bis(dodecyloxy)-phenyl)propoxy)-2,2'-bipyridine, two clearly differing patterns could be observed which were attributed to different stereoisomers.

Chapter 5 deals with the synthesis of dendrons decorated with perfluorinated alkyl chains and their use in the functionalisation of 2,2'-bipyridine ligands. Adsorbed monolayers on graphite of such a ligand were studied with STM. Due to a, apparently, lower propensity to establish monolayers, only few examples of visualised patterns could be observed.

The following three chapters cover the synthesis and STM-visualisation of 2,2'-bipyridine-based ligands (**Chapter 6**), their iridium(III) complexes (**Chapter 7**), and the use thereof in LEEC devices (**Chapter 8**). In **Chapter 6**, simple and more advanced ligands were synthesised and characterised. In the case of the ligands which were functionalised with dendrons presented in **Chapter 2**, STM studies of monolayers on graphite are discussed. **Chapter 7** presents the synthesis and characterisation of iridium(III) complexes obtained from ligands described in the previous chapter. The characterisation comprises measurements of NMR, MS, UV-Vis, photoluminescence, electrochemistry, and, where single crystals could be obtained, their solid state structures. For the complexes bearing dendronised ligands, STM measurements were performed which revealed highly resolved patterns. In the last chapter (**Chapter 8**), results from LEEC devices fabricated with complexes described in **Chapter 7** are shown. The device preparation and the measurement of their characteristics were performed by the group of *H. Bolink* who kindly allowed the publication of their results in this thesis. It could be shown that for all complexes exhibiting an intramolecular π-π stacking, the stability of their devices was increased dramatically.

This thesis has brought together the realms of chemical design with, firstly, studies of the physical behaviour of the envisioned molecules on the surface and, secondly, systematic structural optimisation of iridium(III) complexes for the application in solid state lighting. With the work presented in this thesis, a major breakthrough for long-lived LEECs has been achieved allowing lifetimes of several thousands of hours, an increase of several orders of magnitude compared to the best-performing devices reported to date (see **Chapter 1** and **Chapter 8**).

Chapter 1

Background

1.1
Supramolecular chemistry

1.1.1
History and terminology

For more than 180 years, since urea was synthesised by *F. Wöhler*,[2] molecular chemistry has developed a vast array of highly sophisticated and powerful methods for the construction of ever more complex molecular structures by the making or breaking of covalent bonds between atoms in a controlled and precise fashion.[3] Organic synthesis grew rapidly, leading to a whole series of brilliant achievements. Molecular chemistry has established its power over the covalent bond. Beyond molecular chemistry there lies the field of *supramolecular chemistry*, the goal of which is to gain control over the intermolecular bond.[3]

In contrast to molecular chemistry, the area of *supramolecular chemistry* is still a young one.[4] The term "*supramolecular*" can be traced back at least to 1925.[5] The roots of *supramolecular chemistry* are found in early discoveries, mostly in the field of biological chemistry, amongst there are molecular recognition (1894, *E. Fischer*)[6], the concept of receptors (*P. Ehrlich*)[7], and coordination chemistry (by *A. Werner*, see **Section 1.3**)[8] which would be, at least partially, regarded as *supramolecular chemistry* nowadays. With these three concepts, fixation, recognition, and coordination, the foundations of *supramolecular chemistry* are laid.[3] The term "*Übermoleküle*" was used in the mid-1930's to describe entities of higher organisation, such as the dimer of acetic acid, resulting from the association of coordinately saturated species.[9-11]

Nevertheless, the field of *supramolecular chemistry*, as we know it, started with the selective binding of alkali metal cations by crown ethers[12, 13] and cryptands[14-16]. The concept and term of *supramolecular chemistry* were introduced by *J.-M. Lehn* in 1978.[17] Earlier, *supramolecular chemistry* was defined as organised entities of higher complexity resulting from the association of two or more chemical species held together by intermolecular forces, not by covalent bonds.[18] But the use of covalent bonds to describe interactions is unhelpful, as it mixes interactions that are energetically different.[19] Furthermore, metal ligand bonds or hydrogen bonds can be substantial and strong.

A grander view of *supramolecular chemistry* focuses on the controlled assembly of multiple chemical components. The assembly can involve standard intermolecular interactions, and/or metal coordination. One broad goal is to have the ability to mimic the structure and the function of the assemblies of molecular biology.[19]

Currently, the term "*supramolecular*" has three different meanings:[19]
(a) intermolecular interactions;
(b) applied coordination chemistry;
(c) a strategy of controlled organisation of multiple separate components.

In order to disentangle this confusion, *I. Dance* recommended to use "*intermolecular*" as the adjective for the well-known weak and long interactions between molecules, and to describe elabo-

rate coordination complexes and polymers unambiguously with the terminology of coordination chemistry (see **Section 1.3**). He suggested restricting the use of the adjective "*supramolecular*" to the philosophies and strategies of grand assembly.[19]

To sum up, *supramolecular chemistry* is commonly defined as chemistry "beyond the molecule", as chemistry of tailor-shaped intermolecular interaction. In *supramolecules*, information is stored in the form of structural peculiarities. Moreover, not only the combined action of molecules is called *supramolecular*, but also the combined action of characteristic *parts* of one and the same molecule.[4]

1.1.2 Weak chemical bonds

Supramolecular chemists often use the terminology of chemical bonds (see **Section 1.1.1**). This raises the question of a definition of a chemical bond.

L. Pauling defined in 1939 a chemical bond as follows: "We shall say that there is a chemical bond between two atoms or two groups of atoms in case that forces acting between them are such as to lead to the formation of an aggregate with sufficient stability to make it convenient for the chemist to consider it as an independent chemical species."[20] *Pauling* explained that this definition was meant to include not only the directed valence bond of the organic chemist but also electrostatic bonds (*e.g.* present in the solid state of sodium chloride) or even the weak bond which holds together the two O_2 molecules of O_4.[21] But he did not consider the weak van der Waals forces between molecules as leading to chemical bonding.[22]

Therefore, we will classify bonds into weak bonds (such as hydrogen bonds or π-π interactions, see below) or strong bonds (covalent bonds, coordination bonds). One has to bear in mind though, that in supramolecular chemistry, multiple ligands on one entity bind simultaneously to multiple receptors on another, therefore the understanding of the concept of *multivalency*[23-27] is important. Multivalent interactions tend to be much stronger than the corresponding monovalent ones.[21] The binding of two molecules, both having multiple recognition sites, may occur with an affinity greater than the sum of the corresponding monovalent interactions, a phenomenon that has been defined as the *cluster effect*.[28]

In the following two sections, two interactions playing a major role in supramolecular chemistry are briefly explained.

1.1.2.1 Hydrogen bonding

The hydrogen bond is the most important of all directional intermolecular interactions.[29] A hydrogen bond is the attractive force between, classically, one electronegative atom and a hydrogen

covalently bonded to another electronegative atom.[30] It results from a dipole-dipole force with a hydrogen atom bonded to nitrogen, oxygen or fluorine. The energy of a hydrogen bond (typically 5 – 30 kJ mol^{-1}) is comparable to that of weak covalent bonds (155 kJ mol^{-1}),[31] and "strong" charge-assisted or resonance-assisted X–H···Y (X, Y = O, N) show bond energies of up to 150 kJ mol^{-1}.[32] Unsurprisingly, these bonds can occur intermolecularly or intramolecularly.

As an extrapolation of this type of interaction, the involvement of weak, "unconventional", or "non-classical" hydrogen bonds has been invoked.[22] It has become almost routine to discuss and analyse intermolecular interactions in terms of C–H···O, C–H···N, C–H···F, C–H···Cl, C–H···π (see **Section 1.1.2.2**), and Cl···Cl intermolecular "bonds".[29, 33-35] It is clear that the atoms that come into contact in these intermolecular interactions are not those in the molecular interiors but those on the peripheries.[22] One cannot deny that these weak intermolecular atom–atom bonds can be neatly categorised on the basis of geometrical, spectroscopic, and even energetic criteria and are thus according to these criteria existent rather than non-existent, provided one is prepared to accept a continuum of energies until nearly zero. The question is not whether weak hydrogen bonds "exist" but rather to what extent are they relevant in distinguishing one possible crystal structure from another.[22]

1.1.2.2
π-π Interactions

Strong attractive interactions between π-systems have been known for over half a century.[36] Two different geometries of π-π stacking are observed in crystal structures, and are depicted in **Figure 1.1**.

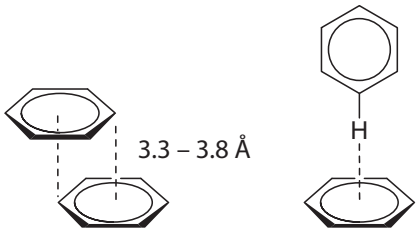

Figure 1.1 Two different possibilities of π-π stacking. Left: face-to-face geometry showing the typical range in distance.[37] Right: edge-to-face geometry.

These interactions control such diverse phenomena as the vertical base-base interactions which stabilise the double helical structure of DNA,[38] the intercalation of drugs into DNA,[38, 39] the packing of aromatic molecules in crystals,[40] the tertiary structures of proteins,[41] the conformational preferences and binding properties of polyaromatic macrocycles,[42] complexation in many host-guest systems,[43] and porphyrin aggregation.[44] To date, no readily accessible or intuitive model has been suggested to explain the experimental observations. Full *ab initio* calculations have been carried out for a limited number of small systems[45] and these do reproduce the experimental re-

sults well, but they do not explain the basic mechanisms of π-π interactions in a way that is helpful or predictive for the practical chemist. *C. A. Hunter* and *J. K. M. Sanders* presented a pictorial model and the rules they derived from it have a general applicability. In essence, the model indicates that the geometries of π-π interactions are controlled by electrostatic interactions but that the major energetic contribution occurs when the attractive interactions between π-electrons and the σ-framework outweigh unfavourable contributions such as π-electron repulsion (**Figure 1.2**).[36] Therefore, it is rather a π-σ attraction than a π-π electronic interaction which leads to favourable interactions. In face-to-face arrangements (**Figure 1.1**), offset geometries are often observed which can be explained with this model (**Figure 1.2**).

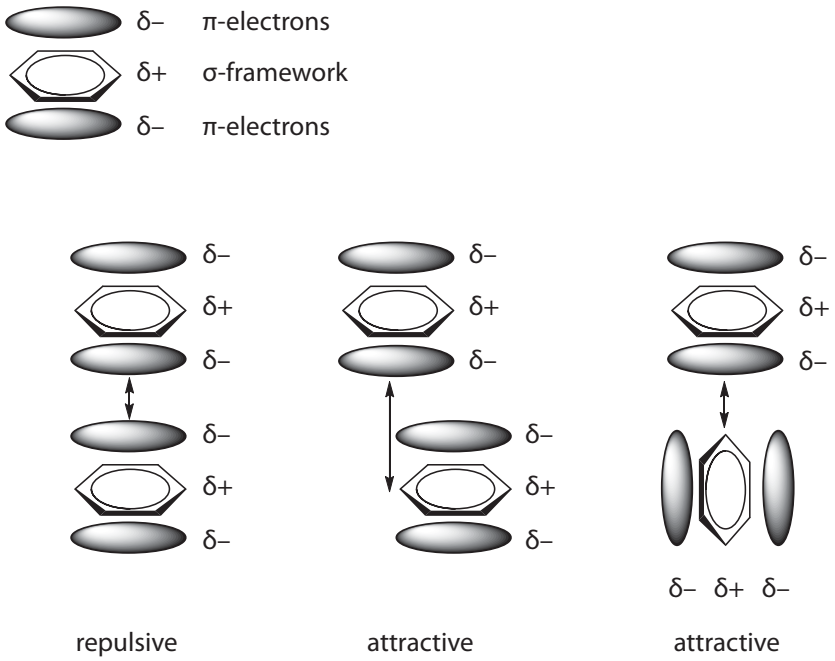

Figure 1.2 Attractive and repulsive arrangements of π-systems.[36] In this model, the π–σ attractions determine the geometry.

Nevertheless, the real origins of π-π stacking are still unclear.[46] In a recent article, *S. Grimme* pointed out that π-π stacking is a widely held misconception.[47] In his article, *Grimme* investigated the true origin of π-π stacking and questioned if it really exists. After all, many intermolecular interactions can equally well be explained with conventional dispersion forces which arise from statistical fluctuations in electron density.

In a series of computations, *Grimme* compares a group of aromatic compounds with their saturated all-trans counterparts with respect to intermolecular separation and stabilisation energy.

In summary, he recommended to use the term "π-π interactions" with care. For systems with about ten carbon atoms or less, there is little theoretical evidence for a special role of the π-orbitals. Thus, the term "π-π stacking" should be used as a geometrical descriptor of the interaction mode in unsaturated molecules and to understand π-π interactions as a special type of electron correla-

tion (dispersion) effect that can only act in large unsaturated systems when they are spatially close, which is only possible in the stacked orientation.

1.1.3 Self-assembly

Molecular self-assembly is a strategy for nanofabrication that involves designing molecules and supramolecular entities so that shape-complementarity causes them to aggregate into desired structures.[48] Self-assembly has a number of advantages as a strategy. Firstly, it carries out many of the most difficult steps in nanofabrication, those involving atomic-level modification of structure using the very highly developed techniques of synthetic chemistry. Secondly, it draws from the enormous wealth of examples in biology for inspiration. Self-assembly is one of the most important strategies used in biology for the development of complex, functional structures. Thirdly, it can incorporate biological structures directly as components in the final systems. Fourthly, because it requires the target structures to be the thermodynamically most stable ones open to the system, it tends to produce structures that are relatively defect-free and self-healing.[49-53]

One area in which self-assembly can emerge are the self-assembled monolayers (SAM).[54] There, the self-assembling process takes place in only two dimensions, *i.e.* on a surface of, for example, being gold, copper or graphite. These monolayers are well suited to measurements with scanning probe techniques (see **Section 1.4**), such as atomic force microscopy (AFM) or, as used in this thesis, scanning tunnelling microscopy (STM).

There is considerable potential for the study of structural questions of chemical interest using these new methods. Conventional three dimensional methods of determining molecular conformation such as single-crystal X-ray crystallography or NMR spectroscopic methods give structures averaged over some 10^{15} molecules. Without any averaging procedure, single molecules can be detected by analysis of surface molecular conformation of two dimensional arrays. For a better resolution, the images can be processed by averaging over 10 – 200 molecules (see also **Chapter 2**).

Dendrimer-functionalised heterocycles, such as 4,4'-bis(3,5-bis(octyloxy)benzyloxy)-2,2'-bipyridine (**14**, see **Chapter 4**) are ideally suited for the formation of SAMs[1, 55-57]. One reason is that the four octyl chains undergo intermolecular interactions between molecules, and molecules and the graphite surface. Although this interaction is quite weak (the adsorption energy per CH_2 group is about –12 kJ mol^{-1}),[58] it is however accumulated over every CH_2 group of the four octyl chains in the molecule. Another reason is the occurrence of π-π stacking of the aryl groups with the graphite surface. This interaction is also weak, but taken over the surface as whole, it is adequate to enable self-assembly to occur.

1.2 Dendrimers

1.2.1 History and terminology

The term "*dendrimer*" comes from the Greek and is a combination of the words dendron, meaning "tree", and meros, meaning "part", and was introduced by *D. A. Tomalia* in 1985.[59] The 1978 publication of *F. Vögtle et al.* laid the foundation of the preparation of dendritic molecules,[60] which have attracted considerable attention in the last decades in the field of supramolecular chemistry, and also in theoretical, physical, polymer, and inorganic chemistry due to their material properties as well as in biotechnology.[61] Such branched or even hyperbranched molecules called arboroles[62], cascade molecules,[60] dendritic molecules, or starburst-dendrimers[59] are constructed from identical monomeric building blocks carrying branching sites which are located in a spherical way around a core. The shells of monomers are called generations (**Figure 1.3**). On the periphery, dendrimers can carry numerous functional groups that can finally lead to a surface congestion due to their steric interactions (dense-packed stage or "starburst").[63, 64]

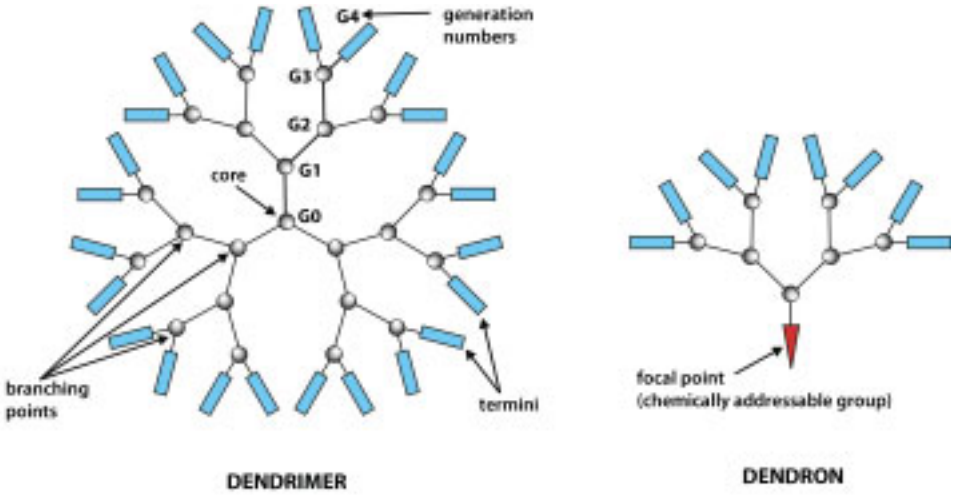

Figure 1.3 Terminology used for dendrimers. Figure based on an image which was published under public domain licensing.[65]

1.2.2 Construction of dendrimers

The synthesis of uniform dendritic molecules can proceed in two iterative ways. Firstly, the *divergent-iterative* pathway (**Figure 1.4**), which was used in the early work in 1978, starts from an initial core with two or more functional groups. These are converted using monomers with protected reac-

tive sites. The removal of the protecting groups and the repeated reaction with monomer units leads to an exponential increase of functional groups on the surface of the spherical molecule.[64]

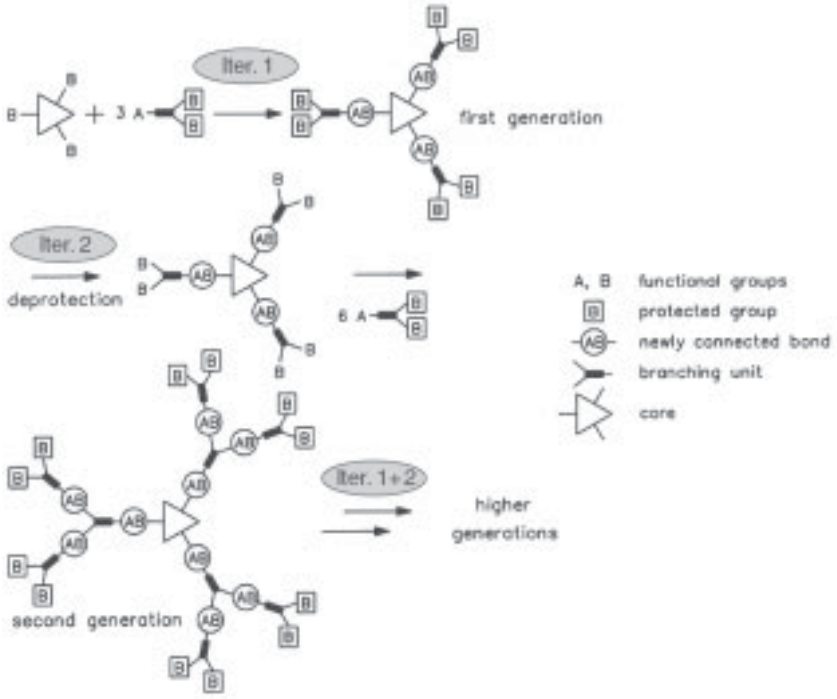

Figure 1.4 Divergent-iterative synthetic pathway for the preparation of dendrimers. Figure taken from literature.[64]

With this method, new dendrimers were prepared in the following years by *R. G. Denkewalter et al.*,[66] *D. A. Tomalia et al.*,[67] *G. R. Newkome et al.*,[68] and by *F. Vögtle et al.*[69] Following a reaction pathway similar to the one used in 1978, *E. W. Meijer et al.* successfully synthesised a polynitrile dendrimer up to the fifth generation on a large scale (**Scheme 1.1**).[70]

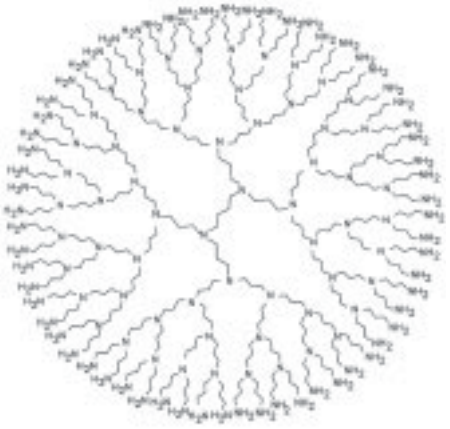

Scheme 1.1 Polyamine dendrimer of the fifth generation obtained on a kilogram scale.

A potential source of structural imperfection is the rapid increase of reactive groups as growth is pursued. Their incomplete conversion leads to defects inside the molecule.[71] In the second major iterative pathway, called *convergent-iterative* synthesis, these problems are avoided by directing the dendritic growth from the surface inwards to a focal point. In a final step, several dendrons are connected with a multifunctional core to yield the desired dendrimer (**Figure 1.5**).[64]

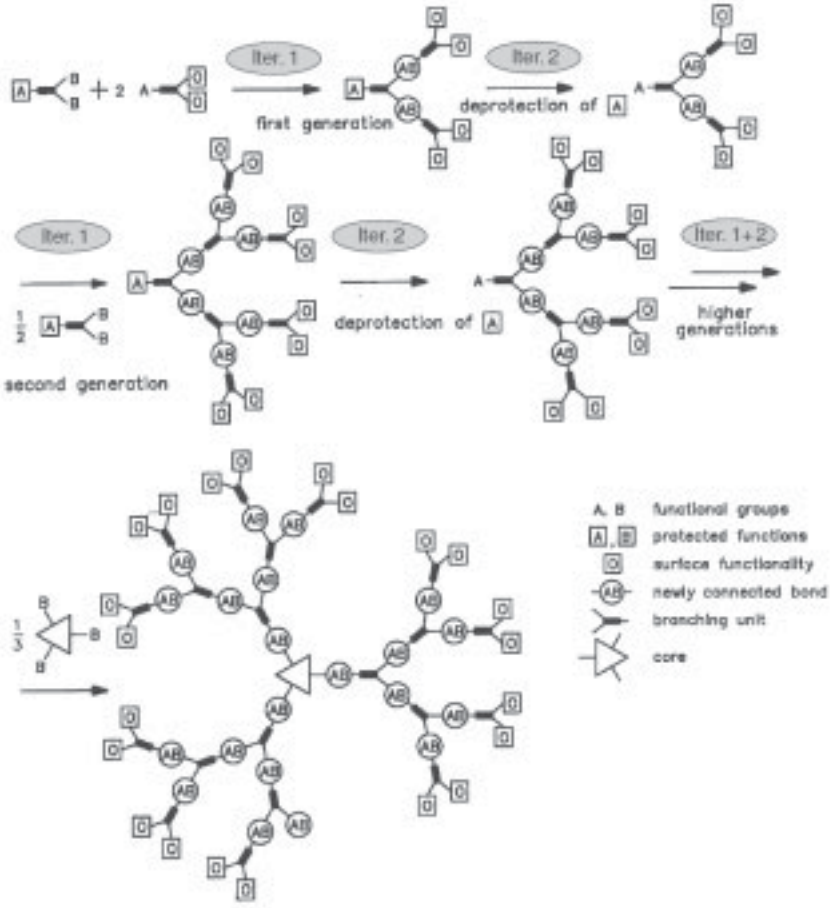

Figure 1.5 Convergent-iterative synthesis of dendritic molecules. Figure taken from literature.[64]

A large family of new dendrimers has been synthesised following this divergent method. *C. J. Hawker* and *J. M. J. Fréchet* developed polyaryl(-benzyl)ether dendrimers (see **Section 1.2.3**),[71] *T. M. Miller* and *T. X. Neenan*,[72] and also *J. S. Moore* and *Z. F. Xu*[73] prepared hydrocarbon dendrimers. The latter have reported the largest monodispersed organic hydrocarbon dendrimer with a molecular mass of 18 kDa and a diameter of 12.5 nm.[74]

Comparison of these two methods shows that generally dendrimers prepared by the divergent approach are more polydispersed than those prepared by the convergent route.[75] In the divergent methodology, a significant feature is the rapid increase in the number of reactive groups at the periphery of the growing macromolecule.[21] Potential problems which may arise as growth is pursued include incomplete reaction of these terminal groups, especially at higher generations when large numbers of reactions have to occur on a sterically hindered dendrimer surface. This would lead to

imperfections in the next generation, or the use of large excess of reagents that are required to force reactions to completion. This, in turn, presents difficulties in purification.[21]

The convergent method, on the other hand, is usually limited to dendrimers of lower generations due to the steric hindrance at the focal points of large dendrons. Stoichiometric reactions are therefore crucial for every step.

1.2.3 Fréchet-type dendrimers

C. J. Hawker and *J. M. J. Fréchet* described the first example of dendrimers constructed by the convergent approach (see previous section).[71, 76] The so-called Fréchet-type dendrimers consist of polyether fragments which are prepared by starting from what will become the periphery of the molecule.[77] The synthesis then progresses inward. In their very first example, the first step is a condensation of two equivalents of benzyl bromide with two phenolic groups of the monomer, *i.e.* 3,5-dihydroxybenzyl alcohol (**Scheme 1.2**). After transformation of the benzylic alcohol functionality into the corresponding leaving group (*e.g.* bromide or mesylate), the procedure is repeated with stepwise addition of the monomer followed again by activation of the benzylic site.[21] As discussed in the previous section, this method of building up dendrimers has been established as the ideal system to construct dendrimers when lower generations are needed. In this thesis, Fréchet-type dendrons were used to study their 2D self-assembled monolayers on graphite.

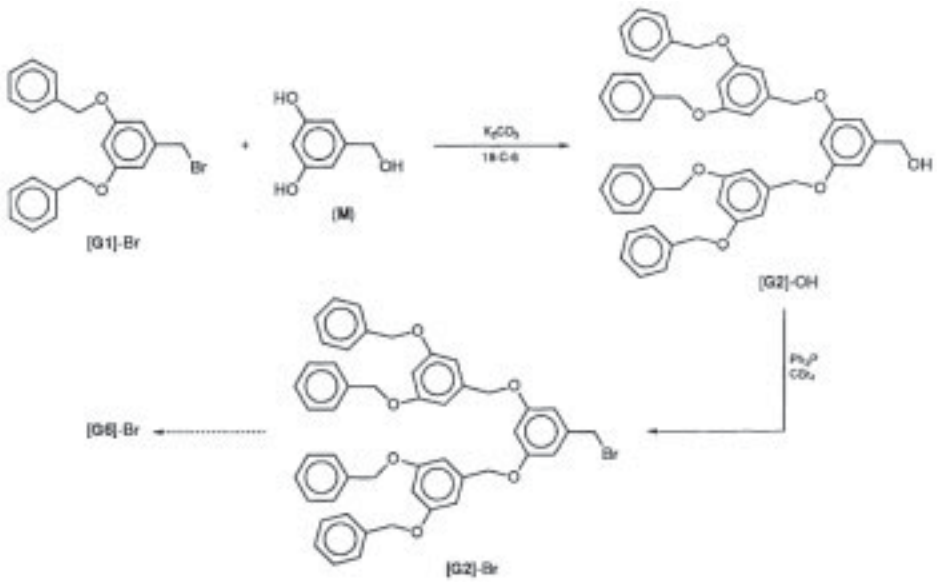

Scheme 1.2 Synthesis of a Fréchet-dendrimer. Figure taken from literature.[71]

1.3 Coordination chemistry

1.3.1 History and concepts

It is difficult to trace back the history in the area of *coordination chemistry*, as there is, in fact, no defined beginning.[78] The synthesis of certain compounds, of which the crucial ingredient is a coordination compound, has been performed, and also documented, in ancient times already. The first scientific evidence for the formation of a coordination compound is the preparation and characterisation of $[Cu(NH_3)_4]^{2+}$ by *A. Libavious*, a physician and alchemist, in 1597.[79] Although he did not isolate the product, *Libavious* observed a blue colouration when a solution of $Ca(OH)_2$ on a bronze surface was treated with NH_4Cl.[80]

The beginning of *coordination chemistry*, as we know it today, is often referred to *A. Werner*. He introduced a theory[8] which allows us to understand the difference between coordinated and ionic chloride in the cobalt ammine chlorides and to explain many of the previously inexplicable isomers.[81]

Coordination compounds, also known as metal complexes, include all metal compounds, aside from metal vapours, plasmas, and alloys.[81] The study of "*coordination chemistry*" is the study of the inorganic chemistry of all alkali and alkaline earth metals, transition metals, lanthanides, actinides, and metalloids. Thus, coordination chemistry is the chemistry of the majority of the periodic table. Metals and metal ions only exist, in the condensed phases at least, surrounded by ligands.

Mononuclear transition metal complexes are prepared by reacting a metal ion (M) with a number of free ligands (L) (**Scheme 1.3**).

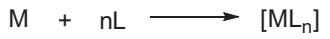

Scheme 1.3 Reaction of a metal ion (M) with a number of free ligands (L).

Whereas the effect of the ligands upon a metal ion is relatively well understood, and moderately easily quantified, the converse effect is not so.[82] In particular, the change from lone pair to bonding pair, consequent upon the formation of the coordinate bond (**Figure 1.6**), has effects upon the other groups which might be bonded to the ligand donor atom(s).

Figure 1.6 Schematic representation of the formation of a coordination compound, emphasising the conversion of the ligand lone pair to a bond pair.

There are several changes which result from coordination of a ligand to a metal.[82]

(a) *Conformation changes* can occur in the equilibrium conformation of the coordinated ligand with respect to the equilibrium conformation of the free ligand. A lone pair from the ligand bonds to a metal. The bonding changes the non-binding interactions in the molecules and we can see changes in bond lengths, angles, and molecular geometry.

If a polydentate ligand binds to a single metal, the resultant complex is a chelate (Greek "chelos", claw). Chelate complexes are more stable, with respect to ligand displacement, than a compound with equivalent monodentate ligands. The coordination follows a pathway in which metal-ligand formation is sequential.

An example of this is the conformational changes of 2,2'-bipyridine (see **Section 1.3.2**) when coordinated to a metal. The conformation is altered from *transoid* to *cisoid*, as shown in **Figure 1.7**. These changes can be monitored by the downfield shifting of the signal for H^3 comparing the ^1H NMR spectrum of the free ligand and complex. This is a consequence of the steric repulsion between the H^3 atoms in the *cisoid* conformation of the complex.

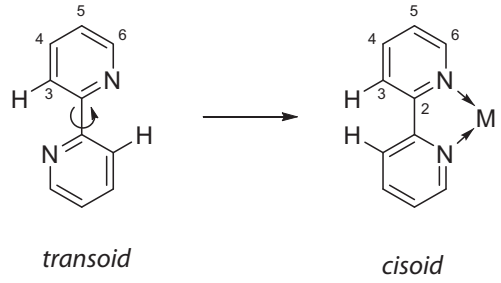

Figure 1.7 Conformational change upon coordination of 2,2'-bipyridine.

(b) *Polarisation changes* may occur upon complexation. If the metal ion to which a ligand is coordinated is in a non-zero oxidation state, it will exert an electrostatic effect upon the bonding electrons of the ligand. This will result in the induction of a net permanent dipole in the ligand, with any associated chemical and physical effects. Even zero-oxidation state metal centres may induce a polarisation in the ligand through electronegativity or induced dipole-dipole effects.

(c) *π-Bonding changes* will take place by the introduction of π-bonding interactions between the metal and the ligand. The coordination process results in a metal-to-ligand or ligand-to-metal transfer of electron density, depending on the nature of the metal centre, its oxidation state, and on the nature of the ligands. This opposes the polarisation effects of the metal ion in many cases.

The understanding of all these effects has led to a better understanding of the chemistry of organometallic and bio-inorganic systems. The explanation gives a versatile description of an enormous range of ligand reactions.

1.3.2 Oligopyridines

Oligopyridines are molecules made (formally) by bonding pyridine subunits together through C–C bonds. The most commons ones are represented in **Scheme 1.4**.

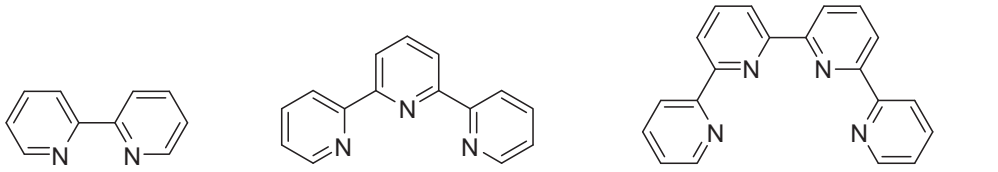

2,2'-bipyridine (bpy) 2,2':6',2''-terpyridine (tpy) 2,2':6',2'':6'',2'''-quaterpyridine (qtpy)

Scheme 1.4 The most common oligopyridines.

The names come from the Greek prefix for the total number of pyridine rings combined with the word "pyridine". The position is specified with the nitrogen at the first position and subsequent rings are denoted with primes.

2,2'-Bipyridine, is, undoubtedly, the most commonly used representative ligand in the class of oligopyridines, and its derivatives are renowned for their ability to form coordination compounds with metal ions of almost all groups in the periodic table.[4] It is a molecular building block *par excellence* for a wide variety of types of molecular and ionic aggregates ("supramolecules", see **Section 1.1**). Pure 2,2'-bipyridine was synthesised and analysed by *F. Blau* in 1889, when he obtained it by distillation of copper picolinate.[83] One year before, in 1888, *Blau* synthesised the first complexes of Fe(II) salts with 2,2'-bipyridine and isolated a series of salts with the composition $[Fe(bpy)_3][X]_2$.[84, 85] As metal complexes usually are readily obtained upon addition of the free ligand bpy to the metal ion, and as the complexes normally exhibit a very high stability, 2,2'-bipyridine complexes are used in analytical chemistry for the determination of metals, especially Fe(II).[86] 2,2'-Bipyridines can also influence biological systems.[87, 88] Their activity is usually a consequence of their ability to complex those metals which are jointly responsible for the enzymatic activity in a living organism. Moreover, they are able to stimulate the activity of some enzymes, probably by removing the metal which inhibits them.[87]

1.3.3 Iridium and its complexes

The element iridium is a very hard, brittle, silvery-white transition metal of the platinum family. Iridium is the second densest element (after osmium by about 0.1 %) and is the most corrosion-resistant metal, even at temperatures as high as 2000 °C.[89] Iridium (Greek "*iridios*", meaning rainbow-like colours, named by the manifold colours of its compounds) was discovered in 1803 by

S. Tennant among insoluble impurities in natural platinum from South America.[90] Iridium is one of the least abundant elements in the Earth's crust. With an average mass fraction of 0.001 ppm in crustal rock, it is four times less abundant than gold, ten times less abundant than platinum, and eighty times less abundant than silver and mercury.[91] An alloy of 90 % platinum and 10 % iridium was used in 1889 to construct the international prototype meter and kilogram mass, kept by the "International Bureau of Weights and Measures" near Paris.[92] Interestingly, iridium has been linked with the extinction of the dinosaurs and many other species 65 million years ago. The unusually high abundance of iridium in the clays of the K–T geologic boundary (Cretaceous and Tertiary periods) was a crucial clue that led to the theory that the extinction was caused by the impact of a massive extraterrestrial object with the Earth, the so-called *Alvarez* hypothesis.[93]

Iridium forms compounds in the oxidation states of −3 and all in the range from −1 to +6, the most common oxidation states are +3 and +4.[91] Trihalides of iridium, *i.e.* IrX_3, are known for all of the halogens. $IrCl_3 \cdot 3H_2O$ was used for the preparation of the Ir(III) complexes presented in **Chapter 7**. In the solid state of the trihalides, in fact for all halides of IrX_n (n = 1, 3, 4, 5, 6), each metal centre is in an octahedral environment.[90]

Iridium(III) complexes, exhibiting a [Xe] d^6 electron configuration, generally adopt the coordination number six. Normally, they possess diamagnetic properties due to the low-spin $t_{2g}^{\ 6}\ e_g^{\ 0}$ configuration in the complex, as the iridium(III) cation (as a third row transition metal) has a large contribution to the ligand field stabilisation energy,[90] with a *g*-factor of 32'000 cm^{-1}.[94] The colour of the complexes, often in the range between yellow and red, is due to two electronic transitions from $t_{2g}^{\ 6}\ e_g^{\ 0}$ to $t_{2g}^{\ 5}\ e_g^{\ 1}$ (*i.e.* $^1A_{1g} \rightarrow {}^1T_{1g}$ and $^1A_{1g} \rightarrow {}^1T_{2g}$, respectively).[90] Charge transfer bands, on the other hand, may lead to other colours also. Like the Co(III) analogues, Ir(III) complexes possess a *kinetically* high stability due to the highly symmetric electronic configuration. The *thermodynamically* stability ranges from "hard" (*e.g.* F^-, OH^-, NH_3; lower stability) to "soft" (*e.g.* I^-, RS^-, PR_3, CO; higher stability) ligands.[90]

A rather unique feature of the Ir(III) chemistry is the ability to establish bonds to carbon atoms to form extraordinarily (air- and water-) stable complexes. Chelate complexes with, for instance, 2-phenylpyridine (Hppy), such as the homoleptic $[Ir(ppy)_3]$ (**Scheme 1.5**), often described as *cyclometallated* or *orthometallated* compounds,[95, 96] are well known and have a broad application in solid state lighting (see **Section 1.5**).

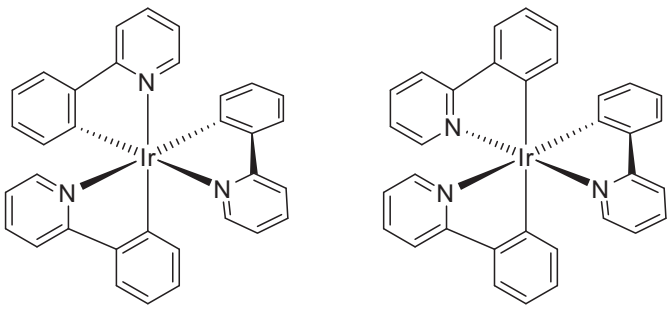

fac *mer*

Scheme 1.5 The two stereoisomers of homoleptic tris(2-phenylpyridine)iridium(III), the *facial* and the *meridional* isomer.

Concerning electronic features of heteroleptic Ir(III) complexes as prepared in **Chapter 7**, calculations of the cations show that both the HOMO and the LUMO are primarily ligand-centred. Whereas the HOMO is mainly found on the phenyl rings of the *C*,*N*-ligands, the LUMO is strictly localised on the *N*,*N*′-ligand (**Figure 1.8**). This is important for colour optimisation regarding the complex's luminescence properties.

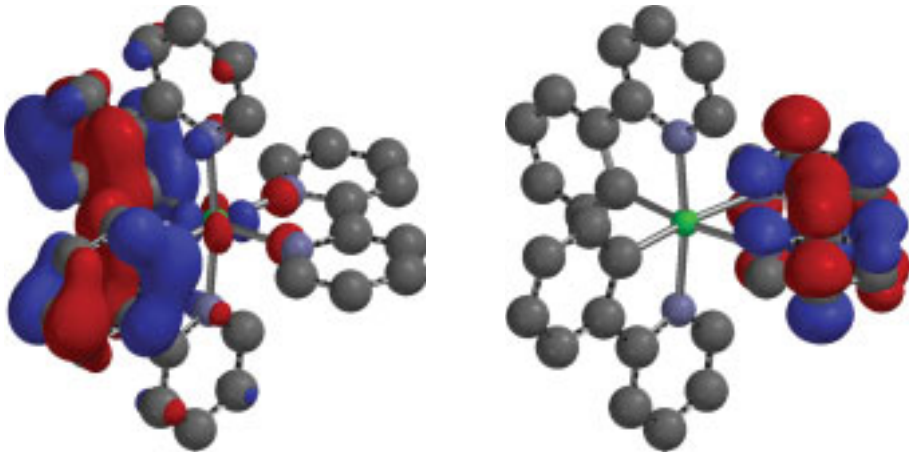

Figure 1.8 Semi-empirical calculations at the PM3 level of the HOMO (left) and LUMO (right) of the solid state structure of the cation in complex **49**.

1.4
Scanning tunnelling microscopy

1.4.1
History

In March 1981, a new type of microscope made its debut.[97] Unlike traditional (optical) microscopes, however, the scanning tunnelling microscope (STM) did not use lenses. Instead, a sharp tip was moved close enough to a conductive surface for the electron wavefunctions of the atoms in the tip to overlap with the wavefunctions of the surface atoms (see also **Section 1.4.2**). The initial results were written up in a manuscript which was submitted to a leading physics journal in June 1981. However, the paper was declined by the editors based on the report of one of the referees who said that the experiment would not give any new insight. Eventually, the results were published in another leading journal, *Applied Physics Letters*, in January 1982.[98] These experiments were conducted in Switzerland at the IBM research centre in Rüschlikon by *G. Binnig* and *H. Rohrer* who awarded the Nobel prize for physics only four years later, in 1986. In terms of science, the real breakthrough for the STM came in 1983 with the experimental observation of one of the most intriguing phenomena in surface science at that time, *i.e.* atom-by-atom imaging of the 7×7 surface reconstruction in Si(111).[99] For the first time it was possible to visualise individual atoms on surfaces in a 3D representation.[97]

Another important strength of STM (beyond topographic imaging and local measurements of surface properties) is the manipulation of surfaces.[21] Single atoms of the surface or adsorbates on it have been systematically moved in STM in order to build nanometer-sized structures (**Figure 1.9**). This can be accomplished by pushing or pulling the atoms with the tip, or even by transfer of atoms to and from the tip. Such experiments establish a lithography on a molecular scale.[100]

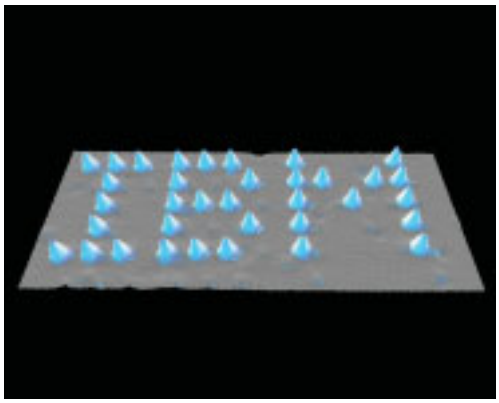

Figure 1.9 An STM image after manipulating the surface with an STM tip. "IBM" was written with Xenon atoms on Ni(110). Image taken from the literature.[101, 102]

It can be safely stated that with the invention of STM,[103] the "doors to the nanoworld were opened"[97]. Indeed, STM has inspired more than 14'000 papers, and there are at least 500 patents related to the various forms of scanning probe microscopes.[97]

1.4.2 Concept

As described in the previous section, the STM is *not* an optical microscope. It works with a sharp metallic tip which scans over the surface at the distance of less than 1 nm.[21] The distance is controlled by the tunnelling current between the tip and the conducting surface. The tunnelling current is a quantum mechanical effect with two properties important for STM. Firstly, it runs between two electrodes through a thin insulator or a vacuum gap, and it decays roughly by a factor of 450 on a length scale of one atomic radius. Secondly, therefore in STM, the tunnelling current flows from the very last atom of the tip apex to single atoms at the surface, inherently providing atomic resolution.[104, 105]

Therefore, STM does not measure the real topography of the surface, but rather a surface of constant tunnelling probability, which is connected with the local density of state near the Fermi level.[104] For example, a molecule adsorbed on top of a metal surface may reduce the local density of states and may actually be imaged as a depression, as, for instance, carbon on Ni(100).[106]

D. Eigler et al. used this peculiarity of STM to visualise not only an atomic landscape, but the electronic landscape also.[107, 108] They were able to image standing electron waves on a copper surface, confined by a "corral" of deposited iron atoms (**Figure 1.10**). The "ripples" in the ring of atoms are the density distribution of a particular set of quantum states of the corral. The authors could explain this phenomenon by solving the classic eigenvalue problem in quantum mechanics: a particle in a hard-wall box.

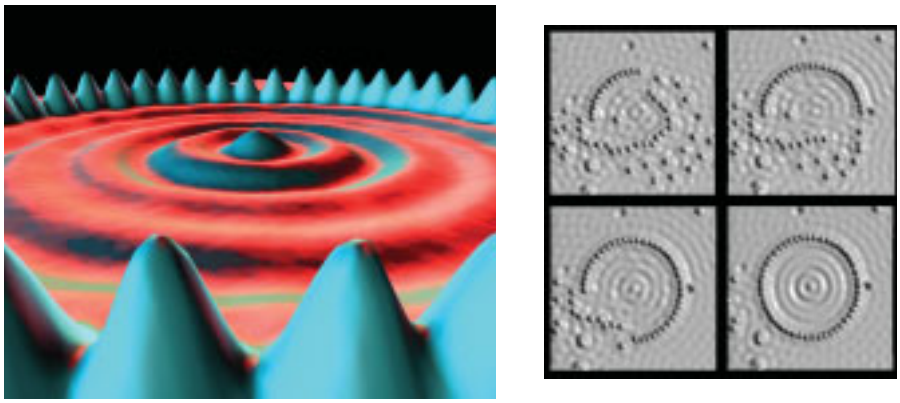

Figure 1.10 Left: Positioning of 48 iron atoms on Cu(111) into a circular ring in order to "corral" some surface state electrons and force them into standing waves inside the circular structure. Right: Various stages during the construction of the circular corral. Images taken from the literature.[107, 108]

The main parts of an STM system are a sample, a tip on a piezo-actuator, electronics to apply a potential and to control the piezo-voltage by a feedback, and a computer to record the data.[109] **Figure 1.11** illustrates a schematic representation of these components.

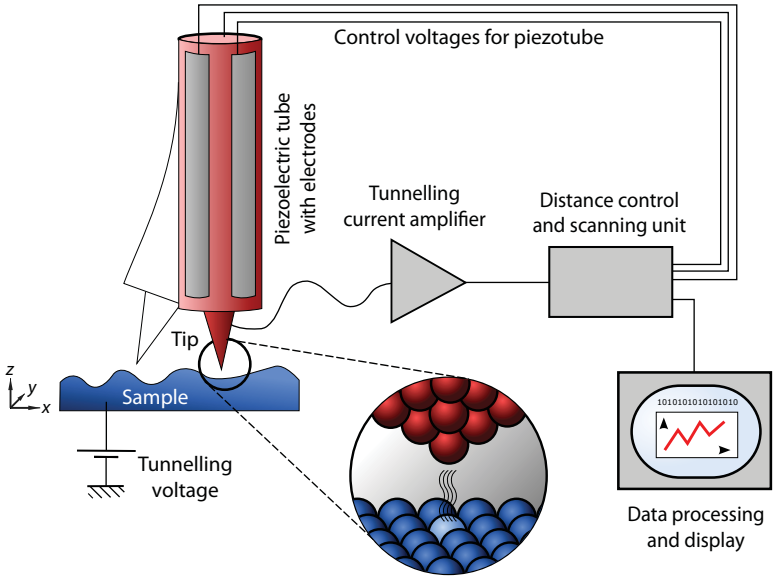

Figure 1.11 Schematic of a scanning tunnelling microscope. Original image[110] was published under a Creative Commons Attribution ShareAlike (cc-by-sa) License[111] and adapted for our needs.

In a standard experiment, the tip is moved in three dimensions by the aforementioned piezoelectric actuators.[21] Using the combination of a coarse approach and piezoelectric transducers, a sharp, metallic probing tip is brought into close proximity with the sample. The distance between the tip and the sample is only a few angstrom units, which means that the electron wavefunctions of tip and sample start to overlap. A bias voltage between tip and sample causes electrons to tunnel through the barrier, as discussed before. An electronic controller guides the tip at a tip–sample distance corresponding to either a constant tunnelling current (*constant current* mode) or a constant height (*constant height* mode). The tunnelling current is in the range of pA to nA and is measured with a preamplifier. The z-position is measured at discrete (x,y)-positions, and this distance is recorded by a computer as a function of the lateral position and displayed as the microscope image (see also **Chapter 2**).

High mechanical stability of the experimental setup turns out to be a prerequisite for successful measurements on the atomic scale.[104, 105] The tip has to be conducting and atomically sharp.[21] The shape of the tip is not that crucial, because the tunnelling current, I_t, decays exponentially with the distance between tip and sample, and, as a consequence, the tunnelling current flows mainly through the atom at the very end of the tip. It is therefore necessary to position the tip at sub-Å precision in the z-direction.[21]

Operational aspects of STM measurements are covered in **Chapter 2**.

1.5 Solid state lighting

1.5.1 History and terminology

Solid state lighting (SSL) is an illumination technology, of which the base is the phenomena of electroluminescence (EL, see **Section 1.5.2**). Its applications are, amongst others, LEDs (light-emitting diodes), OLEDs (organic light-emitting diodes), and, sometimes considered as a sub-category of OLEDs, the LEECs (or LECs, light-emitting electrochemical cells, see **Section 1.5.3**). In this thesis, compounds for the use in LEECs have been prepared. See **Chapter 7** for the synthesis and characterisation of the complexes, and **Chapter 8** for the characterisation and discussion of their LEEC devices which were fabricated and measured by the group of *H. Bolink* in Valencia, Spain.

In 1962, *N. Holonyak*, working at the US company "General Electric", gave the first practical demonstration of LEDs.[112] Over the course of the 1970's, the physics of LED illumination was explained in detail,[113] and by the end of the decade, LEDs had replaced incandescent bulbs for indicator lamps and Nixie tubes (small plasma discharge vacuum tubes) for numeric displays.[114] Starting in the mid- to late 1980's, a new type of SSL source was developed based on organic semiconductors.[115, 116] The performance of these OLED devices improved dramatically in the 1990's until now, a consequence of worldwide efforts to develop full-colour, flat-panel displays. By the turn of the

century, the performance of OLEDs clearly showed that they had the potential for use in general illumination.

The 1990's also saw two major breakthroughs in inorganic LED technology.[114] The performance of LED devices, like that of their organic counterparts, steadily increased during the 1990's. Since LEDs, in fact, SSL devices generally, can be fabricated in all the primary colours, they will, in time, serve as a source of white light for general purposes.

As about 20 % of electricity (in the United States) is used for lighting, and the production of the electricity costs more than $ 60 billion a year,[114] it is obvious that there is a huge demand for efficient lighting technology, at least on an economical level. SSL devices promise to replace conventional light sources, such as incandescent and fluorescent lamps.

Another important application of SSL technology is found in displays. With the success of flat screen displays at the end of the 20th century, the demand for even thinner, foldable, more power efficient models, and displays showing a larger colour gamut, has risen. SSL devices, especially the ones based on organic technology (OLEDs, LEECs), promise to deliver these demands as they can be "printed" onto substrates in contrast to the inorganic devices (LEDs). In fact, displays built on the technology of OLEDs are already in the market, albeit at a high price.

1.5.2
General principles of electroluminescence

Electroluminescence (also called electrogenerated luminescence and abbreviated as EL) involves the generation of species at electrode surfaces that then undergo electron-transfer reactions to form excited states that emit light.[117] For example, application of a voltage to an electrode in the presence of an EL luminophore such as $[Ru(bpy)_3]^{2+}$ results in light emission and allows detection of the emitter at very low concentrations ($< 10 - 11$ mol l^{-1}).[118] The effect of EL is observable in the solid state and in solution.

EL is a means of converting electrical energy into radiative energy. It involves the production of reactive intermediates from stable precursors at the surface of an electrode. These intermediates then react under a variety of conditions to form excited states that emit light.[117]

In *photoluminescence*, emission derives from the excitation of electrons in the HOMO of a particular luminophore (*e.g.* any Ir(III) complex presented in **Chapter 7**) and its radiative return to the ground state (**Figure 1.12**).

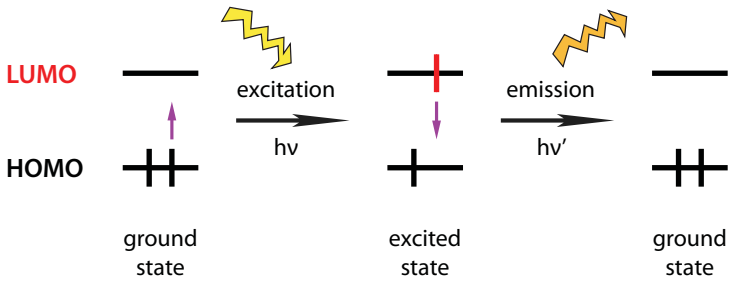

Figure 1.12 The principles of photoluminescence. An electron in the HOMO of a luminophore is excited by a photon, and upon its return to the ground state, a photon is released.

Electroluminescence, on the other hand, is the result of a radiative recombination of electrons and holes (= missing / extracted electrons) in a material (*e.g.* a semiconductor in LEDs, or the emissive layer in LEECs containing the active luminophore). Electrons injected at the cathode reduce the luminophores. On the other side of the applied electric field, *i.e.* at the anode, electrons are withdrawn, and thus, holes are generated. Through a hopping mechanism, electrons migrate through the film eventually meeting an oxidised luminophore which lacks one electron (possesses a hole). This so-formed excited state in the luminophore ("exciton") eventually releases its energy as a photon upon its radiative return to the ground state (**Figure 1.13**). Concomitantly to this process, ions migrate between the electrodes.

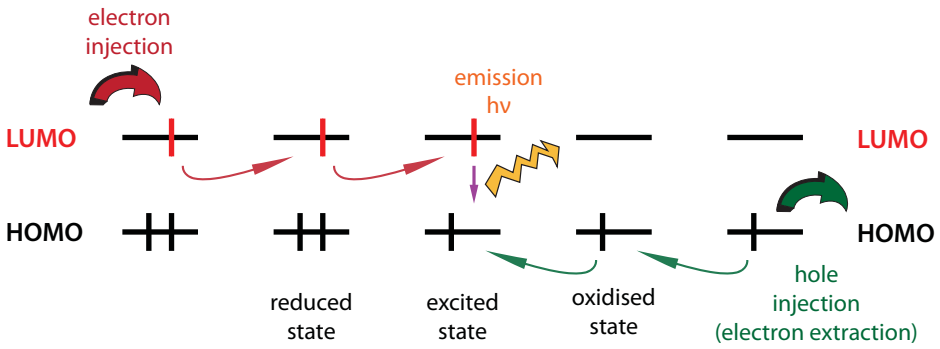

Figure 1.13 The principles of electroluminescence. At the cathode (left hand side), electrons are injected on the luminophore. At the anode (right hand side), electrons are extracted, and thus, holes are generated. Both electrons and holes migrate through the film, eventually meeting each other at a particular luminophore, thus generating an excited state ("exciton"). Upon the return of the electron to the ground state, a photon is released.

1.5.3 OLEDs and LEECs

Organic light-emitting diodes (OLEDs) and, often regarded as a sub-category thereof, *light-emitting electrochemical cells* (LEECs or LECs) are electroluminescent devices of which the emissive

electroluminescent layer is composed of a film of "organic" compounds. In this context, "organic" covers ("inorganic") metal complexes as well; the term is rather used to separate from semiconducting materials such as (*e.g.*) gallium(III) phosphide used in LEDs.

OLEDs

An OLED consists of one or more organic layers sandwiched between two metal electrodes, one of which must be transparent.[114] The organic layers are typically undoped and insulating molecules with a large π-conjugated system or polymers. These materials have essentially no free charges. Hence, the charges that run through the OLED during operation are injected into the organic layers from the electrode contacts. The cathode, which injects electrons into the device, should have a low work function (*i.e.* the minimum energy needed to remove an electron from an uncharged solid), allowing its energy to be close to that of the LUMO of the luminophore. A good energy match between the LUMO and the cathode means that not much energy is lost when electrons are injected. Likewise, the anode should have a high work function and an energy close to that of the HOMO. Typically, the cathode is made of a reactive metal such as calcium, lithium, or magnesium, either singly or alloyed with another metal, while the anode is formed from indium tin oxide (ITO), a transparent conductor with a relatively high work function.[114]

Once electrons and holes are injected into the organic layer, they drift under the influence of the applied field toward the opposite polarity contacts.[114] The electron and hole mobilities in the disordered layer are low, so a high field is required for appreciable current. Thus, the organic layers must be thin (on the order of 100 nm) for low-voltage operation. As electrons and holes hop from site to site, they sometimes land in the same place and form a neutral bound excited state, or exciton (see **Section 1.5.2** above). With properly chosen materials, a significant fraction of these excitons relax by emitting a photon so as to generate light. The colour of the emitted light and the electrical characteristics of the OLED depend on the specific organic material and details of the device design.

For the usage in displays, the advantages of OLEDs compared to traditional LCD screens, of which the light source normally is a fluorescent lamp, or as recently, white LEDs or RGB LEDs have been used as well, are numerous. Firstly, since OLEDs can be printed onto any suitable substrate using an inkjet printer or even screen printing technologies,[119] they can theoretically have a significantly lower cost than LCDs or plasma displays. Printing OLEDs onto flexible substrates opens the door to new applications such as roll-up displays and displays embedded in fabrics or clothing. Secondly, OLEDs enable a greater range of colours (gamut), brightness, contrast and viewing angle than LCDs because OLED pixels directly emit light. Thirdly, OLED displays supposedly use less power than traditional LCD screens.

On the other hand, the major technical problem for OLEDs is the limited lifetime of the organic materials. Furthermore, as three different compounds for each of the three colours red, green, and blue (RGB) are used, they all have differing stabilities resulting in colour shifts during the lifetime of an OLED display. Nevertheless, enormous progress has been made in that field. Many products

(although mostly with small screens) are already on the market, such as displays in mobile phones, in digital cameras, and even a TV screen featuring a 12“ OLED display is commercially available.

As for the usage in general lighting, due to their thin structure and flexibility, OLEDs could be mounted on ceilings or walls. According to the chosen device characteristics and/or through a combination of different devices, very pleasant light temperatures mimicking the spectrum of the sun light can be achieved.

LEECs

The principle of LEECs is essentially a simplified OLED structure. **Figure 1.14** depicts the stack of layers used in a typical LEEC. They are usually composed of two metal electrodes connected by (*i.e.* “sandwiching”) an emissive (“active”) layer containing the luminophore. On the chemical side, the luminophore in the emissive layer is not an uncharged compound (as in OLEDs) but rather an ionic one. The invention of the LEEC (based on a conducting polymer) is attributed to the Nobel laureate *A. J. Heeger*.[120]

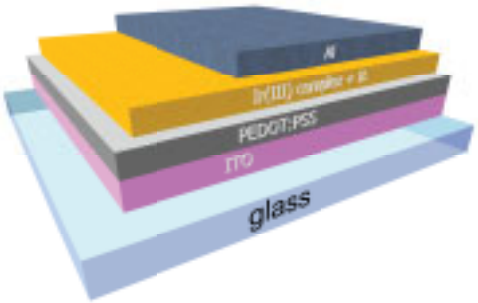

Figure 1.14 Sketch configuration of a double-layer LEEC device. In purple and dark blue the anode (ITO) and cathode (Al), respectively. In dark grey the PEDOT:PSS layer used to improve the reproducibility. In orange the active layer based on a mixture of an Ir(III) complex and ionic liquid (IL).

In contrast to OLEDs, LEEC devices are insensitive to the work function of the electrodes employed.[121, 122] This is due to the generation of a strong interfacial electric field caused by the displacement of the mobile ionic species toward the charged electrodes when an external electric field is applied over the device.[123] Therefore, in contrast to OLEDs, which require rigorous encapsulation to prevent degradation of the electron-injecting layers,[124] air-stable electrodes, such as gold, silver, or aluminium can be used, which is an initial requirement for obtaining unencapsulated devices.

Soon after the initial polymer-based LEEC by *Heeger et al.*, single-component, solid state light-emitting devices based on ionic transition-metal complexes have been reported.[125, 126] In this type of LEECs, the complexes perform all the necessary roles to generate light: (a) the decrease of injection barriers via the displacement of the counterions, (b) the transport of electrons and holes via consecutive reduction and oxidation, respectively, of the complex, and (c) the generation of the photons. The metal complex is an intrinsic molecular semiconductor, in which the HOMO is the t_{2g}

of the metal centre, and the LUMO is a π* orbital of the ligands.[127] On application of a bias in this LEEC, holes and electrons are injected from the anode and the cathode, respectively, into the transition metal complex. These carriers are transported towards the opposite electrode *via* hopping, and may recombine to produce light emission with a characteristic colour that corresponds to the energy gap of the complex. Critical to the operation of these LEECs are the counter ions (*e.g.* $[PF_6]^-$), which are mobile in the film and at room temperature. Their redistribution on the application of a bias assists the injection of electronic carriers.[127]

However, the detailed working principles, such as the electric-field distribution within a device, are still debated,[127, 128] although the internal device operation can be observed directly.[129]

As with OLEDs, the benefits of LEECs in lighting applications and their usage in displays are numerous. Additionally to the advantages mentioned for OLEDs, LEECs operate at very low voltages, yielding high power efficient devices.[123] Furthermore, they are easy and cheap to produce as they can be fabricated using spin-coating techniques rather than the chemical vapour deposition used for OLEDs. This, together with their overall simpler architecture (no encapsulation of the electrodes, fewer layers), LEECs represent a more economical alternative.[130-133]

Unfortunately, LEECs based on ionic transition-metal complexes have limited stability. This has been attributed (in the case of a $[Ru(bpy)_3]^{2+}$-based device) to a water-assisted ligand exchange reaction of the excited state molecule ("exciton") and the subsequent formation of a new complex that functions as an efficient luminance quencher.[134, 135] In **Scheme 1.6**, this degradation process is depicted for the most simple Ir(III) complex described in this thesis, *i.e.* $[Ir(ppy)_2(bpy)][PF_6]$ (**49**, see **Chapter 7** and **Chapter 8**).

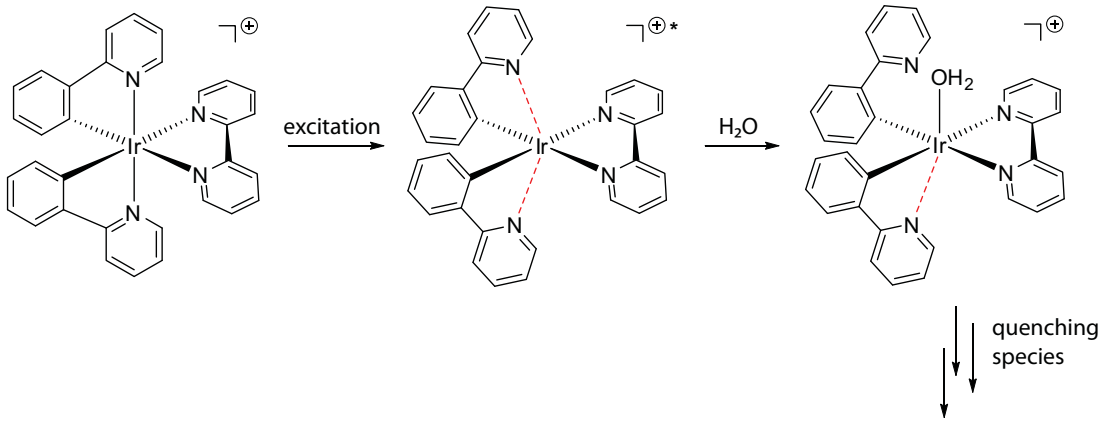

Scheme 1.6 Degradation reactions in the emissive film of LEEC devices using the example of $[Ir(ppy)_2(bpy)][PF_6]$ (**49**). The excited species ("exciton") is hydrolysed by water leading to several quenching species.

This instability renders the usage for LEEC devices in real-world applications useless, as their stability is in the range of hours to days. The best reported LEEC so far has a lifetime of 60 hours.[136]

With the work presented in this thesis, a major breakthrough for long-lived LEECs has been achieved allowing lifetimes of several thousands of hours (see **Chapter 8**).[123, 124, 137]

Chapter 2

Instruments and Methods

2.1
General experimental

Chemicals and reagents

All starting chemicals were commercially available and of reagent grade and were used without further purification except the following compounds. 4,4'-Dinitro-2,2'-bipyridine-*N*,*N'*-dioxide was donated by *C. Brennan* of our group, 3,5-bis(octyloxy)benzaldehyde (**12**) was provided by *L. Scherer*, (+)-TADDOL and (–)-TADDOL were gifts from the *Dieter Seebach* group at the ETH Zürich, and all dichloro-bridged Ir(III) dimers (**41**, **42**, **43**, **44**, **45**, and **46**) including the *C*,*N*-ligands Hpiq and Hdmppz were prepared by *L. Siegfried* as noted in **Chapter 7**.

Solvents

All solvents were commercially available and of HPLC grade. Solvents were dried either by distilling over sodium (THF and diethyl ether) or sodium hydride (dichloromethane), or on a solvent purification system "Pure Solv MD-5" (using several columns) by Innovative Technology inc.

Chromatography

Preparative column chromatography was done using Fluka silica gel 60 (0.040 – 0.063 mm) or Merck aluminium oxide 90 standardised unless otherwise stated. Freshly distilled solvents were used.

TLC was carried out using Merck precoated, aluminium-backed silica gel 60 F_{254} plates and the R_f values were rounded to one significant figure. Visualisation agents are designated as follows: (A) ultraviolet illumination, (B) 7 ml anisaldehyde, 5 ml conc. sulfuric acid and 3 ml glacial acetic acid in 250 ml ethanol, (C) iron(II) chloride solution in methanol (for 2,2'-bipyridine ligands). In the case of B, dipped plates were heated to approximately 200 °C.

Preparative layer chromatography was performed with commercially available Merck silica gel 60 PLC (2 mm) 20 cm square plates. Products were visualised by ultraviolet irradiation.

Microwave reactor

The microwave reactor used in this thesis was a Biotage Initiator (400 W max power) with sealed tubes allowing pressures of up to 20 bar.

2.2 Analytical equipment

Melting point

Melting points were measured with a Stuart Scientific Melting Point Apparatus SMP3.

NMR spectroscopy

^{1}H and ^{13}C NMR spectra were recorded on Bruker AM250 (250 MHz), Bruker DRX400 (400 MHz) or Bruker DRX500 (500 MHz) spectrometers. For full assignments, COSY, DEPT, HMBC, and HMQC experiments were conducted on the Bruker DRX500 by either *K. Harris*, *A. Hernández*, or *V. Jullien*. ^{19}F NMR spectra were recorded on the Bruker DRX400. For ^{1}H and ^{13}C NMR measurements, the chemical shifts δ are relative and internally referenced to either TMS or the residual peak of the solvent (mostly $CDCl_3$ or CD_2Cl_2).

Infrared spectroscopy

Infrared spectra were recorded on a Shimadzu FTIR-8400S spectrophotometer with neat samples using a golden gate attachment.

Mass spectrometry

MALDI-TOF mass spectra were performed on a Vestec Voyager Elite using a supporting matrix (α-cyano-4-hydroxycinnamic acid). ESI mass spectra were recorded on a Bruker Esquire 3000 plus instrument at 250 °C. MALDI-TOF and ESI mass spectra were measured by either *L. Scherer*, *P. Rösel*, or *R. Schmitt*. EI mass spectra were conducted on a Finnigan MAT 312 and 3-nitrobenzyl alcohol was used as supporting matrix. FAB mass spectra were measured on a Finnigan MAT 95Q apparatus. Both FAB and EI measurements were conducted by *P. Nadig*.

UV-Vis spectroscopy

UV-Vis spectroscopy measurements were done either on a Perkin-Elmer Carey 5000 spectrophotometer (for compounds **49**, **50**, **51**, **52**, and **57**) or on an Agilent Technologies UV-Visible 8453 Spectrophotometer (for complexes **47**, **48**, **53**, **54**, **55**, **56**, **58**, **59**, **60**, and **61**). For every compound, at least four different concentrations were measured. The solvent is given in parentheses.

Photoluminescence

The photoluminescence of Ir(III) complexes were performed on a Shimadzu RF-5301PC spectrofluorometer. Solutions from the UV-Vis measurements were used (normally the lowest concentration) and the emission was determined at different excitation wavelengths which were detected in previous excitation spectra. The excitation and emission slits were kept as close as possible, and they were never opened more than 3.0 units. Prior to the measurements, blank samples of the solvent were measured to assure that the solvent does not emit as well.

Photoluminescence lifetime

The lifetime of the photoluminescence was measured with an Edinburgh Instruments mini-τ apparatus equipped with an Edinburgh Instruments EPL-475 picosecond pulsed diode laser (λ_{ex} = 467.0 nm, pulse width = 75.5 ps) with the appropriate wavelength filter. The same solutions (lowest concentration) as for the photoluminescence measurements were used.

Microanalysis

Elemental analyses were measured with a Leco CHN-900 microanalyser by *W. Kirsch*.

High-performance liquid chromatography

Analytical HPLC was performed on a Shimadzu VP system with UV and photodiode array, integration with Class-VP, chiral Daicel OD-H column. For semi-preparative separation, a chiral OD column was used. All solvents used were of HPLC grade.

Electrochemistry

Electrochemical measurements were done on an Eco Chemie Autolab PGSTAT 20 using a glassy carbon working electrode, a platinum mesh for the counter electrode, and a silver wire as the reference electrode. The redox potentials ($E^{ox}_{½}$, $E^{red}_{½}$ [V]) were determined by cyclic voltammetry (CV) and by square wave and differential pulse voltammetry. The compounds were dissolved and measured in dry acetonitrile in the presence of 0.1 M $(n\text{-Bu})_4NPF_6$ unless otherwise stated. The scanning rate for the CV was 100 mV s^{-1} in all cases and ferrocene (Fc) was added as an internal standard at the end of every experiment.

X-ray diffraction

The determination of the cell parameters and the collection of the reflection intensities of the single crystals were performed by *M. Neuburger* on an Enfraf-Nonius Kappa CCD diffractometer (graphite monochromated $Mo_{K\alpha}$ radiation). For the data reduction, solution and refinement, the programs COLLECT,[138] SIR97,[139] and CRYSTALS (version 12)[140] were used. This was done either by *M. Neuburger* or *S. Schaffner*. Visualisation and structural analyses were performed with the software CCDC Mercury (versions 1.4.2 and 2.2), Accelrys DS Visualizer (version 2.0.1.7347) with POV-Ray (version 3.6), PLATON (GUI version 1.15, PLATON.EXE version 2009-01-19),[141] and ORTEP-3 (version 1.05 based on ORTEP-III version 1.0.2)[142].

2.3 Scanning tunnelling microscopy

For the history and technology of scanning probe microscopy (SPM) and scanning tunnelling microscopy (STM) see **Chapter 1**.

2.3.1 Setup

Apparatus

The STM experiments of this thesis were performed on a Digital Instruments Nanoscope III device (**Figure 2.1**) equipped with a low current converter making it capable of detecting currents below 10 pA. All measurements were conducted under ambient conditions, *i.e.* room temperature and aerial atmosphere. To minimise vibrations, the device was mounted on a shock-absorbing rubber plate standing on an air table.

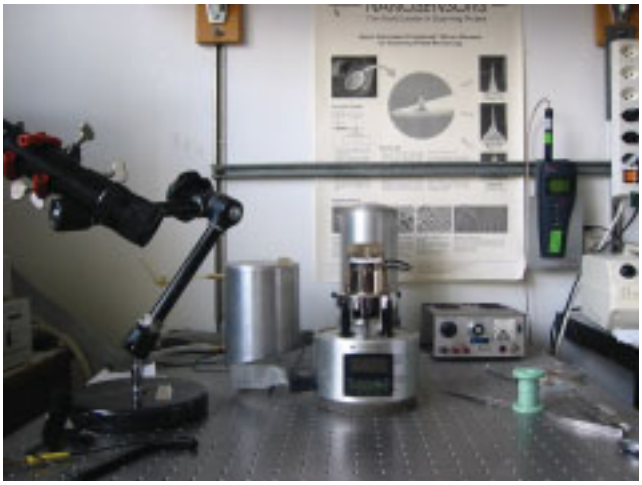

Figure 2.1 The Digital Instruments Nanoscope III STM apparatus used for STM measurements. Image taken from the PhD Thesis of *L. Scherer*[21] with permission of the author.

Substrate

STM devices work with many different substrates, but only highly oriented pyrolytic graphite (HOPG), *i.e.* α-graphite, was used in this work. Cleaning of the surface was performed by cleaving off a few layers of graphite with adhesive tape shortly before the measurements.

The layers in α-graphite are stacked in an ABA manner so that only every 2nd carbon atom has a nearest neighbour orthogonal in the layer below (**Figure 2.2**). Hence, in STM, only three atoms (out of a hexagon) are observed. Therefore, the system exhibits a threefold symmetry and not a sixfold symmetry as expected from a single layer only. This often results in three symmetrical arrangements of domains of molecular monolayers.

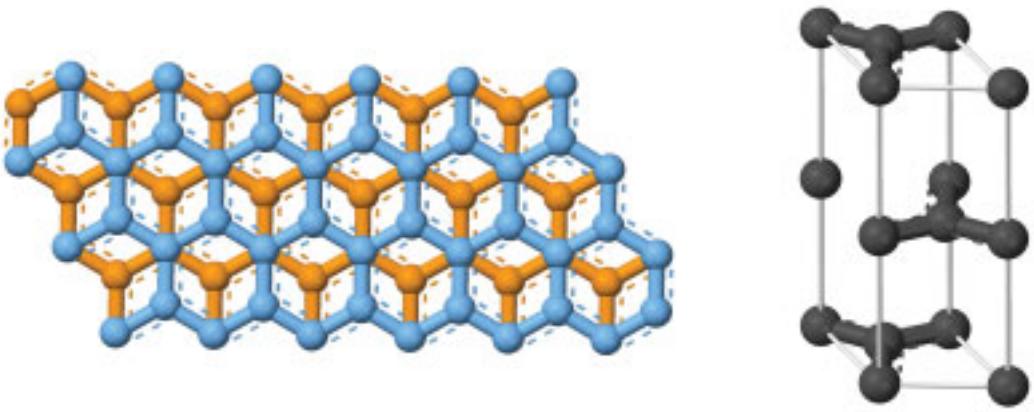

Figure 2.2 Plane view of layer stacking in α-graphite (a) and its unit cell (b). Images were published under public domain licensing.[143]

HOPG is a substrate easy to handle, but there are a lot of artefacts and other peculiarities which have to be taken into consideration.[21] First, graphite steps can lead to misinterpretation. Normally, domains end at a graphite step and do not continue afterwards. Secondly, sometimes bright spots arranged in lines could be detected which do not arise from single molecules or atoms as their size was independent from the recording size and of the compound. Thirdly, in a few instances, stripes are visible which do not correspond to a monolayer as they depend on the recording frequency ν. Moreover, Moiré-patterns (**Figure 2.3**) may be observed which derive from one or more graphite layers which are slightly moved to produce an interference pattern.[144] Interestingly, evaluation of Moiré-patterns between the adsorbate and the substrate lattices allows high-precision determination of intermolecular distances with an error of as little as ± 1 pm.[145, 146]

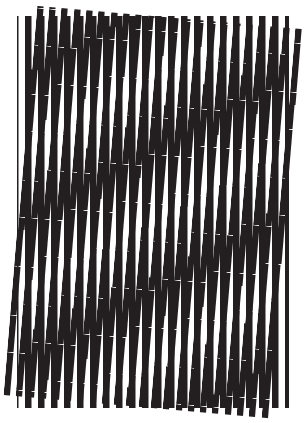

Figure 2.3 A Moiré-pattern which is an interference pattern produced by overlaying similar but slightly offset templates. Image published under the GNU Free Documentation License.[147]

Tip

The tips for STM measurements were made by mechanically cutting a platinum : iridium wire (90:10, d = 0.25 mm).

Sample preparation

There are many possibilities for adsorbing a monolayer onto HOPG. In this thesis, two methods were used: solution casting and measurements at the liquid/solid-interface.

For *solution casting*, the compounds were dissolved in a volatile solvent (mostly hexane) in a concentration of ca. 0.2 mmol l^{-1}. Two drops of the solution were given on the freshly cleaved graphite surface and allowed to evaporate. Then, the tip was approached to the surface yielding an *air/solid-interface*. The sample could be annealed by heating it in an oven for a period of time before measurement.

For the *liquid/solid-interface*, the compounds were dissolved in the non-volatile solvent 1-phenyloctane in the same concentration of ca. 0.2 mmol l^{-1}. Two drops of the solution were given on the freshly cleaved surface again and the tip was approached through the film of solution until it reached the graphite surface. At the *liquid/solid-interface*, one has to consider the fact that these solvents, due to their chemical structure, are also able to form monolayers and, thus, potentially co-adsorb with the dissolved compound. Nevertheless, in the case of 1-phenyloctane, this phenomenum is rather uncommon,[148] although it has been observed before.[56, 149, 150]

Measurement

If not otherwise stated, the normal measuring parameters were as follows: U_{bias} = –700 mV, I_t = 8.0 pA, internal gain = 1.0, proportional gain = 25, and a *Z*-limit of 300 nm. The line frequency ν ("measuring speed") was chosen and balanced carefully according to the image size (the bigger the size the lower the frequency) and the amount of drift present in the setup (the higher the drift the higher the chosen frequency).

As all measurements were conducted under ambient conditions, thermal drift is almost inevitable. Therefore, for all measurements, a subsequent image with the inversed recording direction (up or down) was recorded in order to estimate the drift (**Figure 2.4**).

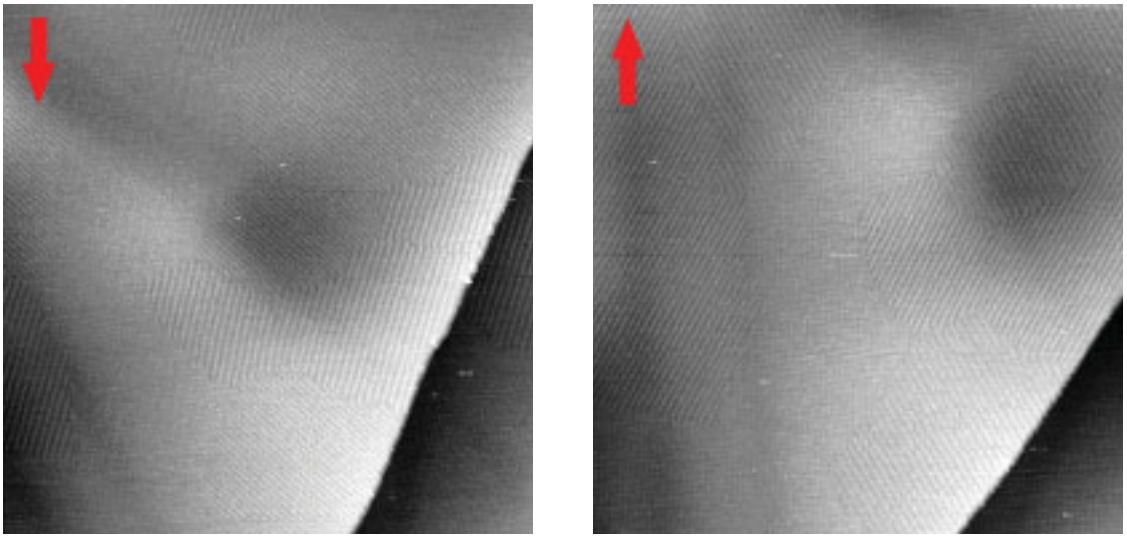

Figure 2.4 Two subsequently recorded STM images with indicated recording direction.

All measurements were performed in the *constant current* mode where the tunnelling current is kept at a constant value by moving the tip in the *z*-position during the acquisition of the image, *i.e.* scanning the sample by rasterising the *x*- and *y*-position. The *z*-position of the tip together with its lateral (*x*,*y*)-position is recorded and displayed as the microscope image.

2.3.2 Processing images

All data processings in this thesis were performed with the software "SXM-Shell", a script collection based on the numeric software Visual Numerics PV-WAVE (version 7.5) with a simple menu-based graphical user interface. SXM was developed at the University of Basel by *D. Brodbeck*, *D. Bürgler*, *R. Hofer*, and *G. Tarrach*. The most common features are described as follows.[21]

Flattening

For every scanline of the image, a polynom of a certain degree is fitted and subtracted from the data. The polynom is fitted using the least-squares method. All images in this thesis were flattened.

Display range

As the relevant data of an image span only over a fraction of nanometres and the *Z*-limit is normally set to 300 nm, the colour code from dark to light is restricted in the *z*-histogram in order to visualise the fine differences. The same effect is achieved by auto-level adjustment features found in numerous image manipulation software as they perform a similar method in order to stretch the luminance histogram of the image. The display range was restricted for all images shown in this thesis.

Topview

Topview is the 2D representation of the three-dimensional data (*x*, *y*, and *z* values from measurements). The colour code can be chosen freely. In this thesis, black to white was the desired visualisation.

Correlation averaging

An interactive correlation averaging procedure was used for many images in this thesis where stated. In a first step, after fast-fourier transformations, undesired artefacts and noise can be eliminated or suppressed in the frequency space by low- and high-pass filtering of the image ("filtered images" as referenced in this thesis). Then, a particular part of the image is selected (normally 10 nm × 10 nm) which is then used as a reference. In a cross-correlation of the selection and the original image, the positions of the best fit are picked. In all these positions, a sub-image with the size of the selection is cut and these sub-images are then averaged. During this step, single locations like scratches or noise can be manually excluded from the averaging process.

For an averaged image in this work, the number of chosen positions for the averaging process is given in their figure capture.

2.3.3
Assigning and overlaying molecules

As the first step in order to discuss an STM image, the pattern was investigated for symmetry elements. In most cases, a *p*1 (no symmetry element apart identity) or a *p*2 (C_2 axis) plane group was found. All subsequent procedures then had to obey these symmetry considerations.

Assigning a pattern to a specific molecular arrangement was performed completely *in silico*. Using Wavefunction Inc. Spartan ´04, the structure of an appropriate molecule was minimised with molecular mechanics methods or semi-empirical PM3 implementations. The exported .pdb-file was imported into PovChem to produce a space-filling representation in a .pov-file which could be rendered using POV-Ray (version 3.6). The .bmp-files so-obtained were pasted into an additional layer in Photoshop (version CS4) over the STM image and resized according to the correct size which was determined by interatomic distance measuring in Spartan ´04.

In Photoshop, the layer containing the molecule was moved and rotated until a reasonable arrangement was found. The occurrence of a higher tunnelling current above an aromatic moiety, as predicted by theoretical calculations,[151] is a general finding which has been observed for a large variety of organic adsorbates on graphite.[148] Therefore, bright spots in an STM image were usually assigned to a "conducting" aromatic ring whereas dark areas correspond to the "nearly insulating" alkyl chains under the herein chosen parameters (see **Section 2.3.1**). The rough approximation of "molecular conductivity" can be affirmed with HOMO-LUMO calculations. The contrast in STM images of organic molecules has often been successfully compared to the respective frontier orbitals according to the polarity of the applied potential.[152-154] **Figure 2.5** illustrates the sum of the HOMO and HOMO–1 molecular orbitals which were calculated semi-empirically at the PM3 level for ligand **29** (see **Chapter 5**). It confirms that the highest and second highest occupied molecular orbitals are found on the benzyl groups (and even extend to the oxygen atoms) giving rise to the highest contrast in an STM image when measured at a negative bias.[155]

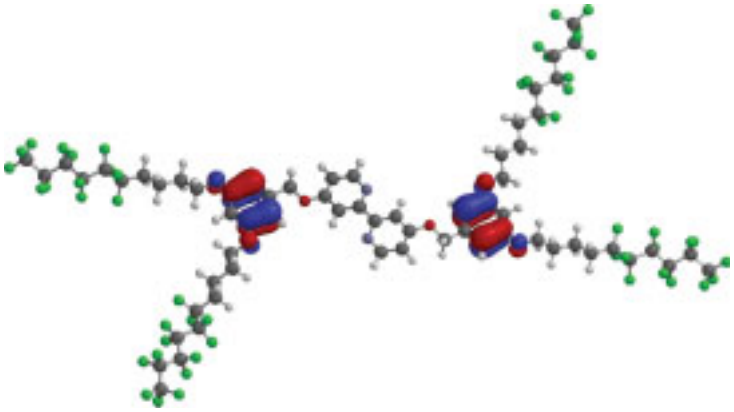

Figure 2.5 Calculated frontier orbitals (sum of HOMO and HOMO–1) for ligand **29**.

Then, the packing in the plane was achieved by duplicating the fitted molecule and moving and rotating it to the appropriate position according to the determined unit cell. The dimensions of the unit cells were obtained by size and angle measurements in Photoshop (averaged over several unit cells). The values were rounded to two significant figures as the experimental error is rather large due to the thermal drift in the setup.

It has to be noted here that the alkyl chains were normally not optimised and fitted to the underlying pattern. Therefore, for some proposed arrangements, alkyl chains may cross each other. It would be highly speculative to optimise the alkyl chains, as normally the aliphatic regions have a very low contrast in STM images which renders atomic assignments impossible. Furthermore, alkyl chains can bend at any position to allow numerous amounts of possible arrangements.

L. Scherer of our group showed a nice example where sheets of an experimentally determined crystal structure could be directly overlaid onto an STM image of a monolayer of the same compound.[156] In another publication by the same author, a similar procedure could be performed. There, the alkyl chains of the adsorbed molecules showed the aforementioned bending.[157]

2.4 LEEC devices

To start with, all the LEECs devices were fabricated by the group of *H. Bolink* in Valencia, Spain. We sent all the Ir(III) complexes discussed in **Chapter 7** to Valencia where they prepared and optimised hundreds of devices tweaking many parameters. A typical device preparation procedure is described in a publication arising from this collaboration.[124]

Chapter 3

Synthesis and STM Imaging of Achiral and Chiral Dendrons

3.1 Introduction and aims

This chapter deals with the syntheses and analyses of achiral and chiral Fréchet-type dendrons[71, 76]. The main purpose of their preparation is the use for coupling to 4,4'-dihydroxy-2,2'-bipyridine which is discussed in **Chapter 4** (see **Section 4.1** for details). The achiral dendrons **3**,[158-160] **4**,[160, 161] **5**,[161] and all 2nd generation dendrons were known (**Scheme 3.1**), although they were mostly synthesised using different methods, whereas the mesylate (**9**) and the chiral analogues (**6**, **7**, **8**, **13**) have not been prepared before.

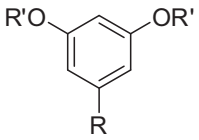

R	R'	
$-CO_2CH_3$	$-C_{12}H_{25}$	**3**
$-CH_2OH$	$-C_{12}H_{25}$	**4**
$-CH_2OSO_2CH_3$	$-C_{12}H_{25}$	**9**
$-CHO$	$-C_{12}H_{25}$	**5**
$-CHOH(CH_2CH_3)$	$-C_{12}H_{25}$	**6** (*rac.*) **7** (*S*) **8** (*R*)
$-CHOH(CH_2CH_3)$	$-C_8H_{17}$	**13** (*rac.*)

Scheme 3.1 All first generation Fréchet-type dendrons presented in this chapter.

All dendrons were adsorbed on HOPG in order to study their monolayer behaviour. Analogues bearing octyl chains had previously been investigated by *L. Scherer* of our group. This work revealed that the molecules showed a high tendency to form monolayers,[21] although this was only observed for 2nd generation systems. The dodecyl chains used in this work proved to be sufficiently different to also form monolayers for 1st generation dendrons.

The syntheses of **3**, **4**, and **9** along with other dendrons possessing different chains lengths were published by our group in 2008.[162]

3.2
Synthesis and discussion

3.2.1
Achiral dendrons

For the synthesis of the achiral dendrons, a well known route was chosen[163, 164], illustrated in **Scheme 3.2**. From the commercially available starting material α-resorcylic acid (**1**) to compound **2**, a simple esterification in methanol proved to be very efficient.[165] Alkylation of **2**, the second step, was done in acetone in the presence of potassium carbonate and 18-crown-6[166, 167] as a catalyst. These conditions were discovered and optimised by *L. Scherer* of our group.[164] The product **3** precipitated out of the reaction mixture upon cooling down to room temperature. The reduction to the alcohol (**4**) was highly efficient and the crude product was even pure enough for microanalysis. Mass spectra and ^{1}H and ^{13}C NMR analyses all showed a very high purity of the compounds.

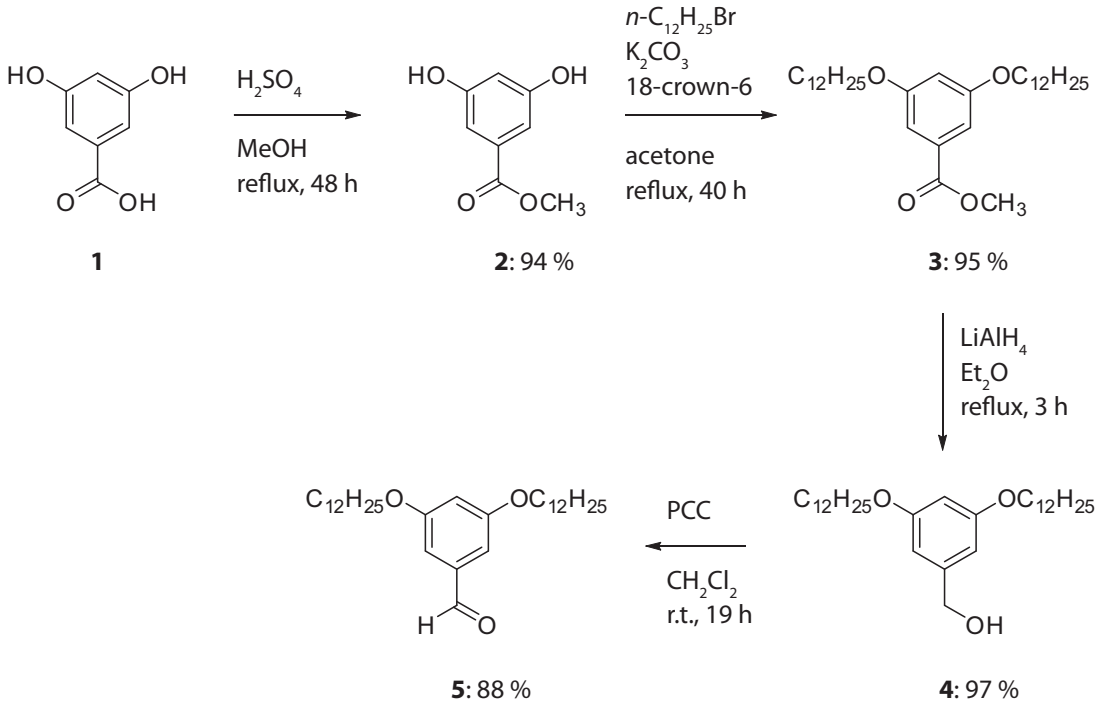

Scheme 3.2 Synthetic pathway to the achiral dendrons **3**, **4**, and **5**.

3.2.2 Chiral dendrons

For the purpose of preparing the chiral dendrons, alcohol **4** was oxidised using PCC (pyridinium chlorochromate) under water free conditions (**Scheme 3.2**). For the alkylation of the aldehyde **5**, diethyl zinc was used leading to the chiral alcohol. According to the double +M-effect of the two *meta*-dodecyloxy chains, the reaction is electronically disfavoured and thus much slower than with benzaldehyde which is often used as a reference system in this type of reaction. An appropriate catalyst was found with diethylaminoethanol[168] which led to the racemate **6** in a yield of 87 % (**Scheme 3.3**). Interestingly, reduction of the aldehyde occurred as a side product of this reaction to give about 10 % of the alcohol **4**. It is assumed[169] that the reaction mechanism proceeds analogously to the *Meerwein-Ponndorf-Verley* reaction[170-174] with zinc(II) as a Lewis acid coordinated by the carbonyl oxygen atom of the aldehyde.

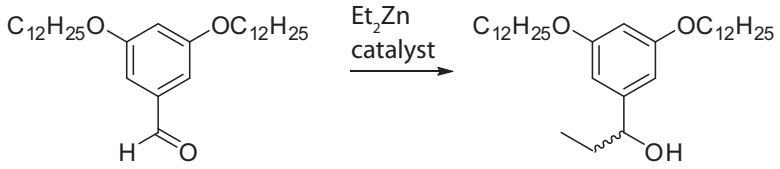

5

6: rac.	87 %	0 % ee
7: (*S*)	71 %	98 % ee
8: (*R*)	42 %	> 90 % ee

Scheme 3.3 Racemic and stereoselective alkylation of the aldehyde **5**. See **Table 3.1** for more details.

To obtain the enantiomerically pure compounds **7** and **8**, chiral catalysts were employed leading to enantioselective reactions and the formation of only one enantiomer in each reaction. *Seebach et al.* discovered in 1991 that a titanium(IV) complex incorporating the chiral ligand TADDOL, catalyses the addition of dialkyl zinc to aldehydes with high enantioselectivity.[169, 175, 176] The catalytically active species is prepared *in situ* from TADDOL as shown in **Scheme 3.4**.

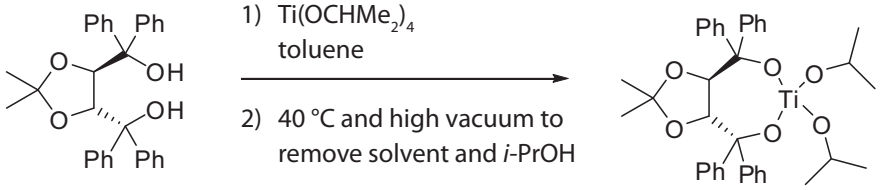

Scheme 3.4 Converting (–)-TADDOL to the active catalyst.

Using the two enantiomers of TADDOL, the alkylated alcohols could be obtained in good yields and very high enantiomeric excesses (**Scheme 3.3** and **Table 3.1**). Starting from (–)-TADDOL, the

(*S*)-enantiomer of the alcohol could be obtained and, accordingly, from (+)-TADDOL, the (*R*)-enantiomer.

Table 3.1 Using different catalysts for the preparation of the chiral alcohols **6**, **7**, and **8**.

Catalyst	Solvent and temperature	Product
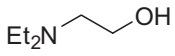	hexane 0 °C → 25 °C	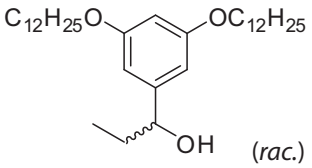 (*rac.*) **6** 87 % yield 0 % ee
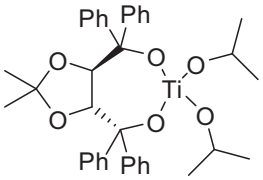 + $Ti(OCHMe_2)_4$	toluene –30 °C → –15 °C	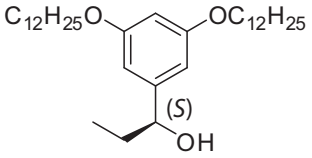 **7** 71 % yield 98 % ee
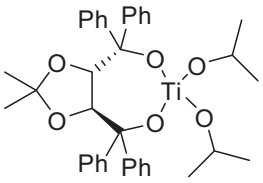 + $Ti(OCHMe_2)_4$	toluene –30 °C → –15 °C	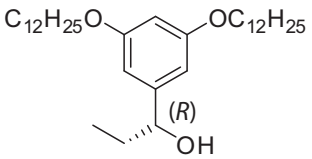 **8** 42 % yield > 90 % ee

Enantiomeric excess was determined with a chiral OD-H column in HPLC experiments (**Figure 3.1**). The absolute configuration of **7** and **8** as the (*S*)-enantiomer, and, respectively, the (*R*)-enantiomer was assumed based upon comparison between similar aldehydes for which the configuration is known.[169, 175, 176] Unfortunately, the retention times were not perfectly reproducible for which the reason remains unknown.[177] Nevertheless, it was still safe to determine the enantiomeric excesses which were, additionally, proved later when the subsequent ligands were analysed (see **Chapter 4**).

Figure 3.1 HPLC Chromatograms of **6**, **7**, and **8** with a chiral column OD-H.

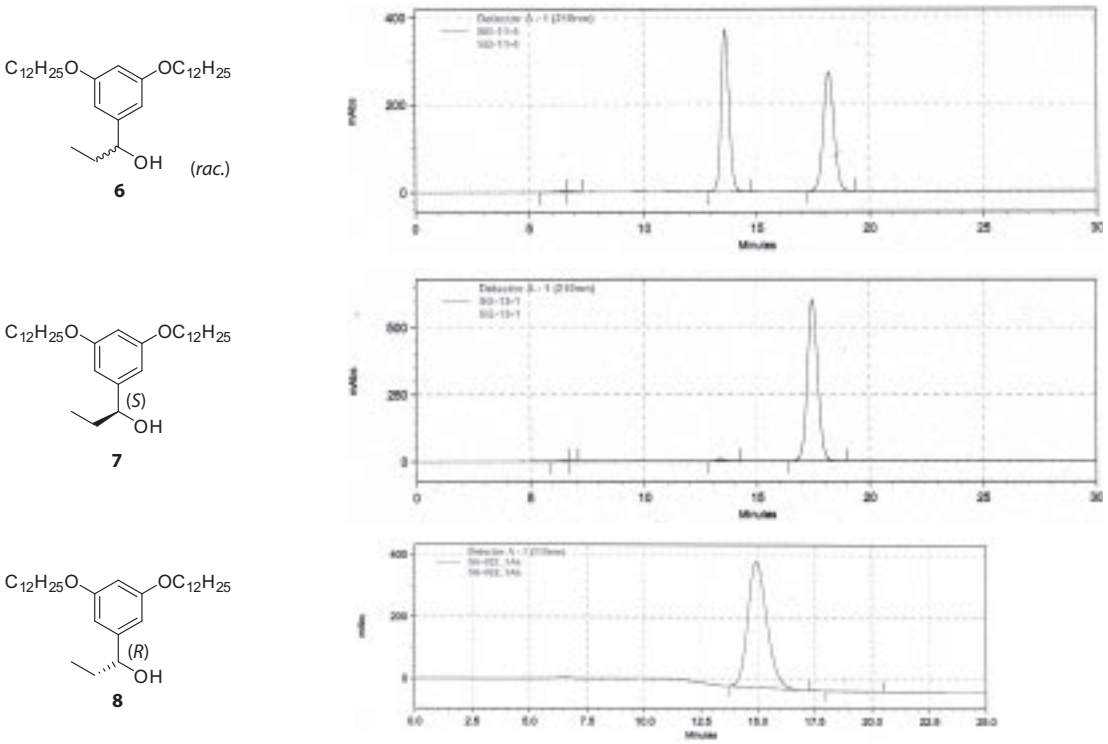

All compounds described in this section were analysed with mass spectrometry, NMR experiments (^{1}H and ^{13}C), infrared spectra, and elemental analyses. They all attested a very high purity of the samples and did not reveal any peculiarities.

3.2.3 Second generation dendrons

In order to obtain second generation dendrons, alcohol **4** was mesylated using standard conditions (**Scheme 3.5**). Without further purification, **9** was used in the subsequent reaction where it was coupled to the dendron core **2** using the same conditions as the addition of the alkyl bromide in the first generation. Ester **10** was isolated in good yields (85 %) and was reduced to the alcohol **11** using the same method as for the first generation synthesis, again achieving almost quantitative yields (98 %) in a very high purity as observed in NMR spectra and elemental analyses.

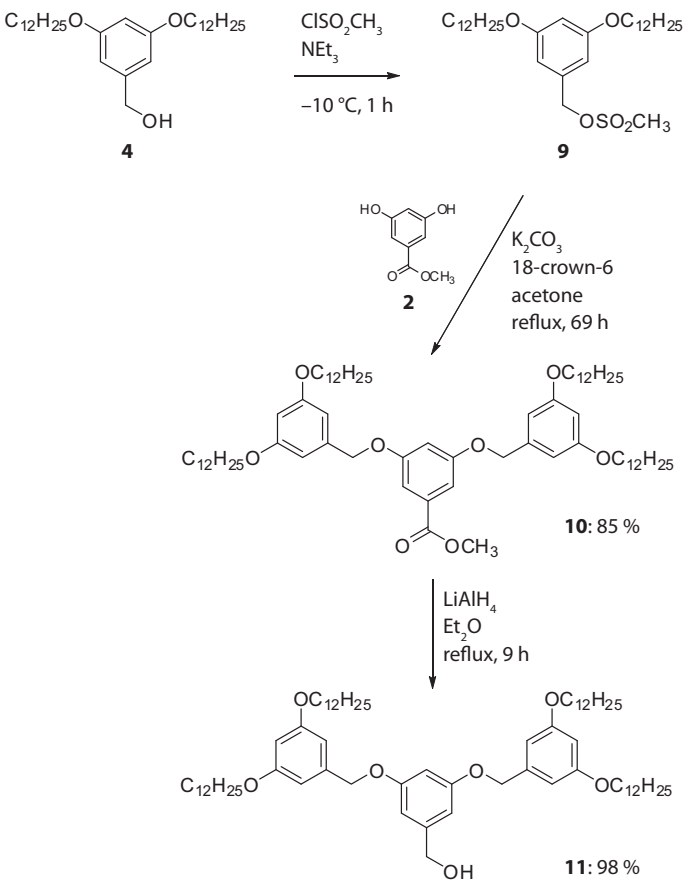

Scheme 3.5 Synthetic route to second generation dendrons **10** and **11**.

3.2.4 Dendrons with different chain lengths

Fréchet dendrons with octyl chains have been used before in our group.[21] Using aldehyde **12**, provided by *L. Scherer*, the racemic secondary alcohol **13** was obtained in 88 % yield (**Scheme 3.6**). The catalyst for the alkylation was diethylaminoethanol, *i.e.* the same as was used for the dodecyl chain alcohol **6**. In the ^{1}H NMR spectrum of **13**, the only change compared to the octyl analogue **6** was the lower intensity of the aliphatic region in the spectrum.

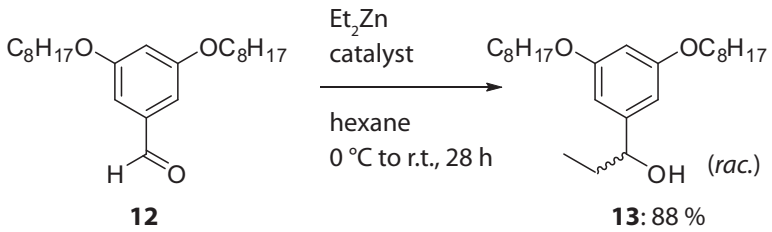

Scheme 3.6 Alkylation of first generation octyl aldehyde.

3.3 STM imaging and discussion

All 1st generation dodecyl decorated dendrons were examined with STM for their monolayer behaviour. Solution casting a hexane solution of each compound onto HOPG tends to form monolayers very easily, resulting in large domains visible just after the approach of the STM tip on the surface.

In a first experiment, a monolayer of dendron **3** was visualised at the air/solid-interface. Very large domains were observed exhibiting a "stripe"-like pattern (**Figure 3.2**).

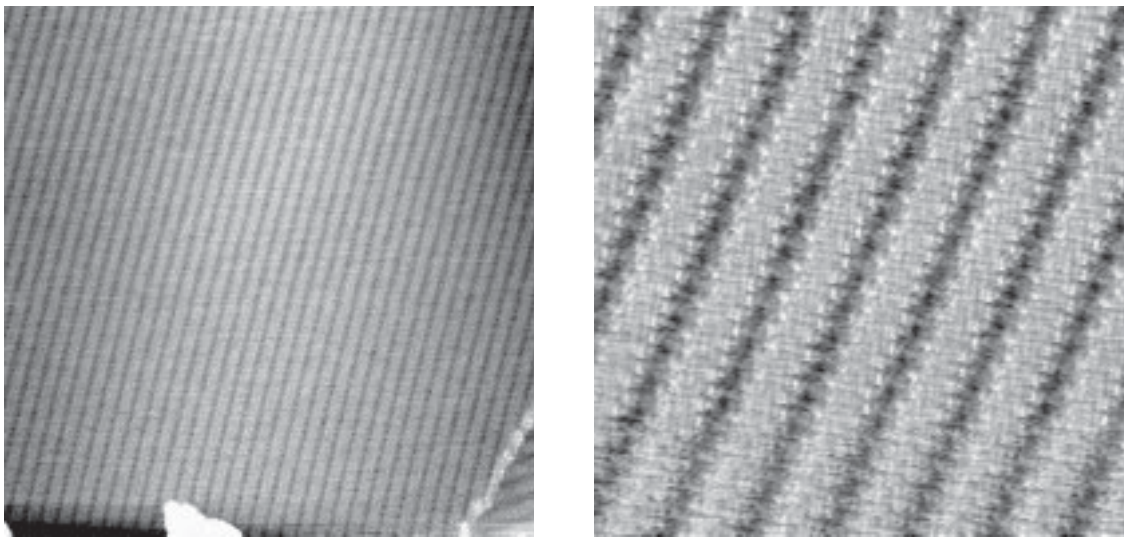

(a) (b)

Figure 3.2 STM images of **3** on HOPG at 150 nm × 150 nm (a) and 30 nm × 30 nm (b). Images recorded with constant scan parameters: U_{bias} = –700 mV, I_t = 8.0 pA, ν = 2.54 Hz (a), ν = 4.07 Hz (b)

After filtering and averaging the image recorded at 30 nm × 30 nm (**Figure 3.2b**), unit cell considerations and attempts of assigning the pattern to an arrangement of molecules of **3** could be performed (**Figure 3.3**). The plane group of the unit cell is probably *p*1, although this remains unsure as there is always drift present in the experimental setup which leads to distortion of the obtained images. The unit cell dimensions are a = 4.1 nm, b = 1.9 nm, α = 92 °. In a rough model, modelled molecules of **3** were overlaid on top of the image in the correct scale. Apart from the alkyl chains which were not modelled in detail and are supposed to take any free space in between, the proposed model fits surprisingly well. It remains unclear though, why there are black and white stripes as they would both originate from the alkyl chains.

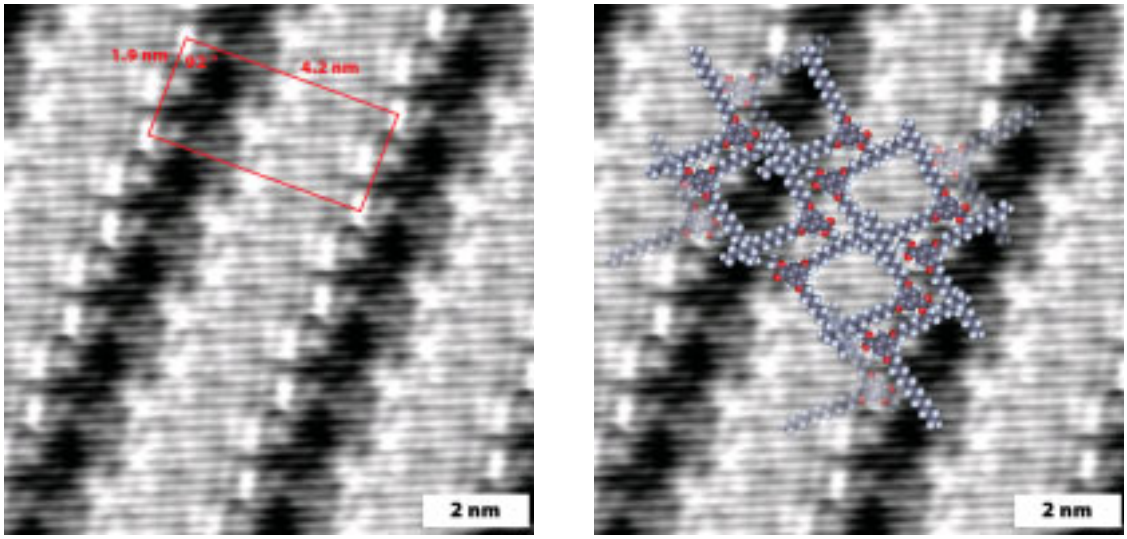

(a) (b)

Figure 3.3 Filtered and averaged images of **Figure 3.2b** with overlaid unit cell (a) and modelled molecules of **3** (b).

Next, alcohol **4** was measured with STM on HOPG after evaporation of a hexane solution. A completely different, "flower"-like hexagonal pattern was observed for alcohol **4** (**Figure 3.4**) compared to the ester **3** which can be explained by hydrogen bonds within a motif of three molecules of **4** (see **Scheme 3.7**) as we will see later.

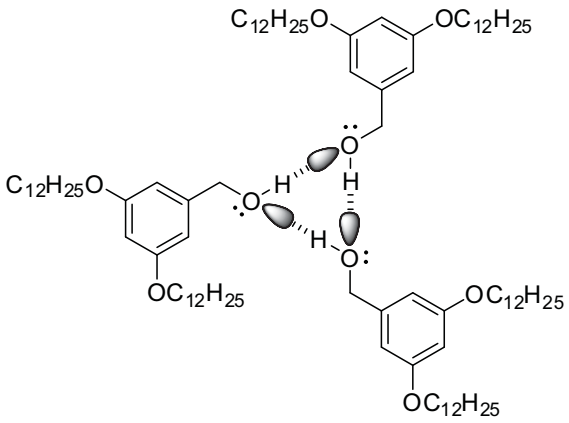

Scheme 3.7 Trimeric motif of molecules of **4**. Hydrogen bonds (hashed) are formed between the hydrogen atoms of the alcohol group and the non-bonding electron pairs of each oxygen atom.

The domains consisted predominantly of trimeric substructures as previously reported by *P. Wu et al.* for 3,5-bis(3,5-bis(dodecyloxy)benzyloxy)benzoic acid,[57] the 2nd generation Fréchet-type dendron bearing dodecyl chains and a carboxylic acid group at the core, and *L. Scherer* for (3,5-bis(3,5-

bis(dodecyloxy)benzyloxy)phenyl)methanol[178], the analogous 2nd generation Fréchet-type dendron bearing octyl chains and an alcohol group at the core.

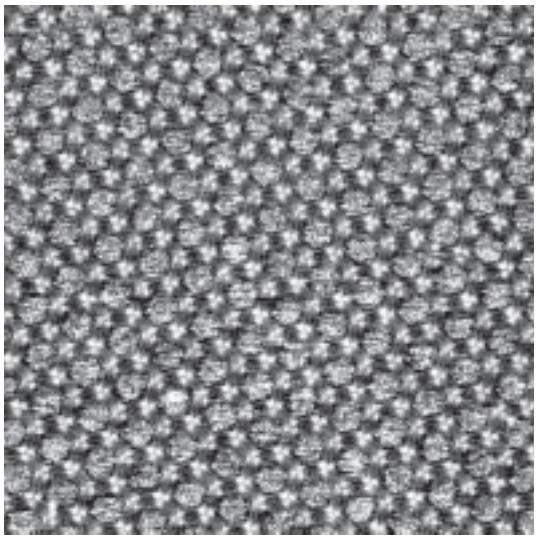

Figure 3.4 Filtered STM image of **4** on HOPG at 50 nm × 50 nm. Scan parameters: U_{bias} = –700 mV, I_t = 8.0 pA, v = 4.07 Hz.

An inset of 10 nm × 10 nm of the image in **Figure 3.4** was averaged (**Figure 3.5**). The bright spots could be assigned to the electron-rich benzene group of each of three molecules.[152, 178] Between the trimeric centres, three weak lines originating from the alkyl chains could be identified. In the centre of each hexagonal array of trimers, a noisy, unresolved part was observed which was smoothed out during the process of averaging. The height of the centre in the raw data (**Figure 3.4**) was roughly the same as for the ordered molecules. In the averaged image (**Figure 3.5**), the height of the centre was lower than the aromatic parts of the fixed molecules. This is an indication of random noise which is generated by mobile molecules.[21] Therefore, the centre could be assigned to one molecule plus six pendant alkyl chains, one from every molecule at the corner of the hexagon, because only three alkyl chains are discovered between the bright spots. At room temperature, the motion of the single molecule in the centre, which has no partners to form an interdigitating pattern or hydrogen bonds with neighbouring molecules, was faster than the time scale of the STM measurements.

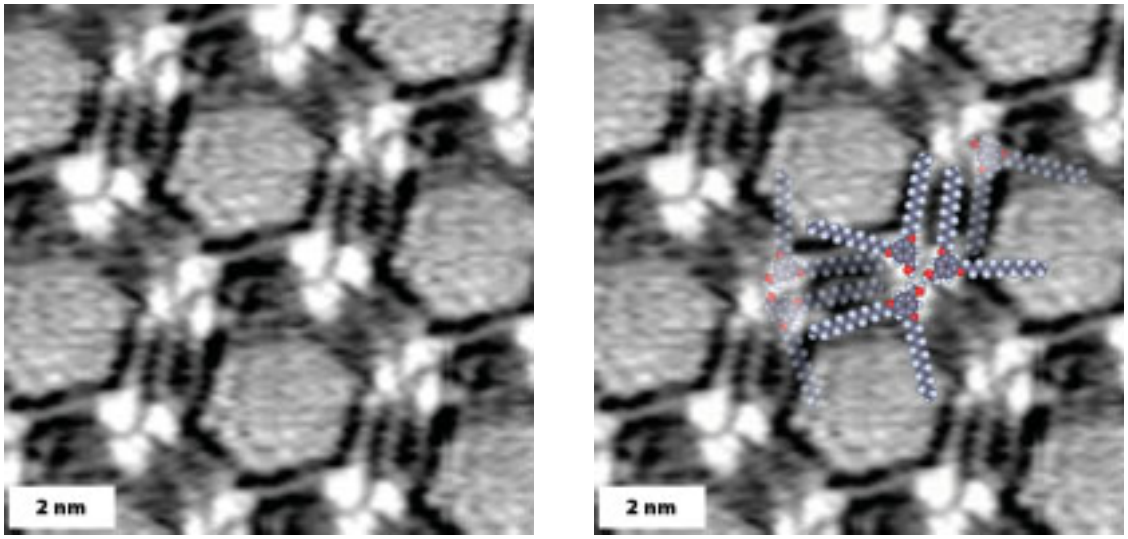

Figure 3.5 (a) Averaged image over 91 positions from **Figure 3.4**. (b) Showing overlaid modelled molecules of **4**.

Neglecting the randomness of the central part, these hexagonal patterns possessed a unit cell with the highest possible symmetry in a *p6mm* plane group (see symmetry elements in **Figure 3.6**) and a unit cell length of 4.6 nm. Without the averaging process, the symmetry is reduced to either a *p*6 or *p*3 plane group, respectively, depending of the arrangement of the alkyl chains.

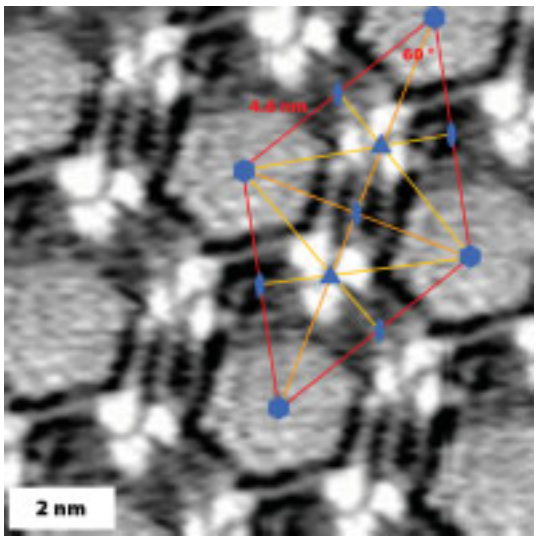

Figure 3.6 Image from **Figure 3.5** depicting the unit cell (red) with its symmetry elements: mirror planes (orange and yellow lines), C_6-axis (blue hexagon), C_3-axis (blue triangle), and C_2-axis (blue ellipses).

Next, aldehyde **5** was dissolved in hexane and solution cast onto HOPG in order to study its monolayer behaviour. In compliance with ester **3**, but in contrast to alcohol **4**, aldehyde **5** forms a "stripe"-like pattern (**Figure 3.7**).

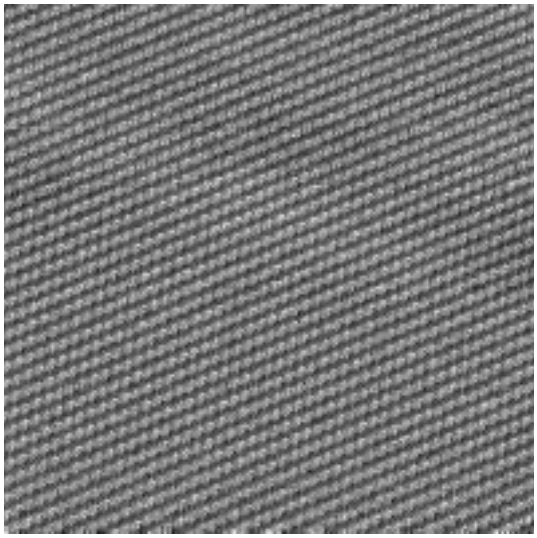

Figure 3.7 STM image of a solution cast monolayer of aldehyde **5** at 75 nm × 75 nm. Scan parameters: U_{bias} = –700 mV, I_t = 8.0 pA, ν = 4.07 Hz.

Averaging a 50 nm × 50 nm image at an inset of 20 nm × 20 nm was performed (**Figure 3.8**). The unit cell's dimensions of the observed pattern are a = 2.2 nm, b = 1.8 nm, α = 80 ° to give an area of 3.9 nm^2. The plane group of the unit cell is *p*1 with no further symmetry elements apart from the identity. Unfortunately, due to insufficient resolution, assigning the pattern to overlaid molecules is impossible.

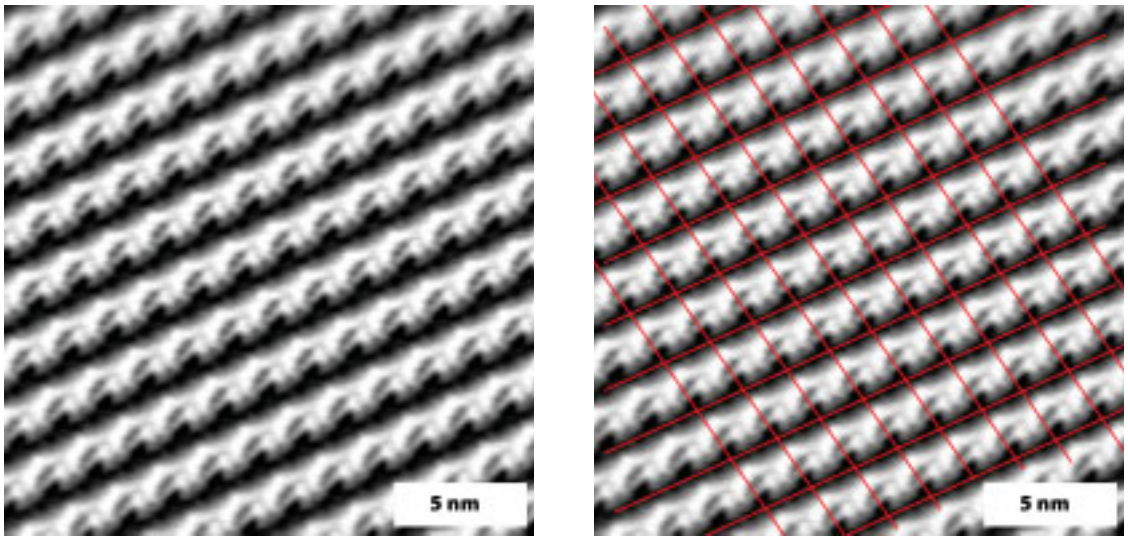

Figure 3.8 Averaged images over 219 positions of monolayers of **5** showing an area of 20 nm × 20 nm (a). The unit cells are depicted in image (b).

In a further experiment, the racemic mixture of alcohol **6** was measured with STM and its monolayer behaviour was studied at the air/solid-interface after evaporation of a hexane solution of **6**. In contrast to the achiral alcohol **4**, no "flower"-like pattern was found but instead, a "stripe"-like pattern as for the ester **3** and the aldehyde **5** was observed (**Figure 3.9**).

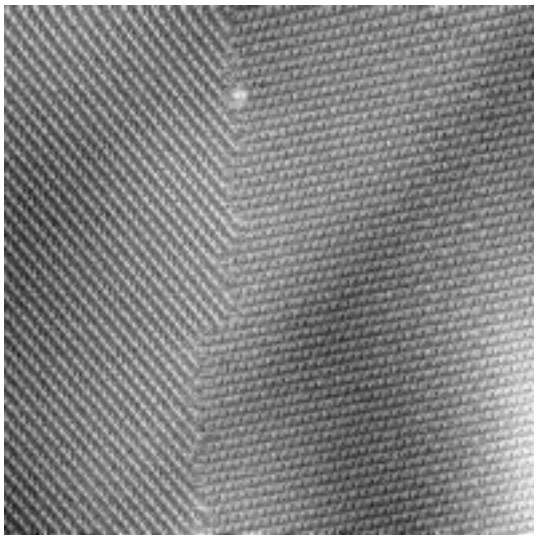

Figure 3.9 STM image of compound **6** on HOPG at 100 nm × 100 nm. Scan parameters: U_{bias} = –700 mV, I_t = 8.0 pA, v = 3.05 Hz.

In the image shown in **Figure 3.9**, large domains were visible. Nonetheless, a domain border could be detected where two domains with different patterns cross. In a smaller area image (**Figure 3.10**), the angle was determined at which the "stripes" cross. The angle is close to 120 ° indicating its origin is the threefold-symmetry of the underlying graphite.

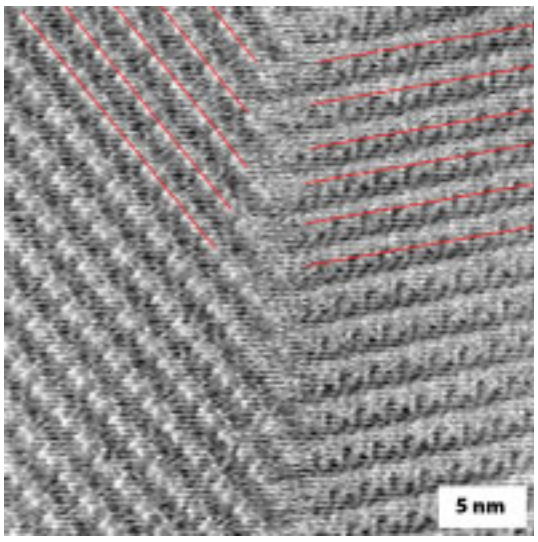

Figure 3.10 STM image of compound **6** on HOPG at 30 nm × 30 nm with overlaid lines emphasising the "stripe"-like pattern. Scan parameters: U_{bias} = –700 mV, I_t = 8.0 pA, v = 6.10 Hz.

Whether these two domains arise from the two enantiomeric molecules present in the racemic mixture of **6** remains unknown as the images obtained at ambient conditions were not resolved enough and differences in patterns arising from each enantiomer would be only marginal, if indeed they can be distinguished at all. **Figure 3.11** shows two averaged images from both domains of **Figure 3.10**. The unit cells are depicted in both images and have the same properties within the experimental error, both possessing a *p*1 plane group. In an attempt of overlaying molecules, (*S*)-**6** (identical to compound **7**) was modelled and assigned to the patterns. Each unit cell contained two molecules giving rise to a dimeric arrangement. The alcohol groups are able to form hydrogen bonds between a pair of molecules which would not be possible if the unit cell contained a racemic pair of molecules. It has to be noted though, that for both domains, (*R*)-**6** (identical to compound **8**) would fit on the pattern as well, although the hydrogen bonds seem to have a more direct interaction for the (*S*)-**6** enantiomer. But due to instrumental drift in the setup (which has a strong influence on the shape and dimensions of the pattern), this cannot be taken as proof.

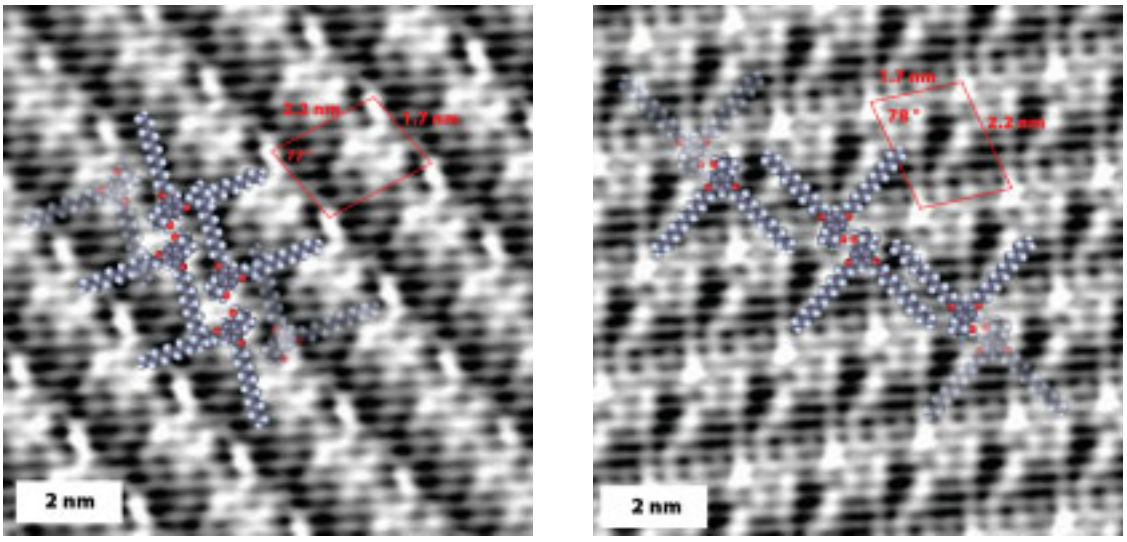

(a) (b)

Figure 3.11 Averaged images from **Figure 3.10** (each domain) both showing an area of 10 nm × 10 nm. (a) Inset of left domain of **Figure 3.10** averaged over 95 positions with depicted unit cell and overlaid molecules ((*S*)-**6**). (b) Inset of right domain of **Figure 3.10** averaged over 99 positions with depicted unit cell and overlaid molecules ((*S*)-**6**).

Furthermore, the enantiomeric pure alcohols **7** and **8** were adsorbed each on HOPG by solution casting of a hexane solution of the appropriate compound. Both compounds were studied with STM and showed a "stripe"-like pattern (**Figure 3.12**). The resolution of the image obtained from the monolayer of **7** was higher than the image of **8** revealing an array of bright spots which correspond to the aromatic ring of **7** whereas for **8**, no fine-structure was visible.

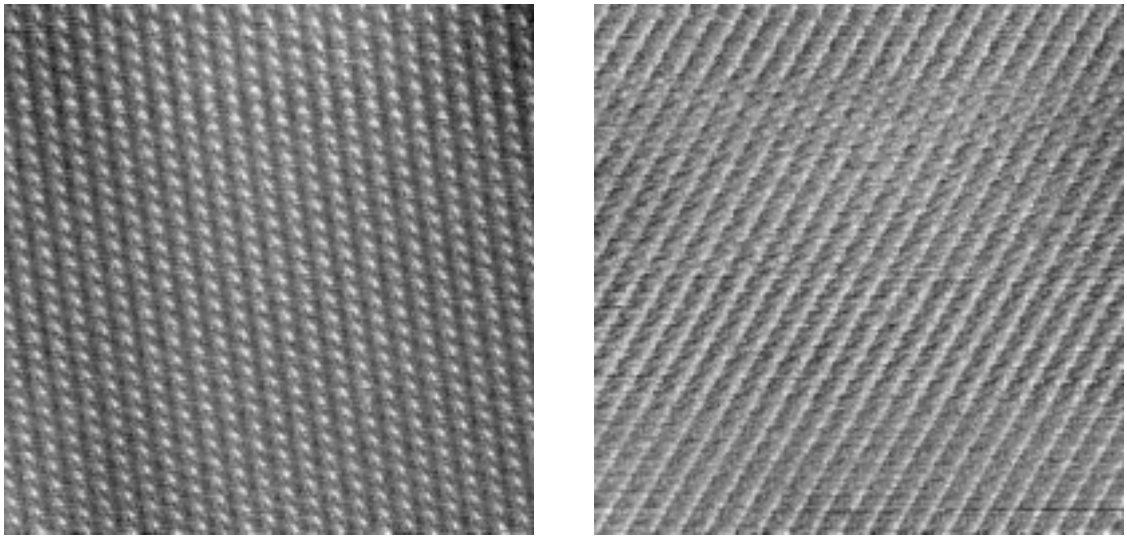

(a) (b)

Figure 3.12 STM images of compound **7** (a) and **8** (b) on HOPG each at a size of 50 nm × 50 nm. Images recorded with constant scan parameters: U_{bias} = –700 mV, I_t = 8.0 pA, v = 3.05 Hz (a), v = 2.54 Hz (b).

For both images of **Figure 3.12**, averaged images were obtained and are shown in **Figure 3.13** with an overlaid grid corresponding to the unit cells. Both images revealed a unit cell in a *p*1 plane group. Their dimensions were, within the experimental error, identical with a = 2.5 nm, b = 1.8 nm, α = 60 ° and 61 °, respectively, giving an area of 3.9 nm^2.

As there is only one bright spot per molecule (one aromatic ring) and only one molecule per unit cell for both compounds, assigning the pattern to a molecular arrangement is obsolete as there is no indication of direction, especially as the alkyl chains are flexible and will occupy any "free space".

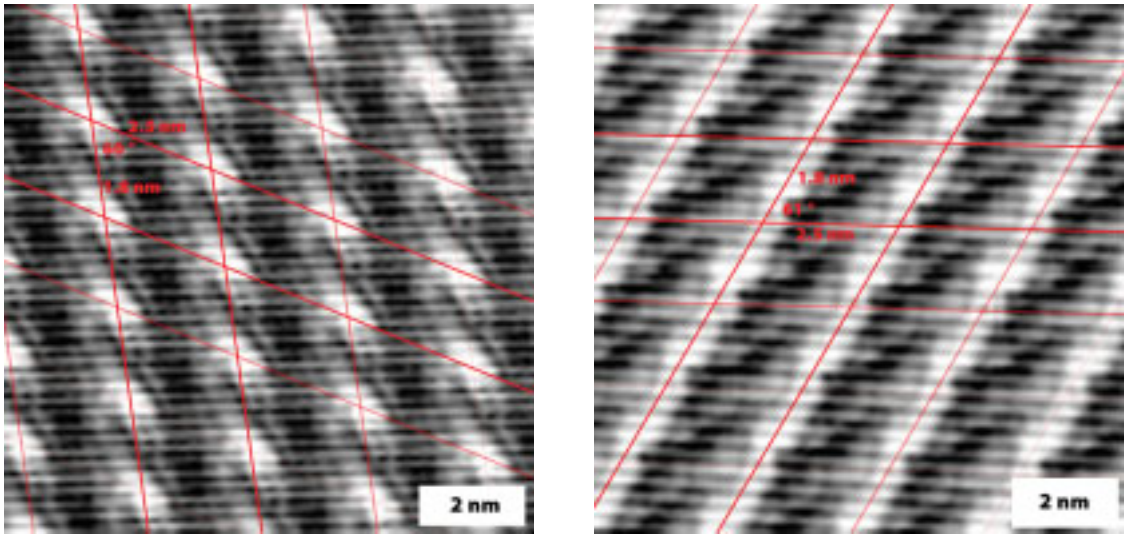

(a) (b)

Figure 3.13 Averaged images of **Figure 3.12** each at an inset of 10 nm × 10 nm with overlaid grid corresponding to the unit cells.

3.4 Experimental part

Preparation of methyl 3,5-dihydroxybenzoate (2)

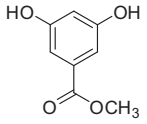

A mixture of 3,5-dihydroxybenzoic acid (**1**) (108 g, 0.700 mol, 1.00 eq) and H_2SO_4 (10 ml) in MeOH (500 ml) was refluxed for 48 h. The solvent was then removed in vacuo, and the residue was redissolved in ethyl acetate (800 ml) and washed twice with saturated aqueous $NaHCO_3$, once with water and once with saturated aqueous NaCl. The organic phase was dried ($MgSO_4$) and evaporated to give the product as an ochre powder (111 g, 0.659 mol, 94 %).

R_f (TLC, silica gel, CH_2Cl_2:MeOH = 10:1): 0.2. **^{1}H NMR** (400 MHz, CD_3OD) δ / ppm 6.90 (d, J = 2.2 Hz, 2H, $H^{2(Ar)}$), 6.45 (t, J = 2.1 Hz, 1H, $H^{4(Ar)}$), 3.83 (s, 3H, $OC\underline{H}_3$). **^{13}C NMR** (101 MHz, CD_3OD) δ / ppm 168.84 ($\underline{C}$=O), 159.95 ($C^{3(Ar)}$), 133.18 ($C^{1(Ar)}$), 108.93 ($C^{2(Ar)}$), 108.40 ($C^{4(Ar)}$), 52.69 ($O\underline{C}H_3$). **IR** (solid): $\tilde{\nu}$ = 3323 (w), 3204 (w), 2627 (w), 2507 (w), 2164 (w), 1983 (w), 1904 (w), 1688 (s), 1601 (m), 1487 (w), 1439 (w), 1294 (s), 1248 (m), 1161 (s), 1101 (m), 993 (s), 908 (w), 868 (w), 847 (m), 764 (s), 667 (m), 592 (w), 554 (w) cm^{-1}. **MS** (EI, *m/z*): 168.0 $[M]^+$ (calc. 168.0), 137.0 $[M\text{-}CH_3O]^+$ (calc. 137.0). **Calcd.** for $C_8H_8O_4$ (168.15) C 57.15, H 4.80; found C 57.09, H 4.78 %.

Preparation of methyl 3,5-bis(dodecyloxy)benzoate (3)

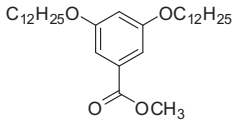

To a mixture of methyl 3,5-dihydroxybenzoate (**2**) (11.3 g, 67.3 mmol, 1.00 eq), 18-crown-6 (3.56 g, 13.5 mmol, 0.200 eq) and potassium carbonate (23.2 g, 168 mmol, 2.50 eq) in dry acetone (200 ml), 1-bromododecane (40.3 ml, 168 mmol, 2.50 eq) was added. Under an inert atmosphere of N_2, the reaction mixture was heated at reflux for 40 h, after which time it was filtered hot and the residue was washed well with boiling acetone. The filtrate was cooled down to 4 °C whereupon white crystals formed which were filtered off, washed well with water (ca. 1 l), cold ethanol and very little of cold acetone. After drying in the desiccator, the desired product could be obtained as a white, cotton-like solid (32.4 g, 64.2 mmol, 95 %).

R_f (TLC, silica gel, hexane: ethyl acetate = 8:1): 0.3. **mp** 61 °C. **^{1}H NMR** (400 MHz, $CDCl_3$) δ / ppm 7.15 (d, ^4J = 2.4 Hz, 2H, $H^{2(Ar)}$), 6.63 (t, ^4J = 2.3 Hz, 1H, $H^{4(Ar)}$), 3.96 (t, ^3J = 6.6 Hz, 4H, $OC\underline{H}_2CH_2CH_2$), 3.89 (s, 3H, $CO_2C\underline{H}_3$), 1.77 (quint, ^3J = 7.0 Hz, 4H, $OCH_2C\underline{H}_2CH_2$), 1.49 – 1.39 (m, 4H, $OCH_2CH_2C\underline{H}_2$), 1.38 – 1.19 (m, 32H, $OCH_2CH_2CH_2(C\underline{H}_2)_8CH_3$), 0.88 (t, ^3J = 6.9 Hz, 6H, $OCH_2CH_2CH_2(CH_2)_8C\underline{H}_3$). **^{13}C NMR** (100 MHz, $CDCl_3$) δ / ppm 167.4 ($\underline{C}O_2CH_3$), 160.6 ($C^{3(Ar)}$), 132.2 ($C^{1(Ar)}$), 108.0 ($C^{2(Ar)}$), 107.0 ($C^{4(Ar)}$), 68.7 ($O\underline{C}H_2(CH_2)_{10}$), 52.6 ($CO_2\underline{C}H_3$), 32.3 ($OCH_2(\underline{C}H_2)_{10}$), 30.1 ($OCH_2(\underline{C}H_2)_{10}$), 30.0 ($OCH_2(\underline{C}H_2)_{10}$), 30.0 ($OCH_2(\underline{C}H_2)_{10}$), 30.0 ($OCH_2(\underline{C}H_2)_{10}$), 29.8 ($OCH_2(\underline{C}H_2)_{10}$), 29.8 ($OCH_2(\underline{C}H_2)_{10}$), 29.6 ($OCH_2(\underline{C}H_2)_{10}$), 26.4 ($OCH_2(\underline{C}H_2)_{10}$), 23.1 ($OCH_2(\underline{C}H_2)_{10}$), 14.5 ($OCH_2(CH_2)_{10}\underline{C}H_3$). **IR** (solid): $\tilde{\nu}$ = 2916 (s), 2846 (m), 1720 (m), 1597 (m), 1466 (m), 1443 (m), 1389 (w), 1319 (s), 1234 (s), 1119 (w), 1049 (m), 995 (m), 856 (w), 764 (m), 717 (w). **MS** (Maldi, *m/z*): 504.4 $[M]^+$ (calc. 504.4). **Calcd.** for $C_{32}H_{56}O_4$ (504.79) C 76.14, H 11.18; found C 76.27, H 10.92 %.

Preparation of 3,5-bis(dodecyloxy)phenylmethanol (**4**)

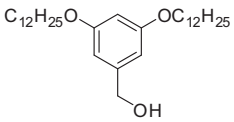

To a suspension of lithium aluminium hydride (2.45 g, 95 % pure, 61.4 mmol, 1.20 eq) in dry Et_2O (500 ml) under an inert atmosphere of N_2, methyl 3,5-bis(dodecyloxy)benzoate (**3**) (25.8 g, 51.2 mmol, 1.00 eq) was added slowly in small portions. The reaction mixture was then heated and stirred at reflux for 3 h, cooled down to room temperature and stirred overnight. It was then quenched by adding 1 M NaOH solution (20 ml) dropwise, whereupon the former grey suspension turned white. The white suspension was filtered over celite and washed with Et_2O. The organic layer of the filtrate was separated and washed two times with water, dried over $MgSO_4$ and evaporated to dryness affording the desired product as a white solid (23.7 g, 49.7 mmol, 97 %) which was analytically pure.

R_f (TLC, silica gel, hexane: ethyl acetate = 7:1): 0.3. **mp** 41 °C. **^{1}H NMR** (400 MHz, $CDCl_3$) δ / ppm 6.50 (d, ^4J = 2.3 Hz, 2H, $H^{2(Ar)}$), 6.37 (t, ^4J = 2.3 Hz, 1H, $H^{4(Ar)}$), 4.61 (s, 2H, $C\underline{H}_2OH$), 3.93 (t, ^3J = 6.6 Hz, 4H, $OC\underline{H}_2CH_2CH_2$), 1.76 (quint, ^3J = 7.0 Hz, 4H, $OCH_2C\underline{H}_2CH_2$), 1.62 (s br, 1H, OH), 1.48 – 1.39 ($OCH_2CH_2C\underline{H}_2$), 1.38 – 1.20 (m, 32H, $OCH_2CH_2CH_2(C\underline{H}_2)_8CH_3$), 0.88 (t, ^3J = 6.9 Hz, 6H, $OCH_2CH_2CH_2(CH_2)_8C\underline{H}_3$). **^{13}C NMR** (100 MHz, $CDCl_3$) δ / ppm 160.9 ($C^{3(Ar)}$), 143.6 ($C^{1(Ar)}$), 105.4 ($C^{2(Ar)}$), 100.9 ($C^{4(Ar)}$), 68.5 ($O\underline{C}H_2(CH_2)_{10}$), 65.9 ($\underline{C}H_2OH$), 32.3 ($OCH_2(\underline{C}H_2)_{10}$), 30.1 ($OCH_2(\underline{C}H_2)_{10}$), 30.1 ($OCH_2(\underline{C}H_2)_{10}$), 30.0 ($OCH_2(\underline{C}H_2)_{10}$), 30.0 ($OCH_2(\underline{C}H_2)_{10}$), 29.8 ($OCH_2(\underline{C}H_2)_{10}$), 29.8 ($OCH_2(\underline{C}H_2)_{10}$), 29.7 ($OCH_2(\underline{C}H_2)_{10}$), 26.5 ($OCH_2(\underline{C}H_2)_{10}$), 23.1 ($OCH_2(\underline{C}H_2)_{10}$), 14.5 ($OCH_2(CH_2)_{10}\underline{C}H_3$). **IR** (solid): $\tilde{\nu}$ = 3510 (w br), 2916 (s), 2854 (m), 1589 (m), 1466 (m), 1396 (w), 1312 (m), 1165 (m), 1011 (m), 833 (m), 710 (m) cm^{-1}. **MS** (Maldi, *m/z*): 476.3 $[M]^+$ (calc. 476.4), 477.3 $[M+H]^+$ (calc. 477.4). **Calcd.** for $C_{31}H_{56}O_3$ (476.78) C 78.09, H 11.84; found C 78.02, H 11.65 %.

Preparation of 3,5-bis(dodecyloxy)benzaldehyde (**5**)

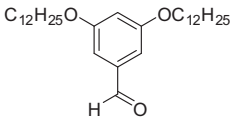

During 30 min, N_2 was blown through CH_2Cl_2 (300 ml) in a flame dried flask. Then, pyridinium chlorochromate (2.26 g, 10.5 mmol, 1.00 eq) was added, whereupon the solution turned bright orange, but after some minutes the colour changed to brown. 3,5-bis(dodecyloxy)phenylmethanol (**4**) (5.00 g, 10.5 mmol, 1.00 eq) was added and the reaction mixture was stirred for 19 h at room temperature under a positive N_2 pressure. The mixture was then filtered over celite and evaporated to dryness to give a dark-brown oil which was purified by column chromatography (Zeochem silica gel, hexane:ethyl acetate = 8:1) yielding the desired product as a white solid (4.36 g, 9.18 mmol, 88 %).

R_f (TLC, silica gel, hexane: ethyl acetate = 8:1): 0.4. **mp** 33 °C. **^{1}H NMR** (400 MHz, $CDCl_3$) δ / ppm 9.89 (s, 1H, $C\underline{H}O$), 6.98 (d, ^4J = 2.3 Hz, 2H, $H^{2(Ar)}$), 6.69 (t, ^4J = 2.3 Hz, 1H, $H^{4(Ar)}$), 3.98 (t, ^3J = 6.6 Hz, 4H, $OC\underline{H}_2CH_2CH_2$), 1.79 (quint, ^3J = 6.6 Hz, 4H, $OCH_2C\underline{H}_2CH_2$), 1.49 – 1.40 (m, 4H, $OCH_2CH_2C\underline{H}_2$), 1.39 – 1.20 (m, 32H, $OCH_2CH_2CH_2(C\underline{H}_2)_8CH_3$), 0.88 (t, ^3J = 6.9 Hz, 6H, $OCH_2CH_2CH_2(CH_2)_8C\underline{H}_3$). **^{13}C NMR** (100 MHz, $CDCl_3$) δ / ppm 192.5 ($\underline{C}HO$), 161.2 ($C^{3(Ar)}$), 138.7 ($C^{1(Ar)}$), 108.4 ($C^{4(Ar)}$), 108.0 ($C^{2(Ar)}$), 68.8 ($O\underline{C}H_2(CH_2)_{10}$), 32.3 ($OCH_2(\underline{C}H_2)_{10}$), 30.1 ($OCH_2(\underline{C}H_2)_{10}$), 30.0 ($OCH_2(\underline{C}H_2)_{10}$), 30.0 ($OCH_2(\underline{C}H_2)_{10}$), 30.0 ($OCH_2(\underline{C}H_2)_{10}$), 29.8 ($OCH_2(\underline{C}H_2)_{10}$), 29.8 ($OCH_2(\underline{C}H_2)_{10}$), 29.5 ($OCH_2(\underline{C}H_2)_{10}$), 26.4 ($OCH_2(\underline{C}H_2)_{10}$), 23.1 ($OCH_2(\underline{C}H_2)_{10}$), 14.5 ($OCH_2(CH_2)_{10}\underline{C}H_3$). **MS** (Maldi, *m/z*): 477.7 $[M+3H]^+$ (calc. 477.4), 445.2 $[M\text{-}CHO]^+$ (calc. 445.4). **IR** (solid): $\tilde{\nu}$ = 2916 (s), 2854 (m), 1705 (m), 1589 (m), 1466 (m), 1389 (w), 1319 (s), 1173 (m), 1057 (m), 941 (m), 839 (w), 717 (w) cm^{-1}. **Calcd.** for $C_{31}H_{54}O_3$ (474.76) C 78.43, H 11.46; found C 78.36, H 11.31 %.

Preparation of (*R*,*S*)-1-(3,5-bis(dodecyloxy)phenyl)propanol (**6**)

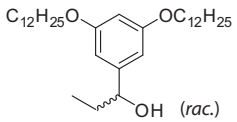

To a mixture of diethylzinc (7.1 ml, ca. 1 M in hexane, 7.1 mmol, 2.3 eq) and 2-diethylaminoethanol (46 µl, 0.35 mmol, 0.11 eq) in hexane (150 ml), 3,5-bis(dodecyloxy)-benzaldehyde (**5**) (1.50 g, 3.16 mmol, 1.00 eq) was added at 0 °C under an argon atmosphere. The cooling bath was removed and the mixture allowed to stir for 24 h at room temperature. The reaction mixture was then cooled down to 0 °C and aqueous 1 M HCl (170 ml) was added. The aqueous layer was separated and extracted once with Et_2O, the combined organic layers were washed twice with saturated aqueous $NaHCO_3$, dried over Na_2SO_4 and evaporated to dryness to give a yellow oil. The crude material was purified by column chromatography (Zeochem silica gel, hexane:ethyl acetate = 8:1) yielding the desired product as a white solid (1.39 g, 2.76 mmol, 87 %) with 0% ee as determined by HPLC analysis (Daicel OD-H, heptane: ^{i}PrOH = 97:3, 0.5 ml/min, 210 nm), t_r 13.6 min ((*R*)-isomer), t_r 18.2 min ((*S*)-isomer).

R_f (TLC, silica gel, hexane: ethyl acetate = 8:1): 0.2. **mp** 43 – 44 °C. **^{1}H NMR** (400 MHz, $CDCl_3$) δ / ppm 6.48 (d, ^4J = 2.1 Hz, 2H, $H^{2(Ar)}$), 6.36 (t, ^4J = 2.1 Hz, 1H, $H^{4(Ar)}$), 4.50 (t, ^3J = 6.6 Hz, 1H, C<u>H</u>OH), 3.93 (t, ^3J = 6.6 Hz, 4H, OC<u>H</u>$_2$CH$_2$), 1.91 (s br, 1H, OH), 1.82 – 1.70 (m, 6H, OCH$_2$C<u>H</u>$_2$CH$_2$ + CHOHC<u>H</u>$_2$CH$_3$), 1.49 – 1.39 (m, 4H, OCH$_2$CH$_2$C<u>H</u>$_2$), 1.39 – 1.20 (m, 32H, OCH$_2$CH$_2$CH$_2$(C<u>H</u>$_2$)$_8$CH$_3$), 0.92 (t, ^3J = 7.2 Hz, 3H, CHOHCH$_2$C<u>H</u>$_3$), 0.88 (t, ^3J = 6.8 Hz, 6H, OCH$_2$CH$_2$CH$_2$(CH$_2$)$_8$C<u>H</u>$_3$). **^{13}C NMR** (100 MHz, $CDCl_3$) δ / ppm 160.8 ($C^{3(Ar)}$), 147.5 ($C^{1(Ar)}$), 104.7 ($C^{2(Ar)}$), 100.6 ($C^{4(Ar)}$), 76.5 (<u>C</u>HOH), 68.4 (O<u>C</u>H$_2$(CH$_2$)$_{10}$), 32.3 (OCH$_2$(<u>C</u>H$_2$)$_{10}$), 32.1 (CHOH<u>C</u>H$_2$CH$_3$), 30.1 (OCH$_2$(<u>C</u>H$_2$)$_{10}$), 30.1 (OCH$_2$(<u>C</u>H$_2$)$_{10}$), 30.0 (OCH$_2$(<u>C</u>H$_2$)$_{10}$), 30.0 (OCH$_2$(<u>C</u>H$_2$)$_{10}$), 29.8 (OCH$_2$(<u>C</u>H$_2$)$_{10}$), 29.8 (OCH$_2$(<u>C</u>H$_2$)$_{10}$), 29.7 (OCH$_2$(<u>C</u>H$_2$)$_{10}$), 26.5 (OCH$_2$(<u>C</u>H$_2$)$_{10}$), 23.1 (OCH$_2$(<u>C</u>H$_2$)$_{10}$), 14.5 (OCH$_2$(CH$_2$)$_{10}$<u>C</u>H$_3$), 10.6 (CHOHCH$_2$<u>C</u>H$_3$). **IR** (solid): $\tilde{\nu}$ = 3364 (w br), 2916 (s), 2847 (s), 1605 (m), 1450 (m), 1319 (w), 1157 (s), 1049 (m), 964 (m), 818 (w), 717 (w) cm^{-1}. **MS** (Maldi, *m/z*): 506.2 [M+2H]$^+$ (calc. 506.5). **Calcd.** for $C_{33}H_{60}O_3$ (504.83) C 78.51, H 11.98; found C 78.45, H 11.73 %.

Preparation of (*S*)-1-(3,5-bis(dodecyloxy)phenyl)propanol (**7**)

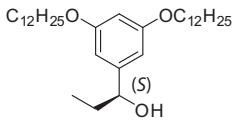

A mixture of (–)-TADDOL (983 mg, 2.11 mmol, 0.20 eq) and tetraisopropyl orthotitanate (758 µl, 2.56 mmol, 0.243 eq) in toluene (15 ml) was stirred for 5 h at room temperature under an argon atmosphere. Toluene and 2-propanol were then removed at 40 °C at high vacuum. To the yellow residue, toluene (30 ml) and tetraisopropyl orthotitanate (3.74 ml, 12.6 mmol, 1.20 eq) were added at room temperature. The reaction mixture was cooled to –30 °C and Et_2Zn (13 ml, ca. 1.0 M in hexane, 13 mmol, 1.2 eq) was added. After 25 min, 3,5-bis(dodecyloxy)benzaldehyde (**5**) (5.00 g in 37 ml of toluene, 10.5 mmol, 1.00 eq) was carefully added to the reaction mixture which was stirred for 63 h at –30 °C. After another 23 h at –20 °C, the temperature was again raised to –15 °C and the mixture stirred for 48 h at this temperature. Then, saturated NH_4Cl (15 ml) and Et_2O (60 ml) were added at –15 °C, the reaction mixture stirred for 3 h, filtered carefully over celite, dried over Na_2SO_4 and evaporated to dryness to give a yellow oil. The crude material was purified twice by column chromatography (Fluka silica gel 60, 0.04-0.063 mm; hexane: ethyl acetate = 10:1 → 8:1) yielding the desired product as a white solid (3.80 g, 7.53 mmol, 71 %) with 98 % ee as determined by HPLC analysis (Daicel OD-H, heptane: ^{i}PrOH = 97:3, 0.5 ml/min, 210 nm), t_r 13.4 ((*R*)-isomer), t_r 17.5 ((*S*)-isomer).

R_f (TLC, silica gel, hexane: ethyl acetate = 8:1): 0.2. **mp** 44 – 45 °C. **$[\alpha]_D^{20}$** = –8.9 ° (c = 1.32 in $CHCl_3$). **^{1}H NMR** (400 MHz, $CDCl_3$) δ / ppm 6.48 (d, ^4J = 2.1 Hz, 2H, $H^{2(Ar)}$), 6.36 (t, ^4J = 2.1 Hz, 1H, $H^{4(Ar)}$), 4.51 (t, ^3J = 6.6 Hz, 1H,

C<u>H</u>OH), 3.93 (t, ^3J = 6.7 Hz, 4H, OC<u>H</u>$_2$CH$_2$), 1.84 – 1.70 (m, 6H, OCH$_2$C<u>H</u>$_2$CH$_2$ + CHOHC<u>H</u>$_2$CH$_3$), 1.71 (s br, 1H, OH), 1.49 – 1.39 (m, 4H, OCH$_2$CH$_2$C<u>H</u>$_2$), 1.38 – 1.20 (m, 32H, OCH$_2$CH$_2$CH$_2$(C<u>H</u>$_2$)$_8$CH$_3$), 0.92 (t, ^3J = 7.5 Hz, 3H, CHOHCH$_2$C<u>H</u>$_3$), 0.88 (t, ^3J = 6.8 Hz, 6H, OCH$_2$CH$_2$CH$_2$(CH$_2$)$_8$C<u>H</u>$_3$). **^{13}C NMR** (100 MHz, CDCl$_3$) δ / ppm 160.8 (C$^{3(Ar)}$), 147.4 (C$^{1(Ar)}$), 104.7 (C$^{2(Ar)}$), 100.6 (C$^{4(Ar)}$), 76.6 (<u>C</u>HOH), 68.5 (O<u>C</u>H$_2$(CH$_2$)$_{10}$), 32.3 (OCH$_2$(<u>C</u>H$_2$)$_{10}$), 32.1 (CHOH<u>C</u>H$_2$CH$_3$), 30.1 (OCH$_2$(<u>C</u>H$_2$)$_{10}$), 30.0 (OCH$_2$(<u>C</u>H$_2$)$_{10}$), 30.0 (OCH$_2$(<u>C</u>H$_2$)$_{10}$), 30.0 (OCH$_2$(<u>C</u>H$_2$)$_{10}$), 29.8 (OCH$_2$(<u>C</u>H$_2$)$_{10}$), 29.8 (OCH$_2$(<u>C</u>H$_2$)$_{10}$), 29.7 (OCH$_2$(<u>C</u>H$_2$)$_{10}$), 26.5 (OCH$_2$(<u>C</u>H$_2$)$_{10}$), 23.1 (OCH$_2$(<u>C</u>H$_2$)$_{10}$), 14.5 (OCH$_2$(CH$_2$)$_{10}$<u>C</u>H$_3$), 10.6 (CHOHCH$_2$<u>C</u>H$_3$). **MS** (Maldi, *m/z*): 506.3 [M+2H]$^+$ (calc. 506.5), 507.2 [M+3H]$^+$ (calc. 507.5). **IR** (solild): $\tilde{\nu}$ = 3364 (w br), 2916 (s), 2847 (s), 1605 (s), 1450 (s), 1319 (m), 1157 (s), 1049 (m), 964 (m), 849 (w), 717 (m) cm^{-1}. **Calcd.** for C$_{33}$H$_{60}$O$_3$ (504.83) C 78.51, H 11.98; found C 78.56, H 11.77 %.

Preparation of (*R*)-1-(3,5-bis(dodecyloxy)phenyl)propan-1-ol (**8**)

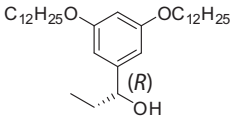

A mixture of (+)-TADDOL (983 mg, 2.11 mmol, 0.200 eq) and tetraisopropyl orthotitanate (758 µl, 2.56 mmol, 0.241 eq) in toluene (15 ml) was stirred for 5 h at room temperature under an argon atmosphere. Toluene and 2-propanol were then removed at 40 °C at high vacuum. To the yellow residue toluene (30 ml) and tetraisopropyl orthotitanate (3.74 ml, 12.6 mmol, 1.19 eq) were added at room temperature, the reaction mixture cooled to –30 °C and Et$_2$Zn (13 ml, ca. 1.0 M in hexane, 13 mmol, 1.2 eq) was added. After 15 min, 3,5-bis(dodecyloxy)benzaldehyde (**5**) (5.04 g in 40 ml of toluene, 10.6 mmol, 1.00 eq) was added to the reaction mixture which was stirred for 140 h at –30 °C. Then, saturated NH$_4$Cl (15 ml) and Et$_2$O (20 ml) were added at –15 °C, the reaction mixture left for 20 h, filtered carefully over celite, dried over MgSO$_4$ und evaporated to dryness to give a yellow oil. The crude material was purified twice by column chromatography (Fluka silica gel 60, 0.040–0.063 mm; hexane: ethyl acetate = 9:1) yielding the desired product as a white solid (2.25 g, 4.46 mmol, 42 %). HPLC measurements did not produce well reproducible retention times due to unknown reasons. It is safe to say though, that this product has a high ee > 90 % as concluded from ee values of the subsequent reaction with this product to the bpy-ligand.

R$_f$ (TLC, silica gel, hexane: ethyl acetate = 5:1): 0.5. **^{1}H NMR** (500 MHz, CDCl$_3$) δ / ppm 6.48 (d, ^4J = 2.2 Hz, 2H, H$^{2(Ar)}$), 6.36 (t, ^4J = 2.2 Hz, 1H, H$^{4(Ar)}$), 4.51 (t, ^3J = 6.4 Hz, 1H, C<u>H</u>OH), 3.93 (t, ^3J = 6.6 Hz, 4H, OC<u>H</u>$_2$CH$_2$), 1.83 – 1.70 (m, 7H, OCH$_2$C<u>H</u>$_2$CH$_2$ + CHOHC<u>H</u>$_2$CH$_3$ + OH), 1.47 – 1.40 (m, 4H, OCH$_2$CH$_2$C<u>H</u>$_2$), 1.37 – 1.22 (m, 32H, OCH$_2$CH$_2$CH$_2$(C<u>H</u>$_2$)$_8$CH$_3$), 0.92 (t, ^3J = 7.4 Hz, 3H, CHOHCH$_2$C<u>H</u>$_3$), 0.88 (t, ^3J = 6.9 Hz, 6H, OCH$_2$CH$_2$CH$_2$(CH$_2$)$_8$C<u>H</u>$_3$). **^{13}C NMR** (126 MHz, CDCl$_3$) δ / ppm 160.51 (C$^{3(Ar)}$), 147.19 (C$^{1(Ar)}$), 104.44 (C$^{2(Ar)}$), 100.37 (C$^{4(Ar)}$), 76.30 (<u>C</u>HOH), 68.19 (O<u>C</u>H$_2$(CH$_2$)$_{10}$), 32.07 (OCH$_2$(<u>C</u>H$_2$)$_{10}$), 31.86 (CHOH<u>C</u>H$_2$CH$_3$), 29.82 (OCH$_2$(<u>C</u>H$_2$)$_{10}$), 29.79 (OCH$_2$(<u>C</u>H$_2$)$_{10}$), 29.75 (OCH$_2$(<u>C</u>H$_2$)$_{10}$), 29.73 (OCH$_2$(<u>C</u>H$_2$)$_{10}$), 29.55 (OCH$_2$(<u>C</u>H$_2$)$_{10}$), 29.50 (OCH$_2$(<u>C</u>H$_2$)$_{10}$), 29.43 (OCH$_2$(<u>C</u>H$_2$)$_{10}$), 26.20 (OCH$_2$(<u>C</u>H$_2$)$_{10}$), 22.84 (OCH$_2$(<u>C</u>H$_2$)$_{10}$), 14.27 (OCH$_2$(CH$_2$)$_{10}$<u>C</u>H$_3$), 10.34 (CHOHCH$_2$<u>C</u>H$_3$). **IR** (solid): $\tilde{\nu}$ = 3342 (w), 3267 (w), 2955 (w), 2916 (s), 2851 (s), 1610 (s), 1599 (s), 1450 (s), 1394 (w), 1342 (w), 1325 (w), 1258 (w), 1161 (s), 1105 (w), 1047 (m), 962 (m), 881 (w), 847 (m), 824 (m), 716 (s), 696 (s), 598 (m), 581 (w), 511 (w) cm^{-1}. **MS** (EI, *m/z*): 504.5 [M]$^+$ (calc. 504.5). **Calcd.** for C$_{33}$H$_{60}$O$_3$ (504.83) C 78.51, H 11.98; found C 78.66, H 11.75 %.

Preparation of 3,5-bis(dodecyloxy)benzyl methanesulfonate (**9**)

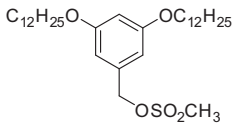

NEt_3 (22 ml, 0.16 mol, 5.0 eq) was added to a solution of 3,5-bis(dodecyloxy)phenylmethanol (**4**) (15.0 g, 31.4 mmol, 1.00 eq) in CH_2Cl_2 (100 ml), previously cooled to –10 °C. Methanesulfonyl chloride (9.7 ml, 0.13 mol, 4.0 eq) was added slowly over a period of 20 min, and then the reaction mixture was stirred at –10 °C for 1 h. The mixture was poured into a mixture of concentrated HCl (20 ml) and crushed ice (200 g), and extracted with CH_2Cl_2. The organic layer was washed with a saturated solution of $NaHCO_3$, dried with Na_2SO_4, and the solvent removed. The desired product was isolated as a yellow solid (18.2 g, 32.8 mmol, 104 %).

^{1}H NMR (400 MHz, $CDCl_3$) δ / ppm 6.52 (d, ^4J = 2.2 Hz, 2H, $H^{2(Ar)}$), 6.45 (t, ^4J = 2.2 Hz, 1H, $H^{4(Ar)}$), 5.15 (s, 2H, $C\underline{H}_2OSO_2Me$), 3.92 (t, ^3J = 6.6 Hz, 4H, $OC\underline{H}_2CH_2CH_2$), 2.92 (s, 3H, $SO_2C\underline{H}_3$), 1.76 (quint, ^3J = 7.0 Hz, 4H, $OCH_2C\underline{H}_2CH_2$), 1.49 – 1.39 (m, 4H, $OCH_2CH_2C\underline{H}_2$), 1.38-1.18 (m, 32H, $OCH_2CH_2CH_2(C\underline{H}_2)_8CH_3$), 0.88 (t, ^3J = 6.9 Hz, 6H, $OCH_2CH_2CH_2(CH_2)_8C\underline{H}_3$). **^{13}C NMR** (100 MHz, $CDCl_3$) δ / ppm 161.1 ($C^{3(Ar)}$), 135.6 ($C^{1(Ar)}$), 107.3 ($C^{2(Ar)}$), 102.5 ($C^{4(Ar)}$), 72.0 ($\underline{C}H_2OSO_2CH_3$), 68.6 ($O\underline{C}H_2(CH_2)_{10}$), 38.8 ($CH_2OSO_2\underline{C}H_3$), 32.3 ($OCH_2(\underline{C}H_2)_{10}$), 30.1 ($OCH_2(\underline{C}H_2)_{10}$), 30.0 ($OCH_2(\underline{C}H_2)_{10}$), 30.0 ($OCH_2(\underline{C}H_2)_{10}$), 30.0 ($OCH_2(\underline{C}H_2)_{10}$), 29.8 ($OCH_2(\underline{C}H_2)_{10}$), 29.8 ($OCH_2(\underline{C}H_2)_{10}$), 29.6 ($OCH_2(\underline{C}H_2)_{10}$), 26.4 ($OCH_2(\underline{C}H_2)_{10}$), 23.1 ($OCH_2(\underline{C}H_2)_{10}$), 14.5 ($OCH_2(CH_2)_{10}\underline{C}H_3$). **IR** (solid): $\tilde{\nu}$ = 2916 (s), 2847 (w), 2600 (s), 2492 (s), 1605 (w), 1474 (s), 1396 (m), 1342 (m), 1173 (s), 1034 (s), 972 (w), 926 (w), 849 (m), 810 (m), 648 (m) cm^{-1}.

Preparation of methyl 3,5-bis(3,5-bis(dodecyloxy)benzyloxy)benzoate (**10**)

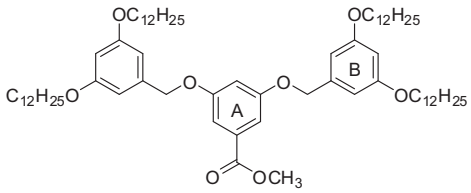

A mixture of methyl 3,5-dihydroxybenzoate (**2**) (2.00 g, 11.9 mmol, 1.00 eq), 3,5-bis(dodecyloxy)benzyl methanesulfonate (**9**) (16.5 g, 29.7 mmol, 2.50 eq), K_2CO_3 (6.57 g, 47.5 mmol, 4.00 eq) and 18-crown-6 (0.63 g, 2.4 mmol, 0.20 eq) in dry acetone (50 ml) was refluxed for 69 h. The solvent was evaporated and the residue was given to water (250 ml) which was extracted three times with CH_2Cl_2 (each about 150 ml). The combined organic layers were dried ($MgSO_4$) and evaporated to dryness to give a brown oil. This crude product was purified by chromatography on silica gel (Fluka silica gel 60, 0.040–0.063 mm; hexane:ethyl acetate = 20:1), followed by a subsequent chromatography on silica gel (Fluka silica gel 60, 0.040–0.063 mm; hexane:ethyl acetate = 80:1), and another chromatography on silica gel (Fluka silica gel 60, 0.040–0.063 mm; hexane:diethyl ether = 33:1) yielding the desired product as a white solid (10.9 g, 10.1 mmol, 85 %).

$\mathbf{R_f}$ (TLC, silica gel, hexane:ethyl acetate = 10:1): 0.5. **^{1}H NMR** (400 MHz, $CDCl_3$) δ / ppm 7.28 (d, J = 2.3 Hz, 2H, $H^{2(A)}$), 6.79 (t, J = 2.3 Hz, 1H, $H^{4(A)}$), 6.55 (d, J = 2.2 Hz, 4H, $H^{2(B)}$), 6.41 (t, J = 2.2 Hz, 2H, $H^{4(B)}$), 4.98 (s, 4H, $Ar_AO\underline{C}H_2Ar_B$), 3.93 (t, J = 6.6 Hz, 8H, $Ar_BOC\underline{H}_2$), 3.90 (s, 3H, $CO_2C\underline{H}_3$), 1.81 – 1.71 (m, 8H, $OCH_2C\underline{H}_2CH_2$), 1.49 – 1.39 (m, 8H, $OCH_2CH_2C\underline{H}_2$), 1.38 – 1.19 (m, 64H, $OCH_2CH_2CH_2(C\underline{H}_2)_8$), 0.88 (t, J = 6.8 Hz, 12H, $O(CH_2)_{11}C\underline{H}_3$). **^{13}C NMR** (101 MHz, $CDCl_3$) δ / ppm 167.19 ($\underline{C}O_2CH_3$), 160.94 ($C^{3(B)}$), 160.17 ($C^{3(A)}$), 138.97 ($C^{1(B)}$), 132.40 ($C^{1(A)}$), 108.76 ($C^{2(A)}$), 107.59 ($C^{4(A)}$), 106.13 ($C^{2(B)}$), 101.31 ($C^{4(B)}$), 70.71 ($Ar_AO\underline{C}H_2Ar_B$), 68.49 ($Ar_BO\underline{C}H_2$), 52.66 ($CO_2\underline{C}H_3$), 32.33 ($OCH_2(\underline{C}H_2)_{10}$), 30.08 ($OCH_2(\underline{C}H_2)_{10}$), 30.05 ($OCH_2(\underline{C}H_2)_{10}$), 30.02 ($OCH_2(\underline{C}H_2)_{10}$), 30.00 ($OCH_2(\underline{C}H_2)_{10}$), 29.82 ($OCH_2(\underline{C}H_2)_{10}$), 29.77 ($OCH_2(\underline{C}H_2)_{10}$), 29.67 ($OCH_2(\underline{C}H_2)_{10}$), 26.47 ($OCH_2(\underline{C}H_2)_{10}$), 23.10 ($OCH_2(\underline{C}H_2)_{10}$), 14.53 ($O(CH_2)_{11}\underline{C}H_3$). **IR** (solid): $\tilde{\nu}$

= 2918 (s), 2851 (m), 1718 (w), 1593 (s), 1462 (w), 1441 (w), 1369 (w), 1350 (w), 1302 (m), 1240 (w), 1171 (s), 1146 (s), 1103 (w), 1055 (m), 1011 (w), 827 (m), 760 (m), 721 (m), 619 (s) cm^{-1}. **MS** (FAB, *m/z*): 1085.9 $[M+H]^+$ (calc. 1085.9); 154.1 [3,5-dihydroxybenzoic acid]$^+$ (calc. 154.0). **Calcd.** for $C_{70}H_{116}O_8$ (1085.67) C 77.44, H 10.77; found C 77.40, H 10.57 %.

Preparation of 3,5-bis(3,5-bis(dodecyloxy)benzyloxy)benzyl alcohol (11)

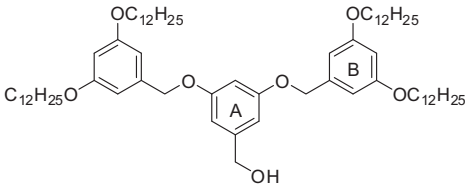

To a suspension of lithium aluminium hydride (319 mg, 95% pure, 7.99 mmol, 1.14 eq) in freshly distilled diethyl ether (200 ml) under an inert atmosphere of N_2, methyl 3,5-bis(3,5-bis(dodecyloxy)benzyloxy) benzoate (**10**) (7.61 g, 7.01 mmol, 1.00 eq) was added slowly in small portions. The reaction mixture was then heated and stirred at reflux for 9 h, cooled down to room temperature and quenched by adding aqueous 1 M NaOH solution (4 ml) dropwise, whereupon the former grey suspension turned white. The white suspension was filtered over celite and washed with diethyl ether. The organic layer was separated and washed twice with water, dried over $MgSO_4$ and evaporated to dryness affording the desired product as a white solid (7.26 g, 6.86 mmol, 98 %) which was analytically pure.

$\mathbf{R_f}$ (TLC, silica gel, hexane:ethyl acetate = 5:1): 0.4. **^{1}H NMR** (400 MHz, $CDCl_3$) δ / ppm 6.61 (d, *J* = 2.2 Hz, 2H, $H^{2(A)}$), 6.56 – 6.52 (m, 5H, $H^{4(A)}$+$H^{2(B)}$), 6.40 (t, *J* = 2.2 Hz, 2H, $H^{4(B)}$), 4.95 (s, 4H, $Ar_AOC\underline{H}_2Ar_B$), 4.63 (s, 2H, $C\underline{H}_2OH$), 3.93 (t, *J* = 6.6 Hz, 8H, $Ar_BOC\underline{H}_2$), 1.82 – 1.71 (m, 8H, $OCH_2C\underline{H}_2CH_2$), 1.49 – 1.39 (m, 8H, $OCH_2CH_2C\underline{H}_2$), 1.39 – 1.19 (m, 64H, $OCH_2CH_2CH_2(C\underline{H}_2)_8$), 0.88 (t, *J* = 6.9 Hz, 12H, $O(CH_2)_{11}C\underline{H}_3$). **^{13}C NMR** (101 MHz, $CDCl_3$) δ / ppm 160.92 ($C^{3(B)}$), 160.57 ($C^{3(A)}$), 143.76 ($C^{1(A)}$), 139.38 ($C^{1(B)}$), 106.10 ($C^{2(A)}$+$C^{2(B)}$), 101.72 ($C^{4(A)}$), 101.18 ($C^{4(B)}$), 70.52 ($Ar_AO\underline{C}H_2Ar_B$), 68.48 ($Ar_BO\underline{C}H_2$), 65.76 ($\underline{C}H_2OH$), 32.34 ($OCH_2(\underline{C}H_2)_{10}$), 30.09 ($OCH_2(\underline{C}H_2)_{10}$), 30.06 ($OCH_2(\underline{C}H_2)_{10}$), 30.03 ($OCH_2(\underline{C}H_2)_{10}$), 30.00 ($OCH_2(\underline{C}H_2)_{10}$), 29.83 ($OCH_2(\underline{C}H_2)_{10}$), 29.77 ($OCH_2(\underline{C}H_2)_{10}$), 29.68 ($OCH_2(\underline{C}H_2)_{10}$), 26.47 ($OCH_2(\underline{C}H_2)_{10}$), 23.11 ($OCH_2(\underline{C}H_2)_{10}$), 14.54 ($O(CH_2)_{11}\underline{C}H_3$). **IR** (solid): $\tilde{\nu}$ = 3354 (w), 2920 (s), 2853 (s), 1597 (s), 1464 (m), 1377 (w), 1344 (w), 1325 (w), 1296 (w), 1167 (m), 1055 (w), 829 (w), 719 (w), 683 (w), 563 (w) cm^{-1}. **MS** (FAB, *m/z*): 1057.9 $[M+H]^+$ (calc. 1057.9); 154.1 [3,5-dihydroxybenzoic acid]$^+$ (calc. 154.0). **Calcd.** for $C_{70}H_{116}O_8$ (1057.66) C 78.36, H 11.05; found C 78.48, H 10.91 %.

Preparation of (*R,S*)-1-(3,5-bis(octyloxy)phenyl)propanol (13)

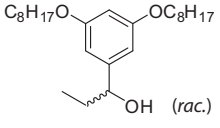

To a mixture of diethylzinc (6.9 ml, ca. 1.0 M in hexane, 6.9 mmol, 2.3 eq) and 2-diethylaminoethanol (45 µl, 0.34 mmol, 0.11 eq) in hexane (110 ml, degassed), 3,5-bis(octyloxy)-benzaldehyde (**12**) (1.11 g, 3.06 mmol, 1.00 eq) in hexane (20 ml) was added at 0 °C under an argon atmosphere. The cooling bath was removed and the mixture allowed to stir for 28 h at room temperature. The reaction mixture was then cooled down to 0 °C and aqueous 1 M HCl (160 ml) was added. The aqueous layer was separated and extracted once with Et_2O, the combined organic layers were washed twice with saturated aqueous $NaHCO_3$, dried over $MgSO_4$ and evaporated to dryness to give a yellow oil. The crude material was purified by column chromatography (Fluka silica gel 60, 0.040–0.063 mm; hexane:ethyl acetate = 8:1) yielding the desired product as a white solid (1.05 g, 2.68 mmol, 88 %).

R_f (TLC, silica gel, hexane: ethyl acetate = 5:1): 0.5. **^{1}H NMR** (500 MHz, $CDCl_3$) δ / ppm 6.48 (d, ^4J = 2.3 Hz, 2H, $H^{2(Ar)}$), 6.36 (t, ^4J = 2.2 Hz, 1H, $H^{4(Ar)}$), 4.51 (t, ^3J = 6.5 Hz, 1H, C<u>H</u>OH), 3.93 (t, ^3J = 6.6 Hz, 4H, O<u>C</u>H_2CH_2CH_2), 1.84 – 1.68 (m, 6H, OCH_2C<u>H</u>$_2$CH_2 + CHOHC<u>H</u>$_2$CH_3), 1.50 – 1.40 (m, 4H, OCH_2CH_2C<u>H</u>$_2$), 1.39 – 1.20 (m, 16H, OCH_2CH_2CH_2(C<u>H</u>$_2$)$_4$CH_3), 0.92 (t, ^3J = 7.4 Hz, 3H, CHOHCH_2C<u>H</u>$_3$), 0.89 (t, ^3J = 7.0 Hz, 6H, OCH_2CH_2CH_2(CH_2)$_4$C<u>H</u>$_3$). **^{13}C NMR** (126 MHz, $CDCl_3$) δ / ppm 160.35 ($C^{3(Ar)}$), 147.05 ($C^{1(Ar)}$), 104.28 ($C^{2(Ar)}$), 100.19 ($C^{4(Ar)}$), 76.17 (<u>C</u>HOH), 68.04 (O<u>C</u>H_2(CH_2)$_6$), 31.84 (OCH_2(<u>C</u>H_2)$_6$), 31.73 (CHOH<u>C</u>H_2CH_3), 29.39 (OCH_2(<u>C</u>H_2)$_6$), 29.29 (OCH_2(<u>C</u>H_2)$_6$), 29.27 (OCH_2(<u>C</u>H_2)$_6$), 26.07 (OCH_2(<u>C</u>H_2)$_6$), 22.69 (OCH_2(<u>C</u>H_2)$_6$), 14.14 (OCH_2(CH_2)$_6$<u>C</u>H_3), 10.23 (CHOHCH_2<u>C</u>H_3). **IR** (solid): $\tilde{\nu}$ = 3375 (w), 2922 (s), 2854 (m), 1595 (s), 1452 (s), 1383 (w), 1348 (w), 1290 (w), 1159 (s), 1047 (s), 966 (w), 833 (m), 694 (m), 579 (m) cm^{-1}. **MS** (EI, *m/z*): 392.3 $[M]^+$ (calc. 392.3). **Calcd.** for $C_{25}H_{44}O_3$ (392.62) C 76.48, H 11.30; found C 76.50, H 11.19 %.

Chapter 4

Synthesis and STM Imaging of Achiral and Chiral Bipyridine Ligands

4.1
Introduction and aims

In this chapter, the syntheses and analyses of achiral and chiral 2,2'-bipyridine-based ligands are presented. The ligands were functionalised in the 4- and 4'-positions with the Fréchet-type dendrons introduced in **Chapter 3**. The main goal of their preparation was their use in monolayer formation, observable in STM measurements. Similar systems have been investigated into detail by *L. Scherer* and other co-workers of our research group. *Scherer* used octyl-decorated Fréchet-type dendrimers[21] whereas in this work, dodecyl-functionalised systems were used. This was done due to the expected higher affinity to form interdigitated arrangements and the possibility to reveal liquid-crystalline properties,[179, 180] which were, in the end, not observed.

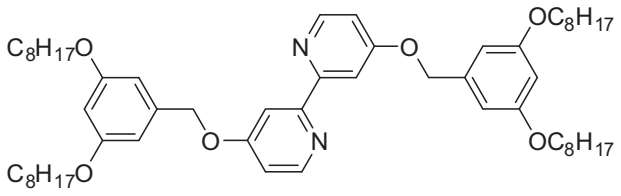

14

Scheme 4.1 Ligand **14** prepared by *L. Scherer*: 2,2'-bipyridine functionalised with Fréchet-type dendrons bearing octyl chains.

It was shown by *L. Scherer* that ligand **14** (**Scheme 4.1**) readily forms monolayer visualisable by STM. Domains with different patterns were observed.[1] The occurrence of these different domains was attributed to the different conformations that ligand **14** is able to adopt by rotation about the bpy–OCH_2Ar axis. In order to gain more support for this statement and to investigate this effect in more detail, chiral analogues of **14** were prepared in this thesis.[181]

By introducing an ethyl group at the benzylic methylene-position, it is supposed to force the molecule into a particular conformation on a flat surface due to steric repulsion with the underlying graphite surface (**Scheme 4.2**).[182-190]

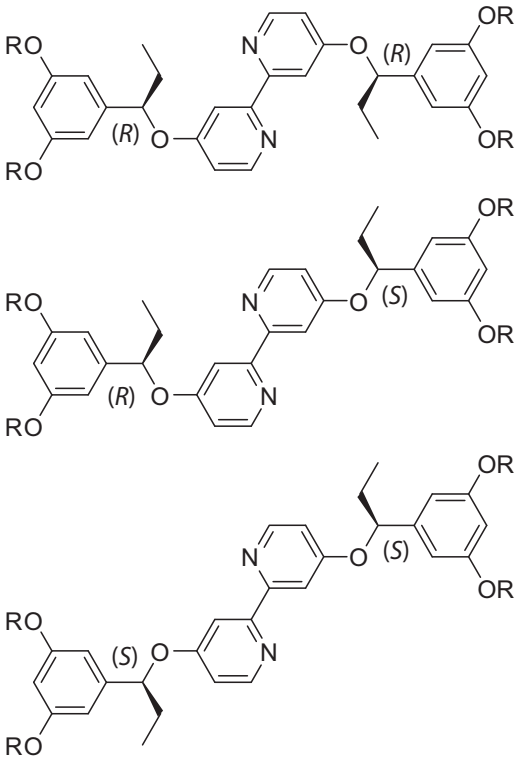

Scheme 4.2 Conformations adopted on a surface for different stereoisomers avoiding steric repulsion of the ethyl group with an underlying surface in the sheet plane.

As the chiral dodecyl-functionalised ligands did not prove to form monolayers easily when solution cast onto HOPG (see **Section 4.3.1**), the chiral octyl analogue was prepared (**Section 4.2.4**) to be able to differentiate whether this effect is due to the introduction of the ethyl group or due to the longer alkyl chains.

Parts of this work have been published already in the diploma work of the author of this thesis.[191]

4.2
Synthesis and discussion

4.2.1
Achiral ligands

The synthetic strategy adopted for the synthesis of the ligands was the reaction of nucleophilic bipyridine derivative 4,4'-dihydroxy-2,2'-bipyridine[192, 193] with an electrophilic dendritic wedge.

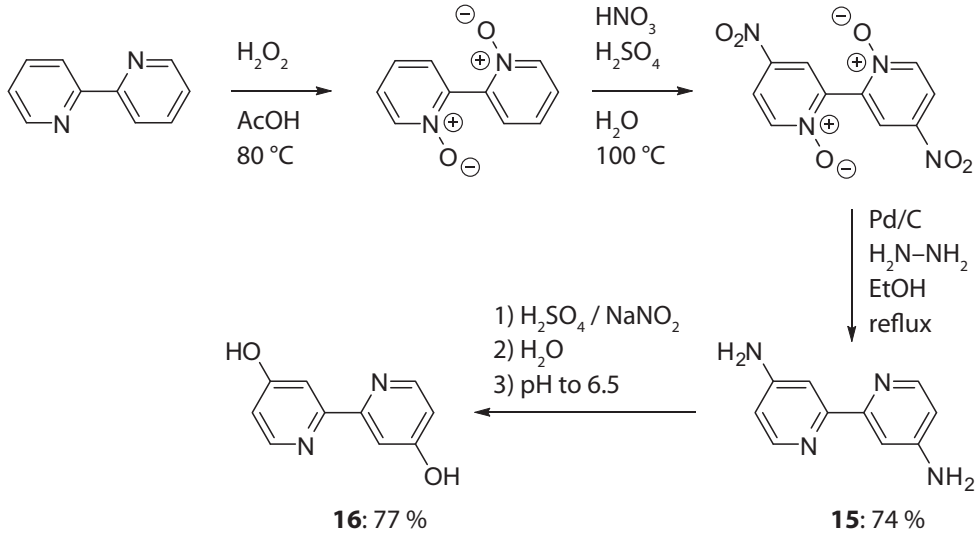

Scheme 4.3 Four step synthesis of 4,4'-dihydroxy-2,2'-bipyridine (**16**) starting from 2,2'-bipyridine.

In the four step synthesis of 4,4'-dihydroxy-2,2'-bipyridine (**16**), the starting material was 2,2'-bipyridine (**Scheme 4.3**).[21] First, the pyridine units were oxidised with H_2O_2 as the oxidising reagent. The 4,4'-dinitro-2,2'-bipyridine-*N*,*N'*-dioxide could then easily be nitrated at the 4- and 4'-positions using a mixture of concentrated nitric acid and concentrated sulfuric acid. In this step, formation of 4-nitropicolinic acid as a side product leads to low yields as shown by *A. Mahmood* in our group.[194] Up to this step, the procedure had followed a report[193] of a former student in our group and the compound 4,4'-dinitro-2,2'-bipyridine-*N*,*N'*-dioxide was kindly offered by *C. Brennan* in our group for further synthesis. Reduction of this compound was performed using a more convenient procedure than before, *i.e.* reduction with iron in acetic acid[193]. It was shown by *Maury et al.*[195] that palladium on activated carbon and hydrazine were much more effective.[196, 197] Using this method, 4,4'-diamino-2,2'-bipyridine (**15**) could be obtained in 74 % yield. Converting the amino groups to the corresponding hydroxyl groups using non-classical *Sandmayer*-conditions[193] yielded the desired 4,4'-dihydroxy-2,2'-bipyridine (**16**) in good yield.

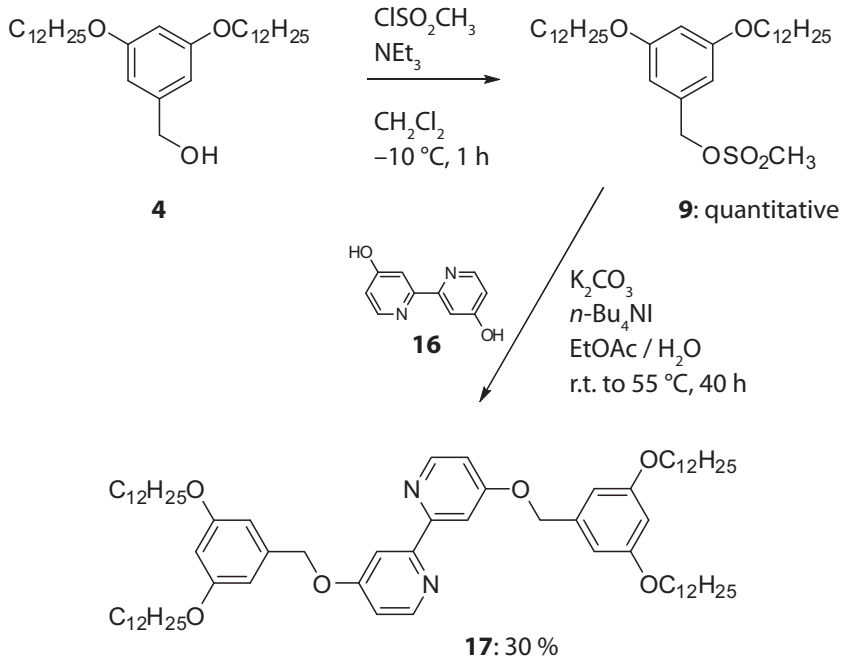

Scheme 4.4 Preparation of the achiral ligand **17**.

Coupling the alcohol to the bipyridine was done in two steps using the mesylate derivative as the electrophile. Mesylates are very good leaving groups and their synthesis is straightforward using standard methods by treating alcohol **4** in dichloromethane with methanesulfonyl chloride for one hour in the presence of triethylamine at –10 °C (**Scheme 4.4**). The crude mesylate **9** was not purified and used directly for the coupling reaction with 4,4'-dihydroxy-2,2'-bipyridine (**16**). The coupling reaction itself was performed under high-concentration phase transfer conditions using *n*-Bu_4NI as the phase transfer catalyst in ethyl acetate and water in the presence of K_2CO_3 as shown previously by *L. Scherer*.[1]

4.2.2 Chiral ligands

In order to obtain the chiral bipyridine ligand, coupling the chiral alcohols **6**, **7**, and **8** to 4,4'-dihydroxy-2,2'-bipyridine (**16**) was the next step. Since the procedure using the mesylate derivatives as used for the achiral ligand **17** occurs at least partially through an S_N1-mechanism because of the neighbouring aryl group, losing chiral information would be inevitable. Therefore, an alternative way to the bipyridine ligand was desired. As shown before by the author, a *Mitsunobu*-type reaction was successful.[191] *Dehaen et al.* reported[198] a way to couple higher generation dendritic polyethers under *Mitsunobu* conditions[199-205] resulting in inversion of the stereocentre of a secondary alcohol.[206] The requirement for this stereospecific reaction is a pK_a below 11 for one of the coupling reagents which is achieved using 4,4'-dihydroxy-2,2'-bipyridine (**16**).

The chiral secondary alcohols **6**, **7**, and **8** were mixed with 4,4'-dihydroxy-2,2'-bipyridine (**16**) and triphenylphosphine. Because crystalline 4,4'-dihydroxy-2,2'-bipyridine (**16**) always contains small amounts of water and the *Mitsunobu* reaction[207] must be carried out under water-free conditions, this mixture was firstly dissolved several times in dichloromethane and evaporated to dryness in order to remove water as an azeotrope. In addition, more DEAD (diethyl azodicarboxylate) and triphenylphosphine than usual was used (3.50 equivalents each). The mixture was finally added to a small amount of THF, and DEAD was added to the suspension under an argon atmosphere. After a few minutes, the mixture turned into a brown solution and it was stirred overnight at room temperature (**Scheme 4.5**).

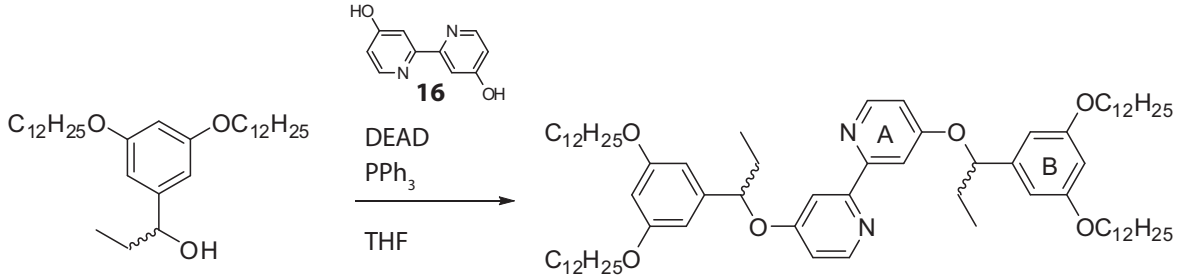

6: *rac.*
7: (*S*)
8: (*R*)

18: diastereomeric mixture
19: (*R*)(*R*)-stereoisomer
20: (*S*)(*S*)-stereoisomer

Scheme 4.5 Mitsunobu reaction to the chiral bipyridine ligands. Ring labels are for NMR spectroscopic assignments (**Figure 4.3**).

One problem in the isolation of the products was the purification because the hydrazine derivatives originating from DEAD and the triphenylphosphine oxide co-elute[208] with the product when performing a silica gel column chromatographic separation. This is attributed to the strong hydrogen-bond forming ability of triphenylphosphine oxide[209] as well as hydrophobic effects[210]. Previously,[191] the product was recrystallised from hexane and ethanol but this has the disadvantage that rather large amounts of product were lost. It was found, however, that with a specific mixture in the eluent for the column chromatography (*i.e.* dichloromethane : methanol = 40 : 1), the order of elution could be changed resulting in faster elution of the product compared to the aforementioned side products yielding the ligand in a very high purity. Alternatively, one could perform the reaction in diethyl ether resulting in precipitation of the side products and removing these by filtration[211], and by using phosphines bearing a basic group (*e.g.* PPh_2Py)[211-213] allowing acid extraction of the oxidised species. Alternative reagents to triphenyl phosphine have also been used[214]. Other strategies reported[215] to facilitate the removal of the undesired products include the use of polymer-supported,[216] acid-sensitive,[217] polymerisable,[218] precipitable,[219] fluorous,[220] and cyclodextrin binding[221] analogues of DEAD.

Due to the inversion at the chiral centre in the chiral alcohol,[222] the enantiopure (*R*)(*R*)-ligand **19** was obtained from the (*S*)-alcohol **7** and the enantiopure (*S*)(*S*)-ligand **20** from the (*R*)-alcohol **8** (**Table 4.1**). The chiral bpy ligand **18** from the reaction with the racemic alcohol **6** consists of three

different stereoisomers as shown in **Figure 4.1**. One might expect four stereoisomers, (*R*)(*R*)-**18** (identical to **19**), (*S*)(*R*)-**18**, (*R*)(*S*)-**18**, and (*S*)(*S*)-**18** (identical to **20**). However, due to the inversion centre in (*S*)(*R*)-**18** and (*R*)(*S*)-**18**, they are achiral, *i.e.* (*meso*)-**18**.

Table 4.1 Chiral bpy-ligands from Mitsunobu reactions showing yields and stereomeric excesses.

Starting material	Product	
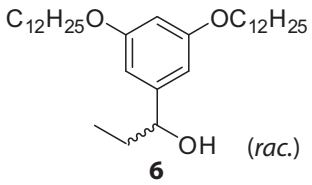 **6**	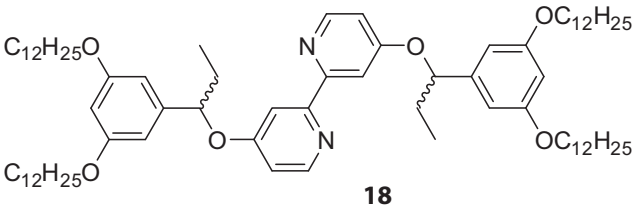 **18**	55 % yield 5 % ee 6 % de
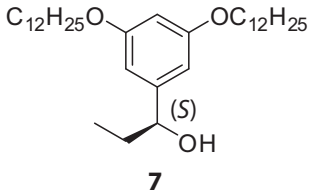 **7**	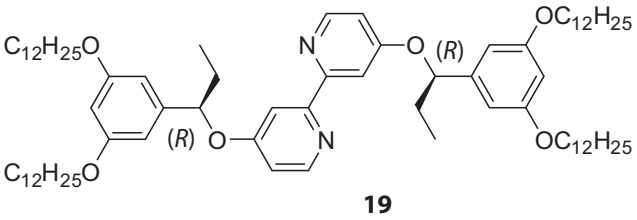 **19**	57 % yield 99 % ee 95 % de
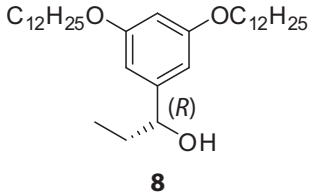 **8**	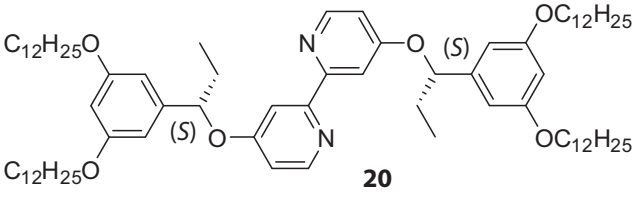 **20**	55 % yield 99 % ee 91 % de

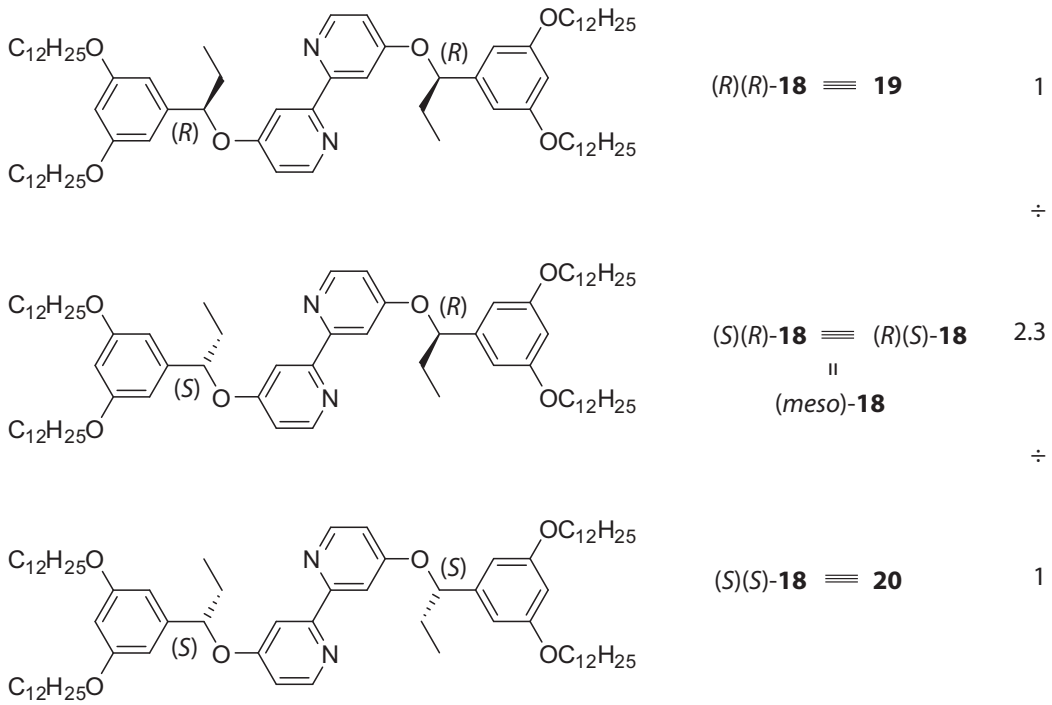

Figure 4.1 Stereoisomers of the chiral bpy-ligand **18** and their ratio determined by HPLC.

The products from the three reactions were analysed using HPLC (**Figure 4.2**) with a chiral OD-H column. Reactions of enantiopure alcohols **7** and **8** yielded ligands **19** and **20**, respectively, with very high enantiomeric and diastereomeric excesses proving the exceptionally high stereospecific character of the *Mitsunobu* reaction. Concerning **18**, (*R*)(*R*)-**18**, (*meso*)-**18**, and (*S*)(*S*)-**18** should occur in a 1 : 2 : 1 ratio at first glance with twice the amount of (*meso*)-**18**. If one takes a closer look though, the (*meso*)-**18** does not necessarily have to be formed in double the amount of (*R*)(*R*)-**18** or (*S*)(*S*)-**18**. When the first alcohol molecule, either being (*R*)-**6** or (*S*)-**6**, was coupled to the bipyridine, the resulting compound is now chiral and reacts differently with the two possible enantiomeric alcohol molecules (*R*)-**6** and (*S*)-**6**. This assumption was proved in the HPLC measurements showing 5 % ee and 6 % ee which converts to a ratio of 1 : 2.3 : 1 of the three stereoisomers in **18** (**Figure 4.1**).

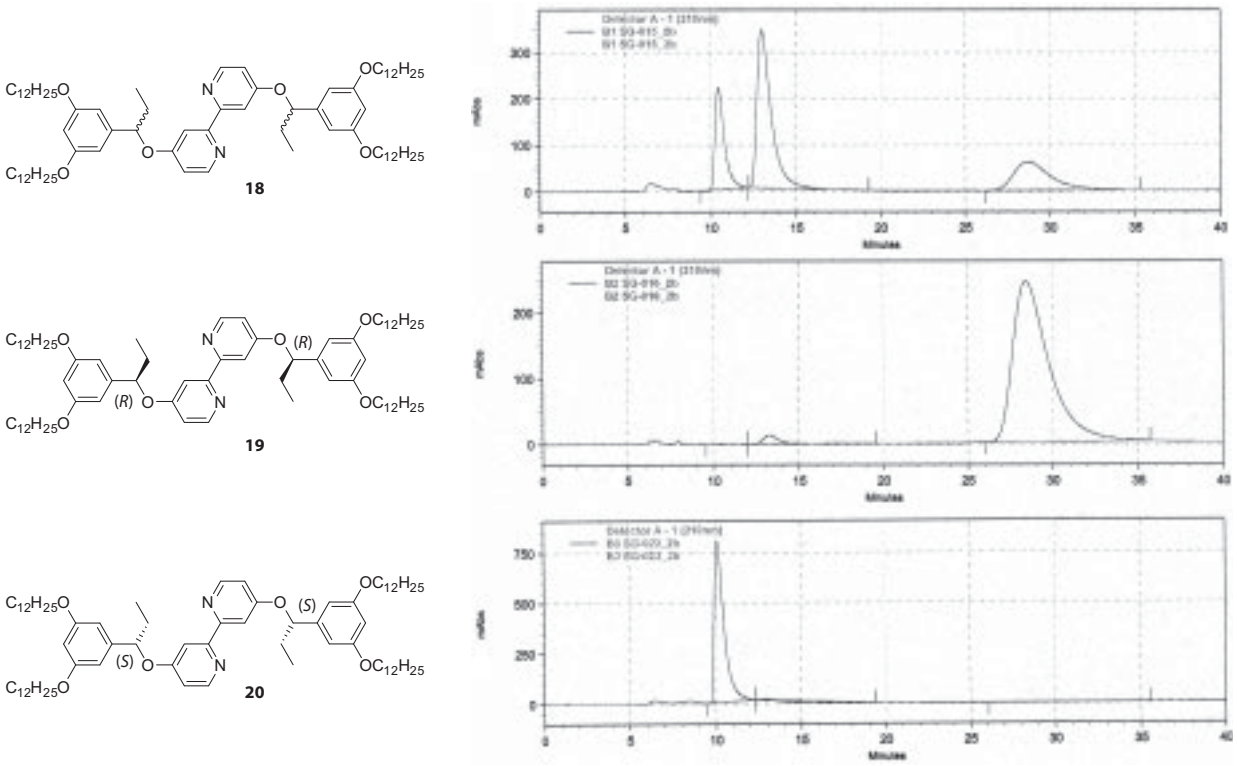

Figure 4.2 HPLC Chromatograms of **18**, **19**, and **20** with a chiral column OD-H.

Interestingly, using the *Mitsunobu* reaction for the coupling of the achiral primary alcohol **4** to 4,4'-dihydroxy-2,2'-bipyridine (**16**) did only yield in traces of the product (**17**) for which the reason remains unknown.

Another interesting observation is visible in the ^{1}H NMR spectra. **Figure 4.3** shows exemplary ^{1}H NMR spectra of compound **19** after two different purification procedures. The bottom spectrum was from a batch where purification was done by silica gel chromatography, recrystallisation from ethanol, preparative layer chromatography and a subsequent recrystallisation from ethanol. First, the broadening of the bipyridine proton ($H^{3(A)}$ and $H^{5(A)}$) peaks in the corresponding NMR spectrum was attributed to a hindered rotation about the bpy–OR or the py–py axis.[191]

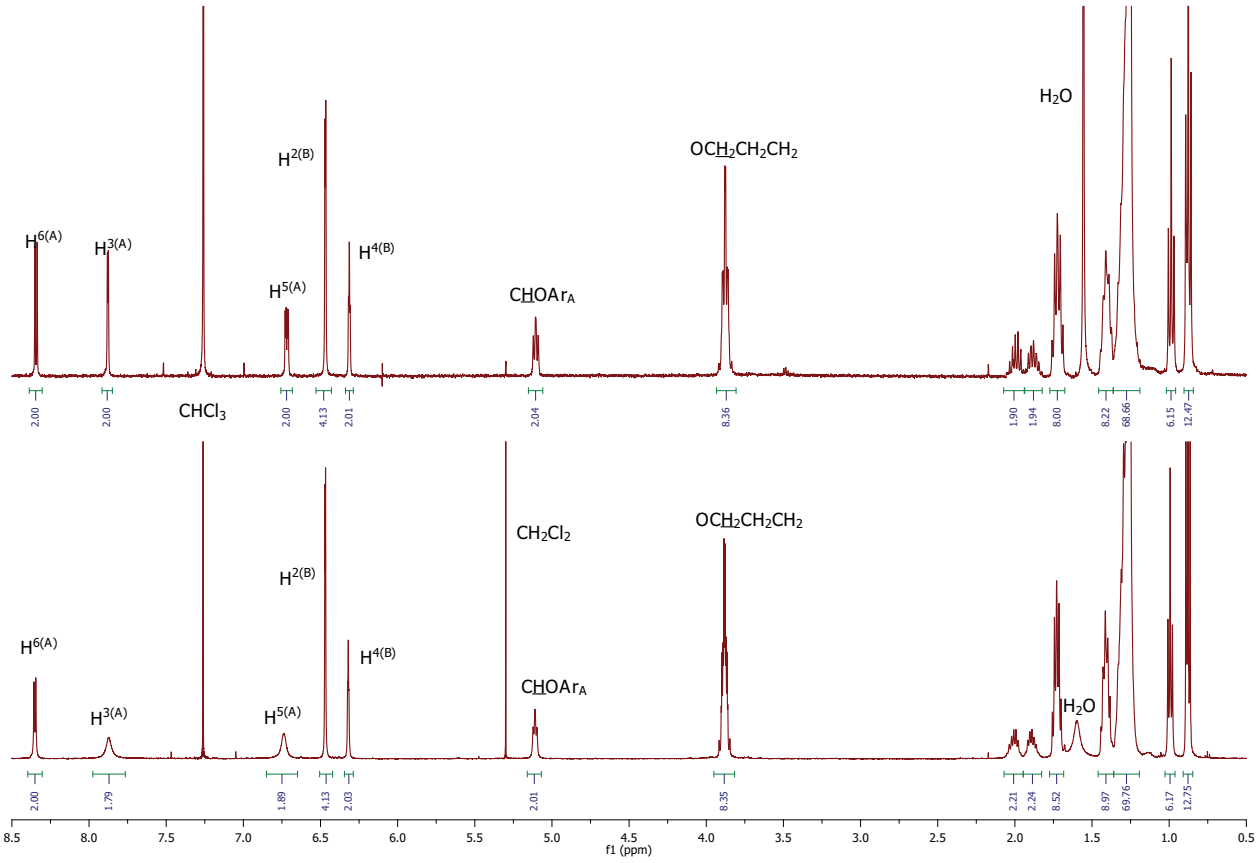

Figure 4.3 400 MHz (top) and 500 MHz (bottom) ^{1}H NMR spectrum of **19** each in $CDCl_3$ at 300 K (top spectrum) and 295 K (bottom), respectively, after two different purification procedures. See **Scheme 4.5** for ring labelling.

However, later it was found that with different purification processes, involving washing the compound with aqueous sodium hydrogencarbonate solution as described in this work and no use of preparative layer chromatography, the peaks for protons $H^{3(A)}$ and $H^{5(A)}$ become sharp (top spectrum in **Figure 4.3**) indicating very small amounts of impurities, *e.g.* protonated product, being responsible for this behaviour. This assumption is confirmed by temperature experiments with the first batch of compound where raising the temperature did not result in sharpening of the corresponding peaks.

4.2.3 Second generation ligands

The synthetic approach to the second generation bipyridine ligand **22** was analogous to the synthesis of the corresponding first generation achiral ligand (**Scheme 4.6**). Converting the second generation alcohol **11** quantitatively to its mesylate derivative **21**, led to the desired electrophile suitable for the following coupling reaction. Crude **21** was reacted with 4,4'-dihydroxy-2,2'-bipyridine (**16**) under similar conditions as for the first generation ligand using high-concentration phase transfer

conditions with *n*-Bu_4NI as the phase transfer catalyst in ethyl acetate and water in the presence of K_2CO_3 as shown previously by *L. Scherer*.[1]

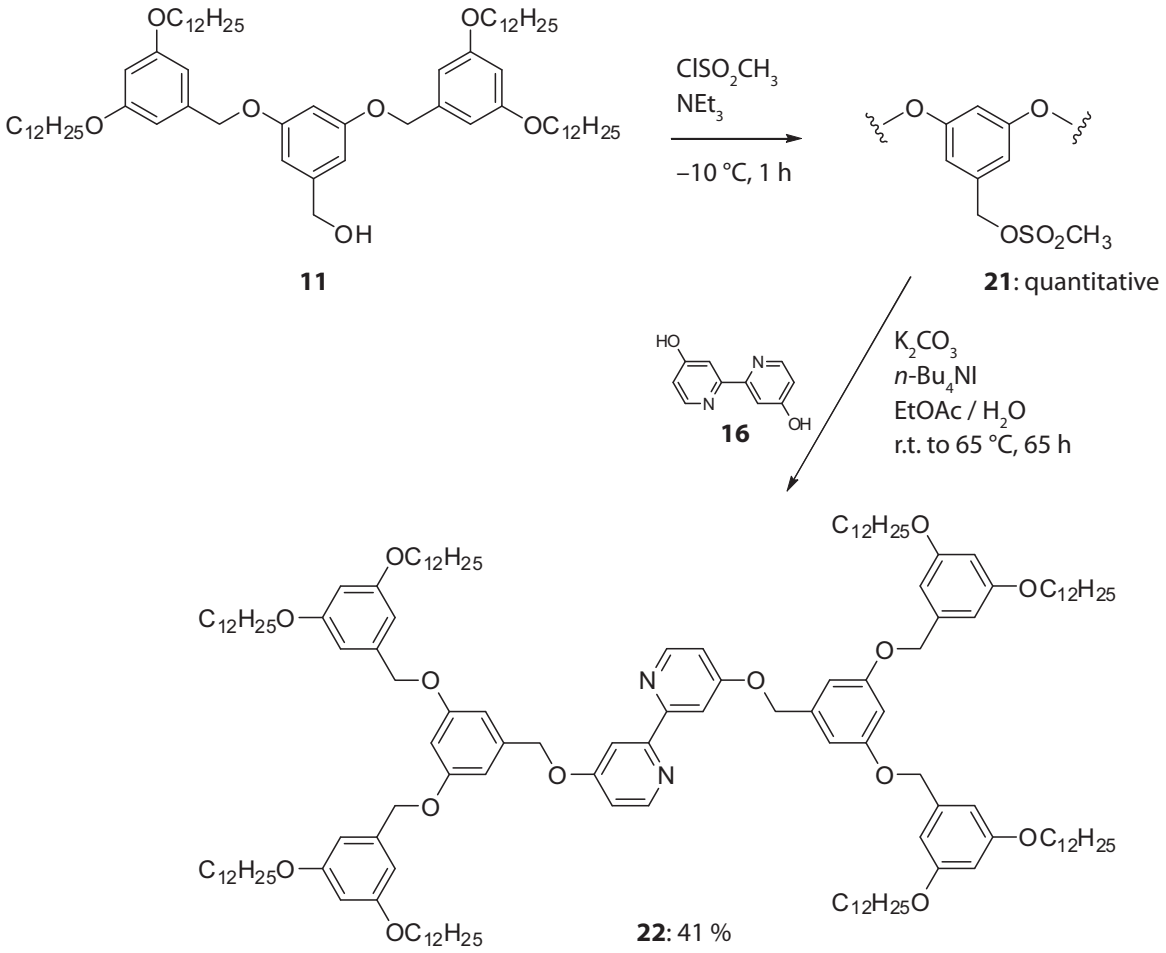

Scheme 4.6 Synthetic route to the second generation bipyridine ligand **22**.

4.2.4 Ligands with different chain lengths

For the synthesis of the chiral ligand **23** bearing octyl chains, the same conditions as for the dodecyl type ligands were used (**Scheme 4.7**). Under *Mitsunobu* conditions, the racemic alcohol **13** was reacted with 4,4'-dihydroxy-2,2'-bipyridine (**16**) yielding a diastereomeric mixture of ligand **23** like its dodecyl analogue **18**. The achiral ligand without the two ethyl groups compared to **23** is already known and was synthesised earlier in our research group by *L. Scherer*.[21]

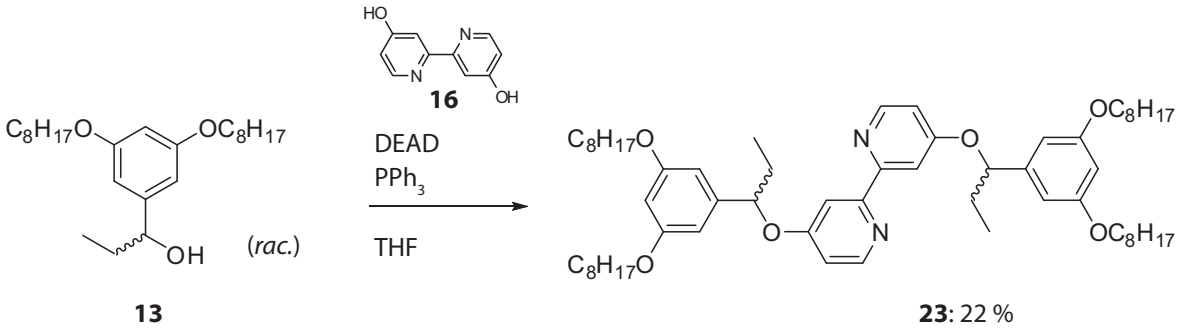

13 **23**: 22 %

Scheme 4.7 Synthesis of the chiral ligand **23** with octyl chains.

4.3 STM imaging and discussion

All achiral and chiral 1st generation ligands presented in this chapter were studied using STM. For that purpose, the molecules were solution cast onto a graphite surface to form a monolayer. Where no monolayer pattern could be observed at the air/solid-interface, established by evaporation of a solution of the compound in hexane on HOPG, additional measurements at the liquid/solid-interface were performed. There, the appropriate ligand was dissolved in 1-phenyloctane, a non-volatile solvent, and two droplets were placed on a fresh surface of HOPG yielding a dynamic adsorption and desorption process (see **Chapter 2** for more details).

As discussed in **Section 4.1**, the ligands introduced in this chapter are able to adopt a variety of conformations. **Scheme 4.8** depicts conformers where the bipyridine unit exhibits a *transoid*-conformation. Rotation around the bpy–OCH_2Ar axis leads to *syn*- and *anti*-conformations when a molecule adopts a planar arrangement. This gives rise to a total of three conformations for 1st generation Fréchet-type decorated bipyridine ligands, neglecting different arrangements of the alkyl chains and assuming the transoid-conformation that is typical of the free bpy domain.

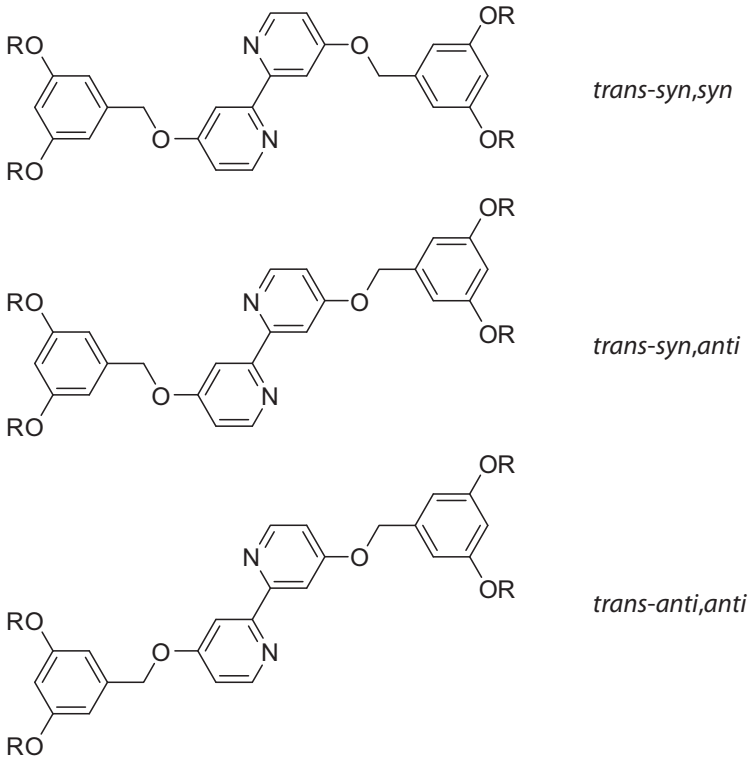

Scheme 4.8 Nomenclature of possible conformations of the ligands.

4.3.1 Air/solid-interface

First, the achiral ligand **17** was measured with STM. The sample (compound **17** deposited on HOPG from a hexane solution) had to be heated for one hour at 70 °C before measuring in order to obtain a monolayer (**Figure 4.4**). In the earlier measurements of the related octyl ligand, the bright area of the obtained image could be assigned clearly to the aromatic part of the molecule and the dark area to the "insulating" alkyl chains.[1] As expected, the black areas found in **Figure 4.4** are larger than the black areas found in STM images with the corresponding octyl ligand.

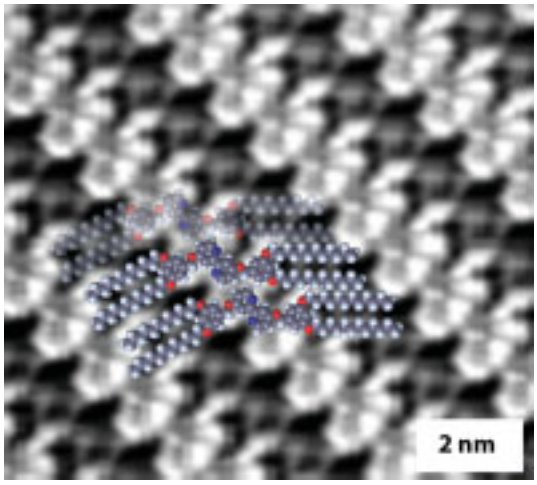

Figure 4.4 STM image (averaged) of the achiral ligand **17** with overlaid molecules in the *syn*,*anti*-conformation, showing an area of 10 nm × 9 nm.

In a next measurement, the chiral ligand **18**, being a mixture of three different stereoisomers, was solution cast onto HOPG (see **Figure 4.1**). One image revealed two different patterns as shown in **Figure 4.5**. The stripe-like pattern in the upper-left corner and in a few other spots in the image shown in **Figure 4.5** was encountered only in this instance. The second pattern was observed in many other instances. The occurrence of these two differing patterns could be attributed to the diastereoisomers present in **18**, (*meso*)-**18** and the enantiomeric pair of (*R*)(*R*)-**18** and (*S*)(*S*)-**18**.

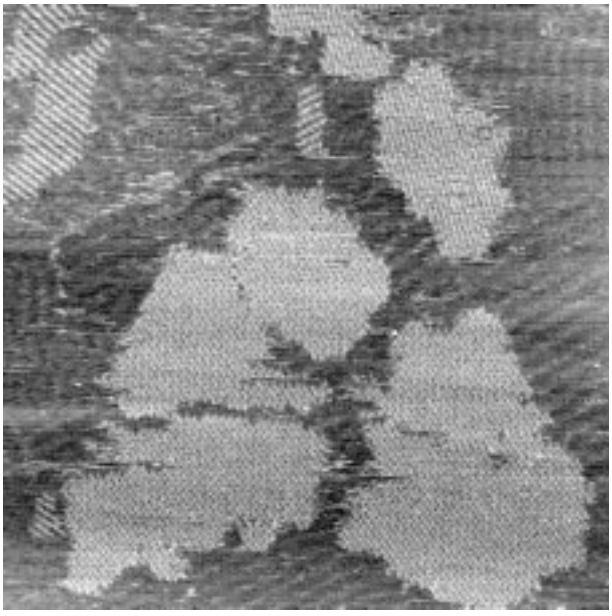

Figure 4.5 STM image of the stereomeric mixture of **18**, showing a 200 nm × 200 nm area.

Figure 4.6 shows an averaged image of the mostly present pattern observed in the monolayer of **18**. The arrangement of the molecules in the monolayer is not trivial, nevertheless **Figure 4.6** shows a possible packing. There, solely (*meso*)-configurated isomers in their *syn*,*anti*-conformation were considered and matched to the bright and dark spots observed in the STM image.

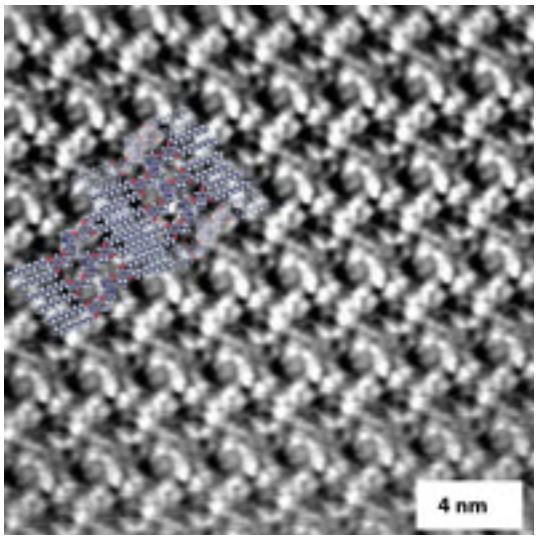

Figure 4.6 STM image (averaged) of a pattern of **18** with overlaid molecules in the *meso*-configuration (*R*,*S*) and the *syn*,*anti*-conformation, showing a 20 nm × 20 nm area.

In a further experiment, the monolayer behaviour of the enantiopure ligand **19** was investigated using STM. Images obtained from these measurements show a stripe-like pattern. **Figure 4.7** shows one possible arrangement of the molecules in their expected *syn*,*syn*-conformation. But due to low resolution, it is difficult to assign the pattern to a specific arrangement.

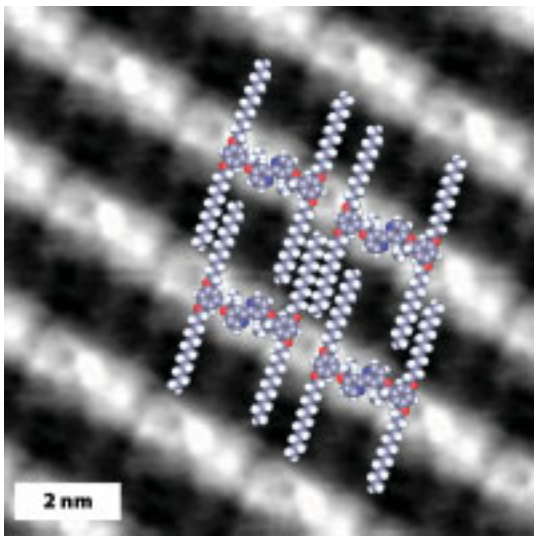

Figure 4.7 STM image (averaged) of a pattern of **19** with overlaid molecules in the *syn*,*syn*-conformation, showing an area of 10 nm × 10 nm.

Unfortunately, STM measurements of the other enantiopure ligand **20** at the air/solid-interface did not result in a visualisable monolayer as observed for the other stereoisomers.

In a proceeding experiment, the octyl chain-analogue of the stereomeric mixture of **18**, ligand **23**, was solution cast onto HOPG. Only for a few instances, patterns from a monolayer could be detected by STM. **Figure 4.8** gives an example of the typical arrangement found in monolayers of the stereomeric mixture in compound **23**. The lines found in the pattern are separated by a distance of 4.6 nm. The angle between lines from other domains is roughly 60 °, reflecting three-fold symmetry of the underlying graphite. Due to lack of better resolved images, no detailed analysis could be performed.

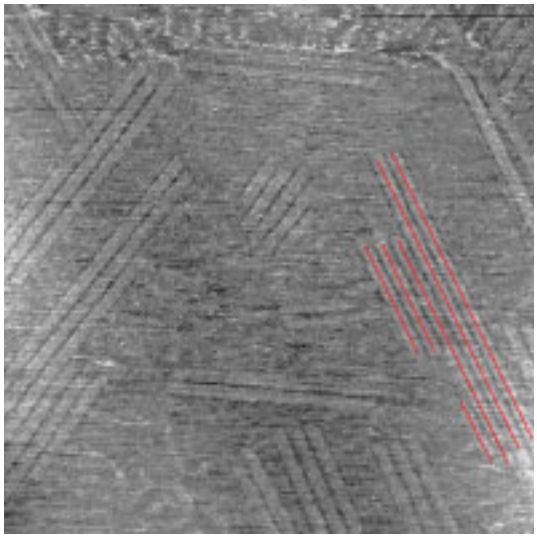

Figure 4.8 STM image of **23** on HOPG at 150 nm × 150 nm using scan parameters: U_{bias} = –700 mV, I_t = 8.0 pA, v = 1.49 Hz.

4.3.2 Liquid/solid-interface

Generally, measuring at the liquid/solid-interface, it was easier to visualise monolayers in STM compared to solution cast samples. Unfortunately, this benefit comes at the expense of inherently augmented drift in the setup. Therefore, images obtained at the liquid/solid-interface need to be carefully studied and it is dangerous to make conclusions without solid foundations. This especially applies to our attempt to differentiate between conformations, as the expected differences in patterns are supposed to be marginal.

In a first experiment, the stereoisomeric mixture of compound **18** was measured at the liquid/solid-interface. As seen in **Figure 4.9**, a direct consequence of the dynamic adsorbing process is the presence of very large domains of which the borders could not be determined even when measured at a large image size of 200 nm × 200 nm. In a dynamic system as is the case for the liquid/solid-

interface, the thermodynamically most stable arrangement will be adopted; hence a "2D single crystal" can be formed. Interestingly, packing defects are still present as observed in **Figure 4.9** with the diagonal, brighter "line". This could be explained by defects of the underlying graphite surface.

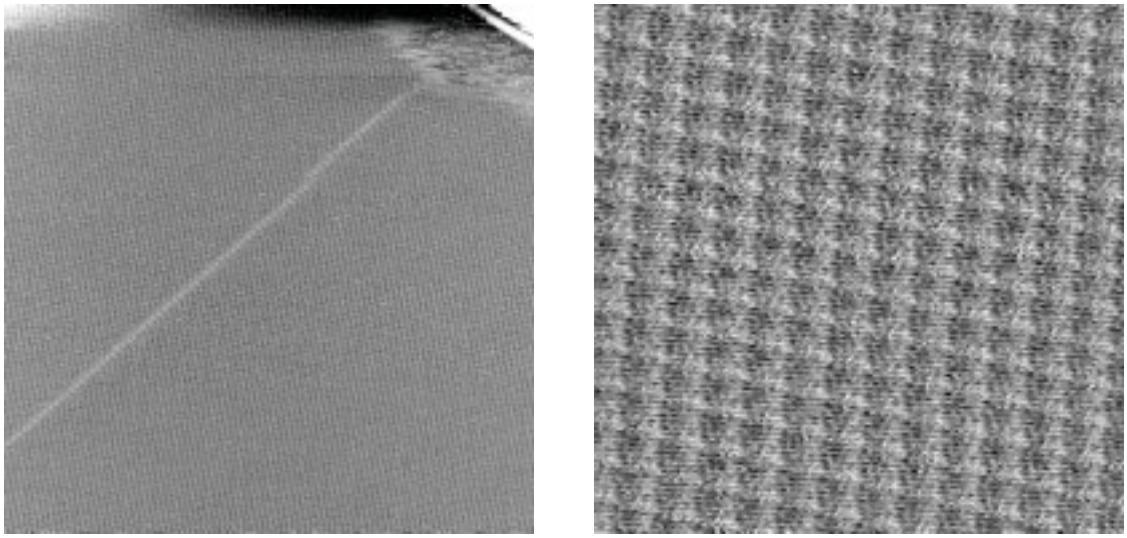

Figure 4.9 STM images of **18** on HOPG at 200 nm × 200 nm (a) and 30 nm × 30 nm (b) using scan parameters: U_{bias} = –800 mV, I_t = 8.0 pA, v = 3.05 Hz (a); U_{bias} = –700 mV, I_t = 8.0 pA, v = 4.07 Hz (b).

An inset (10 nm × 10 nm) of the image in **Figure 4.9b** was averaged over 293 positions (**Figure 4.10**) and shows an overlaid unit cell. The oblique unit cell's plane group is probably $p1$ with no additional symmetry element than the identity. The unit cell dimensions are a = 2.4 nm, b = 2.5 nm, α = 67 °, which gives an area of 5.5 nm^2. Because compound **18** consists of three different stereomers which supposedly would adopt different conformations, no further analysis by overlaying molecules on top of the averaged STM image were performed.

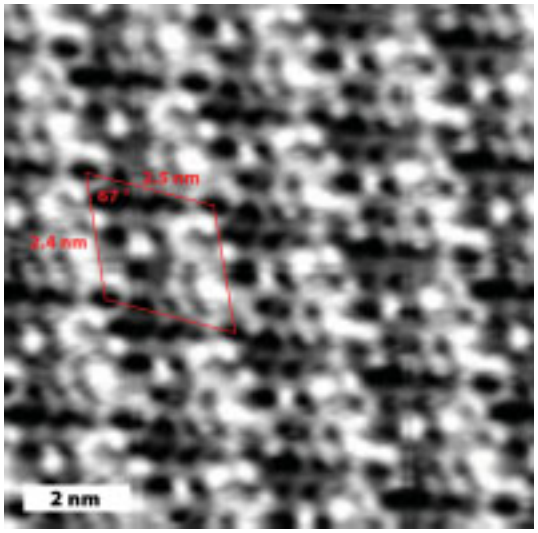

Figure 4.10 Averaged image (10 nm × 10 nm) of **Figure 4.9b** over 293 positions showing the unit cell.

Next, the enantiopure ligand **19** was measured on HOPG at the liquid/solid-interface. With regard to the domain size, the same principles explained for compound **18** apply here, *i.e.* large domains were observed with no evidence of domain borders (**Figure 4.11**).

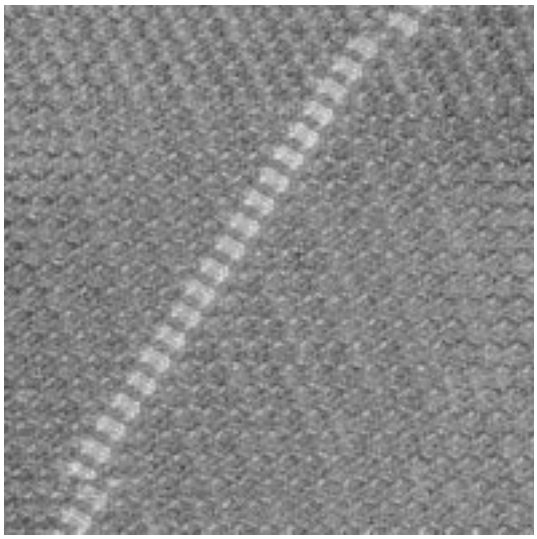

Figure 4.11 STM image of **19** on HOPG at 50 nm × 50 nm using scan parameters: U_{bias} = –800 mV, I_t = 8.0 pA, v = 3.05 Hz.

After averaging over 253 positions, simple unit cell considerations could be done (**Figure 4.12**). The unit cell possesses the shape of a parallelogram and thus exhibits most probably a $p1$ plane group due to the lack of further symmetry elements apart from the identity. The dimensions of the unit cell are a = 2.4 nm, b = 2.4 nm, α = 65 ° yielding an area of 5.1 nm^2.

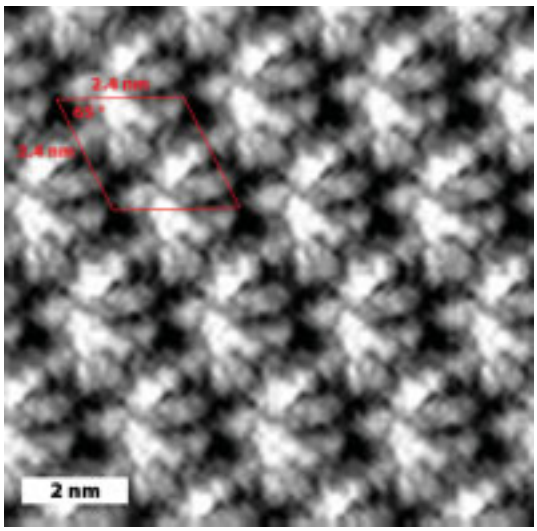

Figure 4.12 Averaged image (10 nm × 10 nm) of ligand **19** over 253 positions showing the unit cell.

Figure 4.13 shows two possible arrangements of molecules of compound **19** overlaid on the same averaged image as in **Figure 4.12**. Being the (*R*)(*R*)-enantiomer, it is supposed to adopt the *syn*,*syn*-conformation. As there is still a noticeable amount of "unused" space, it remains unsure if the arrangements presented are correct.

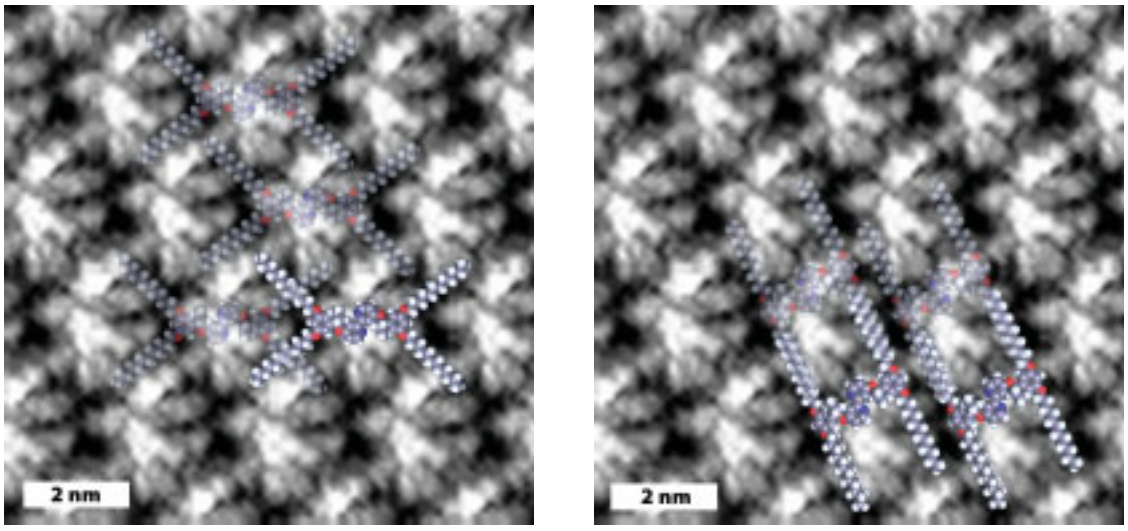

Figure 4.13 Averaged images (10 nm × 10 nm) of **Figure 4.12** with two different arrangements of overlaid molecules of **19** in their *syn*,*syn*-conformation.

The enantiomer of **19**, ligand **20**, was measured next at the liquid/solid-interface using STM. Again, large domains were formed by the monolayer of **20** with no indication of domain borders (**Figure 4.14**).

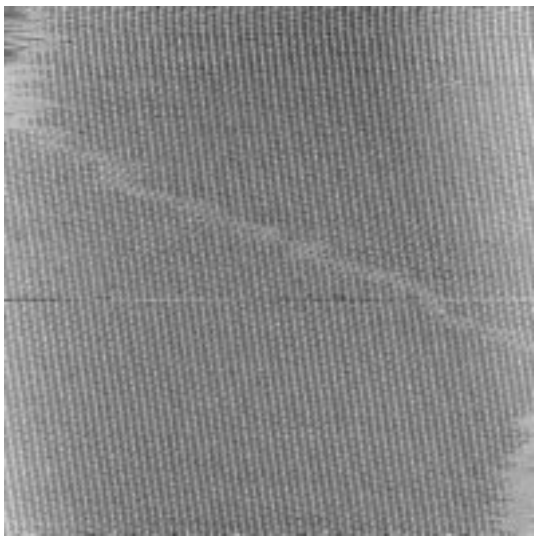

Figure 4.14 STM image of **20** on HOPG at 150 nm × 150 nm using scan parameters: U_{bias} = –800 mV, I_t = 8.0 pA, v = 1.97 Hz.

In **Figure 4.15**, an averaged image (10 nm × 10 nm) is depicted including a representation of the unit cell. The oblique's unit cell plane group is most probably *p*1. The unit cell dimensions are a = 2.7 nm, b = 2.3 nm, α = 58 ° leading to an area of 5.1 nm^2.

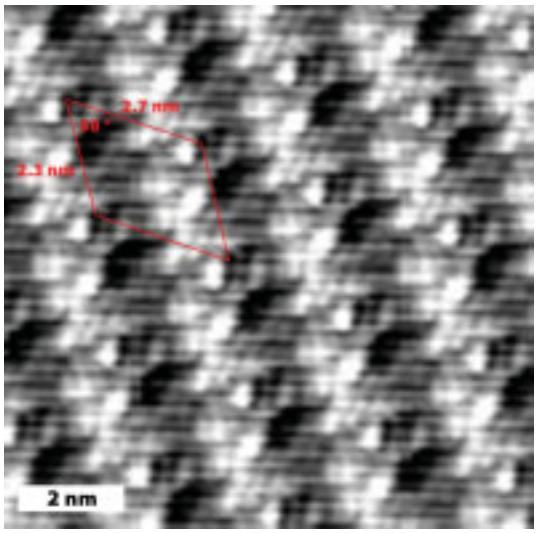

Figure 4.15 Averaged image (10 nm × 10 nm) of ligand **20** over 297 positions showing the unit cell.

As the (*S*)(*S*)-enantiomer supposedly adopts an *anti*,*anti*-conformation in order to avoid steric repulsion of the ethyl group with the underlying graphite (see **Section 4.1** and **Scheme 4.2**), in an attempt to overlay an arrangement of molecules of **20**, two possibilities are given in **Figure 4.16**.

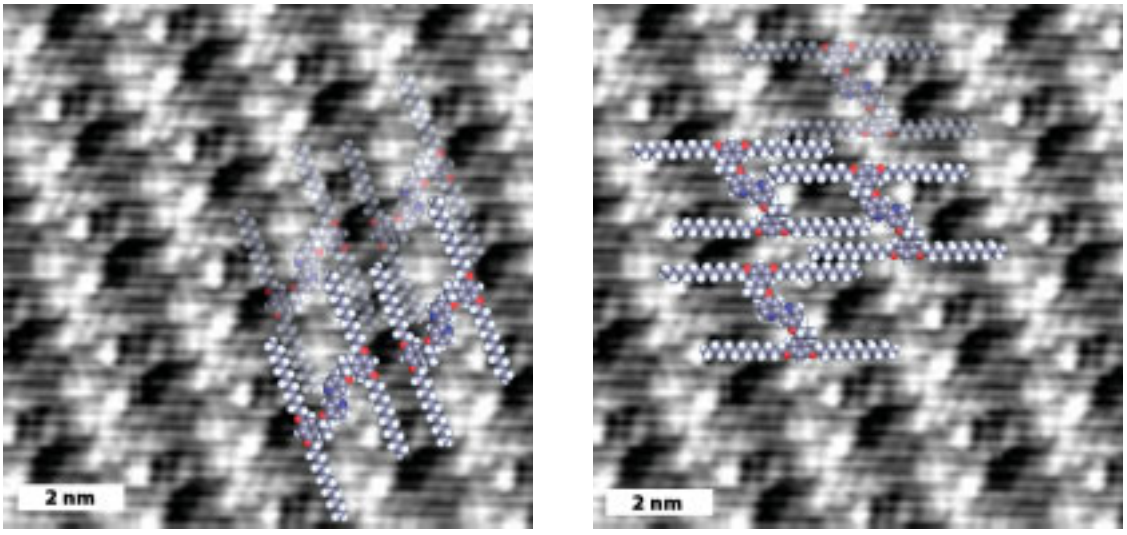

(a) (b)

Figure 4.16 Averaged images (10 × 10 nm^2) of **Figure 4.15** with two different arrangements of overlaid molecules of **20** in their *anti*,*anti*-conformation.

In conclusion, the differences of the observed patterns at the liquid/solid-interface for the three compounds **18**, **19**, and **20** are only marginal. Also, the dimensions of the unit cells are almost identical with respect to the experimental error (**Table 4.2**). Therefore, it is hard to make any assumptions and the attempts of overlying modelled molecules in a particular conformation remain highly delicate.

Table 4.2 Comparison of unit cell dimensions; area = a × b × sin(α).

	18	**19**	**20**
a	2.5 nm	2.4 nm	2.7 nm
b	2.4 nm	2.4 nm	2.3 nm
α	67 °	65 °	58 °
area	5.5 nm^2	5.1 nm^2	5.1 nm^2

4.4 Experimental part

Preparation of 4,4'-diamino-2,2'-bipyridine (15)

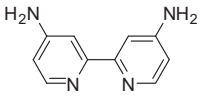

To a mixture of 4,4'-dinitro-2,2'-bipyridine 1,1'-dioxide (20.0 g, 71.9 mmol, 1.00 eq) and 10 % Pd on carbon (4.67 g, 4.39 mmol, 0.0600 eq) in EtOH (700 ml), a solution of hydrazine monohydrate (17.5 ml, 0.359 mol, 5.00 eq) in EtOH (130 ml) was added dropwise over a period of 1 h. The reaction mixture was stirred at 65 °C for 14 h and another 5 h at reflux. The mixture was then filtered hot and washed with cold Et_2O. The filtrate was evaporated to dryness and the residue recrystallised from EtOH to yield the product as a yellow solid (9.94 g, 53.4 mmol, 74 %).

mp 278 – 280 °C (EtOH). **^{1}H NMR** (400 MHz, DMSO-d_6) δ / ppm 8.02 (d, *J* = 5.5 Hz, 2H, H^6), 7.53 (d, *J* = 2.2 Hz, 2H, H^3), 6.44 (dd, *J* = 2.2 Hz, 5.5 Hz, 2H, H^5), 6.03 (s, 4H, NH_2). **^{13}C NMR** (100 MHz, DMSO-d_6) δ / ppm 156.20 (C^4), 154.92 (C^2), 148.92 (C^6), 108.62 (C^5), 105.60 (C^3). **IR** (solid): $\tilde{\nu}$ = 3441 (s), 3286 (m), 3132 (s), 2708 (w), 2060 (w), 1898 (w), 1636 (s), 1589 (s), 1551 (s), 1412 (s), 1335 (m), 1288 (m), 1250 (m), 1126 (w), 1057 (w), 980 (s), 856 (m), 818 (s) cm^{-1}. **MS** (EI, *m/z*): 186.1 $[M]^+$ (calc. 186.1). **Calcd.** for $C_{10}H_{10}N_4$ (186.22) C 64.50, H 5.41, N 30.09; found C 64.44, H 5.42, N 30.05 %.

Preparation of 4,4'-dihydroxy-2,2'-bipyridine (16)

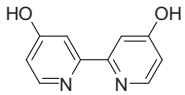

At 0 °C, a solution of $NaNO_2$ (9.50 g, 0.138 mol, 3.70 eq) in conc. H_2SO_4 (70 ml) was prepared. In order to dissolve everything, the mixture was heated to 65 °C whereupon a colourless solution was obtained. It was then cooled down to –10 °C and 4,4'-diamino-2,2'-bipyridine (**15**) (6.95 g, 37.3 mmol, 1.00 eq) in H_2SO_4 (50 ml) was added. The reaction mixture was stirred for 90 min at room temperature and then poured onto 400 g of crushed ice and stirred overnight until no more bubbles (N_2) emerged from the solution. Using aqueous 4 M NaOH, the pH was raised to pH = 6.5. An ochre product precipitated which was separated by filtration, washed well with water and dried under high vacuum to yield the desired product as an ochre solid (5.64 g, 28.6 mmol, 77 %). Due to its insolubility in nearly any organic solvent, it was not possible to obtain an NMR spectrum for this compound.

mp decomp. > 325 °C. **IR** (solid): $\tilde{\nu}$ = 3055 (m), 2754 (br s), 1782 (w), 1589 (s), 1528 (s), 1481 (s), 1389 (s), 1211 (s), 1049 (m), 987 (m), 864 (s), 818 (s), 725 (m), 633 (w), 548 (s) cm^{-1}. **MS** (EI, *m/z*): 188.1 $[M]^+$ (calc. 188.1). **Calcd.** for $C_{10}H_8N_2O_2 \cdot H_2O$ (206.20) C 58.25, H 4.89, N 13.59; found C 58.27, H 4.04, N 13.91 %.

Preparation of 4,4'-bis(3,5-bis(dodecyloxy)benzyloxy)-2,2'-bipyridine (17)

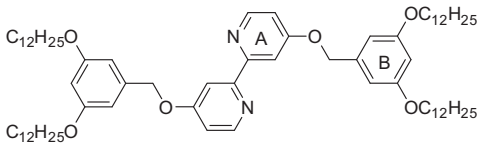

A mixture of crude 3,5-bis(dodecyloxy)benzyl methanesulfonate (**9**) (3.24 g, ca. 80 % pure, 4.67 mmol, 2.50 eq), 4,4'-dihydroxy-2,2'-bipyridine (**16**) (369 mg, 1.87 mmol, 1.00 eq), K_2CO_3 (1.55 g, 11.2 mmol, 6.00 eq) and tetra-*n*-butylammonium iodide (69 mg, 0.187 mmol, 0.10 eq) in a 50 ml vial was stirred vigorously in ethyl acetate (15 ml) and water (15 ml) at room temperature for 34 h. The temperature was raised to 55 °C and the reaction was stirred for another 4 h at this temperature. After cooling to room temperature, water was added and the mixture was extracted three times with ethyl acetate. The combined organic layers were dried over $MgSO_4$ and evaporated to dryness to give a yellow oil. The crude material was purified by silica gel chromatography (Fluka silica gel 60, 0.040–0.063 mm; CH_2Cl_2:MeOH = 40:1) and recrystallisation from EtOH to give the desired product as an off-white solid (624 mg, 0.564 mmol, 30 %).

$\mathbf{R_f}$ (TLC, silica gel, CH_2Cl_2: MeOH = 30:1): 0.2. **mp** 71 °C. **^{1}H NMR** (400 MHz, $CDCl_3$) δ / ppm 8.48 (d, ^3J = 5.7 Hz, 2H, $H^{6(A)}$), 8.06 (d, ^4J = 2.5 Hz, 2H, $H^{3(A)}$), 6.90 (dd, ^3J = 5.7 Hz, ^4J = 2.6 Hz, 2H, $H^{5(A)}$), 6.57 (d, ^4J = 2.1 Hz, 4H, $H^{2(B)}$), 6.42 (t, ^4J = 2.1 Hz, 2H, $H^{4(B)}$), 5.14 (s, 4H, $Ar_AOC\underline{H}_2Ar_B$), 3.94 (t, ^3J = 6.6 Hz, 8H, $OC\underline{H}_2CH_2CH_2$), 1.77 (quint, ^3J = 6.5 Hz, 8H, $OCH_2C\underline{H}_2CH_2$), 1.44 (quint, ^3J = 6.5 Hz, 8H, $OCH_2CH_2C\underline{H}_2$), 1.39 – 1.19 (m, 64H, $OCH_2CH_2CH_2(C\underline{H}_2)_8CH_3$), 0.88 (t, *J* = 6.8 Hz, 12H, $OCH_2CH_2CH_2(CH_2)_8C\underline{H}_3$). **^{13}C NMR** (101 MHz, $CDCl_3$) δ / ppm 166.19 ($C^{2(A)}$), 160.99 ($C^{3(B)}$), 158.28 ($C^{4(A)}$), 150.65 ($C^{6(A)}$), 138.33 ($C^{1(B)}$), 111.87 ($C^{5(A)}$), 107.56 ($C^{3(A)}$), 106.13 ($C^{2(B)}$), 101.48 ($C^{4(B)}$), 70.32 ($Ar_AO\underline{C}H_2Ar_B$), 68.53 ($O\underline{C}H_2(CH_2)_{10}$), 32.33 ($OCH_2(\underline{C}H_2)_{10}$), 30.08 ($OCH_2(\underline{C}H_2)_{10}$), 30.05 ($OCH_2(\underline{C}H_2)_{10}$), 30.01 ($OCH_2(\underline{C}H_2)_{10}$), 29.99 ($OCH_2(\underline{C}H_2)_{10}$), 29.81 ($OCH_2(\underline{C}H_2)_{10}$), 29.76 ($OCH_2(\underline{C}H_2)_{10}$), 29.65 ($OCH_2(\underline{C}H_2)_{10}$), 26.45 ($OCH_2(\underline{C}H_2)_{10}$), 23.10 ($OCH_2(\underline{C}H_2)_{10}$), 14.53 ($OCH_2(CH_2)_{10}\underline{C}H_3$). **IR** (solid): $\tilde{\nu}$ = 2916 (s), 2847 (m), 1582 (s), 1450 (w), 1381 (w), 1296 (m), 1250 (w), 1173 (s), 1034 (w), 872 (w), 825 (m), 679 (w) cm^{-1}. **MS** (Maldi, *m/z*): 1106.0 $[M+H]^+$ (calc. 1105.9). **Calcd.** for $C_{72}H_{116}N_2O_6 \cdot 2H_2O$ (1141.73) C 75.74, H 10.59, N 2.45; found C 75.69, H 10.18, N 2.42 %.

Preparation of 4,4'-bis(1-(3,5-bis(dodecyloxy)phenyl)propoxy)-2,2'-bipyridine (18)

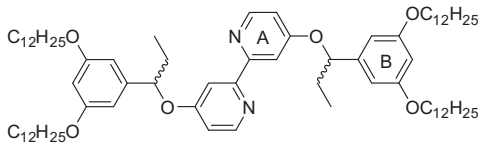

CH_2Cl_2 (3 ml) was added to a mixture of (*R*,*S*)-1-(3,5-bis(dodecyloxy) phenyl)propan-1-ol (**6**) (256 mg, 0.507 mmol, 2.50 eq), 4,4'-dihydroxy-2,2'-bipyridine (**16**) (40.0 mg, 0.203 mmol, 1.0 eq) and PPh_3 (186 mg, 0.710 mmol, 3.50 eq). The solution was evaporated to dryness and CH_2Cl_2 (3 ml) was added. The mixture was evaporated to dryness in order to remove water. Under an argon atmosphere, freshly distilled THF (ca. 3 ml) was added and diethyl azodicarboxylate (0.33 ml, 40 % in toluene, 0.71 mmol, 3.5 eq) was added to the grey suspension which turned to a brown/yellow solution after a few minutes. It was stirred for 18 h at room temperature. The solution was then evaporated to dryness, purified by column chromatography (Fluka silica gel 60, 0.040–0.063 mm; CH_2Cl_2: MeOH = 40:1), dissolved in hexane and the filtered solution was washed with ⅛ sat. aqueous $NaHCO_3$, evaporated to dryness and the white residue was then recrystallised from EtOH to give the desired compound as a cotton-like white solid (129 mg, 0.111 mmol, 55 %) with 5 % ee and 6 % de as determined by HPLC analysis (Daicel OD-H, heptane: ^{i}PrOH = 99:1, 0.5 ml/min, 210 nm), t_r 10.4 ((*S*)(*S*)-isomer), t_r 13.0 ((*meso*)-isomer), t_r 28.7 ((*R*)(*R*)-isomer).

R_f (TLC, silica gel, CH_2Cl_2: MeOH = 30:1): 0.3. **^{1}H NMR** (500 MHz, $CDCl_3$) δ / ppm 8.42 (s br, 2H, $H^{6(A)}$), 8.3 – 7.4 (s br, 2H, $H^{3(A)}$), 7.05 – 6.76 (s br, 2H, $H^{5(A)}$), 6.51 (s br, 4H, $H^{2(B)}$), 6.33 (s br, 2H, $H^{4(B)}$), 5.58 – 5.00 (m, 2H, C$\underline{H}$O-Ar_A), 3.94 – 3.84 (m, 8H, OC$\underline{H}_2CH_2CH_2$), 2.11 – 1.99 (m, 2H, Ar_AOCHC$\underline{H}_aH_bCH_3$), 1.98 – 1.87 (m, 2H, Ar_AO-CHC$H_a\underline{H}_bCH_3$), 1.73 (tt, ^3J = 7.0 Hz, ^3J = 6.9 Hz, 8H, $OCH_2C\underline{H}_2CH_2$), 1.45 – 1.37 (m, 8H, $OCH_2CH_2C\underline{H}_2$), 1.35 – 1.20 (m, 64H, $OCH_2CH_2CH_2(C\underline{H}_2)_8CH_3$), 1.01 (t, ^3J = 7.3 Hz, 6H, Ar_AOCHCH$_a$H$_b$C$\underline{H}_3$), 0.88 (t, ^3J = 7.0 Hz, 12H, $OCH_2CH_2CH_2(CH_2)_8C\underline{H}_3$). **^{13}C NMR** (126 MHz, $CDCl_3$) δ / ppm 165.54 ($C^{2(A)}$), 160.63 ($C^{3(B)}$), 157.76 ($C^{4(A)}$), 150.40 ($C^{6(A)}$), 143.21 ($C^{1(B)}$), 111.17 ($C^{5(A)}$), 109.22 ($C^{3(A)}$), 104.54 ($C^{2(B)}$), 100.54 ($C^{4(B)}$), 81.50 (Ar_AO$\underline{C}$HCH$_2$CH$_3$), 68.19 (O$\underline{C}$H$_2$(CH$_2$)$_{10}$), 32.07(OCH$_2$($\underline{C}$H$_2$)$_{10}$), 31.31 (OCH$_2$($\underline{C}$H$_2$)$_{10}$), 29.82 (Ar_AOCH$\underline{C}$H$_2$CH$_3$), 29.79 (OCH$_2$($\underline{C}$H$_2$)$_{10}$), 29.75 (OCH$_2$($\underline{C}$H$_2$)$_{10}$), 29.72 (OCH$_2$($\underline{C}$H$_2$)$_{10}$), 29.56 (OCH$_2$($\underline{C}$H$_2$)$_{10}$), 29.51 (OCH$_2$($\underline{C}$H$_2$)$_{10}$), 29.40 (OCH$_2$($\underline{C}$H$_2$)$_{10}$), 26.19 (OCH$_2$($\underline{C}$H$_2$)$_{10}$), 22.84 (OCH$_2$($\underline{C}$H$_2$)$_{10}$), 14.28(OCH$_2$(CH$_2$)$_{10}$C$\underline{H}_3$), 10.22 (Ar_AOCHCH$_2$C$\underline{H}_3$). **IR** (solid): $\tilde{\nu}$ = 2920 (s), 2851 (s), 1605 (m), 1583 (s), 1556 (m), 1470 (m), 1452 (s), 1394 (w), 1346 (w), 1286 (m), 1229 (m), 1155 (s), 1045 (m), 997 (m), 893 (w), 851 (s), 820 (m), 719 (m), 696 (s), 679 (m), 638 (m), 606 (s), 581 (s) cm^{-1}. **MS** (Maldi, *m/z*): 1162.7 $[M+2H]^+$ (calc. 1163.0), 1187.9 $[M+Na+4H]^+$ (calc. 1188.0), 1203.7 $[M+K+4H]^+$ (calc. 1203.9). **Calcd.** for $C_{76}H_{124}N_2O_6$ (1161.82) C 78.57, H 10.76, N 2.41; found C 78.50, H 10.51, N 2.64 %.

Preparation of 4,4'-bis((*R*)-1-(3,5-bis(dodecyloxy)phenyl)propoxy)-2,2'-bipyridine (19)

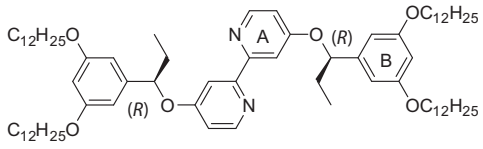

Acetonitrile (5 ml) was added to a mixture of (*S*)-1-(3,5-bis(dodecyloxy) phenyl)propan-1-ol (**7**) (559 mg, 1.11 mmol, 2.50 eq), 4,4'-dihydroxy-2,2'-bipyridine (**16**) (87.3 mg, 0.443 mmol, 1.00 eq) and PPh_3 (406 mg, 1.55 mmol, 3.50 eq). The suspension was evaporated to dryness and toluene (5 ml) was added. It was evaporated to dryness in order to remove water. Under an argon atmosphere, freshly distilled THF (6 ml) was added and diethyl azodicarboxylate (0.71 ml, 40 % in toluene, 1.6 mmol, 3.5 eq) was dropped to the grey suspension which turned into a clear brown solution after a few minutes. It was stirred for 19 h at room temperature. The yellow solution was then evaporated to dryness. The crude material was purified by column chromatography (Fluka silica gel 60, 0.040-0.063 mm; CH_2Cl_2:MeOH = 40:1) followed

by a subsequent chromatography (Fluka silica gel 60, 0.040–0.063 mm; CH_2Cl_2:MeOH = 50:1), dissolved in hexane and the filtered solution was washed with ⅛ sat. aqueous $NaHCO_3$, evaporated to dryness and the white residue was then recrystallised from EtOH to give the desired product as a white solid (295 mg, 0.254 mmol, 57 %) with 99.9 % ee and 95 % de as determined by HPLC analysis (Daicel OD-H, heptane:^{i}PrOH = 99:1, 0.5 ml/min, 210 nm), t_r 10.4 ((*S*)(*S*)-isomer), t_r 13.2 ((*meso*)-isomer), t_r 28.4 ((*R*)(*R*)-isomer).

R_f (TLC, silica gel, CH_2Cl_2: MeOH = 30:1): 0.3. **mp** 49.0 – 49.5 °C. **$[\alpha]_D^{20}$** = +16.0 (c = 0.389 in $CHCl_3$). **^{1}H NMR** (400 MHz, $CDCl_3$) δ / ppm 8.34 (d, ^3J = 5.7 Hz, 2H, $H^{6(A)}$), 7.88 (d, ^4J = 2.4 Hz, 2H, $H^{3(A)}$), 6.72 (dd, ^3J = 5.7 Hz, ^4J = 2.4 Hz, 2H, $H^{5(A)}$), 6.47 (d, ^4J = 2.1 Hz, 4H, $H^{2(B)}$), 6.31 (t, ^4J = 2.0 Hz, 2H, $H^{4(B)}$), 5.11 (t, ^3J = 6.1 Hz, 2H, $C\underline{H}OAr_A$), 3.92 – 3.83 (m, 8H, $OC\underline{H}_2CH_2CH_2$), 2.05 – 1.94 (m, 2H, $Ar_AOCHC\underline{H}_aH_bCH_3$), 1.94 – 1.82 (m, 2H, $Ar_AOCHCH_a\underline{H}_bCH_3$), 1.72 (tt, ^3J = 6.9 Hz, ^3J = 6.8 Hz, 8H, $OCH_2C\underline{H}_2CH_2$), 1.47 – 1.36 (m, 8H, $OCH_2CH_2C\underline{H}_2$), 1.36 – 1.17 (m, 64H, $OCH_2CH_2CH_2(C\underline{H}_2)_8CH_3$), 0.99 (t, ^3J = 7.3 Hz, 6H, $Ar_AOCHCH_a\underline{H}_bC\underline{H}_3$), 0.88 (t, ^3J = 6.8 Hz, 12H, $OCH_2CH_2CH_2(CH_2)_8C\underline{H}_3$). **^{13}C NMR** (125 MHz, $CDCl_3$) δ / ppm 165.5 ($C^{2(A)}$), 160.5 ($C^{3(B)}$), 157.7 ($C^{4(A)}$), 150.2 ($C^{6(A)}$), 143.0 ($C^{1(B)}$), 111.2 ($C^{5(A)}$), 109.0 ($C^{3(A)}$), 104.4 ($C^{2(B)}$), 100.4 ($C^{4(B)}$), 81.5 ($Ar_AO\underline{C}HCH_2CH_3$), 68.1 ($O\underline{C}H_2(CH_2)_{10}$), 31.9 ($OCH_2(\underline{C}H_2)_{10}$), 31.2 ($Ar_AOCH\underline{C}H_2CH_3$), 29.7 ($OCH_2(\underline{C}H_2)_{10}$), 29.7 ($OCH_2(\underline{C}H_2)_{10}$), 29.6 ($OCH_2(\underline{C}H_2)_{10}$), 29.6 ($OCH_2(\underline{C}H_2)_{10}$), 29.4 ($OCH_2(\underline{C}H_2)_{10}$), 29.4 ($OCH_2(\underline{C}H_2)_{10}$), 29.3 ($OCH_2(\underline{C}H_2)_{10}$), 26.1 ($OCH_2(\underline{C}H_2)_{10}$), 22.7 ($OCH_2(\underline{C}H_2)_{10}$), 14.1 ($OCH_2(CH_2)_{10}\underline{C}H_3$), 10.1 ($Ar_AOCHCH_2\underline{C}H_3$). **IR** (solid): $\tilde{\nu}$ = 2916 (s), 2854 (m), 1597 (s), 1458 (m), 1389 (w), 1288 (w), 1250 (w), 1227 (w), 1150 (s), 1049 (m), 1003 (m), 849 (m), 717 (w), 694 (w) cm^{-1}. **MS** (FAB, *m/z*): 1161.9 $[M+H]^+$ (calc. 1162.0); 189.1 [4,4'-dihydroxy-2,2'-bipyridine+H]$^+$ (calc. 189.1). **Calcd.** for $C_{76}H_{124}N_2O_6$ (1161.82) C 78.57, H 10.76, N 2.41; found C 78.52, H 10.59, N 2.60 %.

Preparation of 4,4'-bis((*S*)-1-(3,5-bis(dodecyloxy)phenyl)propoxy)-2,2'-bipyridine (**20**)

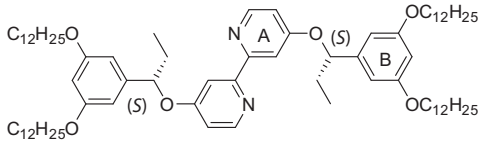

CH_2Cl_2 (5 ml) was added to a mixture of (*R*)-1-(3,5-bis(dodecyloxy)phenyl)propan-1-ol (**8**) (256 mg, 0.507 mmol, 2.50 eq), 4,4'-dihydroxy-2,2'-bipyridine (**16**) (40.0 mg, 0.203 mmol, 1.00 eq) and PPh_3 (186 mg, 0.710 mmol, 3.50 eq). The suspension was evaporated to dryness and CH_2Cl_2 (5 ml) was added. It was evaporated to dryness at high vacuum in order to remove water. Under an argon atmosphere, freshly distilled THF (3 ml) was added and diethyl azodicarboxylate (0.33 ml, 40 % in toluene, 0.71 mmol, 3.5 eq) was dropped to the grey suspension which turned into a clear brown solution after a few minutes. It was stirred for 17 h at room temperature. The reaction mixture was then evaporated to dryness. The crude material was purified by column chromatography (Fluka silica gel 60, 0.040–0.063 mm; CH_2Cl_2:MeOH = 40:1) and recrystallised from EtOH to give the desired product as a white solid (129 mg, 0.111 mmol, 55 %) with 99 % ee and 91 % de as determined by HPLC analysis (Daicel OD-H, heptane: ^{i}PrOH = 99:1, 0.5 ml/min, 210 nm), t_r 10.1 ((*S*)(*S*)-isomer), t_r 12.9 ((*meso*)-isomer), t_r 35.6 ((*R*)(*R*)-isomer).

R_f (TLC, silica gel, CH_2Cl_2: MeOH = 30:1): 0.4. **^{1}H NMR** (500 MHz, $CDCl_3$) δ / ppm 8.35 (d, ^3J = 5.7 Hz, 2H, $H^{6(A)}$), 7.88 (d, ^4J = 2.4 Hz, 2H, $H^{3(A)}$), 6.72 (dd, ^3J = 5.7 Hz, ^4J = 2.5 Hz, 2H, $H^{5(A)}$), 6.47 (d, ^4J = 2.1 Hz, 4H, $H^{2(B)}$), 6.32 (t, ^4J = 2.0 Hz, 2H, $H^{4(B)}$), 5.11 (t, ^3J = 6.3 Hz, 2H, $C\underline{H}OAr_A$), 3.96 – 3.81 (m, 8H, $OC\underline{H}_2CH_2CH_2$), 2.05 – 1.95 (m, 2H, $Ar_AOCHC\underline{H}_aH_bCH_3$), 1.94 – 1.83 (m, 2H, $Ar_AOCHCH_a\underline{H}_bCH_3$), 1.76 – 1.68 (m, 8H, $OCH_2C\underline{H}_2CH_2$), 1.45 – 1.37 (m, 8H, $OCH_2CH_2C\underline{H}_2$), 1.36 – 1.21 (m, 64H, $OCH_2CH_2CH_2(C\underline{H}_2)_8CH_3$), 0.99 (t, ^3J = 7.4 Hz, 6H, $Ar_AOCHCH_a\underline{H}_bC\underline{H}_3$), 0.88 (t, ^3J = 6.9 Hz, 12H, $OCH_2CH_2CH_2(CH_2)_8C\underline{H}_3$). **^{13}C NMR** (126 MHz, $CDCl_3$) δ / ppm 165.54 ($C^{2(A)}$), 160.63 ($C^{3(B)}$), 157.80

($C^{4(A)}$), 150.38 ($C^{6(A)}$), 143.21 ($C^{1(B)}$), 111.27 ($C^{5(A)}$), 109.13 ($C^{3(A)}$), 104.53 ($C^{2(B)}$), 100.55 ($C^{4(B)}$), 81.49 ($Ar_AO\underline{C}HCH_2CH_3$), 68.19 ($O\underline{C}H_2(CH_2)_{10}$), 32.07 ($OCH_2(\underline{C}H_2)_{10}$), 31.35 ($Ar_AOCH\underline{C}H_2CH_3$), 29.82 ($OCH_2(\underline{C}H_2)_{10}$), 29.79 ($OCH_2(\underline{C}H_2)_{10}$), 29.75 ($OCH_2(\underline{C}H_2)_{10}$), 29.72 ($OCH_2(\underline{C}H_2)_{10}$), 29.56 ($OCH_2(\underline{C}H_2)_{10}$), 29.51 ($OCH_2(\underline{C}H_2)_{10}$), 29.40 ($OCH_2(\underline{C}H_2)_{10}$), 26.19 ($OCH_2(\underline{C}H_2)_{10}$), 22.84 ($OCH_2(\underline{C}H_2)_{10}$), 14.28 ($OCH_2(CH_2)_{10}\underline{C}H_3$), 10.23 ($Ar_AOCHCH_2\underline{C}H_3$). **IR** (neat): $\tilde{\nu}$ = 2922 (s), 2853 (s), 1582 (s), 1556 (m), 1468 (s), 1458 (s), 1394 (w), 1344 (w), 1288 (w), 1229 (m), 1153 (s), 1043 (m), 997 (m), 895 (w), 849 (s), 812 (s), 783 (m), 719 (s), 696 (s), 611 (s), 590 (s) cm^{-1}. **MS** (FAB, *m/z*): 1161.9 $[M+H]^+$ (calc. 1162.0); 189.1 [4,4'-dihydroxy-2,2'-bipyridine+H]$^+$ (calc. 189.1). **Calcd.** for $C_{76}H_{124}O_6$ (1161.82) C 78.57, H 10.76, N 2.41; found C 78.29, H 10.60, N 2.60 %.

Preparation of 3,5-bis(3,5-bis(dodecyloxy)benzyloxy)benzyl methanesulfonate (21)

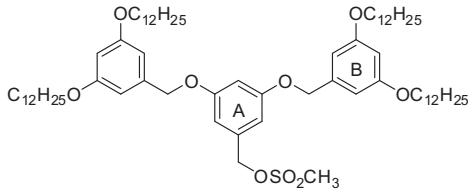

NEt_3 (0.84 ml, 6.0 mmol, 5.0 eq) was added to a solution of 3,5-bis(3,5-bis(dodecyloxy)benzyloxy)benzyl alcohol (**11**) (1.27 g, 1.20 mmol, 1.00 eq) in freshly distilled CH_2Cl_2 (25 ml), previously cooled to –10 °C. Under an inert atmosphere of argon, methanesulfonyl chloride (0.37 ml, 4.8 mol, 4.0 eq) was added slowly over a period of 5 min, and then the reaction mixture was stirred at –10 °C for 1 h. The mixture was poured into a mixture of concentrated HCl (1 ml) and crushed ice (10 g), and extracted with CH_2Cl_2. The organic layer was washed with a saturated solution of $NaHCO_3$, dried with $MgSO_4$, and the solvent removed. The desired product was isolated as a yellow oil (1.47 g, 1.29 mmol, 107 %).

^{1}H NMR (400 MHz, $CDCl_3$) δ / ppm 6.63 – 6.60 (m, 3H, $H^{2(A)}$+$H^{4(A)}$), 6.54 (d, *J* = 2.2 Hz, 4H, $H^{2(B)}$), 6.40 (t, J = 2.2 Hz, 2H, $H^{4(B)}$), 5.15 (s, 2H, $C\underline{H}_2OSO_2CH_3$), 4.96 (s, 4H, $Ar_AOC\underline{H}_2Ar_B$), 3.93 (t, *J* = 6.6 Hz, 8H, $Ar_BOC\underline{H}_2$), 2.85 (s, 3H, $SO_2C\underline{H}_3$), 1.83 – 1.71 (m, 8H, $OCH_2C\underline{H}_2CH_2$), 1.49 – 1.39 (m, 8H, $OCH_2CH_2C\underline{H}_2$), 1.38 – 1.20 (m, 64H, $OCH_2CH_2CH_2(C\underline{H}_2)_8$), 0.88 (t, *J* = 6.9 Hz, 12H, $O(CH_2)_{11}C\underline{H}_3$). **^{13}C NMR** (101 MHz, $CDCl_3$) δ / ppm 160.97 ($C^{3(B)}$), 160.61 ($C^{3(A)}$), 139.02 ($C^{1(B)}$), 135.87 ($C^{1(A)}$), 108.01 ($C^{2(A)}$), 106.08 ($C^{2(B)}$), 103.38 ($C^{4(A)}$), 101.22 ($C^{4(B)}$), 71.85 ($\underline{C}H_2OSO_2CH_3$), 70.60 ($Ar_AO\text{-}\underline{C}H_2Ar_B$), 68.50 ($Ar_BO\underline{C}H_2$), 38.84 ($SO_2\underline{C}H_3$), 32.33 ($OCH_2(\underline{C}H_2)_{10}$), 30.08 ($OCH_2(\underline{C}H_2)_{10}$), 30.05 ($OCH_2(\underline{C}H_2)_{10}$), 30.02 ($OCH_2(\underline{C}H_2)_{10}$), 30.00 ($OCH_2(\underline{C}H_2)_{10}$), 29.82 ($OCH_2(\underline{C}H_2)_{10}$), 29.76 ($OCH_2(\underline{C}H_2)_{10}$), 29.67 ($OCH_2(\underline{C}H_2)_{10}$), 26.47 ($OCH_2(\underline{C}H_2)_{10}$), 23.10 ($OCH_2(\underline{C}H_2)_{10}$), 14.53 ($O(CH_2)_{11}\underline{C}H_3$).

Preparation of 4,4'-bis(3,5-bis(3,5-bis(dodecyloxy)benzyloxy)benzyloxy)-2,2'-bipyridine (**22**)

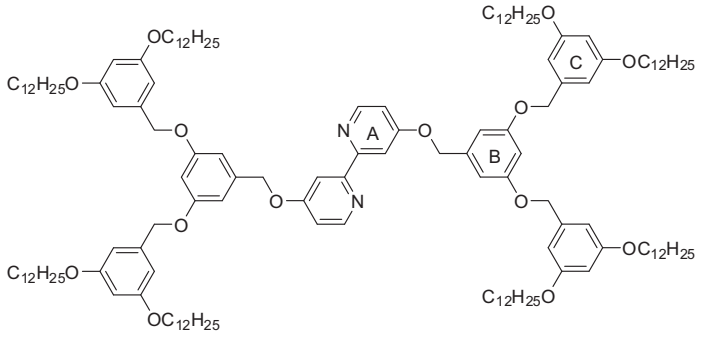

A mixture of crude 3,5-bis(3,5-bis(dodecyloxy) benzyloxy)benzyl methanesulfonate (**21**) (1.27 g, ca. 80 % pure, 0.899 mmol, 2.50 eq), 4,4'-dihydroxy-2,2'-bipyridine (**16**) (71.0 mg, 0.360 mmol, 1.00 eq), K_2CO_3 (298 mg, 2.16 mmol, 6.00 eq) and tetra-*n*-butylammonium iodide (13 mg, 0.036 mmol, 0.10 eq) was stirred vigorously in ethyl acetate (3 ml) and water (3 ml) at 60 °C for 65 h. After cooling to room temperature, water was added and the mixture was extracted three times with ethyl acetate. The combined organic layers were dried over $MgSO_4$ and evaporated to dryness to give a yellow oil. The crude material was purified by column chromatography (Fluka silica gel 60, 0.040–0.063 mm; CH_2Cl_2:MeOH = 30:1), followed by a subsequent column chromatography (Fluka silica gel 60, 0.040–0.063 mm; CH_2Cl_2:MeOH = 100:1 → 70:1 → 50:1), yielding the desired product as an off-white solid (333 mg, 0.147 mmol, 41 %).

R_f (TLC, silica gel, CH_2Cl_2: MeOH = 10:1): 0.4. **^{1}H NMR** (400 MHz, $CDCl_3$) δ / ppm 8.48 (d, ^3J = 5.7 Hz, 2H, $H^{6(A)}$), 8.08 (d, ^4J = 2.5 Hz, 2H, $H^{3(A)}$), 6.90 (dd, ^3J = 5.7 Hz, ^4J = 2.6 Hz, 2H, $H^{5(A)}$), 6.69 (d, ^4J = 2.2 Hz, 4H, $H^{2(B)}$), 6.58 (t, ^4J = 2.2 Hz, 2H, $H^{4(B)}$), 6.55 (d, ^4J = 2.2 Hz, 8H, $H^{2(C)}$), 6.40 (t, ^4J = 2.2 Hz, 4H, $H^{4(C)}$), 5.15 (s, 4H, $Ar_AOC\underline{H}_2Ar_B$), 4.96 (s, 8H, $Ar_BOC\underline{H}_2Ar_C$), 3.93 (t, ^3J = 6.6 Hz, 16H, $Ar_COC\underline{H}_2$), 1.81 – 1.70 (m, 16H, $OCH_2C\underline{H}_2CH_2$), 1.48 – 1.39 (m, 16H, $OCH_2CH_2C\underline{H}_2$), 1.39 – 1.19 (m, 128H, $OCH_2CH_2CH_2(C\underline{H}_2)_8$), 0.87 (t, ^3J = 6.9 Hz, 24H, $O(CH_2)_{11}C\underline{H}_3$). **^{13}C NMR** (126 MHz, $CDCl_3$) δ / ppm 165.87 ($C^{2(A)}$), 160.67 ($C^{3(C)}$), 160.35 ($C^{3(B)}$), 158.01 ($C^{4(A)}$), 150.39 ($C^{6(A)}$), 138.96 ($C^{1(C)}$), 138.25 ($C^{1(B)}$), 111.69 ($C^{5(A)}$), 107.15 ($C^{3(A)}$), 106.56 ($C^{2(B)}$), 105.86 ($C^{2(C)}$), 102.00 ($C^{4(B)}$), 100.98 ($C^{4(C)}$), 70.35 ($Ar_BO\text{-}\underline{C}H_2Ar_C$), 69.94 ($Ar_AO\underline{C}H_2Ar_B$), 68.22 ($Ar_COC\underline{H}_2$), 32.06 ($OCH_2(\underline{C}H_2)_{10}$), 29.82 ($OCH_2(\underline{C}H_2)_{10}$), 29.79 ($OCH_2(\underline{C}H_2)_{10}$), 29.76 ($OCH_2(\underline{C}H_2)_{10}$), 29.74 ($OCH_2(\underline{C}H_2)_{10}$), 29.56 ($OCH_2(\underline{C}H_2)_{10}$), 29.50 ($OCH_2(\underline{C}H_2)_{10}$), 29.41 ($OCH_2(\underline{C}H_2)_{10}$), 26.21 ($OCH_2(\underline{C}H_2)_{10}$), 22.84 ($OCH_2(\underline{C}H_2)_{10}$), 14.27 ($OCH_2(CH_2)_{10}\underline{C}H_3$). **IR** (solid): $\tilde{\nu}$ = 2918 (s), 2849 (m), 1595 (s), 1585 (s), 1450 (m), 1371 (w), 1329 (w), 1294 (w), 1242 (w), 1163 (s), 1057 (w), 1016 (w), 847 (w), 825 (w), 681 (s), 621 (s), 511 (w) cm^{-1}. **Calcd.** for $C_{148}H_{236}N_2O_{14}$ (2267.46) C 78.40, H 10.49, N 1.24; found C 78.45, H 10.23, N 1.13 %.

Preparation of 4,4'-bis(1-(3,5-bis(octyloxy)phenyl)propoxy)-2,2'-bipyridine (**23**)

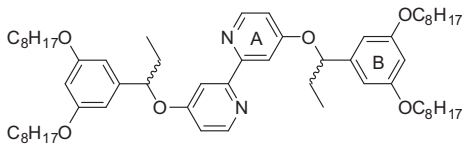

CH_2Cl_2 (3 ml) was added to a mixture of (*R*,*S*)-1-(3,5-bis(dodecyloxy) phenyl)propan-1-ol (**13**) (256 mg, 0.507 mmol, 2.50 eq), 4,4'-dihydroxy-2,2'-bipyridine (**16**) (40.0 mg, 0.203 mmol, 1.0 eq) and PPh_3 (186 mg, 0.710 mmol, 3.50 eq). The solution was evaporated to dryness in order to remove water. Under an argon atmosphere, freshly distilled THF (ca. 3 ml) was added and diethyl azodicarboxylate (0.33 ml, 40 % in toluene, 0.71 mmol, 3.5 eq) was dropped to the grey suspension which turned to a clear brown/yellow solution after a few minutes. It was stirred for 18 h at room temperature. The solution was then evaporated to dryness, purified by column chromatography (Fluka silica gel 60, 0.040–0.063 mm; CH_2Cl_2: MeOH = 40:1). The product was dissolved in hexane and the filtered solution was washed

with ⅛ sat. aqueous $NaHCO_3$, dried over $MgSO_4$ and evaporated to dryness. It was again dissolved in hexane, the white precipitate was filtered off and the solution was evaporated to dryness. The residue was recrystallised from EtOH, then recrystallised from MeOH, and purified by preparative plate chromatography (silica gel, CH_2Cl_2:MeOH = 10:1) to give a pinkish solid, which was recrystallised from EtOH to give the desired product as white crystals (83 mg, 0.089 mmol, 22 %).

R_f (TLC, silica gel, CH_2Cl_2:MeOH = 10:1): 0.5. **^{1}H NMR** (500 MHz, $CDCl_3$) δ / ppm 8.35 (d, ^3J = 5.7 Hz, 2H, $H^{6(A)}$), 7.90 (d, ^4J = 2.4 Hz, 2H, $H^{3(A)}$), 6.72 (dd, ^3J = 5.7 Hz, ^4J = 2.5 Hz, 2H, $H^{5(A)}$), 6.47 (d, ^4J = 2.1 Hz, 4H, $H^{2(B)}$), 6.32 (t, ^4J = 1.9 Hz, 2H, $H^{4(B)}$), 5.10 (t, ^3J = 6.3 Hz, 2H, $C\underline{H}OAr_A$), 3.94 – 3.83 (m, 8H, $OC\underline{H}_2CH_2CH_2$), 2.05 – 1.95 (m, 2H, Ar_A-$OCHC\underline{H}_aH_bCH_3$), 1.93 – 1.83 (m, 2H, $Ar_AOCHCH_a\underline{H}_bCH_3$), 1.77 – 1.69 (m, 8H, $OCH_2C\underline{H}_2CH_2$), 1.46 – 1.37 (m, 8H, $OCH_2CH_2C\underline{H}_2$), 1.36 – 1.21 (m, 32H, $OCH_2CH_2CH_2(C\underline{H}_2)_4CH_3$), 0.99 (t, ^3J = 7.4 Hz, 6H, $Ar_AOCHCH_aH_bC\underline{H}_3$), 0.88 (t, ^3J = 6.9 Hz, 12H, $OCH_2CH_2CH_2(CH_2)_4C\underline{H}_3$). **^{13}C NMR** (126 MHz, $CDCl_3$) δ / ppm 165.54 ($C^{2(A)}$), 160.63 ($C^{3(B)}$), 157.76 ($C^{4(A)}$), 150.40 ($C^{6(A)}$), 143.21 ($C^{1(B)}$), 111.18 ($C^{5(A)}$), 109.21 ($C^{3(A)}$), 104.55 ($C^{2(B)}$), 100.55 ($C^{4(B)}$), 81.50 ($Ar_AO\underline{C}HCH_2CH_3$), 68.18 ($O\underline{C}H_2(CH_2)_{10}$), 31.95 ($OCH_2(\underline{C}H_2)_6$), 31.31 ($Ar_AOCH\underline{C}H_2CH_3$), 29.51 ($OCH_2(\underline{C}H_2)_6$), 29.38 ($OCH_2(\underline{C}H_2)_6$), 29.37 ($OCH_2(\underline{C}H_2)_6$), 26.18 ($OCH_2(\underline{C}H_2)_6$), 22.80 ($OCH_2(\underline{C}H_2)_6$), 14.25 ($OCH_2(CH_2)_6\underline{C}H_3$), 10.22 ($Ar_AOCHCH_2\underline{C}H_3$). **IR** (solid): $\tilde{\nu}$ = 2922 (m), 2854 (w), 1585 (s), 1556 (m), 1454 (m), 1387 (w), 1348 (w), 1281 (m), 1234 (w), 1165 (s), 1059 (w), 1045 (w), 991 (w), 964 (m), 893 (w), 851 (m), 818 (s), 723 (s), 694 (s), 619 (s) cm^{-1}. **MS** (FAB, *m/z*): 937.7 $[M+H]^+$ (calc. 937.7); 189.0 [4,4'-dihydroxy-2,2'-bipyridine+H]$^+$ (calc. 189.1). **Calcd.** for $C_{60}H_{92}N_2O_6$ (937.38) C 76.88, H 9.89, N 2.99; found C 76.81, H 9.63, N 2.84 %.

Chapter 5

Synthesis and STM Imaging of Perfluorinated Dendrons and Ligands

5.1 Introduction and aims

In this chapter, unsuccessful and successful preparative routes to dendrons decorated with perfluorinated and semi-fluorinated alkyl chains and their use in the functionalisation of 2,2'-bipyridine ligands are discussed. The idea behind that was mainly their application in STM visualisation. Compounds bearing perfluorinated alkyl chains should exhibit different two-dimensional phase behaviour[223] which would lead to different monolayer formation on graphite, thus showing different patterns in STM images. The reason for this assumption is the differing interdigitation properties of perfluorinated alkyl chains in contrast to hydrogenated alkyl chains.[148] Additionally, fluorinated methylene groups in monolayers physisorbed on graphite exhibit decreased tunnelling current as indicated in theoretical calculations,[154, 224] thereby potentially changing the typical contrast of STM images with dark grey coloured areas related to the nearly insulating alkyl chains to completely black bands of fluorinated chains.[146] Nevertheless, obtaining physisorbed monolayers of compounds with perfluorinated alkyl chains visualisable by STM techniques is not trivial, as molecular mechanics calculations indicate a substantially smaller adsorption energy of a semi-fluorinated molecule compared to a non-fluorinated molecule.[225]

5.2 Synthesis and discussion

5.2.1 Dendron synthesis

In a first attempt to attach a perfluorinated alkyl chain to the dendritic starting material methyl 3,5-dihydroxybenzoate (**2**), standard procedures as used to prepare the non-fluorinated alkyl chains were applied (**Scheme 5.1**), *i.e.* refluxing the starting materials in acetone in the presence of potassium carbonate and 18-crown-6[166, 167]. The iodo analogue was used instead of the bromo compound because of its commercial availability. Unfortunately, no traces of the desired product were observed in the reaction mixture when analysed by NMR spectroscopy. It seems that the fluorine atoms attached to and next to the carbon atom bearing the iodine atom ("C_α") dramatically lower the reactivity of the compound and render S_N2-reactions difficult. This observation can be understood as perfluoroalkyl iodine compounds show reverse polarisation due to the low electronegativity of the iodine atom which enhances the probability of an attack of nucleophiles at the iodine atom instead of the carbon atom C_α.[226] These halophilic reactions have been well studied and have provided some useful methods for preparing fluoroorganic compounds.[227-235]

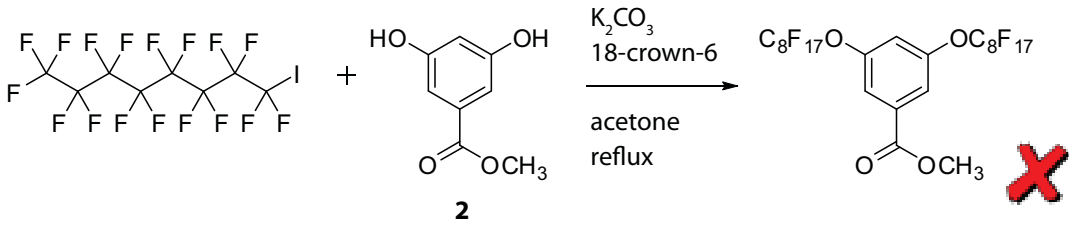

Scheme 5.1 Unsuccessful attempt to attach a perfluorinated alkyl chain to **2**.

In the next attempt, a different perfluorinated alkyl chain with an ethylene spacer was chosen (**Scheme 5.2**). However, since the standard conditions using potassium carbonate as the base in acetone in the presence of catalytic amounts of 18-crown-6[166, 167] did not show any traces of the desired product, a few others methods were applied and are summarised in **Table 5.1**.

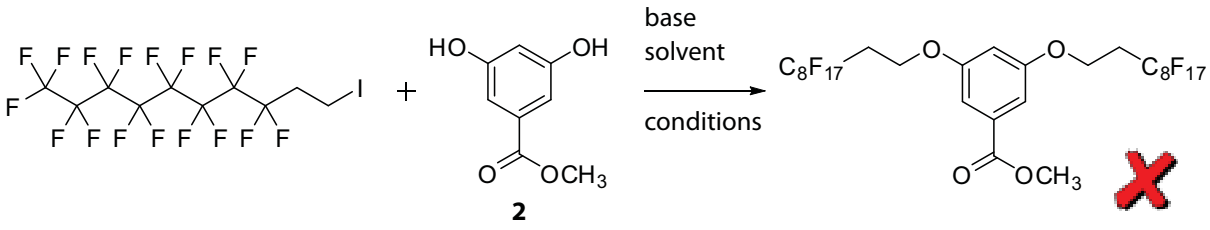

Scheme 5.2 Another unsuccessful attempt to attach a perfluorinated alkyl chain to **2** with an ethylene spacer.

Heating the same starting materials in a sealed tube in a "Biotage Initiator" microwave reactor (entry 1 in **Table 5.1**) did not prove to be successful, nor did any of the other methods shown in **Table 5.1**. Conditions from entry 2 in the table were modified from the literature[236], and, similarly, entry 3[237]. Prior to the two phase reactions (entries 4 and 5 in **Table 5.1**), hydrolysing and elimination propensity of the iodo compound was tested in a reaction of 3,3,4,4,5,5,6,6,7,7,8,8,9,9,10,10,10-heptadecafluoro-1-iododecane in a mixture of water and dichloromethane in the presence of KOH. Only the starting material could be detected.

Table 5.1 Varying reaction conditions used in attempts to synthesise the perfluorinated dendron.

Entry	Base	Solvent	Conditions
1	K_2CO_3 18-crown-6	acetone	160 °C, 60 min (microwave)
2	K_2CO_3 18-crown-6	THF	70 °C, 15 h
3	NaH	DMF	two steps: 1) deprotonation 2) addition of chain each 0 °C → r.t.
4	K_2CO_3 18-crown-6	THF / H_2O / acetone	120 °C, 45 min (microwave)
5	K_2CO_3 18-crown-6	CH_2Cl_2 / H2O Aliquat 336	130 °C, 12 h (microwave)

Treating 3,3,4,4,5,5,6,6,7,7,8,8,9,9,10,10,10-heptadecafluoro-1-iododecane with an excess of KBr in acetone[238] for 2 h at 120 °C in a "Biotage Initiator" microwave reactor did not give the exchange product 3,3,4,4,5,5,6,6,7,7,8,8,9,9,10,10,10-heptadecafluoro-1-bromodecane. Furthermore, using the mesylate derivative obtained from 3,3,4,4,5,5,6,6,7,7,8,8,9,9,10,10,10-heptadecafluorodecane-1-ol under the standard conditions (as in entry 1 of **Table 5.1**) did not give the desired dendron either.[239] One can conclude from all these observations, that an ethylene spacer separating the perfluorinated alkyl chain from the iodine atom at C_α is insufficient to increase the overall reactivity of this compound in S_N2-reactions. A further factor to consider is the unusual solubility effects of perfluorinated compounds.[240]

On the basis of these findings, a perfluorinated alkyl chain with a butylene spacer was chosen for the next attempt. Because 10-bromo-1,1,1,2,2,3,3,4,4,5,5,6,6-tridecafluorodecane (**25**) is not commercially available, it was prepared in three steps (**Scheme 5.3**) adapted from a literature method[241]. Palladium catalysed addition of perfluorohexane iodide to 3-butenoic acid followed by lithium aluminium hydride reduction gave alcohol **24** which has very interesting wettability properties. Even in extremely low concentration, **24** dissolved in dichloromethane forms drops similar to higher viscosity solvents like water (**Figure 5.1**). Conversion into the bromide **25** was done in HBr under standard conditions and in a microwave reactor in a sealed vessel both yielding the desired product in very high yields.

Figure 5.1 Droplets on the glass wall indicating a low wetting effect of **24** in dichloromethane in a test tube.

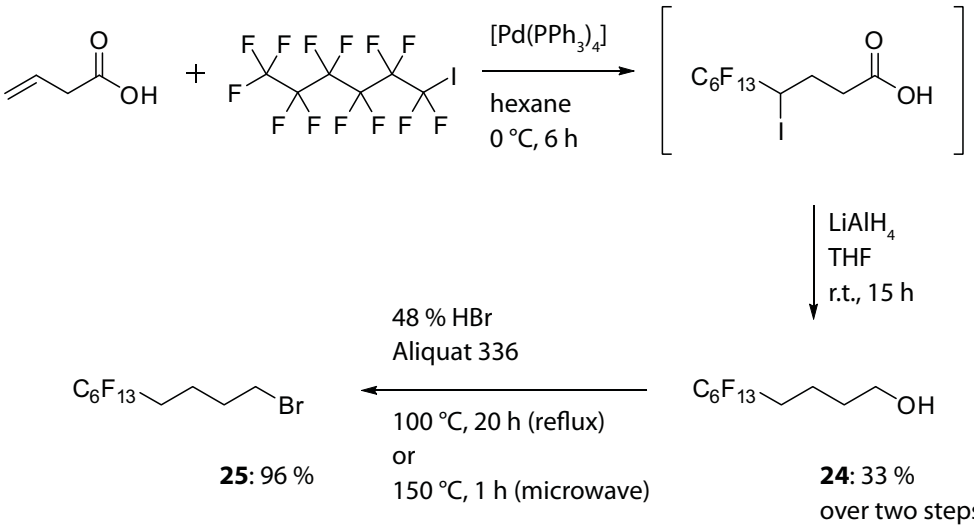

Scheme 5.3 Synthesis of the fluorinated alkyl chain with a butylene spacer (**25**).

An attempt was then made to attach bromide **25** to the dendritic starting material methyl 3,5-dihydroxybenzoate (**2**) using standard conditions in refluxing acetone and in a sealed microwave vessel (**Scheme 5.4**). Both methods yielded the desired product **26** in an almost quantitative yield. Reducing the methyl ester **26** under the same conditions as was used for the non-fluorinated dendrons lead to alcohol **27** in high yields.

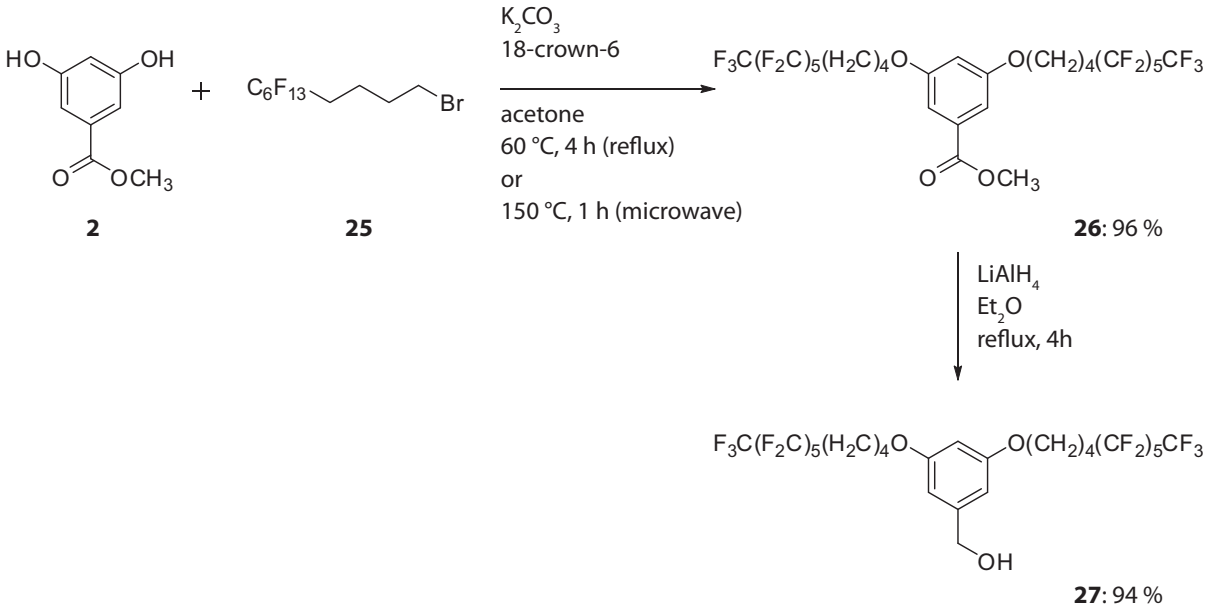

Scheme 5.4 Dendron synthesis with fluorinated alkyl substituents.

5.2.2 Ligand synthesis

In order to obtain the bipyridine ligand **29**, alcohol **27** was mesylated to give the desired electrophile **28** (**Scheme 5.5**). Because alcohol **27** is poorly soluble in dichloromethane, especially at low temperatures, diethyl ether was used as the solvent for the reaction. This did not affect the yields in any way. Using the same conditions as for the non-fluorinated ligands, a two phase reaction was performed coupling crude mesylate **28** to 4,4'-dihydroxy-2,2'-bipyridine (**16**) yielding ligand **29** in moderate 26 % yield, compared to the non-fluorinated ligands **17** (30 %) and **22** (41 %).

A nice feature of ligand **29** is its simplicity in a ^{1}H NMR experiment compared to the non-fluorinated ligands as the overlapping signals of CH_2 groups from the alkyl chains are no longer present (**Figure 5.2**). In the ^{13}C NMR spectrum, carbon atoms couple with the fluorine atoms. This is the reason for the carbon atoms bearing fluorine atoms not being visible in the spectrum because the signal-to-noise ratio is too low to distinguish the signals from noise.

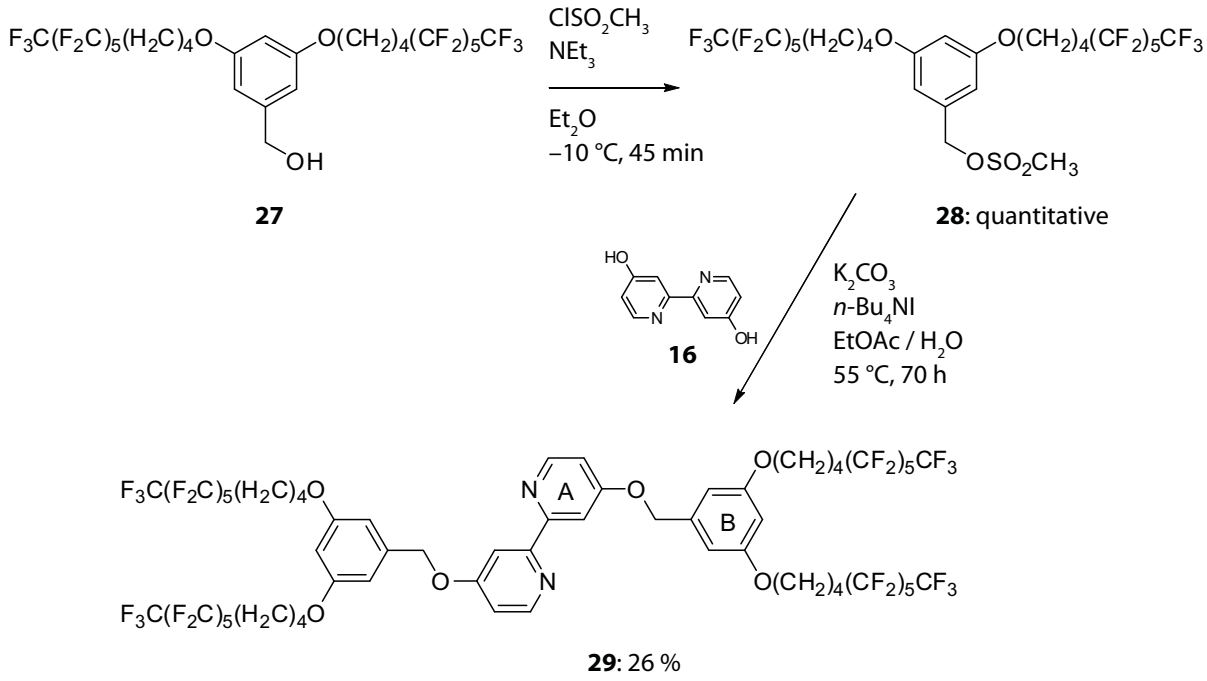

Scheme 5.5 Synthesis of the bipyridine ligand **29**. Ring labels are for NMR spectroscopic assignments (**Figure 5.2**).

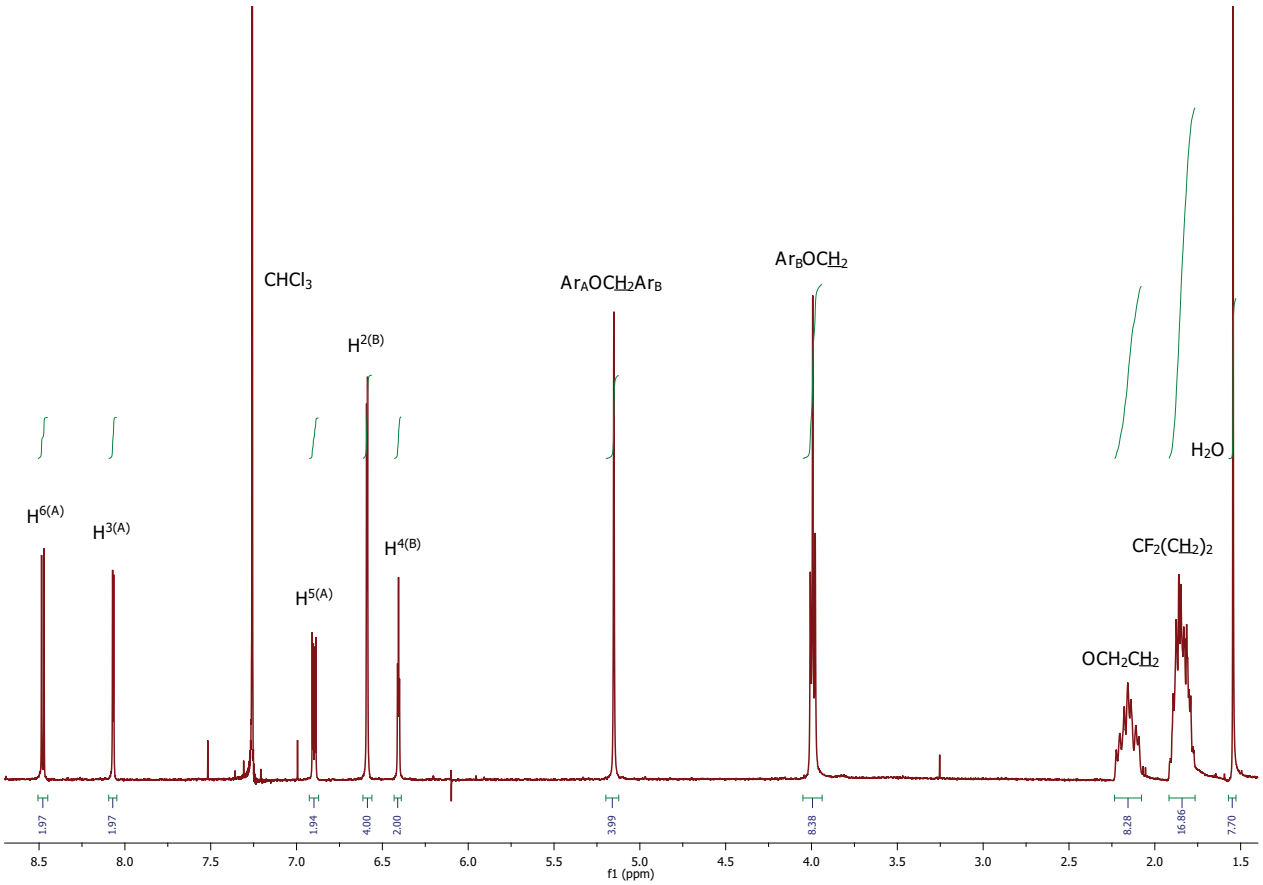

Figure 5.2 ^{1}H NMR spectra of the fluorinated ligand **29** in $CDCl_3$. See **Scheme 5.5** for ring labelling.

5.3
STM imaging and discussion

The semi-fluorinated bipyridine ligand **29** was dissolved in chloroform and solution cast onto a fresh surface of HOPG. Chloroform was used since the compound was insoluble in the commonly used hexane. Judging by the difficulties in visualising the compound in STM measurements, it seems that molecules of **29** do not tend to form monolayers easily. Still, a few images revealing a repetitive pattern were obtained. **Figure 5.3** displays two completely different patterns, where the left one was reproducible and the right one was observed only once. They both show a typical line pattern, but they differ quite dramatically in terms of their size.

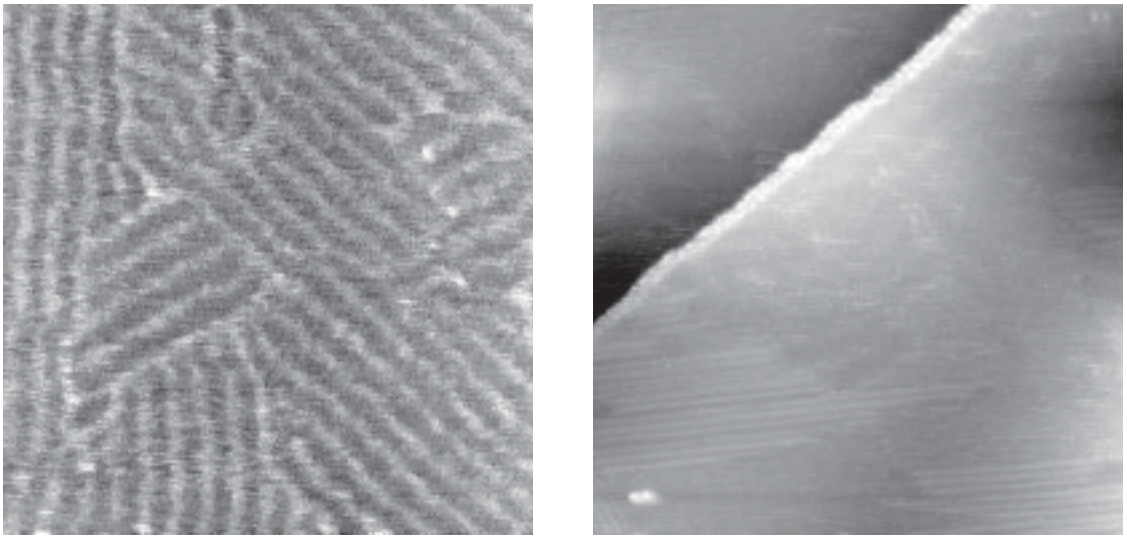

(a) (b)

Figure 5.3 STM images of **29** on HOPG each at 100 nm × 100 nm using scan parameters: U_{bias} = –700 mV, I_t = 8.0 pA, ν = 3.05 Hz (a), ν = 2.54 Hz (b).

In **Figure 5.4**, both patterns are supported by overlaid red lines which are separated in a distance of 5.3 – 6.1 nm in the case of the left image and 1.8 nm for the right image. The angles formed by the different domains in the left image are roughly 120 °, thus reflecting the underlying three-fold symmetry of HOPG.

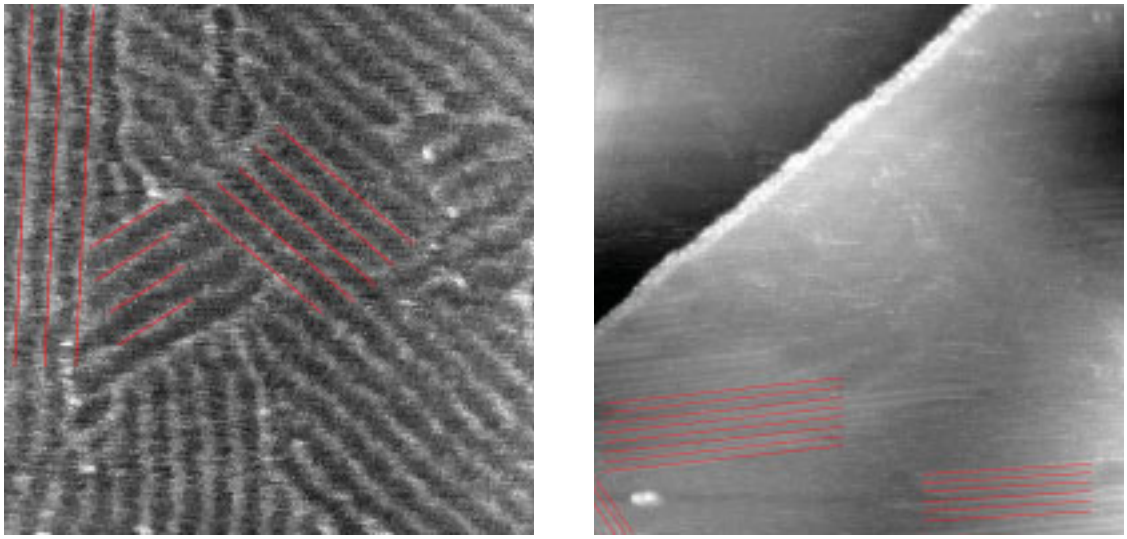

(a) (b)

Figure 5.4 STM images from **Figure 5.3** (100 nm × 100 nm) emphasising the line pattern of the present domains.

In order to have a rough estimation of the molecular size, one molecule of **29** was modelled in a flat conformation *in silico* in **Figure 5.5**. The longest possible distance found in the molecule is between the two outmost fluorine atoms of the "*trans*" C_{10}-chains measuring 4.8 nm. This distance compares with the pattern width of the left image from **Figure 5.4** (5.3 – 6.1 nm). 1.8 Nanometres on the other hand, found as the distance between the lines in the right image of **Figure 5.4**, would compare with the farthest distance in the 2,2'-bipyridine subunit. Hence, one could claim the two observed patterns arising from different conformations of the molecules. Once in its fully extended arrangement (as in **Figure 5.5**), and once in a arrangement where the C_{10}-chains point inwards to the 2,2'-bipyridine core, therefore in its most contracted conformation. More probably, though, is the presence of some sort of tip defect for the pattern showed in the right image of **Figure 5.3**.

Unfortunately, due to low resolution and the unavailability of images with a smaller area, detailed unit cell considerations and molecular fitting models could not be performed.

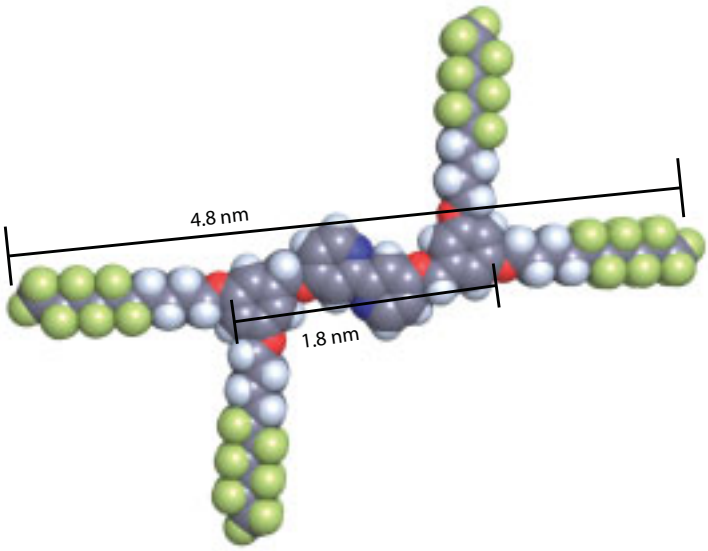

Figure 5.5 Space filling representation of a model of **29** in a flat conformation showing molecular dimensions.

5.4 Experimental part

Preparation of 5,5,6,6,7,7,8,8,9,9,10,10,10-tridecafluorodecan-1-ol (24)

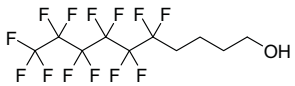

A solution of but-3-enoic acid (2.59 g, 30.1 mmol, 1.10 eq) in hexane (45 ml) was cooled down to 0 °C under an inert atmosphere of N_2, and perfluoro-*n*-hexyl iodide (12.2 g, 27.4 mmol, 1.00 eq) and tetrakis(triphenylphosphine)palladium(0) (1.33 g, 1.15 mmol, 0.0420 eq) were added. The reaction was stirred for 6 h at 0 °C whereupon an orange suspension resulted. The reaction mixture was brought to room temperature and stirred for another 15 min. Water and hexane were given to the suspension and filtered. The filtrate was extracted twice with hexane. The combined organic layers were dried ($MgSO_4$) and evaporated to dryness to give a dark orange solid (5.94 g). The residue from the filtration was dried in the desiccator to give an orange solid (5.00 g).

Both charges were combined (10.8 g in total, assuming 75 % purity, 21 mmol, 1.0 eq), dissolved in THF (350 ml), and added to a slurry of $LiAlH_4$ (4.0 g, 0.11 mol, 5.1 eq) in THF (50 ml) over a period of 45 min. The reaction mixture was left stirring overnight at room temperature and was quenched by very slow addition of water. The mixture was left open overnight under an N_2-flow to reduce volume. It was then filtered and the two phases were separated. The aqueous layer was extracted twice with CH_2Cl_2, and the combined organic layers were dried ($MgSO_4$) and evaporated to dryness to give a brown oil mixed with black solid (4.89 g). The crude material was purified by column chromatography (Fluka silica gel 60, 0.040–0.063 mm; hexane:CH_2Cl_2 = 1:1 → hexane:CH_2Cl_2 = 1:2 → CH_2Cl_2 → CH_2Cl_2:MeOH = 50:1 → CH_2Cl_2:MeOH = 42:1), followed by a subsequent column chromatography (Fluka silica gel 60, 0.040–0.063 mm; hexane:ethyl acetate = 5:1), and another column chromatography (Fluka silica gel 60, 0.040–0.063 mm; CH_2Cl_2:MeOH

= 50:1) to give the desired product in two different fractions, a yellow oil (1.16 g, 2.97 mmol, less pure by NMR) and a white oil (2.43 g, 6.20 mmol, pure by NMR). Both fractions (3.594, 9.16 mmol, 33 % overall yield) were used in subsequent reactions without further purification.

$\mathbf{R_f}$ (TLC, silica gel, CH_2Cl_2: MeOH = 50:1): 0.3. **^{1}H NMR** (400 MHz, $CDCl_3$) δ / ppm 3.65 (s, 2H, C$\underline{H}_2$OH), 2.29 (s, 1H, O$\underline{H}$), 2.21 – 1.96 (m, 2H, C$\underline{H}_2$CH$_2$OH), 1.78 – 1.53 (m, 4H, CF$_2$(C$\underline{H}_2$)$_2$). **^{13}C NMR** (101 MHz, $CDCl_3$) δ / ppm 122 – 108 (m, $\underline{C}F_3(\underline{C}F_2)_5$), 62.36 (C$\underline{H}_2$OH), 32.21 ($\underline{C}H_2CH_2OH$), 30.98 (t, $^2J_{CF}$ = 23 Hz, CF$_2\underline{C}H_2CH_2$), 17.12 (t, $^3J_{CF}$ = 3.9 Hz, $CF_2CH_2\underline{C}H_2$). **^{19}F NMR** (376 MHz, $CDCl_3$) δ / ppm –82.37, –115.97, –123.36, –124.33, –125.00, –127.65.

Preparation of 10-bromo-1,1,1,2,2,3,3,4,4,5,5,6,6-tridecafluorodecane (25)

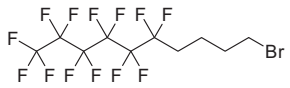

5,5,6,6,7,7,8,8,9,9,10,10,10-tridecafluorodecan-1-ol (**24**) (2.13 g, 5.43 mmol, 1.00 eq) and Aliquat 336 (73 mg, 0.16 mmol, 0.030 eq) as a phase transfer catalyst were given to 48 % aqueous HBr (2.2 ml, 20 mmol, 3.6 eq). The reaction mixture was refluxed for 20 h, cooled down to room temperature and diluted with water (30 ml). The mixture was extracted three times with CH_2Cl_2 and the combined organic extracts were dried ($MgSO_4$) and evaporated to dryness. Purification by column chromatography (Fluka silica gel 60, 0.040–0.063 mm; hexane:CH_2Cl_2 = 1:1) yielded a colourless oil (2.36 g, 5.19 mmol, 96 %).

mp between –20°C and +4 °C. $\mathbf{R_f}$ (TLC, silica gel, hexane:CH_2Cl_2 = 1:1): 0.9. **^{1}H NMR** (400 MHz, $CDCl_3$) δ / ppm 3.42 (t, *J* = 6.5 Hz, 2H, C$\underline{H}_2$Br), 2.17 – 2.02 (m, 2H, C$\underline{H}_2$), 2.00 – 1.90 (m, 2H, C$\underline{H}_2$), 1.85 – 1.73 (m, 2H, C$\underline{H}_2$). **^{13}C NMR** (101 MHz, $CDCl_3$) δ / ppm 120 - 110 (m, $\underline{C}F_3(\underline{C}F_2)_5$), 32.67 ($\underline{C}H_2$), 32.24 ($\underline{C}H_2$), 30.41 (t, $^2J_{CF}$ = 23 Hz, CF$_2\underline{C}H_2CH_2$), 19.41 (t, $^3J_{CF}$ = 3.9 Hz, $CF_2CH_2\underline{C}H_2$). **^{19}F NMR** (376 MHz, $CDCl_3$) δ / ppm –82.29, –115.78, –123.28, –124.26, –124.90, –127.57. **IR** (neat): $\tilde{\nu}$ = 1234 (w), 1186 (w), 1144 (w), 1049 (w), 1016 (w), 787 (w), 735 (w), 692 (w), 669 (w), 642 (m), 625 (m), 598 (m), 565 (s), 550 (s), 542 (s), 532 (s), 523 (s), 513 (s) cm^{-1}. **MS** (EI, *m/z*): 375.0 [M-Br]$^+$ (calc. 375.0). **Calcd.** for $C_{10}H_8BrF_{13}$ (455.05) C 26.39, H 1.77, N 0.00; found C 26.44, H 1.86, N 0.00 %.

Preparation of methyl 3,5-bis(5,5,6,6,7,7,8,8,9,9,10,10,10-tridecafluorodecyloxy) benzoate (26)

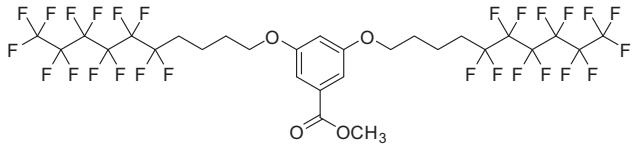

A mixture of 10-bromo-1,1,1,2,2,3,3,4,4,5,5,6,6-tridecafluorodecane (**25**) (2.86 g, 6.28 mmol, 2.50 eq), 3,5-dihydroxybenzoate (**2**) (423 mg, 2.52 mmol, 1.00 eq), 18-crown-6 (133 mg, 0.503 mmol, 0.200 eq), and K_2CO_3 (868 mg, 6.28 mmol, 2.50 eq) in dry acetone (7 ml) was heated to reflux and the mixture was stirred for 4 h under an inert atmosphere of N_2. The solvent was evaporated to dryness and water was added to the residue. This was extracted three times with CH_2Cl_2. The combined organic layers were dried ($MgSO_4$) and evaporated to dryness. The crude material was purified by column chromatography (Fluka silica gel 60, 0.040–0.063 mm; hexane:ethyl acetate = 40:1 → 30:1 → 20:1 → 15:1 → 10:1), followed by a subsequent silica gel chromatography (Fluka silica gel 60, 0.040–0.063 mm; hexane:CH_2Cl_2 = 3:1 → 2:1 → 3:2) yielding the desired product as a white powder (2.22 g, 2.42 mmol, 96 %).

$\mathbf{R_f}$ (TLC, silica gel, hexane:ethyl acetate = 10:1): 0.3. **^{1}H NMR** (500 MHz, $CDCl_3$) δ / ppm 7.17 (d, ^4J = 2.3 Hz, 2H, $H^{Ar(2)}$), 6.63 (t, ^4J = 2.3 Hz, 1H, $H^{Ar(4)}$), 4.02 (t, ^3J = 5.8 Hz, 4H, $OC\underline{H}_2CH_2$), 3.90 (s, 3H, $CO_2C\underline{H}_3$), 2.22 – 2.09 (m, 4H, $OCH_2CH_2CH_2C\underline{H}_2(CF_2)_5CF_3$), 1.92 – 1.85 (m, 4H, $OCH_2C\underline{H}_2CH_2CH_2(CF_2)_5CF_3$), 1.85 – 1.78 (m, 4H, $OCH_2CH_2C\underline{H}_2CH_2(CF_2)_5CF_3$). **^{13}C NMR** (126 MHz, $CDCl_3$) δ / ppm 166.95 ($\underline{C}O_2CH_3$), 160.00 ($C^{3(Ar)}$), 132.21 ($C^{1(Ar)}$), 107.89 ($C^{2(Ar)}$), 106.75 ($C^{4(Ar)}$), 67.64 ($O\underline{C}H_2(CH_2)_3$), 52.40 ($CO_2\underline{C}H_3$), 30.78 (t, $^2J_{CF}$ = 22.5 Hz, $OCH_2CH_2CH_2\underline{C}H_2(CF_2)_5CF_3$), 28.73, ($OCH_2\underline{C}H_2CH_2CH_2(CF_2)_5CF_3$), 17.40 ($OCH_2CH_2\underline{C}H_2CH_2(CF_2)_5CF_3$). **^{19}F NMR** (376 MHz, $CDCl_3$) δ / ppm –81.96, –115.61, –123.09, –124.06, –124.71, –127.32. **IR** (solid): $\tilde{\nu}$ = 2957 (w), 2881 (w), 1717 (m), 1603 (w), 1466 (w), 1450 (w), 1433 (w), 1352 (w), 1302 (m), 1231 (s), 1177 (s), 1138 (s), 1038 (s), 841 (w), 762 (m), 744 (m), 727 (m), 696 (s), 648 (m), 567 (m) cm^{-1}. **MS** (EI, *m/z*): 916.1 $[M]^+$ (calc. 916.1); 168.1 [methyl 3,5-dihydroxybenzoate]$^+$ (calc. 168.0). **Calcd.** for $C_{28}H_{22}F_{26}O_4$ (916.43) C 36.70, H 2.42; found C 36.58, H 2.28 %.

Preparation of 3,5-bis(5,5,6,6,7,7,8,8,9,9,10,10,10-tridecafluorodecyloxy)benzyl alcohol (**27**)

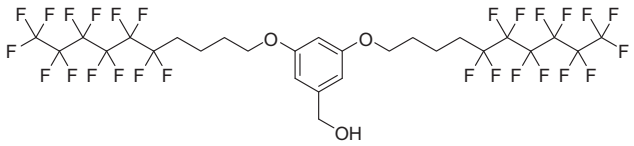

To a suspension of lithium aluminium hydride (108 mg, 95 % pure, 2.70 mmol, 1.38 eq) in freshly distilled diethyl ether (50 ml) under an inert atmosphere of N_2, methyl 3,5-bis(5,5,6,6,7,7,8,8,9,9,10,10,10-tridecafluorodecyloxy)benzoate (**26**) (1.80 g, 1.96 mmol, 1.00 eq) was added slowly in small portions. The reaction mixture was then heated and stirred at reflux for 3.5 h, cooled down to room temperature and quenched by adding 1 aqueous M NaOH solution (0.8 ml) dropwise, whereupon the former grey suspension turned white. The white suspension was filtered over celite and washed with diethyl ether. The filtrate was dried ($MgSO_4$) and evaporated to dryness. The residue was dissolved in CH_2Cl_2 and washed twice with water. The organic layer was dried ($MgSO_4$) and evaporated to dryness affording the product as a white solid (1.64 g, 1.85 mmol, 94 %) which was analytically pure.

$\mathbf{R_f}$ (TLC, silica gel, hexane:ethyl acetate = 5:1): 0.1. **^{1}H NMR** (500 MHz, $CDCl_3$) δ / ppm 6.52 (d, ^4J = 2.1 Hz, 2H, $H^{Ar(2)}$), 6.36 (t, ^4J = 2.2 Hz, 1H, $H^{Ar(4)}$), 4.63 (d, ^3J = 5.4 Hz, 2H, $C\underline{H}_2OH$), 3.99 (t, ^3J = 5.8 Hz, 4H, $OC\underline{H}_2CH_2$), 2.22 – 2.09 (m, 4H, $OCH_2CH_2CH_2C\underline{H}_2(CF_2)_5CF_3$), 1.91 – 1.84 (m, 4H, $OCH_2C\underline{H}_2CH_2CH_2(CF_2)_5CF_3$), 1.84 – 1.77 (m, 4H, $OCH_2CH_2C\underline{H}_2CH_2(CF_2)_5CF_3$), 1.67 (t, ^3J = 5.8 Hz, 1H, OH). **^{13}C NMR** (126 MHz, $CDCl_3$) δ / ppm 160.37 ($C^{3(Ar)}$), 143.59 ($C^{1(Ar)}$), 105.32 ($C^{2(Ar)}$), 100.72 ($C^{4(Ar)}$), 67.38 ($O\underline{C}H_2(CH_2)_3$), 65.47 ($\underline{C}H_2OH$), 30.79 (t, $^2J_{CF}$ = 22.2 Hz, $OCH_2CH_2CH_2\underline{C}H_2(CF_2)_5CF_3$), 28.79 ($OCH_2\underline{C}H_2CH_2CH_2(CF_2)_5CF_3$), 17.42 ($OCH_2CH_2\underline{C}H_2CH_2(CF_2)_5CF_3$). **IR** (neat): $\tilde{\nu}$ = 3497 (w), 2962 (w), 2880 (w), 1612 (w), 1589 (w), 1472 (w), 1404 (w), 1367 (w), 1315 (m), 1244 (s), 1204 (s), 1184 (s), 1169 (s), 1138 (s), 1063 (m), 1034 (s), 964 (w), 920 (w), 839 (w), 789 (w), 694 (s), 642 (s), 569 (m) cm^{-1}. **MS** (EI, *m/z*): 888.1 $[M]^+$ (calc. 888.1). **Calcd.** for $C_{27}H_{22}F_{26}O_3$ (888.42) C 36.50, H 2.50; found C 36.46, H 2.49 %.

Preparation of 3,5-bis(5,5,6,6,7,7,8,8,9,9,10,10,10-tridecafluorodecyloxy)benzyl methanesulfonate (**28**)

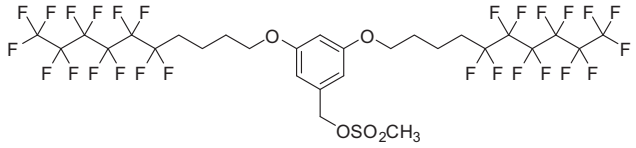

NEt_3 (1.1 ml, 7.7 mmol, 5.0 eq) was added to a solution of 3,5-bis(5,5,6,6,7,7,8,8,9,9,10,10,10-tridecafluorodecyloxy)benzyl alcohol (**27**) (1.37 g, 1.54 mmol, 1.00 eq) in dry Et_2O (20 ml), previously cooled to –18 °C under an argon atmosphere. Methanesulfonyl chloride (0.48 ml, 6.2 mol, 4.0 eq) was added slowly over a period of 15 min, and then the reaction mixture was stirred at –18 °C for 45 min. The mixture was poured into a mixture of concentrated HCl (1 ml) and crushed ice (10 g), and extracted with CH_2Cl_2. The organic layer was washed with a saturated solution of $NaHCO_3$, dried with $MgSO_4$, and the solvent removed. The desired product was isolated as a colourless oil (1.51 g, 1.56 mmol, 101 %).

^{1}H NMR (400 MHz, $CDCl_3$) δ / ppm 6.54 (d, J = 2.2 Hz, 2H, $H^{2(Ar)}$), 6.44 (t, J = 2.2 Hz, 1H, $H^{4(Ar)}$), 5.15 (s, 2H, $C\underline{H}_2OSO_2CH_3$), 3.98 (t, J = 5.7 Hz, 4H, $OC\underline{H}_2CH_2$), 2.94 (s, 3H, $OSO_2C\underline{H}_3$), 2.24 – 2.06 (m, 4H, $OCH_2C\underline{H}_2$), 1.92 – 1.75 (m, 8H, $CF_2(C\underline{H}_2)_2$).

Preparation of 4,4'-bis(3,5-bis(5,5,6,6,7,7,8,8,9,9,10,10,10-tridecafluorodecyloxy) benzyloxy)-2,2'-bipyridine (**29**)

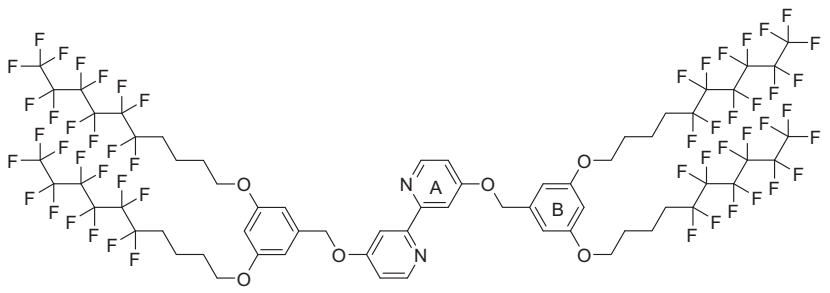

A mixture of crude 3,5-bis(5,5,6,6,7,7,8,8,9,9,10,10,10-tridecafluorodecyloxy)benzyl methanesulfonate (**28**) (564 mg, ca. 80 % pure, 0.467 mmol, 2.50 eq), 4,4'-dihydroxy-2,2'-bipyridine (**16**) (37.0 mg, 0.187 mmol, 1.00 eq), K_2CO_3 (155 mg, 1.12 mmol, 6.00 eq) and tetra-*n*-butylammonium iodide (7 mg, 0.02 mmol, 0.1 eq) was stirred vigorously in ethyl acetate (1.5 ml) and water (1.5 ml) at 55 °C for 68 h. After cooling to room temperature, water was added and the mixture was extracted three times with ethyl acetate. The combined organic layers were dried over $MgSO_4$ and evaporated to dryness to give a yellow oil. The crude material was purified by column chromatography (Normasil silica gel 60, 0.040–0.063 mm; CH_2Cl_2:MeOH = 40:1) and recrystallised from EtOH yielding the desired product as an off-white solid (93 mg, 0.048 mmol, 26 %).

R_f (TLC, silica gel, CH_2Cl_2: MeOH = 10:1): 0.4. **^{1}H NMR** (500 MHz, $CDCl_3$) δ / ppm 8.48 (d, ^3J = 5.7 Hz, 2H, $H^{6(A)}$), 8.07 (d, ^4J = 2.5 Hz, 2H, $H^{3(A)}$), 6.90 (dd, ^3J = 5.7 Hz, ^4J = 2.6 Hz, 2H, $H^{5(A)}$), 6.59 (d, ^4J = 2.1 Hz, 4H, $H^{2(B)}$), 6.41 (t, J = 2.1 Hz, 2H, $H^{4(B)}$), 5.15 (s, 4H, $Ar_AOC\underline{H}_2Ar_B$), 3.99 (t, J = 5.8 Hz, 8H, $OC\underline{H}_2CH_2$), 2.22 – 2.09 (m, 8H, $OCH_2CH_2CH_2C\underline{H}_2(CF_2)_5CF_3$), 1.91 – 1.84 (m, 8H, $OCH_2C\underline{H}_2CH_2CH_2(CF_2)_5CF_3$), 1.84 – 1.78 (m, 8H, $OCH_2CH_2C\underline{H}_2CH_2(CF_2)_5CF_3$). **^{13}C NMR** (126 MHz, $CDCl_3$) δ / ppm 165.88 ($C^{2(A)}$), 160.43 ($C^{3(B)}$), 158.00 ($C^{4(A)}$), 150.44 ($C^{6(A)}$), 138.38 ($C^{1(B)}$), 111.58 ($C^{5(A)}$), 107.35 ($C^{3(A)}$), 106.00 ($C^{2(B)}$), 101.29 ($C^{4(B)}$), 69.90 ($Ar_AOC\underline{H}_2Ar_B$), 67.45 ($OC\underline{H}_2(CH_2)_3$), 30.79 (t, $^2J_{CF}$ = 22.1 Hz, $OCH_2CH_2CH_2C\underline{H}_2(CF_2)_5CF_3$), 28.78 ($OCH_2C\underline{H}_2CH_2CH_2(CF_2)_5CF_3$), 17.42 ($OCH_2CH_2C\underline{H}_2CH_2(CF_2)_5CF_3$). **^{19}F NMR** (376 MHz, CDCl3) δ / ppm –81.94, –115.59, –123.11, –124.05, –124.70, –127.30. **IR** (solid): $\tilde{\nu}$ = 2949 (w), 2880 (w),

1587 (m), 1560 (w), 1456 (w), 1367 (w), 1321 (w), 1296 (w), 1227 (m), 1173 (m), 1140 (s), 1121 (m), 1022 (m), 951 (w), 926 (w), 893 (w), 827 (m), 812 (m), 696 (s), 652 (s), 621 (s), 582 (s) cm^{-1}. **MS** (Maldi, *m/z*): 1929.1 $[M+H]^+$ (calc. 1929.3); 1951.1 $[M+Na]^+$ (calc. 1951.3); 1967.2 $[M+K]^+$ (calc. 1967.2). **Calcd.** for $C_{64}H_{48}F_{52}N_2O_6$ (1928.99) C 39.85, H 2.51, N 1.45; found C 39.80, H 2.52, N 1.30 %.

Chapter 6

Synthesis and STM Imaging of Ligands for Iridium(III) Complexes

6.1
Introduction and aims

This chapter deals mainly with the syntheses of various *N,N'*-ligands based upon either 2,2'-bipyridine or 1,10-phenanthroline for orthometallated Ir(III) complexes (see **Chapter 7**). The more simple ligands, discussed in **Section 6.2.1**, are already known with the exception of the more complex structure of the archetypical dendronised ligand **35** (**Scheme 6.1**). This ligand, together with all the dendronised ligands discussed in **Section 6.2.2**, were unknown to this date, although somehow similar compounds have been prepared by *Kröhnke et al.*,[242], *Neve et al.*,[243-247] *Che et al.*,[248] and *Ziessel et al.*[249, 250] In the cited literature, these ligands were often used for the formation of cyclometallated compounds, mainly Pd(II)- or Pt(II)-complexes. Bearing Fréchet-type dendrons and thus potentially capable of forming stable monolayers on HOPG,[21] ligands **38**, **39**, and **40** were studied using STM imaging.

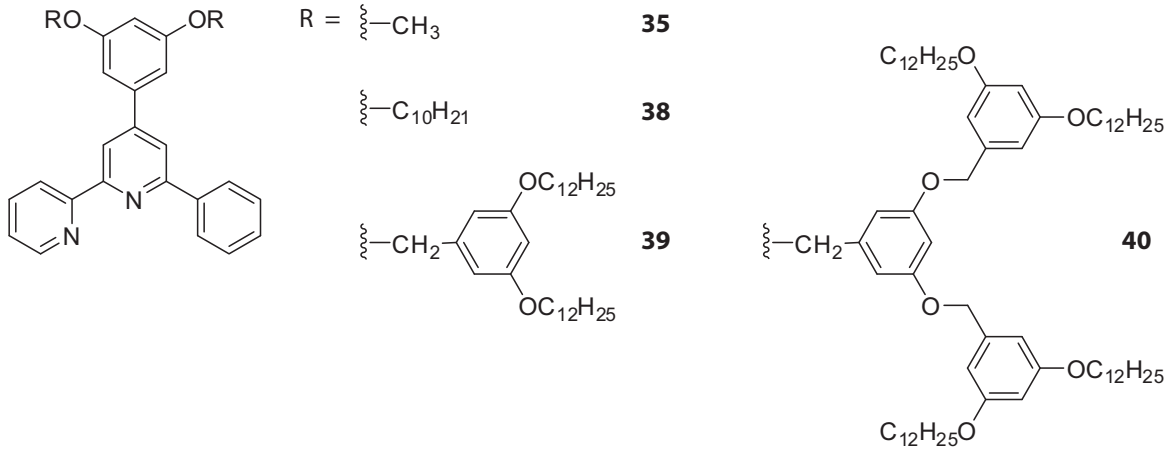

Scheme 6.1 Archetype (**35**) and dendronised (**38**, **39**, **40**) ligands.

6.2
Synthesis and discussion

6.2.1
Simple ligands

Synthesis of monosubstituted phenanthroline 2-phenyl-1,10-phenanthroline (**30**) was done as described in literature.[251-253] As the reaction with phenyllithium needs to occur under water-free conditions, 1,10-phenanthroline monohydrate was dissolved in dichloromethane and evaporated to dryness several times. It was then reacted with 1.25 equivalents of phenyllithium at 0 °C in dry diethyl ether and subsequently quenched with water to give the dihydro-intermediate which was then reoxidised with activated manganese(IV) oxide to ligand **30** (**Scheme 6.2**).

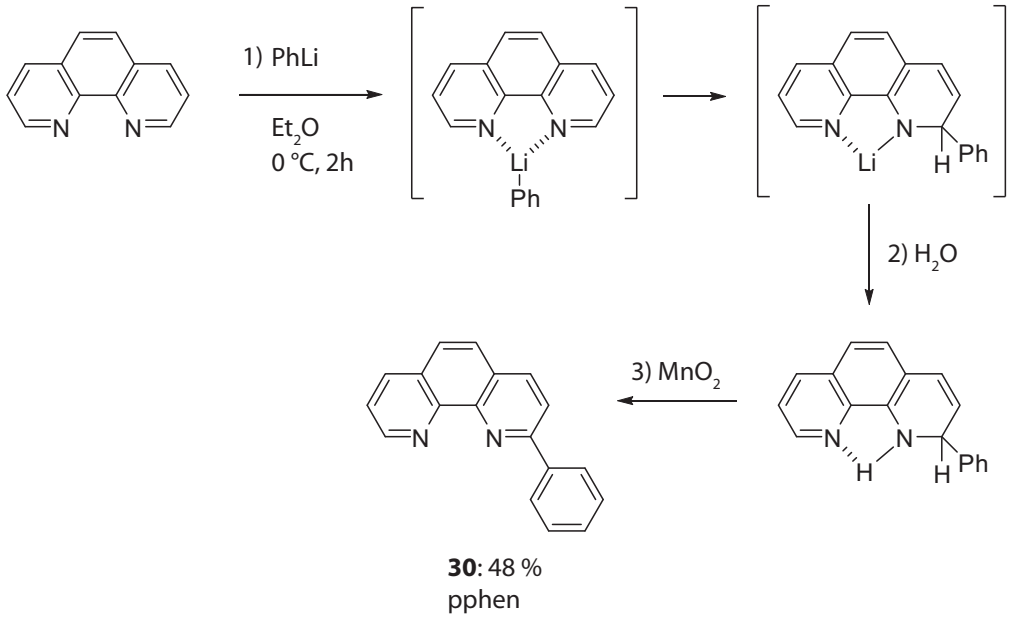

Scheme 6.2 Preparation of 2-phenyl-1,10-phenanthroline (**30**) and the mechanism of its formation.

Recrystallisation in toluene afforded beautiful, big crystals on which X-ray crystallography could be performed. Solving the crystal structure at 173 K revealed a monoclinic crystal system (a = 10.8416(2), b = 21.0804(3), c = 12.2036(2) Å; β = 107.7982(9) °) with two molecules per asymmetric unit in a $P2_1/c$ space group (Z = 8) with acceptable R-factors ($R1$ = 0.0452, $wR2$ = 0.0510, gof = 1.0571). The two molecules of the asymmetric unit are depicted in **Figure 6.1**.

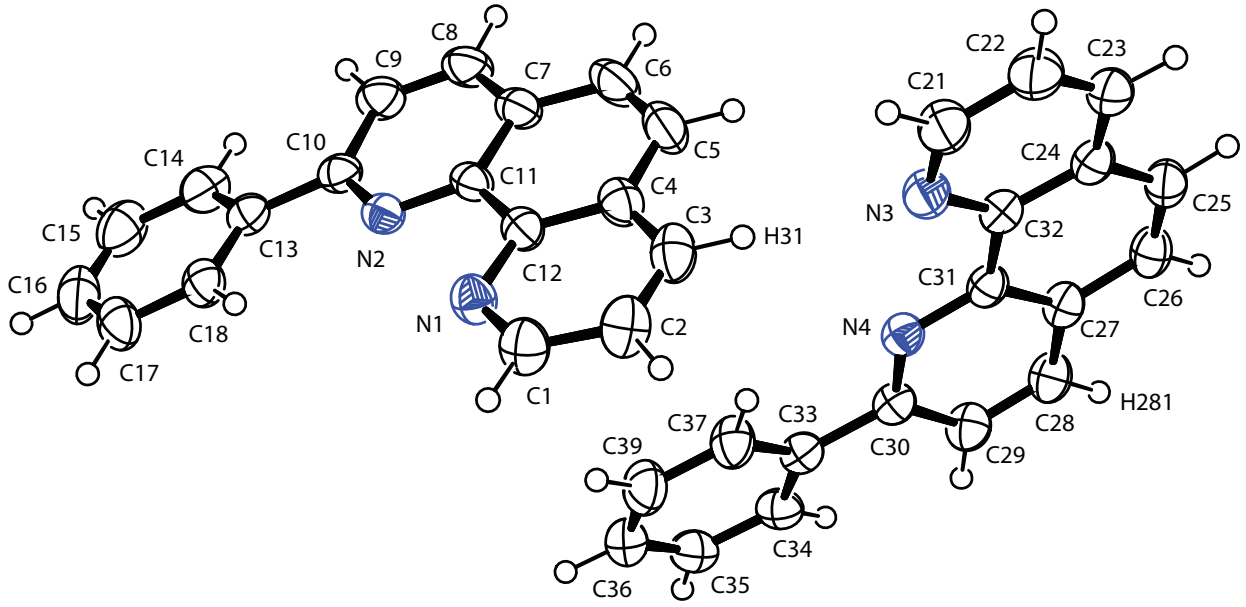

Figure 6.1 ORTEP representation of the solid state structure of the two molecules present in the asymmetric unit of **30**. Thermal ellipsoids are depicted at 50 % probability.
Selected bond lengths (Å) and angles (°) of one of the two molecules (very similar values in the other molecule): N1–C1 = 1.327(3), N1–C12 = 1.358(2), N2–C10 = 1.336(2), N2–C11 = 1.3547(19), C4–C12 = 1.412(2), C7–C11 = 1.416(2), C10–C13 = 1.484(2), C11–C12 = 1.452(2), C5–C6 = 1.348(3); C1–N1–C12 = 117.07(14), C10–N2–C11 = 118.81(14), N1–C12–C11 = 118.28(13), N2–C11–C12 = 118.30(13), N2–C10–C13 = 115.95(14).

The solid state structure of **30** shows close contacts with non-classical hydrogen bonds between N1···H281^{i}–C28^{i} (3.475 Å, 144.5 °; symmetry operator i = 1 – *x*, ½ + *y*, ³⁄₂ – *z*) and N3···H31–C3 (3.513(2) Å, 160.1 °). The torsion angle N1–C12–C11–N2 is –5.2(2) °. The molecule is close to planar, the angle between the least square planes of the rings containing atoms C13 and N2 being 9.11(9) °.

For the preparation of 6-phenyl-2,2'-bipyridine (**31**), 2,2'-bipyridine was reacted with phenyllithium at 0 °C in dry diethyl ether and the intermediate product was oxidised with potassium permanganate to rearomatise the pyridine ring. This strategy is similar to the synthesis of **30** (**Scheme 6.3**).[254]

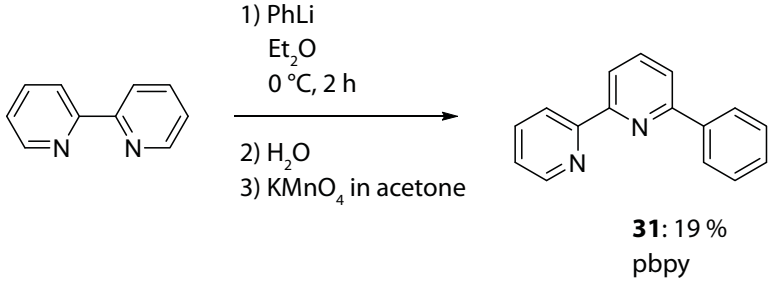

31: 19 %
pbpy

Scheme 6.3 Synthesis of 6-phenyl-2,2'-bipyridine (**31**).

The synthetic strategy adopted for the preparation of 6,6'-diphenyl-2,2'-bipyridine (**32**) was a one step diphenyllation of 2,2'-bipyridine reported for the phenathroline analogue by *J. P. Sauvage et al.*[255] and established for 2,2'-bipyridine by *V. Chaurin* of our group.[256] 4.00 Equivalents of phenyllithium were added to a solution of 2,2'-bipyridine in THF at –78 °C, raised to room temperature and then stirred at reflux for 4 h (**Scheme 6.4**). Quenching with water and subsequent oxidation of the dihydro-intermediate gave the desired ligand **32** in poor yields. Slow evaporation of a dichloromethane : hexane = 1 : 1 solution of **32** afforded long needles suitable for single crystal experiments. Unfortunately, standard methods are not capable of resolving its solid state structure because of a modulation along one crystallographic axis with a highly repetitive pattern where one of the two pendant phenyl rings rotates around 60 ° in every unit cell, so that every 7th unit cell is identical again.[257]

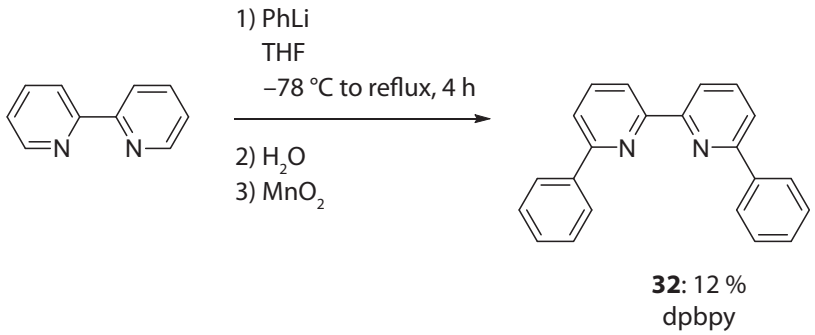

Scheme 6.4 Synthesis of 6,6'-diphenyl-2,2'-bipyridine (**32**).

As the starting point for dendronised ligands based on 6-phenyl-2,2'-bipyridine, ligand **35** was synthesised using a solventless "grinding" method developed for aldol condensation and *Michael* addition and adapted for substituted pyridines by *G. W. V. Cave* and *C. L. Raston* under the principles of "Green Chemistry".[258, 259] Firstly, acetophenone and 3,5-dimethoxybenzaldehyde were put in a mortar in the presence of sodium hydroxide (**Scheme 6.5**). After combining the medium for 30 min with a pestle to give the intermediate chalcone **33**, 2-acetylpyridine was added and ground again for 30 min until the material was too viscous to grind yielding the crude *Michael* addition product **34**. Ring condensation and oxidation to the final ligand **35** was performed under aerial conditions in solution in glacial acetic acid with ammonium acetate as the nitrogen source. A lot of the product was lost during work-up and purification procedures due to the acidic conditions and resulted in 4 % overall yield only for **35**. In another batch, polyethylene glycol 300 (PEG-300) was used as the solvent in the ring condensation reaction as described by *C. Smith.*,[260] a former member of our group, achieving higher overall yields of 24 %.

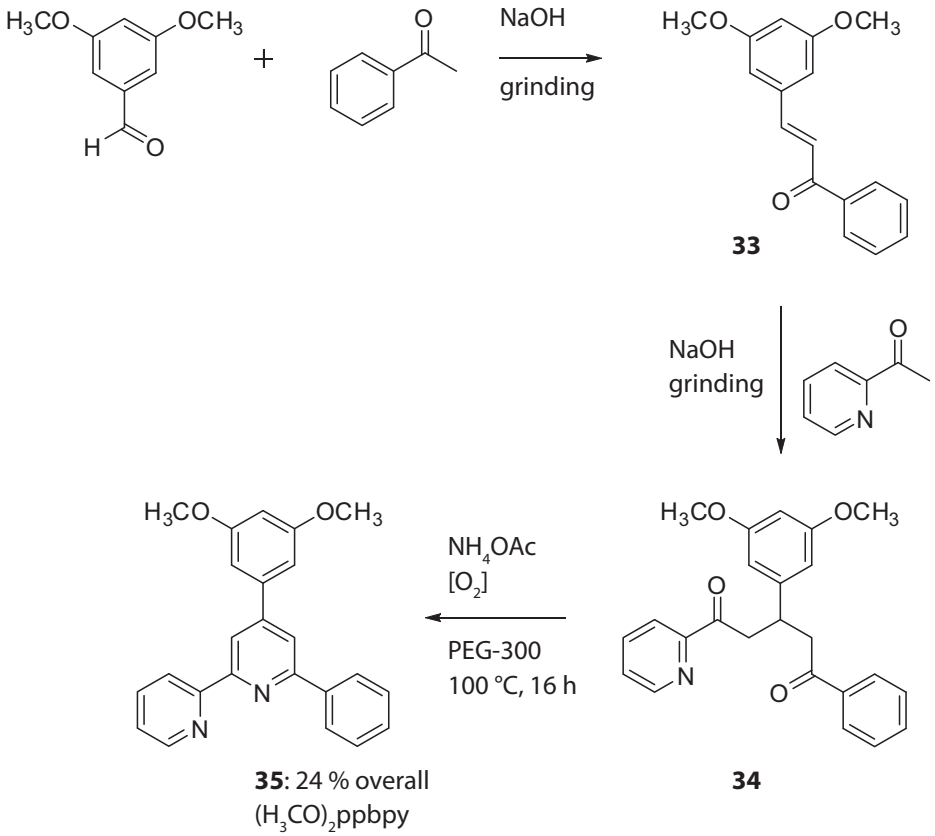

Scheme 6.5 First synthetic approach to ligand **35**.

Because of the disappointingly low yields in the preparation of **35** and its time-consuming purification, a new synthetic approach was tried based on a *Kröhnke*-type[242] synthesis. *Neve et al.* have reported similar compounds, and their preparations[245, 246] were adapted to our needs (**Scheme 6.6**). Chalcone **33** was prepared in methanol[261] and 1-(2-pyridinylcarbonyl)pyridinium iodide (**36**) was obtained from the reaction of 2-acetylpyridine in pyridine in the presence of iodine[262]. Crude chalcone **33** was combined with **36** and ammonium acetate in refluxing methanol which afforded the desired product, ligand **35**. Unfortunately, the yield obtained from this synthetic approach (17 % overall) was even lower than from the "grinding method" (24 % overall yield in its optimised variant).

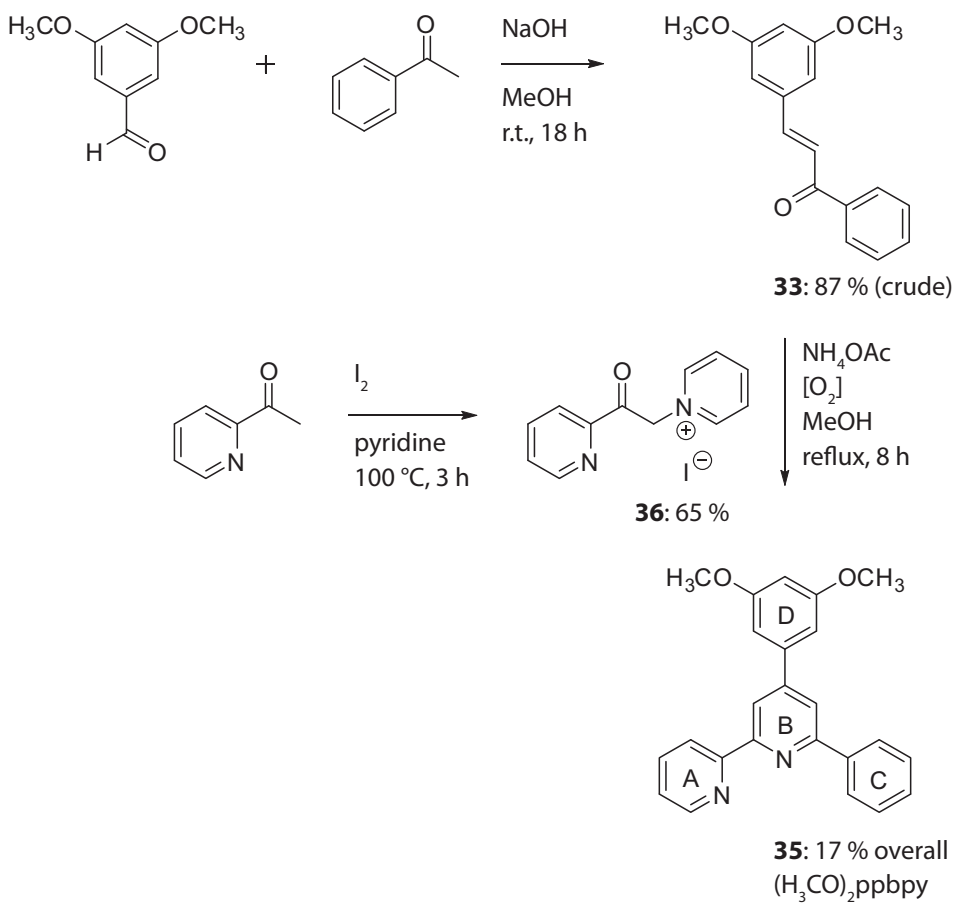

Scheme 6.6 Second synthetic route to ligand **35**. Ring labels are for NMR spectroscopic assignments (**Figure 6.2**).

The ^{1}H NMR spectrum of **35** is shown in **Figure 6.2** and was fully assigned by 2D methods COSY and NOESY; for assignment of the ^{13}C NMR spectrum, HMQC and HMBC methods were used.

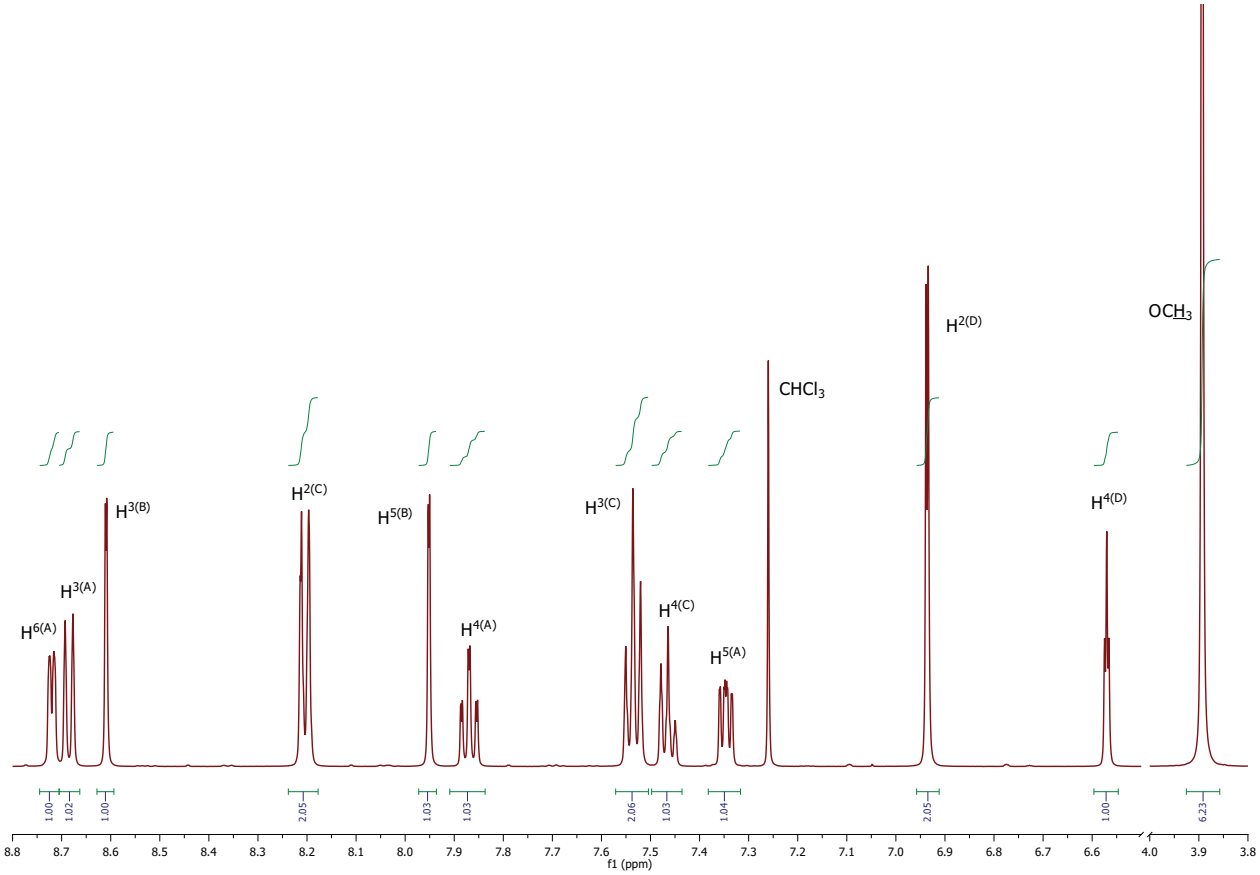

Figure 6.2 ^{1}H NMR spectra of ligand **35** in $CDCl_3$ at 295 K. See **Scheme 6.6** for ring labelling.

Crystals of ligand **35** which were suitable for X-ray crystallography were obtained by slow evaporation of a hexane : diethyl ether = 3 : 2 solution. Solving the crystal structure at 173 K revealed a triclinic crystal system (a = 4.7434(1), b = 8.7761(2), c = 23.1828(4) Å; α = 95.3520(9), β = 92.9223(9), γ = 105.3722(9) °) containing one molecule per asymmetric unit in a $P\bar{1}$ space group (Z = 2) with acceptable R-factors ($R1$ = 0.0557, $wR2$ = 0.0642, gof = 1.0573). The solid state structure of a molecule of **35** is illustrated in **Figure 6.3**. The phenyl ring is disordered over two positions, each with an occupancy of 50 %. C19 and C20 are shared in both conformations and the angle between the least square planes containing the phenyl rings is 56.22(18) °.

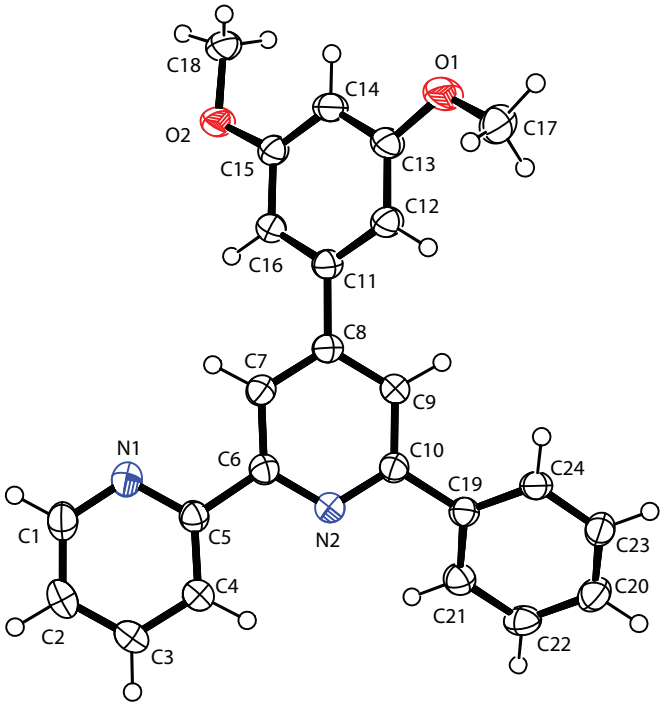

Figure 6.3 ORTEP representation of the solid state structure of one of the two conformers present in **35**. Thermal ellipsoids are depicted at 50 % probability.
Selected bond lengths (Å) and angles (°): N1–C1 = 1.340(3), N1–C5 = 1.345(2), C5–C6 = 1.483(3), N2–C6 = 1.348(2), N2–C10 = 1.342(2), C10–C19 = 1.489(3), C8–C11 = 1.486(3), O1–C13 = 1.368(2), O1–C17 = 1.422(3), O2–C15 = 1.368(2), O2–C18 = 1.430(3);
C1–N1–C5 = 117.99(18), N1–C5–C6 = 117.20(17), N2–C6–C5 = 115.89(16), C6–N2–C10 = 118.10(16), N2–C10–C19 = 116.24(16), C10–C19–C24 = 121.7(2), O1–C13–C14 = 114.79(18), O1–C13–C12 = 124.29(17), C13–O1–C17 = 117.50(18), O2–C15–C14 = 124.02(17), O2–C15–C16 = 115.43(15), C15–O2–C18 = 117.09(16).

The bipyridine unit in the solid state structure of **35** exhibits the expected *transoid* conformation with an angle of 6.05(11) ° between the least square planes of the two rings. The pendant phenyl ring is twisted by 29.45(14) ° (26.80(14) ° for the other conformation not shown in **Figure 6.3**) and the dimethoxy-subsituted ring by 38.60(9) ° compared to the central ring containing N2. The angles of O1–C13–C12 (124.29(17) °) and O2–C15–C16 (115.43(15) °) as well as the dihedral angles of C17–O1–C13–C12 (–12.1(3) °) and C18–O2–C15–C14 (7.6(3) °) indicate a large fraction of sp^2-hybridisation in the oxygen atoms as expected.

The crystal lattice of **35** possesses an inversion centre in its unit cell so that in the packing, the bipyridine parts and dimethoxyphenyl parts of the molecules are located next to each other (**Figure 6.4**).

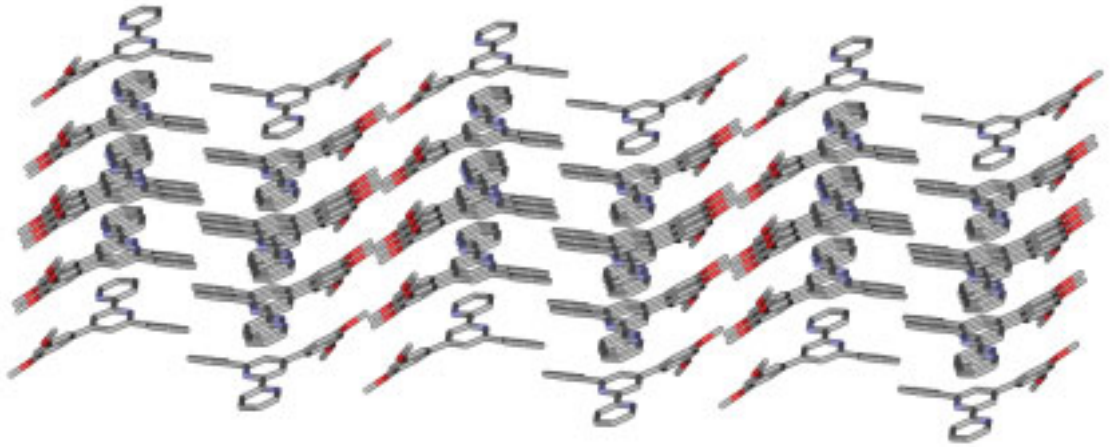

Figure 6.4 Crystal stacking in the solid state structure of **35**. Hydrogen atoms have been omitted for clarity.

6.2.2 Dendronised ligands

In order to apply the standard synthetic procedure for coupling Fréchet-type dendrons to **35**, the methoxy groups had to be deprotected in order to obtain two free phenolic hydroxy groups. Several attempts were tried using standard methods commonly found in the literature. First, BBr_3 in dichloromethane was tried as described before,[263-265] but the desired product could not be isolated. In another attempt, trimethylsilyl iodide was used in acetonitrile,[266-271] but again no traces of the product were found when analysed by NMR spectroscopy. Finally, boiling pyridinium hydrochloride, prepared previously simply by adding aqueous HCl to pyridine and drying under vacuo, was used as the deprotecting reagent affording the desired product in quantitative yields after precipitation in water (**Scheme 6.7**).[272] Pyridinium hydrochloride, exhibiting ionic liquid-properties under these conditions, is a classical reagent for cleavage of aryl methyl ethers at high temperatures avoiding strongly acidic or basic conditions.[273-275] In addition to the classic reflux conditions, microwaving the mixture in a sealed tube at 250 °C for 15 min proved to be effective as well.

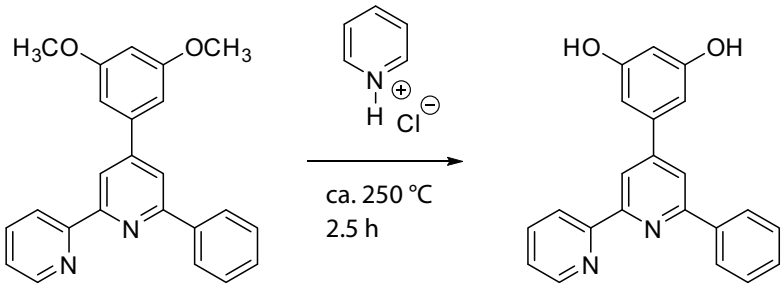

35

37: 99 %
$(HO)_2$ppbpy

Scheme 6.7 Deprotection of methoxy ether groups in ligand **35**.

Because of its similar structure and acidic properties, ligand **37** was used in the same way compound **2** was used in the dendron synthesis. Therefore, ligand **37** was put in a microwave reactor together with the appropriate electrophile (**Table 6.1**) in the presence of potassium carbonate and 18-crown-6[166, 167] with a small amount of acetone. The desired dendronised ligands **38**, **39**, and **40** were produced. These exploited three different dendritic generations (**Scheme 6.8**): 1st generation (**38**), 2nd generation (**39**), and 3rd generation (**40**).

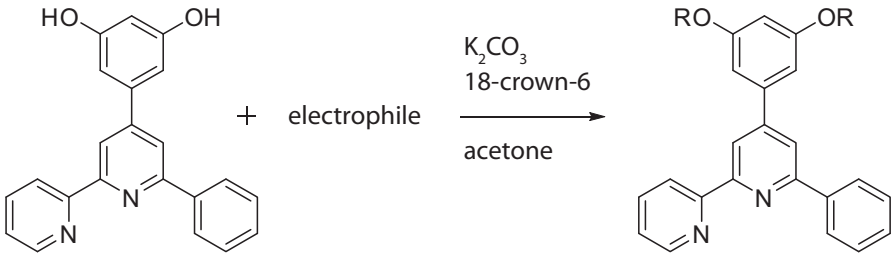

37

Scheme 6.8 Synthesis of dendronised ligands **38**, **39**, and **40** (see **Table 6.1**).

The conditions for the three reactions were slightly different in regards of the temperature so that the mesylate electrophiles were not heated above 100 °C complying with their lower thermal stability. The yield in the reaction with the bromo electrophile was as expected (94 %), but for the mesylate electrophiles the yields were a bit lower (62 %, and, respectively, 75 %). This behaviour is probably due to more difficult purification procedures for high mass molecules and also for the lower purity of the electrophilic starting materials.

Figure 6.5 shows a comparison of the ^{1}H NMR spectra of the dendronised ligands **35**, **38**, **39**, and **40**. It is worth noting the increasing ratio of the integrals of alkyl- to bipyridine-protons and the appearance of new peaks assigned to the additional benzylic CH_2-groups and arylic H^2- and H^4-protons.

Table 6.1 Syntheses starting from ligand **37** (**Scheme 6.8**): 1st generation (**38**), 2nd generation (**39**), and 3rd generation (**40**) Fréchet-type dendronised ligands.

Electrophile and conditions	Product	
n-$C_{10}H_{21}Br$ 120 °C, 60 min	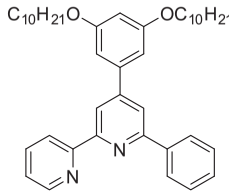 **38** $(H_{21}C_{10}O)_2$ppbpy	94 %
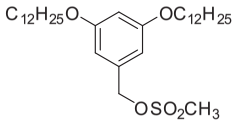 **9** 100 °C, 60 min	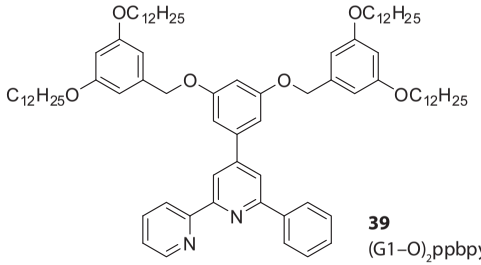 **39** $(G1–O)_2$ppbpy	62 %
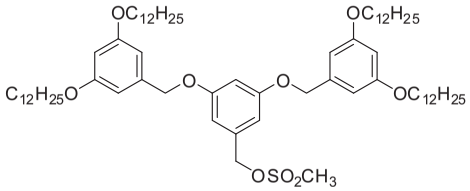 **21** 100 °C, 60 min	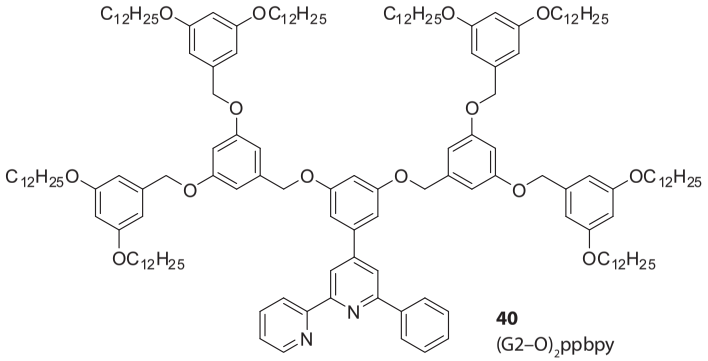 **40** $(G2–O)_2$ppbpy	75 %

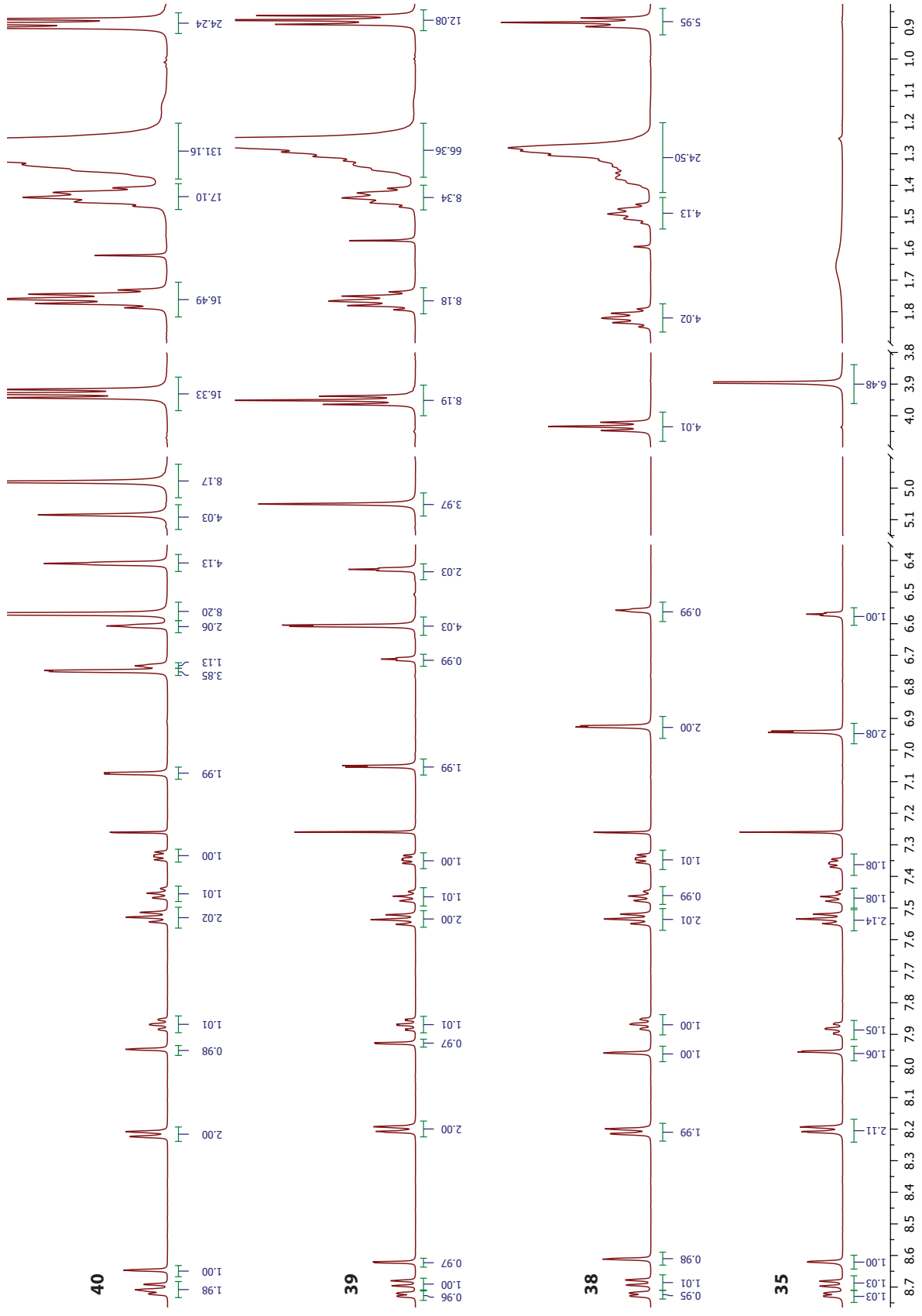

Figure 6.5 ^{1}H NMR spectra of dendronised ligands **35**, **38**, **39**, and **40** (from bottom to top) each in $CDCl_3$ at 295 K.

6.3 STM imaging and discussion

The dendronised ligands **38**, **39**, and **40** were dissolved in hexane and solution cast on HOPG whereupon STM measurements were performed. For compound **38**, a pattern was observed at the air/solid-interface. A series of images with different sizes is depicted in **Figure 6.6**.

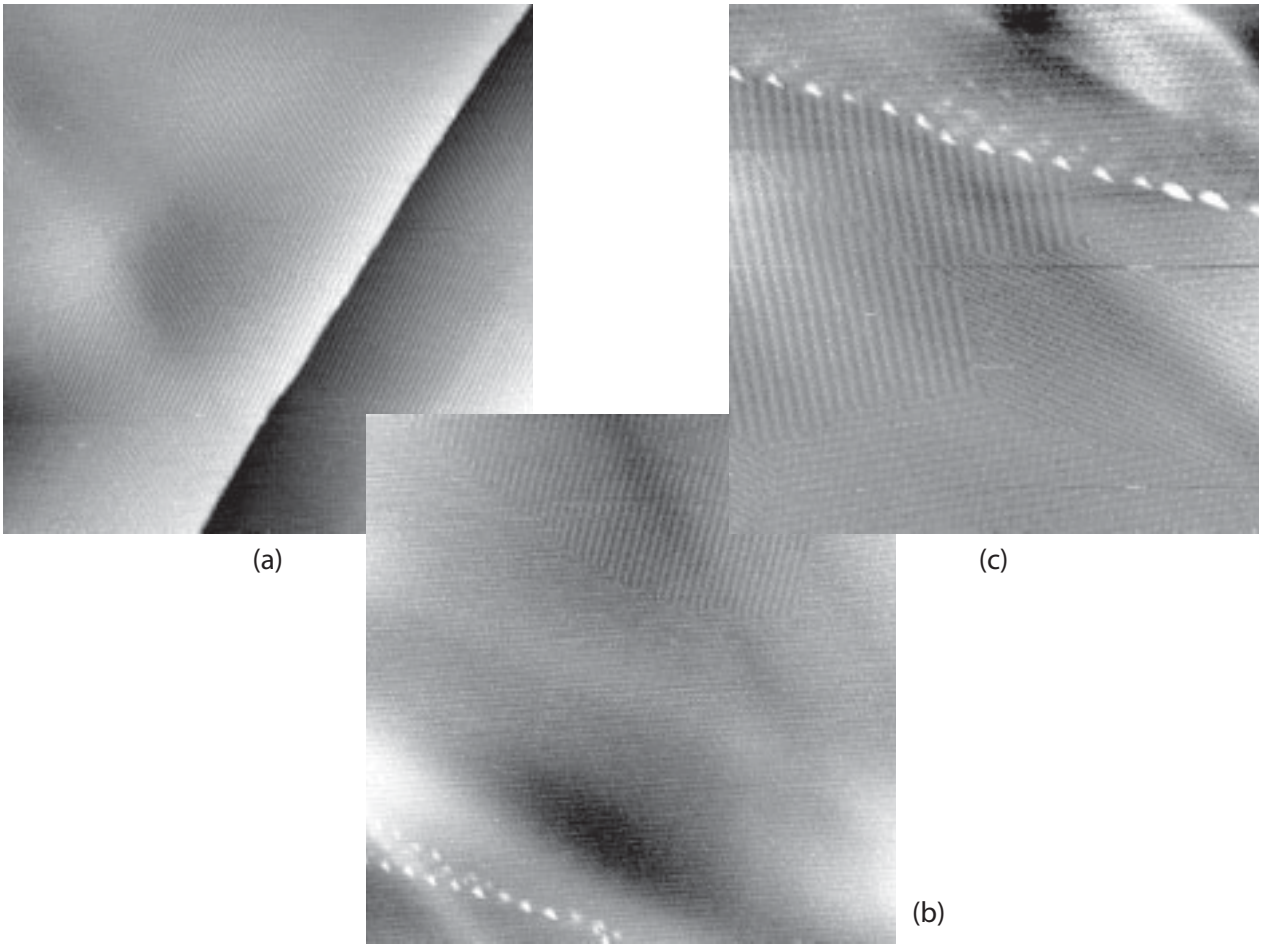

Figure 6.6 STM images of **38** on HOPG at different recording sizes: (a) 200 nm × 200 nm (v = 2.54 Hz), (b) 150 nm × 150 nm (v = 3.05 Hz), (c) 100 nm × 100 nm (v = 4.07 Hz). All images recorded with constant scan parameters: U_{bias} = –700 mV, I_t = 8.0 pA.

The line pattern formed by the monolayer of **38** emerges in different domains of various sizes. In **Figure 6.7**, on the base of one of the images from **Figure 6.6**, the line pattern of three of the present domains is supported by overlaid red lines. The angles formed by the lines are roughly 60 °, therefore the displacement of the domains can be attributed to the three-fold symmetry of the underlying graphite. The distance between the lines varies from 1.4 nm (bottom right domain) and 1.8 nm (bottom left domain) to 2.6 nm (top left domain) which implies a rather strong motional drift in this setup.

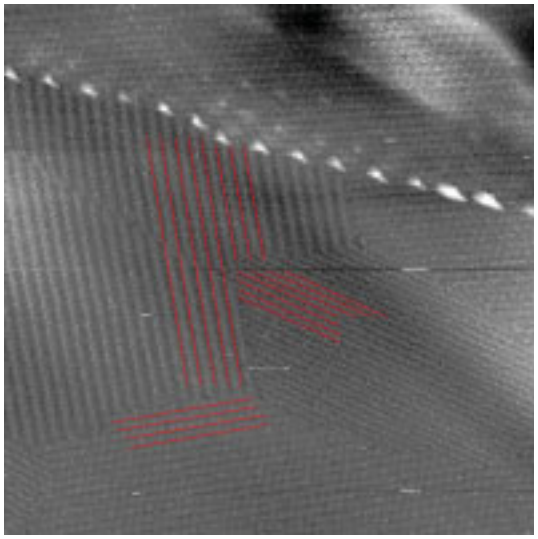

Figure 6.7 STM image from **Figure 6.6c** (100 nm × 100 nm) emphasising the line pattern of three of the present domains.

This distance is in agreement with the molecular size of **38** being roughly 2 nm diagonally in a typical, flat conformation (**Figure 6.8**). The model was calculated *in silico* for one molecule of **38** in order to have a rough estimation of the molecular size.

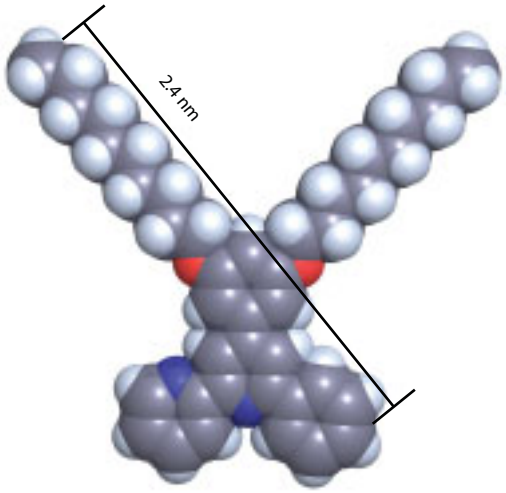

Figure 6.8 Space filling representation of a model of **38** in a flat conformation showing molecular dimensions.

Unfortunately, due to low resolution and the aforementioned drift, averaging images for detailed unit cell considerations or molecular fitting to the observed pattern could not be performed.

6.4 Experimental part

Preparation of 2-phenyl-1,10-phenanthroline (30)

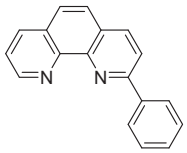

To a suspension of 1,10-phenanthroline (5.00 g, 27.7 mmol, 1.00 eq) in dry Et_2O (300 ml) at 0 °C, phenyllithium (22.4 ml, 34.7 mmol, 1.25 eq, 1.55 M in cyclohexane / Et_2O) was added under an atmosphere of N_2 whereupon the colour of the solution turned red. The reaction mixture was allowed to stir for 2 h at 0 °C after which it was quenched by addition of ice (80 g). The organic layer was separated and the aqueous layer was extracted twice with CH_2Cl_2 (250 ml total). The combined organic layers were dried ($MgSO_4$) and evaporated to a volume of 300 ml under reduced pressure. The solution was then oxidised by stirring with activated MnO_2 (25 g, 0.29 mol, 10 eq). An additional portion of MnO_2 (25 g, 0.29 mol, 10 eq) was added to the mixture after 1 h to ensure complete oxidation. After a total of 6 h, anhydrous $MgSO_4$ (40 g) was added, and the mixture was filtered. The residue was washed well with CH_2Cl_2 and the filtrate was evaporated to dryness to give a sticky solid. The crude material was recrystallised from toluene (10 ml), purified by column chromatography (Fluka silica gel 60, 0.040–0.063 mm; CH_2Cl_2:hexane = 1:1 → CH_2Cl_2 → CH_2Cl_2:MeOH = 100:1 → 40:1) and recrystallised again from toluene (10 ml) affording the desired product as colourless crystals (3.43 g, 13.4 mmol, 48 %).

$\mathbf{R_f}$ (TLC, silica gel, CH_2Cl_2:MeOH = 40:1): 0.2. **^{1}H NMR** (500 MHz, $CDCl_3$) δ / ppm 9.24 (dd, ^3J = 4.2 Hz, ^4J = 1.3 Hz, 1H, $H^{9(phen)}$), 8.34 (d, ^3J = 7.7 Hz, 2H, $H^{2(Ph)}$), 8.29 (d, ^3J = 8.4 Hz, 1H, $H^{4(phen)}$), 8.24 (dd, ^3J = 8.1 Hz, ^4J = 1.1 Hz, 1H, $H^{7(phen)}$), 8.09 (d, ^3J = 8.4 Hz, 1H, $H^{3(phen)}$), 7.80 (d, ^3J = 8.7 Hz, 1H, $H^{5(phen)}$), 7.76 (d, ^3J = 8.7 Hz, 1H, $H^{6(phen)}$), 7.63 (dd, ^3J = 8.0 Hz, ^3J = 4.3 Hz, 1H, $H^{8(phen)}$), 7.54 (t, ^3J = 7.6 Hz, 2H, $H^{3(Ph)}$), 7.47 (t, ^3J = 7.3 Hz, 1H, $H^{4(Ph)}$). **^{13}C NMR** (126 MHz, $CDCl_3$) δ / ppm 157.69 ($C^{2(phen)}$), 150.57 ($C^{9(phen)}$), 146.58 ($C^{10a(phen)}$), 146.24 ($C^{10b(phen)}$), 139.76 ($C^{1(Ph)}$), 136.95 ($C^{4(phen)}$), 136.18 ($C^{7(phen)}$), 129.42 ($C^{4(Ph)}$), 129.18 ($C^{6a(phen)}$), 128.89 ($C^{3(Ph)}$), 128.10 ($C^{2(Ph)}$), 127.65 ($C^{4a(phen)}$), 126.48 ($C^{5(phen)}$), 126.37 ($C^{6(phen)}$), 122.99 ($C^{8(phen)}$), 120.75 ($C^{3(phen)}$). **IR** (solid): $\tilde{\nu}$ = 3036 (w), 2617 (w), 1961 (w), 1904 (w), 1809 (w), 1772 (w), 1695 (w), 1587 (m), 1549 (m), 1510 (w), 1487 (s), 1439 (m), 1385 (s), 1277 (m), 1211 (w), 1182 (w), 1150 (m), 1107 (w), 1086 (m), 1022 (w), 984 (w), 864 (s), 847 (s), 766 (s), 731 (s), 689 (s) cm^{-1}. **MS** (ESI, *m/z*): 535.3 $[2M+Na]^+$ (calc. 535.2), 279.2 $[M+Na]^+$ (calc. 279.1), 257.2 $[M+H]^+$ (calc. 257.1). **Calcd.** for $C_{18}H_{12}N_2$ (256.30) C 84.35, H 4.72, N 10.93; found C 84.33, H 4.86, N 10.82 %.

Preparation of 6-phenyl-2,2'-bipyridine (31)

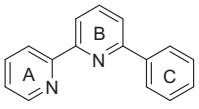

To a solution of 2,2'-bipyridine (7.80 g, 49.9 mmol, 1.00 eq) in dry Et_2O (200 ml), phenyllithium (30.2 ml, 59.9 mmol, 1.20 eq, in dibutylether) was added dropwise at 0 °C whereupon the colour of the solution turned red. After stirring for 2 h at 0 °C, the mixture was hydrolysed by adding H_2O (100 ml). The aqueous phase was separated and extracted three times with Et_2O (each 70 ml). The combined organic layers were dried ($MgSO_4$) and evaporated to dryness. For reoxidation of the rings, the residue was dissolved in acetone (75 ml) and $KMnO_4$ in acetone was added until the colour of the solution stayed purple. Filtering over celite and evaporation of the solvent yielded a brown oil. The crude material was purified by column chromatography (Normasil silica gel 60, 0.040–0.063 mm; Et_2O:hexane = 2:1) and recrystallised from *n*-heptane affording the desired product as an off-white solid (2.20 g, 9.48 mmol, 19 %).

R_f (TLC, silica gel, Et_2O:hexane = 2:1): 0.5. **^{1}H NMR** (500 MHz, $CDCl_3$) δ / ppm 8.75 (d, ^3J = 4.6 Hz, 1H, $H^{6(A)}$), 8.70 (d, ^3J = 8.0 Hz, 1H, $H^{3(A)}$), 8.43 (d,^{3} J = 7.8 Hz, 1H, $H^{3(B)}$), 8.21 (d, ^3J = 7.3 Hz, 2H, $H^{2(C)}$), 7.94 (t, ^3J = 7.8 Hz, 1H, $H^{4(B)}$), 7.90 (td, ^3J = 7.8 Hz, ^4J = 1.7 Hz, , 1H, $H^{4(A)}$), 7.83 (d, ^3J = 7.8 Hz, 1H, $H^{5(B)}$), 7.56 (t, ^3J = 7.5 Hz, 2H, $H^{3(C)}$), 7.49 (t, ^3J = 7.3 Hz, 1H, $H^{4(C)}$), 7.37 (dd, ^3J = 6.9 Hz, ^3J = 5.3 Hz, 1H, $H^{5(A)}$). **^{13}C NMR** (126 MHz, $CDCl_3$) δ / ppm 156.47, 156.41, 155.79, 149.11 ($C^{6(A)}$), 139.40 ($C^{1(C)}$), 137.74 ($C^{4(B)}$), 136.89 ($C^{4(A)}$), 129.06 ($C^{4(C)}$), 128.76 ($C^{3(C)}$), 126.98 ($C^{2(C)}$), 123.77 ($C^{5(A)}$), 121.34 ($C^{3(A)}$), 120.33 ($C^{5(B)}$), 119.33 ($C^{3(B)}$). **IR** (solid): $\tilde{\nu}$ = 3065 (w), 3016 (w), 1987 (w), 1900 (w), 1855 (w), 1809 (w), 1560 (s), 1493 (m), 1475 (m), 1452 (s), 1421 (s), 1398 (s), 1315 (m), 1277 (m), 1259 (m), 1188 (m), 1153 (m), 1095 (m), 1057 (m), 1041 (m), 1020 (m), 987 (s), 964 (m), 922 (m), 910 (w), 899 (w), 827 (m), 791 (s), 754 (s), 716 (s), 689 (s), 642 (s), 615 (s), 581 (s) cm^{-1}. **MS** (ESI, *m/z*): 487.2 $[2M+Na]^+$ (calc. 487.2), 255.1 $[M+Na]^+$ (calc. 255.1). **Calcd.** for $C_{16}H_{12}N_2$ (232.28); C 82.73, H 5.21, N 12.06; found C 82.57, H 5.31, N 11.99 %.

Preparation of 6,6'-diphenyl-2,2'-bipyridine (32)

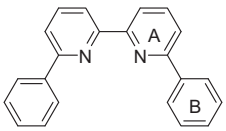

2,2'-Bipyridine (5.50 g, 35.2 mmol, 1.00 eq) was dissolved in THF (130 ml) at –78 °C and phenyllithium (2.0 M solution in dibutylether; 70.9 ml, 0.141 mol, 4.00 eq) was added whereupon the colourless mixture turned into a dark red suspension which was stirred for 15 min at –78 °C. The cooling bath was removed and the mixture was allowed to warm up to room temperature where all remaining solid was dissolved. The solution was stirred at room temperature for 2 h, the temperature was raised and the mixture was stirred at reflux for 4 h. The dark red mixture was cooled down to room temperature again and quenched by slow addition of ice (100 g). THF was removed under vacuo and the remaining two phases were extracted three times with CH_2Cl_2. The combined organic extracts were dried ($MgSO_4$), MnO_2 (70 g, 0.91 mol, 23 eq) was added slowly and the mixture was stirred for 11 h at room temperature. After filtering over Celite, the filtrate was evaporated to dryness. The crude material was purified by column chromatography (Fluka silica gel 60, 0.040–0.063 mm; hexane:CH_2Cl_2 = 2:1 → 1:1) affording the desired product as a white solid (1.26 g, 4.09 mmol, 12 %).

mp 175 – 176 °C. **R_f** (TLC, silica gel, hexane:CH_2Cl_2 = 1:1): 0.5. **^{1}H NMR** (500 MHz, $CDCl_3$) δ / ppm 8.67 (d, ^3J = 7.8 Hz, 2H, $H^{3(A)}$), 8.23 (d, ^3J = 7.4 Hz, 4H, $H^{2(B)}$), 7.97 (t, ^3J = 7.8 Hz, 2H, $H^{4(A)}$), 7.84 (d, ^3J = 7.8 Hz, 2H, $H^{5(A)}$), 7.58 (t, ^3J = 7.6 Hz, 4H, $H^{3(B)}$), 7.50 (t, ^3J = 7.3 Hz, 2H, $H^{4(B)}$). **^{13}C NMR** (126 MHz, $CDCl_3$) δ / ppm 156.36 ($C^{6(A)}$), 155.98 ($C^{2(A)}$), 139.48 ($C^{1(B)}$), 137.66 ($C^{4(A)}$), 129.03 ($C^{4(B)}$), 128.78 ($C^{3(B)}$), 127.00 ($C^{2(B)}$), 120.35 ($C^{5(A)}$), 119.59 ($C^{3(A)}$). **IR** (solid): $\tilde{\nu}$ = 3059 (w), 3040 (w), 1981 (w), 1894 (w), 1813 (w), 1771 (w), 1724 (w), 1690 (w), 1645 (w), 1562 (s), 1495 (m), 1431 (s), 1375 (m), 1288 (m), 1259 (m), 1184 (w), 1151 (m), 1107 (m), 1086 (m), 1020 (m), 987 (m), 920 (m), 806 (m), 754 (s), 687 (s), 625 (s), 582 (s), 453 (s), 434 (s) cm^{-1}. **MS** (ESI, *m/z*): 309.2 $[M+H]^+$ (calc. 309.1), 331.1 $[M+Na]^+$ (calc. 331.1), 639.1 $[2M+Na]^+$ (calc. 639.3). **Calcd.** for $C_{22}H_{16}N_2$ (308.38) C 85.69, H 5.23, N 9.08; found C 85.28, H 5.37, N 8.88 %.

Preparation of 4-(3,5-dimethoxyphenyl)-6-phenyl-2,2'-bipyridine (35)

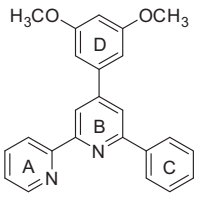

Route A

Acetophenone (6.69 g, 55.7 mmol, 1.00 eq), 3,5-dimethoxybenzaldehyde (9.25 g, 55.7 mmol, 1.00 eq), and powdered NaOH (2.23 g, 55.7 mmol, 1.00 eq) were combined using a mortar and a pestle. The yellow mixture was ground and became stickier, although it never solidified even after 30 min of grinding. 2-Acetylpyridine (6.74 g, 55.7 mmol, 1.00 eq) was added and everything was mixed together until the material was too viscous to grind. The mortar with the substance was placed in a desiccator overnight. The following day, the ochre mixture was powdered and was then transferred to a round-bottom flask. Ammonium acetate (28.9 g, 0.375 mol, 6.70 eq) and PEG-300 (90 ml) were added and the mixture heated to 100 °C and stirred for 16 h. The brown solution was then cooled down to room temperature and water (300 ml) was added whereupon a sticky ochre material precipitated. The supernatant solution was decanted, the residue was washed twice with water (100 ml each) and dissolved in Et_2O (200 ml). The brown solution was evaporated to dryness to give a mixture of a solid and an oil. Everything was dissolved in CH_2Cl_2 and washed once with $NaHCO_3$ (half saturated) and twice with water. The organic layer was dried ($MgSO_4$) and evaporated to dryness to give a brown, sticky oil. The crude material was purified by column chromatography (Normasil silica gel 60, 0.040–0.063 mm; CH_2Cl_2 → Et_2O:hexane = 1:1 → 2:1) followed by a subsequent column chromatography (Fluka silica gel 60, 0.040–0.063 mm; Et_2O:hexane = 1:2 → 2:3 → 1:1 → 2:1) and recrystallised from *n*-heptane affording the desired product as an off-white solid (4.97 g, 13.5 mmol, 24 %).

R_f (TLC, silica gel, Et_2O:hexane = 2:1): 0.5. **^{1}H NMR** (500 MHz, $CDCl_3$) δ / ppm 8.72 (d, ^3J = 4.6 Hz, 1H, $H^{6(A)}$), 8.69 (d, ^3J = 7.9 Hz, 1H, $H^{3(A)}$), 8.62 (d, ^4J = 2.1 Hz, 1H, $H^{3(B)}$), 8.20 (d, ^3J = 7.2 Hz, 2H, $H^{2(C)}$), 7.95 (d, ^4J = 1.3 Hz, 1H, $H^{5(B)}$), 7.88 (t, ^3J = 7.7 Hz, 1H, $H^{4(A)}$), 7.53 (t, ^3J = 7.5 Hz, 2H, $H^{3(C)}$), 7.46 (t, ^3J = 7.3 Hz, 1H, $H^{4(C)}$), 7.36 (t, ^3J = 6.1 Hz, 1H, $H^{5(A)}$), 6.94 (d, ^4J = 2.2 Hz, 2H, $H^{2(D)}$), 6.57 (t, ^4J = 2.1 Hz, 1H, $H^{4(D)}$), 3.89 (s, 6H, $OC\underline{H}_3$). **^{13}C NMR** (126 MHz, $CDCl_3$) δ / ppm 161.43 ($C^{3(D)}$), 157.30 ($C^{6(B)}$), 156.47 ($C^{2(A)}$/$C^{2(B)}$), 156.40 ($C^{2(A)}$/$C^{2(B)}$), 150.56 ($C^{4(B)}$), 149.07 ($C^{6(A)}$), 141.18 ($C^{1(D)}$), 139.56 ($C^{1(C)}$), 137.06 ($C^{4(A)}$), 129.28 ($C^{4(C)}$), 128.91 ($C^{3(C)}$), 127.24 ($C^{2(C)}$), 124.02 ($C^{5(A)}$), 121.81 ($C^{3(A)}$), 118.89 ($C^{5(B)}$), 117.83 ($C^{3(B)}$), 105.65 ($C^{2(D)}$), 101.05 ($C^{4(D)}$), 55.76 ($O\underline{C}H_3$).

Route B

Acetophenone (14.5 ml, 0.124 mol, 1.00 eq) and 3,5-dimethoxybenzaldehyde (20.7 g, 0.124 mol, 1.00 eq) were dissolved in MeOH (10 ml) and NaOH (15.3 g, 0.383 mol, 3.10 eq) in MeOH (157 ml) was added whereupon a small amount of precipitate was formed. The mixture was stirred for 16 h at room temperature until bigger chunks of solid were formed. The mixture was filtered and the residue was washed with ice-cold water (130 ml), ice-cold MeOH (50 ml) and dried in a desiccator to give 3-(3,5-dimethoxyphenyl)-1-phenylprop-2-en-1-one (**33**) as a yellowish solid (29.0 g) which was pure enough (by NMR) to be used for subsequent reactions.

A solution of 2-acetylpyridine (16.8 ml, 0.150 mol, 1.00 eq) in dry pyridine (40 ml) was treated with iodine (38.1 g, 0.150 mol, 1.00 eq) in dry pyridine (110 ml) at room temperature. This mixture was heated and stirred for 3 h at 100 °C whereafter it was cooled down to room temperature and allowed to stand overnight. The crude material was filtered off and the residue was washed with pyridine (100 ml) and cold EtOH (40 ml). Three recrystallisations from 18 % EtOH in H_2O afforded 1-(2-pyridinylcarbonyl)pyridinium iodide (**36**) as creamy crystals (31.9 g, 97.7 mmol, 65 %) which was pure enough (by NMR) to be used for subsequent reactions.

A suspension of 3-(3,5-dimethoxyphenyl)-1-phenylprop-2-en-1-one (**33**) (19.4 g, 72.5 mmol, 1.00 eq), 1-(2-pyridinylcarbonyl)pyridinium iodide (**36**) (23.6 g, 72.5 mmol, 1.00 eq) and ammonium acetate (55.9 g, 0.725 mol, 10.0 eq) was heated to reflux in MeOH (150 ml). The solution was stirred at reflux for 8 h. After cooling to room temperature, the solvent was removed in vacuo. Water (700 ml) was added to the residue and the aqueous phase was extracted three times with EtOAc (total 900 ml). The combined organic extracts were washed once with water (700 ml), dried ($MgSO_4$) and evaporated to dryness to give a brown sticky oil. The crude material was purified by column chromatography (Fluka silica gel 60, 0.040–0.063 mm; CH_2Cl_2:MeOH = 100:1 → hexane:ethyl acetate = 3:1), another column chromatography (Fluka silica gel 60, 0.040–0.063 mm; CH_2Cl_2:MeOH = 100:1 → 50:1), a further column chromatography (Fluka silica gel 60, 0.040-0.063 mm; CH_2Cl_2 → hexane:ethyl acetate = 3:1), followed by a subsequent Alox chromatography (Merck Alox 90; hexane:ethyl acetate:CH_2Cl_2 = 15:1:2 → 10:1:2) yielding the desired product as a white powder (5.34 g, 14.5 mmol, 20 %, 17 % overall).

R_f (TLC, silica gel, hexane: ethyl acetate = 2:1): 0.5. **^{1}H NMR** (500 MHz, $CDCl_3$) δ / ppm 8.72 (d, ^3J = 4.0 Hz, 1H, $H^{6(A)}$), 8.68 (d, ^3J = 8.0 Hz, 1H, $H^{3(A)}$), 8.61 (d, ^4J = 1.4 Hz, 1H, $H^{3(B)}$), 8.20 (d, ^3J = 7.3 Hz, 2H, $H^{2(C)}$), 7.95 (d, ^4J = 1.4 Hz, 1H, $H^{5(B)}$), 7.87 (td, ^3J = 7.7 Hz, ^4J = 1.7 Hz, 1H, $H^{4(A)}$), 7.54 (t, ^3J = 7.5 Hz, 2H, $H^{3(C)}$), 7.46 (t, ^3J = 7.3 Hz, 1H, $H^{4(C)}$), 7.35 (ddd, ^3J = 7.4 Hz, ^3J = 4.8 Hz, ^4J = 0.8 Hz, 1H, $H^{5(A)}$), 6.94 (d, ^4J = 2.2 Hz, 2H, $H^{2(D)}$), 6.57 (t, ^4J = 2.2 Hz, 1H, $H^{4(D)}$), 3.89 (s, 6H, $OC\underline{H}_3$). **^{13}C NMR** (126 MHz, $CDCl_3$) δ / ppm 161.42 ($C^{3(D)}$), 157.26 ($C^{6(B)}$), 156.48 ($C^{2(A)}$/$C^{2(B)}$), 156.41 ($C^{2(A)}$/$C^{2(B)}$), 150.53 ($C^{4(B)}$), 149.19 ($C^{6(A)}$), 141.23 ($C^{1(D)}$), 139.58 ($C^{1(C)}$), 137.03 ($C^{4(A)}$), 129.25 ($C^{4(C)}$), 128.91 ($C^{3(C)}$), 127.24 ($C^{2(C)}$), 123.98 ($C^{5(A)}$), 121.71 ($C^{3(A)}$), 118.84 ($C^{5(B)}$), 117.76 ($C^{3(B)}$), 105.65 ($C^{2(D)}$), 101.01 ($C^{4(D)}$), 55.74 ($O\underline{C}H_3$). **IR** (solid): $\tilde{\nu}$ = 3055 (w), 3009 (w), 2976 (w), 1954 (w), 1595 (s), 1583 (s), 1545 (s), 1445 (s), 1389 (s), 1331 (m), 1286 (m), 1200 (s), 1151 (s), 1063 (s), 987 (w), 928 (w), 906 (w), 849 (m), 825 (s), 791 (s), 770 (s), 731 (m), 689 (s), 662 (s), 652 (s), 640 (s), 617 (s), 579 (m) cm^{-1}. **MS** (ESI, *m/z*): 759.9 $[2M+Na]^+$ (calc. 759.3). **Calcd.** for $C_{24}H_{20}N_2O_2$ (368.43) C 78.24, H 5.47, N 7.60; found C 78.03, H 5.47, N 7.45 %.

Preparation of 4-(3,5-dihydroxyphenyl)-6-phenyl-2,2'-bipyridine (37)

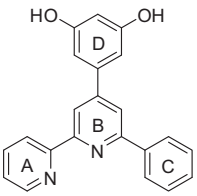

4-(3,5-Dimethoxyphenyl)-6-phenyl-2,2'-bipyridine (**35**) (4.27 g, 11.6 mmol, 1.00 eq) and pyridinium chloride (67 g, 0.58 mol, 50 eq; prepared by slow addition of equimolar amounts of aqueous HCl to ice-cooled pyridine followed by water removal under vacuo) were mixed and stirred at reflux for 2.5 h under an inert atmosphere of N_2. The reaction mixture was cooled down from ca. 250 °C to ca. 160 °C (still molten) and poured into water (2 l) whereupon a white solid immediately precipitated. Measuring with a pH-electrode, the aqueous phase was adjusted from pH = 2.7 to pH = 6.2 with saturated aqueous $NaHCO_3$ (ca. 550 ml). The precipitate was filtered off, washed well with water (1 l), powdered and dried in the desiccator yielding the desired product as an off-white powder (4.18 g, M·H_2O, 11.5 mmol, 99 %).

R_f (TLC, silica gel, CH_2Cl_2:MeOH = 10:1): 0.5. **^{1}H NMR** (500 MHz, CD_3OD) δ / ppm 8.67 (d, ^3J = 4.1 Hz, 1H, $H^{6(A)}$), 8.60 (d, ^3J = 8.0 Hz, 1H, $H^{3(A)}$), 8.43 (d, ^4J = 1.2 Hz, 1H, $H^{3(B)}$), 8.20 (d, ^3J = 7.3 Hz, 2H, $H^{2(C)}$), 8.01 (d, ^4J = 1.3 Hz, 1H, $H^{5(B)}$), 7.98 (td, ^3J = 7.8 Hz, J = 1.6 Hz, 1H, $H^{4(A)}$), 7.52 (t, ^3J = 7.5 Hz, 2H, $H^{3(C)}$), 7.48 – 7.43 (m, 2H, $H^{5(A)}$ + $H^{4(C)}$), 6.78 (d, ^4J = 2.1 Hz, 2H, $H^{2(D)}$), 6.40 (t, ^4J = 2.0 Hz, 1H, $H^{4(D)}$). **^{13}C NMR** (126 MHz, CD_3OD) δ / ppm 160.62 ($C^{3(D)}$), 158.91 ($C^{6(B)}$), 157.75 ($C^{2(A)}$), 157.29 ($C^{2(B)}$), 152.25 ($C^{4(B)}$), 150.17 ($C^{6(A)}$), 141.85 ($C^{1(D)}$), 140.70 ($C^{1(C)}$), 138.96 ($C^{4(A)}$), 130.41 ($C^{4(C)}$), 129.96 ($C^{3(C)}$), 128.30 ($C^{2(C)}$), 125.52 ($C^{5(A)}$), 123.24 ($C^{3(A)}$), 119.49 ($C^{5(B)}$), 118.55 ($C^{3(B)}$), 106.73 ($C^{2(D)}$), 104.60 ($C^{4(D)}$). **IR** (solid): $\tilde{\nu}$ = 3306 (w), 3198 (w), 3061 (w), 2644 (w), 1981 (w), 1794 (w), 1686 (w), 1587 (s), 1549 (s), 1497 (m), 1475 (m),

1443 (w), 1400 (m), 1373 (w), 1344 (w), 1304 (m), 1259 (w), 1159 (s), 1088 (w), 1001 (s), 829 (s), 787 (m), 770 (s), 727 (m), 687 (s), 660 (s), 636 (s), 617 (s) cm^{-1}. **MS** (ESI, *m/z*): 703.6 $[2M+Na]^+$ (calc. 703.2); 363.5 $[M+Na]^+$ (calc. 363.1). **Calcd.** for $C_{22}H_{16}N_2O_2 \cdot H_2O$ (358.39) C 73.73, H 5.06, N 7.82; found C 74.15, H 5.05, N 7.77 %.

Preparation of 4-(3,5-bis(decyloxy)phenyl)-6-phenyl-2,2'-bipyridine (38)

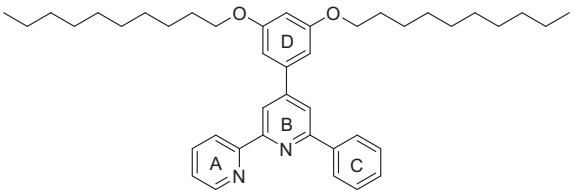

A mixture of 1-bromodecane (0.38 ml, 1.8 mmol, 2.5 eq), 4-(3,5-dihydroxyphenyl)-6-phenyl-2,2'-bipyridine (**37**) (250 mg, 0.734 mmol, 1.00 eq), 18-crown-6 (39 mg, 0.15 mmol, 0.20 eq), and K_2CO_3 (406 mg, 2.94 mmol, 4.00 eq) in dry acetone (3 ml) was placed in a microwave reactor and heated for 60 min at 120 °C under a pressure of 7 bar. The solvent was evaporated to dryness and water (50 ml) was added to the residue. This was extracted three times with ethyl acetate (each 50 ml). The combined organic layers were dried ($MgSO_4$) and evaporated to dryness. The crude material was purified by column chromatography (Merck Alox 90; hexane:ethyl acetate:CH_2Cl_2 = 30:1:2), followed by a subsequent column chromatography (Fluka silica gel 60, 0.040–0.063 mm; hexane:ethyl acetate = 8:1) yielding the desired product as a white solid (428 mg, 0.689 mmol, 94 %).

$\mathbf{R_f}$ (TLC, silica gel, hexane:ethyl acetate = 8:1): 0.4. **^{1}H NMR** (500 MHz, $CDCl_3$) δ / ppm 8.72 (d, ^3J = 4.7 Hz, 1H, $H^{6(A)}$), 8.69 (d, ^3J = 7.9 Hz, 1H, $H^{3(A)}$), 8.61 (s, 1H, $H^{3(B)}$), 8.21 (d, ^3J = 7.5 Hz, 2H, $H^{2(C)}$), 7.96 (s, 1H, $H^{5(B)}$), 7.87 (t, ^3J = 7.7 Hz, 1H, $H^{4(A)}$), 7.53 (t, ^3J = 7.6 Hz, 2H, $H^{3(C)}$), 7.46 (t, J = 7.3 Hz, 1H, $H^{4(C)}$), 7.34 (dd, ^3J = 7.3 Hz, ^3J = 4.9 Hz, 1H, $H^{5(A)}$), 6.93 (d, ^4J = 1.8 Hz, 2H, $H^{2(D)}$), 6.56 (t, ^4J = 1.9 Hz, 1H, $H^{4(D)}$), 4.03 (t, ^3J = 6.5 Hz, 4H, $OC\underline{H}_2CH_2CH_2$), 1.86 – 1.78 (m, 4H, $OCH_2C\underline{H}_2CH_2$), 1.53 – 1.45 (m, 4H, $OCH_2CH_2C\underline{H}_2$), 1.42 – 1.21 (m, 24H, $OCH_2CH_2CH_2(C\underline{H}_2)_6CH_3$), 0.88 (t, ^3J = 6.8 Hz, 6H, $O(CH_2)_9C\underline{H}_3$). **^{13}C NMR** (126 MHz, $CDCl_3$) δ / ppm 160.95 ($C^{3(D)}$), 157.20 ($C^{6(B)}$), 156.54 ($C^{2(A)}$/$C^{2(B)}$), 156.37 ($C^{2(A)}$/$C^{2(B)}$), 150.62 ($C^{4(B)}$), 149.19 ($C^{6(A)}$), 140.98 ($C^{1(D)}$), 139.63 ($C^{1(C)}$), 137.01 ($C^{4(A)}$), 129.21 ($C^{4(C)}$), 128.88 ($C^{3(C)}$), 127.24 ($C^{2(C)}$), 123.93 ($C^{5(A)}$), 121.70 ($C^{3(A)}$), 118.82 ($C^{5(B)}$), 117.73 ($C^{3(B)}$), 106.12 ($C^{2(D)}$), 101.76 ($C^{4(D)}$), 68.43 ($O\underline{C}H_2$), 32.05 ($O(\underline{C}H_2)_9$), 29.75 ($O(\underline{C}H_2)_9$), 29.72 ($O(\underline{C}H_2)_9$), 29.57 ($O(\underline{C}H_2)_9$), 29.48 ($O(\underline{C}H_2)_9$), 29.47 ($O(\underline{C}H_2)_9$), 26.23 ($OCH_2C\underline{H}_2CH_2$), 22.83 ($O(\underline{C}H_2)_9$), 14.27 ($O(CH_2)_9\underline{C}H_3$). **IR** (solid): $\tilde{\nu}$ = 3059 (w), 2922 (s), 2853 (m), 1582 (s), 1551 (m), 1466 (w), 1456 (w), 1385 (m), 1306 (m), 1259 (w), 1173 (s), 1082 (w), 1047 (m), 986 (w), 908 (w), 881 (w), 851 (w), 829 (m), 814 (w), 793 (m), 775 (m), 735 (m), 723 (m), 689 (s), 667 (m), 640 (w), 617 (w), 598 (w), 581 (w) cm^{-1}. **MS** (ESI, *m/z*): 1264.9 $[2M+Na]^+$ (calc. 1263.9). **Calcd.** for $C_{42}H_{56}N_2O_2$ (620.91) C 81.24, H 9.09, N 4.51; found C 81.32, H 9.10, N 4.30 %.

Preparation of 4-(3,5-bis(3,5-bis(dodecyloxy)benzyloxy)phenyl)-6-phenyl-2,2'-bipyridine (**39**)

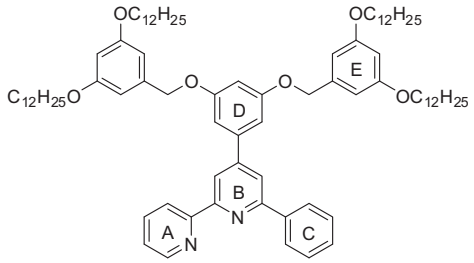

A mixture of 3,5-bis(dodecyloxy)benzyl methanesulfonate (**9**) (611 mg, ca. 80 % pure, 0.881 mmol, 3.00 eq), 4-(3,5-dihydroxyphenyl)-6-phenyl-2,2'-bipyridine (**37**) (100 mg, 0.294 mmol, 1.00 eq), 18-crown-6 (16 mg, 0.059 mmol, 0.20 eq), and K_2CO_3 (162 mg, 1.18 mmol, 4.00 eq) in dry acetone (3 ml) was placed in a microwave reactor and heated for 60 min at 100 °C under a pressure of 2 bar. The solvent was evaporated to dryness and water (50 ml) was added to the residue. This was extracted three times with ethyl acetate (each 50 ml). The combined organic layers were dried ($MgSO_4$) and evaporated to dryness. The crude material was purified by Alox chromatography (Merck Alox 90; hexane:ethyl acetate:CH_2Cl_2 = 45:1:2 → 30:1:2), followed by a subsequent column chromatography (Fluka silica gel 60, 0.040–0.063 mm; hexane:ethyl acetate = 10:1) and another column chromatography (Fluka silica gel 60, 0.040–0.063 mm; hexane:ethyl acetate = 15:1) yielding the desired product as a white solid (229 mg, 0.182 mmol, 62 %).

R_f (TLC, silica gel, hexane:ethyl acetate = 8:1): 0.2. **^{1}H NMR** (500 MHz, $CDCl_3$) δ / ppm 8.72 (d, ^3J = 4.5 Hz, 1H, $H^{6(A)}$), 8.69 (d, ^3J = 7.9 Hz, 1H, $H^{3(A)}$), 8.62 (d, ^4J = 1.2 Hz, 1H, $H^{3(B)}$), 8.20 (d, ^3J = 7.4 Hz, 2H, $H^{2(C)}$), 7.93 (d, ^4J = 1.2 Hz, 1H, $H^{5(B)}$), 7.87 (td, ^3J = 7.7 Hz, ^4J = 1.7 Hz, 1H, $H^{4(A)}$), 7.54 (t, ^3J = 7.6 Hz, 2H, $H^{3(C)}$), 7.46 (t, ^3J = 7.3 Hz, 1H, $H^{4(C)}$), 7.35 (dd, ^3J = 7.0 Hz, ^3J = 5.2 Hz, 1H, $H^{5(A)}$), 7.05 (d, ^4J = 2.1 Hz, 2H, $H^{2(D)}$), 6.71 (t, ^4J = 2.0 Hz, 1H, $H^{4(D)}$), 6.61 (d, ^4J = 2.0 Hz, 4H, $H^{2(E)}$), 6.43 (t, ^4J = 2.0 Hz, 2H, $H^{4(E)}$), 5.05 (s, 4H, $Ar_DOC\underline{H}_2Ar_E$), 3.95 (t, ^3J = 6.6 Hz, 8H, $OC\underline{H}_2CH_2CH_2$), 1.80 – 1.73 (m, 8H, $OCH_2C\underline{H}_2CH_2$), 1.48 – 1.40 (m, 8H, $OCH_2CH_2C\underline{H}_2$), 1.37 – 1.21 (m, 64H, $OCH_2CH_2CH_2(C\underline{H}_2)_8CH_3$), 0.88 (t, ^3J = 6.9 Hz, 12H, $O(CH_2)_{11}C\underline{H}_3$). **^{13}C NMR** (126 MHz, $CDCl_3$) δ / ppm 160.72 ($C^{3(E)}$), 160.56 ($C^{3(D)}$), 157.24 ($C^{6(B)}$), 156.49 ($C^{2(A)}$/$C^{2(B)}$), 156.42 ($C^{2(A)}$/$C^{2(B)}$), 150.30 ($C^{4(B)}$), 149.20 ($C^{6(A)}$), 141.06 ($C^{1(D)}$), 139.54 ($C^{1(C)}$), 138.94 ($C^{1(E)}$), 137.02 ($C^{4(A)}$), 129.24 ($C^{4(C)}$), 128.90 ($C^{3(C)}$), 127.22 ($C^{2(C)}$), 123.96 ($C^{5(A)}$), 121.69 ($C^{3(A)}$), 118.72 ($C^{5(B)}$), 117.64 ($C^{3(B)}$), 106.86 ($C^{2(D)}$), 105.90 ($C^{2(E)}$), 102.51 ($C^{4(D)}$), 101.10 ($C^{4(E)}$), 70.54 ($Ar_DO\underline{C}H_2Ar_E$), 68.25 ($O\underline{C}H_2(CH_2)_{10}CH_3$), 32.07 ($OCH_2(\underline{C}H_2)_{10}CH_3$), 29.82 ($OCH_2(\underline{C}H_2)_{10}CH_3$), 29.79 ($OCH_2(\underline{C}H_2)_{10}CH_3$), 29.76 ($OCH_2(\underline{C}H_2)_{10}CH_3$), 29.74 ($OCH_2(\underline{C}H_2)_{10}CH_3$), 29.57 ($OCH_2(\underline{C}H_2)_{10}CH_3$), 29.50 ($OCH_2(\underline{C}H_2)_{10}CH_3$), 29.42 ($OCH_2(\underline{C}H_2)_{10}CH_3$), 26.21 ($OCH_2CH_2\underline{C}H_2$), 22.84 ($OCH_2(\underline{C}H_2)_{10}CH_3$), 14.28 ($O(CH_2)_{11}\underline{C}H_3$). **IR** (solid): $\tilde{\nu}$ = 3059 (w), 2918 (s), 2849 (s), 1593 (s), 1553 (w), 1450 (m), 1377 (m), 1346 (w), 1325 (w), 1296 (m), 1155 (s), 1053 (s), 1014 (w), 825 (m), 793 (w), 775 (w), 737 (w), 719 (w), 689 (w), 609 (w), 582 (w) cm^{-1}. **MS** (ESI, *m/z*): 1281.0 $[M+Na]^+$ (calc. 1279.9). **Calcd.** for $C_{84}H_{124}N_2O_6$ (1257.89) C 80.21, H 9.94, N 2.23; found C 80.03, H 9.80, N 2.06 %.

Preparation of 4-(3,5-bis(3,5-bis(3,5-bis(dodecyloxy)benzyloxy)benzyloxy)phenyl)-6-phenyl-2,2'-bipyridine (40)

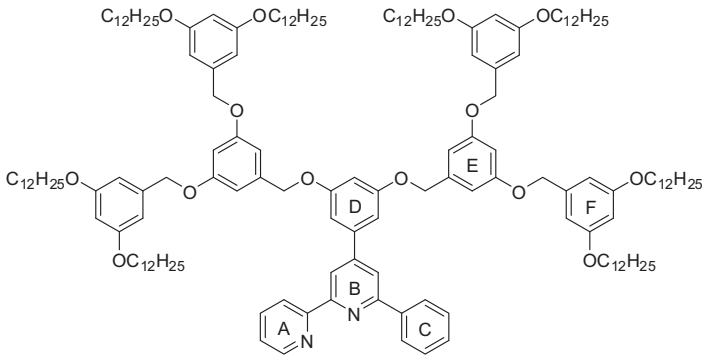

A mixture of 3,5-bis(3,5-bis(dodecyloxy)benzyloxy)benzyl methanesulfonate (**21**) (834 mg, ca. 80 % pure, 0.588 mmol, 2.50 eq), 4-(3,5-dihydroxyphenyl)-6-phenyl-2,2'-bipyridine (**37**) (80 mg, 0.235 mmol, 1.00 eq), 18-crown-6 (12 mg, 0.047 mmol, 0.20 eq), and K_2CO_3 (130 mg, 0.940 mmol, 4.00 eq) in dry acetone (4 ml) was placed in a microwave reactor and heated for 60 min at 100 °C under a pressure of 4 bar. The solvent was evaporated to dryness and water (50 ml) was added to the residue. This was extracted three times with ethyl acetate (each 50 ml). The combined organic layers were dried ($MgSO_4$) and evaporated to dryness. The crude material was purified by column chromatography (Merck Alox 90; hexane:ethyl acetate:CH_2Cl_2 = 45:1:2 → 30:1:2 → 20:1:2), followed by a subsequent column chromatography (Fluka silica gel 60, 0.040–0.063 mm; hexane:ethyl acetate = 20:1) yielding the desired product as a white solid (425 mg, 0.176 mmol, 75 %).

R_f (TLC, silica gel, hexane:ethyl acetate = 8:1): 0.4. **^{1}H NMR** (500 MHz, $CDCl_3$) δ / ppm 8.73 – 8.69 (m, 2H, $H^{6(A)}$ + $H^{3(A)}$), 8.65 (s, 1H, $H^{3(B)}$), 8.22 (d, ^3J = 8.0 Hz, 2H, $H^{2(C)}$), 7.95 (s, 1H, $H^{5(B)}$), 7.87 (t, ^3J = 8.0 Hz, 1H, $H^{4(A)}$), 7.53 (t, ^3J = 7.6 Hz, 2H, $H^{3(C)}$), 7.45 (t, ^3J = 7.0 Hz, 1H, $H^{4(C)}$), 7.34 (dd, ^3J = 7.4 Hz, ^3J = 4.8 Hz, 1H, $H^{5(A)}$), 7.07 (d, ^4J = 1.6 Hz, 2H, $H^{2(D)}$), 6.75 (d, ^4J = 1.6 Hz, 4H, $H^{2(E)}$), 6.73 (s, 1H, $H^{4(D)}$), 6.61 (s, 2H, $H^{4(E)}$), 6.57 (d, ^4J = 1.7 Hz, 8H, $H^{2(F)}$), 6.41 (s, 4H, $H^{4(F)}$), 5.08 (s, 4H, $Ar_DOC\underline{H}_2Ar_E$), 4.98 (s, 8H, $Ar_EOC\underline{H}_2Ar_F$), 3.93 (t, ^3J = 6.6 Hz, 16H, $OC\underline{H}_2CH_2CH_2$), 1.80 – 1.72 (m, 16H, $OCH_2C\underline{H}_2CH_2$), 1.48 – 1.39 (m, 16H, $OCH_2CH_2C\underline{H}_2$), 1.38 – 1.20 (m, 128H, $OCH_2CH_2CH_2(C\underline{H}_2)_8CH_3$), 0.89 (t, ^3J = 6.9 Hz, 24H, $O(CH_2)_{11}C\underline{H}_3$). **^{13}C NMR** (126 MHz, $CDCl_3$) δ / ppm 160.64 ($C^{3(F)}$), 160.50 ($C^{3(D)}$), 160.36 ($C^{3(E)}$), 157.22 ($C^{6(B)}$), 156.45 ($C^{2(A)}$/$C^{2(B)}$), 156.41 ($C^{2(A)}$/$C^{2(B)}$), 150.19 ($C^{4(B)}$), 149.19 ($C^{6(A)}$), 141.07 ($C^{1(D)}$), 139.48 ($C^{1(C)}$), 139.15 ($C^{1(E)}$), 139.02 ($C^{1(F)}$), 136.96 ($C^{4(A)}$), 129.22 ($C^{4(C)}$), 128.88 ($C^{3(C)}$), 127.19 ($C^{2(C)}$), 123.93 ($C^{5(A)}$), 121.64 ($C^{3(A)}$), 118.66 ($C^{5(B)}$), 117.60 ($C^{3(B)}$), 106.88 ($C^{2(D)}$), 106.55 ($C^{2(E)}$), 105.87 ($C^{2(F)}$), 102.43 ($C^{4(D)}$), 101.87 ($C^{4(E)}$), 100.96 ($C^{4(F)}$), 70.41 ($Ar_DO\underline{C}H_2Ar_E$), 70.34 ($Ar_EO\underline{C}H_2Ar_F$), 68.19 ($O\underline{C}H_2(CH_2)_{10}CH_3$), 32.06 ($OCH_2(\underline{C}H_2)_{10}CH_3$), 29.81 ($OCH_2(\underline{C}H_2)_{10}CH_3$), 29.78 ($OCH_2(\underline{C}H_2)_{10}CH_3$), 29.76 ($OCH_2(\underline{C}H_2)_{10}CH_3$), 29.73 ($OCH_2(\underline{C}H_2)_{10}CH_3$), 29.56 ($OCH_2(\underline{C}H_2)_{10}CH_3$), 29.50 ($OCH_2(\underline{C}H_2)_{10}CH_3$), 29.41 ($OCH_2(\underline{C}H_2)_{10}CH_3$), 26.20 ($OCH_2CH_2\underline{C}H_2$), 22.83 ($OCH_2(\underline{C}H_2)_{10}CH_3$), 14.27 ($O(CH_2)_{11}\underline{C}H_3$). **IR** (solid): $\tilde{\nu}$ = 3061 (w), 2920 (s), 2851 (m), 1595 (s), 1452 (m), 1367 (m), 1331 (w), 1308 (w), 1153 (s), 1053 (m), 831 (m), 797 (m), 721 (s), 683 (s), 638 (s), 619 (s) cm^{-1}. **Calcd.** for $C_{160}H_{244}N_2O_{14}$ (2419.65) C 79.42, H 10.16, N 1.16; found C 79.37, H 10.03, N 1.08 %.

Chapter 7

Synthesis and STM Imaging of Cyclometallated Iridium(III) Complexes

7.1
Introduction and aims

In this chapter, syntheses and properties of cyclometallated Ir(III) complexes will be discussed. The desired complexes are obtained *via* a chloro-bridged Ir(III) dimer and are suitable for electroluminescence as it will be shown in **Chapter 8**. Two of the complexes were already known (see **Scheme 7.1**), *i.e.* **47**[276] and **49**[277, 278], and *Neve et al.* synthesised Ir(III) complexes similar to **52** – **56**.[247]

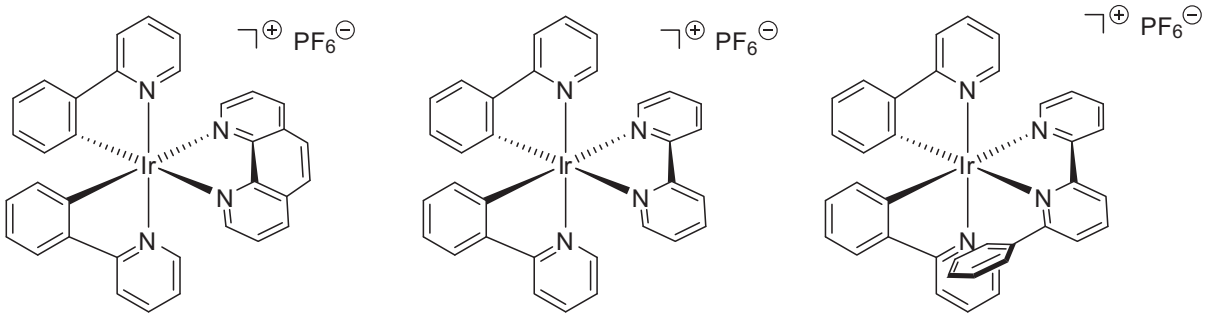

47 **49** **50**

Scheme 7.1 Structures of the previously known complexes **47** and **49** and the model compound **50**.

Because of the very promising findings of a former member of our research group,[123] *K. Doyle* (see **Chapter 8**), in regards of the device stability for complexes having 6-phenyl-derivatised 2,2'-bipyridines, the first complex synthesised and characterised by the author was complex **50** as a model compound. As the device stability was even higher after this ligand modification, this effect was studied in further detail. Therefore, three main goals are pursued in this chapter. Firstly, in order to understand, rationalise, and, ideally, also enhance the aforementioned device stability, a series of *N*,*N'*-ligands, the syntheses of which are mostly described in the previous chapter, was used for the preparation of Ir(III) complexes in a systematic approach. Secondly, as it is of crucial importance for their real-world application in solid state lighting, colour tuning of the emission was investigated by varying the *C*,*N*-ligands which are known to possess a considerable impact on the HOMO/LUMO energy levels (see also **Chapter 1**).[279, 280] Thirdly, monolayer behaviour on surfaces was studied by dendronised Ir(III) complexes to facilitate adsorption on HOPG. The justification of this goal is the relevance of solid state properties in the device. STM studies on HOPG of neutral and charged complexes have been done before,[281-285] also by *L. Scherer* in our research group,[286] but still, there are not too many results published in this field.

In combination with the collaborator's results presented in the following chapter, many of the herein described results were published.[123, 124, 137]

7.2 Synthesis and discussion

7.2.1 Cyclometallated Ir(III) dimers

To start with, all syntheses of the cyclometallated Ir(III) dimers as precursors for the $[Ir(C^N)_2(N^N)]^+[PF_6]^-$ complexes were performed according to the literature[96, 287] by *L. Siegfried* in our group. For $[Ir(ppy\text{-}C,N)_2(\mu\text{-}Cl)]_2$ (**41**), iridium(III) chloride hydrate and 2-phenylpyridine (Hppy) were refluxed in a mixture of 2-ethoxyethanol and water (3:1 v/v) for 24 h (**Scheme 7.2**). After cooling the solution to room temperature, the precipitate was collected, washed with ethanol and acetone, and then dissolved in dichloromethane and filtered. A mixture of toluene and hexane (5:2 v/v) was added to precipitate the desired cyclometallated chloro-bridged Ir(III) dimer **41**. X-Ray crystal structures of these types of compounds[288, 289] imply that the Ir–C bond exerts a significant *trans*-effect which favours formation of the Ir–Cl bridge bonds *trans* to the Ir–C bond.[287] On these grounds, the structure illustrated in **Scheme 7.2** is favoured compared to the isomer where the C- and N-donor atoms lie in a *trans* manner to each other. Although two other isomers which are enantiomers are potentially formed (**Scheme 7.3**), they are not distinguishable in NMR experiments and will lead to the same Ir(III) complexes upon reacting with an *N*,*N*′-ligand.

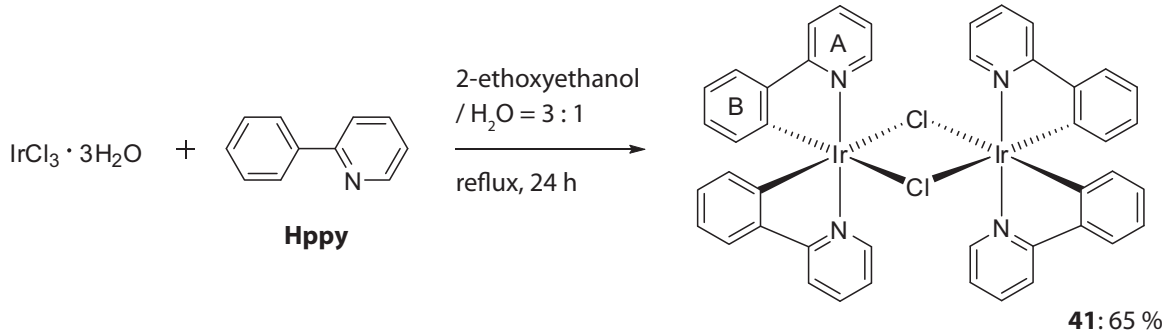

Scheme 7.2 Synthesis of Ir(III) dimer $[Ir(ppy\text{-}C,N)_2(\mu\text{-}Cl)]_2$ (**41**). Ring labels are for NMR spectroscopic assignments (**Figure 7.1**).

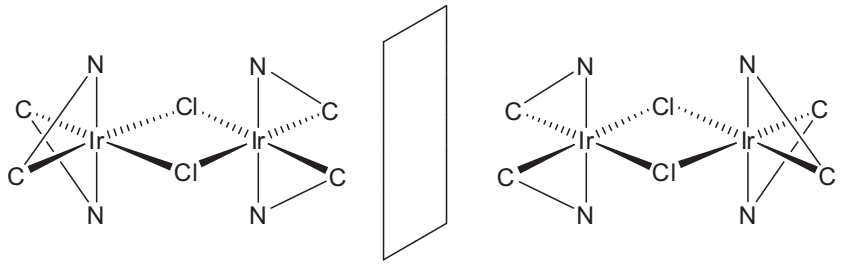

Scheme 7.3 Racemate of $[Ir(C^N)_2(\mu\text{-}Cl)]_2$ which is potentially formed in the synthesis of the cyclometallated Ir(III) dimers (schematic representation).

Figure 7.1 depicts the proton NMR of the cyclometallated Ir(III) dimer **47** illustrating the presence of one species in solution. Proton $H^{6(B)}$, next to the coordinated carbon atom, exhibits a dramatic high-field shift, whereas proton $H^{6(A)}$, neighbouring the N atom, exhibits a shift in the other direction. As we will see later (**Figure 7.2**), the latter proton will shift again dramatically upon complexation with an *N*,*N*′-ligand, making this signal a diagnostic probe for changes in coordination pattern.

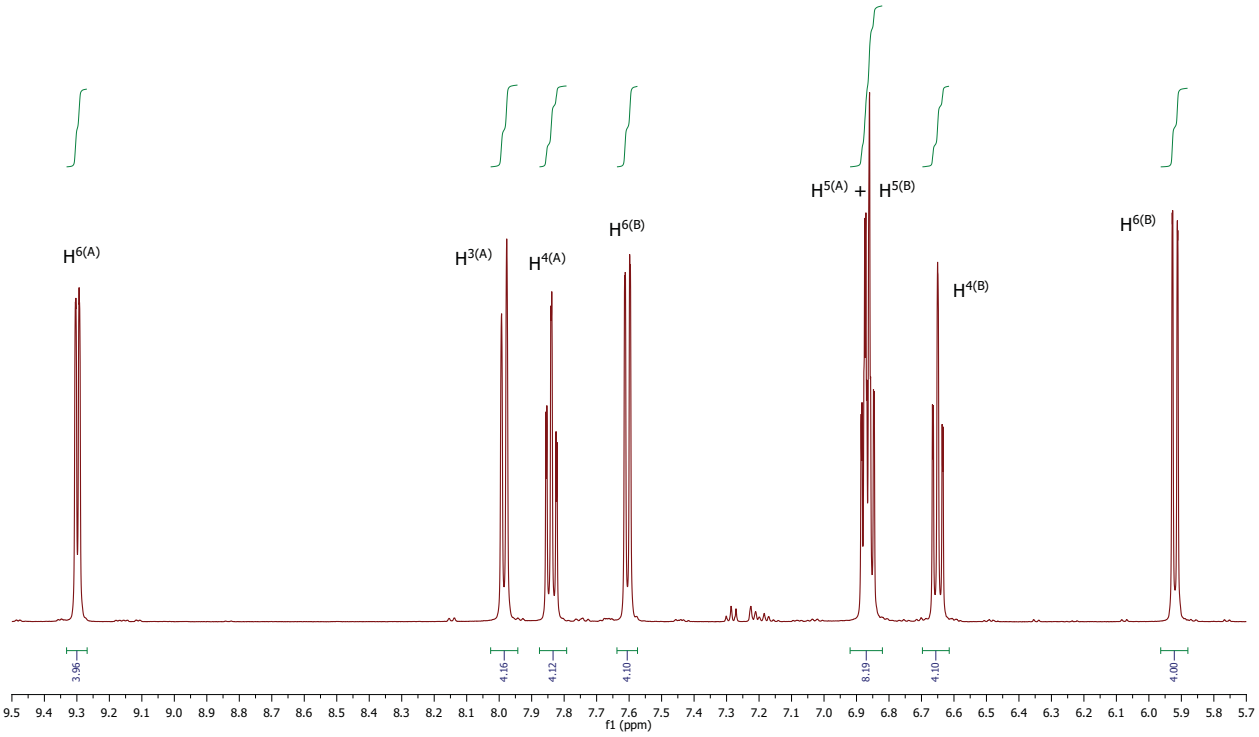

Figure 7.1 500 MHz ^{1}H NMR spectrum of **41** in CD_2Cl_2 at 295 K. Assignment was achieved using COSY and NOESY spectra. See **Scheme 7.2** for ring labelling.

$[Ir(dfppy\text{-}C,N)_2(\mu\text{-}Cl)]_2$ (**42**), $[Ir(bzq\text{-}C,N)_2(\mu\text{-}Cl)]_2$ (**43**), $[Ir(piq\text{-}C,N)_2(\mu\text{-}Cl)]_2$ (**44**), $[Ir(ppz\text{-}C,N)_2(\mu\text{-}Cl)]_2$ (**45**), and $[Ir(dmppz\text{-}C,N)_2(\mu\text{-}Cl)]_2$ (**46**) were synthesised in an analogous manner to **41** using the appropriate *C*,*N*-ligand (**Table 7.1**), albeit 2-methoxyethanol was used as the solvent in the preparation of **43** and **46**. 2-Phenylpyridine (Hppy), 2-(2,4-difluorophenyl)pyridine (Hdfppy), 7,8-benzoquinoline (Hbzq), and 1-phenylpyrazole (Hppz) were commercially available. 1-Phenylisoquinoline (Hpiq)[290] and 3,5-dimethyl-1-phenylpyrazole (Hdmppz)[291] were prepared by *L. Siegfried* as described in the literature (**Scheme 7.4**).

Table 7.1 Synthesis of further Ir(III) dimers.

C,N-ligand	Product	
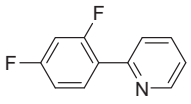 **Hdfppy**	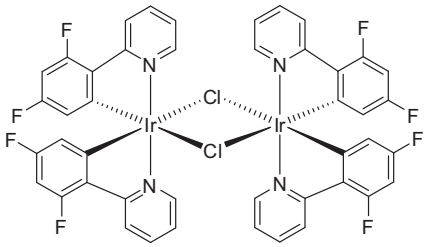	**42**: 48 %
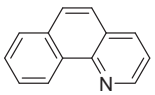 **Hbzq**	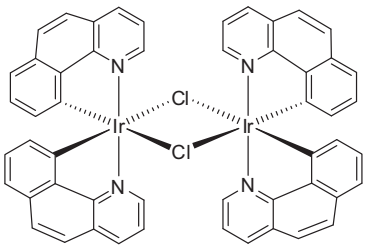	**43**: 67 %
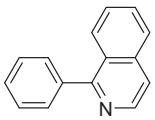 **Hpiq**	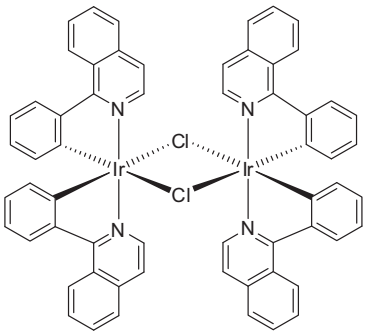	**44**: 58 %
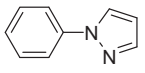 **Hppz**	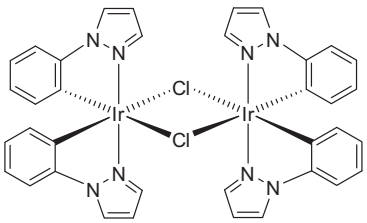	**45**: 59 %
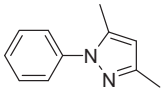 **Hdmppz**	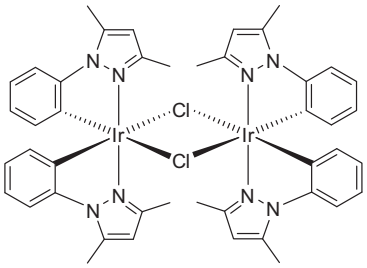	**46**: 58 %

In a *Suzuki*-type reaction,[292-296] 1-chloroisoquinoline, benzeneboronic acid, palladium(II) acetate, sodium carbonate, and tetrabutylammonium bromide were reacted for 40 min in a mixture of water and acetonitrile (1:1 v/v) in a "Biotage Initiator" microwave reactor at 150 °C to give Hpiq after work-up and purification procedures (**Scheme 7.4**).[290] The 3,5-dimethyl-substituted 1-phenylpyrazole *C*,*N*-ligand Hdmppz was prepared in good yields by treating phenylhydrazine hydrochloride with acetylacetone in 1,2-dichloroethane at 70 °C for 24 h *via* a successive hydrazone formation, cyclisation, and double bond isomerisation sequence.[291]

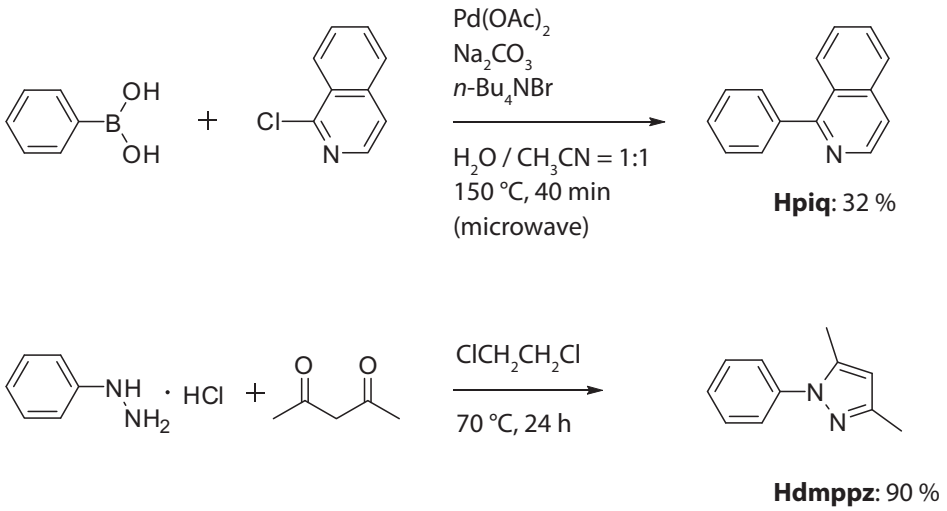

Scheme 7.4 Syntheses of Hpiq and Hdmppz.

7.2.2 Cyclometallated Ir(III) complexes

The heteroleptic Ir(III) complexes were prepared in a similar manner to those for other $[Ir(C\hat{}N)_2(N\hat{}N)]^+$ species.[297] The $[Ir(C\hat{}N)_2(\mu\text{-}Cl)]_2$ precursors were reacted with two equivalents of the desired *N*,*N*′-ligand in a refluxing mixture of dichloromethane and methanol (1:1 v/v) overnight affording the complex $[Ir(C\hat{}N)_2(N\hat{}N)]^+$ as its chloride salt. By adding excess of NH_4PF_6 to the solution, the desired $[PF_6]^-$-salt could be isolated, mostly in quantitative yields, by evaporation of the reaction mixture followed by purification with two subsequent column chromatographies, once with Alox and once with silica (**Scheme 7.5**).

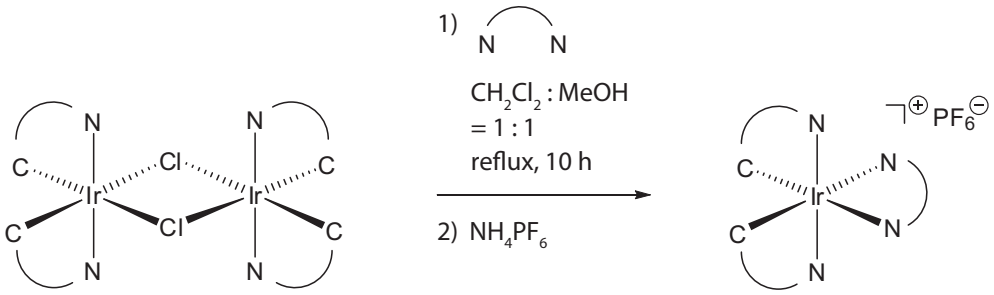

Scheme 7.5 General synthetic pathway to $[Ir(C^N)_2(N^N)][PF_6]$ complexes starting from $[Ir(C^N)_2(\mu\text{-}Cl)]_2$.

7.2.2.1
Ir(III) complexes with different *N,N′*-ligands

In a first attempt, Ir(III) complexes with different *N,N′*-ligands were prepared using the most simple and common *C,N*-ligand, *i.e.* 2-phenylpyridine (Hppy) to give a set of cyclometallated $[Ir(ppy)_2(N^N)][PF_6]$ complexes **47** – **56** (**Table 7.2**) according to the structure given in **Scheme 7.6**.

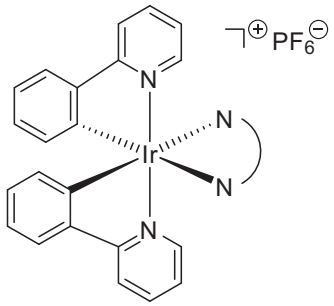

Scheme 7.6 $[Ir(ppy)_2(N^N)][PF_6]$ as the general structure for altering the *N,N′*-ligand.

Table 7.2 Synthesis of a series of $[Ir(ppy)_2(N\hat{}N)][PF_6]$ complexes.

N,N′-ligand	Ir(III) complex (as Scheme 7.6)	*N,N′*-ligand	Ir(III) complex (as Scheme 7.6)
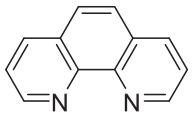 **phen**	**47**: 99 %	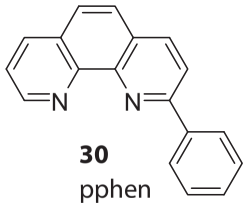 **30** pphen	**48**: 80 %
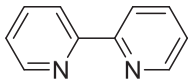 **bpy**	**49**: 98 %	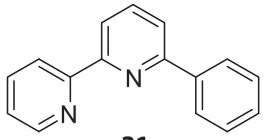 **31** pbpy	**50**: 99 %
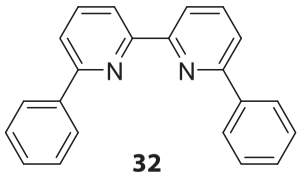 **32** dpbpy	**51**: 89 %	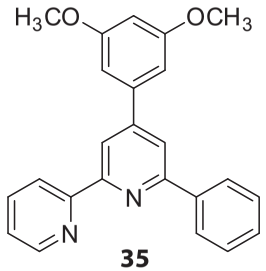 **35** $(H_3CO)_2$ppbpy	**52**: 91 %

***N,N′*-ligand**	**Ir(III) complex** (as **Scheme 7.6**)	***N,N′*-ligand**	**Ir(III) complex** (as **Scheme 7.6**)
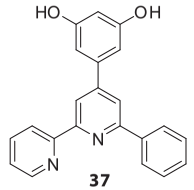 **37** $(HO)_2$ppbpy	**53**: 90 %	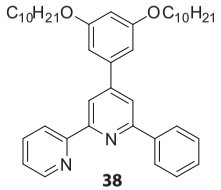 **38** $(H_{21}C_{10}O)_2$ppbpy	**54**: 96 %
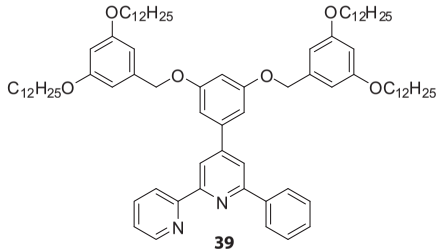 **39** $(G1–O)_2$ppbpy	**55**: 96 %	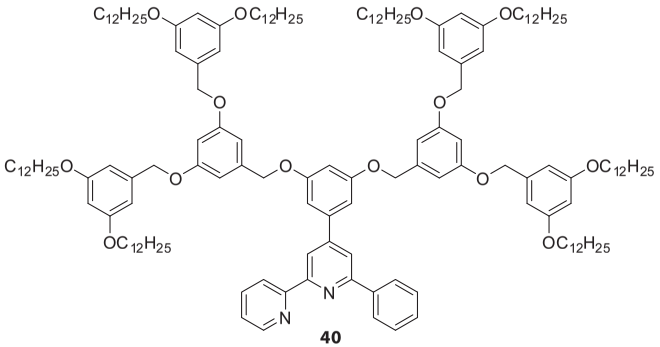 **40** $(G2–O)_2$ppbpy	**56**: 92 %

Preparations of the various *N*,*N*′-ligands were described in **Chapter 6**, and 2,2'-bipyridine (bpy) and 1,10-phenanthroline (phen) were commercially available. The syntheses of complexes **47** – **56** were straightforward yielding orange powders for most of the given examples. Purification of the $[PF_6]^-$-salts had to be adapted for a few compounds. Normally, one chromatographic column on Alox and another on silica was performed each with a mobile phase of first pure dichloromethane to elute the traces of remaining free ligand and then a mixture of dichloromethane and methanol (100:2 v/v) to elute a coloured band containing the desired complex. Nevertheless, due to its high polarity, compound **53** with the two free OH-groups showed such a high affinity for Alox that size exclusion column chromatography using Sephadex LH–20 had to be performed (methanol as the mobile phase) followed by silica column chromatography (CH_2Cl_2:MeOH = 100:5 as the eluent). In contrast, complexes **54** – **56** are high lipophilic because of the alkyl chains from the dendronised *N*,*N*′-ligands. For these compounds, a less polar eluent was chosen using a mixture of dichloromethane and hexane (1:1 v/v) to elute the traces of the free *N*,*N*′-ligands, and then a mixture of dichloromethane and methanol (100:2 v/v) to isolate the desired complexes. All the complexes with *N*,*N*′-ligands bearing a pending phenyl group in the 6-position of bpy (or 2-position in the case of phen) are orange in the solid phase, while complexes **47** and **49** are yellowish-orange and yellow, respectively.

7.2.2.2
Ir(III) complexes with different *C*,*N*-ligands

Because of the exceptionally high performance of **50** in LEECs in respect of the device's lifetime (see **Chapter 8**), 6-phenyl-2,2'-bipyridine (**31**, pbpy) was used as the invariable *N*,*N*′-ligand when we investigated the effect of varying the *C*,*N*-ligand (**Scheme 7.7**). A series of complexes was prepared using the same synthetic pathway as for the compounds **47** – **56** to give complexes **57** – **61** with the generic chemical formula $[Ir(C^N)_2(pbpy)][PF_6]$ (**Table 7.3**).

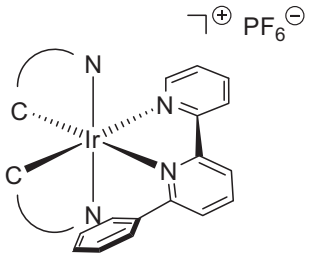

Scheme 7.7 $[Ir(C^N)_2(pbpy)][PF_6]$ as the general structure for the series of different *C*,*N*-ligands.

Table 7.3 Synthesis of a series of $[Ir(C^N)_2(pbpy)][PF_6]$ complexes.

***C,N*-ligand**	**Ir(III) complex** (see **Scheme 7.7**)	***C,N*-ligand**	**Ir(III) complex** (see **Scheme 7.7**)
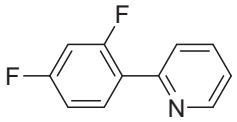 **Hdfppy**	**57**: 87 %	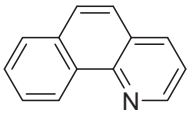 **Hbzq**	**58**: 61 %
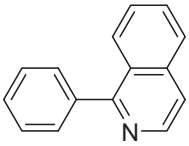 **Hpiq**	**59**: 90 %	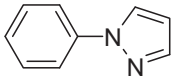 **Hppz**	**60**: 78 %
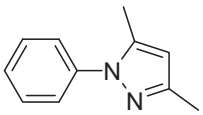 **Hdmppz**	**61**: 99 %		

Purification of the Ir(III) complexes was achieved using the standard method described in the section above. As the precursor $[Ir(bzq\text{-}C,N)_2(\mu\text{-}Cl)]_2$ (**43**) already showed the presence of impurities in its ^1H NMR spectra, purification of the corresponding Ir(III) complex $[Ir(bzq)_2(pbpy)][PF_6]$ (**58**) was more difficult than for the other compounds. Nevertheless, the impurities in **58** revealed a slightly lower polarity so they could be separated after three chromatographic columns. The most striking feature of this series of complexes is their colour. Most the compounds of the series **47** – **56** were orange whereas series **57** – **61** revealed a variety of colours. Complex **57** with dfppy as its *C,N*-ligand possessed a greenish colour which is also reflected in its photoluminescence spectra with a blue shift of the emission (see next section). Complexes **58** and **61** showed an orange colour with a slight reddish (**58**) or, respectively, yellowish (**61**) sheen, whereas **60** was yellow, similar to **49**. In the case of **59**, the powder showed a dramatic colour change being a dark red compound. Unfortunately, the red shift in its emission spectra is not too impressive.

7.3 Characterisation of the cyclometallated Ir(III) complexes

7.3.1 General characterisation

All complexes **47** – **61** were fully characterised with 1D- and 2D-NMR experiments, IR absorption, ESI-MS, UV-Vis absorption, photoluminescence and lifetime spectroscopy, and elemental analysis.

Almost all of the ^{1}H NMR spectra showed well-resolved and sharp peaks and the correct number of protons in the integrals. Compounds **49** and **50** with the first- and second-generation Fréchet dendron in their structure revealed some line broadening which can be attributed to the low intensity signals of the (bi-)pyridine protons compared to the high number of protons of the alkyl chains of the dendrons. Complexes from *N*,*N*′-ligands containing a mirror plane in their py–py axis (bpy, phen), *i.e.* **47** and **49**, possessed a much simpler spectrum due to their higher symmetry leading to the coincidence of all protons of the two *C*,*N*-ligands. As an example, the ^{1}H NMR spectra of **49** is depicted in **Figure 7.2** which could be fully assigned using COSY and NOESY measurements (and HMQC and HMBC methods for assigning the ^{13}C spectrum). Interestingly, the most downfield proton $H^{6(bpy)}$ in the free bpy-ligand was shifted upfield in the complex and $H^{3(bpy)}$ is then the highest peak in the complex.[298] Likewise, proton $H^{6(B)}$ in the complex, next to the N-donor atom in the cyclometallated ligands, underwent a dramatic shift compared to the corresponding peak in the Ir(III) dimer **41** from δ 9.30 to 7.54 ppm (compare with **Figure 7.1**).

Electrospray mass spectrometry (ESI-MS) normally showed the cation of the complex $[M\text{-}PF_6]^+$ as the only peak. But for complexes $[Ir(ppy)_2(dpbpy)][PF_6]$ (**51**), $[Ir(bzq)_2(pbpy)][PF_6]$ (**58**), and $[Ir(piq)_2(pbpy)][PF_6]$ (**59**), a second peak was observed which could be assigned to $[M\text{-}PF_6\text{-}L_{N,N'}]^+$ arising from the loss of the *N*,*N*′-ligand. This could be explained by a weaker N–Ir bond for the coordinating *N*,*N*′-ligand, either due to steric reasons (**51**) or due to electronic reasons (**58**, **59**).

Elemental analyses of the complexes were all within the acceptable limit and indicated the presence of water in some of the compounds.

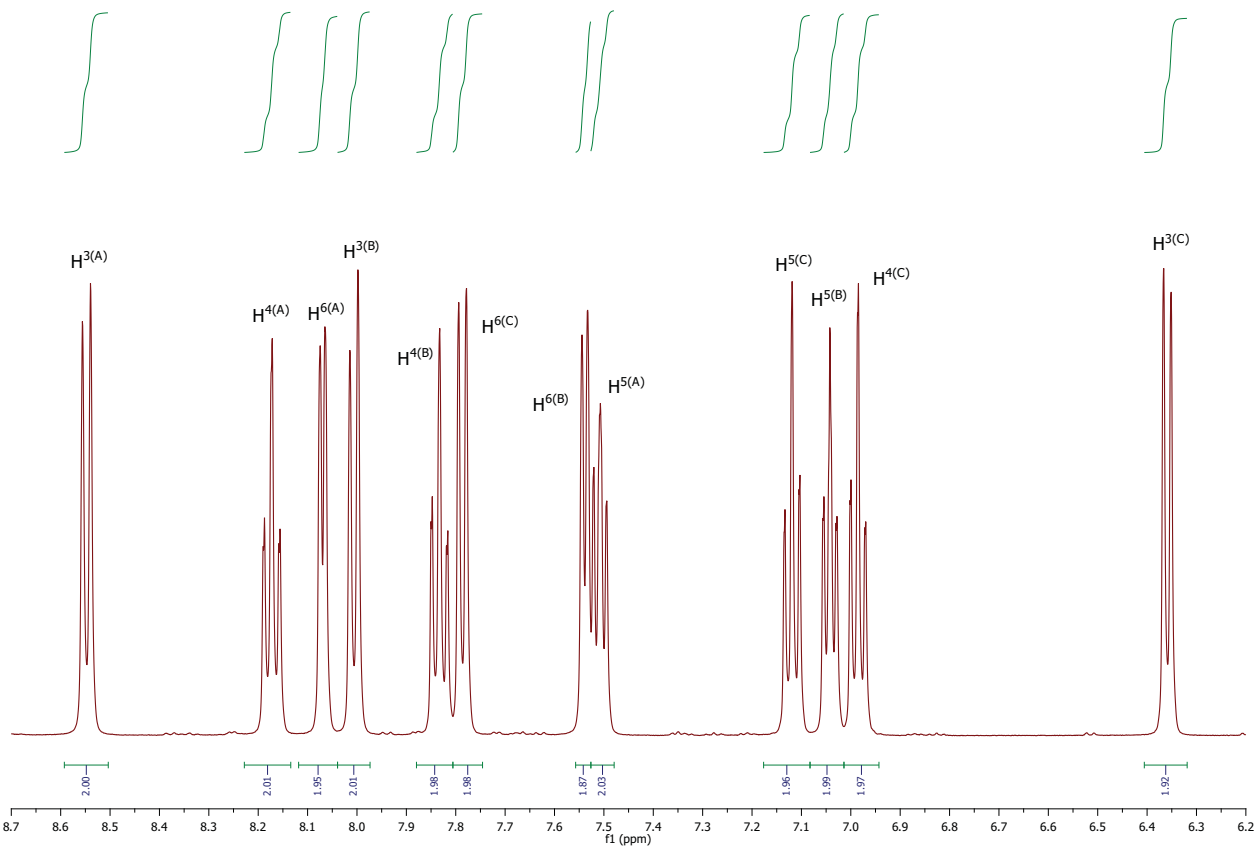

Figure 7.2 500 MHz ^{1}H NMR spectrum of **49** in CD_2Cl_2 at 295 K. Assignment was achieved using COSY and NOESY spectra. See experimental part for ring labelling.

7.3.2 UV-Vis absorption

Of all complexes **47** – **61**, UV-Vis absorption was measured in dichloromethane under ambient conditions with three to four different concentrations each. The absorption coefficient was plotted against the wavelength in **Figure 7.3** for all complexes. Additionally, a few of the complexes (**49** – **52** and **57**) were measured in acetonitrile revealing almost identical characteristics (**Figure 7.4**).

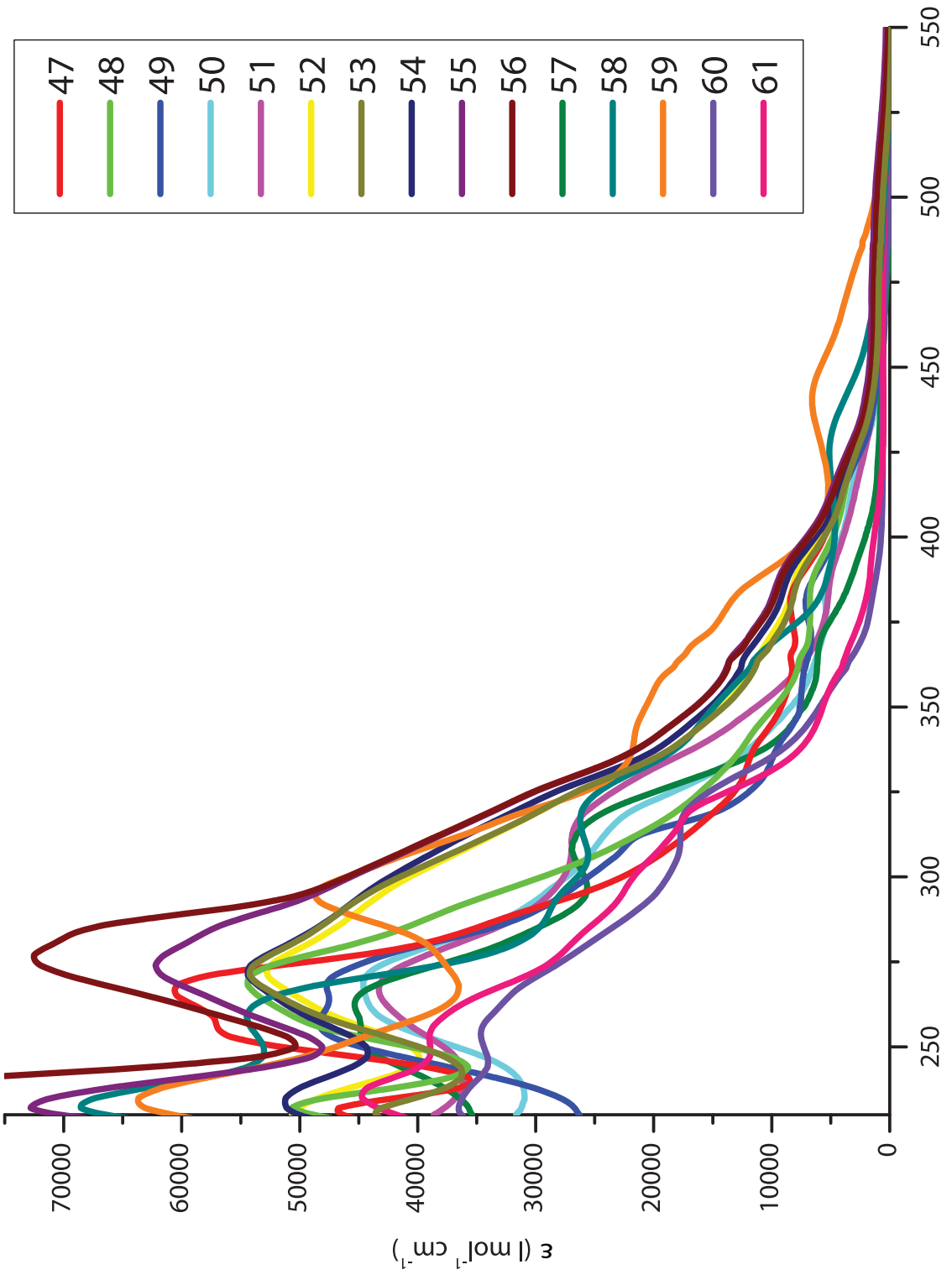

Figure 7.3 UV-Vis absorption spectra of complexes **47** – **61** in aerated CH_2Cl_2.

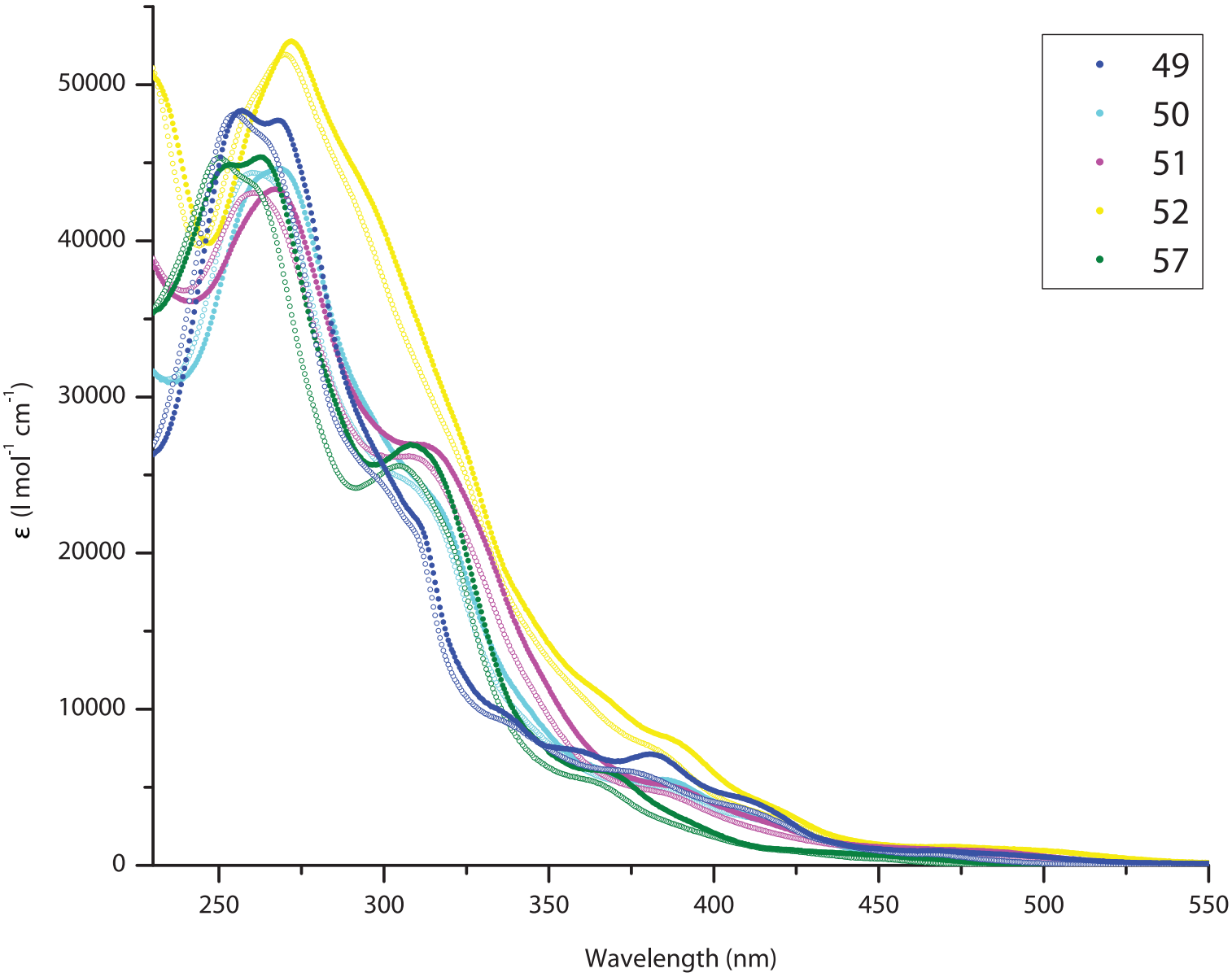

Figure 7.4 Comparison of the UV-Vis spectra of complexes **49**, **50**, **51**, **52**, and **57** in CH_2Cl_2 (closed circles) and CH_3CN (open circles).

Table 7.4 Spectroscopic data for complexes **47** – **61** from UV-Vis absorption measurements in aerated CH_2Cl_2. Italic wavelengths mean shoulder peak. Red coloured numbers are specifically discussed in text.

	λ_{max} [nm] (ε [l·mol^{-1}·cm^{-1}])							
47		*255* (sh, 56'000)	267 (59'000)		*334* (sh, 11'000)	381 (7'800)		467 (910)
48	232 (53'000)		269 (57'000)		*343* (sh, 11'000)	383 (6'700)	*412* (sh, 3'700)	471 (840)
49		257 (48'000)		*308* (sh, 23'000)	*336* (sh, 9'800)	381 (7'000)	*406* (sh, 4'200)	467 (830)
50			267 (44'000)	*311* (sh, 23'000)		*382* (sh, 5'500)	*411* (sh, 3'400)	470 (760)
51			267 (43'000)	*311* (sh, 27'000)		*383* (sh, 5'200)		474 (920)
52			272 (53'000)	*317* (sh, 31'000)		*384* (sh, 8'200)	*412* (sh, 4'000)	471 (1'100)
53			272 (55'000)	*292* (sh, 46'000)		*382* (sh, 8'300)	*419* (sh, 3'500)	471 (1'100)
54	234 (52'000)		272 (56'000)			*384* (sh, 8'900)	*418* (sh, 3'700)	471 (1'100)
55	232 (73'000)		274 (62'000)			*386* (sh, 8'800)		471 (1'100)

	λ_{max} [nm] (ε [l·mol^{-1}·cm^{-1}])								
56	232 (110'000)		276 (73'000)	*283* (sh, 69'000)			*389* (sh, 8'900)	*420* (sh, 3'600)	471 (1'100)
57		252 (45'000)	262 (45'000)		308 (27'000)	*363* (sh, 6'000)			*448* (sh, 620)
58	233 (69'000)		260 (54'000)	*293* (sh, 29'000)	318 (27'000)	*365* (sh, 10'000)		425 (4'900)	
59	234 (64'000)			295 (48'000)		*343* (sh, 21'000)	*381* (sh, 13'000)		440 (6'700)
60		254 (35'000)			*314* (sh, 18'000)				438 (690)
61	236 (45'000)	254 (39'000)		*282* (sh, 26'000)	*318* (sh, 17'000)	*352* (sh, 5'300)	*394* (sh, 1'400)		464 (630)

The absorption spectra show the typical intense, spin-allowed, $^1\pi$-π^* ligand-centred (LC, aromatic rings) bands for Ir(III) complexes in the UV-region (230 – 300 nm) where most complexes exhibit two maxima. The less intense, lower-energy absorption features above 300 nm are assigned to both spin-allowed and spin-forbidden metal-to-ligand charge transfer (MLCT) electronic transitions.[123, 299, 300] The colour of the complexes is mainly related to the lowest-energy MLCT transition, a weak and broad absorption at around 470 nm which gives the most often present orange colour.

It is noteworthy to mention a few irregularities (**Table 7.4**). First, the dendronised complexes **55** and **56** show a dramatic increase of the absorption coefficient in the UV region of the spectra which can be explained by the presence of an augmented number of benzene rings per molecule. Also, complexes **52** – **56** exhibit an almost identical spectra in regards of the lower-energy transitions, especially the lowest one at 471 nm where all compounds possess the same absorption coefficient. This implies that the "outer sphere" of the complex does not have a big influence on the energy of the HOMO and LUMO levels, consistent with the non-conjugated varying part in this series of the corresponding *N*,*N*′-ligands. The hypsochromic shift of the lowest-energy transition of compound **57** explains its greenish-yellow colour. Complex **58** shows an increased absorption coefficient for the lowest-energy transition, albeit it is shifted to higher energy compared to all other complexes. Similarly, compound **59** exhibits a dramatic increase of the absorption coefficient for the lowest-energy absorption at 440 nm, namely by a factor of six which explains its deep red colour.

7.3.3 Photoluminescence and lifetime

Photoluminescence measurements were performed for all complexes **47** – **61** in dichloromethane under ambient conditions, *i.e.* aerated solutions at room temperature. The excitation wavelength was determined from an excitation spectra which was performed for all samples (**Figure 7.5**). In agreement with *Kasha's rule*,[301] the maxima in the emission spectra were independent of the excitation wavelength, at least in the measured range from about 270 – 700 nm. Subsequent emission spectra were recorded under identical conditions (**Figure 7.6**). The ordinate of the graph is originally related to the emission intensity, although the curves were scaled for a better visibility in **Figure 7.6** as quantitative considerations require different measurement setups anyway. Additionally, a few of the complexes (**49** – **52** and **57**) were measured in acetonitrile revealing slightly shifted emission to higher wavelengths, albeit at much lower intensity. This corresponds with the observed diminished lifetime in acetonitrile by a factor between two and three. The unstructured and broad emission bands of complexes **47** – **61** visible in **Figure 7.6** are typical of complexes containing a combination of orthometallating and neutral ligands.[299, 300, 302] Lifetime measurements were performed with the same solutions as used for the luminescence experiments.

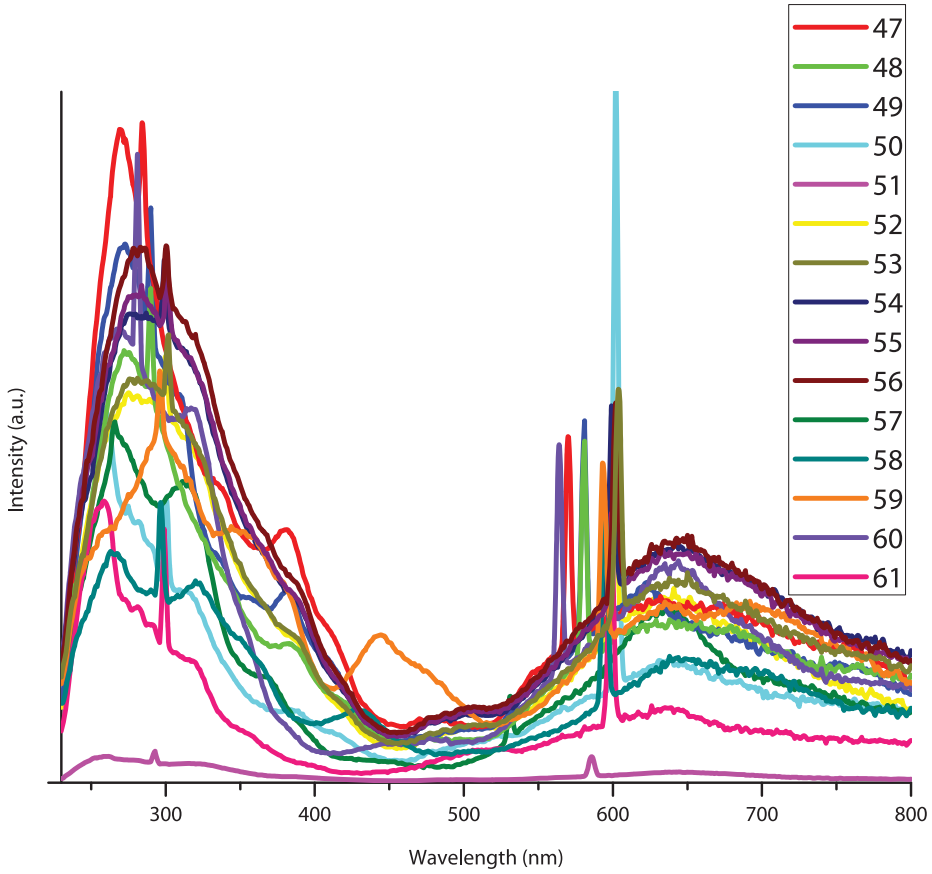

Figure 7.5 Qualitative photoluminescence excitation spectra of complexes **47** – **61** in aerated CH_2Cl_2 measured at each of the complexes' emission maximum. The ordinate (related to intensity) is normalised to the concentration of the samples.

The archetype complexes $[Ir(ppy)_2(phen)][PF_6]$ (**47**) and $[Ir(ppy)_2(bpy)][PF_6]$ (**49**) emit at 573 nm (greenish-yellow) and 582 nm (yellow), respectively (**Table 7.5**). Introduction of the pendant phenyl in the *N*,*N*′-ligand in complexes **48** and **50** results in a bathochromic effect of about 10 nm. Interestingly, the second pendant phenyl ring of 6,6'-diphenyl-2,2'-bipyridine in complex **51** gives a small hypsochromic shift in the emission spectrum and a considerable reduction of its lifetime. Yet, the additional phenyl ring in the 4-position of bipyridine of complex **52** leads to a small bathochromic effect, again of nearly 10 nm to 603 nm (darker orange). A much stronger effect on the emission wavelength was observed upon altering the *C*,*N*-ligand in the complexes. The most blue-shifted emission was found in complex **57** with an exceptionally strong emission with a maximum at 532 nm (intense green) and, concurrently, a doubled lifetime compared to most other complexes. Despite the two maxima in its spectrum, there is no evidence of an independent dual emission of complex **59**, for which assumption there would be no physico-chemical basis. Because of this unusual behaviour, lifetime data of **59** could not be coherently evaluated.

Most lifetimes were in the range of 0.1 – 0.2 µs with the before-mentioned exceptions.

As we will see later in **Chapter 8**, values from photoluminescence do not necessarily reflect electroluminescence values.

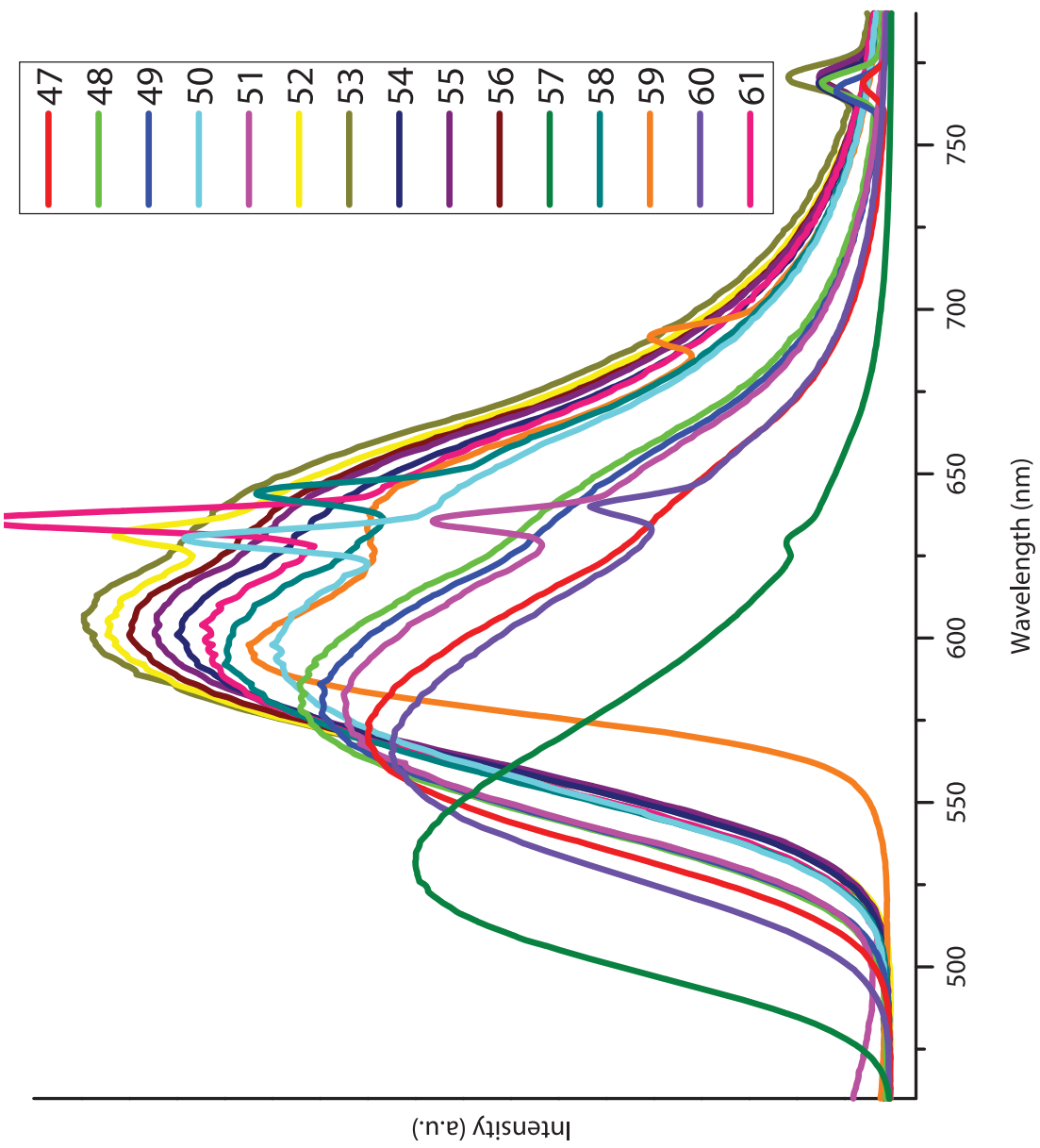

Figure 7.6 Qualitative photoluminescence spectra of complexes **47** – **61** in aerated CH_2Cl_2 excited at variable wavelengths between 313 – 383 nm. The ordinate is scaled for good visibility and does not correspond to the relative intensity. The humps visible in the spectra refer to the second harmonics of the excitation wavelengths.

Table 7.5 Spectroscopic data for complexes **47** – **61** from photoluminescence and lifetime measurements in aerated CH_2Cl_2. Red coloured numbers are specifically discussed in text.

complex	**47**	**48**	**49**	**50**	**51**	**52**	**53**	**54**	**55**	**56**	**57**	**58**	**59**	**60**	**61**
CH_2Cl_2															
λ_{ex} [nm]	382	382	381	313	316	314	383	382	383	383	313	320	344	318	316
λ_{em}[nm]	573	583	582	595	579	603	605	601	602	602	532	596	596, 635	566	599
τ [μs] (χ^2)	0.15 (1.008)	0.17 (1.010)	0.16 (1.055)	0.13 (1.085)	0.098 (1.050)	0.17 (1.068)	0.17 (1.038)	0.17 (1.005)	0.18 (1.024)	0.19 (1.028)	0.32 (1.011)	0.13 (1.047)		0.18 (1.021)	0.13 (1.012)
CH_3CN															
λ_{ex} [nm]			305	312	316	314					307				
λ_{em}[nm]			590	603	589	610					537				
τ [μs] (χ^2)			0.062 (1.017)	0.046 (1.017)	0.055 (1.023)	0.062 (0.995)					0.11 (1.054)				

7.3.4
Cyclic voltammetry

The redox properties of all the cyclometallated Ir(III) complexes **47** – **61** were investigated using cyclic voltammetry (CV) and by square wave and differential pulse voltammetry. The complexes were dissolved and measured in acetonitrile in the presence of 0.1 M $(n\text{-Bu})_4NPF_6$ except for **56** which was not soluble in acetonitrile, therefore it was measured in dichloromethane. The scanning rate for the CV was 100 mV s^{-1} in all cases and ferrocene (Fc) was added as an internal standard at the end of the experiment. A typical example of a CV is shown in **Figure 7.7** for complex **49**.

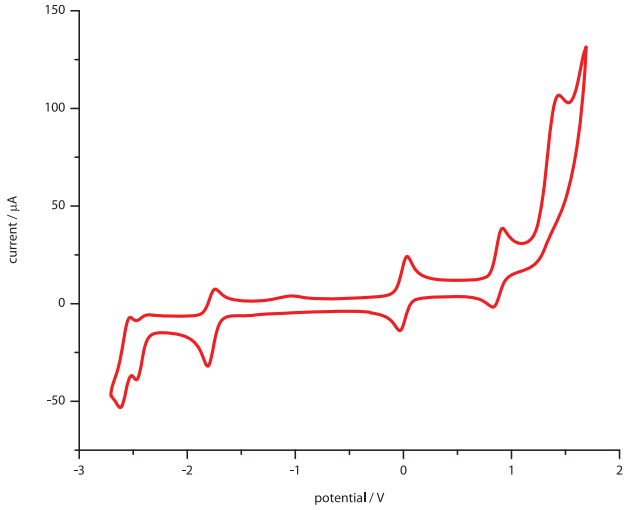

Figure 7.7 Cyclic voltammogram of **49** (1.0 mmol l^{-1}) in argon purged acetonitrile containing 0.1 M $(n\text{-Bu})_4NPF_6$ and Fc as internal standard at a scanning rate of 100 mV s^{-1}. The potential is referenced to Fc/Fc^+.

Table 7.6 depicts the redox potentials of all complexes **47** – **61**. The phenathroline-containing complexes **47** and **48** show a different behaviour revealing a very poorly resolved CV difficult to interpret. Most complexes exhibit a quasi reversible or slightly irreversible one electron-oxidation peak at 0.8 – 0.9 V which is in agreement with literature where the Ir(III) to Ir(IV) oxidation normally occurs in a similar range of potentials in the case of $[Ir(ppy)_2(N\text{^}N)]^+$.[303] For $[Ir(ppz)_2(N\text{^}N)]^+$-type complexes, the observed range of oxidation potentials in literature is much broader, *i.e.* 0.62 – 1.25 V.[132] The potentials in the literature had to be recalculated from the referenced value against SCE (standard calomel electrode) to the Fc/Fc^+ redox couple *via* the equation[304] $V_{Fc/Fc+} = V_{SCE} - 0.41$ V where necessary. In regards of the reduction potentials, most complexes show one reversible and two subsequent irreversible reduction peaks which can be attributed to reduction of every ligand in a monoelectronic process or to the reduction of the Ir(III) metal centre to Ir(II) plus two reduction processes in the ligands. The reduction peaks for the complexes with $[ppy]^-$ as their *C,N*-ligands possess very similar reduction potentials at ~ –1.8, ~ –2.4, and ~ –2.6 V, albeit complex **53** with its two hydroxyl groups has slightly shifted reduction potentials. The shifts in emission wavelength upon variation of the *C,N*-ligands is reflected in the deviant redox potentials for both oxidation and reduction potentials.

Table 7.6 Redox potentials measured for complexes **47** – **61** in acetonitrile (argon-purged). For reversible processes, $E_{½}$ values were calculated from cyclic voltammetry, for irreversible or quasi reversible processes, the values given are peak potentials from square wave measurements.
[a] Irreversible process, peak potential from square wave.
[b] Process only observed in square wave.
[c] Reversible process, but peak potential from square wave.
[d] Solubility problems in acetonitrile lead to intractable measurements.
[e] Compound not soluble in acetonitrile, measured in dichloromethane instead which gives poorly reproducible voltagrams.

	Potential [V] versus Fc/Fc^+	
	$E_{½}^{ox}$	$E_{½}^{red}$
47	1.10[a]	–1.56[a], –2.17[a]
48	0.80[a]	–1.36[a], –1.90[a], –2.55[a]
49	0.87, 1.36[a]	–1.78, –2.44[a], –2.59[a]
50	0.86[a], 1.44[b]	–1.81, –2.46[a], –2.64[a]
51	0.83[a], 1.34[b]	–1.82, –2.41[a], –2.64[a]
52	0.87[c], 1.41[b]	–1.78[c], –2.39[a], –2.62[c]
53	0.81[a], 1.44[a]	–1.44[c], –1.98[c], –2.65[b]
54	0.81[a], 1.36[a]	–1.32[a], –1.73[a], –2.32[a], –2.56[a]
55[d]	0.72[b]	not observed[d]
56[e]	0.83[a], 1.30[a]	not observed[e]
57	1.19[a]	–1.76[c], –2.41[a], –2.53[b]
58	0.74[c], 1.37[a]	–1.30[c], –1.79[a], –2.34[c]
59	0.81[a], 1.11[a], 1.35[a]	–1.28[c], –1.78, –2.14, –2.40
60	0.89[a], 1.53[a]	–1.25, –1.79[a], –2.45[a]
61	0.78, 1.40[a]	–1.24, –1.80[a], –2.50[a]

7.3.5 Crystal structures

In contrast to ligand crystallisation, obtaining single crystals from complexes proved to be much more facile. If not otherwise stated, single crystals were grown by a diffusion method where the complex was dissolved in dichloroethane and placed in a small tube with a perforated cap. This tube was placed in a bigger vial, diethyl ether was added and the vial was closed and left at a dark, calm place for a few weeks. X-ray crystallography was performed at 123 K for all complexes except for **48** and **50** which were measured at 173 K. Crystallographic data are summarised in **Table 7.7**.

Table 7.7 Crystallographic data for Ir(III) complexes.

Complex	Temp. [K]	Crystal system a, b, c [Å] α, β, γ [°] or β [°]	Space group	*R*1	*wR*2	gof
47	123	monoclinic 15.2417(6), 23.0629(9), 18.8709(7) 95.015(2)	*C*2/*c*	0.0219	0.0253	1.0406
48	123	monoclinic 19.0044(4), 25.7833(6), 16.0565(3) 96.260(1)	*C*2/*m*	0.0283	0.0163	0.9963
49	173	orthorhombic 10.8993(2), 15.8290(4), 33.4603(7)	*Pbca*	0.0265	0.0327	0.9771
50	173	monoclinic 17.6215(1), 19.3637(1), 20.6311(1) 92.1545(3)	$P2_1/c$	0.0263	0.0293	1.0952
51	123	monoclinic 13.6575(6), 8.8865(4), 29.8329(12) 95.286(2)	$P2_1/c$	0.0263	0.0254	1.0818
57	123	monoclinic 19.3540(9), 10.2932(5), 18.1712(8) 114.558(2)	$P2_1/c$	0.0172	0.0175	1.0654
59	123	triclinic 9.5172(2), 12.3792(3), 17.8883(4) 79.721(1), 84.041(1), 76.441(1)	$P\bar{1}$	0.0196	0.0208	1.0606
60	123	orthorhombic 10.6947(3), 16.7197(5), 37.9704(11)	*Pbcm*	0.0285	0.0278	1.0662
61	123	monoclinic 12.5994(6), 21.9541(10), 12.8280(6) 95.825(2)	$P2_1/n$	0.0222	0.0201	1.0936

The asymmetric unit of $[Ir(ppy)_2(phen)][PF_6]$ (**47**) contained one cation / anion pair and disordered solvent molecules (dichloroethane) ($Z = 8$). The solid state structure of the cation is given in **Figure 7.8a**.

The cation exhibits a near-octahedral geometry with trans-angles of the donor atoms between 172 – 174 ° and "bite angles" of the ligands ranging from 78 – 81 ° with the smallest angle at the *N*,*N*′-ligand (see figure caption to **Figure 7.8**). The bond lengths of the donor atoms of the *N*,*N*′-ligand (phen, 2.14 and 2.15 Å) to the metal centre are significantly longer than those of the two cyclometallating *C*,*N*-ligands (ppy, 2.00 – 2.05 Å) indicating a slightly weaker bond as expected by the negative partial charge of the coordinating carbon atoms in the $[ppy]^-$-ligands. Surprisingly, the Ir–C and Ir–N bond lengths in $[ppy]^-$ are almost identical.

In the crystal lattice, the cations and anions of **47** form alternating layers (**Figure 7.8b**). Free space in the $[PF_6]^-$-layer is occupied by disordered solvent molecules.

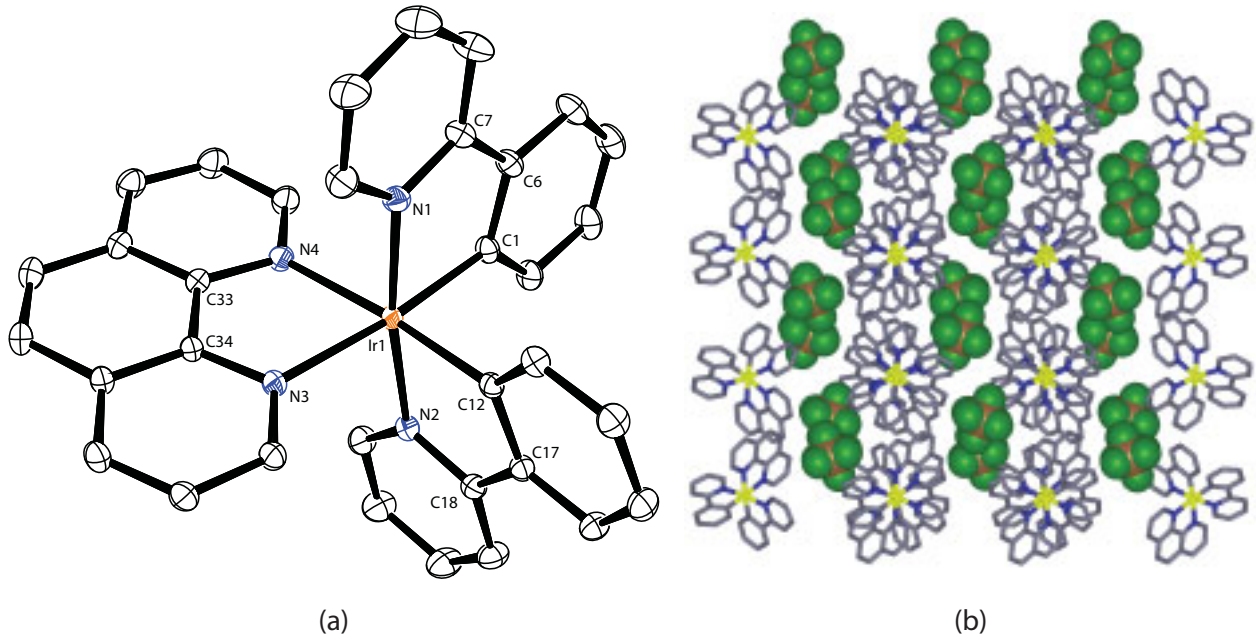

Figure 7.8 (a) ORTEP representation of the solid state structure of the cation present in **47**. Hydrogen atoms, the counterion (PF_6^-), and solvent molecules have been omitted for clarity and thermal ellipsoids are depicted at 50 % probability.
Selected bond lengths (Å) and angles (°):
Ir1–N3 2.1367(10), Ir1–N4 2.1496(12), Ir1–N1 2.0480(12), Ir1–N2 2.0432(11), Ir1–C1 2.0166(12), Ir1–C12 2.0034(14);
N1–Ir1–N2 171.61(5), N3–Ir1–C1 173.95(5), N4–Ir1–C12 173.85(5), N3–Ir1–N4 77.86(4), N1–Ir1–C1 80.61(5), N2–Ir1–C12 80.38(5).
(b) Packing of the cations (stick representation) and anions (space filling representation) in complex **47** as viewed along the crystallographic a axis revealing alternating layers.

In the solid state structure of **48**, there is one molecule per asymmetric unit ($Z = 8$). The cation present in the solid state structure of **48** is shown in **Figure 7.9a**. It exhibits a near-octahedral geometry with trans-angles of the donor atoms ranging from 170 ° – 178 ° and "bite angles" of the coordinating ligands from 77 – 81 °. The most remarkable feature of the structure is the presence of an intramolecular π-π stacking between the pendant phenyl ring (containing C13) of 2-phenyl-1,10-phenanthroline and the coordinated phenyl ring (containing C29) of one of the two cyclometallating *C*,*N*-ligands. The centroids of the two rings are separated by a distance of 3.47 Å, but this segment does not lie perpendicular to the planes built from the rings which intersect at an angle of 8.13(12) °, because they are slightly shifted to provide a stronger interaction. The pendant phenyl ring containing C13 is contorted by angle of 79.59(13) ° to the six-membered ring containing N2. The bond lengths of the metal centre to the six donor atoms are very similar to those in the solid state structure of **47** discussed above with the exception of the lengthening of the Ir–N2 distance in order to make space for the pendant phenyl ring adopting the aforementioned π-π stacking.

The packing involves alternating layers of cations and anions, illustrated in **Figure 7.9b**.

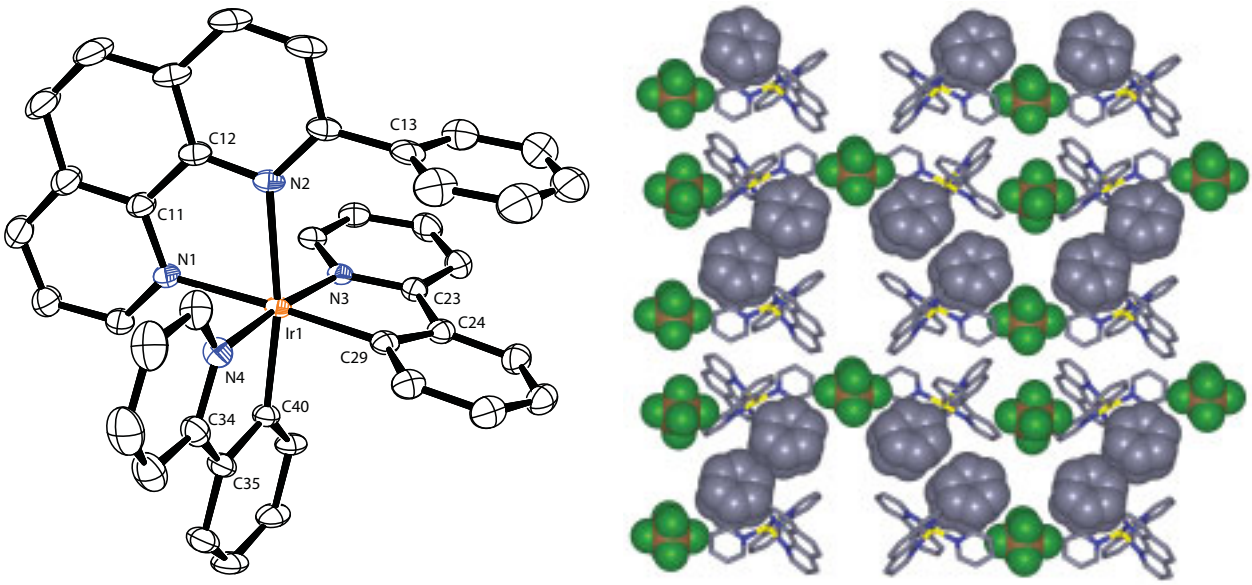

Figure 7.9 (a) ORTEP representation of the solid state structure of the cation present in **48**. Hydrogen atoms and the counterion (PF_6^-) have been omitted for clarity and thermal ellipsoids are depicted at 50 % probability.
Selected bond lengths (Å) and angles (°):
Ir1–N1 2.1449(18), Ir1–N2 2.2259(16), Ir1–N3 2.0417(18), Ir1–N4 2.0467(18), Ir1–C29 2.016(2), Ir1–C40 2.0009(17);
N3–Ir1–N4 174.32(7), N1–Ir1–C29 177.51(7), N2–Ir1–C40 169.71(8), N1–Ir1–N2 76.50(6), N3–Ir1–C29 80.23(7), N4–Ir1–C40 80.56(8).
(b) Packing of the cations (stick representation) and anions (space filling representation) in complex **48** as viewed along the crystallographic a axis emphasising intramolecular π–π interactions (space filling representation).

Crystals of complex **49** were grown by slow evaporation of an NMR sample solution in CD_2Cl_2 and were of good enough quality to distinguish the coordinating N- and C-atoms in the X-ray crystallography measurements. The compound revealed an orthorhombic unit cell adopting a *Pbca* space group where the asymmetric unit contained one cation / anion pair to give rise to eight molecules per unit cell ($Z = 8$).

Figure 7.10a shows the cation present in the crystal structure of **49** which exhibits a near-octahedral geometry with trans-angles of the donor atoms between 172 – 175 ° and "bite angles" of the coordinating ligands ranging from 76 – 81 °, very similar to complex **47** and **48**. All bond lengths of the donor atoms to the metal centre are similar, again with slightly longer bonds for the two nitrogen atoms of the *N*,*N*′-ligand (bpy) to the iridium atom.

The crystal packing shown in **Figure 7.10b** reveals alternating layers of anions and cations as observed for complexes **47** and **48**.

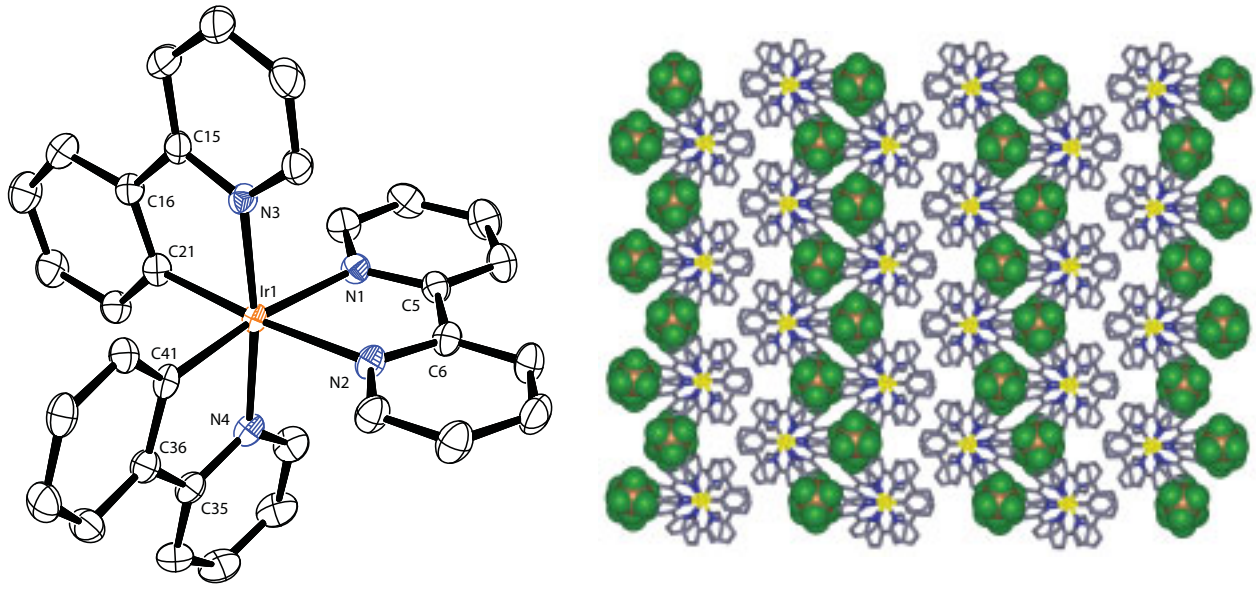

Figure 7.10 (a) ORTEP representation of the solid state structure of the cation present in **49**. Hydrogen atoms and the counterion (PF_6^-) have been omitted for clarity and thermal ellipsoids are depicted at 50 % probability.
Selected bond lengths (Å) and angles (°):
Ir1–N1 2.129(3), Ir1–N2 2.136(3), Ir1–N3 2.047(3), Ir1–N4 2.042(3), Ir1–C21 2.024(4), Ir1–C41 2.004(4); N3–Ir1–N4 172.09(13), N1–Ir1–C41 171.80(15), N2–Ir1–C21 174.92(15), N1–Ir1–N2 76.21(12), N3–Ir1–C21 80.06(16), N4–Ir1–C41 80.68(15).
(b) Packing of the cations (stick representation) and anions (space filling representation) in complex **49** as viewed along the crystallographic b axis.

Single crystals of complex **50** were obtained by slow evaporation of an NMR sample solution in $CDCl_3$. The asymmetric unit of the solid state structure of **50** contains two cation / anion pairs and one solvent molecule, *i.e.* $CDCl_3$ ($Z = 4$). One of the two cations present in the solid state structure of **50** is illustrated in **Figure 7.11a**. Trans-angles of the coordinating atoms range from 168 – 177 ° and "bite angles" of the ligands from 76 – 81 ° affirm the near-octahedral geometry. Bond lengths of the six donating atoms to the metal centre are very similar to the bond lengths in complex **48**, where a lengthening of the Ir–N2 distance was observed as well. Similarly, the distance of the Ir metal centre to the nitrogen atoms of the *N*,*N'*-ligand is elongated in comparison to the distance of the Ir metal centre to the donating atoms in the *C*,*N*-ligands.

Similar to complex **48**, the most striking aspect of the crystal structure of **50** is the occurrence of intramolecular π-π stacking between the pendant phenyl ring of 6-phenyl-2,2'-bipyridine containing C11 and the coordinated phenyl ring of one of the two cyclometallating *C*,*N*-ligands containing C22 and C27.[124] The centroids of the two rings are separated by 3.54 Å, although the two rings are not congruent and their planes intersect at an angle of 8.1(2) °, very similar to the findings in complex **48**. A tilting angle of 58.2(2) ° formed by the pendant phenyl ring containing C11 and the six membered ring containing N2 is considerably lower than that found in complex **48**.

The packing of cations is dominated by intermolecular π-π interactions as highlighted in **Figure 7.11b** involving the aforementioned intramolecular π-π stacking, too. Four face-to-face interactions with quasi-parallel aryl rings are locked on both ends with edge-to-face (C–H···π) interactions, also known for their contribution to increased stability (see **Section 1.1.2.2**).[36] Analogous to all solid state structures of the Ir(III) complexes discusses so far, the packing adopts alternating layers of cations and anions.

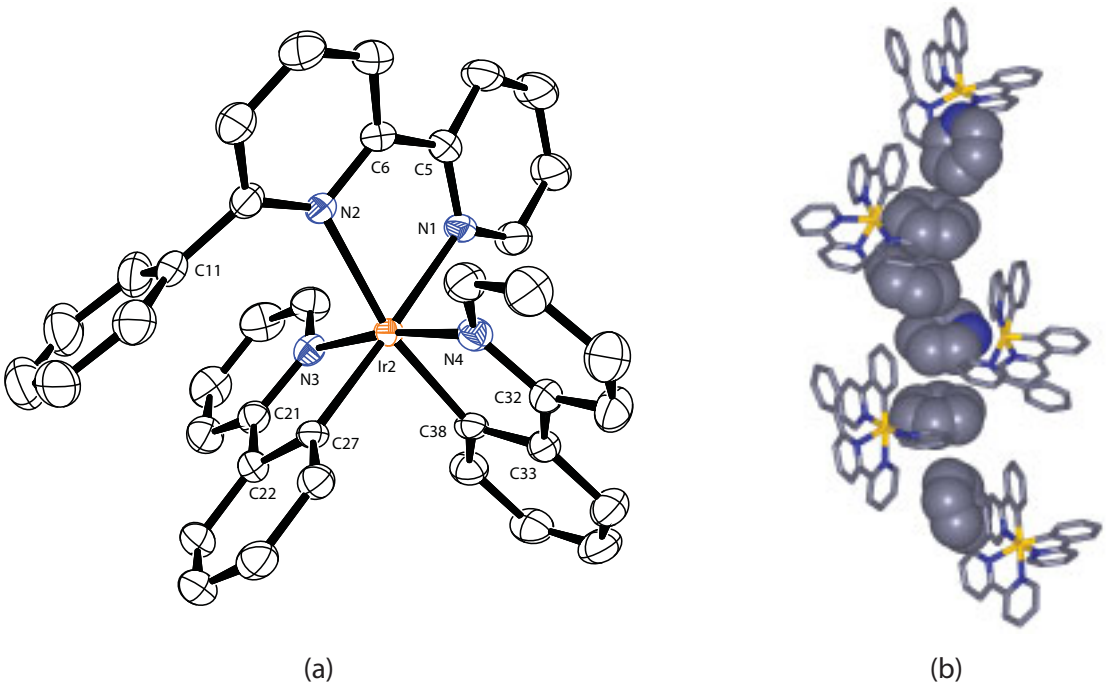

Figure 7.11 (a) ORTEP representation of the solid state structure of one of the cations present in **50**. Hydrogen atoms, the counterion (PF_6^-), and solvent molecules have been omitted for clarity and thermal ellipsoids are depicted at 50 % probability.
Selected bond lengths (Å) and angles (°):
Ir2–N1 2.151(3), Ir2–N2 2.215(3), Ir2–N3 2.036(3), Ir2–N4 2.056(3), Ir2–C27 2.025(3), Ir2–C38 2.004(3); N3–Ir2–N4 171.32(11), N1–Ir2–C27 176.55(12), N2–Ir2–C38 167.59(12), N1–Ir2–N2 75.66(11), N3–Ir2–C27 81.05(13), N4–Ir2–C38 80.62(13).
(b) Packing of the cations in complex **50** highlighting intra- and intermolecular π–π interactions (space filling representation).

In the solid state structure of **51**, there is one molecule per asymmetric unit ($Z = 4$). The cation present in the solid state structure is depicted in **Figure 7.12a**. It possesses a quasi-octahedral geometry with trans-angles of the donor atoms between 173 – 178 ° and "bite angles" of the coordinating ligands ranging from 76 – 80 °, very similar to all of the previously discussed complexes, which also applies to the bond lengths showing no irregularities.

As anticipated, the cation reveals two intramolecular π-π stacking interactions with the two pendant phenyl rings of the *N*,*N*′-ligand (containing C33 and C39) and the coordinated phenyl rings of each of the cyclometallating *C*,*N*-ligands (containing C12 and C1, respectively).[137] The centroids of the involved aryl rings lie both at a distance of 3.49 Å. In this case, both pairs of interacting rings are offset more compared to previously discussed complexes allowing an even better electrostatic attraction. Their least-square planes intersect at an angle of 5.92(15) ° (C1 and C39 containing rings) and 6.64(14) ° (C12 and C33 containing rings), respectively. In contrast to all other complexes introduced in this chapter, the bipyridine unit itself is distorted and the angle between the two pyridine units is 25.14(16) °. The pendant phenyl rings are twisted by an angle of 79.40(15) ° (N3 and C33

containing rings) and 54.36(18) ° (N4 and C39 containing rings), respectively, compared to each of the pyridine rings.

The crystal packing shown in **Figure 7.12b** reveals alternating layers of anions and cations as discussed before for all other complexes.

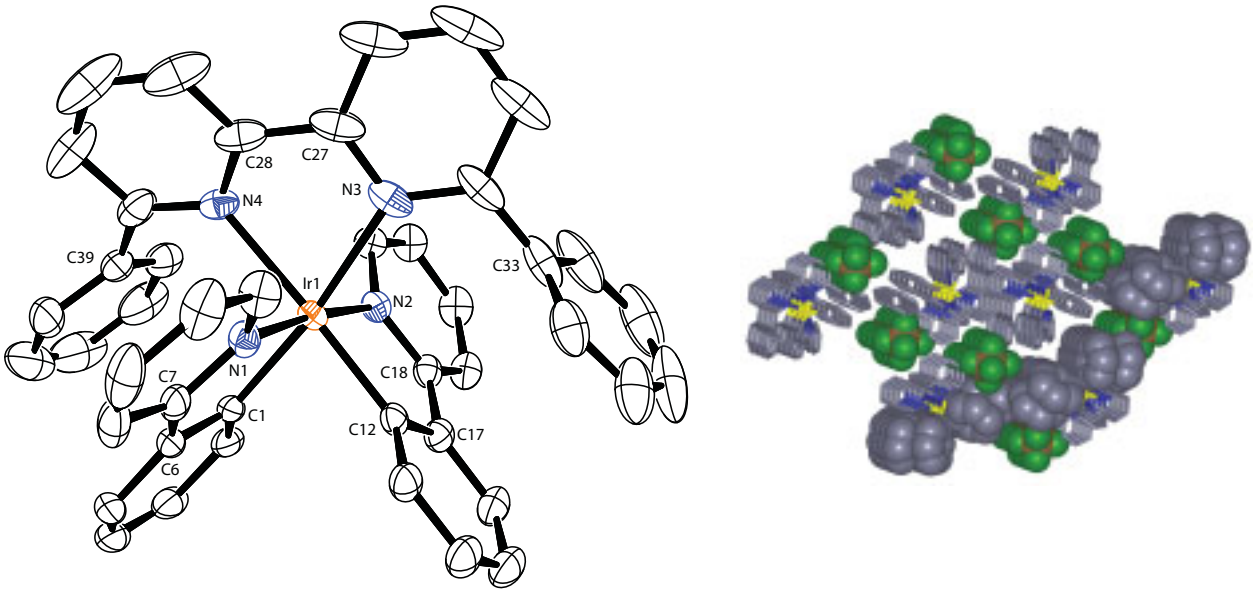

Figure 7.12 (a) ORTEP representation of the solid state structure of one of the cations present in **51**. Hydrogen atoms and the counterion (PF_6^-) have been omitted for clarity and thermal ellipsoids are depicted at 50 % probability).
Selected bond lengths (Å) and angles (°):
Ir1–N3 2.2019(19), Ir1–N4 2.226(2), Ir1–N1 2.0504(17), Ir1–N2 2.0339(17), Ir1–C1 2.012(2), Ir1–C12 2.0120(19);
N1–Ir1–N2 174.31(7), N3–Ir1–C1 172.84(8), N4–Ir1–C12 177.50(7), N3–Ir1–N4 76.17(8), N1–Ir1–C1 80.32(7), N2–Ir1–C12 80.31(7).
(b) Packing of the cations (stick representation) and anions (space filling representation) in complex **51** as viewed along the crystallographic b axis emphasising a few of the present intramolecular π–π interactions (space filling representation).

The asymmetric unit of the solid state structure of complex **57** contains one cation / anion pair ($Z = 4$). The cation present in the solid state structure is shown in **Figure 7.13a**. In agreement with all previously discussed complexes, **57** is no exception and adopts a quasi-octahedral geometry at the metal centre with trans-angles of the donor atoms between 168 – 177 ° and "bite angles" of the coordinating ligands ranging from 76 – 81 °, again with the narrowest angle found in the *N*,*N*′-ligand. Bond lengths of the six donating atoms to the metal centre are very similar to all other aforementioned complexes.

Analogous to all the complexes containing at least one phenyl ring at 6-position of the bipyridine, an intramolecular π-π stacking between that ring (containing C33) and the coordinated phenyl ring of one of the two cyclometallating *C,N*-ligands (containing C1) is found. When compared to the other complexes possessing this intramolecular interaction, the centroids of the two involved rings are separated by a shorter distance of 3.35 Å, and, interestingly, almost congruent with an intersection angle of the two planes formed by the two rings of only 2.22(5) °, thus quasi-coplanar. The shorter distance can be explained by the stronger interaction between the electron richer phenyl ring and the electron poor difluoro-aryl ring as it was observed empirically[305, 306] and confirmed computationally[307-309] before. The pendant phenyl ring is located almost perpendicular to the pyridine ring containing N4 with an angle of 82.85(5) °.

The crystal packing shown in **Figure 7.13b** emphasises the alternating layers of anions and cations as observed before for all other complexes.

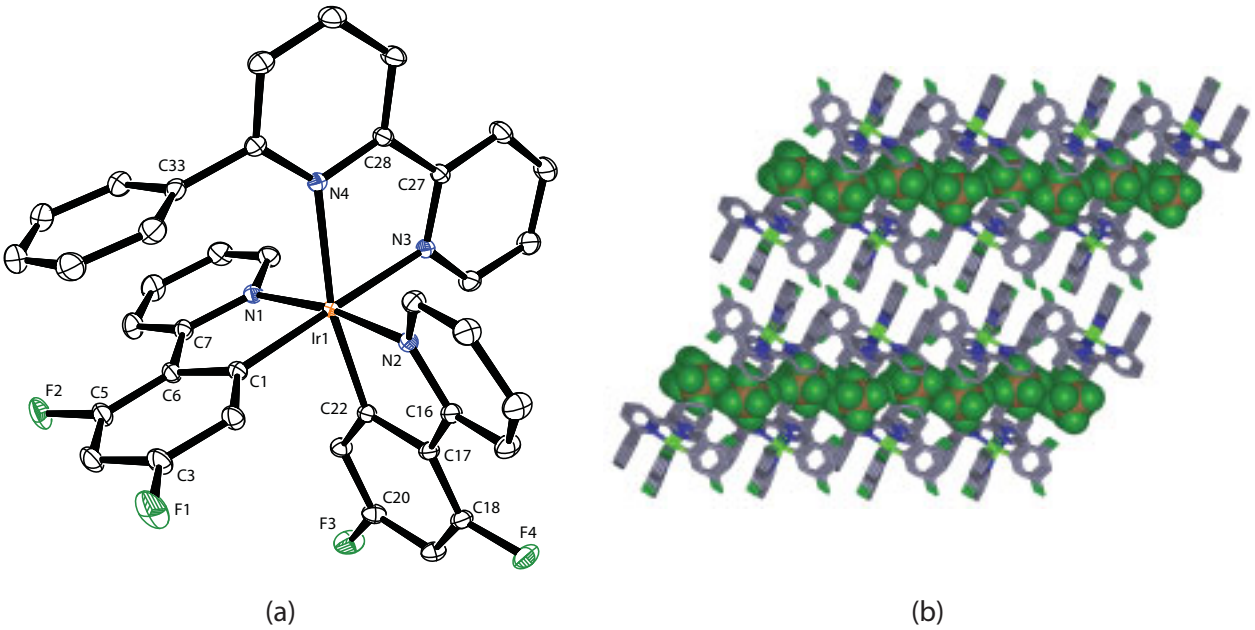

Figure 7.13 (a) ORTEP representation of the solid state structure of the cation present in **57**. Hydrogen atoms and the counterion (PF_6^-) have been omitted for clarity and thermal ellipsoids are depicted at 50 % probability).
Selected bond lengths (Å) and angles (°):
Ir1–N3 2.1383(7), Ir1–N4 2.2168(7), Ir1–N1 2.0455(8), Ir1–N2 2.0463(7), Ir1–C1 2.0099(8), Ir1–C22 2.0011(7);
N1–Ir1–N2 171.64(3), N3–Ir1–C1 177.17(3), N4–Ir1–C22 168.04(3), N3–Ir1–N4 75.69(2), N1–Ir1–C1 80.62(3), N2–Ir1–C22 80.38(3).
(b) Packing of the cations (stick representation) and anions (space filling representation) in complex **57** as viewed along the crystallographic b axis.

Complex **59** crystallised in the centrosymmetric $P\bar{1}$ space group with one molecule in the asymmetric unit (Z = 2). The cation present in the solid state structure is depicted in **Figure 7.14a**. It

possesses a near-octahedral geometry with trans-angles of the donor atoms between 172 – 177 ° and "bite angles" of the coordinating ligands ranging from 76 – 80 °, very similar to all of the previously discussed complexes, which also applies to the bond lengths exhibiting no major differences.

Again, as for all other complexes with a non-coordinating phenyl ring, complex **59** is no exception and an intramolecular π-π stacking is adopted. The pendant phenyl ring of the *N*,*N*′-ligand containing C11 emerges this interaction with the C31-containing cyclometallating aryl ring. Additionally, in regards of the packing in the crystal lattice, intermolecular π-π interactions are observed as highlighted in **Figure 7.14b** where the fused ring containing C23 of an neighbouring molecule provides the continuation of the intramolecular π-π stacking. Centroids of all the three involved rings build an angle of 159.81 °; the selfsame are separated by a distance of 3.50 Å (intramolecular interaction, *i.e.* pendant C11-containing phenyl ring and C31-containing ring) and 4.13 Å (intermolecular interaction, *i.e.* pendant C11-containing phenyl ring and fused ring containing C23 of the adjacent molecule), respectively. The three concerned rings are almost coplanar with intersecting angles of their planes of 10.53(7) ° (intramolecular) and 12.24(8) ° (intermolecular) and are displaced slightly to provide a strong interaction. The least square plane emerging from the pendant (C11-containing) phenyl ring is twisted by 61.37(8) ° to the least square plane of the N2-containing ring.

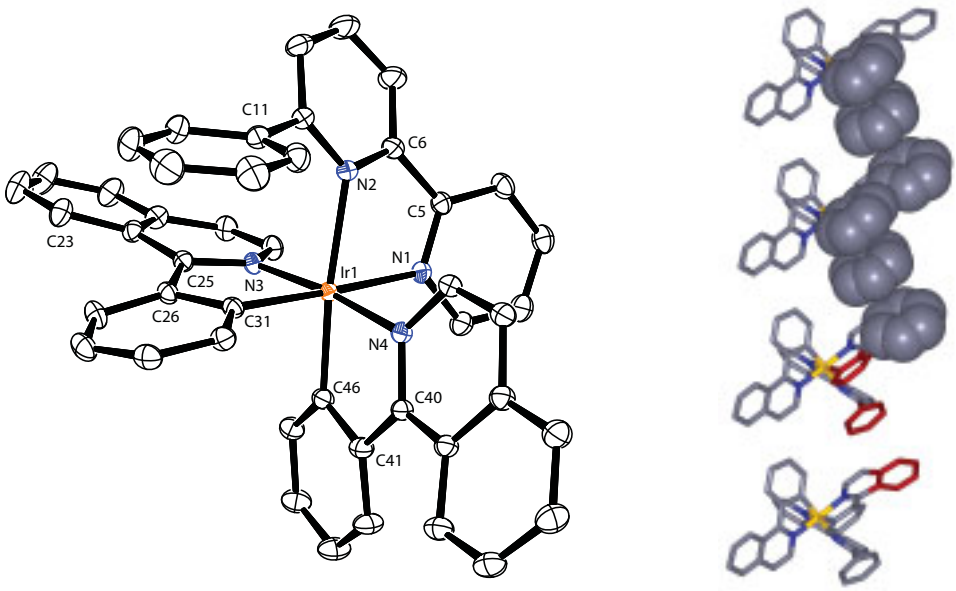

Figure 7.14 (a) ORTEP representation of the solid state structure of the cation present in **59**. Hydrogen atoms, the counterion (PF_6^-), and solvent molecules have been omitted for clarity and thermal ellipsoids are depicted at 50 % probability).
Selected bond lengths (Å) and angles (°):
Ir1–N1 2.1379(11), Ir1–N2 2.2157(11), Ir1–N3 2.0441(11), Ir1–N4 2.0440(11), Ir1–C31 2.0152(12), Ir1–C46 1.9888(13);
N3–Ir1–N4 173.47(4), N1–Ir1–C31 176.79(5), N2–Ir1–C46 172.19(5), N1–Ir1–N2 76.33(4), N3–Ir1–C31 79.56(5), N4–Ir1–C46 79.73(5).
(b) Packing of the cations in complex **59** highlighting intra- and intermolecular π–π interactions (space filling representation and red coloured sticks).

The solid state structure of complex **60** revealed an asymmetric unit containing one molecule ($Z = 4$). The cation is depicted in **Figure 7.15a**. As for all previously discussed complexes, **60** adopts a quasi-octahedral geometry at the metal centre with trans-angles of the donor atoms between 164 – 177 ° and "bite angles" of the coordinating ligands ranging from 76 – 80 °, with the narrowest angle found in the *N*,*N*'-ligand and a slightly more skewed geometry due to the angle built by the trans-donor atoms N2–Ir1–C25 of 164.44(11) ° compared to previously discussed complexes. Bond lengths of the six donating atoms to the metal centre are very similar to all other aforementioned complexes.

Complex **60** exhibits intramolecular π-π stacking between C11- and C34-containing rings, respectively, as is the case for all complexes possessing at least one pendant phenyl ring on the *N*,*N*′-ligand. The centroids of the two rings are separated by a distance of 3.62 Å and the rings are slightly offset with respect to one another. The two planes formed by the two rings intersect at an angle of 13.6(2) °, thus exhibiting an almost parallel geometry. The pendant phenyl ring is twisted by 48.2(2) ° to the ring containing N2.

The crystal packing shown in **Figure 7.15b** highlights the alternating layers of anions and cations as observed before for all other herein discussed complexes.

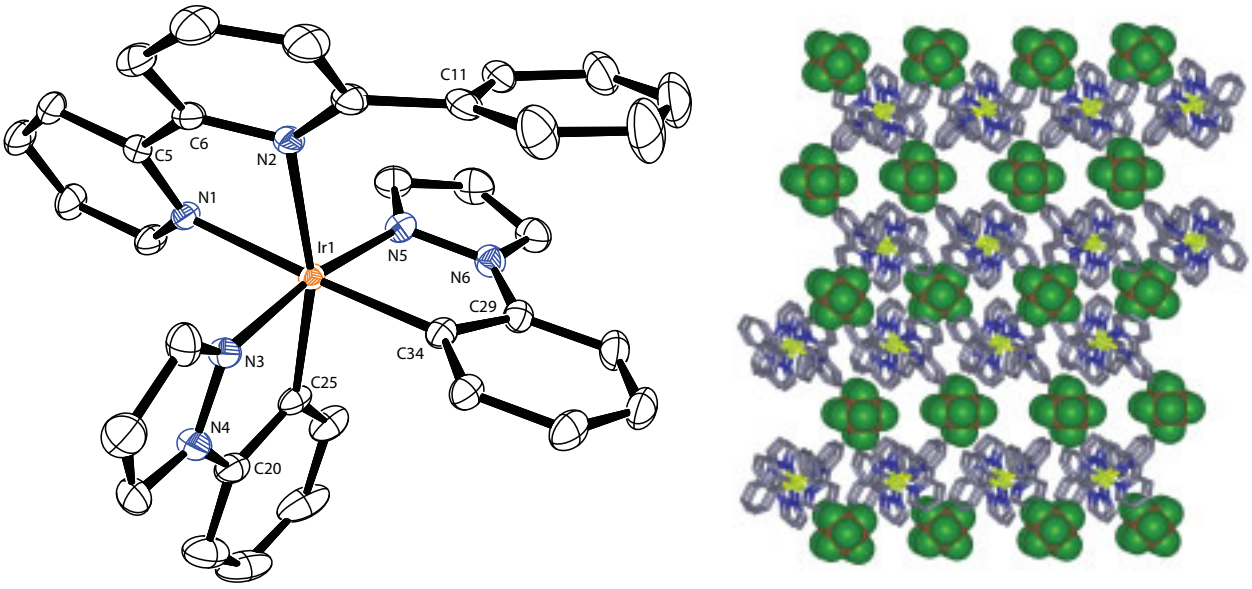

Figure 7.15 (a) ORTEP representation of the solid state structure of the cation present in **60**. Hydrogen atoms, the counterion (PF_6^-), and solvent molecules have been omitted for clarity and thermal ellipsoids are depicted at 50 % probability).
Selected bond lengths (Å) and angles (°):
Ir1–N1 2.121(2), Ir1–N2 2.199(3), Ir1–N3 2.024(3), Ir1–N5 2.012(2), Ir1–C25 2.007(3), Ir1–C34 2.016(3); N3–Ir1–N5 171.15(11), N1–Ir1–C34 177.20(11), N2–Ir1–C25 164.44(11), N1–Ir1–N2 75.98(9), N3–Ir1–C25 80.31(12), N5–Ir1–C34 80.07(11).
(b) Packing of the cations (stick representation) and anions (space filling representation) in complex **60** as viewed along the crystallographic a axis.

In the crystal lattice of complex **61**, there is one cation / anion pair per asymmetric unit ($Z = 4$). The cation present in the solid state structure is depicted in **Figure 7.16a**. It possesses a near-octahedral geometry with trans-angles of the donor atoms between 170 – 177 ° and "bite angles" of the coordinating ligands ranging from 76 – 80 °, very similar to all of the previously discussed complexes, which also applies to the bond lengths revealing no major differences.

Analogous to all other complexes containing at least on phenyl ring at 6-position of the bipyridine, an intramolecular π-π stacking between that ring (containing C33) and the coordinated C11-containing phenyl ring of one of the two cyclometallating *C*,*N*-ligands is found. When compared to the other complexes possessing this intramolecular interaction, the centroids of the two involved rings are separated by a similar distance of 3.51 Å, and offset slightly with an intersection angle of the two planes formed by the two rings of 12.67(8) °. The pendant phenyl ring is twisted to the pyridine ring containing N6 with an angle of 62.87(8) °.

The crystal packing shown in **Figure 7.16b** emphasises the alternating layers of anions and cations as observed before for all other complexes.

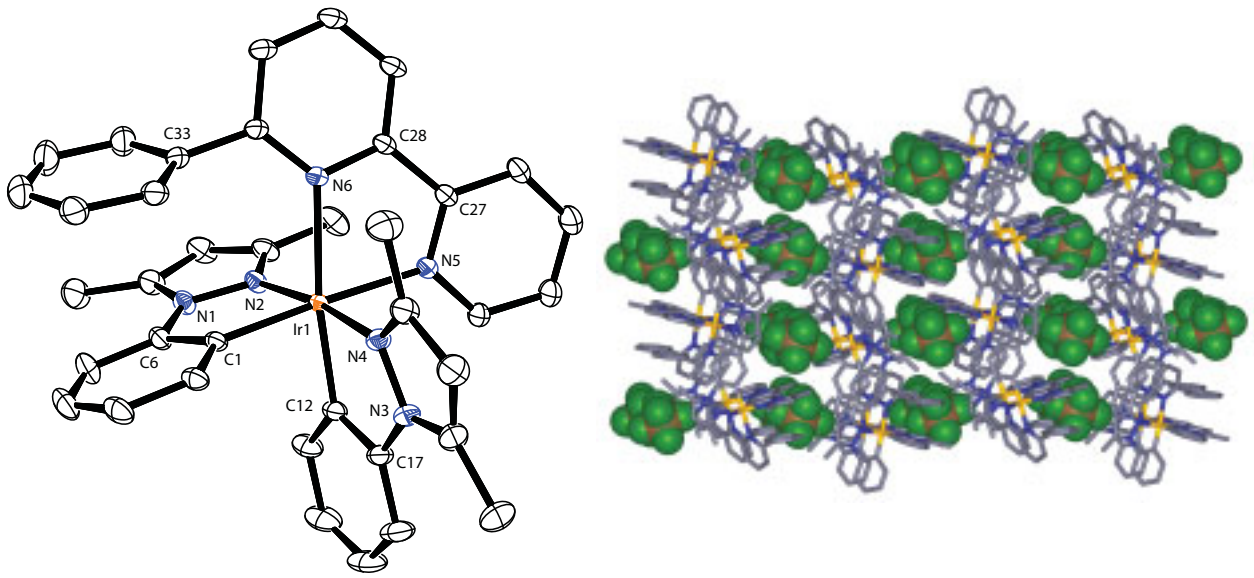

Figure 7.16 (a) ORTEP representation of the solid state structure of the cation present in **61**. Hydrogen atoms and the counterion (PF_6^-) have been omitted for clarity and thermal ellipsoids are depicted at 50 % probability).
Selected bond lengths (Å) and angles (°):
Ir1–N5 2.1540(11), Ir1–N6 2.2425(10), Ir1–N2 2.0344(11), Ir1–N4 2.0483(11), Ir1–C1 2.0216(12), Ir1–C12 2.0088(12);
N2–Ir1–N4 172.12(4), N5–Ir1–C1 177.15(5), N6–Ir1–C12 170.28(5), N5–Ir1–N6 76.06(4), N2–Ir1–C1 79.32(5), N4–Ir1–C12 79.55(5).
(b) Packing of the cations (stick representation) and anions (space filling representation) in complex **61** as viewed along the crystallographic a axis.

From an overview of the solid state structures of the complexes, one can state that they all possess a quasi-octahedral geometry. Bond angles and lengths are, within small margins, in a typical range and very similar in this whole series (**Table 7.8**). The *N*,*N*′-ligand is always at a slightly further distance from the Ir centre. In the *C*,*N*-ligands, the nitrogen atoms are always situated somewhat further from the Ir centre than the negatively charged carbon atoms. As a consequence, the "bite angles" of the *N*,*N*′-ligands is roughly five degrees smaller than that of each *C*,*N*-ligand. If present, the pendant phenyl ring(s) at the *N*,*N*′-ligand give(s) rise to an intramolecular π-π stacking. The rings are located by about 3.5 Å apart with the exception of complexes **57** and **60** in which they are closer and farther apart, respectively. The two π-stacked rings are mostly arranged in an almost parallel manner and the pendant phenyl ring is twisted with regard to the neighbouring pyridine ring by an angle between 48 ° and 83 °. In the crystal lattice, alternating sheets built from the cations and anions, respectively, are found in all the structures.

Table 7.8 Summary of bond lengths and angles of the crystallographic data for all solved complexes.
[a] Ir–N_1 means the shorter, Ir–N_2 means the longer bond from Ir to N of the *N*,*N*′-ligand; Ir–N_3, Ir–N_4, Ir–C_1, and Ir–C_2 mean the distance from Ir to the donating atom, the shorter bond length first.
[b] Of all three trans-angles of the donor atoms, the lowest and the highest are given.
[c] For those complexes adopting an intramolecular π-π stacking, the distance between the centroids of the two involved rings is given. Note that the segment between the centroids normally does not lie perpendicular to the two least-square planes built from the rings, therefore it does not reflect the actual distance between the two planes as they are neither perfectly congruent nor parallel.
[d] As for [c], the intersecting angle of the two involved rings is noted.
[e] The twisting angle(s) of the pendant phenyl ring to the connected pyridine ring is given where applicable.

complex	Ir–N_1[a] [Å]	Ir–N_2[a] [Å]	Ir–N_3[a] [Å]	Ir–N_4[a] [Å]	Ir–C_1[a] [Å]	Ir–C_2[a] [Å]	trans angles[b] [°]	bite angle (N^N) [°]	bite angles (C^N) [°]	distance centroids[c] [Å]	intersecting angle[d] [°]	twisting angle[e] [°]
47	2.1367(10)	2.1496(12)	2.0432(11)	2.0480(12)	2.0034(14)	2.0166(12)	172 – 174	77.86(4)	80.38(5) 80.61(5)			
48	2.1449(18)	2.2259(16)	2.0417(18)	2.0467(18)	2.0009(17)	2.016(2)	170 – 178	76.50(6)	80.23(7) 80.56(8)	3.47	8.13(12)	79.59(13)
49	2.129(3)	2.136(3)	2.042(3)	2.047(3)	2.004(4)	2.024(4)	172 – 175	76.21(12)	80.06(16) 80.68(15)			
50	2.151(3)	2.215(3)	2.036(3)	2.056(3)	2.004(3)	2.025(3)	168 – 177	75.66(11)	80.62(13) 81.05(13)	3.54	8.1(2)	58.2(2)
51	2.2019(19)	2.226(2)	2.0339(17)	2.0504(17)	2.0120(19)	2.012(2)	173 – 178	76.17(8)	80.31(7) 80.32(7)	3.49 (both)	5.92(15) 6.64(14)	54.36(18) 79.40(15)
57	2.1383(7)	2.2168(7)	2.0455(8)	2.0463(7)	2.0011(7)	2.0099(8)	168 – 177	75.69(2)	80.38(3) 80.62(3)	3.35	2.22(5)	82.85(5)
59	2.1379(11)	2.2157(11)	2.0440(11)	2.0441(11)	1.9888(13)	2.0152(12)	172 – 177	76.33(4)	79.56(5) 79.73(5)	3.50	10.53(7)	61.37(8)

complex	Ir–N_1[a] [Å]	Ir–N_2[a] [Å]	Ir–N_3[a] [Å]	Ir–N_4[a] [Å]	Ir–C_1[a] [Å]	Ir–C_2[a] [Å]	trans angles[b] [°]	bite angle (N^N) [°]	bite angles (C^N) [°]	distance centroids[c] [Å]	intersecting angle[d] [°]	twisting angle[e] [°]
60	2.121(2)	2.199(3)	2.012(2)	2.024(3)	2.007(3)	2.016(3)	164 – 177	75.98(9)	80.07(11) 80.31(12)	3.62	13.6(2)	48.2(2)
61	2.1540(11)	2.2425(10)	2.0344(11)	2.0483(11)	2.0088(12)	2.0216(12)	170 – 177	76.06(4)	79.32(5) 79.55(5)	3.51	12.67(8)	62.87(8)

7.4 STM imaging of the cyclometallated Ir(III) complexes and discussion

The dendronised complexes **54**, **55**, **56**, which represent a first, second, and third generation Fréchet-dendronised complex according to the definition pointed out in **Chapter 6**, were examined for their monolayer behaviour on HOPG using the scanning tunnelling microscope. On the air/solid-interface, *i.e.* solution cast samples from acetonitrile (**54**) or hexane (**55** and **56**), unfortunately, no patterns could be observed at all. Dissolving **55** and **56** in 1-phenyloctane (**54** is not soluble therein), in the case of **55**, monolayer formation was seen in the resulting liquid/solid-interface setup. **Figure 7.17** shows the directly observed growing of the domains possessing a repeated pattern in quasi-subsequent images with a size of 200 nm × 200 nm.

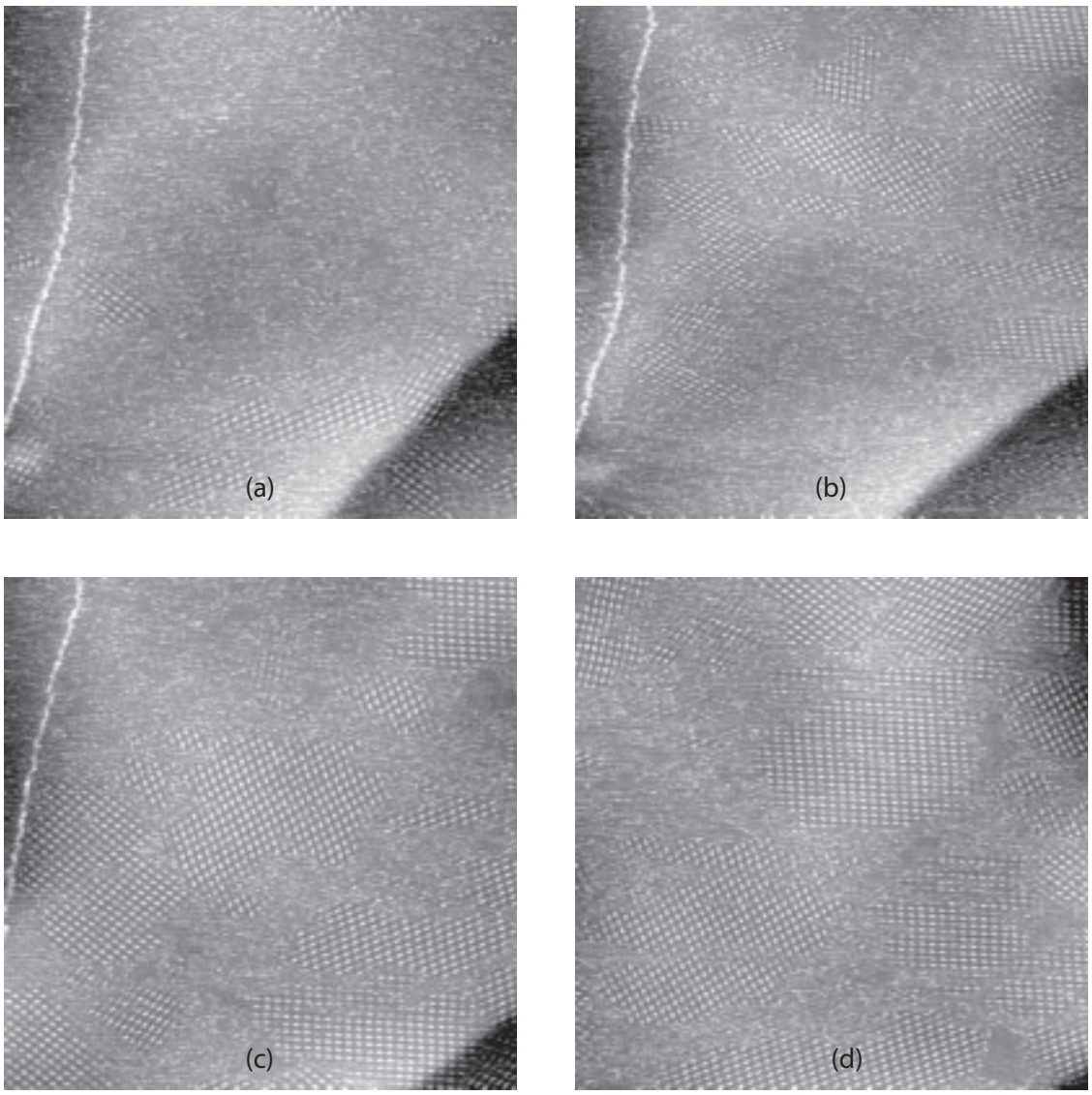

Figure 7.17 Monolayer formation of **55** in 1-phenyloctane on HOPG. All images recorded quasi-subsequently (a → b → c → d) with following scan parameters: U_{bias} = –700 mV, I_t = 8.0 pA, ν = 2.54 Hz, size = 200 nm × 200 nm.

Using a new tip, the monolayer was investigated in more detail and in different scan sizes. Stunningly, even a huge area covering 500 nm × 500 nm could be visualised in high detail. In **Figure 7.18**, the different "zoom" levels are depicted with a set of images recorded quasi-subsequently (although from small to large size) all at the same position.

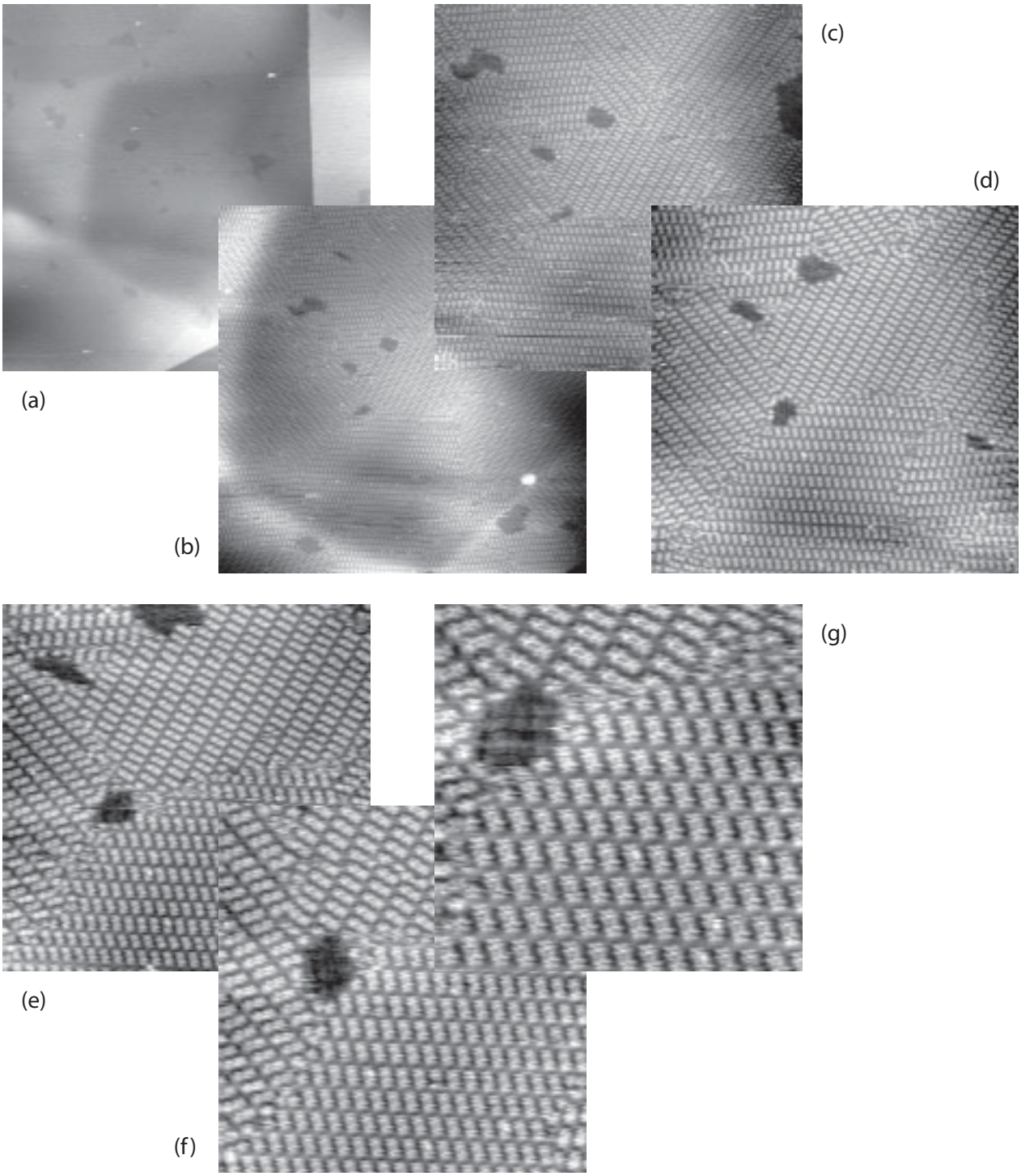

Figure 7.18 STM Images of **55** in 1-phenyloctane on HOPG at different recording sizes: (a) 500 nm × 500 nm (v = 1.00 Hz), (b) 300 nm × 300 nm (v = 1.97 Hz), (c) 200 nm × 200 nm (v = 2.54 Hz), (d) 150 nm × 150 nm (v = 3.05 Hz), (e) 100 nm × 100 nm (v = 4.07 Hz), (f) 75 nm × 75 nm (v = 5.09 Hz), (g) 50 nm × 50 nm (v = 6.10 Hz). All images recorded quasi-reversed-subsequently with constant scan parameters: U_{bias} = –700 mV, I_t = 8.0 pA.

One possible unit cell of the 2D-monolayer is shown in **Figure 7.19** as an overlay on the image from **Figure 7.18g** (50 nm × 50 nm). The oblique unit cell's plane group is most probably *p*2 due to its two-fold axis and the cell parameters are a = 5.0 nm, b = 3.4 nm, α = 66 °.

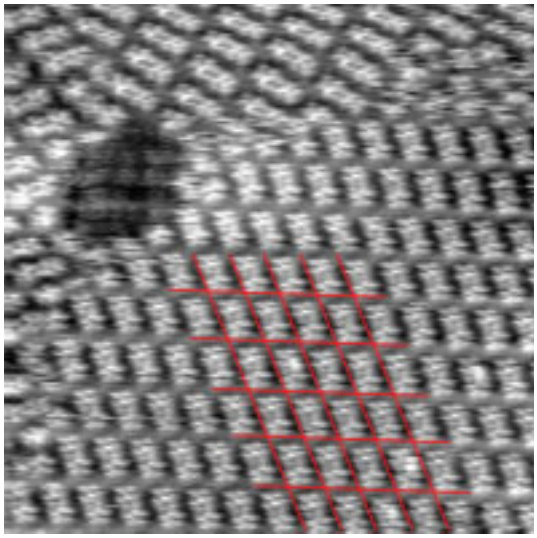

Figure 7.19 Image from **Figure 7.18g** with its corresponding unit cell: a = 5.0 nm, b = 3.4 nm, α = 66 °.

A 10 nm × 10 nm inset of the image from **Figure 7.19** was averaged over 72 positions which is depicted in **Figure 7.20** with two hypothetical overlays of correspondingly sized molecules of **55** adopting a quasi-flat conformation, at least in its dendron part. It should be noted that the alkyl chains were not fitted at all and may intersect in this model, albeit this rough model fits surprisingly well for an interdigitation with other alkyl chains and the black parts in the image associated with insulating "objects" of the monolayer. It remains unknown though whether monolayers exhibiting alkyl chains lying on top of each other exist.

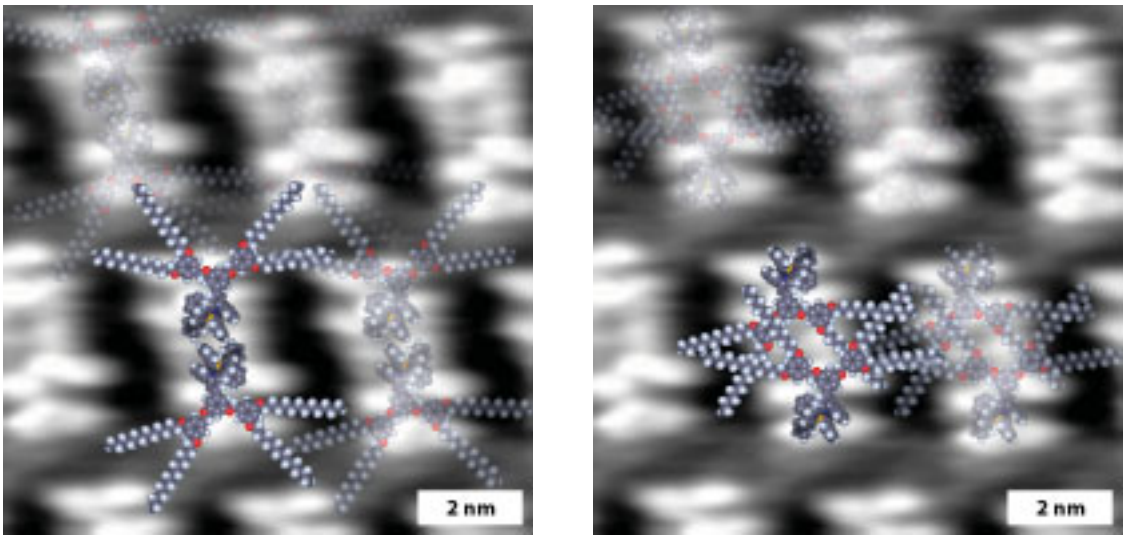

(a) (b)

Figure 7.20 Averaged image over 72 positions with two possible overlays of molecules of **55**.

7.5
Experimental part

Preparation of bis(2-phenylpyridine-*C,N*)(1,10-phenanthroline-*N,N'*)iridium(III) hexafluorophosphate (**47**)

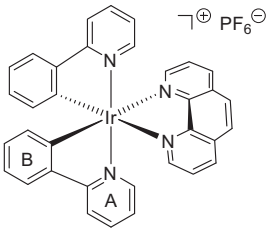

An orange suspension of tetrakis(2-phenylpyridine-*C,N*)di(μ-chloro)diiridium(III) (**41**) (354 mg, 0.330 mmol, 1.00 eq) and 1,10-phenanthroline (119 mg, 0.660 mmol, 2.00 eq) in MeOH (30 ml) and CH_2Cl_2 (30 ml) was refluxed under an inert atmosphere of N_2 in the dark for 14 h. The orange solution was then cooled down to room temperature, and solid ammonium hexafluorophosphate (538 mg, 3.30 mmol, 10.0 eq) was added to the solution. The mixture was stirred for 30 min at room temperature and then evaporated to dryness. The crude material was purified by column chromatography (Merck Alox 90; CH_2Cl_2 → CH_2Cl_2:MeOH = 100:1) yielding the desired product as a yellow solid (538 mg, 0.652 mmol, 99 %).

mp decomp. > 320 °C. **^{1}H NMR** (500 MHz, CD_2Cl_2) δ / ppm 8.67 (dd, ^3J = 8.2 Hz, ^4J = 1.2 Hz, 2H, $H^{4/7(phen)}$), 8.38 (dd, ^3J = 5.0 Hz, ^4J = 1.2 Hz, 2H, $H^{2/9(phen)}$), 8.25 (s, 2H, $H^{5/6(phen)}$), 8.01 (d, ^3J = 8.2 Hz, 2H, $H^{3(A)}$), 7.87 (dd, ^3J = 8.2 Hz, ^3J = 5.0 Hz, 2H, $H^{3/8(phen)}$), 7.82 (d, ^3J = 7.8 Hz, 2H, $H^{6(B)}$), 7.78 (t, ^3J = 7.8 Hz, 2H, $H^{4(A)}$), 7.36 (d, ^3J = 5.7 Hz, 2H, $H^{6(A)}$), 7.17 (t, ^3J = 7.6 Hz, 2H, $H^{5(B)}$), 7.04 (td, ^3J = 7.4 Hz, ^4J = 1.0 Hz, 2H, $H^{4(B)}$), 6.89 (t, ^3J = 6.6 Hz, 2H, $H^{5(A)}$), 6.47 (d, ^3J = 7.5 Hz, 2H, $H^{3(B)}$). **^{13}C NMR** (126 MHz, CD_2Cl_2) δ / ppm 168.22 ($C^{2(A)}$), 151.59 ($C^{2/9(phen)}$), 149.67 ($C^{2(B)}$), 148.94 ($C^{6(A)}$), 147.23 ($C^{10a/10b(phen)}$), 144.28 ($C^{1(B)}$), 138.92 ($C^{4/7(phen)}$), 138.59 ($C^{4(A)}$), 132.19 ($C^{3(B)}$), 131.94 ($C^{4a/6a(phen)}$), 131.13 ($C^{4(B)}$), 128.88 ($C^{5/6(phen)}$), 127.06 ($C^{3/8(phen)}$), 125.32 ($C^{6(B)}$), 123.60 ($C^{5(A)}$), 123.27 ($C^{5(B)}$), 120.26 ($C^{3(A)}$). **IR** (solid): $\tilde{\nu}$ = 3040 (w),2623 (w), 1909 (w), 1801 (w), 1749 (w), 1715 (w), 1609 (m), 1582 (m), 1477 (m), 1418 (m), 1342 (w), 1310 (w), 1269 (m), 1227 (w), 1163 (w), 1148 (w), 1126 (w), 1065 (w), 1032 (w), 1011 (w), 825 (s), 756 (s), 721 (s), 669 (s), 555 (m), 507 (s), 484 (s), 438 (s) cm^{-1}. **MS** (ESI, *m/z*): 681.1 $[M\text{-}PF_6]^+$ (calc. 681.2). **UV-Vis** λ / nm (ε / l mol^{-1} cm^{-1}) (CH_2Cl_2, 1.03E–5 mol l^{-1}) 255 (sh, 56 000), 267 (59 000); (CH_2Cl_2, 2.07E–5 mol l^{-1}) 334 (sh, 11 000); (CH_2Cl_2, 1.03E–4 mol l^{-1}) 381 (7 800); (CH_2Cl_2, 4.13E–4 mol l^{-1}) 467 (910). **Luminescence** (CH_2Cl_2, c = 1.03E–5 mol l^{-1}, λ_{ex} = 382 nm): λ_{em} = 573 nm; lifetime τ = 148 ns (χ^2 = 1.008). **Calcd.** for $C_{34}H_{24}F_6IrN_4P{\cdot}H_2O$ (843.78) C 48.40, H 3.11, N 6.64; found C 48.53, H 3.09, N 6.60 %.

Preparation of bis(2-phenylpyridine-*C,N*)(2-phenyl-1,10-phenanthroline-*N,N'*)iridium(III) hexafluorophosphate (**48**)

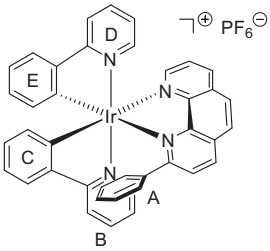

An orange suspension of tetrakis(2-phenylpyridine-*C,N*)di(μ-chloro)diiridium(III) (**41**) (350 mg, 0.326 mmol, 1.00 eq) and 2-phenyl-1,10-phenanthroline (**30**) (167 mg, 0.653 mmol, 2.00 eq) in MeOH (30 ml) and CH_2Cl_2 (30 ml) was refluxed under an inert atmosphere of N_2 in the dark for 12 h. The orange solution was then cooled down to room temperature, and solid ammonium hexafluorophosphate (532 mg, 3.27 mmol, 10.0 eq) was added to the solution. The mixture was stirred for 2 h at room temperature and then evaporated to dryness. The crude material was purified twice by column chromatography (Merck Alox 90; CH_2Cl_2 → CH_2Cl_2:MeOH = 100:1), dissolved in CH_2Cl_2, and precipitated with hexane, washed with hexane, ethyl acetate, tolu-

ene and purified by a subsequent column chromatography (Merck Alox 90; CH_2Cl_2 → CH_2Cl_2:MeOH = 100:2) yielding the desired product as an orange solid (474 mg, 0.526 mmol, 80 %).

^{1}H NMR (500 MHz, CD_2Cl_2) δ / ppm 8.73 (d, *J* = 8.3 Hz, 1H), 8.64 (dd, *J* = 8.2 Hz, *J* = 1.2 Hz, 1H), 8.31 (d, *J* = 8.8 Hz, 1H), 8.26 (d, *J* = 8.8 Hz, 1H), 8.21 (dd, *J* = 5.1 Hz, *J* = 1.3 Hz, 1H), 7.93 (d, *J* = 8.0 Hz, 1H), 7.89 – 7.81 (m, 3H), 7.77 – 7.71 (m, 2H), 7.61 (d, *J* = 7.8 Hz, 1H), 7.54 (d, *J* = 5.7 Hz, 1H), 7.49 (d, *J* = 5.7 Hz, 1H), 7.36 (d, *J* = 7.7 Hz, 1H), 7.05 (d, *J* = 7.6 Hz, 1H), 7.02 (d, *J* = 7.6 Hz, 1H), 6.98 – 6.89 (m, 3H), 6.85 (s br, 2H), 6.69 (t, *J* = 7.5 Hz, 1H), 6.45 (td, *J* = 7.5 Hz, *J* = 1.1 Hz, 1H), 6.10 (d, *J* = 7.6 Hz, 1H), 5.66 (d, *J* = 7.5 Hz, 1H). **^{13}C NMR** (126 MHz, CD_2Cl_2) δ / ppm 169.24, 167.46, 166.83, 151.30, 149.29, 147.74, 147.36, 147.03, 143.44, 143.29, 139.26, 138.70, 138.44, 138.40, 137.86, 132.24, 131.96, 131.19, 130.94, 130.71, 130.16, 129.67, 129.47, 129.02, 128.45, 128.20, 127.67, 126.46, 125.01, 124.84, 123.66, 123.27, 122.65, 121.28, 120.23, 120.17. **IR** (solid): $\tilde{\nu}$ = 3666 (w), 3585 (w), 3045 (w), 1607 (s), 1583 (s), 1564 (m), 1477 (s), 1439 (m), 1421 (s), 1385 (w), 1306 (w), 1269 (m), 1227 (w), 1157 (m), 1063 (w), 1030 (w), 827 (s), 754 (s), 727 (s), 698 (s), 660 (s), 629 (m), 554 (s) cm^{-1}. **MS** (ESI, *m/z*): 757.1 $[M\text{-}PF_6]^+$ (calc. 757.2). **UV-Vis** λ / nm (ε / l mol^{-1} cm^{-1}) (CH_2Cl_2, 1.01E–5 mol l^{-1}) 232 (53 000), 269 (57 000); (CH_2Cl_2, 2.02E–5 mol l^{-1}) 343 (sh, 11 000); (CH_2Cl_2, 1.01E–4 mol l^{-1}) 383 (6 700), 412 (sh, 3 700); (CH_2Cl_2, 4.05E–4 mol l^{-1}) 471 (840). **Luminescence** (CH_2Cl_2, c = 1.01E–5 mol l^{-1}, λ_{ex} = 382 nm): λ_{em} = 583 nm; lifetime τ = 168 ns (χ^2 = 1.010). **Calcd.** for $C_{40}H_{28}F_6IrN_4P{\cdot}H_2O$ (919.87) C 52.23, H 3.29, N 6.09; found C 52.10, H 3.23, N 5.85 %.

Preparation of bis(2-phenylpyridine-*C,N*)(2,2′-bipyridine-*N,N*′)iridium(III) hexafluorophosphate (**49**)

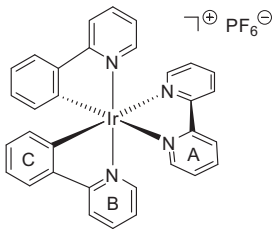

A yellow suspension of tetrakis(2-phenylpyridine-*C,N*)di(μ-chloro)diiridium(III) (**41**) (300 mg, 0.280 mmol, 1.00 eq) and 2,2'-bipyridine (87.0 mg, 0.560 mmol, 2.00 eq) in MeOH (30 ml) and CH_2Cl_2 (30 ml) was refluxed under an inert atmosphere of N_2 in the dark for 16 h. The orange solution was then cooled down to room temperature, and solid ammonium hexafluorophosphate (456 mg, 2.80 mmol, 10.0 eq) was added to the solution. The mixture was stirred for 30 min at room temperature and then evaporated to dryness. The crude material was purified by column chromatography (Merck Alox 90; CH_2Cl_2 → CH_2Cl_2:MeOH = 100:1) yielding the desired product as a yellow solid (438 mg, 0.546 mmol, 98 %).

mp decomp. > 340 °C. **^{1}H NMR** (500 MHz, CD_2Cl_2) δ / ppm 8.55 (d, *J* = 8.2 Hz, 2H, $H^{3(A)}$), 8.17 (t, *J* = 7.9 Hz, 2H, $H^{4(A)}$), 8.07 (d, *J* = 4.8 Hz, 2H, $H^{6(A)}$), 8.01 (d, *J* = 8.2 Hz, 2H, $H^{3(B)}$), 7.83 (t, *J* = 7.8 Hz, 2H, $H^{4(B)}$), 7.79 (d, *J* = 7.8 Hz, 2H, $H^{6(C)}$), 7.54 (d, *J* = 5.6 Hz, 2H, $H^{6(B)}$), 7.51 (t, *J* = 6.6 Hz, 2H, $H^{5(A)}$), 7.12 (t, *J* = 7.5 Hz, 2H, $H^{5(C)}$), 7.04 (t, *J* = 6.6 Hz, 2H, $H^{5(B)}$), 6.98 (t, *J* = 7.4 Hz, 2H, $H^{4(C)}$), 6.36 (d, *J* = 7.6 Hz, 2H, $H^{3(C)}$). **^{13}C NMR** (126 MHz, CD_2Cl_2) δ / ppm 168.13 ($C^{2(B)}$), 156.07 ($C^{2(A)}$), 151.16 ($C^{6(A)}$), 150.29 ($C^{(1C)}$), 148.91 ($C^{6(B)}$), 144.07 ($C^{2(C)}$), 139.82 ($C^{4(A)}$), 138.62 ($C^{4(B)}$), 132.02 ($C^{3(C)}$), 131.11 ($C^{4(C)}$), 128.71 ($C^{5(A)}$), 125.31 ($C^{6(C)}$), 124.95 ($C^{3(A)}$), 123.72 ($C^{5(B)}$), 123.12 ($C^{5(C)}$), 120.27 ($C^{3(B)}$). **IR** (solid): $\tilde{\nu}$ = 3040 (w), 2611 (w), 1898 (w), 1867 (w), 1826 (w), 1790 (w), 1609 (m), 1582 (m), 1477 (m), 1445 (m), 1420 (m), 1313 (m), 1269 (m), 1227 (m), 1163 (m), 1128 (w), 1109 (w), 1065 (m), 1032 (m), 879 (m), 831 (s), 752 (s), 727 (s), 669 (s), 555 (s) cm^{-1}. **MS** (ESI, *m/z*): 657.0 $[M\text{-}PF_6]^+$ (calc. 657.2). **UV-Vis** λ / nm (ε / l mol^{-1} cm^{-1}) (CH_2Cl_2, 1.01E–5 mol l^{-1}) 257 (48 000), 308 (sh, 23 000); (CH_2Cl_2, 1.01E–4 mol l^{-1}) 336 (sh, 9 800), 381 (7 000), 406 (sh, 4 200); (CH_2Cl_2, 4.05E–4 mol l^{-1}) 467 (830). **Luminescence** (CH_2Cl_2, c = 1.01E–5 mol l^{-1}, λ_{ex} = 381 nm): λ_{em} = 582 nm; lifetime τ = 157 ns (χ^2 = 1.055). **Calcd.** for $C_{32}H_{24}F_6IrN_4P{\cdot}H_2O$ (819.76) C 46.88, H 3.20, N 6.83; found C 47.07, H 2.94, N 6.76 %.

Preparation of bis(2-phenylpyridine-*C,N*)(6-phenyl-2,2'-bipyridine-*N,N'*)iridium(III) hexafluorophosphate (**50**)

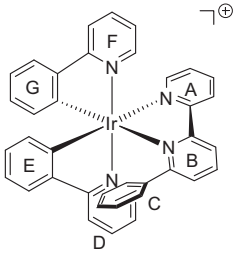

$\neg^{\oplus}$ $PF_6^{\ominus}$ A yellow suspension of tetrakis(2-phenylpyridine-*C,N*)di(μ-chloro)diiridium(III) (**41**) (300 mg, 0.280 mmol, 1.00 eq) and 6-phenyl-2,2'-bipyridine (**31**) (131 mg, 0.562 mmol, 2.01 eq) in MeOH (30 ml) and CH_2Cl_2 (30 ml) was refluxed under an inert atmosphere of N_2 in the dark for 10 h. The orange solution was then cooled down to room temperature, and solid ammonium hexafluorophosphate (365 mg, 2.24 mmol, 8.00 eq) was added to the solution. The mixture was stirred for 30 min at room temperature and then evaporated to dryness. The crude material was purified by column chromatography (Merck Alox 90; CH_2Cl_2 → CH_2Cl_2:MeOH = 100:1) yielding the desired product as an orange solid (487 mg, 0.554 mmol, 99 %).

R_f (TLC, Alox 90; CH_2Cl_2:MeOH = 100:2): 0.3. **^{1}H NMR** (500 MHz, CD_2Cl_2) δ / ppm 8.60 – 8.52 (m, 2H), 8.26 (t, *J* = 7.9 Hz, 1H), 8.15 (td, *J* = 8.1 Hz, *J* = 1.5 Hz, 1H), 7.95 – 7.83 (m, 4H), 7.80 (td, *J* = 7.9 Hz, *J* = 1.4 Hz, 1H), 7.74 (d, *J* = 5.8 Hz, 1H), 7.57 (d, *J* = 7.8 Hz, 1H), 7.52 (dd, *J* = 7.7 Hz, *J* = 1.0 Hz, 1H), 7.44 – 7.40 (m, 2H), 7.27 (d, *J* = 7.8 Hz, 1H), 7.12 (td, *J* = 6.6 Hz, *J*= 1.4 Hz, 1H), 7.09 (td, *J* = 6.3 Hz, *J*= 1.9 Hz, 1H), 6.99 (td, *J* = 7.5 Hz, *J*= 1.0 Hz , 2H), 6.86 (td, *J* = 7.6 Hz, *J* = 1.2 Hz, 1H), 6.78 (t, *J* = 7.7 Hz, 2H), 6.64 (td, *J* = 7.5 Hz, *J*= 0.9 Hz, 1H), 6.56 (s br, 2H), 6.44 (td, *J* = 7.5 Hz, *J* = 1.1 Hz, 1H), 6.00 (d, *J* = 7.6 Hz, 1H), 5.63 (d, *J* = 7.6 Hz, 1H). **^{13}C NMR** (126 MHz, CD_2Cl_2) δ / ppm 169.27, 167.52, 166.23, 157.29, 157.12, 151.29, 150.68, 149.21, 149.20, 146.86, 143.37, 143.17, 140.02, 139.65, 138.58, 138.41, 138.05, 131.74, 131.12, 130.59, 130.38, 129.94, 129.40, 128.26, 128.07, 127.73, 125.38, 124.95, 124.91, 123.89, 123.82, 123.16, 122.74, 121.15, 120.35, 120.19. **IR** (solid): $\tilde{\nu}$ = 3043 (w), 1981 (w), 1607 (w), 1583 (w), 1560 (w), 1477 (m), 1448 (w), 1421 (w), 1315 (w), 1269 (w), 1227 (w), 1163 (w), 1126 (w), 1063 (w), 1030 (w), 829 (s), 754 (s), 729 (s), 694 (s), 613 (m), 581 (m), 555 (m) cm^{-1}. **MS** (ESI, *m/z*): 732.8 $[M\text{-}PF_6]^+$ (calc. 733.2). **UV-Vis** λ / nm (ε / l mol^{-1} cm^{-1}) (CH_2Cl_2, 9.72E–6 mol l^{-1}) 267 (44 000), 311 (sh, 23 000); (CH_2Cl_2, 3.89E–4 mol l^{-1}) 382 (sh, 5 500), 411 (sh, 3 400), 470 (760). **Luminescence** (CH_2Cl_2, c = 9.72E–6 mol l^{-1}, λ_{ex} = 313 nm): λ_{em} = 595 nm; lifetime τ = 125 ns (χ^2 = 1.085). **Calcd.** for $C_{38}H_{28}F_6IrN_4P{\cdot}0.5H_2O$ (886.84) C 51.46, H 3.30, N 6.32; found C 51.54, H 3.17, N 6.28 %.

Preparation of bis(2-phenylpyridine-*C,N*)(6,6'-diphenyl-2,2'-bipyridine-*N,N'*)iridium(III) hexafluorophosphate (**51**)

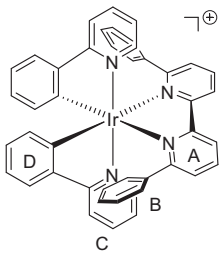

$\neg^{\oplus}$ $PF_6^{\ominus}$ A yellow suspension of tetrakis(2-phenylpyridine-*C,N*)di(μ-chloro)diiridium(III) (**41**) (350 mg, 0.326 mmol, 1.00 eq) and 6,6'-diphenyl-2,2'-bipyridine (**32**) (203 mg, 0.659 mmol, 2.02 eq) in MeOH (35 ml) and CH_2Cl_2 (35 ml) was refluxed under an inert atmosphere of N_2 in the dark for 36 h. Silver(I) hexafluorophosphate (167 mg, 0.659 mmol, 2.02 eq) was added to the mixture which was then refluxed for another 20 h. The yellow suspension was then cooled down to room temperature, and solid ammonium hexafluorophosphate (532 mg, 3.26 mmol, 10.0 eq) was added to the solution. The mixture was stirred for 1 h at room temperature and then evaporated to dryness. The crude material was purified by column chromatography (Merck Alox 90; CH_2Cl_2 → CH_2Cl_2:MeOH = 100:1) yielding the desired product as an orange solid (554 mg, 0.581 mmol, 89 %).

mp 195 – 200 °C. **^{1}H NMR** (500 MHz, CD_2Cl_2) δ / ppm 8.42 (d, ^3J = 8.0 Hz, 2H, $H^{3(A)}$), 8.26 (d, ^3J = 5.7 Hz, 2H, $H^{6(C)}$), 8.15 (t, ^3J = 7.9 Hz, 2H, $H^{4(A)}$), 7.83 (t, ^3J = 7.8 Hz, 2H, $H^{4(C)}$), 7.65 (d, ^3J = 8.2 Hz, 2H, $H^{3(C)}$), 7.34 (d, ^3J = 7.7 Hz, 2H,

$H^{5(A)}$), 7.16 (t, ^3J = 6.6 Hz, 2H, $H^{5(C)}$), 7.11 (d, ^3J = 7.8 Hz, 2H, $H^{6(D)}$), 7.01 (t, ^3J = 7.5 Hz, 2H, $H^{4(B)}$), 6.76 (t, ^3J = 7.8 Hz, 4H, $H^{3(B)}$), 6.60 (d, ^3J = 6.2 Hz, 4H, $H^{2(B)}$), 6.55 (t, ^3J = 7.5 Hz, 2H, $H^{5(D)}$), 6.21 (t, ^3J = 7.5 Hz, 2H, $H^{4(D)}$), 5.24 (d, ^3J = 7.8 Hz, 2H, $H^{3(D)}$). **^{13}C NMR** (126 MHz, CD_2Cl_2) δ / ppm 168.33 ($C^{2(C)}$), 165.56 ($C^{6(A)}$), 159.38 ($C^{2(A)}$), 150.37 ($C^{6(C)}$), 146.81 ($C^{2(D)}$), 141.85 ($C^{1(D)}$), 139.68 ($C^{4(A)}$), 138.41 ($C^{1(B)}$), 138.35 ($C^{4(C)}$), 131.09 ($C^{3(D)}$), 130.01 ($C^{5(A)}$/$C^{4(D)}$), 129.98 ($C^{5(A)}$/$C^{4(D)}$), 128.72 ($C^{4(B)}$), 128.02 ($C^{3(B)}$), 127.51 ($C^{2(B)}$), 124.63 ($C^{3(A)}$), 124.42 ($C^{6(D)}$), 122.37 ($C^{5(C)}$), 121.25 ($C^{5(D)}$), 119.75 ($C^{3(C)}$). **IR** (solid): $\tilde{\nu}$ = 3045 (w), 2627 (w), 1983 (w), 1607 (m), 1585 (m), 1564 (m), 1477 (m), 1452 (m), 1421 (m), 1307 (w), 1271 (w), 1229 (w), 1163 (w), 1128 (w), 1063 (w), 1030 (w), 1003 (w), 827 (s), 752 (s), 729 (s), 694 (s) cm^{-1}. **MS** (ESI, *m/z*): 809.2 $[M\text{-}PF_6]^+$ (calc. 809.2); 501.1 $[M\text{-}PF_6\text{-}L_{N,N'}]^+$ (calc. 501.1). **UV-Vis** λ / nm (ε / l mol^{-1} cm^{-1}) (CH_2Cl_2, 9.99E–6 mol l^{-1}) 267 (43 000), 311 (sh, 27 000); (CH_2Cl_2, 9.99E–5 mol l^{-1}) 383 (sh, 5 200); (CH_2Cl_2, 4.00E–4 mol l^{-1}) 474 (920). **Luminescence** (CH_2Cl_2, c = 9.99E–6 mol l^{-1}, λ_{ex} = 316 nm): λ_{em} = 579 nm; lifetime τ = 98 ns (χ^2 = 1.050). **Calcd.** for $C_{44}H_{32}F_6IrN_4P{\cdot}0.5H_2O$ (962.94) C 54.88, H 3.45, N 5.82; found C 54.82, H 3.36, N 5.80 %.

Preparation of bis(2-phenylpyridine-*C,N*)(4-(3,5-dimethoxyphenyl)-6-phenyl-2,2'-bipyridine-*N,N'*)iridium(III) hexafluorophosphate (**52**)

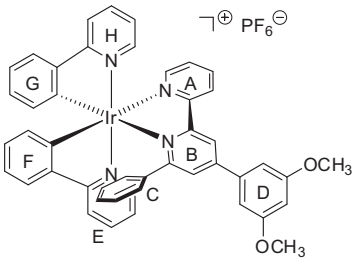

A yellow suspension of tetrakis(2-phenylpyridine-*C,N*)di(μ-chloro)diiridium(III) (**41**) (300 mg, 0.280 mmol, 1.00 eq) and 4-(3,5-dimethoxyphenyl)-6-phenyl-2,2'-bipyridine (**35**) (208 mg, 0.565 mmol, 2.00 eq) in MeOH (30 ml) and CH_2Cl_2 (30 ml) was refluxed under an inert atmosphere of N_2 in the dark for 12 h. The orange solution was then cooled down to room temperature, and solid ammonium hexafluorophosphate (456 mg, 2.80 mmol, 10.0 eq) was added to the solution. The mixture was stirred for 45 min at room temperature and then evaporated to dryness. The crude material was purified by column chromatography (Merck Alox 90; CH_2Cl_2 → CH_2Cl_2:MeOH = 100:1) yielding the desired product as an orange solid (519 mg, 0.512 mmol, 91 %).

^{1}H NMR (500 MHz, CD_2Cl_2) δ / ppm 8.65 (d, J = 1.3 Hz, 1H), 8.63 (d, J = 8.2 Hz, 1H), 8.15 (t, J = 7.9 Hz, 1H), 7.92 – 7.81 (m, 4H), 7.77 (t, J = 7.8 Hz, 1H), 7.70 (d, J = 5.7 Hz, 1H), 7.66 (s, 1H), 7.63 (d, J = 5.7 Hz, 1H), 7.54 (d, J = 7.7 Hz, 1H), 7.40 (t, J = 6.5 Hz, 1H), 7.25 (d, J = 7.8 Hz, 1H), 7.12 – 7.02 (m, 2H), 6.99 – 6.94 (m, 4H), 6.83 (t, J = 7.5 Hz, 1H), 6.77 (t, J = 7.5 Hz, 2H), 6.68 – 6.50 (m, 4H), 6.40 (t, J = 7.4 Hz, 1H), 5.97 (d, J = 7.6 Hz, 1H), 5.59 (d, J = 7.6 Hz, 1H), 3.88 (s, 6H). **^{13}C NMR** (126 MHz, CD_2Cl_2) δ / ppm 169.21, 167.58, 166.30, 162.23, 157.59, 157.18, 151.58, 151.34, 150.75, 149.36, 149.22, 147.26, 143.36, 143.13, 139.70, 138.56, 138.41, 138.12, 137.68, 131.81, 131.15, 130.64, 129.99, 129.46, 128.26, 128.17, 127.83, 127.82, 125.54, 124.99, 124.85, 123.78, 123.16, 122.79, 121.46, 121.15, 120.26, 120.23, 105.87, 102.89, 56.16. **IR** (solid): $\tilde{\nu}$ = 3043 (w), 2947 (w), 2843 (w), 1595 (s), 1539 (w), 1477 (m), 1394 (m), 1308 (w), 1269 (w), 1204 (m), 1155 (s), 1061 (m), 1030 (w), 935 (w), 829 (s), 789 (s), 754 (s), 725 (s), 694 (m), 667 (w), 615 (w), 579 (w), 555 (s) cm^{-1}. **MS** (ESI, *m/z*): 869.2 $[M\text{-}PF_6]^+$ (calc. 869.2). **UV-Vis** λ / nm (ε / l mol^{-1} cm^{-1}) (CH_2Cl_2, 9.93E–6 mol l^{-1}) 272 (53 000), 317 (sh, 31 000); (CH_2Cl_2, 9.93E–5 mol l^{-1}) 384 (sh, 8 200), 412 (sh, 4 000); (CH_2Cl_2, 3.97E–4 mol l^{-1}) 471 (1 100). **Luminescence** (CH_2Cl_2, c = 9.93E–6 mol l^{-1}, λ_{ex} = 314 nm): λ_{em} = 603 nm; lifetime τ = 168 ns (χ^2 = 1.068). **Calcd.** for $C_{46}H_{36}F_6IrN_4O_2P{\cdot}0.5H_2O$ (1013.98) C 54.49, H 3.58, N 5.53; found C 54.52, H 3.71, N 5.45 %.

Preparation of bis(2-phenylpyridine-*C,N*)(4-(3,5-dihydroxyphenyl)-6-phenyl-2,2'-bipyridine-*N,N'*)iridium(III) hexafluorophosphate (**53**)

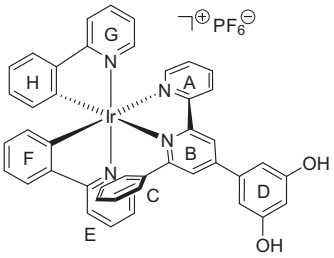

A yellow suspension of tetrakis(2-phenylpyridine-*C,N*)di(μ-chloro)diiridium(III) (**41**) (400 mg, 0.373 mmol, 1.00 eq) and 4-(3,5-dihydroxyphenyl)-6-phenyl-2,2'-bipyridine (**37**) (254 mg, 0.746 mmol, 2.00 eq) in MeOH (30 ml) and CH_2Cl_2 (30 ml) was refluxed under an inert atmosphere of N_2 in the dark for 15 h. The orange solution was then cooled down to room temperature, and solid ammonium hexafluorophosphate (608 mg, 3.73 mmol, 10.0 eq) was added to the solution. The mixture was stirred for 30 min at room temperature and then evaporated to dryness. The crude material was purified with size exclusion chromatography (Sephadex LH–20, 0.025–0.100 mm, MeOH), followed by a subsequent column chromatography (Fluka silica gel 60, 0.040–0.063 mm; CH_2Cl_2 → CH_2Cl_2:MeOH = 100:5) yielding the desired product as an orange solid (662 mg, 0.671 mmol, 90 %).

^{1}H NMR (500 MHz, CD_2Cl_2) δ / ppm 8.84 (d, *J* = 8.3 Hz, 1H), 8.82 (d, *J* = 1.9 Hz, 1H), 8.16 (td, *J* = 8.0 Hz, *J* = 1.6 Hz, 1H), 7.92 – 7.84 (m, 4H), 7.79 (td, *J* = 7.9 Hz, *J* = 1.4 Hz, 1H), 7.74 (d, *J* = 5.8 Hz, 1H), 7.67 (d, *J* = 1.9 Hz, 1H), 7.63 (d, *J* = 5.7 Hz, 1H), 7.57 (dd, *J* = 7.8 Hz, *J* = 1.0 Hz, 1H), 7.40 (ddd, *J* = 7.4 Hz, *J* = 5.6 Hz, *J* = 0.9 Hz, 1H), 7.28 (dd, *J* = 7.8 Hz, *J* = 0.8 Hz, 1H), 7.12 (ddd, *J* = 7.4 Hz, *J* = 5.9 Hz, *J* = 1.4 Hz, 1H), 7.10 – 7.05 (m, 3H), 6.99 (t, *J* = 7.5 Hz, 2H), 6.86 (td, *J* = 7.5 Hz, *J* = 1.3 Hz, 1H), 6.79 (t, *J* = 7.6 Hz, 2H), 6.64 (td, *J* = 7.6 Hz, *J* = 1.0 Hz, 1H), 6.61 (s br, 2H), 6.53 (t, *J* = 2.1 Hz, 1H), 6.43 (td, *J* = 7.5 Hz, *J* = 1.2 Hz, 1H), 6.01 (dd, *J* = 7.7 Hz, *J* = 0.7 Hz, 1H), 5.93 (s, 2H), 5.64 (dd, *J* = 7.5 Hz, *J* = 0.5 Hz, 1H). **^{13}C NMR** (126 MHz, CD_2Cl_2) δ / ppm 169.27, 167.54, 166.19, 158.62, 157.64, 157.43, 150.75, 150.50, 149.34, 149.21, 147.43, 143.41, 143.14, 139.77, 138.49, 138.31, 138.21, 137.23, 131.80, 131.08, 130.63, 129.96, 129.36, 128.22, 127.98, 127.81, 127.18, 125.89, 124.93, 124.85, 123.85, 123.09, 122.71, 121.36, 121.10, 120.24, 120.14, 107.02, 105.67. **IR** (solid): $\tilde{\nu}$ = 3528 (w), 3045 (w), 1607 (s), 1583 (m), 1541 (m), 1477 (s), 1400 (m), 1375 (w), 1306 (w), 1269 (m), 1229 (m), 1161 (m), 1065 (w), 1030 (w), 1005 (m), 827 (s), 787 (s), 752 (s), 727 (s), 694 (s), 667 (s), 554 (s) cm^{-1}. **MS** (ESI, *m/z*): 841.1 $[M\text{-}PF_6]^+$ (calc. 841.2). **UV-Vis** λ / nm (ε / l mol^{-1} cm^{-1}) (CH_2Cl_2, 1.00E–5 mol l^{-1}) 272 (55 000); (CH_2Cl_2, 2.00E–5 mol l^{-1}) 292 (sh, 46 000); (CH_2Cl_2, 1.00E–4 mol l^{-1}) 382 (sh, 8 300), 419 (sh, 3 500); (CH_2Cl_2, 4.00E–4 mol l^{-1}) 471 (1 100). **Luminescence** (CH_2Cl_2, c = 1.00E–5 mol l^{-1}, λ_{ex} = 383 nm): λ_{em} = 605 nm; lifetime τ = 168 ns (χ^2 = 1.038). **Calcd.** for $C_{44}H_{32}F_6IrN_4O_2P\ H_2O$ (1003.95) C 52.64, H 3.41, N 5.58; found C 52.80, H 3.32, N 5.46 %.

Preparation of bis(2-phenylpyridine-*C,N*)(4-(3,5-bis(decyloxy)phenyl)-6-phenyl-2,2'-bipyridine-*N,N'*)iridium(III) hexafluorophosphate (**54**)

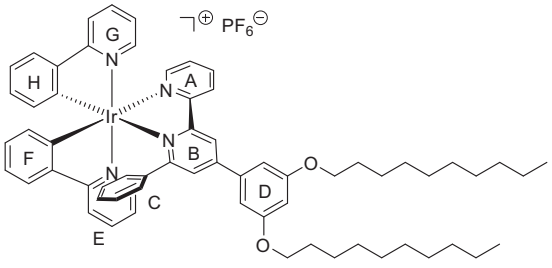

A yellow suspension of tetrakis(2-phenylpyridine-*C,N*)di(μ-chloro)diiridium(III) (**41**) (200 mg, 0.187 mmol, 1.00 eq) and 4-(3,5-bis(decyloxy)phenyl)-6-phenyl-2,2'-bipyridine (**38**) (232 mg, 0.373 mmol, 2.00 eq) in MeOH (30 ml) and CH_2Cl_2 (30 ml) was refluxed under an inert atmosphere of N_2 in the dark for 12 h. The orange solution was then cooled down to room temperature, and solid ammonium hexafluorophosphate (304 mg, 1.87 mmol, 10.0 eq) was added to the solution. The mixture was stirred for 30 min at room temperature and then evaporated to dryness. The crude material was purified by column chromatography (Merck Alox 90; CH_2Cl_2:hexane =

1:1→ CH_2Cl_2 → CH_2Cl_2:MeOH = 100:2), followed by a subsequent column chromatography (Fluka silica gel 60, 0.040–0.063 mm; CH_2Cl_2 → CH_2Cl_2:MeOH = 100:2) yielding the desired product as an orange solid (454 mg, 0.358 mmol, 96 %).

R_f (TLC, silica gel, CH_2Cl_2:MeOH = 100:1): 0.3. **^{1}H NMR** (500 MHz, CD_2Cl_2) δ / ppm 8.66 (d, *J* = 1.6 Hz, 1H), 8.63 (d, *J* = 8.2 Hz, 1H), 8.18 (t, *J* = 7.9 Hz, 1H), 7.95 (d, *J* = 4.8 Hz, 1H), 7.91 – 7.86 (m, 3H), 7.81 (td, *J* = 8.0 Hz, *J* = 1.3 Hz, 1H), 7.74 (d, *J* = 5.7 Hz, 1H), 7.70 (d, *J* = 1.7 Hz, 1H), 7.63 (d, *J* = 5.6 Hz, 1H), 7.58 (d, *J* = 7.7 Hz, 1H), 7.45 (t, *J* = 6.5 Hz, 1H), 7.29 (d, *J* = 7.8 Hz, 1H), 7.14 – 7.07 (m, 2H), 7.01 (t, *J* = 7.5 Hz, 2H), 6.97 (d, *J* = 2.0 Hz, 2H), 6.87 (td, *J* = 7.6 Hz, *J* = 1.1 Hz, 1H), 6.80 (t, *J* = 7.6 Hz, 2H), 6.70 – 6.53 (m, 4H), 6.44 (t, *J* = 7.4 Hz, 1H), 6.01 (d, *J* = 7.7 Hz, 1H), 5.63 (d, *J* = 7.5 Hz, 1H), 4.07 (t, *J* = 6.5 Hz, 4H), 1.87 – 1.80 (m, 4H), 1.54 – 1.47 (m, 4H), 1.44 – 1.26 (m, 24H), 0.92 (t, *J* = 6.9 Hz, 6H). **^{13}C NMR** (126 MHz, CD_2Cl_2) δ / ppm 169.23, 167.64, 166.33, 161.76, 157.53, 157.20, 151.65, 151.28, 150.82, 149.28, 149.20, 147.21, 143.33, 143.13, 139.64, 138.55, 138.42, 138.11, 137.44, 131.78, 131.18, 130.64, 129.99, 129.47, 128.27, 128.20, 127.80, 125.35, 125.00, 124.87, 123.74, 123.18, 122.78, 121.31, 121.17, 120.29, 120.25, 106.28, 103.59, 68.96, 32.30, 29.98, 29.96, 29.78, 29.72, 29.62, 26.39, 23.08, 14.28. **IR** (solid): $\tilde{\nu}$ = 3047 (w), 2922 (w), 2853 (w), 1587 (m), 1541 (w), 1477 (m), 1441 (m), 1412 (m), 1400 (m), 1369 (w), 1298 (w), 1269 (w), 1229 (w), 1161 (s), 1061 (w), 1030 (w), 829 (s), 789 (s), 754 (s), 727 (s), 696 (s), 669 (s), 623 (m), 555 (m) cm^{-1}. **MS** (ESI, *m/z*): 1121.6 $[M\text{-}PF_6]^+$ (calc. 1121.5). **UV-Vis** λ / nm (ε / l mol^{-1} cm^{-1}) (CH_2Cl_2, 1.01E–5 mol l^{-1}) 234 (52 000), 272 (56 000); (CH_2Cl_2, 1.01E–4 mol l^{-1}) 384 (sh, 8 900), 418 (sh, 3 700); (CH_2Cl_2, 4.04E–4 mol l^{-1}) 471 (1 100). **Luminescence** (CH_2Cl_2, c = 1.01E–5 mol l^{-1}, λ_{ex} = 382 nm): λ_{em} = 601 nm; lifetime τ = 174 ns (χ^2 = 1.005). **Calcd.** for $C_{64}H_{72}F_6IrN_4O_2P{\cdot}0.5H_2O$ (1275.47) C 60.27, H 5.77, N 4.39; found C 60.32, H 5.52, N 4.23 %.

Preparation of bis(2-phenylpyridine-*C,N*)(4-(3,5-bis(3,5-bis(dodecyloxy)benzyloxy) phenyl)-6-phenyl-2,2'-bipyridine-*N,N'*)iridium(III) hexafluorophosphate (**55**)

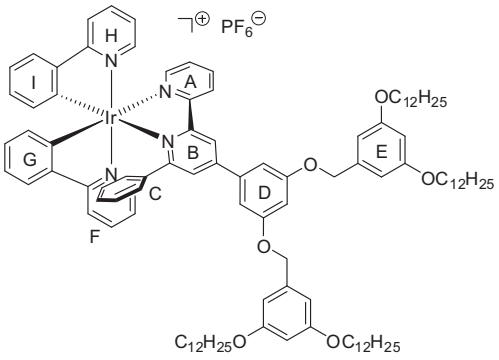

A yellow suspension of tetrakis(2-phenylpyridine-*C,N*)di(μ-chloro) diiridium(III) (**41**) (75 mg, 0.0704 mmol, 1.00 eq) and 4-(3,5-bis(3,5-bis(dodecyloxy)benzyloxy)phenyl)-6-phenyl-2,2'-bipyridine (**39**) (177 mg, 0.141 mmol, 2.00 eq) in MeOH (25 ml) and CH_2Cl_2 (25 ml) was refluxed under an inert atmosphere of N_2 in the dark for 15 h. The orange solution was then cooled down to room temperature, and solid ammonium hexafluorophosphate (115 mg, 0.704 mmol, 10.0 eq) was added to the solution. The mixture was stirred for 30 min at room temperature and then evaporated to dryness. The crude material was purified by column chromatography (Merck Alox 90; CH_2Cl_2:hexane = 1:1 → CH_2Cl_2 → CH_2Cl_2:MeOH = 100:2), followed by a subsequent column chromatography (Fluka silica gel 60, 0.040–0.063 mm; CH_2Cl_2:hexane = 1:1 → CH_2Cl_2 → CH_2Cl_2:MeOH = 100:2) yielding the desired product as an orange solid (253 mg, 0.133 mmol, 96 %).

^{1}H NMR (500 MHz, CD_2Cl_2) δ / ppm 8.66 – 8.62 (m, *J* = 11.6 Hz, 2H), 8.19 (t, *J* = 7.9 Hz, 1H), 7.95 (d, *J* = 5.5 Hz, 1H), 7.92 – 7.86 (m, 3H), 7.80 (t, *J* = 7.8 Hz, 1H), 7.74 (d, *J* = 5.6 Hz, 1H), 7.69 (s, 1H), 7.64 (d, *J* = 5.9 Hz, 1H), 7.59 (d, *J* = 7.8 Hz, 1H), 7.45 (t, *J* = 6.6 Hz, 1H), 7.29 (d, *J* = 7.8 Hz, 1H), 7.14 – 7.07 (m, 4H), 7.01 (t, *J* = 7.5 Hz, 2H), 6.87 (t, *J* = 7.5 Hz, 1H), 6.84 – 6.78 (m, 3H), 6.69 – 6.57 (m, 7H), 6.47 – 6.42 (m, 3H), 6.01 (d, *J* = 7.7 Hz, 1H), 5.63 (d, *J* = 7.6 Hz, 1H), 5.11 (s, 4H), 3.97 (t, *J* = 6.5 Hz, 8H), 1.82 – 1.74 (m, 8H), 1.51 – 1.43 (m, 8H), 1.43 – 1.24 (s, 64H), 0.92 (t, *J* = 6.7 Hz, 12H).

^{13}C NMR (126 MHz, CD_2Cl_2) δ / ppm 169.23, 167.63, 166.35, 161.22, 161.02, 157.60, 157.19, 151.38, 151.27, 150.80, 149.31, 149.21, 147.18, 143.32, 143.12, 139.66, 139.12, 138.54, 138.41, 138.09, 137.85, 137.63, 131.79, 131.19, 130.64, 130.00, 129.49, 128.27, 128.18, 127.79, 125.46, 125.00, 124.87, 123.74, 123.20, 122.77, 121.37, 121.18, 120.28, 120.23, 107.01, 106.08, 104.50, 100.97, 70.76, 68.54, 32.32, 30.07, 30.04, 30.01, 29.99, 29.80, 29.75, 29.65, 26.42, 23.09, 14.28. **IR** (solid): $\tilde{\nu}$ = 2922 (w), 2853 (w), 1593 (m), 1543 (w), 1454 (w), 1371 (w), 1300 (w), 1269 (w), 1157 (m), 1057 (w), 831 (s), 787 (s), 754 (s), 729 (s), 694 (s), 621 (s) cm^{-1}. **MS** (ESI, *m/z*): 1758.4 $[M\text{-}PF_6]^+$ (calc. 1758.0). **UV-Vis** λ / nm (ε / l mol^{-1} cm^{-1}) (CH_2Cl_2, 1.02E–5 mol l^{-1}) 232 (73 000), 274 (62 000); (CH_2Cl_2, 1.02E–4 mol l^{-1}) 386 (sh, 8 800); (CH_2Cl_2, 4.07E–4 mol l^{-1}) 471 (1 100). **Luminescence** (CH_2Cl_2, c = 1.02E–5 mol l^{-1}, λ_{ex} = 383 nm): λ_{em} = 602 nm; lifetime τ = 179 ns (χ^2 = 1.024). **Calcd.** for $C_{106}H_{140}F_6IrN_4O_6P$ (1903.45) C 66.89, H 7.41, N 2.94; found C 66.92, H 7.20, N 2.75 %.

Preparation of bis(2-phenylpyridine-*C,N*)(4-(3,5-bis(3,5-bis(3,5-bis(dodecyloxy) benzyloxy)benzyloxy)phenyl)-6-phenyl-2,2'-bipyridine-*N,N'*)iridium(III) hexafluorophosphate (**56**)

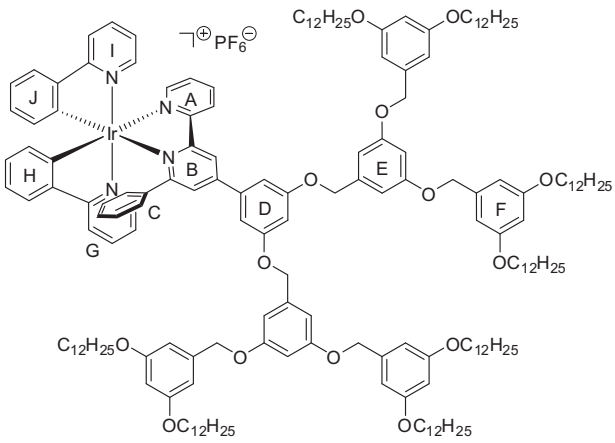

A yellow suspension of tetrakis(2-phenylpyridine-*C,N*) di(μ-chloro)diiridium(III) (**41**) (73 mg, 0.0682 mmol, 1.00 eq) and 4-(3,5-bis(3,5-bis(3,5-bis(dodecyloxy)benzyloxy)benzyloxy)phenyl)-6-phenyl-2,2'-bipyridine (**40**) (330 mg, 0.136 mmol, 2.00 eq) in MeOH (25 ml) and CH_2Cl_2 (25 ml) was refluxed under an inert atmosphere of N_2 in the dark for 11 h. The orange solution was then cooled down to room temperature, and solid ammonium hexafluorophosphate (111 mg, 0.682 mmol, 10.0 eq) was added to the solution. The mixture was stirred for 30 min at room temperature and then evaporated to dryness. The crude material was purified by column chromatography (Merck Alox 90; CH_2Cl_2:hexane = 1:1 → CH_2Cl_2 → CH_2Cl_2:MeOH = 100:2), followed by a subsequent column chromatography (Fluka silica gel 60, 0.040–0.063 mm; CH_2Cl_2:hexane = 1:1 → CH_2Cl_2 → CH_2Cl_2:MeOH = 100:2) yielding the desired product as an orange solid (385 mg, 0.126 mmol, 92 %).

^{1}H NMR (500 MHz, CD_2Cl_2) δ / ppm 8.65 – 8.61 (m, 2H), 8.13 (td, *J* = 8.1 Hz, *J* = 1.4 Hz, 1H), 7.93 (d, *J* = 4.6 Hz, 1H), 7.90 – 7.85 (m, 3H), 7.79 (td, *J* = 8.0 Hz, *J* = 1.3 Hz, 1H), 7.74 (d, *J* = 5.8 Hz, 1H), 7.70 (d, *J* = 1.7 Hz, 1H), 7.66 (d, *J* = 5.5 Hz, 1H), 7.58 (d, *J* = 7.2 Hz, 1H), 7.41 (t, *J* = 6.6 Hz, 1H), 7.29 (d, *J* = 7.4 Hz, 1H), 7.14 – 7.06 (m, 4H), 7.03 – 6.97 (m, 2H), 6.87 (td, *J* = 7.6 Hz, *J* = 1.1 Hz, 1H), 6.84 (t, *J* = 2.0 Hz, 1H), 6.79 (t, *J* = 7.6 Hz, 2H), 6.68 – 6.53 (s br, 3H), 6.76 (d, *J* = 2.1 Hz, 4H), 6.65 (t, *J* = 7.5 Hz, 1H), 6.60 (t, *J* = 2.1 Hz, 1H), 6.56 (d, *J* = 2.1 Hz, 8H), 6.44 (td, *J* = 7.5 Hz, *J* = 0.9 Hz, 1H), 6.41 (t, *J* = 2.1 Hz, 4H), 6.01 (d, *J* = 7.4 Hz, 1H), 5.63 (d, *J* = 7.4 Hz, 1H), 5.15 (s, 4H), 4.99 (s, 8H), 3.95 (t, *J* = 6.6 Hz, 16H), 1.81 – 1.74 (m, 16H), 1.50 – 1.43 (m, 16H), 1.42 – 1.25 (m, 128H), 0.92 (t, *J* = 6.9 Hz, 24H). **^{13}C NMR** (126 MHz, CD_2Cl_2) δ / ppm 169.38, 167.77, 166.48, 161.33, 161.11, 160.74, 157.77, 157.33, 151.50, 151.48, 150.89, 149.53, 149.40, 147.40, 143.49, 143.27, 139.86, 139.64, 139.58, 138.68, 138.55, 138.27, 137.81, 131.97, 131.35, 130.80, 130.17, 129.63, 128.43, 128.27, 127.96, 125.67, 125.15, 125.01, 123.91, 123.35, 122.95, 121.57, 121.33, 120.41, 120.36, 107.21, 106.86, 106.27, 104.74, 101.96, 101.08, 70.78, 70.65, 68.66, 32.49, 30.25, 30.22, 30.20, 30.17, 29.98, 29.93, 29.83, 26.59, 23.26, 14.46. **IR** (solid): $\tilde{\nu}$ = 3051 (w), 2922 (s), 2851 (m), 1593 (s), 1452 (m), 1371 (w), 1296 (w), 1155 (s), 1053 (m),

833 (s), 789 (m), 756 (s), 729 (s), 694 (m), 683 (s), 619 (w), 581 (w), 557 (w) cm^{-1}. **MS** (ESI, *m/z*): 2919.5 $[M\text{-}PF_6]^+$ (calc. 2918.9). **UV-Vis** λ / nm (ε / l mol^{-1} cm^{-1}) (CH_2Cl_2, 1.05E–5 mol l^{-1}) 232 (110 000), 276 (73 000), 283 (sh, 69 000); (CH_2Cl_2, 1.05E–4 mol l^{-1}) 389 (sh, 8 900), 420 (sh, 3 600); (CH_2Cl_2, 4.19E–4 mol l^{-1}) 471 (1 100). **Luminescence** (CH_2Cl_2, c = 1.05E–5 mol l^{-1}, λ_{ex} = 383 nm): λ_{em} = 602 nm; lifetime τ = 186 ns (χ^2 = 1.028). **Calcd.** for $C_{182}H_{260}F_6IrN_4O_{14}P$ (3065.21) C 71.31, H 8.55, N 1.83; found C 71.21, H 8.46, N 1.78 %.

Preparation of bis(2-(2,4-difluorophenyl)pyridine-*C,N*)(6-phenyl-2,2'-bipyridine-*N,N'*) iridium(III) hexafluorophosphate (**57**)

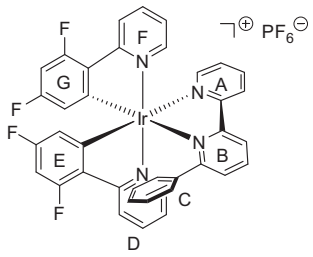

A yellow suspension of tetrakis(2-(2,4-difluorophenyl)pyridine-*C,N*)di(μ-chloro) diiridium(III) (**42**) (350 mg, 0.288 mmol, 1.00 eq) and 6-phenyl-2,2'-bipyridine (**31**) (134 mg, 0.579 mmol, 2.00 eq) in MeOH (30 ml) and CH_2Cl_2 (30 ml) was refluxed under an inert atmosphere of N_2 in the dark for 17 h. The yellow solution was then cooled down to room temperature, and solid ammonium hexafluorophosphate (469 mg, 2.88 mmol, 10.0 eq) was added to the solution. The mixture was stirred for 7 h at room temperature and then evaporated to dryness. The crude material was purified by column chromatography (Merck Alox 90; CH_2Cl_2 → CH_2Cl_2:MeOH = 100:1) yielding the desired product as a yellow solid (477 mg, 0.502 mmol, 87 %).

^{1}H NMR (500 MHz, CD_2Cl_2) δ / ppm 8.63 (dd, *J* = 12.8 Hz, *J* = 8.2 Hz, 2H), 8.31 (t, *J* = 7.9 Hz, 1H), 8.28 – 8.19 (m, 3H), 7.96 (t, *J* = 7.8 Hz, 1H), 7.92 (d, *J* = 5.4 Hz, 1H), 7.87 (t, *J* = 7.9 Hz, 1H), 7.72 (d, *J* = 5.7 Hz, 1H), 7.56 – 7.48 (m, 3H), 7.23 – 6.00 (s br, 2H), 7.19 (t, *J* = 6.7 Hz, 1H), 7.17 – 7.11 (m, 2H), 6.95 (s br, 2H), 6.59 – 6.52 (m, 1H), 6.21 – 6.13 (m, 1H), 5.48 (dd, *J* = 8.5 Hz, *J* = 2.2 Hz, 1H), 5.08 (dd, *J* = 8.8 Hz, *J* = 2.2 Hz, 1H). **^{13}C NMR** (126 MHz, CD_2Cl_2) δ / ppm 166.21, 165.86, 165.81, 164.25, 164.19, 157.13, 156.94, 155.32, 155.27, 150.59, 150.49, 150.43, 149.54, 149.51, 140.76, 140.56, 139.81, 139.67, 137.95, 130.93, 129.86, 128.67, 128.18, 127.37, 126.04, 124.67, 124.49, 124.38, 123.35, 113.99 (dd, $^2J_{CF}$ = 17.7 Hz, $^4J_{CF}$ = 2.8 Hz), 113.34 (dd, $^2J_{CF}$ = 18.3 Hz, $^4J_{CF}$ = 2.6 Hz), 99.82 (t, $^2J_{CF}$ = 26.6 Hz, $C^{3(E/G)}$), 98.15 (t, $^2J_{CF}$ = 27.2 Hz, $C^{3(G/E)}$). **^{19}F NMR** (376 MHz, CD_2Cl_2) δ / ppm –73.31, –75.20, –106.68, –109.48, –109.86, –111.09. **IR** (solid): $\tilde{\nu}$ = 3090 (w), 2924 (w), 1981 (w), 1601 (s), 1574 (s), 1479 (m), 1450 (m), 1431 (m), 1404 (m), 1294 (m), 1248 (m), 1165 (m), 1103 (m), 1068 (w), 1043 (w), 987 (m), 825 (s), 777 (s), 756 (s), 717 (s), 696 (s), 613 (w), 555 (m) cm^{-1}. **MS** (ESI, *m/z*): 805.0 $[M\text{-}PF_6]^+$ (calc. 805.2). **UV-Vis** λ / nm (ε / l mol^{-1} cm^{-1}) (CH_2Cl_2, 9.94E–6 mol l^{-1}) 252 (45 000), 262 (45 000), 308 (27 000); (CH_2Cl_2, 9.94E–5 mol l^{-1}) 363 (sh, 6 000); (CH_2Cl_2, 3.98E–4 mol l^{-1}) 448 (sh, 620). **Luminescence** (CH_2Cl_2, c = 9.94E–6 mol l^{-1}, λ_{ex} = 313 nm): λ_{em} = 532 nm; lifetime τ = 318 ns (χ^2 = 1.011). **Calcd.** for $C_{38}H_{24}F_{10}IrN_4P$ (949.80) C 48.05, H 2.55, N 5.90; found C 48.25, H 2.70, N 5.83 %.

Preparation of bis(7,8-benzoquinoline-*C,N*)(6-phenyl-2,2'-bipyridine-*N,N'*)iridium(III) hexafluorophosphate (**58**)

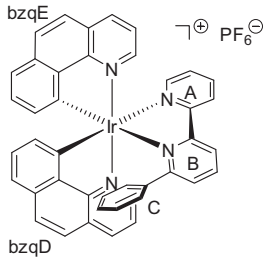

A yellow suspension of tetrakis(7,8-benzoquinoline-*C,N*)di(μ-chloro)diiridium(III) (**43**) (350 mg, 0.300 mmol, 1.00 eq) and 6-phenyl-2,2'-bipyridine (**31**) (139 mg, 0.599 mmol, 2.00 eq) in MeOH (30 ml) and CH_2Cl_2 (30 ml) was refluxed under an inert atmosphere of N_2 in the dark for 13 h. The orange solution was then cooled down to room temperature, and solid ammonium hexafluorophosphate (488 mg, 3.00 mmol, 10.0 eq) was added to the solution. The mixture was stirred for 30 min at room temperature and then evaporated to dryness. The crude material was purified by column chromatography (Merck Alox 90; CH_2Cl_2 → CH_2Cl_2:MeOH = 100:1; followed by two subsequent Fluka silica gel 60 chromatographies, 0.040–0.063 mm; CH_2Cl_2 → CH_2Cl_2:MeOH = 100:1) yielding the desired product as a yellow-orange solid (337 mg, 0.364 mmol, 61 %).

R_f (TLC, silica gel, CH_2Cl_2:MeOH = 100:1): 0.2. **^{1}H NMR** (500 MHz, CD_2Cl_2) δ / ppm 8.59 (d, *J* = 8.0 Hz, 1H), 8.53 (d, *J* = 8.2 Hz, 1H), 8.46 (d, *J* = 7.9 Hz, 1H), 8.33 – 8.28 (m, 2H), 8.24 (d, *J* = 5.3 Hz, 1H), 8.10 (t, *J* = 8.0 Hz, 1H), 8.07 (d, *J* = 5.4 Hz, 1H), 7.80 (d, *J* = 8.8 Hz, 1H), 7.74 (q, *J* = 8.8 Hz, 2H), 7.67 (d, *J* = 8.8 Hz, 1H), 7.59 – 7.54 (m, 2H), 7.54 – 7.49 (m, 2H), 7.41 (d, *J* = 7.9 Hz, 1H), 7.33 (d, *J* = 6.5 Hz, 1H), 7.07 (d, *J* = 7.8 Hz, 1H), 7.04 (t, *J* = 7.6 Hz, 1H), 6.66 (t, *J* = 7.6 Hz, 1H), 6.55 (t, *J* = 8.5 Hz, 1H), 6.24 (s br, 4H), 5.86 (d, *J* = 7.3 Hz, 1H), 5.65 (d, *J* = 7.2 Hz, 1H). **^{13}C NMR** (126 MHz, CD_2Cl_2) δ / ppm 166.57, 158.37, 157.64, 157.62, 157.17, 150.93, 148.40, 148.05, 147.60, 143.43, 140.60, 140.16, 139.64, 137.64, 137.46, 134.47, 134.38, 130.69, 130.23, 130.11, 130.05, 129.20, 128.89, 128.87, 128.06, 127.95, 127.79, 127.62, 127.16, 125.26, 124.25, 123.66, 123.47, 122.67, 121.69, 121.14, 119.54. **IR** (solid): $\tilde{\nu}$ = 3034 (w), 1620 (w), 1595 (w), 1566 (m), 1485 (w), 1447 (s), 1406 (m), 1329 (m), 1292 (w), 1219 (w), 1190 (w), 1165 (w), 1140 (w), 1107 (w), 1084 (w), 1051 (w), 1022 (w), 1003 (w), 932 (w), 818 (s), 775 (s), 756 (s), 716 (s), 694 (s), 654 (s), 625 (s), 554 (s) cm^{-1}. **MS** (ESI, *m/z*): 781.1 $[M\text{-}PF_6]^+$ (calc. 781.2); 549.6 $[M\text{-}PF_6\text{-}L_{N,N'}]^+$ (calc. 549.1). **UV-Vis** λ / nm (ε / l mol^{-1} cm^{-1}) (CH_2Cl_2, 1.02E–5 mol l^{-1}) 233 (69 000), 260 (54 000); (CH_2Cl_2, 2.04E–5 mol l^{-1}) 293 (sh, 29 000), 318 (27 000), 365 (sh, 10 000); (CH_2Cl_2, 1.02E–4 mol l^{-1}) 425 (4 900). **Luminescence** (CH_2Cl_2, c = 1.02E–5 mol l^{-1}, λ_{ex} = 320 nm): λ_{em} = 596 nm; lifetime τ = 126 ns (χ^2 = 1.047). **Calcd.** for $C_{42}H_{28}F_6IrN_4P{\cdot}H_2O$ (943.89) C 53.44, H 3.20, N 5.94; found C 53.36, H 3.00, N 5.83 %.

Preparation of bis(1-phenylisoquinoline-*C,N*)(6-phenyl-2,2'-bipyridine-*N,N'*)iridium(III) hexafluorophosphate (**59**)

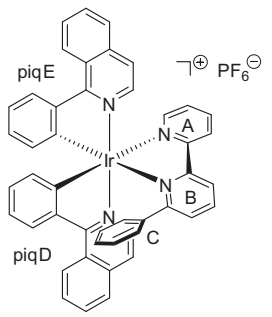

A red suspension of tetrakis(1-phenylisoquinoline-*C,N*)di(μ-chloro)diiridium(III) (**44**) (350 mg, 0.275 mmol, 1.00 eq) and 6-phenyl-2,2'-bipyridine (**31**) (128 mg, 0.550 mmol, 2.00 eq) in MeOH (30 ml) and CH_2Cl_2 (30 ml) was refluxed under an inert atmosphere of N_2 in the dark for 15 h. The red solution was then cooled down to room temperature, and solid ammonium hexafluorophosphate (448 mg, 2.75 mmol, 10.0 eq) was added to the solution. The mixture was stirred for 30 min at room temperature and then evaporated to dryness. The crude material was purified by column chromatography (Merck Alox 90; CH_2Cl_2 → CH_2Cl_2:MeOH = 100:2) , followed by a subsequent column chromatography (Fluka silica gel 60, 0.040–0.063 mm; CH_2Cl_2 → CH_2Cl_2:MeOH = 100:2) yielding the desired product as a red solid (484 mg, 0.495 mmol, 90 %).

^{1}H NMR (500 MHz, CD_2Cl_2) δ / ppm 8.92 (d, *J* = 8.4 Hz, 1H), 8.89 – 8.84 (m, 1H), 8.61 – 8.56 (m, 2H), 8.23 – 8.18 (m, 2H), 8.15 (t, *J* = 7.9 Hz, 1H), 8.02 (d, *J* = 7.9 Hz, 1H), 8.00 – 7.96 (m, 1H), 7.89 – 7.81 (m, 5H), 7.78 (d, *J* = 6.4 Hz, 1H), 7.64 (d, *J* = 5.3 Hz, 1H), 7.54 (d, *J* = 6.4 Hz, 1H), 7.51 (d, *J* = 6.4 Hz, 1H), 7.41 (d, *J* = 7.7 Hz, 1H), 7.40 – 7.35 (m, 2H), 7.11 (t, *J* = 7.6 Hz, 1H), 6.95 (t, *J* = 7.5 Hz, 1H), 6.84 (t, *J* = 7.4 Hz, 1H), 6.75 (t, *J* = 7.6 Hz, 2H), 6.70 (t, *J* = 7.6 Hz, 1H), 6.64 (s br, 2H), 6.39 (t, *J* = 7.4 Hz, 1H), 6.26 (d, *J* = 7.7 Hz, 1H), 5.68 (d, *J* = 7.6 Hz, 1H). **^{13}C NMR** (126 MHz, CD_2Cl_2) δ / ppm 170.19, 168.91, 165.67, 157.31, 156.86, 154.21, 150.70, 150.60, 144.99, 144.55, 141.59, 140.58, 139.89, 139.66, 138.23, 137.44, 137.36, 132.57, 132.31, 132.09, 131.27, 131.12, 131.07, 130.28, 130.05, 129.82, 129.34, 129.28, 128.96, 128.15, 128.06, 127.87, 127.80, 127.49, 127.23, 126.75, 126.54, 125.48, 124.07, 122.85, 122.07, 121.33, 120.67. **IR** (solid): $\tilde{\nu}$ = 3043 (w), 1597 (w), 1576 (m), 1539 (m), 1501 (w), 1447 (s), 1381 (m), 1350 (m), 1296 (w), 1273 (m), 1225 (w), 1153 (m), 1121 (w), 1040 (m), 1001 (w), 831 (s), 816 (s), 754 (s), 729 (s), 694 (s), 675 (s), 625 (s), 581 (m), 555 (s) cm^{-1}. **MS** (ESI, *m/z*): 833.2 $[M\text{-}PF_6]^+$ (calc. 833.2); 601.5 $[M\text{-}PF_6\text{-}L_{N,N'}]^+$ (calc. 601.1). **UV-Vis** λ / nm (ε / l mol^{-1} cm^{-1}) (CH_2Cl_2, 1.01E–5 mol l^{-1}) 234 (64 000); (CH_2Cl_2, 2.02E–5 mol l^{-1}) 295 (48 000), 343 (sh, 21 000), 381 (sh, 13 000); (CH_2Cl_2, 1.01E–4 mol l^{-1}) 440 (6 700). **Luminescence** (CH_2Cl_2, c = 1.01E–5 mol l^{-1}, λ_{ex} = 344 nm): λ_{em} = 596 nm, 635 nm. **Calcd.** for $C_{46}H_{32}F_6IrN_4P{\cdot}H_2O$ (995.97) C 55.47, H 3.44, N 5.63; found C 55.56, H 3.30, N 5.62 %.

Preparation of bis(1-phenylpyrazole-*C,N*)(6-phenyl-2,2'-bipyridine-*N,N'*)iridium(III) hexafluorophosphate (**60**)

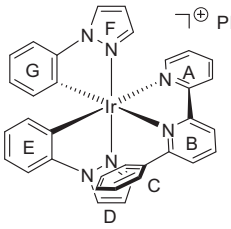

A yellow suspension of tetrakis(1-phenylpyrazole-*C,N*)di(μ-chloro)diiridium(III) (**45**) (340 mg, 0.331 mmol, 1.00 eq) and 6-phenyl-2,2'-bipyridine (**31**) (154 mg, 0.661 mmol, 2.00 eq) in MeOH (30 ml) and CH_2Cl_2 (30 ml) was refluxed under an inert atmosphere of N_2 in the dark for 13 h. The yellow solution was then cooled down to room temperature, and solid ammonium hexafluorophosphate (539 mg, 3.31 mmol, 10.0 eq) was added to the solution. The mixture was stirred for 1 h at room temperature and then evaporated to dryness. The crude material was purified by column chromatography (Merck Alox 90; CH_2Cl_2 → CH_2Cl_2:MeOH = 100:1), washed with hexane, ethyl acetate, Et_2O, toluene and purified by a further column chromatographic separation (Merck Alox 90; CH_2Cl_2 → CH_2Cl_2:MeOH = 100:2). The desired product was isolated as a yellow solid (444 mg, 0.519 mmol, 78 %).

^{1}H NMR (500 MHz, CD_2Cl_2) δ / ppm 8.48 (t, *J* = 7.6 Hz, 2H), 8.31 – 8.26 (m, 2H), 8.18 (t, *J* = 8.0 Hz, 1H), 8.15 (d, *J* = 2.9 Hz, 1H), 8.03 (d, *J* = 2.9 Hz, 1H), 7.61 (d, *J* = 7.8 Hz, 1H), 7.48 (t, *J* = 6.6 Hz, 1H), 7.27 (d, *J* = 2.2 Hz, 1H), 7.16 (d, *J* = 7.9 Hz, 1H), 7.05 – 6.98 (m, 2H), 6.88 – 6.80 (m, 4H), 6.78 (t, *J* = 2.5 Hz, 1H), 6.74 – 6.42 (s br, 2 H), 6.64 (t, *J* = 7.6 Hz, 1H), 6.56 (t, *J* = 2.6 Hz, 1H), 6.39 (t, *J* = 7.4 Hz, 2H), 6.03 (d, *J* = 7.6 Hz, 1H), 5.51 (d, *J* = 7.5 Hz, 1H). **^{13}C NMR** (126 MHz, CD_2Cl_2) δ / ppm 166.33, 158.17, 157.97, 150.72, 142.63, 142.45, 139.98, 139.86, 138.65, 138.36, 133.20, 132.46, 129.65, 129.40, 129.14, 128.36, 127.64, 127.57, 127.44, 127.29, 127.24, 126.04, 125.16, 123.79, 122.86, 121.96, 111.98, 111.79, 108.76, 108.63. **IR** (solid): $\tilde{\nu}$ = 3144 (w), 3055 (w), 1597 (w), 1562 (w), 1479 (m), 1448 (m), 1412 (m), 1335 (w), 1277 (w), 1231 (w), 1165 (w), 1111 (w), 1057 (m), 1034 (w), 966 (w), 918 (w), 825 (s), 743 (s), 694 (s), 656 (s), 609 (m), 554 (s) cm^{-1}. **MS** (ESI, *m/z*): 711.0 $[M\text{-}PF_6]^+$ (calc. 711.2). **UV-Vis** λ / nm (ε / l mol^{-1} cm^{-1}) (CH_2Cl_2, 2.07E–5 mol l^{-1}) 254 (35 000), 314 (sh, 18 000); (CH_2Cl_2, 4.13E–4 mol l^{-1}) 438 (690). **Luminescence** (CH_2Cl_2, c = 1.03E–5 mol l^{-1}, λ_{ex} = 318 nm): λ_{em} = 566 nm; lifetime τ = 179 ns (χ^2 = 1.021). **Calcd.** for $C_{34}H_{26}F_6IrN_6P{\cdot}H_2O$ (873.81) C 46.73, H 3.23, N 9.62; found C 46.34, H 3.00, N 9.33 %.

Preparation of bis(3,5-dimethyl-1-phenylpyrazole-*C,N*)(6-phenyl-2,2'-bipyridine-*N,N'*) iridium(III) hexafluorophosphate (**61**)

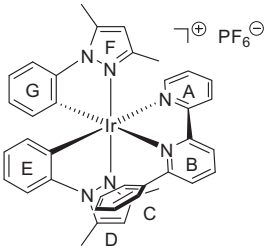

A yellow suspension of tetrakis(3,5-dimethyl-1-phenylpyrazole-*C,N*)di(μ-chloro) diiridium(III) (**46**) (350 mg, 0.307 mmol, 1.00 eq) and 6-phenyl-2,2'-bipyridine (**31**) (143 mg, 0.614 mmol, 2.00 eq) in MeOH (30 ml) and CH_2Cl_2 (30 ml) was refluxed under an inert atmosphere of N_2 in the dark for 10 h. The orange solution was then cooled down to room temperature, and solid ammonium hexafluorophosphate (500 mg, 3.07 mmol, 10.0 eq) was added to the solution. The mixture was stirred for 1 h at room temperature and then evaporated to dryness. The crude material was purified by column chromatography (Merck Alox 90, CH_2Cl_2 → CH_2Cl_2:MeOH = 100:2) yielding the desired product as a yellow-orange solid (554 mg, 0.608 mmol, 99 %).

^{1}H NMR (500 MHz, CD_2Cl_2) δ / ppm 8.54 (d, *J* = 7.0 Hz, 1H), 8.53 (d, *J* = 7.7 Hz, 1H), 8.22 (t, *J* = 7.9 Hz, 1H), 8.11 (td, *J* = 8.2 Hz, *J* = 1.5 Hz, 1H), 7.82 (d, *J* = 4.7 Hz, 1H), 7.43 (dd, *J* = 7.7 Hz, *J* = 1.0 Hz, 1H), 7.37 (ddd, *J* = 7.2 Hz, *J* = 5.8 Hz, *J* = 0.9 Hz, 1H), 7.32 (d, *J* = 8.2 Hz, 1H), 7.06 (t, *J* = 7.5 Hz, 1H), 7.01 (td, *J* = 7.9 Hz, *J* = 1.3 Hz, 1H), 6.87 – 6.81 (m, 3H), 6.78 (td, *J* = 7.5 Hz, *J* = 1.0 Hz, 1H), 6.74 – 6.24 (s br, 2H), 6.60 (td, *J* = 7.9 Hz, *J* = 1.3 Hz, 1H), 6.48 (td, *J* = 7.4 Hz, *J* = 0.9 Hz, 1H), 6.21 (s, 1H), 6.08 (s, 1H), 6.02 (dd, *J* = 7.6 Hz, *J* = 1.2 Hz, 1H), 5.82 (dd, *J* = 7.5 Hz, *J* = 1.2 Hz, 1H), 2.79 (s, 3H), 2.71 (s, 3H), 1.67 (s, 3H), 1.62 (s, 3H). **^{13}C NMR** (126 MHz, CD_2Cl_2) δ / ppm 166.67, 157.90, 157.59, 150.16, 149.96, 149.88, 144.35, 142.02, 141.50, 139.85, 139.46, 137.82, 133.04, 132.88, 130.88, 130.60, 129.22, 127.63, 126.14, 125.21, 124.83, 123.72, 123.08, 121.77, 113.10, 112.99, 110.71, 110.07, 15.04, 14.65, 12.97, 11.88. **IR** (solid): $\tilde{\nu}$ = 3053 (w), 2986 (w), 2922 (w), 1597 (w), 1553 (w), 1470 (m), 1443 (s), 1421 (w), 1396 (w), 1275 (w), 1225 (w), 1150 (w), 1122 (w), 1082 (w), 1059 (w), 1036 (w), 997 (w), 831 (s), 775 (s), 741 (s), 714 (s), 694 (s), 656 (s), 640 (s), 555 (s) cm^{-1}. **MS** (ESI, *m/z*): 767.1 $[M\text{-}PF_6]^+$ (calc. 767.2). **UV-Vis** λ / nm (ε / l mol^{-1} cm^{-1}) (CH_2Cl_2, 2.03E–5 mol l^{-1}) 236 (45 000), 254 (39 000), 282 (sh, 26 000), 318 (sh, 17 000); (CH_2Cl_2, 1.02E–4 mol l^{-1}) 352 (sh, 5 300); (CH_2Cl_2, 4.06E–4 mol l^{-1}) 394 (sh, 1 400), 464 (630).**Luminescence** (CH_2Cl_2, c = 1.02E–5 mol l^{-1}, λ_{ex} = 316 nm): λ_{em} = 599 nm; lifetime τ = 113 ns (χ^2 = 1.012). **Calcd.** for $C_{38}H_{34}F_6IrN_6P{\cdot}0.5H_2O$ (920.91) C 49.56, H 3.83, N 9.13; found C 49.40, H 3.77, N 8.95 %.

Chapter 8

Light-Emitting Electrochemical Cells

8.1
Introduction and aims

This chapter deals with the main application for which the Ir(III) complexes discussed in **Chapter 7** were prepared. Cyclometallated Ir(III) complexes possess electroluminescent properties which can be used in light-emitting electrochemical cells (LEECs) (see **Chapter 1** for more information). This work was done in collaboration with the group of *H. Bolink* from Valencia, Spain. It has to be stated here that all experiments presented in this chapter – *i.e.* the device preparation, the measurement of their characteristics, and the optimisation of their parameters – were performed by their group. *H. Bolink et al.* kindly agreed with the publication of their results in this thesis. As the results originate from to the group of *H. Bolink*, the discussion of the devices presented in this chapter will be brief and without any details. Therefore, this chapter will just give a short overview of the achieved results.

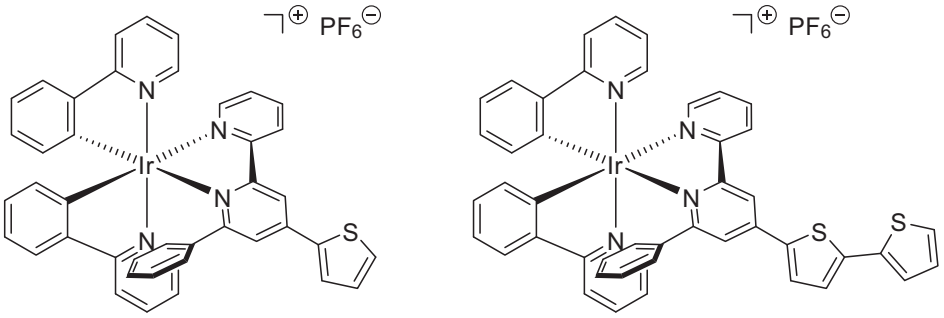

62 **63**

Scheme 8.1 Ir(III) complexes prepared by *K. Doyle*.

The LEEC project was started by *K. Doyle*, a former member of our research group. LEEC devices from compounds **62** and **63** (**Scheme 8.1**), prepared by *K. Doyle*, showed an incredible augmentation of the lifetime (**Figure 8.1**) compared with the best-performing LEECs known to date.[123] **Figure 8.1** shows the characteristics of devices made using complex **62**.

As it turned out, the lifetime of the devices is critically dependent on the amount of ionic liquid (IL, here: 1-butyl-3-methylimidazolium hexafluorophosphate) mixed with the active Ir(III) complex in the emissive layer of the device. This can be explained by the higher mobility of the ions in the film at a higher concentration of the IL.[310] With the lower amount of IL (0.013 %), a half-life $t_{½}$ of more than 600 hours could be measured. Compared with the record lifetime for a previously reported iridium based LEEC (60 hours),[136] this lifetime is an enormous improvement.

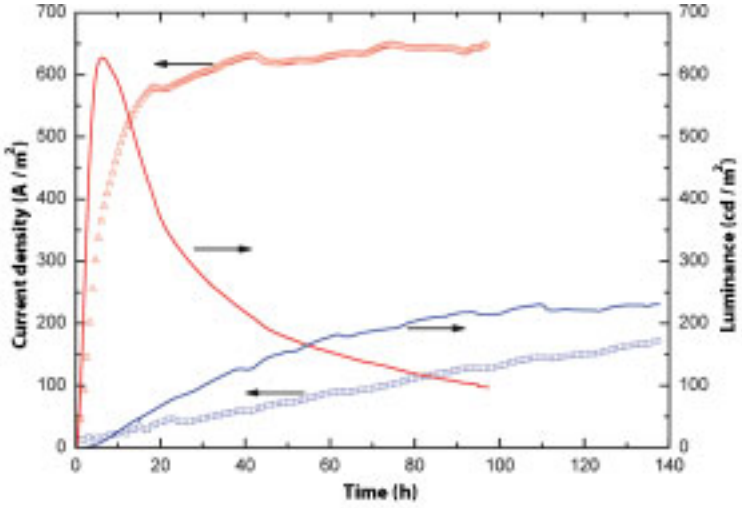

Figure 8.1 Luminance (lines) and current density (symbols) versus time of an LEEC device from compound **62** (ITO / PEDOT : PSS / **62** : IL / Al) containing 0.013 % (blue) and 0.026 % (red) of ionic liquid, at an applied bias of 3 V. Graph taken from the publication.[123]

A very nice feature of the crystal structures of compounds **62** and **63**, and, as it turned out, crucial for their long lifetimes in LEEC devices, is an intramolecular face-to-face π-π stacking (**Figure 8.2**) similar to that observed for the related complexes described in **Chapter 7**.

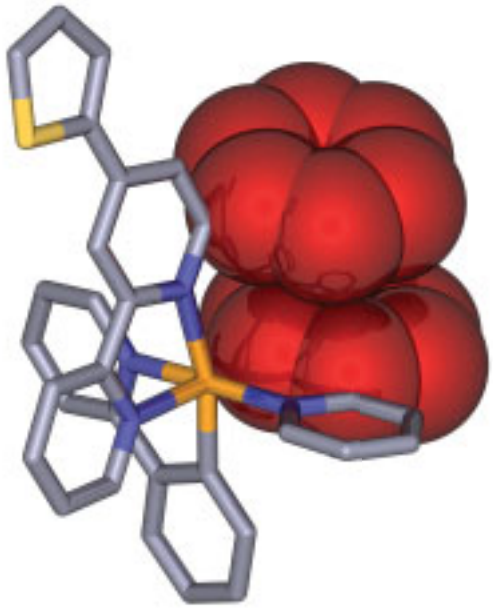

Figure 8.2 Solid state structure of one of the cations present in **62** emphasising the intramolecular π-π stacking (space filling representation in red). Hydrogen atoms and the counterion (PF_6^-) have been omitted for clarity.

In a simple model, the intramolecular π-π stacking found in **62** and similar Ir(III) complexes bearing a pendant phenyl ring (see **Chapter 7**) helps protect the metal centre – on a steric basis – against penetration of water molecules, and hence reduces the possibility of the formation of degradation products.[123] On a more sophisticated level, density functional theory (DFT) calculations performed by the group of *E. Ortí et al.* on the cations in **49** and **50** (**Scheme 8.2**, see below for explanations) at the B3LYP/(6-311G** + LANL2DZ) level revealed detailed insights.[124] Metal-centred (MC) states result from the excitation of one electron from the occupied t_{2g} (dπ) HOMO to the unoccupied e_g (dσ*) orbitals of the metal.[311] These ^{3}MC states were calculated after geometry relaxation. The relevant dσ* orbital in the cation of **49** is σ-antibonding between the metal centre and the nitrogen atom (N_{ppy}) of the [ppy]$^-$ ligands. Electron promotion thus leads to the elongation of the Ir–N_{ppy} bond, from 2.08 Å in the ground state (S_0) to 2.50 Å in the resulting ^{3}MC state, and to the virtual decoordination of the two N_{ppy} atoms. The rupture of the metal-ligand bonds and consequently the opening of the complex enhances the reactivity of the complex in the excited ^{3}MC state and facilitates its degradation. For the cation of complex **50**, the intramolecular π-π stacking prevents the weakening of the Ir–N_{ppy} bond of the [ppy]$^-$ ligand involved in that interaction and this bond only lengthens from 2.08 Å in S_0 to 2.24 Å in the ^{3}MC state. The pendant phenyl ring of **50** thus exerts a cage effect that restricts the opening of the structure of the complex in the excited ^{3}MC state. This makes the complex more robust reducing the possibility of degradation reactions.[124]

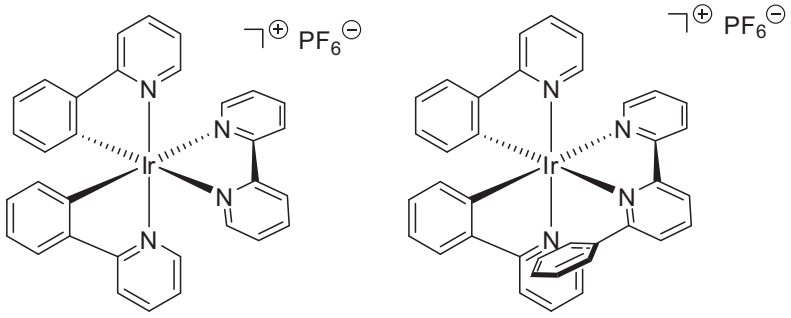

49 **50**

Scheme 8.2 "Model compounds" [Ir(ppy)$_2$(bpy)][PF$_6$] (**49**) and [Ir(ppy)$_2$(pbpy)][PF$_6$] (**50**).

Due to the surprising results of LEEC devices of complex **62**, the model compound **50** (**Scheme 8.2**) was synthesised by the author in order to study the effect of the pendant phenyl ring in a more simple molecule. Surprisingly, LEEC devices of **50** showed even better results compared to devices of complex **62**. The lifetime of the device of **50** could be increased to more than 3000 hours at an average luminance of 200 cd m^{-2} while operating at a driving voltage of 3 V (see **Section 8.2.2**).[124]

Based on these findings, two main goals were pursued in this project (see also **Section 7.1**). Firstly, further improvements of the lifetime of devices obtained from complexes similar to **50** were desired. This was done – on the chemical side – by altering the *N*,*N*′-ligand of the Ir(III) complexes. Secondly, colour tuning of the emission was investigated by varying the *C*,*N*-ligands.

Some of the results described below have been published.[123, 124, 137]

8.2
Device performance and discussion

As stated earlier, all devices described in this section were fabricated and characterised by the group of *H. Bolink* in Valencia, Spain. The reference for a typical procedure is given in **Chapter 2**. The multilayer stack of the herein described LEECs consisted of ITO / PEDOT:PSS / Ir(III) complex : IL / Al.

The results for every Ir(III) complex (**47** – **61**) shown in this chapter depict the most optimised device concerning their lifetime. For every compound, devices with many different parameters were prepared and run, *e.g.* by variation of the driving bias, the amount of ionic liquid in the emissive layer, and the layer thicknesses. While this is convenient to find the best-performing device characteristics for every compound, the comparability of the different compounds itself suffers with this approach. Therefore, the lifetime and the achieved peak luminance values are incommensurable between the different complexes. Furthermore, as the luminance is dependent – unfortunately not in a linear manner – on the applied voltage, comparisons of the results have to be undertaken very carefully. Therefore, in this context, "best-performing" means satisfying a balance between overall brightness, the turn-on-time t_{on}, and the half-life $t_{½}$, as these parameters are not independent of each other.

In the literature, device stabilities are reported in different ways.[124] Normally, it is given either as the time taken to reach half of the maximum luminance ($t_{½}$), or as the total photon flux (E ($t_{⅕}$) in Joules) emitted up to the time the luminance reaches ⅕th of the maximum value ($t_{⅕}$) for a cell area of 3 mm^2.[134, 312] The latter method overcomes, at least partially, the aforementioned problem with the intrinsic dependency of the luminance and the applied bias.

It has to be noted that the sequence of LEEC devices presented below does not necessarily reflect the chronological order in which the devices were fabricated and measured.

8.2.1
Phenanthroline based complexes

LEEC devices with the two phenanthroline based Ir(III) complexes [Ir(ppy)$_2$(phen)][PF$_6$] (**47**) and [Ir(ppy)$_2$(pphen)][PF$_6$] (**48**) in their emissive layer revealed rather long lifetimes (**Figure 8.3**) compared to previously reported Ir(III)-based LEEC devices. However, they were not among the best-performing devices as we will see later. The LEEC device containing complex **47** showed a shorter lifetime compared with the device containing complex **48**, but **47** was run at a higher bias which increased the overall luminance and, at the same time, diminished its lifetime. For both compounds, the best-performing LEEC devices were obtained with a Ir(III) complex : ionic liquid molar ratio of 4:1. As mentioned above, "best-performing" means a satisfying balance between all characteristics of the device, as these parameters are not independent of each other.

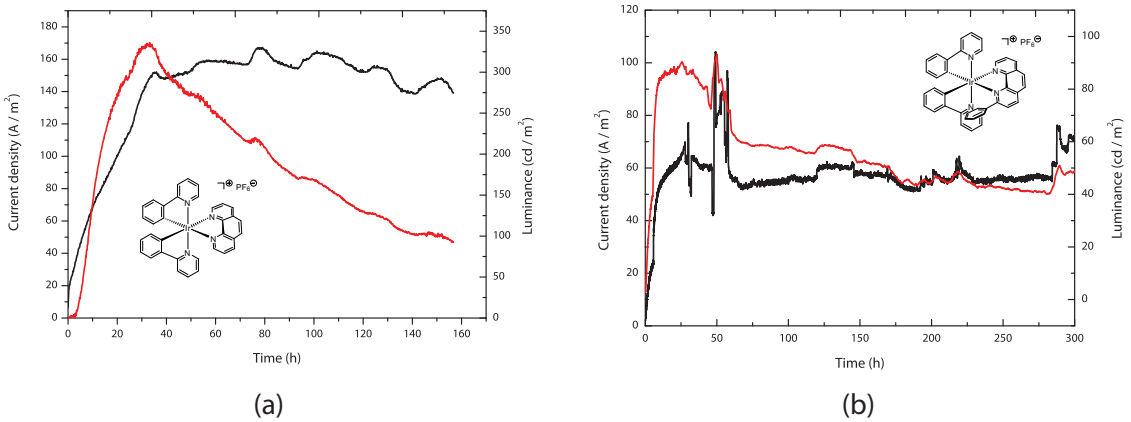

Figure 8.3 Luminance (red) and current density (black) versus time of LEEC devices from phenanthroline based complexes. (a) Compound **47** : IL = 4:1, at an applied bias of 4 V. (b) Compound **48** : IL = 4:1, at an applied bias of 3 V.

8.2.2
Simple bipyridine based complexes

Next, the simple bipyridine based complexes were incorporated into devices (**Figure 8.4**), *i.e.* compounds $[Ir(ppy)_2(bpy)][PF_6]$ (**49**), $[Ir(ppy)_2(pbpy)][PF_6]$ (**50**), and $[Ir(ppy)_2(dpbpy)][PF_6]$ (**51**). As it turned out, the stability of their LEEC devices was increased dramatically by the additional phenyl ring(s) at the 6(,6')-position(s) of the 2,2'-bipyridine ligand due to the π-π stacking which gives rise to an improved stability of the excited molecules. The device containing complex **50** proved to be the most stable LEEC ever reported with achieved lifetimes over 3000 hours while possessing a peak brightness of 300 cd m^{-2} operating at an applied bias of 3 V.[124] Note that these results were achieved with further optimisations of the devices and are not taken from the graph depicted in **Figure 8.4**. Although these results are outstanding, the long lifetime comes at the expense of a very long turn-on time of several hundred hours and is indicative of a low ionic mobility in the emissive thin film. To speed up the occurrence of the electroluminescence, either a higher ratio of ionic liquid in the active layer would help,[310] or several short high-voltage pulses can be applied.[313]

As for the LEEC with **51** as the active component, although there is a double intramolecular π-π stacking present in the solid state structure (see **Chapter 7**), this, surprisingly, did not improve the lifetime of the device compared to the device of **50**, where the complex exhibits only a single π-π stacking.[137] One reason for this is attributed to the distortion of the planarity of the bpy ligand domain when the two attached phenyl groups π-stack with the phenyl groups of the $[ppy]^-$ ligands. Furthermore, quantum chemical calculations show that the energy difference between the emitting triplet and the metal-centred triplet state has decreased which renders the complex more susceptible to emission losses and degradation reactions.[137] Nevertheless, lifetimes of around 1300 hours for complex **51** are very impressive and have no equal in the literature to date (April 2009).

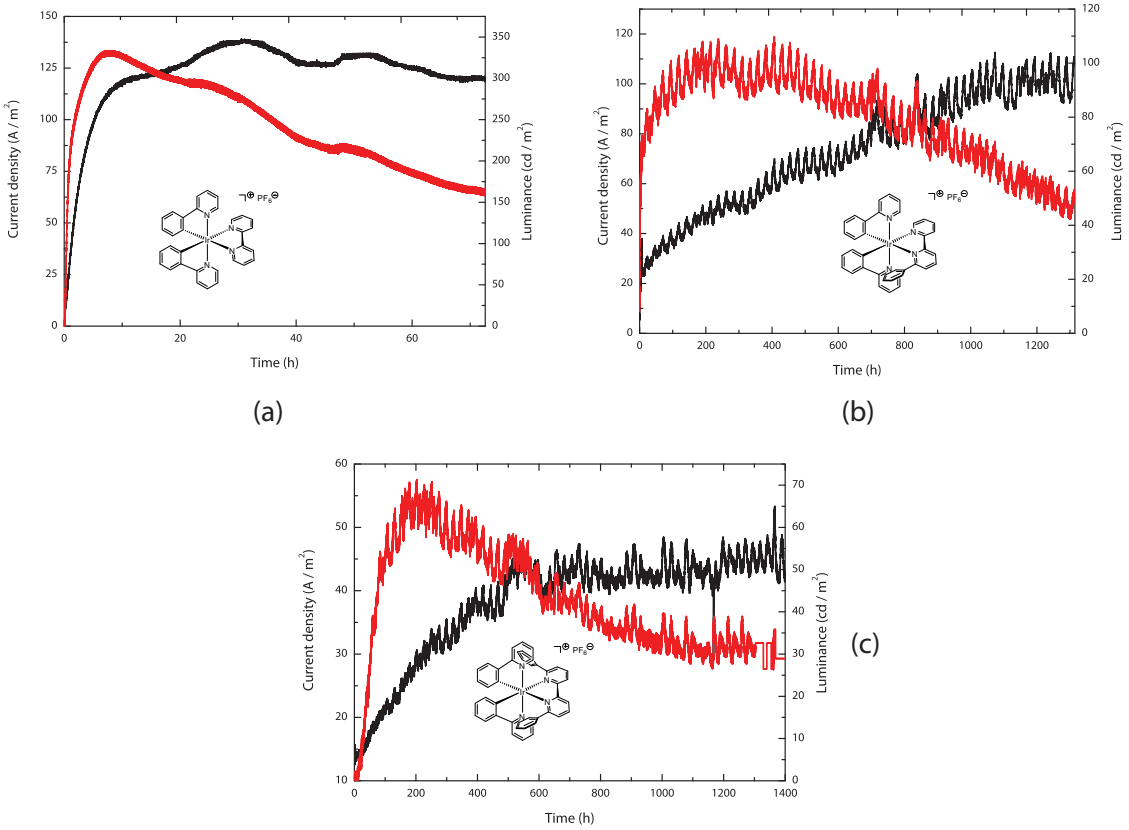

Figure 8.4 Luminance (red) and current density (black) versus time of LEEC devices from simple bipyridine based complexes. (a) Compound **49** : IL = 4:1, at an applied bias of 3 V. (b) Compound **50** : IL = 4:1, at an applied bias of 3 V. (c) Compound **51** : IL = 4:1, at an applied bias of 3 V.
The wavy fine structure in the graphs of devices of **50** and **51** is due to temperature fluctuations in the clean room because the cooling system switched off during the nights.[314]

8.2.3
Archetype and dendronised based complexes

LEEC devices fabricated from Ir(III) complexes bearing dendronised bpy-ligands, *i.e.* $[Ir(ppy)_2((HO)_2ppbpy)][PF_6]$ (**53**), $[Ir(ppy)_2((H_3CO)_2ppbpy)][PF_6]$ (**52**), and $[Ir(ppy)_2((H_{21}C_{10}O)_2ppbpy)][PF_6]$ (**54**), revealed diverse results (**Figure 8.5**). The LEEC containing complex **53** showed very short lifetimes in the range of less than an hour. This dramatic decrease of device stability is most likely associated with different film properties, as the polar hydroxy-groups may bind differently with the surface and thus affect the morphology of the film in a negative manner.[315]

Devices from complexes **52** and **54**, however, revealed great stabilities again to give LEECs with rather long lifetimes. At an applied bias of 3 V, the LEEC device containing complex **54** with the C_{10}-chains showed higher overall and peak brightness of > 250 cd m^{-2} in contrast to ~ 170 cd m^{-2} for the LEEC containing complex **52**. This can be attributed to a higher quantum efficiency in the

film of **54**, as the molecules, due to the long aliphatic chain, are located at a higher distance from each other.[280] This quasi-lower concentration reduces intermolecular quenching effects which are known for aggregates.[316, 317] Interestingly, there are examples where aggregates of nanoparticles exhibit higher efficiencies than within a film of well-dispersed nanoparticles as the aggregates can act as a buffer layer in an electroluminescent device.[318]

Devices of $[Ir(ppy)_2((G1–O)_2ppbpy)][PF_6]$ (**55**) and $[Ir(ppy)_2((G2–O)_2ppbpy)][PF_6]$ (**56**) featured increased molecular size and increased lipophilicity due to the higher ratio of aliphatic chains. Unfortunately, these devices did not reveal any electroluminescence, as no injection and transport process could be observed. It was suggested that the reason for this unexpected behaviour is that the molecules inside the active layer are located too far from each other which then renders the charge transport (which occurs *via* a hopping mechanism) impossible. Moreover, PF_6^- anions could be trapped in the bulky groups of the Fréchet-type dendrons leading to an overall low mobility of the anions.[319, 320]

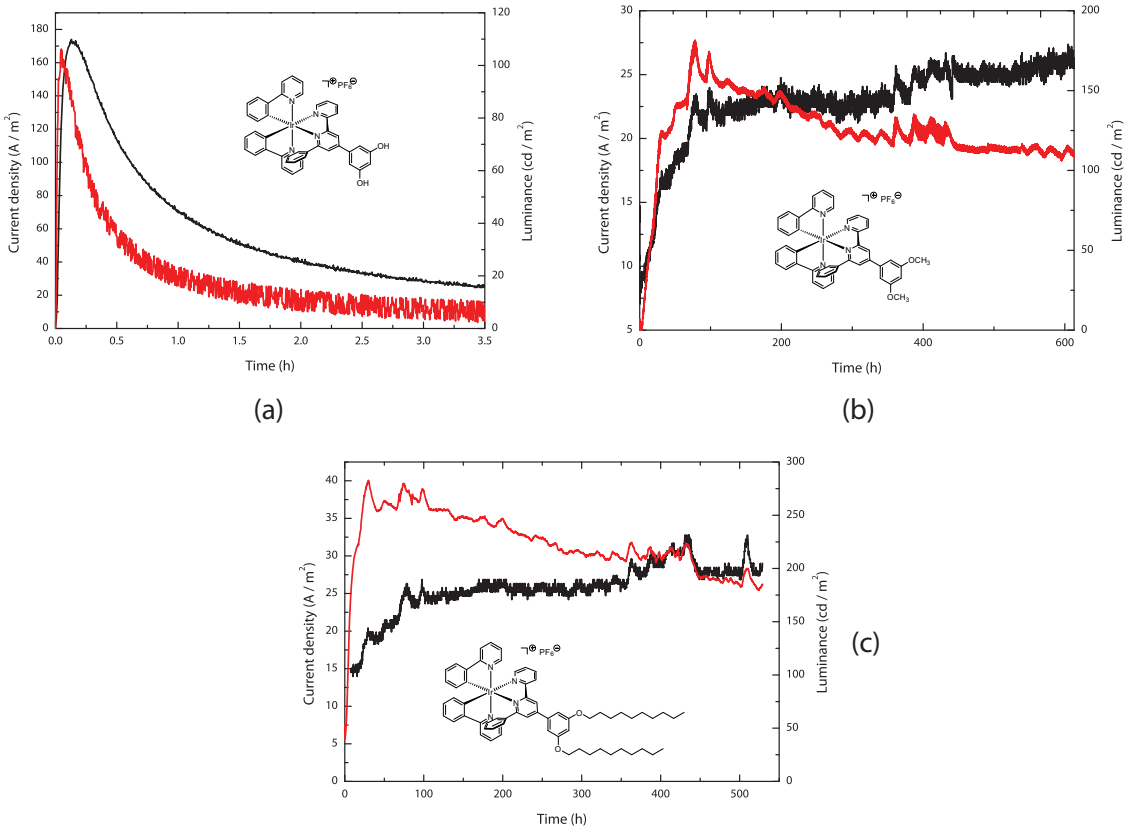

Figure 8.5 Luminance (red) and current density (black) versus time of LEEC devices from archetype and dendronised based complexes. (a) Compound **53** : IL = 1:1, at an applied bias of 3 V. (b) Compound **52** : IL = 4:1, at an applied bias of 3 V. (c) Compound **54** : IL = 4:1, at an applied bias of 3 V.

8.2.4
Modified phenyl-pyridine based complexes

Complexes with *C,N*-ligands other than $[ppy]^-$ were incorporated into LEEC devices, namely $[Ir(dfppy)_2(pbpy)][PF_6]$ (**57**), $[Ir(bzq)_2(pbpy)][PF_6]$ (**58**), and $[Ir(piq)_2(pbpy)][PF_6]$ (**59**) and their luminance and current density values versus time are given in **Figure 8.6**. They all showed rather long lifetimes of several hundreds of hours, again supposedly due to the intramolecular π-π stacking between the pendant phenyl ring of pbpy and one of the carbon-coordinating rings of the *C,N*-ligands. This π-π stacking was confirmed for complexes **57** and **59** where single crystal structures were obtained (see **Chapter 7**).

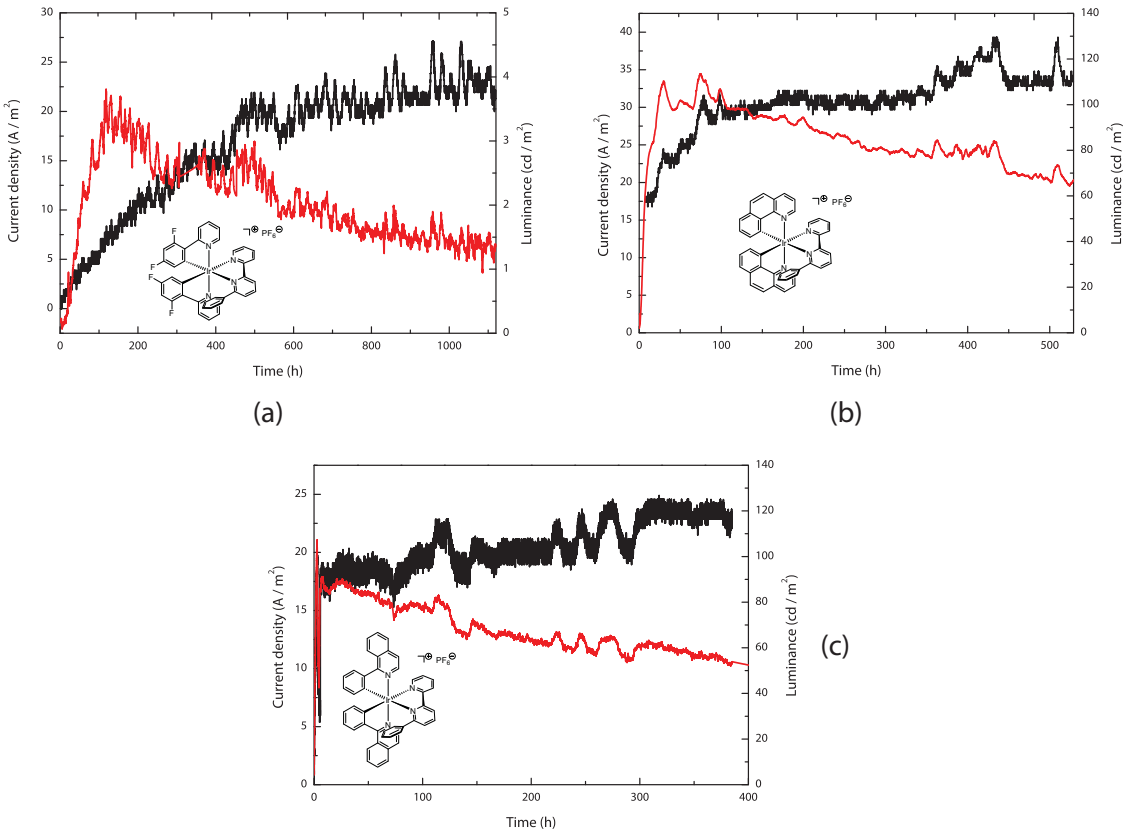

Figure 8.6 Luminance (red) and current density (black) versus time of LEEC devices from modified phenyl-pyridine based complexes. (a) Compound **57** : IL = 4:1, at an applied bias of 3 V. (b) Compound **58** : IL = 4:1, at an applied bias of 3 V. (c) Compound **59** : IL = 4:1, at an applied bias of 3 V.

However, in case of **57**, the long lifetime is accompanied by very low luminance values which renders its application in solid state lighting useless. Operating the device at higher voltages would increase the brightness, but again, at the same time, it diminishes the stability. Nevertheless, the electroluminescence spectrum of the LEEC containing **57** showed a remarkable hypsochromic effect as is the case in photoluminescence (**Chapter 7**) with a maximum emission at 564 nm compared to 588 nm for model compound **50** (**Figure 8.7**). Interestingly, there is a considerable discrepancy

between the electroluminescence and the photoluminescence spectra of complex **57**. In solution, **57** emits at a maximum wavelength of 532 nm (**Chapter 7**), whereas in solid state, *i.e.* in a LEEC device, the maximum is found at the aforementioned 564 nm.

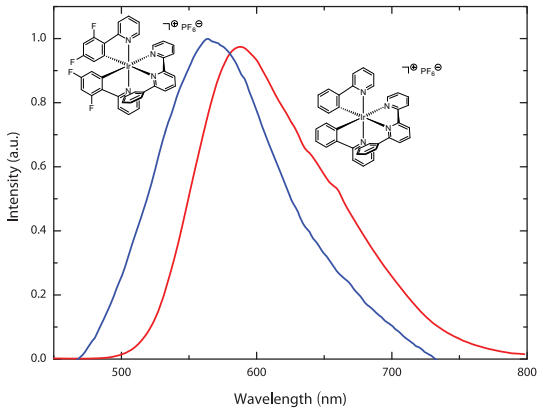

Figure 8.7 Electroluminescence spectra of the LEEC containing **57** (blue line) compared with the device containing **50** (red line).

8.2.5
Pyrazole based complexes

Complexes of pyrazole based *C,N*-ligands were used for fabrication of LEEC devices. $[Ir(ppz)_2(pbpy)][PF_6]$ (**60**) and $[Ir(dmppz)_2(pbpy)][PF_6]$ (**61**) showed again a high stability of the devices giving rise to lifetimes of several hundreds of hours (**Figure 8.8**). Particularly, the LEEC containing complex **61** revealed remarkable results. Then again, the LEEC device with **60** as its active layer showed much higher luminance values (peak value above 200 cd m^{-2}) compared to **61** (peak value below 100 cd m^{-2}) which explains – to a certain extent – the shorter lifetime.

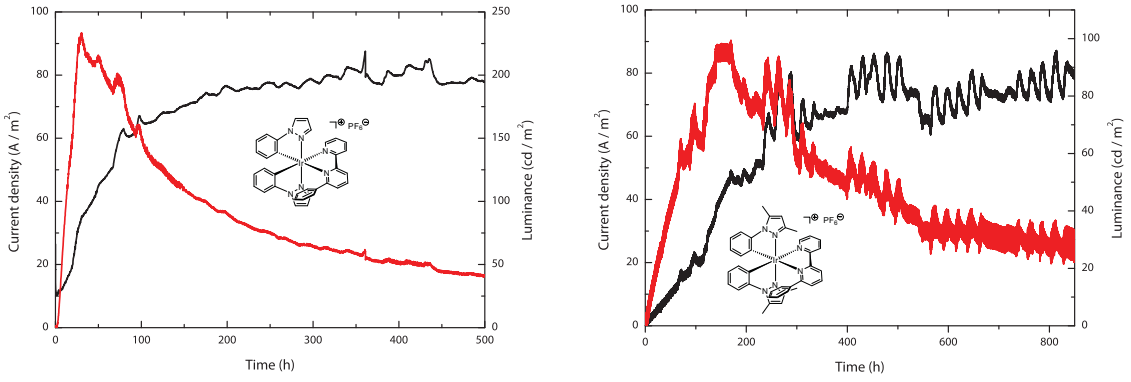

(a) (b)

Figure 8.8 Luminance (red) and current density (black) versus time of LEEC devices from pyrazole based complexes. (a) Compound **60** : IL = 4:1, at an applied bias of 3 V. (b) Compound **61** : IL = 4:1, at an applied bias of 3 V.

8.3 Conclusions

In conclusion, LEEC devices with cyclometallated Ir(III) complexes described in **Chapter 7** as their active component mostly showed remarkable device characteristics, in particular brightness and lifetime values. If there is a pendant phenyl ring at the *N*,*N*′-ligand (*e.g.* ligand pbpy) which exhibits an intramolecular π-π stacking, the lifetime of the LEEC devices was exceptionally augmented. This intramolecular interaction was proven in solid state structures for all instances except complex **58**, and complex **52** and related complexes thereof (**53**, **54**, **55**, and **56**), where no crystal structures could be obtained (see **Chapter 7**).

Selected results are summarised in **Table 8.1**. The values were calculated by members of the group of *H. Bolink*. Again, it has to be noted that evaluation and comparison of these results need to be done carefully, as the parameters are inherently dependant on each other which makes it difficult to speak of "best-performing" devices.

The most stable LEEC were devices with complexes **50** and **51** (**Table 8.1**). Unfortunately, this high stability comes at the expense of a very long turn-on time. In order to decrease the time until the device reaches an acceptable brightness (in terms of real-world applications), the devices were also prebiased with several short high-voltage pulses. This procedure, in return, increased the lifetimes even more.[124] The highest luminance values were obtained with LEEC devices containing either complex **50** or **54**, both at about 290 cd m^{-2}. In the case of **54**, the device thereof also achieved the highest current efficiency. Concordantly, it revealed a very high total photon flux > 17 J. The best value in this category is achieved by the LEEC containing complex **61** (18.7 J) which shows rather balanced characteristics of lifetime, turn-on time, and luminance values. In this series, even the "worst"-performing device being **60** with a total photon flux of 3.55 J showed an increase of overall stability by an order of magnitude compared with the best value reported in the literature (0.27 J)[312].

Table 8.1 Characterisations of LEEC devices with a multilayer stack consisting of ITO / PEDOT:PSS / Ir(III) complex : IL (4:1) / Al, at an applied bias of 3 V. Red numbers indicate best values. All values were calculated by the group of *H. Bolink*.
[a] Time to reach the maximum luminance.
[b] Time from voltage turn-on to the time where the luminance is half of the maximum value.
[c] Time from voltage turn-on to the time where the luminance is one fifth of the maximum value.
[d] Total photon flux emitted up to the time $t_{1/5}$ for a cell area of 3 mm^2.
[e] Maximum luminance value, *i.e.* luminance at t_{on}.
[f] Maximum efficiency value.
[g] Prebiased devices, *i.e.* devices where several short high-voltage pulses were conducted in order to reduce the turn-on time.

Complex	t_{on} [a] [h]	$t_{1/2}$ [b] [h]	$t_{1/5}$ [c] [h]	E ($t_{1/5}$) [d] [J]	**Brightness** [e] [cd m^{-2}]	**Efficiency** [f] [cd A^{-1}]
47	6.4	73	241		63	5.8
48	27	230	400		92	2.8
50	237	1288	1900	13.6	109	3.1
50[g]	510	3000			290	9.7
51	199	1284	1960	6.9	71	2.7
51[g]	262	2566			102	3.2
52	77	910	1700	17.3	183	8.2
54	33	750	1150	17.4	284	14.7
58	73	690		6.19	113	6.2
59	16	500		6.14	90	7.1
60	30	140	476	3.55	236	7.9
61	200	2000	3200	18.7	102	4.6

Appendix A: References

[1] E. C. Constable, B. A. Hermann, C. E. Housecroft, L. Merz, L. J. Scherer, *Chem. Commun.*, **2004**, 928-929.

[2] F. Wöhler, *Ann. Phys. Chem.*, **1828**, *88*, 253-256.

[3] J. M. Lehn, *Supramolecular Chemistry*, VCH Verlagsgesellschaft, Weinheim, **1995**.

[4] F. Vögtle, *Supramolecular Chemistry*, John Wiley & Sons Ltd., Chichester, **1991**.

[5] M. Bergmann, *Z. Angew. Chem.*, **1925**, *38*, 1141-1144.

[6] E. Fischer, *Ber. Dtsch. Chem. Ges.*, **1894**, *27*, 2985-2993.

[7] P. Ehrlich, *Studies on Immunity*, Wiley, New York, **1906**.

[8] A. Werner, *Z. Anorg. Chem.*, **1893**, *3*, 267-330.

[9] K. L. Wolf, H. Frahm, H. Harms, *Z. Phys. Chem. B*, **1937**, *36*, 237-287.

[10] K. L. Wolf, H. Dunken, K. Merkel, *Z. Phys. Chem. B*, **1940**, *46*, 287-312.

[11] K. L. Wolf, R. Wolff, *Angew. Chem.*, **1949**, *61*, 191-201.

[12] C. J. Pedersen, *J. Am. Chem. Soc.*, **1967**, *89*, 2495-2496.

[13] C. J. Pedersen, *J. Am. Chem. Soc.*, **1967**, *89*, 7017-7036.

[14] B. Dietrich, J. M. Lehn, J. P. Sauvage, *Tetrahedron Lett.*, **1969**, 2885-2888.

[15] B. Dietrich, J. M. Lehn, J. P. Sauvage, J. Blanzat, *Tetrahedron*, **1973**, *29*, 1629-1645.

[16] B. Dietrich, J. M. Lehn, J. P. Sauvage, *Tetrahedron*, **1973**, *29*, 1647-1658.

[17] J. M. Lehn, *Pure Appl. Chem.*, **1978**, *50*, 871-892.

[18] J. M. Lehn, *Angew. Chem. Int. Ed.*, **1988**, *27*, 89-112.

[19] I. Dance, *New J. Chem.*, **2003**, *27*, 1-2.

[20] L. Pauling, *The Nature of the Chemical Bond*, 2nd ed., Cornell University Press, Ithaca, **1939**.

[21] L. J. Scherer, PhD Thesis, University of Basel, **2006**.

[22] J. D. Dunitz, A. Gavezzotti, *Angew. Chem. Int. Ed.*, **2005**, *44*, 1766-1787.

[23] M. Mammen, S. K. Choi, G. M. Whitesides, *Angew. Chem. Int. Ed.*, **1998**, *37*, 2755-2794.

[24] J. J. Lundquist, E. J. Toone, *Chem. Rev.*, **2002**, *102*, 555-578.

[25] G. Ercolani, *J. Am. Chem. Soc.*, **2003**, *125*, 16097-16103.

[26] P. I. Kitov, D. R. Bundle, *J. Am. Chem. Soc.*, **2003**, *125*, 16271-16284.

[27] J. D. Badjic, A. Nelson, S. J. Cantrill, W. B. Turnbull, J. F. Stoddart, *Acc. Chem. Res.*, **2005**, *38*, 723-732.

[28] Y. C. Lee, R. T. Lee, *Acc. Chem. Res.*, **1995**, *28*, 321-327.

[29] T. Steiner, *Angew. Chem. Int. Ed.*, **2002**, *41*, 48-76.

[30] http://en.wikipedia.org/w/index.php?title=Hydrogen_bond&oldid=284054865

[31] P. Muller, *Pure Appl. Chem.*, **1994**, *66*, 1077-1184.

[32] G. Gilli, P. Gilli, in *XIIIth International Workshop on Horizons in Hydrogen Bond Research*, Elsevier Science Bv, Swieradow, Poland, **1999**, pp. 1-15.

[33] R. Taylor, O. Kennard, *J. Am. Chem. Soc.*, **1982**, *104*, 5063-5070.

[34] G. R. Desiraju, *Acc. Chem. Res.*, **1991**, *24*, 290-296.

[35] G. R. Desiraju, *Acc. Chem. Res.*, **1996**, *29*, 441-449.

[36] C. A. Hunter, J. K. M. Sanders, *J. Am. Chem. Soc.*, **1990**, *112*, 5525-5534.

[37] C. Janiak, *J. Chem. Soc.-Dalton Trans.*, **2000**, 3885-3896.

[38] W. Saenger, *Principles of Nucleic Acid Structure*, Springer-Verlag, New York, **1984**.

[39] L. P. G. Wakelin, *Med. Res. Rev.*, **1986**, *6*, 275-340.

[40] G. R. Desiraju, A. Gavezzotti, *J. Chem. Soc.-Chem. Commun.*, **1989**, 621-623.
[41] S. K. Burley, G. A. Petsko, *Adv. Protein Chem.*, **1988**, *39*, 125-189.
[42] C. A. Hunter, P. Leighton, J. K. M. Sanders, *J. Chem. Soc.-Perkin Trans. 1*, **1989**, 547-552.
[43] B. Askew, P. Ballester, C. Buhr, K. S. Jeong, S. Jones, K. Parris, K. Williams, J. Rebek, *J. Am. Chem. Soc.*, **1989**, *111*, 1082-1090.
[44] A. E. Alexander, *J. Chem. Soc.*, **1937**, 1813-1816.
[45] J. Langlet, P. Claverie, F. Caron, J. C. Boeuve, *Int. J. Quantum Chem.*, **1981**, *20*, 299-338.
[46] http://chem.vander-lingen.nl/articles/Handle_with_care:__pi_-_pi_stacking/id/126/itemid/310
[47] S. Grimme, *Angew. Chem. Int. Ed.*, **2008**, *47*, 3430-3434.
[48] G. M. Whitesides, in *Fourth Foresight Conference on Molecular Nanotechnology*, Palo Alto, **1995**.
[49] G. M. Whitesides, J. P. Mathias, C. T. Seto, *Science*, **1991**, *254*, 1312-1319.
[50] R. J. Jackman, J. L. Wilbur, G. M. Whitesides, *Science*, **1995**, *269*, 664-666.
[51] E. Kim, Y. N. Xia, G. M. Whitesides, *Nature*, **1995**, *376*, 581-584.
[52] A. Kumar, N. L. Abbott, E. Kim, H. A. Biebuyck, G. M. Whitesides, *Acc. Chem. Res.*, **1995**, *28*, 219-226.
[53] E. Kim, G. M. Whitesides, *Chem. Mat.*, **1995**, *7*, 1257-1264.
[54] A. Ulman, *Chem. Rev.*, **1996**, *96*, 1533-1554.
[55] S. A. Prokhorova, S. S. Sheiko, A. Mourran, R. Azumi, U. Beginn, G. Zipp, C. H. Ahn, M. N. Holerca, V. Percec, M. Moller, *Langmuir*, **2000**, *16*, 6862-6867.
[56] I. Widmer, U. Hubler, M. Stöhr, L. Merz, H. J. Güntherodt, B. A. Hermann, P. Samori, J. P. Rabe, P. B. Rheiner, G. Greiveldinger, P. Murer, *Helv. Chim. Acta*, **2002**, *85*, 4255-4263.
[57] P. Wu, Q. H. Fan, G. J. Deng, Q. D. Zeng, C. Wang, C. L. Bai, *Langmuir*, **2002**, *18*, 4342-4344.
[58] S. X. Yin, C. Wang, X. H. Qiu, B. Xu, C. L. Bai, in *Asia-Pacific Surface and Interface Analysis Conference (APSIAC 2000)*, John Wiley & Sons Ltd, Beijing, Peoples R China, **2000**, pp. 248-252.
[59] D. A. Tomalia, H. Baker, J. Dewald, M. Hall, G. Kallos, S. Martin, J. Roeck, J. Ryder, P. Smith, *Polym. J.*, **1985**, *17*, 117-132.
[60] E. Buhleier, W. Wehner, F. Vögtle, *Synthesis*, **1978**, 155-158.
[61] G. R. Newkome, C. N. Moorefield, F. Vögtle, *Dendritic Molecules*, 1st ed., VCH, Weinheim, **1996**.
[62] G. R. Newkome, Z. Q. Yao, G. R. Baker, V. K. Gupta, *J. Org. Chem.*, **1985**, *50*, 2003-2004.
[63] P. G. de Gennes, H. Hervet, *Journal De Physique Lettres*, **1983**, *44*, L351-L360.
[64] N. Feuerbacher, F. Vögtle, in *Dendrimers, Vol. 197*, Springer-Verlag Berlin, Berlin, **1998**, pp. 1-18.
[65] http://en.wikipedia.org/w/index.php?title=Dendrimer&oldid=281429891
[66] R. G. Denkewalter, J. Kolc, W. J. Lukasvage, US Patent 4,289,872, **1981**.
[67] D. A. Tomalia, A. M. Naylor, W. A. Goddard, *Angew. Chem. Int. Ed.*, **1990**, *29*, 138-175.
[68] G. R. Newkome, C. N. Moorefield, G. R. Baker, A. L. Johnson, R. K. Behera, *Angew. Chem. Int. Ed.*, **1991**, *30*, 1176-1178.
[69] H. B. Mekelburger, W. Jaworek, F. Vögtle, *Angew. Chem. Int. Ed.*, **1992**, *31*, 1571-1576.
[70] E. M. M. de Brabander-van den Berg, E. W. Meijer, *Angew. Chem. Int. Ed.*, **1993**, *32*, 1308-1311.
[71] C. J. Hawker, J. M. J. Fréchet, *J. Chem. Soc.-Chem. Commun.*, **1990**, 1010-1013.
[72] T. M. Miller, T. X. Neenan, *Chem. Mat.*, **1990**, *2*, 346-349.
[73] J. S. Moore, Z. F. Xu, *Macromolecules*, **1991**, *24*, 5893-5894.
[74] Z. F. Xu, J. S. Moore, *Angew. Chem. Int. Ed.*, **1993**, *32*, 1354-1357.
[75] M. L. Mansfield, *Macromolecules*, **1993**, *26*, 3811-3814.
[76] C. J. Hawker, J. M. J. Fréchet, *J. Am. Chem. Soc.*, **1990**, *112*, 7638-7647.

[77] S. M. Grayson, J. M. J. Fréchet, *Chem. Rev.*, **2001**, *101*, 3819-3867.
[78] L. H. Gade, *Koordinationschemie*, 1st ed., Wiley-VCH, Weinheim, **1998**.
[79] H. Kopp, *Geschichte der Chemie*, 1st ed., Braunschweig, **1843**.
[80] L. H. Gade, *Chemie in unserer Zeit*, **2002**, *36*, 168-175.
[81] http://en.wikipedia.org/w/index.php?title=Complex_(chemistry)&oldid=274547840
[82] E. C. Constable, *Metals and Ligand Reactivity - An Introduction to the Organic Chemistry of Metal Complexes*, 2nd ed., VCH, Weinheim, **1995**.
[83] F. Blau, *Monatsh. Chem.*, **1889**, *10*, 375-388.
[84] F. Blau, *Ber. Dtsch. Chem. Ges.*, **1888**, *21*, 1077-1078.
[85] F. Blau, *Monatsh. Chem.*, **1898**, *19*, 647-689.
[86] W. W. Brandt, F. P. Dwyer, E. C. Gyarfas, *Chem. Rev.*, **1954**, *54*, 959-1017.
[87] J. W. Earl, I. R. Kennedy, *Phytochemistry*, **1975**, *14*, 1507-1512.
[88] K. V. Thimann, S. Satler, *Proc. Natl. Acad. Sci. U. S. A.*, **1979**, *76*, 2770-2773.
[89] http://en.wikipedia.org/w/index.php?title=Iridium&oldid=284146245
[90] A. F. Holleman, E. Wiberg, N. Wiberg, *Lehrbuch der Anorganischen Chemie*, 101st ed., Walter de Gruyter, Berlin, **1995**.
[91] N. N. Greenwood, A. Earnshaw, *Chemistry of the Elements*, 2nd ed., Butterworth-Heinemann, Oxford, **1997**.
[92] J. Emsley, *Nature's Building Blocks: An A-Z Guide to the Elements*, 1st ed., Oxford University Press, Oxford, **2003**.
[93] L. W. Alvarez, W. Alvarez, F. Asaro, H. V. Michel, *Science*, **1980**, *208*, 1095-1108.
[94] C. K. Jorgensen, *Modern Aspects of Ligand Field Theory*, Elsevier, New York, **1971**.
[95] G. W. Parshall, *Acc. Chem. Res.*, **1970**, *3*, 139-144.
[96] M. Nonoyama, *Bull. Chem. Soc. Jpn.*, **1974**, *47*, 767-768.
[97] C. Gerber, H. P. Lang, *Nat. Nanotechnol.*, **2006**, *1*, 3-5.
[98] G. Binnig, H. Rohrer, C. Gerber, E. Weibel, *Appl. Phys. Lett.*, **1982**, *40*, 178-180.
[99] G. Binnig, H. Rohrer, C. Gerber, E. Weibel, *Phys. Rev. Lett.*, **1983**, *50*, 120-123.
[100] S. Kramer, R. R. Fuierer, C. B. Gorman, *Chem. Rev.*, **2003**, *103*, 4367-4418.
[101] D. M. Eigler, E. K. Schweizer, *Nature*, **1990**, *344*, 524-526.
[102] http://www.almaden.ibm.com/vis/stm/atomo.html
[103] G. Binnig, H. Rohrer, *Helv. Phys. Acta*, **1982**, *55*, 726-735.
[104] G. Friedbacher, H. Fuchs, *Pure Appl. Chem.*, **1999**, *71*, 1337-1357.
[105] E. Meyer, H.-J. Hug, R. Bennewitz, *Scanning Probe Microscopy - The lab on a Tip*, Springer-Verlag, Heidelberg, **2003**.
[106] C. Klink, L. Olesen, F. Besenbacher, I. Stensgaard, E. Laegsgaard, N. D. Lang, *Phys. Rev. Lett.*, **1993**, *71*, 4350-4353.
[107] M. F. Crommie, C. P. Lutz, D. M. Eigler, *Science*, **1993**, *262*, 218-220.
[108] http://www.almaden.ibm.com/vis/stm/corral.html
[109] L. Merz, PhD Thesis, University of Basel, **2004**.
[110] http://en.wikipedia.org/wiki/File:ScanningTunnelingMicroscope_schematic.png
[111] http://creativecommons.org/licenses/by-sa/2.0/at/deed.en_GB
[112] N. Holonyak, S. F. Bevacqua, *Appl. Phys. Lett.*, **1962**, *1*, 82-83.
[113] A. A. Bergh, P. J. Dean, *Light Emitting Diodes*, Clarendon Press, Oxford, **1976**.
[114] A. A. Bergh, G. Craford, A. Duggal, R. Haitz, *Phys. Today*, **2001**, *54*, 42-47.

[115] C. W. Tang, S. A. VanSlyke, *Appl. Phys. Lett.*, **1987**, *51*, 913-915.

[116] J. H. Burroughes, D. D. C. Bradley, A. R. Brown, R. N. Marks, K. Mackay, R. H. Friend, P. L. Burns, A. B. Holmes, *Nature*, **1990**, *347*, 539-541.

[117] M. M. Richter, *Chem. Rev.*, **2004**, *104*, 3003-3036.

[118] P. McCord, A. J. Bard, *Journal of Electroanalytical Chemistry*, **1991**, *318*, 91-99.

[119] D. A. Pardo, G. E. Jabbour, N. Peyghambarian, *Adv. Mater.*, **2000**, *12*, 1249-1252.

[120] Q. B. Pei, G. Yu, C. Zhang, Y. Yang, A. J. Heeger, *Science*, **1995**, *269*, 1086-1088.

[121] J. Gao, J. Dane, *Appl. Phys. Lett.*, **2003**, *83*, 3027-3029.

[122] J. H. Shin, A. Dzwilewski, A. Iwasiewicz, S. Xiao, A. Fransson, G. N. Ankah, L. Edman, *Appl. Phys. Lett.*, **2006**, *89*, 3.

[123] S. Graber, K. Doyle, M. Neuburger, C. E. Housecroft, E. C. Constable, R. D. Costa, E. Ortí, D. Repetto, H. J. Bolink, *J. Am. Chem. Soc.*, **2008**, *130*, 14944-14945.

[124] H. J. Bolink, E. Coronado, R. D. Costa, E. Ortí, M. Sessolo, S. Graber, K. Doyle, M. Neuburger, C. E. Housecroft, E. C. Constable, *Adv. Mater.*, **2008**, *20*, 3910-3913.

[125] J. K. Lee, D. S. Yoo, E. S. Handy, M. F. Rubner, *Appl. Phys. Lett.*, **1996**, *69*, 1686-1688.

[126] F. G. Gao, A. J. Bard, *J. Am. Chem. Soc.*, **2000**, *122*, 7426-7427.

[127] J. D. Slinker, J. A. DeFranco, M. J. Jaquith, W. R. Silveira, Y. W. Zhong, J. M. Moran-Mirabal, H. G. Craighead, H. D. Abruna, J. A. Marohn, G. G. Malliaras, *Nat. Mater.*, **2007**, *6*, 894-899.

[128] Q. Pei, A. J. Heeger, *Nat. Mater.*, **2008**, *7*, 167-167.

[129] J. Gao, J. Dane, *Appl. Phys. Lett.*, **2004**, *84*, 2778-2780.

[130] J. D. Slinker, A. A. Gorodetsky, M. S. Lowry, J. J. Wang, S. Parker, R. Rohl, S. Bernhard, G. G. Malliaras, *J. Am. Chem. Soc.*, **2004**, *126*, 2763-2767.

[131] R. T. Wegh, E. J. Meijer, E. A. Plummer, L. De Cola, K. Brunner, A. van Dijken, J. W. Hofstraat, in *8th Conference on Organic Light-Emitting Materials and Devices* (Eds.: Z. H. Kafafi, P. A. Lane), Spie-Int Soc Optical Engineering, Denver, CO, **2004**, pp. 48-58.

[132] A. B. Tamayo, S. Garon, T. Sajoto, P. I. Djurovich, I. M. Tsyba, R. Bau, M. E. Thompson, *Inorg. Chem.*, **2005**, *44*, 8723-8732.

[133] H. C. Su, C. C. Wu, F. C. Fang, K. T. Wong, *Appl. Phys. Lett.*, **2006**, *89*, 3.

[134] G. Kalyuzhny, M. Buda, J. McNeill, P. Barbara, A. J. Bard, *J. Am. Chem. Soc.*, **2003**, *125*, 6272-6283.

[135] L. J. Soltzberg, J. D. Slinker, S. Flores-Torres, D. A. Bernards, G. G. Malliaras, H. D. Abruna, J. S. Kim, R. H. Friend, M. D. Kaplan, V. Goldberg, *J. Am. Chem. Soc.*, **2006**, *128*, 7761-7764.

[136] H. J. Bolink, L. Cappelli, E. Coronado, M. Grätzel, E. Ortí, R. D. Costa, P. M. Viruela, M. K. Nazeeruddin, *J. Am. Chem. Soc.*, **2006**, *128*, 14786-14787.

[137] R. D. Costa, E. Ortí, H. J. Bolink, S. Graber, C. E. Housecroft, M. Neuburger, S. Schaffner, E. C. Constable, *Chem. Commun.*, **2009**, 2029-2031.

[138] *Collect* Software, Bruker Nonius BV: Delft, **1997-2001**.

[139] A. Altomare, M. C. Burla, M. Camalli, G. L. Cascarano, C. Giacovazzo, A. Guagliardi, A. G. G. Moliterni, G. Polidori, R. Spagna, *J. Appl. Crystallogr.*, **1999**, *32*, 115-119.

[140] P. W. Betteridge, J. R. Carruthers, R. I. Cooper, K. Prout, D. J. Watkin, *J. Appl. Crystallogr.*, **2003**, *36*, 1487-1487.

[141] A. L. Spek, *J. Appl. Crystallogr.*, **2003**, *36*, 7-13.

[142] L. J. Farrugia, *J. Appl. Crystallogr.*, **1997**, *30*, 565-565.

[143] http://en.wikipedia.org/w/index.php?title=Graphite&oldid=280726617

[144] K. Kobayashi, *Phys. Rev. B*, **1994**, *50*, 4749-4755.
[145] J. P. Rabe, S. Buchholz, *Science*, **1991**, *253*, 424-427.
[146] A. Stabel, L. Dasaradhi, D. Ohagan, J. P. Rabe, *Langmuir*, **1995**, *11*, 1427-1430.
[147] http://en.wikipedia.org/w/index.php?title=Moir%C3%A9_pattern&oldid=278324245
[148] M. M. S. Abdel-Mottaleb, S. De Feyter, M. Sieffert, M. Klapper, K. Müllen, F. C. De Schryver, *Langmuir*, **2003**, *19*, 8256-8261.
[149] B. Venkataraman, J. J. Breen, G. W. Flynn, *J. Phys. Chem.*, **1995**, *99*, 6608-6619.
[150] W. Mamdouh, H. Uji-i, J. S. Ladislaw, A. E. Dulcey, V. Percec, F. C. De Schryver, S. De Feyter, *J. Am. Chem. Soc.*, **2006**, *128*, 317-325.
[151] R. Lazzaroni, A. Calderone, G. Lambin, J. P. Rabe, J. L. Brédas, *Synthetic Metals*, **1991**, *41-43*, 525-528.
[152] L. J. Scherer, L. Merz, E. C. Constable, C. E. Housecroft, M. Neuburger, B. A. Hermann, *J. Am. Chem. Soc.*, **2005**, *127*, 4033-4041.
[153] R. Lim, J. Li, S. F. Y. Li, Z. Feng, S. Valiyaveettil, *Langmuir*, **2000**, *16*, 7023-7030.
[154] R. Lazzaroni, A. Calderone, J. L. Brédas, J. P. Rabe, *J. Chem. Phys.*, **1997**, *107*, 99-105.
[155] C. L. Claypool, F. Faglioni, W. A. Goddard, H. B. Gray, N. S. Lewis, R. A. Marcus, *J. Phys. Chem. B*, **1997**, *101*, 5978-5995.
[156] B. A. Hermann, L. J. Scherer, C. E. Housecroft, E. C. Constable, *Adv. Funct. Mater.*, **2006**, *16*, 221-235.
[157] E. C. Constable, M. Häusler, B. A. Hermann, C. E. Housecroft, M. Neuburger, S. Schaffner, L. J. Scherer, *CrystEngComm*, **2007**, *9*, 176-180.
[158] Y. Azefu, H. Tamiaki, R. Sato, K. Toma, *Bioorg. Med. Chem.*, **2002**, *10*, 4013-4022.
[159] G. Pickaert, R. Ziessel, *Synthesis*, **2004**, 2716-2726.
[160] I. Bury, B. Heinrich, C. Bourgogne, D. Guillon, B. Donnio, *Chem.-Eur. J.*, **2006**, *12*, 8396-8413.
[161] J.-F. Eckert, N. Armaroli, F. Barigelletti, P. Ceroni, J.-F. Nicoud, J.-F. Nierengarten, *Proc. - Electrochem. Soc.*, **2000**, *8*, 256-266.
[162] E. C. Constable, S. Graber, B. A. Hermann, C. E. Housecroft, M. S. Malarek, L. J. Scherer, *Eur. J. Org. Chem.*, **2008**, 2644-2651.
[163] P. B. Rheiner, D. Seebach, *Chem.-Eur. J.*, **1999**, *5*, 3221-3236.
[164] L. J. Scherer, Diploma work, University of Birmingham, **2001**.
[165] J. Zhu, R. Beugelmans, S. Bourdet, J. Chastanet, G. Roussi, *J. Org. Chem.*, **1995**, *60*, 6389-6396.
[166] G. W. Gokel, H. D. Durst, *Synthesis*, **1976**, 168-184.
[167] S. A. Dibiase, G. W. Gokel, *J. Org. Chem.*, **1978**, *43*, 447-452.
[168] R. Noyori, S. Suga, K. Kawai, S. Okada, M. Kitamura, N. Oguni, M. Hayashi, T. Kaneko, Y. Matsuda, *J. Organomet. Chem.*, **1990**, *382*, 19-37.
[169] D. Seebach, D. A. Plattner, A. K. Beck, Y. M. Wang, D. Hunziker, W. Petter, *Helv. Chim. Acta*, **1992**, *75*, 2171-2209.
[170] H. Meerwein, R. Schmidt, *Justus Liebigs Ann. Chem.*, **1925**, *444*, 221-238.
[171] A. Verley, *Bull. Soc. Chim.*, **1925**, *37*, 537-542.
[172] W. Ponndorf, *Z. Angew. Chem.*, **1926**, *39*, 138-143.
[173] R. V. Oppenauer, *Recueil Des Travaux Chimiques Des Pays-Bas*, **1937**, *56*, 137-144.
[174] A. L. Wilds, *Org. React.*, **1944**, *2*, 178-223.
[175] B. Schmidt, D. Seebach, *Angew. Chem. Int. Ed.*, **1991**, *30*, 1321-1323.
[176] D. Seebach, A. K. Beck, B. Schmidt, Y. M. Wang, *Tetrahedron*, **1994**, *50*, 4363-4384.
[177] R. Kovàsy, personal communication, **2005**.

[178] L. Merz, H. Güntherodt, L. J. Scherer, E. C. Constable, C. E. Housecroft, M. Neuburger, B. A. Hermann, in *Symposium on Chemistry-A European Conference - Stimulating Concepts in Chemistry*, Wiley-VCH Verlag Gmbh, Strasbourg, FRANCE, **2005**, pp. 2307-2318.

[179] T. Kajitani, Y. Miwa, N. Igawa, M. Katoh, S. Kohmoto, M. Yamamoto, K. Yamaguchi, K. Kishikawa, *J. Mater. Chem.*, **2004**, *14*, 2612-2621.

[180] P. Keg, A. Lohani, D. Fichou, Y. M. Lam, Y. L. Wu, B. S. Ong, S. G. Mhaisalkar, *Macromol. Rapid Commun.*, **2008**, *29*, 1197-1202.

[181] X. Shao, X. C. Luo, X. Q. Hu, K. Wu, *J. Phys. Chem. B*, **2006**, *110*, 15393-15402.

[182] S. De Feyter, P. C. M. Grim, M. Rucker, P. Vanoppen, C. Meiners, M. Sieffert, S. Valiyaveettil, K. Müllen, F. C. De Schryver, *Angew. Chem. Int. Ed.*, **1998**, *37*, 1223-1226.

[183] H. B. Fang, L. C. Giancarlo, G. W. Flynn, *J. Phys. Chem. B*, **1998**, *102*, 7311-7315.

[184] S. De Feyter, A. Gesquiere, P. C. M. Grim, F. C. De Schryver, S. Valiyaveettil, C. Meiners, M. Sieffert, K. Müllen, *Langmuir*, **1999**, *15*, 2817-2822.

[185] S. De Feyter, A. Gesquiere, M. M. S. Abdel-Mottaleb, P. C. M. Grim, F. C. De Schryver, C. Meiners, M. Sieffert, S. Valiyaveettil, K. Müllen, *Acc. Chem. Res.*, **2000**, *33*, 520-531.

[186] L. C. Giancarlo, G. W. Flynn, *Acc. Chem. Res.*, **2000**, *33*, 491-501.

[187] P. Jonkheijm, A. Miura, M. Zdanowska, F. J. M. Hoeben, S. De Feyter, A. Schenning, F. C. De Schryver, E. W. Meijer, *Angew. Chem. Int. Ed.*, **2004**, *43*, 76-80.

[188] Y. G. Cai, S. L. Bernasek, *J. Phys. Chem. B*, **2005**, *109*, 4514-4519.

[189] K. H. Ernst, *Chimia*, **2008**, *62*, 471-475.

[190] N. Katsonis, A. Minoia, T. Kudernac, T. Mutai, H. Xu, H. Uji-i, R. Lazzaroni, S. De Feyter, B. L. Feringa, *J. Am. Chem. Soc.*, **2008**, *130*, 386-387.

[191] S. Graber, Diploma work, University of Basel, **2004**.

[192] F. H. Case, *J. Org. Chem.*, **1962**, *27*, 640-641.

[193] Praktikumsbericht, **1995**.

[194] E. C. Constable, C. E. Housecroft, B. M. Kariuki, A. Mahmood, *Supramol. Chem.*, **2006**, *18*, 299-303.

[195] O. Maury, J. P. Guegan, T. Renouard, A. Hilton, P. Dupau, N. Sandon, L. Toupet, H. Le Bozec, *New J. Chem.*, **2001**, *25*, 1553-1566.

[196] A. Hilton, T. Renouard, O. Maury, H. Le Bozec, I. Ledoux, J. Zyss, *Chem. Commun.*, **1999**, 2521-2522.

[197] P. Kavanagh, D. Leech, *Tetrahedron Lett.*, **2004**, *45*, 121-123.

[198] B. Forier, W. Dehaen, *Tetrahedron*, **1999**, *55*, 9829-9846.

[199] O. Mitsunobu, M. Yamada, *Bull. Chem. Soc. Jpn.*, **1967**, *40*, 2380-2382.

[200] O. Mitsunobu, *Synthesis*, **1981**, 1-28.

[201] D. L. Hughes, R. A. Reamer, J. J. Bergan, E. J. J. Grabowski, *J. Am. Chem. Soc.*, **1988**, *110*, 6487-6491.

[202] D. Camp, I. D. Jenkins, *J. Org. Chem.*, **1989**, *54*, 3045-3049.

[203] D. Camp, I. D. Jenkins, *J. Org. Chem.*, **1989**, *54*, 3049-3054.

[204] D. Crich, H. Dyker, R. J. Harris, *J. Org. Chem.*, **1989**, *54*, 257-259.

[205] D. L. Hughes, **1992**, *42*, 335-656.

[206] H. Loibner, E. Zbiral, *Helv. Chim. Acta*, **1976**, *59*, 2100-2113.

[207] K. C. K. Swamy, N. N. B. Kumar, E. Balaraman, K. V. P. P. Kumar, *Chem. Rev.*, **2009**, *109*, 2511-2651.

[208] I. D. Jenkins, *Encyclopedia of Organic Reagents*, **1995**, *8*, 5380.

[209] M. C. Etter, P. W. Baures, *J. Am. Chem. Soc.*, **1988**, *110*, 639-640.

[210] R. Castro, K. R. Nixon, J. D. Evanseck, A. E. Kaifer, *J. Org. Chem.*, **1996**, *61*, 7298-7303.

[211] D. Camp, I. D. Jenkins, *Aust. J. Chem.*, **1988**, *41*, 1835-1839.
[212] M. Von Itzstein, M. J. Jenkins, M. Mocerino, *Carbohydr. Res.*, **1990**, *208*, 287-288.
[213] M. Von Itzstein, M. Mocerino, *Synthetic Communications*, **1990**, *20*, 2049-2058.
[214] I. A. O'Neil, S. Thompson, C. L. Murray, S. B. Kalindjian, *Tetrahedron Lett.*, **1998**, *39*, 7787-7790.
[215] T. Y. S. But, P. H. Toy, *J. Am. Chem. Soc.*, **2006**, *128*, 9636-9637.
[216] L. D. Arnold, H. I. Assil, J. C. Vederas, *J. Am. Chem. Soc.*, **1989**, *111*, 3973-3976.
[217] G. W. Starkey, J. J. Parlow, D. L. Flynn, *Bioorg. Med. Chem. Lett.*, **1998**, *8*, 2385-2390.
[218] A. G. M. Barrett, R. S. Roberts, J. Schroder, *Org. Lett.*, **2000**, *2*, 2999-3001.
[219] A. P. Dobbs, C. McGregor-Johnson, *Tetrahedron Lett.*, **2002**, *43*, 2807-2810.
[220] S. Dandapani, D. P. Curran, *J. Org. Chem.*, **2004**, *69*, 8751-8757.
[221] J. C. Poupon, A. A. Boezio, A. B. Charette, *Angew. Chem. Int. Ed.*, **2006**, *45*, 1415-1420.
[222] S. Schenk, J. Weston, E. Anders, *J. Am. Chem. Soc.*, **2005**, *127*, 12566-12576.
[223] R. M. Overney, E. Meyer, J. Frommer, D. Brodbeck, R. Luthi, L. Howald, H. J. Güntherodt, M. Fujihira, H. Takano, Y. Gotoh, *Nature*, **1992**, *359*, 133-135.
[224] G. Lambin, M. H. Delvaux, A. Calderone, R. Lazzaroni, J. L. Brédas, T. C. Clarke, J. P. Rabe, *Mol. Cryst. Liq. Cryst.*, **1993**, *235*, 75-82.
[225] A. Gesquière, M. M. S. Abdel-Mottaleb, S. De Feyter, F. C. De Schryver, M. Sieffert, K. Müllen, A. Calderone, R. Lazzaroni, J. L. Brédas, *Chem.-Eur. J.*, **2000**, *6*, 3739-3746.
[226] T. Umemoto, *Chem. Rev.*, **1996**, *96*, 1757-1777.
[227] J. Banus, H. J. Emeleus, R. N. Haszeldine, *J. Chem. Soc.*, **1951**, 60-64.
[228] W. T. Miller, E. Bergman, A. H. Fainberg, *J. Am. Chem. Soc.*, **1957**, *79*, 4159-4164.
[229] H. Blancou, A. Commeyras, *J. Fluor. Chem.*, **1982**, *20*, 255-265.
[230] S. Benefice, H. Blancou, A. Commeyras, *Tetrahedron*, **1984**, *40*, 1541-1544.
[231] I. Ruppert, K. Schlich, W. Volbach, *Tetrahedron Lett.*, **1984**, *25*, 2195-2198.
[232] Q. Y. Chen, Z. Y. Yang, *J. Fluor. Chem.*, **1985**, *28*, 399-411.
[233] W.-Y. Huang, H.-Z. Zhang, *J. Fluor. Chem.*, **1990**, *50*, 133-140.
[234] H. Meinert, A. Knoblich, J. Mader, H. A. Brune, *J. Fluor. Chem.*, **1992**, *59*, 379-385.
[235] J. L. Howell, B. J. Muzzi, N. L. Rider, E. M. Aly, M. K. Abouelmagd, *J. Fluor. Chem.*, **1995**, *72*, 61-68.
[236] N. Mureau, F. Guittard, S. Geribaldi, *Tetrahedron Lett.*, **2000**, *41*, 2885-2889.
[237] S. Dieng, B. Bertaina, A. Cambon, *J. Fluor. Chem.*, **1985**, *28*, 425-440.
[238] A. Streitwieser, C. H. Heathcock, E. M. Kosower, *Organische Chemie*, 2nd ed., VCH, Weinheim, **1994**.
[239] L. Sachno, Wahlpraktikum, **2008**.
[240] L. P. Barthel-Rosa, J. A. Gladysz, *Coord. Chem. Rev.*, **1999**, 587-605.
[241] S. R. Wilson, V. Cayetano, M. Yurchenko, *Tetrahedron*, **2002**, *58*, 4041-4047.
[242] F. Kröhnke, *Synthesis*, **1976**, 1-24.
[243] F. Neve, M. Ghedini, A. Crispini, *Chem. Commun.*, **1996**, 2463-2464.
[244] F. Neve, A. Crispini, S. Campagna, *Inorg. Chem.*, **1997**, *36*, 6150-6156.
[245] F. Neve, M. Ghedini, O. Francescangeli, S. Campagna, *Liq. Cryst.*, **1998**, *24*, 673-680.
[246] F. Neve, A. Crispini, S. Campagna, S. Serroni, *Inorg. Chem.*, **1999**, *38*, 2250-2258.
[247] F. Neve, A. Crispini, *Eur. J. Inorg. Chem.*, **2000**, 1039-1043.
[248] S. W. Lai, M. C. W. Chan, T. C. Cheung, S. M. Peng, C. M. Che, *Inorg. Chem.*, **1999**, *38*, 4046-4055.
[249] S. Diring, P. Retailleau, R. Ziessel, *Synlett*, **2007**, 3027-3031.
[250] S. Diring, P. Retailleau, R. Ziessel, *J. Org. Chem.*, **2007**, *72*, 10181-10193.

[251] F. H. Case, R. Sasin, *J. Org. Chem.*, **1955**, *20*, 1330-1336.
[252] M. S. Goodman, A. D. Hamilton, J. Weiss, *J. Am. Chem. Soc.*, **1995**, *117*, 8447-8455.
[253] E. C. Riesgo, X. Q. Jin, R. P. Thummel, *J. Org. Chem.*, **1996**, *61*, 3017-3022.
[254] T. Kauffmann, J. Konig, A. Woltermann, *Chem. Ber.-Recl.*, **1976**, *109*, 3864-3868.
[255] C. O. Dietrich-Buchecker, P. A. Marnot, J. P. Sauvage, *Tetrahedron Lett.*, **1982**, *23*, 5291-5294.
[256] V. Chaurin, PhD Thesis, University of Basel, **2007**.
[257] M. Neuburger, personal communication, **2007**.
[258] G. W. V. Cave, C. L. Raston, *J. Chem. Soc.-Perkin Trans. 1*, **2001**, 3258-3264.
[259] G. W. V. Cave, C. L. Raston, *J. Chem. Educ.*, **2005**, *82*, 468-469.
[260] C. B. Smith, C. L. Raston, A. N. Sobolev, *Green Chem.*, **2005**, *7*, 650-654.
[261] A. Budakoti, M. Abid, A. Azam, *Eur. J. Med. Chem.*, **2006**, *41*, 63-70.
[262] S. M. Treffert-Ziemelis, J. Golus, D. P. Strommen, J. R. Kincaid, *Inorg. Chem.*, **1993**, *32*, 3890-3894.
[263] J. F. W. McOmie, M. L. Watts, D. E. West, *Tetrahedron*, **1968**, *24*, 2289-2292.
[264] F. Melin, S. Choua, M. Bernard, P. Turek, J. Weiss, *Inorg. Chem.*, **2006**, *45*, 10750-10757.
[265] V. Percec, M. N. Holerca, S. Nummelin, J. L. Morrison, M. Glodde, J. Smidrkal, M. Peterca, B. M. Rosen, S. Uchida, V. S. K. Balagurusamy, M. J. Sienkowska, P. A. Heiney, *Chem.-Eur. J.*, **2006**, *12*, 6216-6241.
[266] T. L. Ho, G. A. Olah, *Angew. Chem. Int. Ed.*, **1976**, *15*, 774-775.
[267] T. L. Ho, G. A. Olah, *Synthesis*, **1977**, 417-418.
[268] M. E. Jung, M. A. Lyster, *J. Org. Chem.*, **1977**, *42*, 3761-3764.
[269] E. Keinan, D. Perez, *J. Org. Chem.*, **1987**, *52*, 4846-4851.
[270] G. Pattenden, N. A. Pegg, R. W. Kenyon, *J. Chem. Soc.-Perkin Trans. 1*, **1991**, 2363-2372.
[271] Y. Matsuya, K. Sasaki, M. Nagaoka, H. Kakuda, N. Toyooka, N. Imanishi, H. Ochiai, H. Nemoto, *J. Org. Chem.*, **2004**, *69*, 7989-7993.
[272] P. Rösel, personal communication, **2008**.
[273] V. Prey, *Ber. Dtsch. Chem. Ges.*, **1942**, *75*, 350-356.
[274] C. R. Schmid, C. A. Beck, J. S. Cronin, M. A. Staszak, *Org. Process Res. Dev.*, **2004**, *8*, 670-673.
[275] V. N. Kozhevnikov, A. C. Whitwood, D. W. Bruce, *Chem. Commun.*, **2007**, 3826-3828.
[276] M. S. Lowry, W. R. Hudson, R. A. Pascal, S. Bernhard, *J. Am. Chem. Soc.*, **2004**, *126*, 14129-14135.
[277] Y. Ohsawa, S. Sprouse, K. A. King, M. K. Dearmond, K. W. Hanck, R. J. Watts, *J. Phys. Chem.*, **1987**, *91*, 1047-1054.
[278] K. A. King, R. J. Watts, *J. Am. Chem. Soc.*, **1987**, *109*, 1589-1590.
[279] M. K. Nazeeruddin, E. Baranoff, in *IV International Krutyn Summer School 2008*, Krutyn, Poland, **2008**.
[280] C. Rothe, C.-J. Chiang, V. Jankus, K. Abdullah, X. Zeng, R. Jitchati, A. S. Batsanov, M. R. Bryce, A. P. Monkman, *Adv. Funct. Mater.*, **2009**, *19*, 2038-2044.
[281] Y. Kim, E. C. Long, J. K. Barton, C. M. Lieber, *Langmuir*, **1992**, *8*, 496-500.
[282] I. Sakata, K. Miyamura, *Chem. Commun.*, **2003**, 156-157.
[283] H. Furukawa, J. Kim, K. E. Plass, O. M. Yaghi, *J. Am. Chem. Soc.*, **2006**, *128*, 8398-8399.
[284] Y. Kikkawa, E. Koyama, S. Tsuzuki, K. Fujiwara, K. Miyake, H. Tokuhisa, M. Kanesato, *Langmuir*, **2006**, *22*, 6910-6914.
[285] Robert D. P. Sang Bok Kim, Jason S. D'Acchioli, Brennan J. Walder, Gene B. Carpenter, Dwight A. Sweigart, *Angew. Chem.*, **2009**, *121*, 1794-1797.
[286] L. J. Scherer, unpublished work, University of Basel, **2004**.
[287] S. Sprouse, K. A. King, P. J. Spellane, R. J. Watts, *J. Am. Chem. Soc.*, **1984**, *106*, 6647-6653.

[288] R. J. Hoare, O. S. Mills, *J. Chem. Soc.-Dalton Trans.*, **1972**, 2138-2141.
[289] J. M. Patrick, A. H. White, M. I. Bruce, M. J. Beatson, D. S. Black, G. B. Deacon, N. C. Thomas, *J. Chem. Soc.-Dalton Trans.*, **1983**, 2121-2123.
[290] K. Zhang, Z. Chen, Y. Zou, C. L. Yang, J. G. Qin, Y. Cao, *Organometallics*, **2007**, *26*, 3699-3707.
[291] K. Y. Lee, J. M. Kim, J. N. Kim, *Tetrahedron Lett.*, **2003**, *44*, 6737-6740.
[292] N. Miyaura, A. Suzuki, *J. Chem. Soc.-Chem. Commun.*, **1979**, 866-867.
[293] A. R. Martin, Y. Yang, *Acta Chemica Scandinavica*, **1993**, *47*, 221-230.
[294] A. O. Aliprantis, J. W. Canary, *J. Am. Chem. Soc.*, **1994**, *116*, 6985-6986.
[295] N. Miyaura, A. Suzuki, *Chem. Rev.*, **1995**, *95*, 2457-2483.
[296] A. Torrado, B. Iglesias, S. Lopez, A. R. Delera, *Tetrahedron*, **1995**, *51*, 2435-2454.
[297] K. Doyle, personal communication, **2007**.
[298] J. Beves, personal communication, **2008**.
[299] A. B. Tamayo, B. D. Alleyne, P. I. Djurovich, S. Lamansky, I. Tsyba, N. N. Ho, R. Bau, M. E. Thompson, *J. Am. Chem. Soc.*, **2003**, *125*, 7377-7387.
[300] H. J. Bolink, L. Cappelli, S. Cheylan, E. Coronado, R. D. Costa, N. Lardies, M. K. Nazeeruddin, E. Ortí, *J. Mater. Chem.*, **2007**, *17*, 5032-5041.
[301] M. Kasha, *Faraday Discuss.*, **1950**, 14-19.
[302] J. Li, P. I. Djurovich, B. D. Alleyne, M. Yousufuddin, N. N. Ho, J. C. Thomas, J. C. Peters, R. Bau, M. E. Thompson, *Inorg. Chem.*, **2005**, *44*, 1713-1727.
[303] K. K. W. Lo, C. K. Chung, T. K. M. Lee, L. H. Lui, K. H. K. Tsang, N. Y. Zhu, *Inorg. Chem.*, **2003**, *42*, 6886-6897.
[304] L. Flamigni, A. Barbieri, C. Sabatini, B. Ventura, F. Barigelletti, in *Photochemistry and Photophysics of Coordination Compounds II, Vol. 281*, Springer-Verlag Berlin, Berlin, **2007**, pp. 143-203.
[305] C. R. Patrick, G. S. Prosser, *Nature*, **1960**, *187*, 1021-1021.
[306] W. A. Duncan, F. L. Swinton, *Trans. Faraday Soc.*, **1966**, *62*, 1082-1089.
[307] A. P. West, S. Mecozzi, D. A. Dougherty, *J. Phys. Org. Chem.*, **1997**, *10*, 347-350.
[308] B. W. Gung, J. C. Amicangelo, *J. Org. Chem.*, **2006**, *71*, 9261-9270.
[309] M. P. Waller, A. Robertazzi, J. A. Platts, D. E. Hibbs, P. A. Williams, *J. Comput. Chem.*, **2006**, *27*, 491-504.
[310] S. T. Parker, J. D. Slinker, M. S. Lowry, M. P. Cox, S. Bernhard, G. G. Malliaras, *Chem. Mat.*, **2005**, *17*, 3187-3190.
[311] F. Alary, J. L. Heully, L. Bijeire, P. Vicendo, *Inorg. Chem.*, **2007**, *46*, 3154-3165.
[312] J. D. Slinker, J. Rivnay, J. S. Moskowitz, J. B. Parker, S. Bernhard, H. D. Abruna, G. G. Malliaras, *J. Mater. Chem.*, **2007**, *17*, 2976-2988.
[313] E. S. Handy, A. J. Pal, M. F. Rubner, *J. Am. Chem. Soc.*, **1999**, *121*, 3525-3528.
[314] H. J. Bolink, personal communication, **2009**.
[315] H. J. Bolink, personal communication, **2009**.
[316] R. Jakubiak, C. J. Collison, W. C. Wan, L. J. Rothberg, B. R. Hsieh, *J. Phys. Chem. A*, **1999**, *103*, 2394-2398.
[317] L. Zhang, Y. H. Niu, A. K. Y. Jen, W. B. Lin, *Chem. Commun.*, **2005**, 1002-1004.
[318] J. H. Park, S. I. Park, T. H. Kim, O. O. Park, *Thin Solid Films*, **2007**, *515*, 3085-3089.
[319] R. D. Costa, personal communication, **2008**.
[320] R. D. Costa, personal communication, **2009**.

Appendix B: Crystal structure data

2-phenyl-1,10-phenanthroline (**30**)

```
data_sg-087-1
_audit_creation_date·····07-12-06
_audit_creation_method·CRYSTALS_ver_12.84

_oxford_structure_analysis_title···'12061316·sg-087-1_173k'
_chemical_name_systematic·····?
_chemical_melting_point···?

_cell_length_a·····10.8416(2)
_cell_length_b·····21.0804(3)
_cell_length_c·····12.2036(2)
_cell_angle_alpha·····90
_cell_angle_beta····107.7982(9)
_cell_angle_gamma·····90
_cell_volume·····2655.59(8)

_symmetry_cell_setting·····'Monoclinic'·
_symmetry_space_group_name_H-M···'P·21/c·'·
_symmetry_space_group_name_Hall···'-P·2ybc'·
loop_
·_symmetry_equiv_pos_as_xyz
·'x,y,z'
·'-x,-y,-z'
·'-x,y+1/2,-z+1/2'
·'x,-y+1/2,z+1/2'

loop_
·_atom_type_symbol
·_atom_type_scat_dispersion_real
·_atom_type_scat_dispersion_imag
·_atom_type_scat_Cromer_Mann_a1
·_atom_type_scat_Cromer_Mann_b1
·_atom_type_scat_Cromer_Mann_a2
·_atom_type_scat_Cromer_Mann_b2
·_atom_type_scat_Cromer_Mann_a3
·_atom_type_scat_Cromer_Mann_b3
·_atom_type_scat_Cromer_Mann_a4
·_atom_type_scat_Cromer_Mann_b4
·_atom_type_scat_Cromer_Mann_c
·_atom_type_scat_source···
·'C·····0.0033····0.0016···2.3100···20.8439···1.0200···10.2075···1.5886···0.5687
···'0.8650···31.4512····0.2156'·'International·Tables·Vol·C·4.2.6.8·and·6.1.1.4'
·'H·····0.0000···0.0000···0.4930··10.5109···0.3229··26.1257···0.1402···3.1424
····0.0408··57.7998····0.0030'·'International·Tables·Vol·C·4.2.6.8·and·6.1.1.4'
·'N·····0.0061···0.0033···12.2126···0.0057···3.1322···9.8933···2.0125··28.9975
····1.1663···0.5826·-11.5290·'International·Tables·Vol·C·4.2.6.8·and·6.1.1.4'

_cell_formula_units_Z·····8

·#·Given·Formula·=·C18·H12·N2·
#·Dc·=·····1.28·Fooo····1072.00·Mu·=·····0.76·M·=····512.61
#·Found·Formula·=·C18·H12·N2·
#·Dc·=·····1.28·FOOO····1072.00·Mu·=·····0.76·M·=····512.61

_chemical_formula_sum·····'C18·H12·N2'
_chemical_formula_moiety·····'C18·H12·N2'
_chemical_compound_source·····'·'
_chemical_formula_weight·····256.31

·
_cell_measurement_reflns_used·····11074
_cell_measurement_theta_min·····1
_cell_measurement_theta_max·····28
_cell_measurement_temperature·····173
·
_exptl_crystal_description·····'plate'·
_exptl_crystal_colour·····'colorless'·
_exptl_crystal_size_min·····0.22·
_exptl_crystal_size_mid·····0.33·
_exptl_crystal_size_max·····0.42·
·
_exptl_crystal_density_diffrn····1.282·
_exptl_crystal_density_meas·····?·
#·Non-dispersive·F(000):·
_exptl_crystal_F_000·····1072·
_exptl_absorpt_coefficient_mu····0.076·
·
#·Sheldrick·geometric·approximatio·0.98·0.98·
#·No·experimental·values·of·Tmin/max·available·
_exptl_absorpt_correction_type····multi-scan·
_exptl_absorpt_process_details···'DENZO/SCALEPACK·(Otwinowski·&·Minor,·1997)''
_exptl_absorpt_correction_T_min··0.98·
_exptl_absorpt_correction_T_max··0.98·
#·For·a·Kappa·CCD,·set·Tmin·to·1.0·and·
#·Tmax·to·the·ratio·of·max:min·frame·scales·in·scale_all.log·
_diffrn_measurement_device_type···'Nonius·KappaCCD'·
_diffrn_radiation_monochromator···'graphite'·
_diffrn_radiation_type·····'Mo·K\a'·
_diffrn_radiation_wavelength·····0.71073
_diffrn_measurement_method·····'\f·&·\w·scans'·
·
#·If·a·reference·occurs·more·than·once,·delete·the·author·
#·and·date·from·subsequent·references.·
_computing_data_collection·····'COLLECT·(Nonius,·1997-2001).'·
_computing_cell_refinement·····'DENZO/SCALEPACK·(Otwinowski·&·Minor,·1997)''
_computing_data_reduction·····'DENZO/SCALEPACK·(Otwinowski·&·Minor,·1997)''
_computing_structure_solution····'SIR92·(Altomare·et·al.,·1994)'·
_computing_structure_refinement···'CRYSTALS·(Betteridge·et·al.,·2003)'·
_computing_publication_material···'CRYSTALS·(Betteridge·et·al.,·2003)'·
_computing_molecular_graphics····'CAMERON·(Watkin·et·al.,·1996)'·
·
_diffrn_standards_interval_time···?·
_diffrn_standards_interval_count·?·
_diffrn_standards_number·····0·
_diffrn_standards_decay_%·····0·

_diffrn_ambient_temperature·····173
_diffrn_reflns_number·····22145·
_reflns_number_total·····6320·
_diffrn_reflns_av_R_equivalents···0.050·
#·Number·of·reflections·with·Friedels·Law·is·6320·
#·Number·of·reflections·without·Friedels·Law·is·0·
#·Theoretical·number·of·reflections·is·about·6334·
·
·
_diffrn_reflns_theta_min·····1.932·
_diffrn_reflns_theta_max·····27.890·
_diffrn_measured_fraction_theta_max·0.999·
·
_diffrn_reflns_theta_full·····27.890·
_diffrn_measured_fraction_theta_full·0.999·
·
·
_diffrn_reflns_limit_h_min·····-14·
_diffrn_reflns_limit_h_max·····14·
_diffrn_reflns_limit_k_min·····-27·
_diffrn_reflns_limit_k_max·····27·
_diffrn_reflns_limit_l_min·····-16·
_diffrn_reflns_limit_l_max·····16·
_reflns_limit_h_min·····-14·
_reflns_limit_h_max·····13·
_reflns_limit_k_min·····0·
_reflns_limit_k_max·····27·
_reflns_limit_l_min·····0·
_reflns_limit_l_max·····16·
·
_oxford_diffrn_Wilson_B_factor···0.00·
_oxford_diffrn_Wilson_scale·····0.00·
·
_atom_sites_solution_primary·····direct·#heavy,direct,difmap,geom
#·_atom_sites_solution_secondary·difmap
_atom_sites_solution_hydrogens···geom
·
_refine_diff_density_min·····-0.17·
_refine_diff_density_max·····0.16·
·
·
_refine_ls_number_reflns·····3871·
_refine_ls_number_restraints·····0·
_refine_ls_number_parameters·····361·
·
#_refine_ls_R_factor_ref·0.0452·
_refine_ls_wR_factor_ref·····0.0510·
_refine_ls_goodness_of_fit_ref···1.0571·
·
#_reflns_number_all·6279·
_refine_ls_R_factor_all·····0.0861·
_refine_ls_wR_factor_all·····0.0845·
·
#·The·I/u(I)·cutoff·below·was·used·for·refinement·as·
#·well·as·the··gt·R-factors:
_refine_threshold_expression·····I>1.0\s(I)
_reflns_number_gt·····3871·
_refine_ls_R_factor_gt·····0.0452·
_refine_ls_wR_factor_gt·····0.0510·
·
_refine_ls_shift/su_max·····0.000322·
·
·#·choose·from:·rm·(reference·molecule·of·known·chirality),·
#·ad·(anomolous·dispersion·-·Flack),·rmad·(rm·and·ad),·
#·syn·(from·synthesis),·unk·(unknown)·or··(not·applicable).·
_chemical_absolute_configuration···'.'·
·
·
_refine_ls_structure_factor_coef··F·
_refine_ls_matrix_type·····full
_refine_ls_hydrogen_treatment·····constr·····#·none,·undef,·noref,·refall,
·····#·refxyz,·refU,·constr·or·mixed
_refine_ls_weighting_scheme·····calc·

_refine_ls_weighting_details·
;
·Method,·part·1,·Chebychev·polynomial,·(Watkin,·1994,·Prince,·1982)·
·[weight]·=·1.0/[A·0·*T·0·(x)+A·1·*T·1·(x)·....+A·n·1·*T·n·1·(x)]·
·where·A·i·are·the·Chebychev·coefficients·listed·below·and·x=·Fcalc/Fmax·
·Method·=·Robust·Weighting·(Prince,·1982)·
·W·=·[weight]·*·[1-(deltaF/6*sigmaF)^2^]^2^·
·A·i·are:·
·0.722·0.771·0.405·
;
·
·
#·Check·this·file·using·the·IUCr·facility·at:·
#·http://checkcif.iucr.org/·
·
#·The·content·below·is·held·in·the·file·'script/refcif.dat'.·This·is·a·text·
#·file·which·you·may·edit·to·reflect·local·conditions.·
#·Items·which·need·looking·at·are·represented·by·a·'?'.·
#·Items·for·which·there·are·choices·are·prefixed·with·'choose·from'.·
·
_publ_contact_letter·
;·
·Please·consider·this·CIF·submission·for·
·publication·as·a·Short·Format·Paper·in·Acta·
·Crystallographica·E.·The·figures·will·be·
·sent·by·e-mail.·
;·
_publ_contact_author_name·····'Anthony·Other'·
_publ_contact_author_address·
;·
·Chemical·Crystallography·Laboratory,·
·Department·of·Chemistry,·
·University·of·Nowhere,·
·Nowhere,·NO1·4T,·UK.·
;·
·
_publ_contact_author_phone·····'+44·1865·000000'·
_publ_contact_author_fax·····'+44·1865·000000'·
_publ_contact_author_email·····'a.n.other@chem.no.ac.uk'·
_publ_requested_journal·····'Section·E'·
_publ_requested_category·····EO·#·choose·from:·FI·FM·FO·CI·CM·CO·AD·
_publ_requested_coeditor_name····'Prof·William·Clegg'·
·
_publ_section_title·
#·Title·of·paper···generally·just·the·systematic·or·trivial·name·
;·?·
·
·
#·The·loop·structure·below·should·contain·the·names·and·addresses·of·all·
#·authors,·in·the·required·order·of·publication.·Repeat·as·necessary.·
loop_
·_publ_author_name·
·_publ_author_address·
·_publ_author_footer·
·'Other,·Anthony·N.''·#·Author·1·

;·
·?·#·Address·for·author·1·
;·
·

·?·#·Footnote·for·author·1·
;·
·'Else,·S.·O.''·#·Author·2·
;·
·?·#·Address·2·
;·
·
?·#·Footnote·2·
;·
·

·
_publ_section_abstract·
#·Text·of·the·abstract·
#·(a)·The·Abstract·must·be·self-contained·and·comprehensible·
#·without·the·rest·of·the·paper.·This·means·no·references·
#·to·atom·names·or·to·compound·numbers;·compounds·must·be·
#·identified·as·the·title·compound,·or·by·name·or·by·some·other·
#·means·such·as·derivatives·of·each·other·(e.g.·"the·
#·corresponding·ketone").·
#·(b)·The·chemical·formula·of·"the·title·compound"·must·be·given.·
#·(c)·Any·crystallographic·molecular·symmetry·should·be·
#·mentioned,·and·also·the·presence·of·more·than·one·molecule·
#·in·the·asymmetric·unit·(i.e.·anything·other·than·Z'=1).·
;·
?·
;·
·
_publ_section_comment·
#·Text·of·the·paper·
#·Note·that·atoms·are·referenced·as·N2,·not·N(2)·or·N·2·
#·If·text·containing·()·occur·within·(),·the·outer·ones·should·be·[]·
#·Figures·should·be·referenced·as·Fih.·
;·
·
;·
·
_publ_section_acknowledgements····#·Acknowledgments·
;·
·
?·
;·
·
_publ_section_figure_captions·
#·Captions·to·figures···Start·each·caption·on·a·new·line·after·a·blank·line·
;·
Fig.·1.·
The·title·compound·with·displacement·ellipsoids·drawn·at·the·50%·
probability·level.·H·atoms·are·shown·as·spheres·of·
arbitary·radius.·
·
;·
·
_publ_section_exptl_refinement·
#·Some·potentially·useful·phrases·are·donated·by·Bill·Clegg:·
;·
In·the·absence·of·significant·anomalous·scattering,·Friedel·pairs·were·
merged.·
·
The·absolute·configuration·was·arbitrarily·assigned.·
·
The·relatively·large·ratio·of·minimum·to·maximum·corrections·applied·
in·the·multiscan·process·(1:nnn)·reflect·changes·in·the·illuminated·
volume·of·the·crystal.·
·
Changes·in·illuminated·volume·were·kept·to·a·minimum,·and·were·
taken·into·account·(G\"orbitz,·1999)·by·the·multi-scan·inter-frame·
scaling·(DENZO/SCALEPACK,·Otwinowski·&·Minor,·1997).·
·
·
G\"orbitz,·C.·H.·(1999).·Acta·Cryst.·B55,·1090-1098.·
·
·
·
·
The·H·atoms·were·all·located·in·a·difference·map,·but·those·
attached·to·carbon·atoms·were·repositioned·geometrically.·
The·H·atoms·were·initially·refined·with·soft·restraints·on·the·
bond·lengths·and·angles·to·regularise·their·geometry·
(C---H·in·the·range·0.93--0.98),·
N---H·in·the·range·0.86--0.89·
·
N---H·to·0.86·
C---H·=·0.82·
\%A)·
and·
U-iso-(H)·(in·the·range·1.2-1.5·times·U-eq-of·the·parent·atom),·
after·which·the·positions·were·refined·with·riding·constraints.·
·
;·
·
_publ_section_exptl_prep·
#·Brief·details·or·a·reference.·Include·solvent·if·known·
;·
?·
;·
·
·
#·PROCESSING·SUMMARY·(IUCr·Office·Use·Only):·
_journal_date_recd_electronic·····?·
_journal_date_to_coeditor·····?·
_journal_date_from_coeditor·····?·
_journal_date_accepted·····?·
_journal_date_printers_first·····?·
_journal_date_printers_final·····?·
_journal_date_proofs_out·····?·
_journal_date_proofs_in·····?·
_journal_coeditor_name·····?·
_journal_coeditor_code·····?·
_journal_coeditor_notes·····?·
_journal_techeditor_code·····?·
_journal_techeditor_notes·····?·
_journal_coden_ASTM·····?·
_journal_name_full·····?·
_journal_year·····?·
_journal_volume·····?·
_journal_issue·····?·
_journal_page_first·····?·
_journal_page_last·····?·
_journal_suppl_publ_number····?·
_journal_suppl_publ_pages·····?·
·
#·End·of·'script/refcif.dat'·

·
·
·
·
#·Insert·your·own·references·if·required···in·alphabetical·order·
_publ_section_references·
;·
Altomare,·A.,·Cascarano,·G.,·Giacovazzo,·G.,·Guagliardi,·A.,·Burla,·M.C.,·
Polidori,·G.·&·Camalli,·M.·(1994).·J.·Appl.·Cryst.·27,·435.·
·
·
Betteridge,·P.W.,·Carruthers,·J.R.,·Cooper,·R.I.,·
Prout,·K.·&·Watkin,·D.J.·(2003).·J.·Appl.·Cryst.·36,·1487.·
·
Larson,·A.C.·(1970)·Crystallographic·Computing,·Ed·Ahmed,·F.R.,·
Munksgaard,·Copenhagen,·291-294.·
·
Nonius·(1997-2001).·COLLECT.·Nonius·BV,·Delft,·The·Netherlands.·
·
Otwinowski,·Z.·&·Minor,·W.·(1997).·Methods·in·Enzymology,·Vol.·276,·
edited·by·C.·W.·Carter·Jr·&·R.·M.·Sweet,·pp.·307--326.·
New·York:·Academic·Press.·
·
Prince,·E.·
Mathematical·Techniques·in·Crystallography·
and·Materials·Science·
Springer-Verlag,·New·York,·1982.·
·
·
Watkin·D.J.·(1994).·
Acta·Cryst.·A50,·411-437.·
·
·
Watkin,·D.J.,·Prout,·C.K.·&·Pearce,·L.J.·(1996).·CAMERON,·Chemical·
Crystallography·Laboratory,·Oxford,·UK.·
;·

·
#·Reqiuv·=·arithmetic·mean·of·Ui·i.e.·Ueqiv·=·(U1+U2+U3)/3·

·
#·Replace·last·...·with·number·of·unfound·hydrogen·atomsattached·to·an·atom.·

·
#·___·refinement_flags_···
#·...no·refinement·constraints···········S·special·position·constraint·on·site·
#·G·rigid·group·refinement·of·site·····R·riding·atom·
#·D·distance·or·angle·restraint·on·site·T·thermal·displacement·constraints·
#·U·Uiso·or·Uij·restraint·(rigid·bond)···P·partial·occupancy·constraint·

·
·
loop_
·_atom_site_label·
·_atom_site_type_symbol·
·_atom_site_fract_x·
·_atom_site_fract_y·
·_atom_site_fract_z·
·_atom_site_U_iso_or_equiv·
·_atom_site_occupancy·
·_atom_site_adp_type·
·_atom_site_refinement_flags_posn·
·_atom_site_refinement_flags_adp·
·_atom_site_refinement_flags_occupancy·
·_atom_site_disorder_assembly·
·_atom_site_disorder_group·
·_atom_site_attached_hydrogens·
C1·C·0.30103(18)·0.61026(9)·0.55878(16)·0.0493·1.0000·Uani·.·.·.·.·.·.·.·
C2·C·0.33789(19)·0.55853(9)·0.50471(16)·0.0519·1.0000·Uani·.·.·.·.·.·.·.·
C3·C·0.28837(18)·0.50038(9)·0.51578(14)·0.0503·1.0000·Uani·.·.·.·.·.·.·.·
C4·C·0.20269(17)·0.49394(8)·0.58157(13)·0.0424·1.0000·Uani·.·.·.·.·.·.·.·

C5·C·0.14669(19)·0.43438(8)·0.59626(17)·0.0529·1.0000·Uani·.·.·.·.·.·.·.·
C6·C·0.06409(19)·0.42984(8)·0.65897(17)·0.0541·1.0000·Uani·.·.·.·.·.·.·.·
C7·C·0.03328(16)·0.48378(7)·0.71632(14)·0.0421·1.0000·Uani·.·.·.·.·.·.·.·
C8·C·0.04935(17)·0.48119(8)·0.78501(16)·0.0494·1.0000·Uani·.·.·.·.·.·.·.·
C9·C·-0.06796(16)·0.53355(8)·0.84365(16)·0.0458·1.0000·Uani·.·.·.·.·.·.·.·
C10·C·-0.00348(14)·0.59066(8)·0.83426(13)·0.0369·1.0000·Uani·.·.·.·.·.·.·.·
C11·C·0.0844(14)·0.54344(7)·0.70724(12)·0.0349·1.0000·Uani·.·.·.·.·.·.·.·
C12·C·0.17346(15)·0.54885(7)·0.63512(12)·0.0358·1.0000·Uani·.·.·.·.·.·.·.·
C13·C·-0.01319(14)·0.64842(8)·0.90061(13)·0.0387·1.0000·Uani·.·.·.·.·.·.·.·
C14·C·0.07242(17)·0.64790(10)·0.98755(15)·0.0510·1.0000·Uani·.·.·.·.·.·.·.·
C15·C·-0.0791(2)·0.70278(11)·1.04865(18)·0.0628·1.0000·Uani·.·.·.·.·.·.·.·
C16·C·-0.0257(2)·0.75860(10)·1.02580(17)·0.0601·1.0000·Uani·.·.·.·.·.·.·.·
C17·C·0.03453(19)·0.75983(9)·0.94095(16)·0.0518·1.0000·Uani·.·.·.·.·.·.·.·
C18·C·0.04023(16)·0.70549(8)·0.87867(14)·0.0427·1.0000·Uani·.·.·.·.·.·.·.·
C21·C·0.30597(18)·0.34021(9)·0.34723(16)·0.0538·1.0000·Uani·.·.·.·.·.·.·.·
C22·C·0.29983(18)·0.28483(10)·0.28228(16)·0.0542·1.0000·Uani·.·.·.·.·.·.·.·
H1·H·0.2100(16)·0.23383(9)·0.33442(15)·0.0466·1.0000·Uani·.·.·.·.·.·.·.·
C24·C·0.44942(14)·0.23860(8)·0.44948(14)·0.0385·1.0000·Uani·.·.·.·.·.·.·.·
C25·C·0.52830(16)·0.18690(8)·0.50708(15)·0.0416·1.0000·Uani·.·.·.·.·.·.·.·
C26·C·0.61013(16)·0.19321(8)·0.61486(15)·0.0423·1.0000·Uani·.·.·.·.·.·.·.·
C27·C·0.61954(15)·0.25251(7)·0.67410(13)·0.0372·1.0000·Uani·.·.·.·.·.·.·.·
C28·C·0.70945(16)·0.26212(8)·0.78262(14)·0.0428·1.0000·Uani·.·.·.·.·.·.·.·
C29·C·0.71756(16)·0.31988(8)·0.83521(14)·0.0424·1.0000·Uani·.·.·.·.·.·.·.·
C30·C·0.63146(14)·0.36877(7)·0.78021(13)·0.0355·1.0000·Uani·.·.·.·.·.·.·.·
C31·C·0.53971(14)·0.30427(7)·0.62282(13)·0.0346·1.0000·Uani·.·.·.·.·.·.·.·
C32·C·0.45167(14)·0.29706(7)·0.50676(13)·0.0368·1.0000·Uani·.·.·.·.·.·.·.·
C33·C·0.63249(14)·0.43166(7)·0.83577(14)·0.0364·1.0000·Uani·.·.·.·.·.·.·.·
C34·C·0.69861(15)·0.44137(8)·0.95218(14)·0.0404·1.0000·Uani·.·.·.·.·.·.·.·
C35·C·0.69561(16)·0.49992(8)·1.00302(15)·0.0455·1.0000·Uani·.·.·.·.·.·.·.·
C36·C·0.62897(17)·0.54989(9)·0.93883(16)·0.0493·1.0000·Uani·.·.·.·.·.·.·.·
C37·C·0.56439(17)·0.48273(8)·0.77237(15)·0.0461·1.0000·Uani·.·.·.·.·.·.·.·
C39·C·0.56355(18)·0.54123(9)·0.82362(17)·0.0532·1.0000·Uani·.·.·.·.·.·.·.·
N1·N·0.22165(14)·0.60692(6)·0.62254(12)·0.0422·1.0000·Uani·.·.·.·.·.·.·.·
N2·N·0.07152(12)·0.59544(6)·0.76582(11)·0.0353·1.0000·Uani·.·.·.·.·.·.·.·
N3·N·0.37822(13)·0.34733(7)·0.45541(12)·0.0457·1.0000·Uani·.·.·.·.·.·.·.·
N4·N·0.54505(12)·0.36098(6)·0.67673(11)·0.0355·1.0000·Uani·.·.·.·.·.·.·.·
H11·H·0.3356·0.6522·0.5499·0.0619·1.0000·Uiso·R·.·.·.·.·.·.·.·
H21·H·0.3998·0.5647·0.4620·0.0647·1.0000·Uiso·R·.·.·.·.·.·.·.·
H31·H·0.3134·0.4634·0.4808·0.0600·1.0000·Uiso·R·.·.·.·.·.·.·.·
H51·H·0.1684·0.3974·0.5588·0.0628·1.0000·Uiso·R·.·.·.·.·.·.·.·
H61·H·0.0262·0.3895·0.6679·0.0636·1.0000·Uiso·R·.·.·.·.·.·.·.·
H81·H·-0.0932·0.4414·0.7900·0.0587·1.0000·Uiso·R·.·.·.·.·.·.·.·
H91·H·-0.1266·0.5321·0.8913·0.0548·1.0000·Uiso·R·.·.·.·.·.·.·.·
H141·H·-0.1096·0.6080·1.0057·0.0629·1.0000·Uiso·R·.·.·.·.·.·.·.·
H151·H·-0.1241·0.7014·1.1081·0.0750·1.0000·Uiso·R·.·.·.·.·.·.·.·
H161·H·-0.0285·0.7969·1.0676·0.0700·1.0000·Uiso·R·.·.·.·.·.·.·.·
H171·H·0.0738·0.7990·0.9275·0.0592·1.0000·Uiso·R·.·.·.·.·.·.·.·
H181·H·0.0832·0.7062·0.8195·0.0480·1.0000·Uiso·R·.·.·.·.·.·.·.·
H211·H·0.2527·0.3765·0.3104·0.0608·1.0000·Uiso·R·.·.·.·.·.·.·.·
H221·H·0.2430·0.2833·0.2024·0.0629·1.0000·Uiso·R·.·.·.·.·.·.·.·
H231·H·0.3707·0.1940·0.2939·0.0578·1.0000·Uiso·R·.·.·.·.·.·.·.·
H251·H·0.5221·0.1462·0.4660·0.0513·1.0000·Uiso·R·.·.·.·.·.·.·.·
H261·H·0.6641·0.1582·0.6533·0.0543·1.0000·Uiso·R·.·.·.·.·.·.·.·
H281·H·0.7668·0.2280·0.8206·0.0535·1.0000·Uiso·R·.·.·.·.·.·.·.·
H291·H·0.7837·0.3272·0.9101·0.0515·1.0000·Uiso·R·.·.·.·.·.·.·.·
H341·H·0.7481·0.4065·0.9982·0.0497·1.0000·Uiso·R·.·.·.·.·.·.·.·
H351·H·0.7442·0.5054·1.0847·0.0562·1.0000·Uiso·R·.·.·.·.·.·.·.·
H361·H·0.6259·0.5911·0.9727·0.0599·1.0000·Uiso·R·.·.·.·.·.·.·.·
H371·H·0.5162·0.4764·0.6901·0.0557·1.0000·Uiso·R·.·.·.·.·.·.·.·
H391·H·0.5170·0.5757·0.7776·0.0628·1.0000·Uiso·R·.·.·.·.·.·.·.·
```

```
loop_
 _atom_site_aniso_label
 _atom_site_aniso_U_11
 _atom_site_aniso_U_22
 _atom_site_aniso_U_33
 _atom_site_aniso_U_23
 _atom_site_aniso_U_13
 _atom_site_aniso_U_12
C1·0.0584(11)·0.0427(9)·0.0516(10)·0.0078(8)·0.0241(9)·0.0038(8)·
C2·0.0609(11)·0.0526(11)·0.0470(10)·0.0074(8)·0.0239(9)·0.0110(9)·
C3·0.0587(11)·0.0502(10)·0.0396(9)·-0.0028(8)·0.0117(8)·0.0147(8)·
C4·0.0473(9)·0.0389(8)·0.0351(8)·-0.0026(7)·0.0041(7)·0.0036(7)·
C5·0.0632(11)·0.0354(9)·0.0556(11)·-0.0118(8)·0.0115(9)·0.0000(8)·
C6·0.0625(11)·0.0321(9)·0.0639(12)·-0.0076(8)·0.0138(10)·-0.0115(8)·
C7·0.0410(8)·0.0340(8)·0.0455(9)·0.0001(7)·0.0046(7)·-0.0052(6)·
C8·0.0435(9)·0.0384(9)·0.0635(11)·0.0029(8)·0.0119(8)·-0.0121(7)·
C9·0.0405(9)·0.0439(9)·0.0540(10)·0.0063(8)·0.0161(8)·-0.0054(7)·
C10·0.0307(7)·0.0388(8)·0.0377(8)·0.0041(6)·0.0051(6)·-0.0004(6)·
C11·0.0353(7)·0.0294(7)·0.0339(7)·0.0004(6)·0.0016(6)·-0.0024(6)·
C12·0.0380(8)·0.0322(7)·0.0328(7)·0.0012(6)·0.0044(6)·0.0021(6)·
C13·0.0325(7)·0.0416(9)·0.0388(8)·-0.0021(7)·0.0060(6)·0.0040(6)·
C14·0.0441(9)·0.0606(11)·0.0476(10)·-0.0012(8)·0.0131(8)·0.0013(8)·
C15·0.0554(11)·0.0816(15)·0.0531(11)·-0.0112(10)·0.0191(9)·0.0128(10)·
C16·0.0618(12)·0.0567(12)·0.0526(11)·-0.0114(9)·0.0036(9)·0.0220(10)·
C17·0.0587(11)·0.0378(9)·0.0490(10)·0.0017(7)·0.0017(8)·0.0106(8)·
C18·0.0448(9)·0.0386(9)·0.0399(8)·0.0037(7)·0.0061(7)·0.0077(7)·
C21·0.0488(10)·0.0529(11)·0.0481(10)·-0.0008(8)·-0.0025(8)·0.0122(8)·
C22·0.0453(9)·0.0535(12)·0.0433(9)·-0.0062(9)·0.0009(8)·0.0063(9)·
C23·0.0398(9)·0.0526(10)·0.0472(9)·-0.0096(8)·0.0129(7)·0.0011(7)·
C24·0.0342(8)·0.0424(9)·0.0421(8)·0.0007(7)·0.0164(7)·0.0018(6)·
C25·0.0444(9)·0.0370(8)·0.0481(9)·-0.0007(7)·0.0209(7)·0.0022(7)·
C26·0.0481(9)·0.0363(8)·0.0472(9)·0.0079(7)·0.0217(7)·0.0087(7)·
C27·0.0391(8)·0.0359(8)·0.0393(8)·0.0067(6)·0.0163(7)·0.0050(6)·
C28·0.0458(9)·0.0416(9)·0.0408(9)·0.0096(7)·0.0129(7)·0.0118(7)·
C29·0.0424(8)·0.0457(9)·0.0353(8)·0.0063(7)·0.0064(7)·0.0081(7)·
C30·0.0338(7)·0.0376(8)·0.0353(7)·0.0049(6)·0.0105(6)·0.0017(6)·
C31·0.0326(7)·0.0354(8)·0.0382(8)·0.0048(6)·0.0143(6)·0.0025(6)·
C32·0.0326(7)·0.0396(8)·0.0387(8)·0.0013(6)·0.0115(6)·0.0027(6)·
C33·0.0334(7)·0.0385(8)·0.0374(8)·0.0042(6)·0.0109(6)·0.0009(6)·
C34·0.0384(8)·0.0395(8)·0.0404(8)·0.0056(7)·0.0077(7)·-0.0038(7)·
C35·0.0421(9)·0.0403(10)·0.0438(9)·-0.0033(7)·0.0108(7)·-0.0062(7)·
C36·0.0455(9)·0.0454(10)·0.0569(11)·-0.0095(8)·0.0154(8)·0.0034(8)·
C37·0.0488(9)·0.0458(9)·0.0394(9)·0.0018(7)·0.0071(7)·0.0118(7)·
C39·0.0537(10)·0.0441(10)·0.0575(11)·0.0026(8)·0.0107(9)·0.0142(8)·
N1·0.0485(8)·0.0365(7)·0.0443(7)·0.0023(6)·0.0179(6)·0.0002(6)·
N2·0.0348(6)·0.0328(7)·0.0351(6)·0.0021(5)·0.0061(5)·-0.0014(5)·
N3·0.0419(7)·0.0449(8)·0.0426(7)·-0.0009(6)·0.0016(6)·0.0082(6)·
N4·0.0355(6)·0.0338(7)·0.0365(6)·0.0047(5)·0.0100(5)·0.0026(5)·

_refine_ls_extinction_method·
····'None'
 _oxford_refine_ls_scale·0.3340(6)·
loop_
 ·_geom_bond_atom_site_label_1
 ·_geom_bond_site_symmetry_1
 ·_geom_bond_atom_site_label_2
 ·_geom_bond_site_symmetry_2
 ·_geom_bond_distance
 ·_geom_bond_publ_flag
C1·-C2·-·1.395(3)····yes

C1·-N1·-·1.327(2)····yes
C1·-H11·-·0.979····no
C2·-C3·-·1.361(3)····yes
C2·-H21·-·0.976····no
C3·-C4·-·1.408(3)····yes
C3·-H31·-·0.958····no
C4·-C5·-·1.430(2)····yes
C4·-C12·-·1.412(2)····yes
C5·-C6·-·1.347(3)····yes
C5·-H51·-·0.968····no
C6·-C7·-·1.427(2)····yes
C6·-H61·-·0.965····no
C7·-C8·-·1.403(3)····yes
C7·-C11·-·1.416(2)····yes
C8·-C9·-·1.364(3)····yes
C8·-H81·-·0.975····no
C9·-C10·-·1.414(2)····yes
C9·-H91·-·0.984····no
C10·-C13·-·1.484(2)····yes
C10·-N2·-·1.336(2)····yes
C11·-C12·-·1.452(2)····yes
C11·-N2·-·1.3546(19)····yes
C12·-N1·-·1.358(2)····yes
C13·-C14·-·1.398(2)····yes
C13·-C18·-·1.396(2)····yes
C14·-C15·-·1.390(3)····yes
C14·-H141·-·0.987····no
C15·-C16·-·1.377(3)····yes
C15·-H151·-·0.990····no
C16·-C17·-·1.383(3)····yes
C16·-H161·-·0.961····no
C17·-C18·-·1.387(2)····yes
C17·-H171·-·0.965····no
C18·-H181·-·0.972····no
C21·-C22·-·1.401(3)····yes
C21·-N3·-·1.322(2)····yes
C21·-H211·-·0.980····no
C22·-C23·-·1.362(3)····yes
C22·-H221·-·0.981····no
C23·-C24·-·1.405(2)····yes
C23·-H231·-·0.975····no
C24·-C25·-·1.430(2)····yes
C24·-C32·-·1.413(2)····yes
C25·-C26·-·1.350(2)····yes
C25·-H251·-·0.985····no
C26·-C27·-·1.432(2)····yes
C26·-H261·-·0.969····no
C27·-C28·-·1.399(2)····yes
C27·-C31·-·1.414(2)····yes
C28·-C29·-·1.367(2)····yes
C28·-H281·-·0.971····no
C29·-C30·-·1.415(2)····yes
C29·-H291·-·0.987····no
C30·-C33·-·1.488(2)····yes
C30·-N4·-·1.3327(19)····yes
C31·-C32·-·1.454(2)····yes
C31·-N4·-·1.357(2)····yes
C32·-N3·-·1.358(2)····yes
C33·-C34·-·1.397(2)····yes
C33·-C37·-·1.398(2)····yes

C34·-C35·-·1.386(2)····yes
C34·-H341·-·0.980····no
C35·-C36·-·1.378(2)····yes
C35·-H351·-·0.982····no
C36·-C39·-·1.380(3)····yes
C36·-H361·-·0.966····no
C37·-C39·-·1.384(2)····yes
C37·-H371·-·0.989····no
C39·-H391·-·0.962····no
loop_
 ·_geom_angle_atom_site_label_1
 ·_geom_angle_site_symmetry_1
 ·_geom_angle_atom_site_label_2
 ·_geom_angle_site_symmetry_2
 ·_geom_angle_atom_site_label_3
 ·_geom_angle_site_symmetry_3
 ·_geom_angle
 ·_geom_angle_publ_flag
C2·-C1·-N1·-·124.54(17)····yes
C2·-C1·-H11·-·118.6····no
N1·-C1·-H11·-·116.8····no
C1·-C2·-C3·-·118.58(17)····yes
C1·-C2·-H21·-·119.5····no
C3·-C2·-H21·-·121.9····no
C2·-C3·-C4·-·119.50(16)····yes
C2·-C3·-H31·-·121.3····no
C4·-C3·-H31·-·118.8····no
C3·-C4·-C5·-·122.40(16)····yes
C3·-C4·-C12·-·117.73(16)····yes
C5·-C4·-C12·-·119.87(16)····yes
C4·-C5·-C6·-·121.00(16)····yes
C4·-C5·-H51·-·118.3····no
C6·-C5·-H51·-·120.7····no
C5·-C6·-C7·-·121.17(16)····yes
C5·-C6·-H61·-·120.4····no
C7·-C6·-H61·-·118.4····no
C6·-C7·-C8·-·123.36(16)····yes
C6·-C7·-C11·-·119.90(16)····yes
C8·-C7·-C11·-·116.73(15)····yes
C7·-C8·-C9·-·120.40(16)····yes
C7·-C8·-H81·-·118.9····no
C9·-C8·-H81·-·120.7····no
C8·-C9·-C10·-·119.36(16)····yes
C8·-C9·-H91·-·120.7····no
C10·-C9·-H91·-·119.9····no
C9·-C10·-C13·-·122.35(14)····yes
C9·-C10·-N2·-·121.69(15)····yes
C13·-C10·-N2·-·115.95(14)····yes
C7·-C11·-C12·-·118.79(14)····yes
C7·-C11·-N2·-·122.87(15)····yes
C12·-C11·-N2·-·118.30(13)····yes
C11·-C12·-C4·-·119.16(14)····yes
C11·-C12·-N1·-·118.28(13)····yes
C4·-C12·-N1·-·122.56(15)····yes
C10·-C13·-C14·-·122.23(16)····yes
C10·-C13·-C18·-·119.99(14)····yes
C14·-C13·-C18·-·117.77(16)····yes
C13·-C14·-C15·-·120.78(19)····yes
C13·-C14·-H141·-·119.4····no
C15·-C14·-H141·-·119.8····no
C14·-C15·-C16·-·120.55(19)····yes
C14·-C15·-H151·-·119.1····no
C16·-C15·-H151·-·120.4····no
C15·-C16·-C17·-·119.45(18)····yes
C15·-C16·-H161·-·121.8····no
C17·-C16·-H161·-·118.7····no
C16·-C17·-C18·-·120.35(19)····yes
C16·-C17·-H171·-·118.5····no
C18·-C17·-H171·-·121.1····no
C13·-C18·-C17·-·121.08(17)····yes
C13·-C18·-H181·-·118.5····no
C17·-C18·-H181·-·120.4····no
C22·-C21·-N3·-·124.82(17)····yes
C22·-C21·-H211·-·118.1····no
N3·-C21·-H211·-·117.1····no
C21·-C22·-C23·-·118.10(17)····yes
C21·-C22·-H221·-·119.8····no
C23·-C22·-H221·-·122.1····no
C22·-C23·-C24·-·119.58(16)····yes
C22·-C23·-H231·-·122.0····no
C24·-C23·-H231·-·118.4····no
C23·-C24·-C25·-·121.66(15)····yes
C23·-C24·-C32·-·118.05(15)····yes
C25·-C24·-C32·-·120.26(15)····yes
C24·-C25·-C26·-·121.34(15)····yes
C24·-C25·-H251·-·118.4····no
C26·-C25·-H251·-·120.3····no
C25·-C26·-C27·-·120.14(15)····yes
C25·-C26·-H261·-·121.1····no
C27·-C26·-H261·-·118.8····no
C26·-C27·-C28·-·121.73(16)····yes
C26·-C27·-C31·-·120.70(14)····yes
C28·-C27·-C31·-·117.54(15)····yes
C27·-C28·-C29·-·119.99(15)····yes
C27·-C28·-H281·-·120.3····no
C29·-C28·-H281·-·119.7····no
C28·-C29·-C30·-·119.20(15)····yes
C28·-C29·-H291·-·119.9····no
C30·-C29·-H291·-·120.9····no
C29·-C30·-C33·-·121.41(14)····yes
C29·-C30·-N4·-·122.05(15)····yes
C33·-C30·-N4·-·116.54(13)····yes
C27·-C31·-C32·-·118.76(14)····yes
C27·-C31·-N4·-·122.37(14)····yes
C32·-C31·-N4·-·118.84(13)····yes
C31·-C32·-C24·-·118.68(14)····yes
C31·-C32·-N3·-·119.06(14)····yes
C24·-C32·-N3·-·122.21(14)····yes
C30·-C33·-C34·-·121.61(14)····yes
C30·-C33·-C37·-·120.33(14)····yes
C34·-C33·-C37·-·118.05(15)····yes
C33·-C34·-C35·-·120.71(15)····yes
C33·-C34·-H341·-·119.6····no
C35·-C34·-H341·-·119.7····no
C34·-C35·-C36·-·120.41(16)····yes
C34·-C35·-H351·-·118.7····no
C36·-C35·-H351·-·120.8····no
C35·-C36·-C39·-·119.66(17)····yes
C35·-C36·-H361·-·121.6····no
C39·-C36·-H361·-·118.7····no

C33·-C37·-C39·-·120.76(16)····yes
C33·-C37·-H371·-·119.0····no
C39·-C37·-H371·-·120.3····no
C37·-C39·-C36·-·120.41(17)····yes
C37·-C39·-H391·-·119.0····no
C36·-C39·-H391·-·120.6····no
C12·-N1·-C1·-·117.07(14)····yes
C11·-N2·-C10·-·118.81(13)····yes
C32·-N3·-C21·-·117.20(15)····yes
C31·-N4·-C30·-·118.77(13)····yes
```

4-(3,5-dimethoxyphenyl)-6-phenyl-2,2'-bipyridine (**35**)

```
data_CRYSTALS_cif·
 _audit_creation_date·····07-08-28
 _audit_creation_method·CRYSTALS_ver_12.84
·
 _oxford_structure_analysis_title··'B281057·sg072-2_173k'
 _chemical_name_systematic·····?
 _chemical_melting_point·····?
·
 _cell_length_a·····4.74340(10)
 _cell_length_b·····8.7761(2)
 _cell_length_c·····23.1828(4)
 _cell_angle_alpha·····95.3520(9)
 _cell_angle_beta··92.9223(9)
 _cell_angle_gamma·····105.3722(9)
 _cell_volume·····923.60(3)
·
 _symmetry_cell_setting·····'Triclinic'·
 _symmetry_space_group_name_H-M···'P·-1·'·
 _symmetry_space_group_name_Hall···'-P·1'·
loop_
 ·_symmetry_equiv_pos_as_xyz
 'x,y,z'
 '-x,-y,-z'

loop_
 _atom_type_symbol
 _atom_type_scat_dispersion_real
 _atom_type_scat_dispersion_imag
 _atom_type_scat_Cromer_Mann_a1
 _atom_type_scat_Cromer_Mann_b1
 _atom_type_scat_Cromer_Mann_a2
 _atom_type_scat_Cromer_Mann_b2
 _atom_type_scat_Cromer_Mann_a3
 _atom_type_scat_Cromer_Mann_b3
 _atom_type_scat_Cromer_Mann_a4
 _atom_type_scat_Cromer_Mann_b4
 _atom_type_scat_Cromer_Mann_c
 _atom_type_scat_source··
'C'·····0.0033·-0.0016·····2.3100··20.8439···1.0200··10.2075···1.5886···0.5687
···0.8650·51.6512···0.2156·'International·Tables·Vol·C·4.2.6.8·and·6.1.1.4'
'H'·····0.0000·-0.0000···0.4930··10.5109···0.3229··26.1257···0.1402···3.1424
···0.0408·57.7998···0.0030·'International·Tables·Vol·C·4.2.6.8·and·6.1.1.4'
'N'·····0.0061·-0.0033··12.2126···0.0057···3.1322···9.8933···2.0125··28.9975
···1.1663···0.5826·-11.5290·'International·Tables·Vol·C·4.2.6.8·and·6.1.1.4'
'O'·····0.0106·-0.0060···3.0485··13.2771···2.2868···5.7011···1.5463···0.3239
···0.8670··32.9089···0.2508·'International·Tables·Vol·C·4.2.6.8·and·6.1.1.4'
·
·
_cell_formula_units_Z·····2

#·Given·Formula·=·C24·H20·N2·O2·
#·Dc·=·····1.32·Fooo·=····388.00·Mu·=·····0.85·M·=····368.44
#·Found·Formula·=·C24·H20·N2·O2·
#·Dc·=·····1.32·FOOO·=····388.00·Mu·=·····0.85·M·=····368.44

_chemical_formula_sum·····'C24·H20·N2·O2'
_chemical_formula_moiety·····'C24·H20·N2·O2'
_chemical_compound_source·····?
_chemical_formula_weight·····368.44
·
·
·
_cell_measurement_reflns_used·····8813
_cell_measurement_theta_min·····1
_cell_measurement_theta_max·····28
_cell_measurement_temperature·····173
·
_exptl_crystal_description·····'plate'·
_exptl_crystal_colour·····'colorless'·
_exptl_crystal_size_min·····0.08·
_exptl_crystal_size_mid·····0.11·
_exptl_crystal_size_max·····0.39·
·
_exptl_crystal_density_diffrn···1.325·
_exptl_crystal_density_meas·····?·
#·Non-dispersive·F(000):··
_exptl_crystal_F_000·····388·
_exptl_absorpt_coefficient_mu····0.085·
·
#·Sheldrick·geometric·approximatio·0.99·0.99·
_exptl_absorpt_correction_type····multi-scan·
_exptl_absorpt_process_details····'DENZO/SCALEPACK·(Otwinowski·&·Minor,·1997)'·
_exptl_absorpt_correction_T_min··0.99·
_exptl_absorpt_correction_T_max··0.99·
#·For·a·Kappa·CCD,·set·Tmin·to·1.0·and·
#·Tmax·to·the·ratio·of·max:min·frame·scales·in·scale_all.log·
_diffrn_measurement_device_type····'Nonius·KappaCCD'·
_diffrn_radiation_monochromator····'graphite'·
_diffrn_radiation_type·····'Mo·Ka'
_diffrn_radiation_wavelength·····0.71073
_diffrn_measurement_method·····'\f·&·\w·scans'·
·
#·If·a·reference·occurs·more·than·once,·delete·the·author.
#·and·date·from·subsequent·references.·
_computing_data_collection·····'COLLECT·(Nonius,·1997-2001)'·
_computing_cell_refinement·····'DENZO/SCALEPACK·(Otwinowski·&·Minor,·1997)''
_computing_data_reduction·····'DENZO/SCALEPACK·(Otwinowski·&·Minor,·1997)''
_computing_structure_solution····'SIR92·(Altomare·et·al.,·1994)'·
_computing_structure_refinement··'CRYSTALS·(Betteridge·et·al.,·2003)'·
_computing_publication_material··'CRYSTALS·(Betteridge·et·al.,·2003)'·
_computing_molecular_graphics····'CAMERON·(Watkin·et·al.,·1996)'·
·
_diffrn_standards_interval_time···?·
_diffrn_standards_interval_count··?·
_diffrn_standards_number·····0·
_diffrn_standards_decay_%·····?·
·
_diffrn_ambient_temperature·····173
_diffrn_refins_number·····17415·
_refins_number_total·····4426·
_diffrn_refins_av_R_equivalents···0.035·
#·Number·of·reflections·with·Friedels·Law·is·4426·
#·Number·of·reflections·without·Friedels·Law·is·0·
#·Theoretical·number·of·reflections·is·about·4405·
·
·
_diffrn_refins_theta_min·····1.770·
_diffrn_refins_theta_max·····27.874·
_diffrn_measured_fraction_theta_max·1.000·
·
_diffrn_refins_theta_full·····27.874·

_diffrn_measured_fraction_theta_full·1.000·
·
·
_diffrn_refins_limit_h_min·····-6·
_diffrn_refins_limit_h_max·····6·
_diffrn_refins_limit_k_min·····-11·
_diffrn_refins_limit_k_max·····11·
_diffrn_refins_limit_l_min·····-5·
_diffrn_refins_limit_l_max·····30·
_refins_limit_h_min·····-6·
_refins_limit_h_max·····6·
_refins_limit_k_min·····-11·
_refins_limit_k_max·····11·
_refins_limit_l_min·····-5·
_refins_limit_l_max·····30·
·
_oxford_diffrn_Wilson_B_factor···0.00·
_oxford_diffrn_Wilson_scale·····0.00·
·
_atom_sites_solution_primary·····direct·#heavy,direct,difmap,geom
#·_atom_sites_solution_secondary··difmap
_atom_sites_solution_hydrogens···geom
·
_refine_diff_density_min·····-0.40·
_refine_diff_density_max·····0.39·
·
·
_refine_ls_number_reflns·····3026·
_refine_ls_number_restraints····48·
_refine_ls_number_parameters····289·
·
#·refine_ls_R_factor_ref·0.0557·
_refine_ls_wR_factor_ref·····0.0642·
_refine_ls_goodness_of_fit_ref···1.0573·
·
#_refins_number_all·4399·
_refine_ls_R_factor_all·····0.0821·
_refine_ls_wR_factor_all·····0.0938·
·
#·The·I/u(I)·cutoff·below·was·used·for·refinement·as·
#·well·as·the·gt·R-factors:
_refins_threshold_expression·····I>1.0\s(I)
_refins_number_gt·····3026·
_refine_ls_R_factor_gt·····0.0557·
_refine_ls_wR_factor_gt·····0.0642·
·
_refine_ls_shift/su_max·····0.000919·
·
#·choose·from:·rm·(reference·molecule·of·known·chirality),·
#·ad·(anomolous·dispersion·-·Flack),·rmad·(rm·and·ad),·
#·syn·(from·synthesis),·unk·(unknown)·or··(not·applicable).·
_chemical_absolute_configuration···'·'
·
·
_refine_ls_structure_factor_coef··F·
_refine_ls_matrix_type·····full
_refine_ls_hydrogen_treatment·····noref·····#·none,·undef,·noref,·refall,
·····refxyz,·refU,·constr·or·mixed·····#·refxyz,·refU,·constr·or·mixed
_refine_ls_weighting_scheme·····calc·
_refine_ls_weighting_details·
·

;
·Method,·part·1,·Chebychev·polynomial,·(Watkin,·1994,·Prince,·1982).
·[weight]·=·1.0/[a^0*T^0*(x)+a^1*T^1*(x)·...+a^n-1*T^n-1*(x)]·
·Where·A^i^·are·the·Chebychev·coefficients·listed·below·and·x=·Fcalc/Fmax·
·Method···Robust·Weighting·(Prince,·1982)·
·W·=·[weight]·*·[1-(delta2/6*sigma2)^2^]^2^·
·A^i^·are:·
·0.644·0.605·0.278·
;
·
·
·
·Check.this.file.using.the.IUCr·facility·at:·
·http://checkcif.iucr.org/·
·
·The·content·below·is·held·in·the·file·'script/refcif.dat'.··This·is·a·text·
·file·which·you·may·edit·to·reflect·local·conditions.·
·Items·which·need·looking·at·are·represented·by·a·'?'.·
·Items·for·which·there·are·choices·are·prefixed·with·'choose·from'.·
·
_publ_contact_letter·
;·
·Please·consider·this·CIF·submission·for·
·publication·as·a·Short·Format·Paper·in·Acta·
·Crystallographica·E.··The·figures·will·be·
·sent·by·e-mail.·
;·
_publ_contact_author_name·····'Anthony·Other'·
_publ_contact_author_address·
;·
·Chemical·Crystallography·Laboratory,·
·Department·of·Chemistry,·
·University·of·Nowhere,·
·Nowhere,·NO1·4T,·UK.·
;·
·
_publ_contact_author_phone·····'+44·1865·000000'·
_publ_contact_author_fax·····'+44·1865·000000'·
_publ_contact_author_email····'a.n.other@cham.no.ac.uk'·
_publ_requested_journal·····'Section·E'·
_publ_requested_category·····EO·#·choose·from:·FI·FM·FO·CI·CM·CO·AD·
_publ_requested_coeditor_name····'Prof·William·Clegg'·
·
_publ_section_title·
;·Title·of·paper···generally·just·the·systematic·or·trivial·name·
;·?·
·
;·The·loop·structure·below·should·contain·the·names·and·addresses·of·all·
·authors,·in·the·required·order·of·publication.·Repeat·as·necessary.·
;·
loop_·
·_publ_author_name·
·_publ_author_address·
·_publ_author_footnote·
·'Other,·Anthony·N.'·#·Author·1·
;·
·?·#·Address·for·author·1·
;·
·
;·?·#·Footnote·for·author·1·
```

```
·
'Else,·S.·O.'·#·Author·
·
·?·#·Address·
·
·
·?·#·Footnote·
·
·
·
·
_publ_section_abstract·
#·Text·of·the·abstract·
#·(a)·The·Abstract·must·be·self-contained·and·comprehensible·
#·without·the·rest·of·the·paper.·This·means·no·references·
#·to·atom·names·or·to·compound·numbers;·compounds·must·be·
#·identified·as·the·title·compound,·or·by·name·or·by·some·other·
#·means·such·as·derivatives·of·each·other·(e.g.·"the·
#·corresponding·ketone").·
#·(b)·The·chemical·formula·of·"the·title·compound"·must·be·given.·
#·(c)·Any·crystallographic·molecular·symmetry·should·be·
#·mentioned,·and·also·the·presence·of·more·than·one·molecule.·
#·in·the·asymmetric·unit·(i.e.·anything·other·than·Z'=1).·
·
?·
·
_publ_section_comment·
#·Text·of·the·paper·
#·Note·that·atoms·are·referenced·as·N2,·not·N(2)·or·N·2·
#·If·text·containing·()·occur·within·(),·the·outer·ones·should·be·[].·
#·Figures·should·be·referenced·as·Fih.·
·
?·
·
·
_publ_section_acknowledgements···#·Acknowledgments·
·
?·
·
·
_publ_section_figure_captions·
#·Captions·to·figures···Start·each·caption·on·a·new·line·after·a·blank·line·
·
Fig.·1.·
The·title·compound·with·displacement·ellipsoids·drawn·at·the·50%·
probability·level.·H·atoms·are·shown·as·spheres·of·
arbitary·radius.·
·
·
·
·
_publ_section_exptl_refinement·
#·Some·potentially·useful·phrases·are·donated·by·Bill·Clegg:·
·
In·the·absence·of·significant·anomalous·scattering,·Friedel·pairs·were·
merged.·
·
The·absolute·configuration·was·arbitrarily·assigned.·
·
The·relatively·large·ratio·of·minimum·to·maximum·corrections·applied·
in·the·multiscan·process·(1:nn)·reflect·changes·in·the·illuminated·
volume·of·the·crystal.·
·
Changes·in·illuminated·volume·were·kept·to·a·minimum,·and·were·


taken·into·account·(G\"orbitz,·1999)·by·the·multi-scan·inter-frame·
scaling·(DENZO/SCALEPACK,·Otwinowski·&·Minor,·1997).·
·
·
G\"orbitz,·C.·H.·(1999).·Acta·Cryst.·B55,·1090-1098.·
·
·
·
The·H·atoms·were·all·located·in·a·difference·map,·but·those·
attached·to·carbon·atoms·were·repositioned·geometrically.·
The·H·atoms·were·initially·refined·with·soft·restraints·on·the·
bond·lengths·and·angles·to·regularise·their·geometry·
(C---H·in·the·range·0.93--0.98,·
N---H·in·the·range·0.86--0.89·
N---H·to·0.86·
O---H·--0.82·
·\%A)·
and·
U-iso·(H)·(in·the·range·1.2-1.5·times·U-eq·of·the·parent·atom),·
after·which·the·positions·were·refined·with·riding·constraints.·
·
·
·
_publ_section_exptl_prep·
#·Brief·details·or·a·reference.·Include·solvent·if·known·
·
?·
·
·
·
·
#·PROCESSING·SUMMARY·(IUCr·Office·Use·Only):··
_journal_date_recd_electronic·····?·
_journal_date_to_coeditor·····?·
_journal_date_from_coeditor·····?·
_journal_date_accepted·····?·
_journal_date_printers_first·····?·
_journal_date_printers_final·····?·
_journal_date_proofs_out·····?·
_journal_date_proofs_in·····?·
_journal_coeditor_name·····?·
_journal_coeditor_code·····?·
_journal_coeditor_notes·····?·
_journal_techeditor_code·····?·
_journal_techeditor_notes·····?·
_journal_coden_ASTM·····?·
_journal_name_full·····?·
_journal_year·····?·
_journal_volume·····?·
_journal_issue·····?·
_journal_page_first·····?·
_journal_page_last·····?·
_journal_suppl_publ_number·····?·
_journal_suppl_publ_pages·····?·
·
#·End·of·'script/refcif.dat'·
·
·
·
·
#·Insert·your·own·references·if·required···in·alphabetical·order·


_publ_section_references·
·
Altomare,·A.,·Cascarano,·G.,·Giacovazzo,·C.,·Guagliardi,·A.,·Burla,·M.C.,·
Polidori,·G.·&·Camalli,·M.·(1994).·J.·Appl.·Cryst.·27,·435.·
·
Betteridge,·P.W.,·Carruthers,·J.R.,·Cooper,·R.I.,·
Prout,·K.·&·Watkin,·D.J.·(2003).·J.·Appl.·Cryst.·36,·1487.·
·
Larson,·A.C.·(1970).·Crystallographic·Computing,·Ed·Ahmed,·F.R.,·
Munksgaard,·Copenhagen,·291-294.·
·
Nonius·(1997-2001).·COLLECT.·Nonius·BV,·Delft,·The·Netherlands.·
·
Otwinowski,·Z.·&·Minor,·W.·(1997).·Methods·in·Enzymology,·Vol.·276,·
edited·by·C.·W.·Carter·Jr·&·R.·M.·Sweet,·pp.·307--326.·
New·York:·Academic·Press.·
·
Prince,·E.·
Mathematical·Techniques·in·Crystallography·
and·Materials·Science·
Springer-Verlag,·New·York,·1982.·
·
Watkin·D.J.·(1994).·
Acta·Cryst.·A50,·411-437.·
·
Watkin,·D.J.,·Prout,·C.K.·&·Pearce,·L.J.·(1996).·CAMERON,·Chemical·
Crystallography·Laboratory,·Oxford,·UK.·
·
·
·
#·Uequiv·=·arithmetic·mean·of·Ui·i.e.·Ueqiv·=·(U1+U2+U3)/3·


·
#·Replace·last···with·number·of·unfound·hydrogen·atomsattached·to·an·atom.·
·
#····refinement_flags_···
#·..no·refinement·constraints··········S·special·position·constraint·on·site·
#·G·rigid·group·refinement·of·site·····R·riding·atom·
#·D·distance·or·angle·restraint·on·site·T·thermal·displacement·constraints·
#·U·Uiso·or·Uij·restraint·(rigid·bond)···P·partial·occupancy·constraint·
·
·
·
loop_·
_atom_site_label·
_atom_site_type_symbol·
_atom_site_fract_x·
_atom_site_fract_y·
_atom_site_fract_z·
_atom_site_U_iso_or_equiv·
_atom_site_occupancy·
_atom_site_adp_type·
_atom_site_refinement_flags_posn·
_atom_site_refinement_flags_adp·
_atom_site_refinement_flags_occupancy·
_atom_site_disorder_assembly·
_atom_site_disorder_group·
_atom_site_attached_hydrogens·
O1·O·0.8097(4)·0.75513(17)·0.09165(7)·0.0522·1.0000·Uani·.·.·.·.·.·
O2·O·0.5857(4)·0.19191(16)·0.05722(6)·0.0419·1.0000·Uani·.·.·.·.·.·
N1·N·-0.4574(4)·0.0420(2)·0.24404(7)·0.0381·1.0000·Uani·D·U·.·.·.·
N2·N·-0.0178(3)·0.37759(18)·0.33387(7)·0.0307·1.0000·Uani·.·.·.·.·.·
C1·C·-0.7352(5)·-0.0778(2)·0.24873(10)·0.0402·1.0000·Uani·D·U·.·.·.·.·
C2·C·-0.8802(7)·-0.0928(4)·0.29773(12)·0.0733·1.0000·Uani·D·U·.·.·.·.·
C3·C·-0.7808(7)·0.0196(4)·0.34488(13)·0.0898·1.0000·Uani·D·U·.·.·.·.·
C4·C·-0.5345(5)·0.1427(3)·0.34173(10)·0.0484·1.0000·Uani·D·U·.·.·.·.·
C5·C·-0.3962(4)·0.1498(2)·0.29068(8)·0.0299·1.0000·Uani·D·U·.·.·.·.·
C6·C·-0.1290(4)·0.2796(2)·0.28505(8)·0.0293·1.0000·Uani·.·.·.·.·.·.·
C7·C·-0.0005(4)·0.2962(2)·0.23256(8)·0.0307·1.0000·Uani·.·.·.·.·.·.·
C8·C·0.2510(4)·0.4191(2)·0.22916(8)·0.0296·1.0000·Uani·.·.·.·.·.·.·
C9·C·0.3633(4)·0.5198(2)·0.27985(8)·0.0311·1.0000·Uani·.·.·.·.·.·.·
C10·C·0.2265(4)·0.4955(2)·0.33116(8)·0.0288·1.0000·Uani·.·.·.·.·.·.·
C11·C·0.3996(4)·0.4404(2)·0.17441(8)·0.0304·1.0000·Uani·.·.·.·.·.·.·
C12·C·0.5299(4)·0.5940(2)·0.16023(8)·0.0337·1.0000·Uani·.·.·.·.·.·.·
C13·C·0.6778(5)·0.6117(2)·0.11020(9)·0.0360·1.0000·Uani·.·.·.·.·.·.·
C14·C·0.7031(5)·0.4796(2)·0.07471(8)·0.0368·1.0000·Uani·.·.·.·.·.·.·
C15·C·0.5735(4)·0.3290(2)·0.08902(8)·0.0320·1.0000·Uani·.·.·.·.·.·.·
C16·C·0.4188(4)·0.3085(2)·0.13873(8)·0.0313·1.0000·Uani·.·.·.·.·.·.·
C17·C·0.7454(6)·0.8923(2)·0.11921(10)·0.0487·1.0000·Uani·.·.·.·.·.·.·
C18·C·0.7731(5)·0.2076(3)·0.01047(9)·0.0417·1.0000·Uani·.·.·.·.·.·.·
C19·C·0.3463(4)·0.1579(2)·0.38650(8)·0.0289·1.0000·Uani·.·.·.·.·.·.·
C20·C·0.5677(5)·0.7907(3)·0.49011(9)·0.0416·1.0000·Uani·.·.·.·.·.·.·
C21·C·0.3008(9)·0.5355(5)·0.43888(17)·0.0353·0.5000·Uani·.·.·.·.·.·.·
C22·C·0.4120(9)·0.6271(5)·0.49117(17)·0.0387·0.5000·Uani·.·.·.·.·.·.·
C23·C·0.6120(9)·0.8497(5)·0.43968(18)·0.0372·0.5000·Uani·.·.·.·.·.·.·
C24·C·0.5080(8)·0.7572(5)·0.38705(16)·0.0317·0.5000·Uani·.·.·.·.·.·.·
C31·C·0.1618(8)·0.6182(5)·0.43028(17)·0.0346·0.5000·Uani·.·.·.·.·.·.·
C32·C·0.2748(10)·0.7162(5)·0.48108(17)·0.0393·0.5000·Uani·.·.·.·.·.·.·
C33·C·0.7557(9)·0.7724(5)·0.44643(17)·0.0371·0.5000·Uani·.·.·.·.·.·.·
C34·C·0.6433(9)·0.6733(5)·0.39589(17)·0.0335·0.5000·Uani·.·.·.·.·.·.·
H11·H·-0.8061(·-0.1565·0.2159·0.0460·1.0000·Uiso·.·.·.·.·.·.·.·.·.·
H21·H·-1.0493(·-0.1810·0.2995·0.0757·1.0000·Uiso·.·.·.·.·.·.·.·.·.·
H31·H·-0.8839·0.0127·0.3796·0.0902·1.0000·Uiso·.·.·.·.·.·.·.·.·.·
H41·H·-0.4601·0.2221·0.3743·0.0527·1.0000·Uiso·.·.·.·.·.·.·.·.·.·
H71·H·-0.0850·0.2231·0.1988·0.0361·1.0000·Uiso·.·.·.·.·.·.·.·.·.·
H91·H·0.5361·0.6062·0.2794·0.0361·1.0000·Uiso·.·.·.·.·.·.·.·.·.·
H121·H·0.5164·0.6857·0.1849·0.0407·1.0000·Uiso·.·.·.·.·.·.·.·.·.·
H141·H·0.8098·0.4936·0.0406·0.0447·1.0000·Uiso·.·.·.·.·.·.·.·.·.·
H161·H·0.3263·0.2035·0.1481·0.0369·1.0000·Uiso·.·.·.·.·.·.·.·.·.·
H171·H·0.8503·0.9847·0.1025·0.0585·1.0000·Uiso·.·.·.·.·.·.·.·.·.·
H172·H·0.8033·0.9038·0.1600·0.0585·1.0000·Uiso·.·.·.·.·.·.·.·.·.·
H173·H·0.5383·0.8809·0.1138·0.0585·1.0000·Uiso·.·.·.·.·.·.·.·.·.·
H181·H·0.7619·0.1043·-0.0085·0.0500·1.0000·Uiso·.·.·.·.·.·.·.·.·.·
H182·H·0.8715·0.2559·0.0256·0.0500·1.0000·Uiso·.·.·.·.·.·.·.·.·.·
H183·H·0.7111·0.2701·-0.0169·0.0500·1.0000·Uiso·.·.·.·.·.·.·.·.·.·
H201·H·0.6404·0.8581·0.5261·0.0488·1.0000·Uiso·.·.·.·.·.·.·.·.·.·
H211·H·0.1910·0.4260·0.4390·0.0419·0.5000·Uiso·.·.·.·.·.·.·.·.·.·
H221·H·0.3844·0.5814·0.5272·0.0473·0.5000·Uiso·.·.·.·.·.·.·.·.·.·
H231·H·0.7182·0.9595·0.4395·0.0426·0.5000·Uiso·.·.·.·.·.·.·.·.·.·
H241·H·0.5463·0.8023·0.3511·0.0375·0.5000·Uiso·.·.·.·.·.·.·.·.·.·
H311·H·-0.0441·0.5639·0.4249·0.0414·0.5000·Uiso·.·.·.·.·.·.·.·.·.·
H321·H·0.1457·0.7323·0.5102·0.0474·0.5000·Uiso·.·.·.·.·.·.·.·.·.·
H331·H·0.9606·0.8283·0.4518·0.0423·0.5000·Uiso·.·.·.·.·.·.·.·.·.·
H341·H·0.7732·0.6564·0.3669·0.0398·0.5000·Uiso·.·.·.·.·.·.·.·.·.·
loop_·
_atom_site_aniso_label·
_atom_site_aniso_U_11·
_atom_site_aniso_U_22·
_atom_site_aniso_U_33·
_atom_site_aniso_U_23·
_atom_site_aniso_U_13·
_atom_site_aniso_U_12·
O1·O·0.0823(12)·0.0282(7)·0.0479(9)·0.0094(6)·0.0282(8)·0.0119(8)·


O2·O·0.0584(9)·0.0293(7)·0.0379(8)·0.0019(6)·0.0194(7)·0.0091(6)·
N1·O·0.0368(9)·0.0356(9)·0.0375(9)·-0.0027(7)·0.0019(7)·0.0046(7)·
N2·O·0.0307(8)·0.0301(8)·0.0299(8)·0.0025(6)·0.0038(6)·0.0060(6)·
C1·O·0.0360(10)·0.0332(10)·0.0462(11)·-0.0033(8)·-0.0011(9)·0.0038(8)·
C2·O·0.0640(17)·0.0648(16)·0.0603(16)·-0.0094(13)·0.0184(13)·-0.0329(14)·
C3·O·0.079(2)·0.095(2)·0.0529(15)·-0.0177(15)·0.0332(14)·-0.0476(17)·
C4·O·0.0429(12)·0.0500(13)·0.0389(11)·-0.0051(9)·0.0124(9)·-0.0090(10)·
C5·O·0.0269(9)·0.0295(9)·0.0323(9)·0.0023(7)·0.0016(7)·0.0063(7)·
C6·O·0.0283(9)·0.0291(9)·0.0299(9)·0.0028(7)·0.0018(7)·0.0068(7)·
C7·O·0.0307(9)·0.0319(9)·0.0279(9)·0.0005(7)·0.0012(7)·0.0072(7)·
C8·O·0.0302(9)·0.0316(9)·0.0272(9)·0.0037(7)·0.0045(7)·0.0081(7)·
C9·O·0.0304(9)·0.0301(9)·0.0302(9)·0.0026(7)·0.0047(7)·0.0035(7)·
C10·O·0.0289(9)·0.0281(9)·0.0289(9)·0.0016(7)·0.0020(7)·0.0072(7)·
C11·O·0.0301(9)·0.0325(9)·0.0278(9)·0.0040(7)·0.0027(7)·0.0070(7)·
C12·O·0.0416(11)·0.0293(9)·0.0310(9)·0.0028(7)·0.0077(8)·0.0103(8)·
C13·O·0.0470(12)·0.0275(9)·0.0339(10)·-0.0081(8)·0.0097(8)·0.0083(8)·
C14·O·0.0460(11)·0.0342(10)·0.0312(9)·0.0062(8)·0.0128(8)·0.0102(8)·
C15·O·0.0374(10)·0.0291(9)·0.0296(9)·0.0016(7)·0.0051(7)·0.0091(8)·
C16·O·0.0348(10)·0.0290(9)·0.0285(9)·0.0047(7)·0.0040(7)·0.0053(7)·
C17·O·0.0794(17)·0.0282(10)·0.0388(11)·0.0049(8)·0.0045(11)·0.0148(11)·
C18·O·0.0521(13)·0.0396(11)·0.0338(10)·0.0013(8)·0.0138(9)·0.0123(10)·
C19·O·0.0278(9)·0.0309(9)·0.0278(9)·0.0032(7)·0.0027(7)·0.0075(7)·
C20·O·0.0408(11)·0.0471(12)·0.0329(10)·-0.0066(9)·-0.0005(8)·0.0094(9)·
C21·O·0.0328(19)·0.038(2)·0.0334(19)·0.0045(16)·0.0022(15)·0.0066(17)·
C22·O·0.039(2)·0.052(2)·0.0265(18)·0.0076(17)·0.0034(16)·0.0127(19)·
C23·O·0.032(2)·0.036(2)·0.039(2)·-0.0069(16)·0.0040(16)·0.0047(17)·
C24·O·0.0306(18)·0.037(2)·0.0267(17)·0.0039(15)·0.0052(14)·0.0073(16)·
C31·O·0.0303(19)·0.039(2)·0.034(2)·-0.0009(16)·0.0042(15)·0.0099(17)·
C32·O·0.040(2)·0.048(2)·0.0300(18)·-0.0020(17)·0.0054(16)·0.0149(19)·
C33·O·0.032(2)·0.039(2)·0.035(2)·0.0027(16)·0.0014(16)·-0.0003(17)·
C34·O·0.0323(19)·0.0350(19)·0.0324(19)·0.0031(15)·0.0085(15)·0.0067(16)·


_refine_ls_extinction_method·
····'None'·
_oxford_refine_ls_scale·0.5565(15)·
loop_·
·_geom_bond_atom_site_label_1·
·_geom_bond_site_symmetry_1·
·_geom_bond_atom_site_label_2·
·_geom_bond_site_symmetry_2·
·_geom_bond_distance·
·_geom_bond_publ_flag·
O1·.·C13·.·1.368(2)···yes·
O1·.·C17·.·1.422(3)···yes·
O2·.·C13·.·1.368(2)···yes·
O2·.·C18·.·1.430(2)···yes·
N1·.·C1·.·1.340(2)···yes·
N1·.·C5·.·1.346(2)···yes·
N2·.·C6·.·1.347(2)···yes·
N2·.·C10·.·1.342(2)···yes·
C1·.·C2·.·1.357(3)···yes·
C1·.·H11·.·0.960···no·
C2·.·C3·.·1.375(4)···yes·
C2·.·H21·.·0.961···no·
C3·.·C4·.·1.376(3)···yes·
C3·.·H31·.·0.960···no·
C4·.·C5·.·1.381(3)···yes·
C4·.·H41·.·0.961···no·
C5·.·C6·.·1.483(2)···yes·
C6·.·C7·.·1.391(3)···yes·


C7·.·C8·.·1.392(3)···yes·
C7·.·H71·.·0.960···no·
C8·.·C9·.·1.392(3)···yes·
C8·.·C11·.·1.486(2)···yes·
C9·.·C10·.·1.391(3)···yes·
C9·.·H91·.·0.959···no·
C10·.·C19·.·1.489(2)···yes·
C11·.·C12·.·1.403(3)···yes·
C11·.·C16·.·1.384(3)···yes·
C12·.·C13·.·1.386(3)···yes·
C12·.·H121·.·0.962···no·
C13·.·C14·.·1.393(3)···yes·
C14·.·C15·.·1.381(3)···yes·
C14·.·H141·.·0.960···no·
C15·.·C16·.·1.398(3)···yes·
C16·.·H161·.·0.960···no·
C17·.·H171·.·0.960···no·
C17·.·H172·.·0.960···no·
C17·.·H173·.·0.961···no·
C18·.·H181·.·0.959···no·
C18·.·H182·.·0.962···no·
C18·.·H183·.·0.959···no·
C19·.·C21·.·1.382(6)···yes·
C19·.·C24·.·1.403(4)···yes·
C19·.·C31·.·1.402(4)···yes·
C20·.·C34·.·1.385(4)···yes·
C20·.·C22·.·1.433(5)···yes·
C20·.·C23·.·1.327(5)···yes·
C20·.·C32·.·1.366(5)···yes·
C20·.·C33·.·1.408(5)···yes·
C20·.·H201·.·0.967···no·
C21·.·C22·.·1.386(6)···yes·
C21·.·H211·.·0.959···no·
C22·.·H221·.·0.960···no·
C23·.·C24·.·1.390(5)···yes·
C23·.·H231·.·0.962···no·
C24·.·H241·.·0.962···no·
C31·.·C32·.·1.384(5)···yes·
C31·.·H311·.·0.962···no·
C32·.·H321·.·0.959···no·
C33·.·C34·.·1.384(5)···yes·
C33·.·H331·.·0.961···no·
C34·.·H341·.·0.961···no·
loop_·
·_geom_angle_atom_site_label_1·
·_geom_angle_site_symmetry_1·
·_geom_angle_atom_site_label_2·
·_geom_angle_site_symmetry_2·
·_geom_angle_atom_site_label_3·
·_geom_angle_site_symmetry_3·
·_geom_angle·
·_geom_angle_publ_flag·
C13·.·O1·.·C17·.·117.49(17)···yes·
C15·.·O2·.·C18·.·117.07(15)···yes·
C1·.·N1·.·C5·.·117.99(17)···yes·
C6·.·N2·.·C10·.·118.09(15)···yes·
N1·.·C1·.·C2·.·123.0(2)···yes·
N1·.·C1·.·H11·.·118.5···no·
C2·.·C1·.·H11·.·118.6···no·
C1·.·C2·.·C3·.·119.0(2)···yes·


C1·.·C2·.·H21·.·120.5···no·
C3·.·C2·.·H21·.·120.5···no·
C2·.·C3·.·C4·.·119.5(2)···yes·
C2·.·C3·.·H31·.·120.2···no·
C4·.·C3·.·H31·.·120.4···no·
C3·.·C4·.·C5·.·118.5(2)···yes·
C3·.·C4·.·H41·.·120.8···no·
C5·.·C4·.·H41·.·120.7···no·
C4·.·C5·.·N1·.·122.11(17)···yes·
C4·.·C5·.·C6·.·120.68(16)···yes·
N1·.·C5·.·C6·.·117.20(16)···yes·
C5·.·C6·.·N2·.·115.88(16)···yes·
C5·.·C6·.·C7·.·121.49(16)···yes·
N2·.·C6·.·C7·.·122.62(16)···yes·
C6·.·C7·.·C8·.·119.72(16)···yes·
C6·.·C7·.·H71·.·120.1···no·
C8·.·C7·.·H71·.·120.1···no·
C7·.·C8·.·C9·.·117.17(16)···yes·
C7·.·C8·.·C11·.·121.82(16)···yes·
C9·.·C8·.·C11·.·121.05(16)···yes·
C8·.·C9·.·C10·.·120.36(17)···yes·
C8·.·C9·.·H91·.·119.8···no·
C10·.·C9·.·H91·.·119.8···no·
C9·.·C10·.·N2·.·122.09(16)···yes·
C9·.·C10·.·C19·.·121.66(16)···yes·
N2·.·C10·.·C19·.·116.25(15)···yes·
C8·.·C11·.·C12·.·119.87(16)···yes·
C8·.·C11·.·C16·.·119.84(16)···yes·
C12·.·C11·.·C16·.·120.24(17)···yes·
C11·.·C12·.·C13·.·119.15(17)···yes·
C11·.·C12·.·H121·.·120.4···no·
C13·.·C12·.·H121·.·120.4···no·
C12·.·C13·.·O1·.·124.30(18)···yes·
C12·.·C13·.·C14·.·120.91(17)···yes·
O1·.·C13·.·C14·.·114.79(17)···yes·
C13·.·C14·.·C15·.·119.44(17)···yes·
C13·.·C14·.·H141·.·120.4···no·
C15·.·C14·.·H141·.·120.2···no·
C14·.·C15·.·O2·.·124.03(17)···yes·
C14·.·C15·.·C16·.·120.53(17)···yes·
O2·.·C15·.·C16·.·115.44(16)···yes·
C15·.·C16·.·C11·.·119.71(17)···yes·
C15·.·C16·.·H161·.·120.2···no·
C11·.·C16·.·H161·.·120.1···no·
O1·.·C17·.·H171·.·109.5···no·
O1·.·C17·.·H172·.·109.5···no·
H171·.·C17·.·H172·.·109.5···no·
O1·.·C17·.·H173·.·109.4···no·
H171·.·C17·.·H173·.·109.4···no·
H172·.·C17·.·H173·.·109.4···no·
O2·.·C18·.·H181·.·109.5···no·
O2·.·C18·.·H182·.·109.3···no·
H181·.·C18·.·H182·.·109.4···no·
O2·.·C18·.·H183·.·109.5···no·
H181·.·C18·.·H183·.·109.7···no·
H182·.·C18·.·H183·.·109.4···no·
C10·.·C19·.·C21·.·119.7(2)···yes·
C10·.·C19·.·C24·.·121.6(2)···yes·
C21·.·C19·.·C24·.·118.6(3)···yes·
C10·.·C19·.·C31·.·120.7(2)···yes·


C10·.·C19·.·C34·.·120.4(2)···yes·
C31·.·C19·.·C34·.·118.8(3)···yes·
C19·.·C21·.·C22·.·119.3···no·
C22·.·C21·.·H211·.·119.5···no·
C20·.·C22·.·C21·.·118.6(3)···yes·
C20·.·C22·.·H221·.·121.0···no·
C21·.·C22·.·H221·.·120.4···no·
C20·.·C23·.·C24·.·121.7(3)···yes·
C20·.·C23·.·H231·.·119.2···no·
C24·.·C23·.·H231·.·119.1···no·
C19·.·C24·.·C23·.·119.9(3)···yes·
C19·.·C24·.·H241·.·120.1···no·
C23·.·C24·.·H241·.·120.0···no·
C19·.·C31·.·C32·.·120.2(3)···yes·
C19·.·C31·.·H311·.·119.8···no·
C32·.·C31·.·H311·.·120.0···no·
C31·.·C32·.·C20·.·120.7(3)···yes·
C31·.·C32·.·H321·.·119.6···no·
C20·.·C32·.·H321·.·119.7···no·
C20·.·C33·.·C34·.·119.5(3)···yes·
C20·.·C33·.·H331·.·120.1···no·
C34·.·C33·.·H331·.·120.4···no·
C19·.·C34·.·C33·.·120.9(3)···yes·
C19·.·C34·.·H341·.·119.6···no·
C33·.·C34·.·H341·.·119.6···no·
```

bis(2-phenylpyridine-*C*,*N*)(1,10-phenanthroline-*N*,*N*')iridium(III) hexafluorophosphate (**47**)

```
data_sg084_1_123k
_audit_creation_date·····08-10-22
_audit_creation_method·CRYSTALS_ver_12.84
·
_oxford_structure_analysis_title···'sg084_1_123k_Om·in·C2/c'
_chemical_name_systematic·····?
_chemical_melting_point·····?
·
_cell_length_a·····15.2417(6)
_cell_length_b·····23.0629(9)
_cell_length_c·····18.8709(7)
_cell_angle_alpha·····90
_cell_angle_beta·····95.015(2)
_cell_angle_gamma·····90
_cell_volume·····6608.1(4)
·
_symmetry_cell_setting·····'Monoclinic'·
_symmetry_space_group_name_H-M···'C·2/c'·
_symmetry_space_group_name_Hall···'-C·2yc'·
loop_·
·_symmetry_equiv_pos_as_xyz·
·'x,y,z'·
·'-x,-y,-z'·
·'x+1/2,y+1/2,z'·
·'-x+1/2,-y+1/2,-z'·
·'-x,y,-z+1/2'·
·'x,-y,z+1/2'·
·'-x+1/2,y+1/2,-z+1/2'·
·'x+1/2,-y+1/2,z+1/2'·


loop_·
_atom_type_symbol·
_atom_type_scat_dispersion_real·
_atom_type_scat_dispersion_imag·
_atom_type_scat_Cromer_Mann_a1·
_atom_type_scat_Cromer_Mann_b1·
_atom_type_scat_Cromer_Mann_a2·
_atom_type_scat_Cromer_Mann_b2·
_atom_type_scat_Cromer_Mann_a3·
_atom_type_scat_Cromer_Mann_b3·
_atom_type_scat_Cromer_Mann_a4·
_atom_type_scat_Cromer_Mann_b4·
_atom_type_scat_Cromer_Mann_c·
_atom_type_scat_source··
C·····0.0033···0.0016···2.3100···20.8439···1.0200···10.2075···1.5886···0.5687·
N·····0.0061···0.0033···12.2126···0.0057···9.1222···9.8933···0.0125···28.9975·
H·····0.0000···0.0000···0.4930···10.5109···0.3229···26.1257···0.1402···3.1424·
O·····0.0048···0.0032···3.0485···13.2771···2.2868···5.7011···1.5463···0.3239·
F·····0.0070···0.0032···3.5392···10.2825···2.6412···4.2944···1.5170···0.2615·
P·····0.1023···0.0942···6.4345···1.9067···4.1791···27.1570···1.7800···0.5260·
Ir····-1.4908···68.1645···1.1149·'International·Tables·Vol·C·4.2.6.8·and·6.1.1.4'·
Cl····0.8650···51.6512···0.2156·'International·Tables·Vol·C·4.2.6.8·and·6.1.1.4'·
·····5.8338···45.0011···11.4722·'International·Tables·Vol·C·4.2.6.8·and·6.1.1.4'·
·····0.0106···0.0060···3.0485···13.2771···2.2868···5.7011···1.5463···0.3239·
·····0.8670···32.9089···0.2508·'International·Tables·Vol·C·4.2.6.8·and·6.1.1.4'·
·····0.1484···0.1585···11.4604···0.0104···7.1964···1.1662···6.2556···18.5194·
·····1.6455···47.7784···-9.5574·'International·Tables·Vol·C·4.2.6.8·and·6.1.1.4'·
```

```
.
;
_cell_formula_units_Z·····8

#·Given·Formula·=·C34·H24·Cl0.25·F6·Ir1·N4·O0.25·P1·
#·Dc·=·····1.69·Fooo···3416.00·Mu·····41.74·M·····838.64
#·Found·Formula·=·C35·H26.00·Cl1·F6·Ir1·N4·P1·
#·Dc·=·····1.76·FOOO···3416.00·Mu·····42.37·M·····875.25

_chemical_formula_sum·····C35·H26·Cl1·F6·Ir1·N4·P1'
_chemical_formula_moiety·····'C34·H24·Ir·N4,·0.5(C2·H4·Cl2),·F6·P'
_chemical_compound_source·····?
_chemical_formula_weight·····875.25

_cell_measurement_reflns_used·····0
_cell_measurement_theta_min·····0
_cell_measurement_theta_max·····0
_cell_measurement_temperature·····123

_exptl_crystal_description·····'block'·
_exptl_crystal_colour·····'yellow'·
_exptl_crystal_size_min·····0.04·
_exptl_crystal_size_mid·····0.11·
_exptl_crystal_size_max·····0.23

_exptl_crystal_density_diffrn····1.759·
_exptl_crystal_density_meas·····?·
#·Non-dispersive·F(000)·
_exptl_crystal_F_000·····3415.999·
_exptl_absorpt_coefficient_mu····4.237·

#·Sheldrick·geometric·approximatio·0.63·0.84·
_exptl_absorpt_correction_type····multi-scan·
_exptl_absorpt_process_details····'DENZO/SCALEPACK·(Otwinowski·&·Minor,·1997)'·
_exptl_absorpt_correction_T_min···0.63·
_exptl_absorpt_correction_T_max···0.84·
#·For·a·Kappa·CCD,·set·Tmin·to·1.0·and·
#·Tmax·to·the·ratio·of·max:min·frame·scales·in·scale_all.log·
_diffrn_measurement_device_type···'Nonius·KappaCCD'·
_diffrn_radiation_monochromator···'graphite'·
_diffrn_radiation_type·····'Mo·K\a'
_diffrn_radiation_wavelength·····0.71073
_diffrn_measurement_method·····'f·&·w·scans'·

#·If·a·reference·occurs·more·than·once,·delete·the·author.
#·and·date·from·subsequent·references.
_computing_data_collection·····'COLLECT·(Nonius,·1997-2001)·'·
_computing_cell_refinement·····'DENZO/SCALEPACK·(Otwinowski·&·Minor,·1997)'·
_computing_data_reduction·····'DENZO/SCALEPACK·(Otwinowski·&·Minor,·1997)'·
_computing_structure_solution····'SIR97·(Altomare·et·al.,·1999)'·
_computing_structure_refinement···'CRYSTALS·(Betteridge·et·al.,·2003)'·
_computing_publication_material···'CRYSTALS·(Betteridge·et·al.,·2003)'·
_computing_molecular_graphics·····'CAMERON·(Watkin·et·al.,·1996)'·

_diffrn_standards_interval_time···?·
_diffrn_standards_interval_count···?·
_diffrn_standards_number·····0·
_diffrn_standards_decay_%·····?·

_diffrn_ambient_temperature·····123
_diffrn_reflns_number·····233040·
_reflns_number_total·····43275·
_diffrn_reflns_av_R_equivalents···0.043·
#·Number·of·reflections·with·Friedels·Law·is·43275·
#·Number·of·reflections·without·Friedels·Law·is·0·
#·Theoretical·number·of·reflections·is·about·46409·

_diffrn_reflns_theta_min·····2.072·
_diffrn_reflns_theta_max·····57.601·
_diffrn_measured_fraction_theta_max·0.932·

_diffrn_reflns_theta_full·····42.049·
_diffrn_measured_fraction_theta_full·0.995·

_diffrn_reflns_limit_h_min·····-36·
_diffrn_reflns_limit_h_max·····36·
_diffrn_reflns_limit_k_min·····-47·
_diffrn_reflns_limit_k_max·····47·
_diffrn_reflns_limit_l_min·····-44·
_diffrn_reflns_limit_l_max·····44·
_reflns_limit_h_min···········-36·
_reflns_limit_h_max···········35·
_reflns_limit_k_min···········-47·
_reflns_limit_k_max···········47·
_reflns_limit_l_min···········0·
_reflns_limit_l_max···········44·

_oxford_diffrn_Wilson_B_factor···0.00·
_oxford_diffrn_Wilson_scale·····0.00·

_atom_sites_solution_primary·····direct·#heavy,direct,difmap,geom
#·atom_sites_solution_secondary··difmap
_atom_sites_solution_hydrogens···geom

_refine_diff_density_min·····-1.25·
_refine_diff_density_max·····3.12·

_refine_ls_number_reflns·····19927·
_refine_ls_number_restraints····661·
_refine_ls_number_parameters····478·

#_refine_ls_R_factor_ref·0.0219·
_refine_ls_wR_factor_ref·····0.0253·
_refine_ls_goodness_of_fit_ref····1.0406·

#_refine_number_all·43269·
_refine_ls_R_factor_all·····0.0765·
_refine_ls_wR_factor_all·····0.0472·

#·The·I/u(I)·cutoff·below·was·used·for·refinement·as·
#·well·as·the·`gt·R·factors:
_refins_threshold_expression·····I>3.0\s(I)
_refine_number_gt·····19927·
_refine_ls_R_factor_gt·····0.0219·
_refine_ls_wR_factor_gt·····0.0253·

_refine_ls_shift/su_max·····0.005071·

#·choose·from:·rm·(reference·molecule·of·known·chirality),·
#·ad·(anomalous·dispersion···Flack),·rmad·(rm·and·ad),·
#·syn·(from·synthesis),·unk·(unknown)·or··(not·applicable)·
_chemical_absolute_configuration·'.'·

_refine_ls_structure_factor_coef·F·
_refine_ls_matrix_type·····full·
_refine_ls_hydrogen_treatment·····constr·····#·none,·undef,·noref,·refall,
·····························#·refxyz,·refU,·constr·or·mixed
_refine_ls_weighting_scheme·····calc·
_refine_ls_weighting_details·
;
·Method,·part·1,·Chebychev·polynomial,·(Watkin,·1994,·Prince,·1982)·
·[weight]·=·1.0/[A~0~*T~0~(x)+A~1~*T~1~(x)···+A~n-1~*T~n-1~(x)]·
·where·A~i~·are·the·Chebychev·coefficients·listed·below·and·x=·Fcalc/Fmax·
·Method·=·Robust·Weighting·(Prince,·1982)·
·W·=·[weight]·*·[1-(deltaF/6*sigmaF)^2^]^2^·
·A~i~·are:·
·0.749·0.169·0.537·
;
_refine_ls_weighting_scheme·····calc·
_refine_ls_weighting_details·
;
·Method,·part·1,·Chebychev·polynomial,·(Watkin,·1994,·Prince,·1982)·
·[weight]·=·1.0/[A~0~*T~0~(x)+A~1~*T~1~(x)···+A~n-1~*T~n-1~(x)]·
·where·A~i~·are·the·Chebychev·coefficients·listed·below·and·x=·Fcalc/Fmax·
·Method·=·Robust·Weighting·(Prince,·1982)·
·W·=·[weight]·*·[1-(deltaF/6*sigmaF)^2^]^2^·
·A~i~·are:·
·0.749·0.169·0.537·
;

#·Check·this·file·using·the·IUCr·facility·at·
#·http://checkcif.iucr.org/

#·The·content·below·is·held·in·the·file·'script/refcif.dat'.·This·is·a·text·
#·file·which·you·may·edit·to·reflect·local·conditions.·
#·Items·which·need·looking·at·are·represented·by·a·'?'.·
#·Items·for·which·there·are·choices·are·prefixed·with·'choose·from'.·

_publ_contact_letter·
;·
·Please·consider·this·CIF·submission·for·
·publication·as·a·Short·Format·Paper·in·Acta·
·Crystallographica·E.·The·figures·will·be·
·sent·by·e-mail.·
;·
_publ_contact_author_name·····'Anthony·Other'·
_publ_contact_author_address·
;·
·Chemical·Crystallography·Laboratory,·
·Department·of·Chemistry,·
·University·of·Nowhere,·
·Nowhere,·NO1·4T,·UK.·
;·

_publ_contact_author_phone·····'+44·1865·000000'·
_publ_contact_author_fax·····'+44·1865·000000'·
_publ_contact_author_email·····'a.n.other@chem.no.ac.uk'·
_publ_requested_journal·····Section·E'·
_publ_requested_category·····E0·#·choose·from:·FI·FM·FO·CI·CM·CO·AD·
_publ_requested_coeditor_name····'Prof·William·Clegg'·

_publ_section_title·
#·Title·of·paper···generally·just·the·systematic·or·trivial·name·
;·?·

;·
·
#·The·loop·structure·below·should·contain·the·names·and·addresses·of·all·
#·authors,·in·the·required·order·of·publication.··Repeat·as·necessary.·
loop_·
·_publ_author_name·
·_publ_author_address·
·_publ_author_footnote·
·'Other,·Anthony·N.'·#·Author·1·
;·
·?·#·Address·for·author·1·
;·
·
;·#·Footnote·for·author·1·
;·
·
'Else,·S.·O.'·#·Author·2·
;·
·?·#·Address·2·
;·
·
;·?·#·Footnote·2·
;·
·

_publ_section_abstract·
#·Text·of·the·abstract·
#·(a)·The·Abstract·must·be·self-contained·and·comprehensible·
#·without·the·rest·of·the·paper.·This·means·no·references·
#·to·atom·names·or·to·compound·numbers;·compounds·must·be·
#·identified·as·the·title·compound,·or·by·name·or·by·some·other·
#·means·such·as·derivatives·of·each·other·(e.g.·"the·
#·corresponding·ketone").·
#·(b)·The·chemical·formula·of·"the·title·compound"·must·be·given.·
#·(c)·Any·crystallographic·molecular·symmetry·should·be·
#·mentioned,·and·also·the·presence·of·more·than·one·molecule·
#·in·the·asymmetric·unit·(i.e.·anything·other·than·Z'=1).·
;·
·?·
;·
·

_publ_section_comment·
#·Text·of·the·paper·
#·Note·that·atoms·are·referenced·as·N2,·not·N(2)·or·N-2~.·
#·If·text·containing·()·occur·within·(),·the·outer·ones·should·be·[]·
#·Figures·should·be·referenced·as·Fih.·
;·
·
;·?·
;·
·

_publ_section_acknowledgements····#·Acknowledgments·
;·
·
;·?·
;·
·

_publ_section_figure_captions·
#·Captions·to·figures·-·Start·each·caption·on·a·new·line·after·a·blank·line.·
;·
·
Fig.·1.·
The·title·compound·with·displacement·ellipsoids·drawn·at·the·50%·
probability·level.·H·atoms·are·shown·as·spheres·of·
arbitary·radius.·
;·
·
;·?·
;·
·

_publ_section_exptl_refinement·
#·Some·potentially·useful·phrases·are·donated·by·Bill·Cleggː·
;·
In·the·absence·of·significant·anomalous·scattering,·Friedel·pairs·were·
merged.·
;·
·
The·absolute·configuration·was·arbitrarily·assigned.·
;·
·
The·relatively·large·ratio·of·minimum·to·maximum·corrections·applied·
in·the·multiscan·process·(1:nnn)·reflect·changes·in·the·illuminated·
volume·of·the·crystal.·
;·
·
Changes·in·illuminated·volume·were·kept·to·a·minimum,·and·were·
taken·into·account·(G\"orbitz,·1999)·by·the·multi-scan·inter-frame·
scaling·(DENZO/SCALEPACK,·Otwinowski·&·Minor,·1997).·
;·
·
;·"orbitz,·C.·H.·(1999).·Acta·Cryst.·B55,·1090-1098.·
;·
·
;·
·
The·H·atoms·were·all·located·in·a·difference·map,·but·those·
attached·to·carbon·atoms·were·repositioned·geometrically.·
The·H·atoms·were·initially·refined·with·soft·restraints·on·the·
bond·lengths·and·angles·to·regularise·their·geometry·
(C---H·in·the·range·0.93--0.98,·
N---H·in·the·range·0.86--0.89·
N---H·to·0.86·
O---H·--·0.82·
\tA)·
and·
U~iso~(H)·(in·the·range·1.2-1.5·times·U~eq~·of·the·parent·atom),·
after·which·the·positions·were·refined·with·riding·constraints.·
;·
·
;·
·

_publ_section_exptl_prep·
#·Brief·details·or·a·reference.··Include·solvent·if·known·
;·
·
;·
·
;·
·

#·PROCESSING·SUMMARY·(IUCr·Office·Use·Only):·
_journal_date_recd_electronic·····?·
_journal_date_to_coeditor·····?·
_journal_date_from_coeditor·····?·
_journal_date_accepted·····?·
_journal_date_printers_first·····?·
_journal_date_printers_final·····?·
_journal_date_proofs_out·····?·
_journal_date_proofs_in·····?·
_journal_coeditor_name·····?·
_journal_coeditor_code·····?·
_journal_coeditor_notes·····?·
_journal_techeditor_code·····?·
_journal_techeditor_notes·····?·
_journal_coden_ASTM·····?·

_journal_name_full·····?·
_journal_year·····?·
_journal_volume·····?·
_journal_issue·····?·
_journal_page_first·····?·
_journal_page_last·····?·
_journal_suppl_publ_number·····?·
_journal_suppl_publ_pages·····?·

#·End·of·'script/refcif.dat'·
;·
·
;·
·
#·Insert·your·own·references·if·required···in·alphabetical·order·
_publ_section_references·
;·
Altomare,·A.,·Burla,·M.C.,·Camalli,·M.,·Cascarano,·G.L.,·Giacovazzo,·C.,·
Guagliardi,·A.,·Grazia,·A.,·Moliterni,·G.,·Polidori,·G.·&·Spagna,·R.·
(1999).·J.·App.·Cryst.·32,·115-119.·
;·
·
Betteridge,·P.W.,·Carruthers,·J.R.,·Cooper,·R.I.,·
Prout,·K.·&·Watkin,·D.J.·(2003).·J.·Appl.·Cryst.·36,·1487.·
;·
·
Larson,·A.C.·(1970).·Crystallographic·Computing,·Ed·Ahmed,·F.R.,·
Munksgaard,·Copenhagen,·291-294.·
;·
·
Nonius·(1997-2001).·COLLECT.·Nonius·BV,·Delft,·The·Netherlands.·
;·
·
Otwinowski,·Z.·&·Minor,·W.·(1997).·Methods·in·Enzymology,·Vol.·276,·
edited·by·C.·W.·Carter·Jr·&·R.·M.·Sweet,·pp.·307--326.·
New·York:·Academic·Press.·
;·
·
Prince,·E.·
Mathematical·Techniques·in·Crystallography·
and·Materials·Science.·
Springer-Verlag,·New·York,·1982.·
;·
·
Watkin·D.J.·(1994).·
Acta·Cryst,·A50,·411-437.·
;·
·
Watkin,·D.J.,·Prout,·C.K.·&·Pearce,·L.J.·(1996).·CAMERON,·Chemical·
Crystallography·Laboratory,·Oxford,·UK.·
;·
·

#·Uequiv·=·arithmetic·mean·of·U1·i.e.·Ueqiv·=·(U1+U2+U3)/3·
;·
·
#·Replace·last·'.·with·number·of·unfound·hydrogen·atomsattached·to·an·atom.·
;·
·
#·...·refinement_flags_...·
#·..no·refinement·constraints··········S·special·position·constraint·on·site·
#·G·rigid·group·refinement·of·site·····R·riding·atom·
#·D·distance·or·angle·restraint·on·site·T·thermal·displacement·constraints·
#·U·Uiso·or·Uij·restraint·(rigid·bond)··P·partial·occupancy·constraint·
;·
·
loop_·
·_atom_site_label·
·_atom_site_type_symbol·
·_atom_site_fract_x·
·_atom_site_fract_y·
·_atom_site_fract_z·
·_atom_site_U_iso_or_equiv·
·_atom_site_occupancy·
·_atom_site_adp_type·
·_atom_site_refinement_flags_posn·
·_atom_site_refinement_flags_adp·
·_atom_site_refinement_flags_occupancy·
·_atom_site_disorder_assembly·
·_atom_site_disorder_group·
·_atom_site_attached_hydrogens·
Ir1·Ir·0.245687(2)·0.500656(3)·0.49556333(17)·0.0124·1.0000·Uani·.·.·.·.·.·.·
N1·N·0.31579(9)·0.43143(5)·0.53845(7)·0.0158·1.0000·Uani·.·.·.·.·.·.·
N2·N·0.17748(7)·0.57462(5)·0.46750(5)·0.0147·1.0000·Uani·.·.·.·.·.·.·
N3·N·0.30613(7)·0.50417(6)·0.39767(5)·0.0141·1.0000·Uani·.·.·.·.·.·.·
N4·N·0.16837(8)·0.43949(5)·0.43079(6)·0.0156·1.0000·Uani·.·.·.·.·.·.·
C1·C·0.18329(8)·0.48920(6)·0.58445(6)·0.0151·1.0000·Uani·.·.·.·.·.·.·
C2·C·0.11149(9)·0.52018(7)·0.60708(7)·0.0189·1.0000·Uani·.·.·.·.·.·.·
C3·C·0.07551(10)·0.50607(8)·0.67007(8)·0.0227·1.0000·Uani·.·.·.·.·.·.·
C4·C·0.10900(12)·0.46039(9)·0.71245(8)·0.0247·1.0000·Uani·.·.·.·.·.·.·
C5·C·0.17982(11)·0.42861(8)·0.69141(8)·0.0223·1.0000·Uani·.·.·.·.·.·.·
C6·C·0.21622(9)·0.44277(6)·0.62787(7)·0.0171·1.0000·Uani·.·.·.·.·.·.·
C7·C·0.29086(9)·0.41165(6)·0.60200(7)·0.0178·1.0000·Uani·.·.·.·.·.·.·
C8·C·0.33618(13)·0.36604(8)·0.63681(10)·0.0265·1.0000·Uani·.·.·.·.·.·.·
C9·C·0.40617(15)·0.34034(9)·0.60700(12)·0.0299·1.0000·Uani·.·.·.·.·.·.·
C10·C·0.43149(12)·0.36129(8)·0.54285(11)·0.0263·1.0000·Uani·.·.·.·.·.·.·
C11·C·0.38458(10)·0.40683(7)·0.51003(8)·0.0213·1.0000·Uani·.·.·.·.·.·.·
C12·C·0.32483(9)·0.55928(6)·0.54678(7)·0.0137·1.0000·Uani·.·.·.·.·.·.·
C13·C·0.40747(8)·0.55009(6)·0.58500(7)·0.0163·1.0000·Uani·.·.·.·.·.·.·
C14·C·0.45463(9)·0.59606(7)·0.61844(8)·0.0200·1.0000·Uani·.·.·.·.·.·.·
C15·C·0.42135(12)·0.65237(7)·0.61394(9)·0.0210·1.0000·Uani·.·.·.·.·.·.·
C16·C·0.34153(10)·0.66315(6)·0.57459(8)·0.0187·1.0000·Uani·.·.·.·.·.·.·
C17·C·0.29402(8)·0.61715(5)·0.54158(6)·0.0146·1.0000·Uani·.·.·.·.·.·.·
C18·C·0.21015(9)·0.62459(6)·0.49832(6)·0.0155·1.0000·Uani·.·.·.·.·.·.·
C19·C·0.16420(11)·0.67673(7)·0.48749(9)·0.0217·1.0000·Uani·.·.·.·.·.·.·
C20·C·0.08380(12)·0.67798(8)·0.44405(11)·0.0267·1.0000·Uani·.·.·.·.·.·.·
C21·C·0.05418(13)·0.62696(8)·0.41140(11)·0.0250·1.0000·Uani·.·.·.·.·.·.·
C22·C·0.10133(10)·0.57630(7)·0.42489(8)·0.0196·1.0000·Uani·.·.·.·.·.·.·
C23·C·0.03994(9)·0.53961(6)·0.38050(7)·0.0170·1.0000·Uani·.·.·.·.·.·.·
C24·C·0.40538(10)·0.53697(6)·0.31438(7)·0.0190·1.0000·Uani·.·.·.·.·.·.·
C25·C·0.37393(10)·0.49648(8)·0.26505(6)·0.0194·1.0000·Uani·.·.·.·.·.·.·
C26·C·0.30519(9)·0.45885(6)·0.28109(6)·0.0164·1.0000·Uani·.·.·.·.·.·.·
C27·C·0.26745(12)·0.41580(7)·0.23276(7)·0.0212·1.0000·Uani·.·.·.·.·.·.·
C28·C·0.19970(12)·0.38188(7)·0.25019(8)·0.0221·1.0000·Uani·.·.·.·.·.·.·
C29·C·0.16338(10)·0.38838(6)·0.31751(7)·0.0185·1.0000·Uani·.·.·.·.·.·.·
C30·C·0.09225(11)·0.35482(7)·0.33820(9)·0.0222·1.0000·Uani·.·.·.·.·.·.·
C31·C·0.06147(13)·0.36440(8)·0.40362(10)·0.0233·1.0000·Uani·.·.·.·.·.·.·
C32·C·0.10111(10)·0.40728(7)·0.44858(8)·0.0199·1.0000·Uani·.·.·.·.·.·.·
C33·C·0.19967(8)·0.43009(5)·0.36608(6)·0.0149·1.0000·Uani·.·.·.·.·.·.·
C34·C·0.27222(8)·0.46520(5)·0.34803(6)·0.0141·1.0000·Uani·.·.·.·.·.·.·
P1·P·0.35469(3)·0.71662(2)·0.32865(3)·0.0229·1.0000·Uani·.·.·.·.·.·.·
F1·F·0.27427(14)·0.69359(8)·0.40777(8)·0.0493·1.0000·Uani·.·.·.·.·.·.·
F2·F·0.33615(14)·0.74007(7)·0.24854(8)·0.0441·1.0000·Uani·.·.·.·.·.·.·
F3·F·0.43369(13)·0.76204(8)·0.34197(11)·0.0489·1.0000·Uani·.·.·.·.·.·.·
F4·F·0.42689(12)·0.67050(8)·0.31345(10)·0.0495·1.0000·Uani·.·.·.·.·.·.·
F5·F·0.42096(12)·0.66955(7)·0.30178(10)·0.0466·1.0000·Uani·.·.·.·.·.·.·
F6·F·0.28858(12)·0.76384(8)·0.35428(9)·0.0454·1.0000·Uani·.·.·.·.·.·.·
C51·C·0.6376(16)·0.2465(8)·0.1082(6)·0.0737·0.1500·Uani·D·U·.·.·.·.·
C52·C·0.6083(3)·0.2294(2)·0.1803(3)·0.0522·0.5500·Uani·D·U·.·.·.·.·
C61·C·0.7372(4)·0.2616(3)·0.0361(3)·0.0636·0.3000·Uani·D·U·.·.·.·.·
Cl51·Cl·0.6615(3)·0.21816(14)·0.0243(3)·0.0803·0.2500·Uani·D·U·.·.·.·.·

_publ_section_exptl_refinement·
#·Some·potentially·useful·phrases·are·donated·by·Bill·Cleggː·
;·
In·the·absence·of·significant·anomalous·scattering,·Friedel·pairs·were·
merged.·
;·
·
The·absolute·configuration·was·arbitrarily·assigned.·
;·
·
The·relatively·large·ratio·of·minimum·to·maximum·corrections·applied·
in·the·multiscan·process·(1:nnn)·reflect·changes·in·the·illuminated·
volume·of·the·crystal.·
;·
·
Changes·in·illuminated·volume·were·kept·to·a·minimum,·and·were·
taken·into·account·(G\"orbitz,·1999)·by·the·multi-scan·inter-frame·
scaling·(DENZO/SCALEPACK,·Otwinowski·&·Minor,·1997).·
;·
·
;·"orbitz,·C.·H.·(1999).·Acta·Cryst.·B55,·1090-1098.·
;·
·
;·
·
The·H·atoms·were·all·located·in·a·difference·map,·but·those·
attached·to·carbon·atoms·were·repositioned·geometrically.·
The·H·atoms·were·initially·refined·with·soft·restraints·on·the·
bond·lengths·and·angles·to·regularise·their·geometry·
(C---H·in·the·range·0.93--0.98,·
N---H·in·the·range·0.86--0.89·
N---H·to·0.86·
O---H·--·0.82·
\tA)·
and·
U~iso~(H)·(in·the·range·1.2-1.5·times·U~eq~·of·the·parent·atom),·
after·which·the·positions·were·refined·with·riding·constraints.·
;·
·
;·
·

_publ_section_exptl_prep·
#·Brief·details·or·a·reference.··Include·solvent·if·known·
;·
·
;·
·
;·
·

_atom_site_aniso_label·
·_atom_site_aniso_U_11·
·_atom_site_aniso_U_22·
·_atom_site_aniso_U_33·
·_atom_site_aniso_U_23·
·_atom_site_aniso_U_13·
·_atom_site_aniso_U_12·
Ir1·-0.013252(11)·0.013262(12)·0.011061(10)·-0.00057(2)·0.003140(7)·-0.00031(2)·
N1·0.0172(4)·0.0143(4)·0.0162(4)·0.0008(3)·0.0034(3)·0.0011(3)·
N2·0.0148(3)·0.0159(4)·0.0134(3)·0.0000(2)·0.0009(3)·0.0001(3)·
N3·0.0151(3)·0.0147(4)·0.0127(2)·-0.0002(3)·0.0031(2)·-0.0005(3)·
N4·0.0159(3)·0.0152(4)·0.0160(3)·-0.0011(3)·0.0035(3)·-0.0016(3)·
C1·0.0142(3)·0.0184(5)·0.0132(3)·-0.0004(2)·0.0035(3)·-0.0012(3)·
C2·0.0177(4)·0.0225(6)·0.0175(4)·-0.0015(4)·0.0063(4)·0.0005(4)·
C3·0.0193(4)·0.0315(9)·0.0183(4)·-0.0026(5)·0.0080(3)·-0.0015(5)·
C4·0.0228(6)·0.0353(8)·0.0171(4)·0.0025(5)·0.0078(4)·-0.0043(5)·
C5·0.0215(5)·0.0289(7)·0.0171(4)·-0.0062(4)·0.0050(4)·-0.0026(4)·
C6·0.0169(4)·0.0202(5)·0.0147(4)·0.0026(3)·0.0034(3)·-0.0015(3)·
C7·0.0180(4)·0.0186(5)·0.0169(4)·0.0033(3)·0.0022(3)·-0.0005(3)·
C8·0.0265(6)·0.0263(7)·0.0265(6)·0.0117(5)·0.0017(5)·0.0042(5)·
C9·0.0284(9)·0.0248(8)·0.0364(10)·0.0090(7)·0.0010(7)·0.0076(6)·
C10·0.0237(6)·0.0239(7)·0.0318(7)·0.0021(5)·0.0028(6)·0.0079(5)·
C11·0.0206(5)·0.0221(6)·0.0216(5)·0.0003(4)·0.0048(4)·0.0052(4)·
C12·0.0143(4)·0.0153(4)·0.0118(3)·0.0002(3)·0.0032(3)·-0.0013(3)·
C13·0.0145(4)·0.0192(5)·0.0154(4)·0.0005(3)·0.0016(3)·0.0006(3)·
C14·0.0158(4)·0.0237(6)·0.0201(5)·0.0000(4)·-0.0004(4)·-0.0025(4)·

C15·0.0198(6)·0.0216(6)·0.0211(5)·-0.0023(4)·-0.0007(4)·-0.0060(5)·
C16·0.0197(5)·0.0162(5)·0.0200(4)·-0.0011(3)·0.0014(4)·-0.0033(4)·
C17·0.0154(4)·0.0153(4)·0.0132(3)·-0.0003(3)·0.0017(3)·-0.0006(3)·
C18·0.0163(4)·0.0153(4)·0.0148(3)·0.0010(3)·0.0009(3)·-0.0001(3)·
C19·0.0224(5)·0.0157(5)·0.0263(6)·0.0013(4)·-0.0016(5)·0.0014(4)·
C20·0.0247(6)·0.0202(6)·0.0340(8)·0.0027(5)·-0.0047(6)·0.0049(5)·
C21·0.0203(6)·0.0239(7)·0.0293(7)·0.0023(5)·-0.0065(6)·0.0026(5)·
C22·0.0182(4)·0.0204(5)·0.0195(5)·0.0000(4)·-0.0030(4)·-0.0001(4)·
C23·0.0188(4)·0.0174(5)·0.0155(4)·-0.0010(3)·0.0054(3)·-0.0027(3)·
C24·0.0217(5)·0.0185(5)·0.0178(4)·0.0004(3)·0.0079(4)·-0.0021(4)·
C25·0.0235(4)·0.0208(5)·0.0147(3)·0.0002(4)·0.0069(3)·0.0016(5)·
C26·0.0208(4)·0.0165(4)·0.0123(3)·-0.0007(3)·0.0034(3)·0.0013(3)·
C27·0.0288(6)·0.0214(5)·0.0138(4)·-0.0043(3)·0.0034(4)·0.0002(5)·
C28·0.0287(6)·0.0210(6)·0.0164(4)·-0.0054(4)·0.0013(4)·-0.0063(5)·
C29·0.0217(5)·0.0161(5)·0.0174(4)·-0.0029(3)·0.0009(4)·-0.0021(4)·
C30·0.0223(5)·0.0195(5)·0.0246(6)·-0.0040(4)·0.0005(5)·-0.0053(4)·
C31·0.0218(6)·0.0215(6)·0.0269(7)·-0.0021(5)·0.0039(5)·-0.0073(5)·
C32·0.0199(5)·0.0198(5)·0.0207(5)·-0.0023(4)·0.0054(4)·-0.0051(4)·
C33·0.0173(4)·0.0130(4)·0.0145(3)·-0.0010(3)·0.0017(3)·-0.0001(3)·
C34·0.0169(4)·0.0139(4)·0.0118(3)·-0.0003(3)·0.0026(3)·0.0008(3)·
P1·0.02552(18)·0.01803(16)·0.02504(17)·-0.00161(12)·0.00161(14)·0.00050(13)·
F1·0.0708(12)·0.0466(9)·0.0288(6)·0.0080(6)·-0.0059(7)·0.0050(8)·
F2·0.0768(13)·0.0305(6)·0.0247(5)·-0.0008(5)·0.0032(7)·0.0066(7)·
F3·0.0461(9)·0.0349(7)·0.0662(12)·-0.0164(7)·0.0071(8)·-0.0179(7)·
F4·0.0412(8)·0.0494(9)·0.0573(10)·-0.0049(8)·0.0010(7)·-0.0218(7)·
F5·0.0469(8)·0.0297(6)·0.0622(10)·-0.0174(6)·-0.0014(8)·0.0137(6)·
F6·0.0475(9)·0.0526(9)·0.0367(7)·-0.0096(7)·0.0064(7)·0.0243(8)·
C51·0.047(6)·0.070(7)·0.099(6)·0.050(6)·-0.017(6)·0.001(6)·
C52·0.052(2)·0.036(2)·0.061(3)·0.0160(18)·-0.035(2)·-0.0171(18)·
C61·0.048(7)·0.024(3)·0.133(7)·0.008(4)·-0.035(4)·0.002(2)·
Cl51·0.081(2)·0.0357(13)·0.112(3)·-0.0108(17)·-0.060(2)·-0.0063(15)·
Cl52·0.112(2)·0.0532(13)·0.0531(13)·-0.0083(10)·-0.0360(13)·0.0190(14)·
Cl61·0.0478(17)·0.085(3)·0.061(2)·-0.018(2)·0.0018(16)·0.0014(17)·
C171·0.037(2)·0.082(4)·0.086(4)·-0.009(3)·-0.008(3)·-0.012(2)·

_refine_ls_extinction_method·
····'None'
_oxford_refine_ls_scale·0.12382(5)·
loop_·
·_geom_bond_atom_site_label_1·
·_geom_bond_site_symmetry_1·
·_geom_bond_atom_site_label_2·
·_geom_bond_site_symmetry_2·
·_geom_bond_distance·
·_geom_bond_publ_flag·
Ir1·..N1·..2.0480(13)····yes·
Ir1·..N2·..2.0433(11)····yes·
Ir1·..N3·..2.1367(9)····yes·
Ir1·..N4·..2.1496(11)····yes·
Ir1·..C1·..2.0167(12)····yes·
Ir1·..C12·..2.0034(13)····yes·
N1·..C17·..1.3675(18)····yes·
N1·..C11·..1.344(2)····yes·
N2·..C18·..1.3650(17)····yes·
N2·..C22·..1.3537(17)····yes·
N3·..C23·..1.3308(17)····yes·
N3·..C34·..1.3667(16)····yes·
N4·..C32·..1.3325(18)····yes·
N4·..C33·..1.3666(16)····yes·
C1·..C2·..1.4043(19)····yes·
```

```
C1··-C6··-1.4135(18)···yes
C2··-C3··-1.3934(19)···yes
C2··-H21··0.953····no
C3··-C4··1.394(3)···yes
C3··-H31··0.951····no
C4··-C5··1.391(3)···yes
C4··-H41··0.944····no
C5··-C6··1.4031(19)···yes
C5··-H51··0.928····no
C6··-C7··1.465(2)···yes
C7··-C8··1.391(2)···yes
C8··-C9··1.382(3)···yes
C8··-H81··0.906····no
C9··-C10··1.389(3)···yes
C9··-H91··0.940····no
C10··-C11··1.386(2)···yes
C10··-H101··0.926····no
C11··-H111··0.934····no
C12··-C13··1.4116(19)···yes
C12··-C17··1.4154(19)···yes
C13··-C14··1.400(2)···yes
C13··-H131··0.946····no
C14··-C15··1.394(2)···yes
C14··-H141··0.919····no
C15··-C16··1.391(2)···yes
C15··-H151··0.946····no
C16··-C17··1.3997(18)···yes
C16··-H161··0.954····no
C17··-C18··1.4654(17)···yes
C18··-C19··1.398(2)···yes
C19··-C20··1.389(2)···yes
C19··-H191··0.940····no
C20··-C21··1.395(3)···yes
C20··-H201··0.929····no
C21··-C22··1.384(2)···yes
C21··-H211··0.927····no
C22··-H221··0.923····no
C23··-C24··1.4042(18)···yes
C23··-H231··0.959····no
C24··-C25··1.375(2)···yes
C24··-H241··0.945····no
C25··-C26··1.413(2)···yes
C25··-H251··0.936····no
C26··-C27··1.4342(19)···yes
C26··-C34··1.4074(17)···yes
C27··-C28··1.359(2)···yes
C27··-H271··0.932····no
C28··-C29··1.437(2)···yes
C28··-H281··0.935····no
C29··-C30··1.415(2)···yes
C29··-C33··1.4081(17)···yes
C30··-C31··1.376(3)···yes
C30··-H301··0.957····no
C31··-C32··1.405(3)···yes
C31··-H311··0.932····no
C32··-H321··0.953····no
C33··-C34··1.4353(18)···yes
P1··-F1··1.5882(16)···yes
P1··-F2··1.6072(16)···yes
P1··-F3··1.5992(16)···yes

P1··-F4··1.6000(16)···yes
P1··-F5··1.5954(15)···yes
P1··-F6··1.5877(15)···yes
C51··-C52··1.520(9)···yes
C51··-C151··1.780(9)···yes
C51··-H511··0.960····no
C51··-H512··0.960····no
C52··-C152··1.477(6)···yes
C52··-C171··1.644(7)···yes
C52··-H521··0.960····no
C52··-H522··0.960····no
C61··-C61·4_655·1.544(9)···yes
C61··-C151·4_655·2.050(9)···yes
C61··-C151···1.529(8)···yes
C61··-C161···1.875(7)···yes
C61··-H611··0.960····no
C61··-H612··0.960····no
C152··-C152·5_655·1.445(8)···yes
C161··-C171···1.819(9)···yes
loop_
·geom_angle_atom_site_label_1
·geom_angle_site_symmetry_1
·geom_angle_atom_site_label_2
·geom_angle_site_symmetry_2
·geom_angle_atom_site_label_3
·geom_angle_site_symmetry_3
·geom_angle
·geom_angle_publ_flag
N1··-Ir1··-N2··-171.61(5)···yes
N1··-Ir1··-N3··-97.00(5)···yes
N2··-Ir1··-N3··-89.56(5)···yes
N1··-Ir1··-N4··-87.38(5)···yes
N2··-Ir1··-N4··-99.17(4)···yes
N3··-Ir1··-N4··-77.86(4)···yes
N1··-Ir1··-C1··-80.61(5)···yes
N2··-Ir1··-C1··-93.36(5)···yes
N3··-Ir1··-C1··-173.95(5)···yes
N4··-Ir1··-C1··-96.43(5)···yes
N1··-Ir1··-C12··-93.68(4)···yes
N2··-Ir1··-C12··-80.37(5)···yes
N3··-Ir1··-C12··-96.00(5)···yes
N4··-Ir1··-C12··-173.85(5)···yes
C1··-Ir1··-C12··-89.71(5)···yes
Ir1··-N1··-C7··-115.55(10)···yes
Ir1··-N1··-C11··-124.71(10)···yes
C7··-N1··-C11··-119.68(13)···yes
Ir1··-N2··-C18··-115.85(8)···yes
Ir1··-N2··-C22··-124.63(10)···yes
C18··-N2··-C22··-119.40(12)···yes
Ir1··-N3··-C23··-127.79(9)···yes
Ir1··-N3··-C34··-113.69(8)···yes
C23··-N3··-C34··-118.52(10)···yes
Ir1··-N4··-C32··-128.19(10)···yes
Ir1··-N4··-C33··-113.29(8)···yes
C32··-N4··-C33··-118.23(11)···yes
Ir1··-C1··-C2··-128.54(10)···yes
Ir1··-C1··-C6··-114.32(9)···yes
C2··-C1··-C6··-117.12(12)···yes
C1··-C2··-C3··-121.29(14)···yes
C1··-C2··-H21··-119.6··no

C3··-C2··-H21··-119.0··no
C2··-C3··-C4··-120.71(14)···yes
C2··-C3··-H31··-121.5···no
C4··-C3··-H31··-117.8···no
C3··-C4··-C5··-119.49(13)···yes
C3··-C4··-H41··-120.9···no
C5··-C4··-H41··-119.6···no
C4··-C5··-C6··-119.74(14)···yes
C4··-C5··-H51··-120.7···no
C6··-C5··-H51··-119.5···no
C1··-C6··-C5··-121.65(13)···yes
C1··-C6··-C7··-115.15(11)···yes
C5··-C6··-C7··-123.20(13)···yes
C6··-C7··-N1··-114.34(12)···yes
C6··-C7··-C8··-125.54(13)···yes
N1··-C7··-C8··-120.12(14)···yes
C7··-C8··-C9··-120.07(16)···yes
C7··-C8··-H81··-119.7···no
C9··-C8··-H81··-120.2···no
C8··-C9··-C10··-119.25(16)···yes
C8··-C9··-H91··-121.1···no
C10··-C9··-H91··-119.6···no
C9··-C10··-C11··-118.77(17)···yes
C9··-C10··-H101··-121.9···no
C11··-C10··-H101··-119.3···no
C10··-C11··-N1··-122.10(15)···yes
C10··-C11··-H111··-117.5···no
N1··-C11··-H111··-120.4···no
Ir1··-C12··-C13··-128.16(11)···yes
Ir1··-C12··-C17··-114.88(9)···yes
C13··-C12··-C17··-116.92(12)···yes
C12··-C13··-C14··-121.11(13)···yes
C12··-C13··-C131··-120.4···no
C14··-C13··-H131··-118.4···no
C13··-C14··-C15··-120.55(13)···yes
C13··-C14··-H141··-120.0···no
C15··-C14··-H141··-119.4···no
C14··-C15··-C16··-119.70(14)···yes
C14··-C15··-H151··-121.9···no
C16··-C15··-H151··-118.4···no
C15··-C16··-C17··-119.76(14)···yes
C15··-C16··-H161··-119.5···no
C17··-C16··-H161··-120.7···no
C12··-C17··-C16··-121.88(12)···yes
C12··-C17··-C18··-114.64(11)···yes
C16··-C17··-C18··-123.46(12)···yes
C17··-C18··-N2··-113.98(11)···yes
C17··-C18··-C19··-125.71(12)···yes
N2··-C18··-C19··-120.30(12)···yes
C18··-C19··-C20··-119.90(14)···yes
C18··-C19··-H191··-118.4···no
C20··-C19··-H191··-121.7···no
C19··-C20··-C21··-119.30(15)···yes
C19··-C20··-H201··-119.8···no
C21··-C20··-H201··-120.9···no
C20··-C21··-C22··-118.52(15)···yes
C20··-C21··-H211··-122.2···no
C22··-C21··-H211··-119.3···no
C21··-C22··-N2··-122.54(14)···yes
C21··-C22··-H221··-118.9···no

N2··-C22··-H221··-118.6···no
N3··-C23··-C24··-122.41(12)···yes
N3··-C23··-H231··-119.1····no
C24··-C23··-H231··-118.4···no
C23··-C24··-C25··-119.50(13)···yes
C23··-C24··-H241··-120.2···no
C25··-C24··-H241··-120.3···no
C24··-C25··-C26··-119.54(11)···yes
C24··-C25··-H251··-120.8···no
C26··-C25··-H251··-119.7···no
C25··-C26··-C27··-123.54(12)···yes
C25··-C26··-C34··-117.25(12)···yes
C27··-C26··-C34··-119.20(13)···yes
C26··-C27··-C28··-121.05(13)···yes
C26··-C27··-H271··-118.1····no
C28··-C27··-H271··-120.8···no
C27··-C28··-C29··-120.90(13)···yes
C27··-C28··-H281··-120.3···no
C29··-C28··-H281··-118.8···no
C28··-C29··-C30··-123.42(13)···yes
C28··-C29··-C33··-119.14(13)···yes
C30··-C29··-C33··-117.44(13)···yes
C29··-C30··-C31··-119.30(14)···yes
C29··-C30··-H301··-121.1····no
C31··-C30··-H301··-119.6····no
C30··-C31··-C32··-119.50(15)···yes
C30··-C31··-H311··-122.8····no
C32··-C31··-H311··-117.7····no
C31··-C32··-N4··-122.69(14)···yes
C31··-C32··-H321··-117.3····no
N4··-C32··-H321··-120.0····no
C29··-C33··-N4··-122.83(12)···yes
C29··-C33··-C34··-119.85(11)···yes
N4··-C33··-C34··-117.32(10)···yes
C33··-C34··-C26··-119.82(11)···yes
C33··-C34··-N3··-117.48(10)···yes
C26··-C34··-N3··-122.70(11)···yes
F1··-P1··-F2··-179.29(12)···yes
F1··-P1··-F3··-89.67(11)···yes
F2··-P1··-F3··-89.74(11)···yes
F1··-P1··-F4··-91.24(11)···yes
F2··-P1··-F4··-89.34(10)···yes
F3··-P1··-F4··-178.41(11)···yes
F1··-P1··-F5··-89.95(11)···yes
F2··-P1··-F5··-89.66(10)···yes
F3··-P1··-F5··-90.38(10)···yes
F4··-P1··-F5··-88.32(10)···yes
F1··-P1··-F6··-90.87(10)···yes
F2··-P1··-F6··-89.52(9)····yes
F3··-P1··-F6··-89.54(11)···yes
F4··-P1··-F6··-91.75(11)···yes
F5··-P1··-F6··-179.18(10)···yes
C52··-C51··-C151··-143.2(13)···yes
C52··-C51··-H511··-98.7····no
C151··-C51··-H511··-98.1····no
C52··-C51··-H512··-102.7····no
C151··-C51··-H512··-102.2····no
H511··-C51··-H512··-109.5····no
C51··-C52··-C152··-145.3(10)···yes
C152··-C52··-C171··-131.1(5)···yes

C51··-C52··-H521··-102.4····no
C152··-C52··-H521··-98.1····no
C171··-C52··-H521··-77.1····no
C51··-C52··-H522··-98.4····no
C152··-C52··-H522··-100.8····no
C171··-C52··-H522··-127.0····no
H521··-C52··-H522··-109.5····no
C61·4_655·C61··-C151··-83.7(6)···yes
C151·4_655·C61··-C151···-131.5(3)···yes
C61·4_655·C61··-C161···-114.1(6)···yes
C151·4_655·C61··-C161···-161.9(3)···yes
C61·4_655·C61··-H611··-108.4····no
C151·4_655·C61··-H611··-80.2····no
C151···C61··-H611··-123.1····no
C161···C61··-H611··-108.6····no
C61·4_655·C61··-H612··-107.8····no
C151·4_655·C61··-H612··-82.4····no
C151···C61··-H612··-119.2····no
C161···C61··-H612··-108.4····no
H611··-C61··-H612··-109.5····no
C51···C151···C61·4_655·129.3(8)····yes
C51···C151···C61···-80.8(8)····yes
C61·4_655·C151···C61···-48.5(3)···yes
C52···C152···C152·5_655·176.0(3)···yes
C61···C161···C171···82.6(3)····yes
C52···C171···C161···78.4(4)····yes
```

bis(2-phenylpyridine-*C*,*N*)(2-phenyl-1,10-phenanthroline-*N*,*N*')iridium(III) hexafluorophosphate (**48**)

```
data_sg88_1_f19
_audit_creation_date·····08-09-03
_audit_creation_method·CRYSTALS_ver_12.84
;
_oxford_structure_analysis_title··'sg88_1_f19_123k_0m·in·C2/m'
_chemical_name_systematic·····?
_chemical_melting_point·····?
;
_cell_length_a·····19.0044(4)
_cell_length_b·····25.7833(6)
_cell_length_c·····16.0565(3)
_cell_angle_alpha·····90
_cell_angle_beta·····96.2600(10)
_cell_angle_gamma·····90
_cell_volume·····7820.7(3)
;
_symmetry_cell_setting·····'Monoclinic'·
_symmetry_space_group_name_H-M···'C·2/m·'·
_symmetry_space_group_name_Hall···'-C·2y'·
loop_
·_symmetry_equiv_pos_as_xyz
·'x,y,z'
·'-x,-y,-z'
·'x+1/2,y+1/2,z'
·'-x+1/2,-y+1/2,-z'
·'-x,y,-z'
·'x,-y,z'
·'-x+1/2,y+1/2,-z'
·'x+1/2,-y+1/2,z'

loop_
_atom_type_symbol
_atom_type_scat_dispersion_real
_atom_type_scat_dispersion_imag
_atom_type_scat_Cromer_Mann_a1
_atom_type_scat_Cromer_Mann_b1
_atom_type_scat_Cromer_Mann_a2
_atom_type_scat_Cromer_Mann_b2
_atom_type_scat_Cromer_Mann_a3
_atom_type_scat_Cromer_Mann_b3
_atom_type_scat_Cromer_Mann_a4
_atom_type_scat_Cromer_Mann_b4
_atom_type_scat_Cromer_Mann_c
_atom_type_scat_source··
·C·····0.0033···0.0016····2.3100···20.8439···1.0200···10.2075···1.5886···0.5687
····0.8650···51.6512···0.2156·'International·Tables·Vol·C·4.2.6.8·and·6.1.1.4'
·H·····0.0000···0.0000···0.4930···10.5109···0.3229···26.1257···0.1402···3.1424
····0.0408···57.7998···0.0030·'International·Tables·Vol·C·4.2.6.8·and·6.1.1.4'
·N·····0.0061···0.0033···12.2126···0.0057···3.1322···9.8933···2.0125···28.9975
····1.1663···0.5826···11.5290·'International·Tables·Vol·C·4.2.6.8·and·6.1.1.4'
·F·····0.0171···0.0103···3.5392···10.2825···2.6412···4.2944···1.5170···0.2615
····1.0243···26.1476···0.2776·'International·Tables·Vol·C·4.2.6.8·and·6.1.1.4'
·P·····0.1023···0.0942···6.4345···1.9067···4.1791···27.1570···1.7800···0.5260
····1.4908···68.1645···1.1149·'International·Tables·Vol·C·4.2.6.8·and·6.1.1.4'
·Ir····-1.4442···7.9887···27.3049···1.1928···16.7296···8.8655···15.6115···0.4179
····5.8338···45.0011···11.4722·'International·Tables·Vol·C·4.2.6.8·and·6.1.1.4'
·Cl·····0.1484···0.1585···11.4604···0.0104···7.1964···1.1662···6.2556···18.5194
····1.8455···47.7784···0.5574·'International·Tables·Vol·C·4.2.6.8·and·6.1.1.4'
·Cl·····0.0106···0.0060···3.0485···13.2771···2.2868···5.7011···1.5463···0.3239
····0.8670···32.9089···0.2508·'International·Tables·Vol·C·4.2.6.8·and·6.1.1.4'
```

```
·
·
_cell_formula_units_Z·····8

#·Given·Formula·=·C40·H28·C10.25·F6·Ir1·N4·O0.25·P1·
#·Dc·=·····1.55·Fooo·=····3536.00·Mu·=·····35.14·M·=····914.73
#·Found·Formula·=·C40·H28·F6·Ir1·N4·P1·
#·Dc·=·····1.53·FOOO·=····3536.00·Mu·=·····35.16·M·=····901.87

_chemical_formula_sum·····'C40·H28·F6·Ir1·N4·P1'
_chemical_formula_moiety·····'C40·H28·Ir·N4,·F6·P'
_chemical_compound_source·····?
_chemical_formula_weight·····901.87
·
·
_cell_measurement_reflns_used·····0
_cell_measurement_theta_min·····0
_cell_measurement_theta_max·····0
_cell_measurement_temperature·····123
·
_exptl_crystal_description·····'needle'·
_exptl_crystal_colour·····'yellow'·
_exptl_crystal_size_min·····0.04·
_exptl_crystal_size_mid·····0.07·
_exptl_crystal_size_max·····0.21·
·
_exptl_crystal_density_diffrn····1.532·
_exptl_crystal_density_meas·····?·
#·Non-dispersive·F(000):·
_exptl_crystal_F_000·····3536·
_exptl_absorpt_coefficient_mu····3.516·
·
#·Sheldrick·geometric·approximatio·0.78·0.87·
#·No·experimental·values·of·Tmin/max·available·
_exptl_absorpt_correction_type····multi-scan·
_exptl_absorpt_process_details····'DENZO/SCALEPACK·(Otwinowski·&·Minor,·1997)'·
_exptl_absorpt_correction_T_min··0.78·
_exptl_absorpt_correction_T_max··0.87·
#·For·a·Kappa·CCD,·set·Tmin·to·1.0·and·
#·Tmax·to·the·ratio·of·max:min·frame·scales·in·scale_all.log·
_diffrn_measurement_device_type····'Nonius·KappaCCD'·
_diffrn_radiation_monochromator····'graphite'·
_diffrn_radiation_type·····'Mo·K\a'·
_diffrn_radiation_wavelength·····0.71073
_diffrn_measurement_method·····'\f·&·\w·scans'·
·
#·If·a·reference·occurs·more·than·once,·delete·the·author·
#·and·date·from·subsequent·references.·
_computing_data_collection····'COLLECT·(Nonius,·1997-2001).'·
_computing_cell_refinement·····'DENZO/SCALEPACK·(Otwinowski·&·Minor,·1997)'·
_computing_data_reduction·····'DENZO/SCALEPACK·(Otwinowski·&·Minor,·1997)'·
_computing_structure_solution····'SIR97·(Altomare·et·al.,·1999)'·
_computing_structure_refinement····'CRYSTALS·(Batteridge·et·al.,·2003)'·
_computing_publication_material····'CRYSTALS·(Batteridge·et·al.,·2003)'·
_computing_molecular_graphics·····'CAMERON·(Watkin·et·al.,·1996)'·
·
_diffrn_standards_interval_time··?·
_diffrn_standards_interval_count·?·
_diffrn_standards_number·····0·
_diffrn_standards_decay_%·····?·

·
_diffrn_ambient_temperature·····123·
_diffrn_reflns_number·····88828·
_reflns_number_total·····17233·
_diffrn_reflns_av_R_equivalents···0.034·
#·Number·of·reflections·with·Friedels·Law·is·17233·
#·Number·of·reflections·without·Friedels·Law·is·0·
#·Theoretical·number·of·reflections·is·about·18528·
·
·
_diffrn_reflns_theta_min·····1.927·
_diffrn_reflns_theta_max·····35.998·
_diffrn_measured_fraction_theta_max·0.912·
·
_diffrn_reflns_theta_full·····26.279·
_diffrn_measured_fraction_theta_full·0.995·
·
·
_diffrn_reflns_limit_h_min·····-30·
_diffrn_reflns_limit_h_max·····31·
_diffrn_reflns_limit_k_min·····-42·
_diffrn_reflns_limit_k_max·····42·
_diffrn_reflns_limit_l_min·····-19·
_diffrn_reflns_limit_l_max·····25·
_reflns_limit_h_min·····-30·
_reflns_limit_h_max·····31·
_reflns_limit_k_min·····0·
_reflns_limit_k_max·····42·
_reflns_limit_l_min·····0·
_reflns_limit_l_max·····25·
·
_oxford_diffrn_Wilson_B_factor···0.00·
_oxford_diffrn_Wilson_scale·····0.00·
·
_atom_sites_solution_primary·····direct·#heavy,direct,difmap,geom
#·_atom_sites_solution_secondary··difmap
_atom_sites_solution_hydrogens··geom
·
_refine_diff_density_min·····-1.55·
_refine_diff_density_max·····2.38·
·
·
_refine_ls_number_reflns·····12062·
_refine_ls_number_restraints·····624·
_refine_ls_number_parameters·····484·
·
#·refine_ls_R_factor_ref·0.0283·
_refine_ls_wR_factor_ref·····0.0162·
_refine_ls_goodness_of_fit_ref···0.9963·
·
#_reflns_number_all·17187·
_refine_ls_R_factor_all·····0.0443·
_refine_ls_wR_factor_all·····0.0191·
·
#·The·I/u(I)·cutoff·below·was·used·for·refinement·as·
#·well·as·the·_gt·R-factors:
_refine_threshold_expression·····I>3.0\s(I)
_reflns_number_gt·····12062·
_refine_ls_R_factor_gt·····0.0283·
_refine_ls_wR_factor_gt·····0.0163·

·
·
_refine_ls_shift/su_max·····0.003568·
·
#·choose·from:·rm·(reference·molecule·of·known·chirality),·
#·ad·(anomolous·dispersion···Flack),·rmad·(rm·and·ad),·
#·syn·(from·synthesis),·unk·(unknown)·or··(not·applicable).·
_chemical_absolute_configuration·'.'.·
·
·
_refine_ls_structure_factor_coef··F·
_refine_ls_matrix_type·····full·
_refine_ls_hydrogen_treatment·····constr·····#·none,·undef,·noref,·refall,
·refxyz,·refU,·constr·or·mixed
_refine_ls_weighting_scheme·····calc·
_refine_ls_weighting_details·
;
·Method,·part·1,·Chebychev·polynomial,·(Watkin,·1994,·Prince,·1982)·
·[weight]·=·1.0/[A·0·*T·0·(x)+A·1·*T·1·(x)·....+A·n·1·]*T·n·1·(x)]·
·where·A·i··are·the·Chebychev·coefficients·listed·below·and·x=·Fcalc/Fmax·
·Method··Robust·Weighting·(Prince,·1982)·
·W=·[weight]·*·[1-(deltaF/6*sigmaF)^2^]^2^.
·A·1··are:·
·0.795E·01··1.27··0.228··0.548·
;
·
·
·
#·Check·this·file·using·the·IUCr·facility·at:·
#·http://checkcif.iucr.org/·
·
#·The·content·below·is·held·in·the·file·'script/refcif.dat'.·This·is·a·text·
#·file·which·you·may·edit·to·reflect·local·conditions.·
#·items·which·need·looking·at·are·represented·by·a·'?'.·
#·Items·for·which·there·are·choices·are·prefixed·with·'choose·from'.·
·
_publ_contact_letter·
;·
·Please·consider·this·CIF·submission·for·
·publication·as·a·Short·Format·Paper·in·Acta·
·Crystallographica·E.·The·figures·will·be·
·sent·by·e-mail.·
;·
_publ_contact_author_name·····'Anthony·Other'·
_publ_contact_author_address·
;·
·Chemical·Crystallography·Laboratory,·
·Department·of·Chemistry,·
·University·of·Nowhere,·
·Nowhere,·NO1·4Y,·UK.·
;·
·
_publ_contact_author_phone·····'+44·1865·000000'·
_publ_contact_author_fax·····'+44·1865·000000'·
_publ_contact_author_email·····'a.n.other@chem.no.ac.uk'·
_publ_requested_journal·····'Section·E'·
_publ_requested_category·····EO·#·choose·from:·FI·FM·FO·CI·CM·CO·AD·
_publ_requested_coeditor_name····'Prof·William·Clegg'·

_publ_section_title·
#·Title·of·paper·--·generally·just·the·systematic·or·trivial·name·
```

```
; ? 
; 
 
# The loop structure below should contain the names and addresses of all 
# authors, in the required order of publication. Repeat as necessary. 
loop_ 
 _publ_author_name 
 _publ_author_address 
 _publ_author_footnote 
 'Other, Anthony N.' # Author 1 
; 
 ? # Address for author 1 
; 
; 
 ? # Footnote for author 1 
; 
 'Else, S. O.' # Author 2 
; 
 ? # Address 2 
; 
; 
 ? # Footnote 2 
; 
 
 
_publ_section_abstract 
# Text of the abstract 
# (a) The Abstract must be self-contained and comprehensible 
# without the rest of the paper. This means no references 
# to atom names or to compound numbers; compounds must be 
# identified as the title compound, or by name or by some other 
# means such as derivatives of each other (e.g. "the 
# corresponding ketone"). 
# (b) The chemical formula of "the title compound" must be given. 
# (c) Any crystallographic molecular symmetry should be 
# mentioned, and also the presence of more than one molecule 
# in the asymmetric unit (i.e. anything other than Z'=1). 
; 
? 
; 
_publ_section_comment 
# Text of the paper 
# Note that atoms are referenced as N2, not N(2) or N~2~ 
# If text containing () occur within (), the outer ones should be [] 
# Figures should be referenced as Fih. 
; 
? 
; 
_publ_section_acknowledgements    # Acknowledgments 
; 
? 
; 
_publ_section_figure_captions 
# Captions to figures - Start each caption on a new line after a blank line 
; 
Fig. 1. 
The title compound with displacement ellipsoids drawn at the 50% 
probability level. H atoms are shown as spheres of 
arbitary radius. 
 
; 
 
_publ_section_exptl_refinement 
# Some potentially useful phrases are donated by Bill Clegg: 
; 
In the absence of significant anomalous scattering, Friedel pairs were 
merged. 
 
The absolute configuration was arbitrarily assigned. 
 
The relatively large ratio of minimum to maximum corrections applied 
in the multiscan process (1:nnn) reflect changes in the illuminated 
volume of the crystal. 
 
Changes in illuminated volume were kept to a minimum, and were 
taken into account (G\"orbitz, 1999) by the multi-scan inter-frame 
scaling (DENZO/SCALEPACK, Otwinowski & Minor, 1997). 
 
 
G\"orbitz, C. H. (1999). Acta Cryst. B55, 1090-1098. 
 
 
 
 
The H atoms were all located in a difference map, but those 
attached to carbon atoms were repositioned geometrically. 
The H atoms were initially refined with soft restraints on the 
bond lengths and angles to regularise their geometry 
(C---H in the range 0.93--0.98, 
N---H in the range 0.86--0.89 
N---H to 0.86 
O---H = 0.82 
\%A) 
and 
U~iso~(H) (in the range 1.2-1.5 times U~eq~ of the parent atom), 
after which the positions were refined with riding constraints. 
 
; 
 
_publ_section_exptl_prep 
# Brief details or a reference. Include solvent if known 
; 
? 
; 
 
 
# PROCESSING SUMMARY (IUCr Office Use Only): 
_journal_date_recd_electronic     ? 
_journal_date_to_coeditor         ? 
_journal_date_from_coeditor       ? 
_journal_date_accepted            ? 
_journal_date_printers_first      ? 
_journal_date_printers_final      ? 
_journal_date_proofs_out          ? 
_journal_date_proofs_in           ? 
_journal_coeditor_name            ? 
_journal_coeditor_code            ? 
_journal_coeditor_notes           ? 
_journal_techeditor_code          ? 
_journal_techeditor_notes         ? 
_journal_coden_ASTM               ? 
_journal_name_full                ? 
_journal_year                     ? 
_journal_volume                   ? 
_journal_issue                    ? 
_journal_page_first               ? 
_journal_page_last                ? 
_journal_suppl_publ_number        ? 
_journal_suppl_publ_pages         ? 
 
# End of 'script/refcif.dat' 
 
 
 
# Insert your own references if required - in alphabetical order 
_publ_section_references 
; 
Altomare, A., Burla, M.C., Camalli, M., Cascarano, G.L., Giacovazzo, C., 
Guagliardi, A., Grazia, A., Moliterni, G., Polidori, G. & Spagna, R. 
(1999). J. App. Cryst. 32, 115-119. 
 
Betteridge, P.W., Carruthers, J.R., Cooper, R.I., 
Prout, K. & Watkin, D.J. (2003). J. Appl. Cryst. 36, 1487. 
 
Larson, A.C. (1970) Crystallographic Computing, Ed Ahmed, F.R., 
Munksgaard, Copenhagen, 291-294. 
 
Nonius (1997-2001). COLLECT. Nonius BV, Delft, The Netherlands. 
 
Otwinowski, Z. & Minor, W. (1997). Methods in Enzymology, Vol. 276, 
edited by C. W. Carter Jr & R. M. Sweet, pp. 307--326. 
New York: Academic Press. 
 
Prince, E. 
Mathematical Techniques in Crystallography 
and Materials Science 
Springer-Verlag, New York, 1982. 
 
Watkin D.J. (1994). 
Acta Cryst, A50, 411-437. 
 
Watkin, D.J., Prout, C.K. & Pearce, L.J. (1996). CAMERON, Chemical 
Crystallography Laboratory, Oxford, UK. 
; 

# Uequiv = arithmetic mean of Ui i.e. Ueqiv = (U1+U2+U3)/3

# Replace last . with number of unfound hydrogen atomsattached to an atom.

# ..._refinement_flags_... 
# . no refinement constraints           S special position constraint on site
# G rigid group refinement of site      R riding atom
# D distance or angle restraint on site T thermal displacement constraints
# U Uiso or Uij restraint (rigid bond)  P partial occupancy constraint


loop_
_atom_site_label
_atom_site_type_symbol
_atom_site_fract_x
_atom_site_fract_y
_atom_site_fract_z
_atom_site_U_iso_or_equiv
_atom_site_occupancy
_atom_site_adp_type
_atom_site_refinement_flags_posn
_atom_site_refinement_flags_adp
_atom_site_refinement_flags_occupancy
_atom_site_disorder_assembly
_atom_site_disorder_group
_atom_site_attached_hydrogens
Ir1 Ir 0.202471(4) 0.266336(3) 0.275421(4) 0.0182 1.0000 Uani . . . . . . . . . .
N1 N 0.17316(9) 0.32021(7) 0.36741(11) 0.0216 1.0000 Uani . . . . . . . . .
N2 N 0.08730(8) 0.27868(7) 0.23900(11) 0.0223 1.0000 Uani . . . . . . . . .
N3 N 0.17566(8) 0.19810(7) 0.32825(10) 0.0190 1.0000 Uani . . . . . . . . .
N4 N 0.2376(1) 0.33088(7) 0.21833(11) 0.0241 1.0000 Uani . . . . . . . . .
C1 C 0.21655(11) 0.33992(9) 0.43025(14) 0.0267 1.0000 Uani . . . . . . . . .
C2 C 0.19692(13) 0.38070(10) 0.47993(16) 0.0329 1.0000 Uani . . . . . . . . .
C3 C 0.13045(14) 0.40207(10) 0.46440(17) 0.0352 1.0000 Uani . . . . . . . . .
C4 C 0.08324(13) 0.38149(10) 0.39926(16) 0.0312 1.0000 Uani . . . . . . . . .
C5 C 0.01223(14) 0.40019(12) 0.38005(19) 0.0404 1.0000 Uani . . . . . . . . .
C6 C -0.03235(14) 0.37740(12) 0.31971(18) 0.0416 1.0000 Uani . . . . . . . . .
C7 C -0.00980(11) 0.33482(11) 0.27239(16) 0.0320 1.0000 Uani . . . . . . . . .
C8 C -0.05639(12) 0.30780(12) 0.21360(17) 0.0381 1.0000 Uani . . . . . . . . .
C9 C -0.03126(11) 0.26711(13) 0.17164(15) 0.0354 1.0000 Uani . . . . . . . . .
C10 C 0.04125(10) 0.25342(9) 0.18393(13) 0.0259 1.0000 Uani . . . . . . . . .
C11 C 0.10684(11) 0.34061(9) 0.35153(14) 0.0245 1.0000 Uani . . . . . . . . .
C12 C 0.06092(10) 0.31771(9) 0.28511(13) 0.0245 1.0000 Uani . . . . . . . . .
C13 C 0.06390(11) 0.20982(10) 0.13362(14) 0.0291 1.0000 Uani . . . . . . . . .
C14 C 0.09573(15) 0.21869(13) 0.06059(15) 0.0417 1.0000 Uani . . . . . . . . .
C15 C 0.11068(17) 0.17696(16) 0.01072(18) 0.0504 1.0000 Uani . . . . . . . . .
C16 C 0.09494(16) 0.12813(16) 0.0322(2) 0.0522 1.0000 Uani . . . . . . . . .
C17 C 0.06307(17) 0.11840(14) 0.1045(2) 0.0513 1.0000 Uani . . . . . . . . .
C18 C 0.04739(14) 0.15948(12) 0.15534(19) 0.0397 1.0000 Uani . . . . . . . . .
C19 C 0.14164(10) 0.19473(9) 0.39754(13) 0.0234 1.0000 Uani . . . . . . . . .
C20 C 0.11994(11) 0.14795(10) 0.42793(14) 0.0278 1.0000 Uani . . . . . . . . .
C21 C 0.13325(13) 0.10274(10) 0.38477(16) 0.0320 1.0000 Uani . . . . . . . . .
C22 C 0.16920(12) 0.10585(9) 0.31430(15) 0.0286 1.0000 Uani . . . . . . . . .
C23 C 0.19096(10) 0.15420(8) 0.28693(13) 0.0223 1.0000 Uani . . . . . . . . .
C24 C 0.22777(10) 0.16337(9) 0.21293(12) 0.0222 1.0000 Uani . . . . . . . . .
C25 C 0.25365(12) 0.12368(10) 0.16553(14) 0.0288 1.0000 Uani . . . . . . . . .
C26 C 0.28567(13) 0.13549(11) 0.09489(14) 0.0307 1.0000 Uani . . . . . . . . .
C27 C 0.29179(12) 0.18710(11) 0.07146(14) 0.0313 1.0000 Uani . . . . . . . . .
C28 C 0.26738(11) 0.22674(10) 0.11922(12) 0.0265 1.0000 Uani . . . . . . . . .
C29 C 0.23442(10) 0.21594(8) 0.19121(12) 0.0214 1.0000 Uani . . . . . . . . .
C30 C 0.19753(15) 0.36099(9) 0.16321(14) 0.0312 1.0000 Uani . . . . . . . . .
C31 C 0.22417(18) 0.40450(11) 0.12789(17) 0.0411 1.0000 Uani . . . . . . . . .
C32 C 0.29478(18) 0.41777(11) 0.15003(19) 0.0446 1.0000 Uani . . . . . . . . .
C33 C 0.33575(16) 0.38749(11) 0.20657(17) 0.0380 1.0000 Uani . . . . . . . . .
C34 C 0.30709(12) 0.34369(9) 0.24104(14) 0.0269 1.0000 Uani . . . . . . . . .
C35 C 0.34423(10) 0.30803(9) 0.30104(13) 0.0248 1.0000 Uani . . . . . . . . .
C36 C 0.41456(12) 0.31517(10) 0.33577(15) 0.0319 1.0000 Uani . . . . . . . . .
C37 C 0.44561(11) 0.27900(12) 0.39204(15) 0.0359 1.0000 Uani . . . . . . . . .
C38 C 0.40769(10) 0.23602(12) 0.41353(14) 0.0315 1.0000 Uani . . . . . . . . .
C39 C 0.33751(10) 0.22921(10) 0.37931(13) 0.0256 1.0000 Uani . . . . . . . . .
C40 C 0.30415(9) 0.26519(9) 0.32340(11) 0.0210 1.0000 Uani . . . . . . . . .
P1 P 0.32581(5) 0.0000 0.34063(6) 0.0282 1.0000 Uani S T . . . . . .
P2 P -0.00690(8) 0.0000 0.25814(16) 0.0807 1.0000 Uani S T . . . . . .
F1 F 0.37544(16) 0.0000 0.26672(19) 0.0593 1.0000 Uani S T . . . . . .
F2 F 0.27757(12) 0.0000 0.41522(15) 0.0399 1.0000 Uani S T . . . . . .
F3 F 0.39574(12) 0.0000 0.40706(17) 0.0426 1.0000 Uani S T . . . . . .
F4 F 0.25729(13) 0.0000 0.27339(15) 0.0418 1.0000 Uani S T . . . . . .
F5 F 0.32558(9) 0.06189(5) 0.34167(12) 0.0390 1.0000 Uani . . . . . . . . .
F11 F 0.0710(2) 0.0000 0.2356(5) 0.1411 1.0000 Uani S T . . . . . .
F12 F -0.0865(2) 0.0000 0.2693(4) 0.1137 1.0000 Uani S T . . . . . .
F13 F 0.0232(3) 0.0000 0.3512(4) 0.1391 1.0000 Uani S T . . . . . .
F14 F -0.0365(3) 0.0000 0.1633(4) 0.1340 1.0000 Uani S T . . . . . .
F15 F -0.00696(13) 0.06152(9) 0.2608(2) 0.0988 1.0000 Uani . . . . . . . . .
H11 H 0.2617 0.3259 0.4414 0.0330 1.0000 Uiso R . . . . . . .
H21 H 0.2288 0.3933 0.5240 0.0402 1.0000 Uiso R . . . . . . .
H31 H 0.1164 0.4296 0.4971 0.0431 1.0000 Uiso R . . . . . . .
H51 H -0.0033 0.4283 0.4100 0.0492 1.0000 Uiso R . . . . . . .
H61 H -0.0792 0.3891 0.3081 0.0488 1.0000 Uiso R . . . . . . .
H81 H -0.1046 0.3179 0.2048 0.0458 1.0000 Uiso R . . . . . . .
H91 H -0.0625 0.2481 0.1343 0.0430 1.0000 Uiso R . . . . . . .
H141 H 0.1056 0.2523 0.0452 0.0512 1.0000 Uiso R . . . . . . .
H151 H 0.1324 0.1829 -0.0375 0.0602 1.0000 Uiso R . . . . . . .
H161 H 0.1052 0.1012 -0.0019 0.0618 1.0000 Uiso R . . . . . . .
H171 H 0.0522 0.0850 0.1202 0.0619 1.0000 Uiso R . . . . . . .
H181 H 0.0271 0.1530 0.2025 0.0490 1.0000 Uiso R . . . . . . .
H191 H 0.1324 0.2252 0.4251 0.0286 1.0000 Uiso R . . . . . . .
H201 H 0.0973 0.1468 0.4762 0.0345 1.0000 Uiso R . . . . . . .
H211 H 0.1187 0.0708 0.4023 0.0388 1.0000 Uiso R . . . . . . .
H221 H 0.1783 0.0760 0.2857 0.0357 1.0000 Uiso R . . . . . . .
H251 H 0.2490 0.0897 0.1817 0.0363 1.0000 Uiso R . . . . . . .
H261 H 0.3029 0.1096 0.0629 0.0381 1.0000 Uiso R . . . . . . .
H271 H 0.3128 0.1948 0.0233 0.0380 1.0000 Uiso R . . . . . . .
H281 H 0.2735 0.2611 0.1023 0.0333 1.0000 Uiso R . . . . . . .
H301 H 0.1506 0.3516 0.1488 0.0389 1.0000 Uiso R . . . . . . .
H311 H 0.1954 0.4237 0.0902 0.0499 1.0000 Uiso R . . . . . . .
H321 H 0.3147 0.4470 0.1273 0.0552 1.0000 Uiso R . . . . . . .
H331 H 0.3827 0.3962 0.2228 0.0478 1.0000 Uiso R . . . . . . .
H361 H 0.4393 0.3443 0.3206 0.0400 1.0000 Uiso R . . . . . . .
H371 H 0.4922 0.2841 0.4159 0.0431 1.0000 Uiso R . . . . . . .
H381 H 0.4282 0.2113 0.4511 0.0389 1.0000 Uiso R . . . . . . .
H391 H 0.3130 0.2000 0.3950 0.0320 1.0000 Uiso R . . . . . . .
loop_
_atom_site_aniso_label
_atom_site_aniso_U_11
_atom_site_aniso_U_22
_atom_site_aniso_U_33
_atom_site_aniso_U_23
_atom_site_aniso_U_13
_atom_site_aniso_U_12
Ir1 0.01346(3) 0.02203(3) 0.01826(3) 0.00191(3) -0.002286(18) 0.00046(3) 
N1 0.0178(7) 0.0229(7) 0.0234(7) 0.0008(6) -0.0008(5) 0.0029(6) 
N2 0.0155(6) 0.0288(8) 0.0214(7) 0.0043(6) -0.0037(5) 0.0016(6) 
N3 0.0140(6) 0.0213(7) 0.0212(7) 0.0013(6) -0.0007(5) -0.0003(5) 
N4 0.0257(8) 0.0229(8) 0.0232(7) 0.0024(6) 0.0008(6) -0.0007(6) 
C1 0.0220(8) 0.0289(10) 0.0282(10) -0.0022(8) -0.0025(7) 0.0020(7) 
C2 0.0315(11) 0.0346(12) 0.0317(11) -0.0076(9) -0.0006(9) 0.0024(9) 
C3 0.0353(12) 0.0304(11) 0.0396(13) -0.0052(10) 0.0029(10) 0.0077(9) 
C4 0.0273(10) 0.0305(11) 0.0355(11) -0.0002(9) 0.0019(8) 0.0083(8) 
C5 0.0308(11) 0.0407(14) 0.0497(15) -0.0023(12) 0.0038(10) 0.0180(10) 
C6 0.0245(10) 0.0519(16) 0.0478(14) 0.0000(12) 0.0011(10) 0.0172(11) 
C7 0.0177(8) 0.0411(13) 0.0360(11) 0.0073(10) -0.0018(8) 0.0084(8) 
C8 0.0169(8) 0.0595(17) 0.0364(12) 0.0040(11) -0.0041(8) 0.0074(10) 
C9 0.0163(8) 0.0551(15) 0.0324(10) 0.0013(11) -0.0078(7) -0.0005(10) 
C10 0.0173(8) 0.0375(11) 0.0217(8) 0.0033(8) -0.0036(6) -0.0006(7) 
C11 0.0194(8) 0.0246(9) 0.0291(9) 0.0033(7) 0.0005(7) 0.0041(7) 
C12 0.0176(8) 0.0298(10) 0.0253(9) 0.0058(7) -0.0008(6) 0.0033(7) 
C13 0.0181(8) 0.0444(13) 0.0228(9) -0.0017(8) -0.0066(7) -0.0011(8) 
C14 0.0409(13) 0.0590(18) 0.0248(10) 0.0044(11) 0.0020(9) 0.0028(12) 
C15 0.0436(15) 0.080(2) 0.0255(11) -0.0052(13) -0.0048(10) 0.0116(16) 
C16 0.0354(13) 0.076(2) 0.0427(15) -0.0252(16) -0.0086(12) 0.0069(14) 
C17 0.0387(14) 0.0470(17) 0.068(2) -0.0147(15) 0.0035(14) -0.0020(13) 
C18 0.0283(11) 0.0453(15) 0.0456(14) -0.0040(12) 0.0047(10) -0.0036(10) 
C19 0.0168(7) 0.0290(10) 0.0238(8) 0.0007(7) 0.0003(6) -0.0004(7) 
C20 0.0220(9) 0.0336(11) 0.0281(10) 0.0058(8) 0.0043(7) -0.0013(8) 
C21 0.0307(11) 0.0277(11) 0.0380(12) 0.0036(9) 0.0046(9) -0.0070(8) 
C22 0.0280(10) 0.0232(9) 0.0346(11) -0.0012(8) 0.0027(8) -0.0026(8) 
C23 0.0188(8) 0.0249(9) 0.0225(8) -0.0012(7) -0.0006(6) 0.0006(6) 
C24 0.0186(7) 0.0270(9) 0.0204(8) -0.0003(7) -0.0007(6) 0.0010(7) 
C25 0.0278(10) 0.0301(11) 0.0279(10) -0.0023(8) 0.0000(8) 0.0046(8) 
C26 0.0274(10) 0.0399(12) 0.0246(9) -0.0049(9) 0.0014(8) 0.0065(9) 
C27 0.0290(10) 0.0445(13) 0.0203(9) 0.0008(8) 0.0018(7) 0.0039(9) 
C28 0.0244(8) 0.0339(11) 0.0208(8) 0.0030(7) 0.0006(7) 0.0021(8) 
C29 0.0165(7) 0.0280(9) 0.0187(8) 0.0003(7) -0.0031(6) 0.0015(6) 
C30 0.0416(12) 0.0258(10) 0.0254(10) 0.0041(8) -0.0001(9) 0.0034(9) 
C31 0.0627(17) 0.0284(11) 0.0317(12) 0.0075(9) 0.0030(11) 0.0025(12) 
C32 0.0627(18) 0.0280(12) 0.0443(15) 0.0072(11) 0.0116(13) -0.0093(12) 
C33 0.0439(14) 0.0314(12) 0.0398(13) 0.0000(10) 0.0088(11) -0.0124(10) 
C34 0.0279(10) 0.0268(10) 0.0268(10) -0.0025(7) 0.0060(7) -0.0061(8) 
C35 0.0183(8) 0.0295(10) 0.0264(9) -0.0044(7) 0.0016(7) -0.0057(7) 
C36 0.0218(9) 0.0406(13) 0.0333(11) -0.0078(9) 0.0033(8) -0.0100(9) 
C37 0.0145(8) 0.0589(17) 0.0331(11) -0.0085(11) -0.0027(7) -0.0020(9) 
C38 0.0175(8) 0.0479(13) 0.0274(9) -0.0020(10) -0.0050(7) 0.0054(9) 
C39 0.0148(7) 0.0360(11) 0.0248(8) 0.0020(8) -0.0025(6) 0.0019(7) 
C40 0.0156(7) 0.0255(8) 0.0215(7) -0.0009(7) -0.0001(6) -0.0005(7) 
P1 0.0288(4) 0.0172(3) 0.0395(4) 0.0000 0.0082(3) 0.0000 
P2 0.0423(7) 0.0282(5) 0.1643(19) 0.0000 -0.0220(9) 0.0000 
F1 0.0625(17) 0.0578(17) 0.0642(17) 0.0000 0.0364(14) 0.0000 
F2 0.0414(12) 0.0329(11) 0.0483(13) 0.0000 0.0186(10) 0.0000 
F3 0.0322(11) 0.0272(10) 0.0659(16) 0.0000 -0.0056(10) 0.0000 
F4 0.0502(13) 0.0240(10) 0.0482(13) 0.0000 -0.0082(11) 0.0000 
F5 0.0417(8) 0.0166(6) 0.0578(10) 0.0029(6) 0.0018(7) -0.0030(6) 
F11 0.055(2) 0.0417(19) 0.326(6) 0.0000 0.019(3) 0.0000 
F12 0.064(2) 0.0423(18) 0.235(5) 0.0000 0.019(3) 0.0000 
F13 0.168(4) 0.055(2) 0.178(5) 0.0000 -0.059(4) 0.0000 
F14 0.138(4) 0.097(3) 0.158(4) 0.0000 -0.028(4) 0.0000 
F15 0.0576(13) 0.0332(10) 0.199(3) 0.0054(15) -0.0171(17) 0.0053(10) 

_refine_ls_extinction_method 
    'None'
_oxford_refine_ls_scale 0.08720(3) 
loop_
 _geom_bond_atom_site_label_1
 _geom_bond_site_symmetry_1
 _geom_bond_atom_site_label_2
 _geom_bond_site_symmetry_2
 _geom_bond_distance
 _geom_bond_publ_flag
Ir1 . N1 . 2.1448(18)    yes
Ir1 . N2 . 2.2259(16)    yes
Ir1 . N3 . 2.0418(17)    yes
Ir1 . N4 . 2.0466(18)    yes
Ir1 . C29 . 2.016(2)    yes
Ir1 . C40 . 2.0008(17)    yes
N1 . C1 . 1.332(3)    yes
N1 . C11 . 1.364(3)    yes
N2 . C10 . 1.343(3)    yes
N2 . C12 . 1.376(3)    yes
N3 . C19 . 1.349(3)    yes
N3 . C23 . 1.359(3)    yes
N4 . C30 . 1.348(3)    yes
N4 . C34 . 1.372(3)    yes
C1 . C2 . 1.395(3)    yes
C1 . H11 . 0.931    no
C2 . C3 . 1.376(4)    yes
C2 . H21 . 0.938    no
C3 . C4 . 1.406(4)    yes
C3 . H31 . 0.939    no
C4 . C5 . 1.435(3)    yes
C4 . C11 . 1.405(3)    yes
C5 . C6 . 1.350(4)    yes
C5 . H51 . 0.935    no
C6 . C7 . 1.427(4)    yes
C6 . H61 . 0.939    no
C7 . C8 . 1.407(4)    yes
C7 . C12 . 1.408(3)    yes
C8 . C9 . 1.361(4)    yes
C8 . H81 . 0.948    no
C9 . C10 . 1.415(3)    yes
C9 . H91 . 0.935    no
C10 . C13 . 1.476(3)    yes
C11 . C12 . 1.430(3)    yes
C13 . C14 . 1.396(4)    yes
C13 . C18 . 1.389(4)    yes
C14 . C15 . 1.389(5)    yes
C14 . H141 . 0.927    no
C15 . C16 . 1.347(6)    yes
C15 . H151 . 0.930    no
C16 . C17 . 1.390(5)    yes
C16 . H161 . 0.918    no
C17 . C18 . 1.389(4)    yes
C17 . H171 . 0.927    no
C18 . H181 . 0.902    no
C19 . C20 . 1.381(3)    yes
C19 . H191 . 0.928    no
C20 . C21 . 1.393(4)    yes
C20 . H201 . 0.927    no
C21 . C22 . 1.386(3)    yes
C21 . H211 . 0.922    no
C22 . C23 . 1.399(3)    yes
C22 . H221 . 0.923    no
C23 . C24 . 1.462(3)    yes
C24 . C25 . 1.397(3)    yes
C24 . C29 . 1.408(3)    yes
C25 . C26 . 1.378(3)    yes
C25 . H251 . 0.922    no
C26 . C27 . 1.391(4)    yes
C26 . H261 . 0.925    no
C27 . C28 . 1.388(3)    yes
C27 . H271 . 0.930    no
C28 . C29 . 1.401(3)    yes
C28 . H281 . 0.938    no
C30 . C31 . 1.378(4)    yes
C30 . H301 . 0.929    no
C31 . C32 . 1.393(4)    yes
C31 . H311 . 0.915    no
C32 . C33 . 1.373(4)    yes
C32 . H321 . 0.934    no
C33 . C34 . 1.394(3)    yes
C33 . H331 . 0.929    no
C34 . C35 . 1.457(3)    yes
C35 . C36 . 1.403(3)    yes
C35 . C40 . 1.410(3)    yes
C36 . C37 . 1.385(4)    yes
C36 . H361 . 0.932    no
C37 . C38 . 1.386(4)    yes
C37 . H371 . 0.935    no
C38 . C39 . 1.397(3)    yes
C38 . H381 . 0.933    no
C39 . C40 . 1.395(3)    yes
C39 . H391 . 0.934    no
P1 . F5 6_555 1.5957(14)    yes
P1 . F1 . 1.594(3)    yes
P1 . F2 . 1.586(2)    yes
P1 . F3 . 1.611(2)    yes
P1 . F4 . 1.598(2)    yes
P1 . F5 . 1.5957(14)    yes
P2 . F15 6_555 1.587(2)    yes
P2 . F11 . 1.562(5)    yes
P2 . F12 . 1.543(5)    yes
P2 . F13 . 1.540(6)    yes
P2 . F14 . 1.565(6)    yes
P2 . F15 . 1.587(2)    yes
loop_
 _geom_angle_atom_site_label_1
 _geom_angle_site_symmetry_1
 _geom_angle_atom_site_label_2
 _geom_angle_site_symmetry_2
 _geom_angle_atom_site_label_3
 _geom_angle_site_symmetry_3
 _geom_angle
 _geom_angle_publ_flag
N1 . Ir1 . N2 . 76.50(6)    yes
N1 . Ir1 . N3 . 100.17(7)    yes
N2 . Ir1 . N3 . 87.11(6)    yes
N1 . Ir1 . N4 . 84.47(7)    yes
N2 . Ir1 . N4 . 97.20(7)    yes
N3 . Ir1 . N4 . 174.33(7)    yes
N1 . Ir1 . C29 . 177.51(7)    yes
N2 . Ir1 . C29 . 105.99(7)    yes
N3 . Ir1 . C29 . 80.23(8)    yes
N4 . Ir1 . C29 . 94.99(8)    yes
N1 . Ir1 . C40 . 93.26(7)    yes
N2 . Ir1 . C40 . 169.71(8)    yes
N3 . Ir1 . C40 . 95.84(8)    yes
N4 . Ir1 . C40 . 80.56(8)    yes
C29 . Ir1 . C40 . 84.25(8)    yes
Ir1 . N1 . C1 . 125.65(14)    yes
Ir1 . N1 . C11 . 115.16(14)    yes
C1 . N1 . C11 . 118.52(19)    yes
Ir1 . N2 . C10 . 130.94(15)    yes
Ir1 . N2 . C12 . 111.65(12)    yes
C10 . N2 . C12 . 117.35(17)    yes
Ir1 . N3 . C19 . 124.19(15)    yes
Ir1 . N3 . C23 . 115.99(13)    yes
C19 . N3 . C23 . 119.75(18)    yes
Ir1 . N4 . C30 . 125.02(16)    yes
Ir1 . N4 . C34 . 115.36(14)    yes
C30 . N4 . C34 . 119.6(2)    yes
N1 . C1 . C2 . 122.6(2)    yes
N1 . C1 . H11 . 118.6    no
C2 . C1 . H11 . 118.8    no
C1 . C2 . C3 . 119.7(2)    yes
C1 . C2 . H21 . 120.1    no
C3 . C2 . H21 . 120.2    no
C2 . C3 . C4 . 118.9(2)    yes
C2 . C3 . H31 . 120.9    no
C4 . C3 . H31 . 120.3    no
C3 . C4 . C5 . 122.8(2)    yes
C3 . C4 . C11 . 118.2(2)    yes
C5 . C4 . C11 . 118.9(2)    yes
C4 . C5 . C6 . 120.7(2)    yes
C4 . C5 . H51 . 119.4    no
C6 . C5 . H51 . 119.9    no
C5 . C6 . C7 . 121.0(2)    yes
C5 . C6 . H61 . 120.6    no
C7 . C6 . H61 . 118.3    no
C6 . C7 . C8 . 122.3(2)    yes
C6 . C7 . C12 . 120.1(2)    yes
C8 . C7 . C12 . 117.6(2)    yes
C7 . C8 . C9 . 119.0(2)    yes
C7 . C8 . H81 . 119.4    no
C9 . C8 . H81 . 121.6    no
C8 . C9 . C10 . 120.8(2)    yes
C8 . C9 . H91 . 119.3    no
C10 . C9 . H91 . 119.9    no
C9 . C10 . N2 . 121.7(2)    yes
C9 . C10 . C13 . 116.8(2)    yes
N2 . C10 . C13 . 121.46(18)    yes
C4 . C11 . N1 . 122.1(2)    yes
C4 . C11 . C12 . 120.75(19)    yes
N1 . C11 . C12 . 117.17(19)    yes
C11 . C12 . C7 . 118.3(2)    yes
C11 . C12 . N2 . 118.33(17)    yes
C7 . C12 . N2 . 123.3(2)    yes
C10 . C13 . C14 . 120.9(2)    yes
C10 . C13 . C18 . 119.2(2)    yes
C14 . C13 . C18 . 119.7(3)    yes
C13 . C14 . C15 . 119.5(3)    yes
C13 . C14 . H141 . 119.8    no
C15 . C14 . H141 . 120.7    no
C14 . C15 . C16 . 120.8(3)    yes
C14 . C15 . H151 . 119.3    no
C16 . C15 . H151 . 119.9    no
C15 . C16 . C17 . 120.8(3)    yes
C15 . C16 . H161 . 119.2    no
C17 . C16 . H161 . 120.0    no
C16 . C17 . C18 . 119.6(3)    yes
C16 . C17 . H171 . 121.7    no
C18 . C17 . H171 . 118.6    no
C17 . C18 . C13 . 119.7(3)    yes
C17 . C18 . H181 . 119.5    no
C13 . C18 . H181 . 120.8    no
N3 . C19 . C20 . 122.4(2)    yes
N3 . C19 . H191 . 118.1    no
C20 . C19 . H191 . 119.5    no
```

```
C19·,·C20·,·C21·,·118.5(2)····yes
C19·,·C20·,·H20·,·120.4·····no
C21·,·C20·,·H20·,·121.0·····no
C20·,·C21·,·C22·,·119.3(2)····yes
C20·,·C21·,·H21·,·121.2·····no
C22·,·C21·,·H21·,·119.5·····no
C21·,·C22·,·C23·,·119.8(2)····yes
C21·,·C22·,·H22·,·119.6·····no
C23·,·C22·,·H22·,·120.7·····no
C22·,·C23·,·N3·,·120.14(19)···yes
C22·,·C23·,·C24·,·125.7(2)····yes
N3·,·C23·,·C24·,·114.12(18)···yes
C23·,·C24·,·C25·,·123.5(2)····yes
C23·,·C24·,·C29·,·114.87(19)···yes
C25·,·C24·,·C29·,·121.6(2)····yes
C24·,·C25·,·C26·,·120.0(2)····yes
C24·,·C25·,·H25·,·119.6·····no
C26·,·C25·,·H25·,·120.4·····no
C25·,·C26·,·C27·,·119.4(2)····yes
C25·,·C26·,·H26·,·120.9·····no
C27·,·C26·,·H26·,·119.7·····no
C26·,·C27·,·C28·,·120.8(2)····yes
C26·,·C27·,·H27·,·119.0·····no
C28·,·C27·,·H27·,·120.2·····no
C27·,·C28·,·C29·,·121.0(2)····yes
C27·,·C28·,·H28·,·118.5·····no
C29·,·C28·,·H28·,·120.5·····no
C24·,·C29·,·C28·,·117.12(18)···yes
C24·,·C29·,·Ir1·,·114.36(14)···yes
C28·,·C29·,·Ir1·,·128.27(17)···yes
N4·,·C30·,·C31·,·122.2(3)····yes
N4·,·C30·,·H301·,·118.1·····no
C31·,·C30·,·H301·,·119.8·····no
C30·,·C31·,·C32·,·118.8(3)····yes
C30·,·C31·,·H311·,·119.4·····no
C32·,·C31·,·H311·,·121.8·····no
C31·,·C32·,·C33·,·119.3(3)····yes
C31·,·C32·,·H321·,·121.2·····no
C33·,·C32·,·H321·,·119.5·····no
C32·,·C33·,·C34·,·120.3(3)····yes
C32·,·C33·,·H331·,·120.3·····no
C34·,·C33·,·H331·,·119.4·····no
C33·,·C34·,·N4·,·119.7(2)····yes
C33·,·C34·,·C35·,·126.3(2)····yes
N4·,·C34·,·C35·,·114.00(19)···yes
C34·,·C35·,·C36·,·123.5(2)····yes
C34·,·C35·,·C40·,·115.23(17)···yes
C36·,·C35·,·C40·,·121.3(2)····yes
C35·,·C36·,·C37·,·119.4(2)····yes
C35·,·C36·,·H361·,·119.2·····no
C37·,·C36·,·H361·,·121.4·····no
C36·,·C37·,·C38·,·120.3(2)····yes
C36·,·C37·,·H371·,·119.3·····no
C38·,·C37·,·H371·,·120.4·····no
C37·,·C38·,·C39·,·120.2(2)····yes
C37·,·C38·,·H381·,·121.0·····no
C39·,·C38·,·H381·,·118.8·····no
C38·,·C39·,·C40·,·121.1(2)····yes
C38·,·C39·,·H391·,·118.6·····no
C40·,·C39·,·H391·,·120.3·····no

C35·,·C40·,·C39·,·117.69(17)···yes
C35·,·C40·,·Ir1·,·114.61(15)···yes
C39·,·C40·,·Ir1·,·127.57(16)···yes
F5·6_555·P1·,·F1·,·90.60(7)····yes
F5·6_555·P1·,·F2·,·89.40(7)····yes
F1·,·P1·,·F2·,·179.06(17)·····yes
F5·6_555·P1·,·F3·,·89.77(7)····yes
F1·,·P1·,·F3·,·88.89(16)·····yes
F2·,·P1·,·F3·,·90.17(14)·····yes
F5·6_555·P1·,·F4·,·90.24(7)····yes
F1·,·P1·,·F4·,·90.11(16)·····yes
F2·,·P1·,·F4·,·90.83(14)·····yes
F3·,·P1·,·F4·,·179.00(15)·····yes
F5·6_555·P1·,·F5·,·178.72(15)···yes
F1·,·P1·,·F5·,·90.60(7)····yes
F2·,·P1·,·F5·,·89.40(7)····yes
F3·,·P1·,·F5·,·89.77(7)····yes
F4·,·P1·,·F5·,·90.24(7)····yes
F15·6_555·P2·,·F11·,·90.55(12)···yes
F15·6_555·P2·,·F12·,·89.62(12)···yes
F11·,·P2·,·F12·,·173.3(4)·····yes
F15·6_555·P2·,·F13·,·88.60(16)···yes
F11·,·P2·,·F13·,·87.9(4)·····yes
F12·,·P2·,·F13·,·98.7(4)·····yes
F15·6_555·P2·,·F14·,·91.41(16)···yes
F11·,·P2·,·F14·,·91.3(4)·····yes
F12·,·P2·,·F14·,·82.0(3)·····yes
F13·,·P2·,·F14·,·179.3(4)·····yes
F15·6_555·P2·,·F15·,·176.9(3)···yes
F11·,·P2·,·F15·,·90.55(12)···yes
F12·,·P2·,·F15·,·89.62(12)···yes
F13·,·P2·,·F15·,·88.60(16)···yes
F14·,·P2·,·F15·,·91.41(16)···yes
```

```
#·Given·Formula·=·C32·H24·F6·Ir1·N4·P1·
#·Dc·=·····1.84·Fooo·=···3120.00·Mu·=·····47.51·M·=····801.75
#·Found·Formula·=·C32·H24·F6·Ir1·N4·P1·
#·Dc·=·····1.84·FOOO·=···3120.00·Mu·=·····47.51·M·=····801.75

_chemical_formula_sum··········'C32·H24·F6·Ir1·N4·P1'
_chemical_formula_moiety·····'C32·H24·Ir·N4,·F6·P'
_chemical_compound_source·····?
_chemical_formula_weight·····801.75
·
·
_cell_measurement_reflns_used·····18226
_cell_measurement_theta_min·····1
_cell_measurement_theta_max·····28
_cell_measurement_temperature·····173
·
_exptl_crystal_description·····'plate'·
_exptl_crystal_colour·····'yellow'·
_exptl_crystal_size_min·····0.13·
_exptl_crystal_size_mid·····0.17·
_exptl_crystal_size_max·····0.48·
·
_exptl_crystal_density_diffrn····1.845·
_exptl_crystal_density_meas···?·
#·Non-dispersive·F(000):··
_exptl_crystal_F_000·····3120·
_exptl_absorpt_coefficient_mu····4.751·
·
#·Sheldrick·geometric·approximatio·0.45·0.54·
#·No·experimental·values·of·Tmin/max·available·
_exptl_absorpt_correction_type···multi-scan·
_exptl_absorpt_process_details····'DENZO/SCALEPACK·(Otwinowski·&·Minor,·1997)'·
_exptl_absorpt_correction_T_min··0.45·
_exptl_absorpt_correction_T_max··0.54·
#·For·a·Kappa·CCD,·set·Tmin·to·1.0·and·
#·Tmax·to·the·ratio·of·max:min·frame·scales·in·scale_all.log·
_diffrn_measurement_device_type···'Nonius·KappaCCD'·
_diffrn_radiation_monochromator···'graphite'·
_diffrn_radiation_type·····'Mo·K\a'·
_diffrn_radiation_wavelength·····0.71073
_diffrn_measurement_method····'\f·a·\w·scans'·
·
#·If·a·reference·occurs·more·than·once,·delete·the·author·
#·and·date·from·subsequent·references.·
_computing_data_collection·····'COLLECT·(Nonius,·1997-2001).'·
_computing_cell_refinement·····'DENZO/SCALEPACK·(Otwinowski·&·Minor,·1997)'·
_computing_data_reduction·····'DENZO/SCALEPACK·(Otwinowski·&·Minor,·1997)'·
_computing_structure_solution····'SIR92·(Altomare·et·al.,·1994)'·
_computing_structure_refinement···'CRYSTALS·(Betteridge·et·al.,·2003)'·
_computing_publication_material···'CRYSTALS·(Betteridge·et·al.,·2003)'·
_computing_molecular_graphics·····'CAMERON·(Watkin·et·al.,·1996)'·
·
_diffrn_standards_interval_time··?·
_diffrn_standards_interval_count·?·
_diffrn_standards_number·····0·
_diffrn_standards_decay_%·····?·
·
_diffrn_ambient_temperature·····173
_diffrn_reflns_number·····35191·
_reflns_number_total·····4906·
·
·
_diffrn_reflns_av_R_equivalents···0.047·
#·Number·of·reflections·with·Friedels·Law·is·6906·
#·Number·of·reflections·without·Friedels·Law·is·0·
#·Theoretical·number·of·reflections·is·about·6931·
·
·
_diffrn_reflns_theta_min·····1.217·
_diffrn_reflns_theta_max·····27.945·
_diffrn_measured_fraction_theta_max·0.995·
·
_diffrn_reflns_theta_full·····27.945·
_diffrn_measured_fraction_theta_full·0.995·
·
·
·
_diffrn_reflns_limit_h_min·····-14·
_diffrn_reflns_limit_h_max·····14·
_diffrn_reflns_limit_k_min·····-19·
_diffrn_reflns_limit_k_max·····20·
_diffrn_reflns_limit_l_min·····-43·
_diffrn_reflns_limit_l_max·····44·
_reflns_limit_h_min·····0·
_reflns_limit_h_max·····14·
_reflns_limit_k_min·····0·
_reflns_limit_k_max·····20·
_reflns_limit_l_min·····0·
_reflns_limit_l_max·····44·
·
_oxford_diffrn_Wilson_B_factor···0.00·
_oxford_diffrn_Wilson_scale···0.00·
·
_atom_sites_solution_primary·····direct·#heavy,direct,difmap,geom
#·_atom_sites_solution_secondary···difmap
_atom_sites_solution_hydrogens···geom
·
_refine_diff_density_min·····-2.11·
_refine_diff_density_max·····1.62·
·
·
_refine_ls_number_reflns·····4194·
_refine_ls_number_restraints····0·
_refine_ls_number_parameters····397·
·
#_refine_ls_R_factor_ref·0.0265·
_refine_ls_wR_factor_ref·····0.0327·
_refine_ls_goodness_of_fit_ref···0.9771·
·
#_refins_number_all·6839·
_refine_ls_R_factor_all·····0.0456·
_refine_ls_wR_factor_all·····0.0358·
·
#·The·I/u(I)·cutoff·below·was·used·for·refinement·as·
#·well·as·the·gt·R-factors:
_refins_threshold_expression····I>2.0\s(I)
_refins_number_gt·····4194·
_refine_ls_R_factor_gt·····0.0265·
_refine_ls_wR_factor_gt·····0.0327·
·
_refine_ls_shift/su_max·····0.003846·
·
#·choose·from:·rm·(reference·molecule·of·known·chirality),·

#·ad·(anomolous·dispersion···Flack),·rmad·(rm·and·ad),·
#·syn·(from·synthesis),·unk·(unknown)·or··(not·applicable).·
_chemical_absolute_configuration··'.'·
·
·
_refine_ls_structure_factor_coef··F·
_refine_ls_matrix_type·····full
_refine_ls_hydrogen_treatment·····constr·····#·none,·undef,·noref,·refall,
·····refxyz,·refU,·constr·or·mixed
_refine_ls_weighting_scheme·····calc·
_refine_ls_weighting_details·
;
·Method-·Modified.Sheldrick.
·w=1/[\s^2^(F^2^)+·(·0.022P)^2^+·0.022P]·
·,where·P=(max(Fo^2^,0)·+·2Fc^2^)/3·
;
·
·
·
#·Check·this·file·using·the·IUCr·facility·at:·
#·http://checkcif.iucr.org/.·

#·The·content·below·is·held·in·the·file·'script/refcif.dat'.·This·is·a·text·
#·file·which·you·may·edit·to·reflect·local·conditions.·
#·Items·which·need·looking·at·are·represented·by·a·'?'.·
#·Items·for·which·there·are·choices·are·prefixed·with·'choose·from'.·
·
_publ_contact_letter·
;·
·Please·consider·this·CIF·submission·for·
·publication·as·a·Short·Format·Paper·in·Acta·
·Crystallographica·E.·The·figures·will·be·
·sent·by·e-mail.·
;·
_publ_contact_author_name·····'Anthony·Other'·
_publ_contact_author_address·
;·
·Chemical·Crystallography·Laboratory,·
·Department·of·Chemistry,·
·University·of·Nowhere,·
·Nowhere,·NO1·4T,·UK.·
;·
·
_publ_contact_author_phone·····'+44·1865·000000'·
_publ_contact_author_fax·····'+44·1865·000000'·
_publ_contact_author_email····'a.n.other@chem.no.ac.uk'·
_publ_requested_journal·····'Section·E'·
_publ_requested_category·····EO·#·choose·from:·FI·FM·FO·CI·CM·CO·AD·
_publ_requested_coeditor_name····'Prof·William·Clegg'·
·
_publ_section_title·
#·Title·of·paper···generally·just·the·systematic·or·trivial·name·
;·?·
;·
·
#·The·loop·structure·below·should·contain·the·names·and·addresses·of·all·
#·authors,·in·the·required·order·of·publication.·Repeat·as·necessary.·
loop_·
·_publ_author_name·
·_publ_author_address·

·_publ_author_footnote·
·''Other,·Anthony·N.''·#·Author·1·
;·
·?·#·Address·for·author·1·
;·
;·
·?·#·Footnote·for·author·1·
;·
·'Else,·S.·O.''·#·Author·2·
;·
·?·#·Address·2·
;·
;·
·?·#·Footnote·2·
;·
·
·
_publ_section_abstract·
#·Text·of·the·abstract·
#·(a)·The·Abstract·must·be·self-contained·and·comprehensible·
#·without·the·rest·of·the·paper.·This·means·no·references·
#·to·atom·names·or·to·compound·numbers;·compounds·must·be·
#·identified·as·the·title·compound,·or·by·name·or·by·some·other·
#·means·such·as·derivatives·of·each·other·(e.g.·"the·
#·corresponding·ketone").··
#·(b)·The·chemical·formula·of·"the·title·compound"·must·be·given..·
#·(c)·Any·crystallographic·molecular·symmetry·should·be·
#·mentioned,·and·also·the·presence·of·more·than·one·molecule·
#·in·the·asymmetric·unit·(i.e.·anything·other·than·Z'=1)..·
;·
·?·
;·
_publ_section_comment·
#·Text·of·the·paper·
#·Note·that·atoms·are·referenced·as·N2,·not·N(2)·or·N-2·.·
#·If·text·containing·()·occur·within·(),·the·outer·ones·should·be·[]·
#·Figures·should·be·referenced·as·Fih.·
;·
?·
;·
_publ_section_acknowledgements····#·Acknowledgments·
;·
?·
;·
_publ_section_figure_captions·
#·Captions·to·figures·--·Start·each·caption·on·a·new·line·after·a·blank·line·
;·
Fig.·1..·
The·title·compound·with·displacement·ellipsoids·drawn·at·the·50%·
probability·level.·H·atoms·are·shown·as·spheres·of·
arbitrary·radius..·
·
;·
·
_publ_section_exptl_refinement·
#·Some·potentially·useful·phrases·are·donated·by·Bill·Clegg:·
;·
In·the·absence·of·significant·anomalous·scattering,·Friedel·pairs·were·
merged.·
·

The·absolute·configuration·was·arbitrarily·assigned.·
·
The·relatively·large·ratio·of·minimum·to·maximum·corrections·applied·
in·the·multiscan·process·(1:nnn)·reflect·changes·in·the·illuminated·
volume·of·the·crystal..·
·
Changes·in·illuminated·volume·were·kept·to·a·minimum,·and·were·
taken·into·account·(G\"orbitz,·1999)·by·the·multi-scan·inter-frame·
scaling·(DENZO/SCALEPACK,·Otwinowski·&·Minor,·1997)..·
·
·
G\"orbitz,·C.·H.·(1999).·Acta·Cryst.·B55,·1090-1098.·
·
·
·
The·H·atoms·were·all·located·in·a·difference·map,·but·those·
attached·to·carbon·atoms·were·repositioned·geometrically..·
The·H·atoms·were·initially·refined·with·soft·restraints·on·the·
bond·lengths·and·angles·to·regularise·their·geometry·
(C---H·in·the·range·0.93--0.98,·
N---H·in·the·range·0.86--0.89·
N---H·to·0.86·
O---H·=·0.82·
\%A).·
and·
U-iso-(H)·(in·the·range·1.2-1.5·times·U-eq·of·the·parent·atom),·
after·which·the·positions·were·refined·with·riding·constraints..·
·
;·
·
_publ_section_exptl_prep·
#·Brief·details·or·a·reference.·Include·solvent·if·known·
;·
?·
;·
·
·
#·PROCESSING·SUMMARY·(IUCr·Office·Use·Only):·
_journal_date_recd_electronic·····?·
_journal_date_to_coeditor·····?·
_journal_date_from_coeditor·····?·
_journal_date_accepted·····?·
_journal_date_printers_first·····?·
_journal_date_printers_final·····?·
_journal_date_proofs_out·····?·
_journal_date_proofs_in·····?·
_journal_coeditor_name·····?·
_journal_coeditor_code·····?·
_journal_coeditor_notes·····?·
_journal_techeditor_code·····?·
_journal_techeditor_notes·····?·
_journal_coden_ASTM·····?·
_journal_name_full·····?·
_journal_year·····?·
_journal_volume·····?·
_journal_issue·····?·
_journal_page_first·····?·
_journal_page_last·····?·
_journal_suppl_publ_number·····?·

_journal_suppl_publ_pages·····?·
·
#·End·of·'script/refcif.dat'·
·
·
·
#·Insert·your·own·references·if·required·--·in·alphabetical·order.·
_publ_section_references·
;·
Altomare,·A.,·Cascarano,·G.,·Giacovazzo,·C.,·Guagliardi,·A.,·Burla,·M.C.,·
Polidori,·G.·&·Camalli,·M.·(1994).·J.·Appl.·Cryst.·27,·435.·
·
Betteridge,·P.W.,·Carruthers,·J.R.,·Cooper,·R.I.,·
Prout,·K.·&·Watkin,·D.J.·(2003).·J.·Appl.·Cryst.·36,·1487.·
·
Larson,·A.C.·(1970).·Crystallographic·Computing,·Ed·Ahmed,·F.R.,·
Munksgaard,·Copenhagen,·291-294.·
·
Nonius·(1997-2001).·COLLECT.·Nonius·BV,·Delft,·The·Netherlands.·
·
Otwinowski,·Z.·&·Minor,·W.·(1997).·Methods·in·Enzymology,·Vol.·276,·
edited·by·C.·W.·Carter·Jr·&·R.·M.·Sweet,·pp.·307--326.·
New·York:·Academic·Press.·
·
Watkin,·D.J.,·Prout,·C.K.·&·Pearce,·L.J.·(1996).·CAMERON,·Chemical·
Crystallography·Laboratory,·Oxford,·UK.·
;·
·

#·Ueqiv·=·arithmetic·mean·of·Ui·i.e.·Ueqiv·=·(U1+U2+U3)/3·
·
·
#·Replace·last·..·with·number·of·unfound·hydrogen·atomsattached·to·an·atom.·
·
#·___·refinement_flags____·
#·.·no·refinement·constraints···········S·special·position·constraint·on·site·
#·G·rigid·group·refinement·of·site·····R·riding·atom·
#·D·distance·angle·restraint·on·site·T·thermal·displacement·constraints·
#·U·Uiso·or·Uij·restraint·(rigid·bond)···P·partial·occupancy·constraint·

·
loop_·
·_atom_site_label·
·_atom_site_type_symbol·
·_atom_site_fract_x·
·_atom_site_fract_y·
·_atom_site_fract_z·
·_atom_site_U_iso_or_equiv·
·_atom_site_occupancy·
·_atom_site_adp_type·
·_atom_site_refinement_flags_posn·
·_atom_site_refinement_flags_adp·
·_atom_site_refinement_flags_occupancy·
·_atom_site_disorder_assembly·
·_atom_site_disorder_group·
·_atom_site_attached_hydrogens·
Ir1·Ir·0.2375932(13)·0.249744(10)·0.638826(4)·0.0178·1.0000·Uani·.·.·.·.·.·
N1·N·0.1127(3)·0.1745(2)·0.60539(10)·0.0222·1.0000·Uani·.·.·.·.·.·
N2·N·0.2192(3)·0.3165(2)·0.58368(10)·0.0226·1.0000·Uani·.·.·.·.·.·
N3·N·0.0922(3)·0.3048(2)·0.66732(10)·0.0210·1.0000·Uani·.·.·.·.·.·
N4·N·0.3928(3)·0.1918(2)·0.61810(10)·0.0226·1.0000·Uani·.·.·.·.·.·
C1·C·0.0616(4)·0.1020(3)·0.61854(14)·0.0296·1.0000·Uani·.·.·.·.·.·
```

bis(2-phenylpyridine-*C*,*N*)(2,2'-bipyridine-*N*,*N*')iridium(III) hexafluorophosphate (**49**)

```
data_sg080-1_173k
_audit_creation_date·····07-10-09
_audit_creation_method·CRYSTALS_ver_12.84
·
_oxford_structure_analysis_title··'10090908·sg080-1_173k'
_chemical_name_systematic·····?
_chemical_melting_point·····?
·
_cell_length_a·····10.8993(2)
_cell_length_b·····15.8290(4)
_cell_length_c·····33.4603(7)
_cell_angle_alpha·····90
_cell_angle_beta·····90
_cell_angle_gamma·····90
_cell_volume·····5772.7(2)
·
_symmetry_cell_setting·····'Orthorhombic'·
_symmetry_space_group_name_H-M···'P·b·c·a'·
_symmetry_space_group_name_Hall···'-P·2ac·2ab'·
loop_·
·_symmetry_equiv_pos_as_xyz·
·'x,y,z'·
·'-x,-y,-z'·
·'-x+1/2,y+1/2,z'·
·'x+1/2,-y+1/2,-z'·
·'x,-y+1/2,z+1/2'·
·'-x,y+1/2,-z+1/2'·
·'-x+1/2,-y,z+1/2'·
·'x+1/2,y,-z+1/2'·
·
loop_·
·_atom_type_symbol·
·_atom_type_scat_dispersion_real·
·_atom_type_scat_dispersion_imag·
·_atom_type_scat_Cromer_Mann_a1·
·_atom_type_scat_Cromer_Mann_b1·
·_atom_type_scat_Cromer_Mann_a2·
·_atom_type_scat_Cromer_Mann_b2·
·_atom_type_scat_Cromer_Mann_a3·
·_atom_type_scat_Cromer_Mann_b3·
·_atom_type_scat_Cromer_Mann_a4·
·_atom_type_scat_Cromer_Mann_b4·
·_atom_type_scat_Cromer_Mann_c·
·_atom_type_scat_source·
·'C·····0.0033····0.0016····2.3100···20.8439···1.0200···10.2075···1.5886···0.5687
····0.8650···51.6512····0.2156·'International·Tables·Vol·C·4.2.6.8·and·6.1.1.4'
·'H·····0.0000····0.0000····0.4930···10.5109···0.3229···26.1257···0.1402···3.1424
····0.0408···57.7998····0.0030·'International·Tables·Vol·C·4.2.6.8·and·6.1.1.4'
·'Ir····-1.4442····7.9887···27.3049···1.5928···16.7296···8.8655···15.6115···0.4179
····5.8338···45.0011···11.4722·'International·Tables·Vol·C·4.2.6.8·and·6.1.1.4'
·'N·····0.0061····0.0033···12.2126····0.0057···3.1322···9.8933····2.0125···28.9975
····1.1663····0.5826···-11.5290·'International·Tables·Vol·C·4.2.6.8·and·6.1.1.4'
·'P·····0.1023····0.0942····6.4345···1.9067···4.1791···27.1570···1.7800···0.5260
····1.4908···68.1645····1.1149·'International·Tables·Vol·C·4.2.6.8·and·6.1.1.4'
·'F·····0.0171····0.0103····3.5392···10.2825····2.6412···4.2944···1.5170···0.2615
····1.0243···26.1476····0.2776·'International·Tables·Vol·C·4.2.6.8·and·6.1.1.4'
·
·
_cell_formula_units_Z·····8
```

bis(2-phenylpyridine-*C*,*N*)(6-phenyl-2,2'-bipyridine-*N*,*N'*)iridium(III) hexafluorophosphate (**50**)

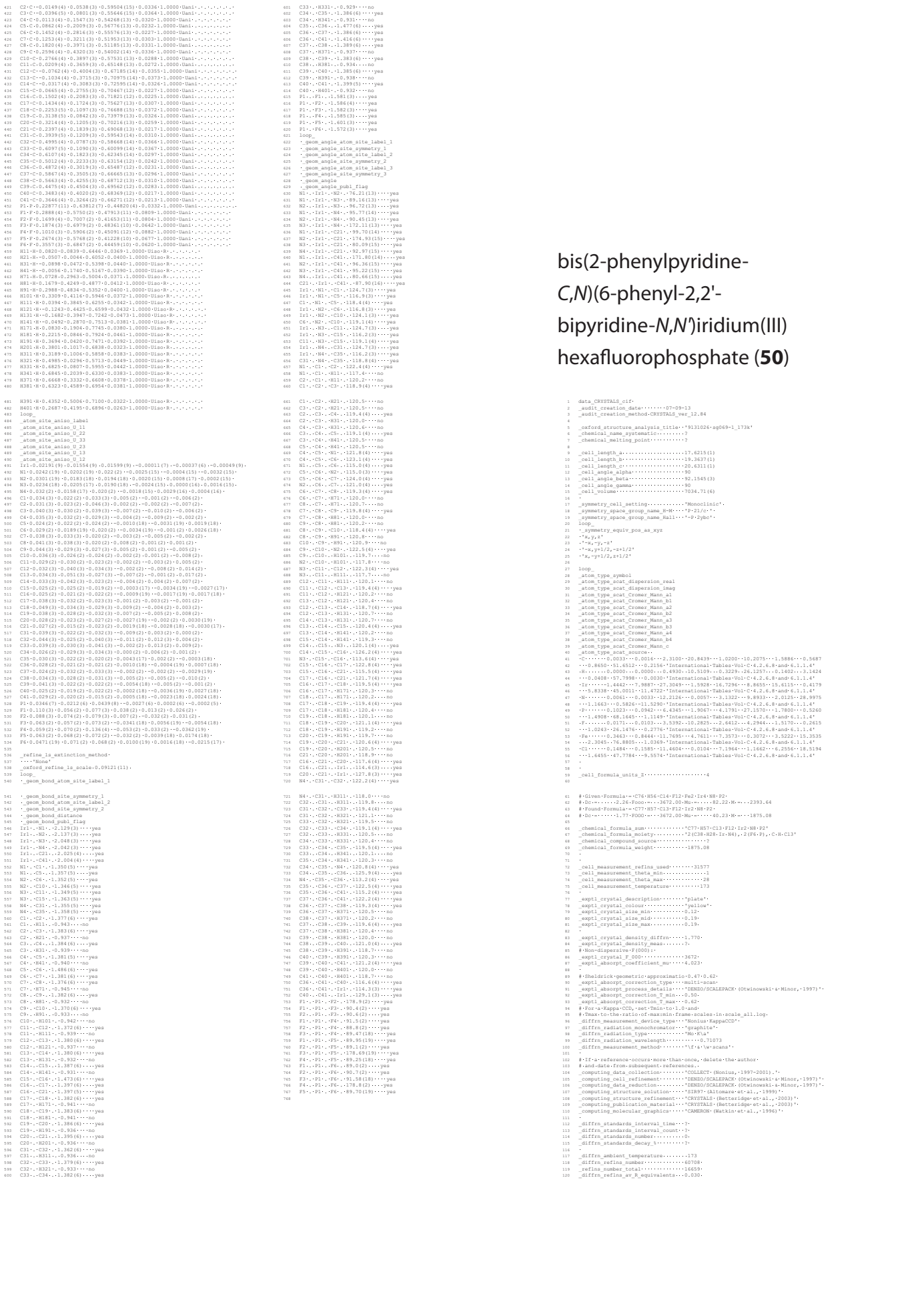

```
#·Number·of·reflections·with·Friedels·Law·is·16659·
#·Number·of·reflections·without·Friedels·Law·is·0·
#·Theoretical·number·of·reflections·is·about·16693·
·
·
_diffrn_refns_theta_min·····1.826·
_diffrn_refns_theta_max·····27.824·
_diffrn_measured_fraction_theta_max·0.998·
·
_diffrn_refns_theta_full·····27.824·
_diffrn_measured_fraction_theta_full·0.998·
·
·
_diffrn_refns_limit_h_min·····-23·
_diffrn_refns_limit_h_max·····23·
_diffrn_refns_limit_k_min·····-25·
_diffrn_refns_limit_k_max·····25·
_diffrn_refns_limit_l_min·····-27·
_diffrn_refns_limit_l_max·····27·
_refns_limit_h_min·····-23·
_refns_limit_h_max·····23·
_refns_limit_k_min·····0·
_refns_limit_k_max·····25·
_refns_limit_l_min·····0·
_refns_limit_l_max·····27·
·
_oxford_diffrn_Wilson_B_factor···0.00·
_oxford_diffrn_Wilson_scale·····0.00·
·
_atom_sites_solution_primary·····direct·#heavy,direct,difmap,geom
#·atom_sites_solution_secondary···difmap
_atom_sites_solution_hydrogens···geom
·
_refine_diff_density_min·····-1.36·
_refine_diff_density_max·····2.37·
·
·
_refine_ls_number_refns·····12712·
_refine_ls_number_restraints····1271·
_refine_ls_number_parameters····938·
·
#_refine_ls_R_factor_ref·0.0263·
_refine_ls_wR_factor_ref·····0.0293·
_refine_ls_goodness_of_fit_ref···1.0952·
·
#_refine_number_all·16554·
_refine_ls_R_factor_all·····0.0359·
_refine_ls_wR_factor_all·····0.0381·
·
#·The·I/u(I)·cutoff·below·was·used·for·refinement·as·
#·well·as·the·_gt·R-factors:
_refns_threshold_expression·····I>3.0\s(I)
_refns_number_gt·····12712·
#_refine_ls_R_factor_gt·0.0263·
_refine_ls_wR_factor_gt·····0.0293·
·
_refine_ls_shift/su_max·····0.002112·
·
#·choose·from:·rm·(reference·molecule·of·known·chirality),·
#·ad·(anomolous·dispersion···Flack),·rmad·(rm·and·ad),·


#·syn·(from·synthesis),·unk·(unknown)·or··(not·applicable)·
_chemical_absolute_configuration·''·
·
·
_refine_ls_structure_factor_coef·F·
_refine_ls_matrix_type·····full
_refine_ls_hydrogen_treatment····constr·····#·none,·undef,·noref,·refall,
·····#·refxyz,·refU,·constr·or·mixed
_refine_ls_weighting_scheme·····calc·
_refine_ls_weighting_details·
;
·Method,·part·1,·Chebychev·polynomial,·(Watkin,·1994,·Prince,·1982):·
·[weight]·=·1.0/[A~0~*T~0~(x)+A~1~*T~1~(x)+...+A~n-1~*T~n-1~(x)]·
·where·A~i~·are·the·Chebychev·coefficients·listed·below·and·x=·Fcalc/Fmax·
·Method·=·Robust·Weighting·(Prince,·1982):·
·W·=·[weight]·*·[1-(deltaF/6*sigmaF)·^2^]^2^·
·A~i~·are:·
·0.284·0.983E-01·0.108·
;
·
·
#·Check·this·file·using·the·IUCr·facility·at:·
#·http://checkcif.iucr.org/·


#·The·content·below·is·held·in·the·file·'script/refcif.dat'.·This·is·a·text·
#·file·which·you·may·edit·to·reflect·local·conditions.·
#·Items·which·need·looking·at·are·represented·by·a·'?'.·
#·Items·for·which·there·are·choices·are·prefixed·with·'choose·from'.·


_publ_contact_letter·
;?·
·Please·consider·this·CIF·submission·for·
·publication·as·a·Short·Format·Paper·in·Acta·
·Crystallographica·E.·The·figures·will·be·
·sent·by·e-mail.·
;?·
_publ_contact_author_name·····'Anthony·Other'·
_publ_contact_author_address·
;?·
·Chemical·Crystallography·Laboratory,·
·Department·of·Chemistry,·
·University·of·Nowhere,·
·Nowhere,·NO1·4T,·UK.·
;?·


_publ_contact_author_phone·····'+44·1865·000000'·
_publ_contact_author_fax·····'+44·1865·000000'·
_publ_contact_author_email·····'a.n.other@chem.no.ac.uk'·
_publ_requested_journal·····'Section·E'·
_publ_requested_category·····#·choose·from:·FI·FM·FO·CI·CM·CO·AD·
_publ_requested_coeditor_name····'Prof·William·Clegg'·


_publ_section_title·
#·Title·of·paper···generally·just·the·systematic·or·trivial·name·
;?·
·
·
#·The·loop·structure·below·should·contain·the·names·and·addresses·of·all·
#·authors,·in·the·required·order·of·publication.·Repeat·as·necessary.·


loop_
_publ_author_name·
_publ_author_address·
_publ_author_footnote·
'Other,·Anthony·N.'·#·Author·1·
;?·
·?·#·Address·for·author·1·
;?·
·
;?·#·Footnote·for·author·1·
;?·
·
'Else,·S.·O.'·#·Author·2·
;?·
·?·#·Address·2·
;?·
·
·
?·#·Footnote·2·
;?·
·


_publ_section_abstract·
#·Text·of·the·abstract·
#·(a)·The·Abstract·must·be·self-contained·and·comprehensible·
#·without·the·rest·of·the·paper.·This·means·no·references·
#·to·atom·names·or·to·compound·numbers;·compounds·must·be·
#·identified·as·the·title·compound,·or·by·name·or·by·some·other·
#·means·such·as·derivatives·of·each·other·(e.g.·"the·
#·corresponding·ketone").·
#·(b)·The·chemical·formula·of·"the·title·compound"·must·be·given.·
#·(c)·Any·crystallographic·molecular·symmetry·should·be·
#·mentioned,·and·also·the·presence·of·more·than·one·molecule·
#·in·the·asymmetric·unit·(i.e.·anything·other·than·Z'=1).·
;?·
·
;?·


_publ_section_comment·
#·Text·of·the·paper·
#·Note·that·atoms·are·referenced·as·N2,·not·N(2)·or·N·2·
#·If·text·containing·()·occur·within·(),·the·outer·ones·should·be·[].·
#·Figures·should·be·referenced·as·Fih.·
;?·
·
;?·


_publ_section_acknowledgements···#·Acknowledgments·
;?·
·
;?·


_publ_section_figure_captions·
#·Captions·to·figures···Start·each·caption·on·a·new·line·after·a·blank·line·
;?·
·
Fig.·1.·
The·title·compound·with·displacement·ellipsoids·drawn·at·the·50%·
probability·level.·H·atoms·are·shown·as·spheres·of·
arbitary·radius.·
;
·
;?·


_publ_section_exptl_refinement·
#·Some·potentially·useful·phrases·are·donated·by·Bill·Clegg:·
;?·


In·the·absence·of·significant·anomalous·scattering,·Friedel·pairs·were·
merged.·
·
The·absolute·configuration·was·arbitrarily·assigned.·
·
The·relatively·large·ratio·of·minimum·to·maximum·corrections·applied·
in·the·multiscan·process·(1:nnn)·reflect·changes·in·the·illuminated·
volume·of·the·crystal.·
·
Changes·in·illuminated·volume·were·kept·to·a·minimum,·and·were·
taken·into·account·(G\^orbitz,·1999)·by·the·multi-scan·inter-frame·
scaling·(DENZO/SCALEPACK,·Otwinowski·&·Minor,·1997).·
·
·
G\^orbitz,·C.·H.·(1999).·Acta·Cryst.·B55,·1090-1098.·
·
·
·
·
The·H·atoms·were·all·located·in·a·difference·map,·but·those·
attached·to·carbon·atoms·were·repositioned·geometrically.·
The·H·atoms·were·initially·refined·with·soft·restraints·on·the·
bond·lengths·and·angles·to·regularise·their·geometry·
(C---H·in·the·range·0.93--0.98,·
N---H·in·the·range·0.86--0.89·
N---H·to·0.86·
O---H·--·0.82·
\hA)·
and.·
U~iso·(H)·(in·the·range·1.2·-1.5·times·U·eq·of·the·parent·atom),·
after·which·the·positions·were·refined·with·riding·constraints.·
·
;·


_publ_section_exptl_prep·
#·Brief·details·or·a·reference.·Include·solvent·if·known·
;·
·
;·


_publ_section_exptl_refinement·
#·PROCESSING·SUMMARY·(IUCr·Office·Use·Only)·
_journal_date_recd_electronic·····?·
_journal_date_to_coeditor·····?·
_journal_date_from_coeditor·····?·
_journal_date_accepted·····?·
_journal_date_printers_first·····?·
_journal_date_printers_final·····?·
_journal_date_proofs_out·····?·
_journal_date_proofs_in·····?·
_journal_coeditor_name·····?·
_journal_coeditor_code·····?·
_journal_coeditor_notes·····?·
_journal_techeditor_code·····?·
_journal_techeditor_notes·····?·
_journal_coden_ASTM·····?·
_journal_name_full·····?·
_journal_year·····?·
_journal_volume·····?·
_journal_issue·····?·


_journal_page_first·····?·
_journal_page_last·····?·
_journal_suppl_publ_number·····?·
_journal_suppl_publ_pages·····?·
·
#·End·of·'script/refcif.dat'·


·
#·Insert·your·own·references·if·required···in·alphabetical·order·
_publ_section_references·
;·
Altomare,·A.,·Burla,·M.C.,·Camalli,·M.,·Cascarano,·G.L.,·Giacovazzo,·C.,·
Guagliardi,·A.,·Grazia,·A.,·Moliterni,·G.,·Polidori,·G.·&·Spagna,·R.·
(1999).·J.·App.·Cryst.·32,·115-119.·
·
Betteridge,·P.W.,·Carruthers,·J.R.,·Cooper,·R.I.,·
Prout,·K.·&·Watkin,·D.J.·(2003).·J.·Appl.·Cryst.·36,·1487.·
·
Larson,·A.C.·(1970).·Crystallographic·Computing,·Ed·Ahmed,·F.R.,·
Munksgaard,·Copenhagen,·291-294.·
·
Nonius·(1997-2001).·COLLECT.·Nonius·BV,·Delft,·The·Netherlands.·
·
Otwinowski,·Z.·&·Minor,·W.·(1997).·Methods·in·Enzymology,·Vol.·276,·
edited·by·C.·W.·Carter·Jr·&·R.·M.·Sweet,·pp.·307---326.·
New·York:·Academic·Press.·
·
Prince,·E.·
Mathematical·Techniques·in·Crystallography·
and·Materials·Science·
Springer-Verlag,·New·York,·1982.·
·
Watkin·D.J.·(1994).·
Acta·Cryst.,·A50,·411-437.·
·
Watkin,·D.J.,·Prout,·C.K.·&·Pearce,·L.J.·(1996).·CAMERON,·Chemical·
Crystallography·Laboratory,·Oxford,·UK.·
;?·


#·Ueqiv·=··arithmetic·mean·of·Ui·i.e.·Ueqiv·=·(U1+U2+U3)/3·
·
#·Replace·last·..·with·number·of·unfound·hydrogen·atomsattached·to·an·atom.·
·
#·___·refinement_flags_...·
#·-·no·refinement·constraints···S·special·position·constraint·on·site·
#·G·rigid·group·refinement·of·site·····R·riding·atom·
#·D·distance·or·angle·restraint·on·site·T·thermal·displacement·constraints·
#·U·Uiso·or·Uij·restraint·(rigid·bond)···P·partial·occupancy·constraint·


loop_
_atom_site_label·
_atom_site_type_symbol·
_atom_site_fract_x·
_atom_site_fract_y·
_atom_site_fract_z·
_atom_site_U_iso_or_equiv·
_atom_site_occupancy·
_atom_site_adp_type·
·


_atom_site_refinement_flags_posn·
_atom_site_refinement_flags_adp·
_atom_site_refinement_flags_occupancy·
_atom_site_disorder_assembly·
_atom_site_disorder_group·
_atom_site_attached_hydrogens·
Ir1·Ir·0.96621(7)·0.190787(6)·0.451190(6)·0.0202·1.0000·Uani·····
Ir2·Ir·0.508995(7)·0.229520(6)·0.521045(6)·0.0203·1.0000·Uani·····
N1·N·0.42402(16)·0.19195(16)·0.45223(14)·0.0259·1.0000·Uani·····
N2·N·0.40247(16)·0.27909(15)·0.55064(14)·0.0234·1.0000·Uani·····
N3·N·0.50240(16)·0.14796(15)·0.58285(14)·0.0257·1.0000·Uani·····
N4·N·0.53284(16)·0.31218(15)·0.46269(14)·0.0262·1.0000·Uani·····
N51·N·0.92315(16)·0.15972(15)·0.52443(13)·0.0240·1.0000·Uani·····
N52·N·0.89783(16)·0.24841(15)·0.42739(14)·0.0234·1.0000·Uani·····
N53·N·0.97592(16)·0.11273(15)·0.38693(14)·0.0259·1.0000·Uani·····
N54·N·1.04011(15)·0.26818(15)·0.51232(13)·0.0225·1.0000·Uani·····
C1·C·0.4322(2)·0.1388(2)·0.4119(19)·0.0344·1.0000·Uani·····
C2·C·0.3734(3)·0.1147(3)·0.3709(2)·0.0450·1.0000·Uani·····
C3·C·0.3043(3)·0.1482(3)·0.3715(2)·0.0492·1.0000·Uani·····
C4·C·0.2953(2)·0.2034(3)·0.4125(2)·0.0417·1.0000·Uani·····
C5·C·0.3565(2)·0.2245(2)·0.45231(17)·0.0299·1.0000·Uani·····
C6·C·0.35061(19)·0.2811(2)·0.49977(18)·0.0280·1.0000·Uani·····
C7·C·0.2946(2)·0.3332(2)·0.4933(2)·0.0390·1.0000·Uani·····
C8·C·0.2949(2)·0.3842(2)·0.5398(2)·0.0415·1.0000·Uani·····
C9·C·0.3428(2)·0.3793(2)·0.5940(2)·0.0362·1.0000·Uani·····
C10·C·0.3948(2)·0.32458(19)·0.59946(18)·0.0283·1.0000·Uani·····
C11·C·0.4378(2)·0.3126(2)·0.66139(18)·0.0321·1.0000·Uani·····
C12·C·0.4842(3)·0.3627(3)·0.6894(2)·0.0452·1.0000·Uani·····
C13·C·0.5207(3)·0.3486(3)·0.7505(3)·0.0624·1.0000·Uani·····
C14·C·0.5079(4)·0.2871(4)·0.7813(3)·0.0651·1.0000·Uani·····
C15·C·0.4612(3)·0.2383(3)·0.7536(2)·0.0603·1.0000·Uani·····
C16·C·0.4266(3)·0.2504(2)·0.6933(2)·0.0422·1.0000·Uani·····
C17·C·0.4544(2)·0.2945(2)·0.5769(2)·0.0350·1.0000·Uani·····
C18·C·0.4552(3)·0.0397(2)·0.6193(2)·0.0444·1.0000·Uani·····
C19·C·0.5084(3)·0.0391(2)·0.6709(2)·0.0439·1.0000·Uani·····
C20·C·0.5572(2)·0.0940(2)·0.6784(2)·0.0376·1.0000·Uani·····
C21·C·0.5542(2)·0.14898(19)·0.63482(17)·0.0285·1.0000·Uani·····
C22·C·0.6018(2)·0.21083(19)·0.63869(17)·0.0270·1.0000·Uani·····
C23·C·0.6567(2)·0.2223(2)·0.68823(19)·0.0349·1.0000·Uani·····
C24·C·0.6981(2)·0.2828(3)·0.6892(2)·0.0405·1.0000·Uani·····
C25·C·0.6857(2)·0.3317(2)·0.6410(2)·0.0371·1.0000·Uani·····
C26·C·0.6306(2)·0.32039(19)·0.59122(18)·0.0282·1.0000·Uani·····
C27·C·0.5878(18)·0.26013(18)·0.58938(16)·0.0233·1.0000·Uani·····
C28·C·0.4985(2)·0.3743(2)·0.46413(19)·0.0339·1.0000·Uani·····
C29·C·0.5212(3)·0.4295(2)·0.4270(2)·0.0427·1.0000·Uani·····
C30·C·0.5798(3)·0.4205(2)·0.3853(2)·0.0453·1.0000·Uani·····
C31·C·0.6154(2)·0.3571(2)·0.3832(2)·0.0403·1.0000·Uani·····
C32·C·0.5919(2)·0.3034(2)·0.42276(17)·0.0293·1.0000·Uani·····
C33·C·0.6276(2)·0.2348(2)·0.42779(17)·0.0293·1.0000·Uani·····
C34·C·0.6873(2)·0.2142(2)·0.3892(2)·0.0395·1.0000·Uani·····
C35·C·0.7175(2)·0.1493(3)·0.3976(2)·0.0451·1.0000·Uani·····
C36·C·0.6892(2)·0.1047(2)·0.4428(2)·0.0411·1.0000·Uani·····
C37·C·0.6294(2)·0.1251(2)·0.4816(2)·0.0352·1.0000·Uani·····
C38·C·0.59733(18)·0.19033(18)·0.47489(17)·0.0252·1.0000·Uani·····
C39·C·0.6981(3)·-0.0389(3)·0.2278(3)·0.0650·1.0000·Uani·····
C51·C·0.9329(2)·0.10642(19)·0.56617(17)·0.0300·1.0000·Uani·····
C52·C·0.8810(2)·0.0904(2)·0.61220(19)·0.0351·1.0000·Uani·····
C53·C·0.8166(2)·0.1306(2)·0.61634(19)·0.0370·1.0000·Uani·····
C54·C·0.8056(2)·0.1857(2)·0.57434(19)·0.0333·1.0000·Uani·····
C55·C·0.86015(19)·0.19947(18)·0.52918(16)·0.0249·1.0000·Uani·····
C56·C·0.85209(19)·0.25544(18)·0.48087(16)·0.0243·1.0000·Uani·····
C57·C·0.8056(2)·0.31122(2)·0.48995(18)·0.0307·1.0000·Uani·····
C58·C·0.8025(2)·0.3634(2)·0.44326(19)·0.0348·1.0000·Uani·····
C59·C·0.8402(2)·0.3536(2)·0.38640(19)·0.0343·1.0000·Uani·····
C60·C·0.8839(2)·0.2941?(19)·0.37827(17)·0.0274·1.0000·Uani·····
C61·C·0.9134(2)·0.2785(2)·0.31381(17)·0.0290·1.0000·Uani·····
C62·C·0.9591(3)·0.3249(2)·0.2813(2)·0.0383·1.0000·Uani·····
C63·C·0.9819(3)·0.3095(3)·0.2195(2)·0.0477·1.0000·Uani·····
C64·C·0.9579(3)·0.2500(3)·0.1889(2)·0.0476·1.0000·Uani·····
C65·C·0.9119(2)·0.2038(3)·0.2200(2)·0.0424·1.0000·Uani·····
C66·C·0.8903(2)·0.2179(2)·0.28295(18)·0.0325·1.0000·Uani·····
C67·C·0.9245(2)·0.0622(2)·0.39534(19)·0.0329·1.0000·Uani·····
C68·C·0.9120(3)·0.0099(2)·0.3505(2)·0.0431·1.0000·Uani·····
C69·C·0.9536(3)·0.0095(2)·0.2949(2)·0.0454·1.0000·Uani·····
C70·C·1.0069(3)·0.0605(2)·0.2860(2)·0.0382·1.0000·Uani·····
C71·C·1.0176(2)·0.11284(19)·0.33199(16)·0.0268·1.0000·Uani·····
C72·C·1.0689(2)·0.17153(19)·0.32761(17)·0.0281·1.0000·Uani·····
C73·C·1.1157(2)·0.1824(2)·0.2753(2)·0.0390·1.0000·Uani·····
C74·C·1.1590(2)·0.2416(3)·0.2732(2)·0.0445·1.0000·Uani·····
C75·C·1.1554(2)·0.2905(3)·0.3219(2)·0.0406·1.0000·Uani·····
C76·C·1.1100(2)·0.2791(2)·0.37450(18)·0.0295·1.0000·Uani·····
C77·C·1.0662(19)·0.21965(18)·0.37871(16)·0.0244·1.0000·Uani·····
C78·C·1.0117(2)·0.33264(18)·0.51617(17)·0.0277·1.0000·Uani·····
C79·C·1.0443(2)·0.3828(2)·0.55589(19)·0.0334·1.0000·Uani·····
C80·C·1.1074(2)·0.3661(2)·0.5943(2)·0.0370·1.0000·Uani·····
C81·C·1.1371(2)·0.3008(2)·0.59058(19)·0.0347·1.0000·Uani·····
C82·C·1.1041(2)·0.25137(19)·0.54866(16)·0.0262·1.0000·Uani·····
C83·C·1.1337(2)·0.18275(19)·0.53617(17)·0.0280·1.0000·Uani·····
C84·C·1.2001(2)·0.1564(2)·0.5665(2)·0.0379·1.0000·Uani·····
C85·C·1.2277(2)·0.0925(2)·0.5486(2)·0.0429·1.0000·Uani·····
C86·C·1.1895(2)·0.0547(2)·0.5011(2)·0.0407·1.0000·Uani·····
C87·C·1.1224(2)·0.0800(2)·0.47180(19)·0.0325·1.0000·Uani·····
C88·C·1.09297(18)·0.14442(18)·0.48871(16)·0.0249·1.0000·Uani·····
P1·P·0.74764(5)·0.49925(5)·0.26962(4)·0.0277·1.0000·Uani·····
P2·P·0.85145(5)·0.49664(8)·0.59166(7)·0.0566·1.0000·Uani·····
F1·F·0.73257(16)·0.41789(12)·0.26466(12)·0.0444·1.0000·Uani·····
F2·F·0.76080(16)·0.58060(13)·0.27605(14)·0.0491·1.0000·Uani·····
F3·F·0.74653(19)·0.50446(15)·0.19256(12)·0.0573·1.0000·Uani·····
F4·P·0.74700(14)·0.49333(12)·0.34710(10)·0.0384·1.0000·Uani·····
F5·F·0.65755(13)·0.51287(13)·0.26789(12)·0.0402·1.0000·Uani·····
F6·F·0.74652(15)·0.48545(16)·0.27190(16)·0.0562·1.0000·Uani·····
F11·F·0.76686(19)·0.4687(2)·0.5745(2)·0.0899·1.0000·Uani·D·U·····
F12·F·0.9336(2)·0.5231(2)·0.6068(2)·0.1081·1.0000·Uani·D·U·····
F13·F·0.8650(3)·0.4986(3)·0.51743(18)·0.1220·1.0000·Uani·D·U·····
F14·P·0.8351(3)·0.4863(3)·0.66474(17)·0.1344·1.0000·Uani·D·U·····
F15·P·0.8794(2)·0.41843(19)·0.5896(2)·0.1051·1.0000·Uani·D·U·····
F16·P·0.8186(3)·0.57071(18)·0.5892(3)·0.1259·1.0000·Uani·D·U·····
C11·C1·0.69861(12)·0.03579(10)·0.27969(10)·0.0892·1.0000·Uani·····
C12·C1·0.71482(13)·-0.10911(11)·0.27755(10)·0.0936·1.0000·Uani·····
C13·C1·0.61365(14)·-0.04194(18)·0.18434(12)·0.1248·1.0000·Uani·····
H1·O·0.4798·0.1165·0.4124·0.0411·1.0000·Uiso·R·····
H21·H·0.3805·0.0771·0.3430·0.0525·1.0000·Uiso·R·····
H31·H·0.2645·0.1332·0.3441·0.0574·1.0000·Uiso·R·····
H41·H·0.2488·0.2268·0.4142·0.0482·1.0000·Uiso·R·····
H71·H·0.2617·0.3334·0.4577·0.0458·1.0000·Uiso·R·····
H81·H·0.2609·0.4217·0.5345·0.0491·1.0000·Uiso·R·····
H91·H·0.3407·0.4121·0.6272·0.0430·1.0000·Uiso·R·····
H121·H·0.4912·0.4052·0.6685·0.0551·1.0000·Uiso·R·····
H131·H·0.5536·0.3810·0.7691·0.0743·1.0000·Uiso·R·····
H141·H·0.5319·0.2783·0.8220·0.0782·1.0000·Uiso·R·····


H151·H·0.4526·0.1966·0.7755·0.0715·1.0000·Uiso·R·····
H161·H·0.3949·0.2165·0.6730·0.0523·1.0000·Uiso·R·····
H171·H·0.4186·0.0948·0.5414·0.0429·1.0000·Uiso·R·····
H181·H·0.4205·0.0040·0.6137·0.0522·1.0000·Uiso·R·····
H191·H·0.5104·0.0015·0.7000·0.0532·1.0000·Uiso·R·····
H201·H·0.5935·0.0948·0.7138·0.0465·1.0000·Uiso·R·····
H231·H·0.6644·0.1889·0.7206·0.0409·1.0000·Uiso·R·····
H241·H·0.7349·0.2908·0.7222·0.0481·1.0000·Uiso·R·····
H251·H·0.7143·0.3728·0.6415·0.0441·1.0000·Uiso·R·····
H261·H·0.6222·0.3532·0.5581·0.0343·1.0000·Uiso·R·····
H281·H·0.4573·0.3799·0.4919·0.0401·1.0000·Uiso·R·····
H291·H·0.4967·0.4728·0.4301·0.0510·1.0000·Uiso·R·····
H301·H·0.5952·0.4573·0.3590·0.0542·1.0000·Uiso·R·····
H311·H·0.6558·0.3498·0.3550·0.0491·1.0000·Uiso·R·····
H341·H·0.7058·0.2447·0.3578·0.0483·1.0000·Uiso·R·····
H351·H·0.7577·0.1351·0.3718·0.0543·1.0000·Uiso·R·····
H361·H·0.7103·0.0603·0.4475·0.0491·1.0000·Uiso·R·····
H371·H·0.6104·0.0947·0.5127·0.0427·1.0000·Uiso·R·····
H391·H·0.7395·-0.0337·0.1979·0.0763·1.0000·Uiso·R·····
H511·H·0.9771·0.0795·0.5632·0.0361·1.0000·Uiso·R·····
H521·H·0.8899·0.0527·0.6404·0.0421·1.0000·Uiso·R·····
H531·H·0.7806·0.1207·0.6469·0.0453·1.0000·Uiso·R·····
H541·H·0.7620·0.2135·0.5756·0.0394·1.0000·Uiso·R·····
H571·H·0.7768·0.3159·0.5270·0.0369·1.0000·Uiso·R·····
H581·H·0.7752·0.4038·0.4503·0.0411·1.0000·Uiso·R·····
H591·H·0.8368·0.3866·0.3522·0.0413·1.0000·Uiso·R·····
H621·H·0.9739·0.3665·0.3018·0.0463·1.0000·Uiso·R·····
H631·H·1.0142·0.3404·0.1983·0.0573·1.0000·Uiso·R·····
H641·H·0.9724·0.2401·0.1466·0.0563·1.0000·Uiso·R·····
H651·H·0.8953·0.1632·0.1990·0.0499·1.0000·Uiso·R·····
H661·H·0.8597·0.1862·0.3048·0.0392·1.0000·Uiso·R·····
H671·H·0.8966·0.0630·0.4331·0.0391·1.0000·Uiso·R·····
H681·H·0.8758·-0.0247·0.3573·0.0512·1.0000·Uiso·R·····
H691·H·0.9459·-0.0249·0.2637·0.0525·1.0000·Uiso·R·····
H701·H·1.0363·0.0607·0.2492·0.0460·1.0000·Uiso·R·····
H731·H·1.1173·0.1494·0.2421·0.0461·1.0000·Uiso·R·····
H741·H·1.1909·0.2487·0.2383·0.0522·1.0000·Uiso·R·····
H751·H·1.1828·0.3313·0.3195·0.0490·1.0000·Uiso·R·····
H761·H·1.1084·0.3117·0.4074·0.0352·1.0000·Uiso·R·····
H781·H·0.9684·0.3437·0.4913·0.0326·1.0000·Uiso·R·····
H791·H·1.0230·0.4271·0.5564·0.0400·1.0000·Uiso·R·····
H801·H·1.1299·0.3986·0.6225·0.0442·1.0000·Uiso·R·····
H811·H·1.1800·0.2889·0.6159·0.0412·1.0000·Uiso·R·····
H841·H·1.2255·0.1826·0.5991·0.0451·1.0000·Uiso·R·····
H851·H·1.2721·0.0749·0.5690·0.0502·1.0000·Uiso·R·····
H861·H·1.2089·0.0119·0.4884·0.0480·1.0000·Uiso·R·····
H871·H·1.0966·0.0536·0.4404·0.0392·1.0000·Uiso·R·····
loop_
_atom_site_aniso_label·
_atom_site_aniso_U_11·
_atom_site_aniso_U_22·
_atom_site_aniso_U_33·
_atom_site_aniso_U_23·
_atom_site_aniso_U_13·
_atom_site_aniso_U_12·
Ir1·1.01947(6)·0.02125(6)·0.01996(6)·0.00083(4)·-0.00001(4)·0.00264(4)·
Ir2·0.01797(6)·0.02201(6)·0.02081(6)·-0.00109(5)·-0.00006(4)·0.00086(4)·
N1·0.0141(11)·0.0325(15)·0.0258(14)·-0.0041(12)·-0.0027(10)·-0.0012(11)·
N2·0.0202(12)·0.0273(14)·0.0230(13)·-0.0024(11)·0.0027(10)·0.0014(11)·
N3·0.0254(14)·0.0241(13)·0.0277(14)·0.0014(12)·0.0054(11)·0.0002(11)·


N4·0.0240(14)·0.0270(14)·0.0274(14)·0.0037(12)·-0.0004(11)·-0.0009(11)·
N51·0.0248(13)·0.0250(14)·0.0222(13)·0.0012(11)·0.0021(10)·-0.0016(11)·
N52·0.0213(13)·0.0268(14)·0.0221(13)·0.0001(11)·-0.0007(10)·0.0029(11)·
N53·0.0254(14)·0.0233(13)·0.0285(14)·-0.0018(11)·-0.0031(11)·0.0040(11)·
N54·0.0209(12)·0.0241(13)·0.0224(13)·-0.0003(11)·0.0018(10)·0.0003(11)·
C1·0.0287(17)·0.039(2)·0.0354(19)·-0.0115(16)·-0.0003(15)·0.0018(15)·
C2·0.039(2)·0.056(3)·0.039(2)·-0.019(2)·-0.0077(17)·0.000(2)·
C3·0.037(2)·0.063(3)·0.046(2)·-0.020(2)·-0.0120(18)·-0.002(2)·
C4·0.0261(18)·0.056(2)·0.043(2)·-0.0118(19)·-0.0095(16)·0.0046(17)·
C5·0.0268(18)·0.0363(19)·0.0262(16)·-0.0020(15)·-0.0029(13)·0.0012(15)·
C6·0.0201(15)·0.0344(18)·0.0296(17)·-0.0005(14)·0.0004(13)·0.0026(13)·
C7·0.0303(18)·0.049(2)·0.037(2)·-0.0023(18)·-0.0023(15)·0.0114(17)·
C8·0.037(2)·0.040(2)·0.048(2)·-0.0013(18)·-0.0049(17)·0.0165(18)·
C9·0.0370(19)·0.0356(19)·0.0262(19)·-0.0079(16)·0.0047(16)·0.0075(16)·
C10·0.0256(16)·0.0314(17)·0.0282(17)·-0.0006(14)·0.0059(13)·0.0013(14)·
C11·0.0272(17)·0.043(2)·0.0259(16)·-0.0085(15)·0.0056(13)·0.0064(15)·
C12·0.042(2)·0.050(2)·0.044(2)·-0.0197(19)·0.0014(18)·0.0051(19)·
C13·0.049(3)·0.084(4)·0.053(3)·-0.043(3)·-0.008(2)·0.011(3)·
C14·0.072(3)·0.087(4)·0.036(2)·-0.007(3)·-0.007(2)·0.037(3)·
C15·0.074(3)·0.073(3)·0.034(2)·0.008(2)·0.003(2)·0.028(3)·
C16·0.049(2)·0.049(2)·0.0293(19)·0.0035(17)·0.0077(17)·0.0087(19)·
C17·0.0323(18)·0.0308(18)·0.042(2)·0.0024(16)·0.0005(16)·-0.0060(15)·
C18·0.041(2)·0.032(2)·0.060(3)·0.0066(19)·-0.006(2)·-0.0084(17)·
C19·0.049(2)·0.032(2)·0.051(2)·0.0137(18)·0.009(2)·0.0015(18)·
C20·0.040(2)·0.037(2)·0.036(2)·0.0056(16)·0.0002(16)·0.0060(17)·
C21·0.0279(16)·0.0301(17)·0.0277(16)·0.0001(14)·0.0028(13)·0.0035(14)·
C22·0.0253(16)·0.0334(18)·0.0223(15)·-0.0002(13)·0.0000(13)·0.0034(13)·
C23·0.0305(18)·0.046(2)·0.0273(17)·-0.0002(16)·-0.0043(14)·0.0062(16)·
C24·0.0293(18)·0.059(3)·0.0327(19)·-0.0096(18)·-0.0054(15)·0.0016(18)·
C25·0.0249(18)·0.041(2)·0.041(2)·-0.0134(17)·-0.0054(16)·-0.0084(16)·
C26·0.0258(16)·0.0284(17)·0.0305(17)·-0.0050(14)·0.0017(13)·-0.0023(13)·
C27·0.0171(14)·0.0286(16)·0.0241(15)·-0.0041(13)·-0.0006(12)·-0.0002(12)·
C28·0.0329(18)·0.0332(19)·0.0357(19)·0.0059(15)·-0.0017(15)·-0.0030(15)·
C29·0.048(2)·0.034(2)·0.046(2)·-0.0104(18)·0.0030(19)·0.0029(18)·
C30·0.047(2)·0.045(2)·0.044(2)·-0.0155(19)·0.0057(19)·-0.0062(19)·
C31·0.039(2)·0.049(2)·0.0329(19)·-0.0038(18)·0.0088(16)·-0.0065(18)·
C32·0.0249(16)·0.0390(19)·0.0241(16)·0.0017(15)·0.0016(13)·-0.0044(15)·
C33·0.0232(15)·0.0396(19)·0.0249(16)·-0.0076(15)·0.0001(13)·-0.0004(14)·
C34·0.0323(19)·0.050(2)·0.037(2)·-0.0059(18)·0.0081(16)·0.0003(17)·
C35·0.0288(19)·0.057(3)·0.050(2)·-0.012(2)·0.0082(17)·0.0025(19)·
C36·0.0343(19)·0.040(2)·0.048(2)·-0.0129(19)·-0.0036(17)·0.0130(17)·
C37·0.0308(18)·0.0340(19)·0.038(2)·-0.0048(16)·-0.0017(15)·0.0075(15)·
C38·0.0176(14)·0.0305(17)·0.0298(16)·-0.0098(14)·-0.0024(12)·0.0014(13)·
C39·0.058(3)·0.078(4)·0.060(3)·0.017(3)·0.015(3)·0.001(3)·
C51·0.0347(18)·0.0287(17)·0.0266(16)·0.0018(14)·-0.0008(14)·0.0012(15)·
C52·0.046(2)·0.0313(18)·0.0280(18)·-0.0051(15)·-0.0037(16)·-0.0024(16)·
C53·0.042(2)·0.039(2)·0.0301(18)·0.0020(16)·0.0106(16)·-0.0066(17)·
C54·0.0316(18)·0.0369(19)·0.0317(18)·-0.0017(16)·0.0070(15)·-0.0002(15)·
C55·0.0249(15)·0.0274(16)·0.0224(15)·-0.0015(13)·0.0013(12)·-0.0026(13)·
C56·0.0199(14)·0.0281(16)·0.0247(15)·-0.0031(13)·-0.0007(12)·0.0030(12)·
C57·0.0259(16)·0.0350(19)·0.0313(18)·-0.0040(15)·0.0028(14)·0.0042(15)·
C58·0.0349(19)·0.0328(19)·0.0369(19)·-0.0008(15)·-0.0014(15)·0.0134(15)·
C59·0.0379(19)·0.0314(18)·0.0332(18)·0.0053(15)·-0.0030(15)·0.0111(16)·
C60·0.0250(16)·0.0301(17)·0.0268(16)·0.0013(14)·-0.0013(13)·0.0047(13)·
C61·0.0249(16)·0.0371(19)·0.0247(16)·0.0078(14)·-0.0022(13)·0.0072(14)·
C62·0.045(2)·0.037(2)·0.0336(19)·0.0115(16)·0.0025(17)·0.0077(17)·
C63·0.047(2)·0.061(3)·0.036(2)·0.021(2)·0.0077(18)·0.009(2)·
C64·0.046(2)·0.071(3)·0.0257(18)·0.008(2)·-0.0037(17)·0.021(2)·
C65·0.039(2)·0.056(3)·0.0309(19)·-0.0049(18)·-0.0060(16)·0.0177(19)·
C66·0.0272(17)·0.043(2)·0.0274(17)·0.0001(15)·-0.0021(14)·0.0092(15)·
```

```
C67·0.0335(18)·0.0315(18)·0.0334(19)·-0.0009(15)·-0.0017(15)·-0.0008(15)·
C68·0.051(2)·0.032(2)·0.046(2)·-0.0032(18)·-0.0080(19)·-0.0060(18)·
C69·0.059(3)·0.033(2)·0.043(2)·-0.0103(18)·-0.010(2)·0.0048(19)·
C70·0.049(2)·0.034(2)·0.0309(19)·-0.0046(16)·-0.0008(17)·0.0088(17)·
C71·0.0258(16)·0.0300(17)·0.0244(15)·-0.0056(14)·-0.0017(12)·0.0099(14)·
C72·0.0255(16)·0.0342(18)·0.0245(16)·0.0012(14)·0.0016(13)·0.0086(14)·
C73·0.036(2)·0.052(2)·0.0300(18)·-0.0041(17)·0.0072(16)·0.0086(18)·
C74·0.037(2)·0.066(3)·0.0318(19)·0.0016(19)·0.0126(16)·-0.002(2)·
C75·0.0343(19)·0.054(2)·0.034(2)·0.0064(18)·0.0069(16)·-0.0078(18)·
C76·0.0243(16)·0.0350(18)·0.0293(17)·0.0020(15)·0.0009(13)·-0.0009(14)·
C77·0.0208(14)·0.0299(17)·0.0224(15)·0.0041(13)·0.0008(12)·0.0082(13)·
C78·0.0281(16)·0.0265(16)·0.0289(17)·-0.0040(13)·0.0038(13)·-0.0006(13)·
C79·0.0381(19)·0.0286(17)·0.0342(18)·-0.0030(15)·0.0095(15)·-0.0038(15)·
C80·0.041(2)·0.038(2)·0.0323(19)·-0.0090(16)·0.0018(16)·-0.0098(17)·
C81·0.0345(19)·0.039(2)·0.0298(18)·0.0001(16)·-0.0065(15)·-0.0059(16)·
C82·0.0256(16)·0.0313(17)·0.0215(15)·0.0016(13)·-0.0003(13)·-0.0039(13)·
C83·0.0234(16)·0.0323(18)·0.0279(17)·0.0052(14)·-0.0032(13)·0.0009(14)·
C84·0.0328(19)·0.040(2)·0.040(2)·0.0055(17)·-0.0092(16)·-0.0008(17)·
C85·0.0320(19)·0.044(2)·0.051(2)·0.0079(19)·-0.0123(18)·0.0104(17)·
C86·0.037(2)·0.033(2)·0.051(2)·0.0077(18)·-0.0046(18)·0.0113(16)·
C87·0.0318(18)·0.0285(17)·0.0367(19)·0.0013(15)·-0.0057(15)·0.0054(15)·
C88·0.0203(14)·0.0285(16)·0.0258(16)·0.0068(13)·-0.0011(12)·0.0020(13)·
P1·0.0310(5)·0.0256(4)·0.0265(4)·0.0027(3)·0.0031(3)·0.0033(3)·
P2·0.0692(8)·0.0537(7)·0.0475(7)·0.0017(6)·0.0098(6)·0.0208(6)·
F1·0.0621(16)·0.0244(11)·0.0459(14)·-0.0048(10)·-0.0084(12)·0.0043(11)·
F2·0.0556(15)·0.0266(12)·0.0655(17)·0.0061(11)·0.0042(13)·-0.0071(11)·
F3·0.090(2)·0.0558(16)·0.0267(12)·0.0093(11)·0.0125(12)·0.0300(15)·
F4·0.0497(14)·0.0385(12)·0.0264(11)·0.0025(9)·-0.0017(10)·0.0094(10)·
F5·0.0321(12)·0.0430(13)·0.0452(13)·0.0030(11)·-0.0044(10)·0.0065(10)·
F6·0.0317(13)·0.0627(18)·0.0750(19)·0.0147(15)·0.0145(12)·0.0100(12)·
F11·0.069(2)·0.090(3)·0.112(3)·0.024(2)·0.016(2)·0.0032(19)·
F12·0.091(2)·0.104(3)·0.126(3)·-0.037(3)·-0.030(2)·0.021(2)·
F13·0.143(3)·0.159(4)·0.067(2)·-0.009(3)·0.037(2)·-0.062(3)·
F14·0.124(3)·0.221(5)·0.059(2)·0.009(3)·0.016(2)·0.070(3)·
F15·0.090(3)·0.070(2)·0.157(4)·0.004(3)·0.019(3)·0.023(2)·
F16·0.125(3)·0.054(2)·0.192(4)·-0.024(3)·-0.079(3)·0.029(2)·
C11·0.1001(13)·0.0695(10)·0.0985(13)·-0.0113(9)·0.0096(11)·-0.0037(9)·
C12·0.1117(14)·0.0886(12)·0.0829(11)·0.0252(10)·0.0349(10)·0.0362(11)·
C13·0.0985(15)·0.186(3)·0.0879(14)·0.0161(15)·-0.0286(12)·-0.0253(16)·

_refine_ls_extinction_coef·114(11)·
_refine_ls_extinction_method·
····'Larson·(1970),·Equation·22'
_oxford_refine_ls_scale·0.07642(6)·
loop_
·_geom_bond_atom_site_label_1
·_geom_bond_site_symmetry_1
·_geom_bond_atom_site_label_2
·_geom_bond_site_symmetry_2
·_geom_bond_distance
·_geom_bond_publ_flag
Ir1··N51··2.148(3)····yes
Ir1··N52··2.199(3)····yes
Ir1··N53··2.043(3)····yes
Ir1··N54··2.068(3)····yes
Ir1··C77··2.017(3)····yes
Ir1··C88··2.004(3)····yes
Ir2··N1··2.151(3)····yes
Ir2··N2··2.215(3)····yes
Ir2··N3··2.036(3)····yes

Ir2··N4··2.056(3)····yes
Ir2··C27··2.025(3)····yes
Ir2··C38··2.004(3)····yes
N1··C1··1.335(5)····yes
N1··C5··1.347(5)····yes
N2··C6··1.366(4)····yes
N2··C10··1.349(5)····yes
N3··C17··1.340(5)····yes
N3··C21··1.362(5)····yes
N4··C28··1.348(5)····yes
N4··C32··1.362(5)····yes
N51··C51··1.351(5)····yes
N51··C55··1.358(4)····yes
N52··C56··1.365(4)····yes
N52··C60··1.354(5)····yes
N53··C67··1.349(5)····yes
N53··C71··1.374(5)····yes
N54··C78··1.348(4)····yes
N54··C82··1.370(4)····yes
C1··C2··1.394(5)····yes
C1··H11··0.942····no
C2··C3··1.381(7)····yes
C2··H21··0.939····no
C3··C4··1.376(6)····yes
C3··H31··0.930····no
C4··C5··1.392(5)····yes
C4··H41··0.938····no
C5··C6··1.475(5)····yes
C6··C7··1.390(5)····yes
C7··C8··1.378(6)····yes
C7··H71··0.941····no
C8··C9··1.379(6)····yes
C8··H81··0.945····no
C9··C10··1.403(5)····yes
C9··H91··0.936····no
C10··C11··1.479(5)····yes
C11··C12··1.381(6)····yes
C11··C16··1.390(6)····yes
C12··C13··1.420(7)····yes
C12··H121··0.939····no
C13··C14··1.372(9)····yes
C13··H131··0.928····no
C14··C15··1.365(9)····yes
C14··H141··0.942····no
C15··C16··1.384(7)····yes
C15··H151··0.939····no
C16··H161··0.950····no
C17··C18··1.375(6)····yes
C17··H171··0.948····no
C18··C19··1.391(7)····yes
C18··H181··0.928····no
C19··C20··1.372(6)····yes
C19··H191··0.945····no
C20··C21··1.393(5)····yes
C20··H201··0.952····no
C21··C22··1.462(5)····yes
C22··C23··1.399(5)····yes
C22··C27··1.411(5)····yes
C23··C24··1.380(6)····yes
C23··H231··0.936····no

C24··C25··1.385(6)····yes
C24··H241··0.936····no
C25··C26··1.404(5)····yes
C25··H251··0.942····no
C26··C27··1.393(5)····yes
C26··H261··0.941····no
C28··C29··1.382(6)····yes
C28··H281··0.947····no
C29··C30··1.378(6)····yes
C29··H291··0.947····no
C30··C31··1.380(7)····yes
C30··H301··0.942····no
C31··C32··1.395(6)····yes
C31··H311··0.946····no
C32··C33··1.473(5)····yes
C33··C34··1.401(5)····yes
C33··C38··1.417(5)····yes
C34··C35··1.374(7)····yes
C34··H341··0.943····no
C35··C36··1.379(7)····yes
C35··H351··0.943····no
C36··C37··1.403(6)····yes
C36··H361··0.940····no
C37··C38··1.388(5)····yes
C37··H371··0.942····no
C39··C12··1.799(7)····yes
C39··C12'··1.722(6)····yes
C39··C13··1.710(7)····yes
C39··H391··0.977····no
C51··C52··1.379(5)····yes
C51··H511··0.941····no
C52··C53··1.379(6)····yes
C52··H521··0.942····no
C53··C54··1.385(6)····yes
C53··H531··0.932····no
C54··C55··1.390(5)····yes
C54··H541··0.938····no
C55··C56··1.476(5)····yes
C56··C57··1.387(5)····yes
C57··C58··1.382(6)····yes
C57··H571··0.935····no
C58··C59··1.383(6)····yes
C58··H581··0.933····no
C59··C60··1.399(5)····yes
C59··H591··0.937····no
C60··C61··1.477(5)····yes
C61··C62··1.394(6)····yes
C61··C66··1.390(6)····yes
C62··C63··1.384(6)····yes
C62··H621··0.942····no
C63··C64··1.374(8)····yes
C63··H631··0.942····no
C64··C65··1.382(7)····yes
C64··H641··0.938····no
C65··C66··1.395(5)····yes
C65··H651··0.939····no
C66··H661··0.941····no
C67··C68··1.384(6)····yes
C67··H671··0.936····no
C68··C69··1.384(7)····yes

C68··H681··0.939····no
C69··C70··1.379(7)····yes
C69··H691··0.934····no
C70··C71··1.395(5)····yes
C70··H701··0.937····no
C71··C72··1.457(5)····yes
C72··C73··1.398(5)····yes
C72··C77··1.409(5)····yes
C73··C74··1.379(7)····yes
C73··H731··0.937····no
C74··C75··1.384(7)····yes
C74··H741··0.940····no
C75··C76··1.389(5)····yes
C75··H751··0.928····no
C76··C77··1.389(5)····yes
C76··H761··0.929····no
C78··C79··1.382(5)····yes
C78··H781··0.928····no
C79··C80··1.379(6)····yes
C79··H791··0.938····no
C80··C81··1.372(6)····yes
C80··H801··0.939····no
C81··C82··1.401(5)····yes
C81··H811··0.933····no
C82··C83··1.454(5)····yes
C83··C84··1.402(5)····yes
C83··C88··1.405(5)····yes
C84··C85··1.385(6)····yes
C84··H841··0.941····no
C85··C86··1.378(6)····yes
C85··H851··0.937····no
C86··C87··1.396(5)····yes
C86··H861··0.939····no
C87··C88··1.399(5)····yes
C87··H871··0.931····no
P1··F1··1.600(2)····yes
P1··F2··1.597(3)····yes
P1··F3··1.592(3)····yes
P1··F4··1.603(2)····yes
P1··F5··1.608(2)····yes
P1··F6··1.588(3)····yes
P2··F11··1.612(4)····yes
P2··F12··1.557(4)····yes
P2··F13··1.559(4)····yes
P2··F14··1.559(4)····yes
P2··F15··1.593(4)····yes
P2··F16··1.547(3)····yes
loop_
·_geom_angle_atom_site_label_1
·_geom_angle_site_symmetry_1
·_geom_angle_atom_site_label_2
·_geom_angle_site_symmetry_2
·_geom_angle_atom_site_label_3
·_geom_angle_site_symmetry_3
·_geom_angle
·_geom_angle_publ_flag
N51··Ir1··N52··75.81(11)····yes
N51··Ir1··N53··97.52(11)····yes
N52··Ir1··N53··94.64(11)····yes
N51··Ir1··N54··89.15(11)····yes

N52··Ir1··N54··92.08(11)····yes
N53··Ir1··N54··171.51(11)····yes
N51··Ir1··C77··176.74(12)····yes
N52··Ir1··C77··101.71(12)····yes
N53··Ir1··C77··80.48(13)····yes
N54··Ir1··C77··93.08(13)····yes
N51··Ir1··C88··97.49(12)····yes
N52··Ir1··C88··169.95(12)····yes
N53··Ir1··C88··93.67(13)····yes
N54··Ir1··C88··80.20(13)····yes
C77··Ir1··C88··85.24(13)····yes
N1··Ir2··N2··75.66(11)····yes
N1··Ir2··N3··95.53(11)····yes
N2··Ir2··N3··95.43(11)····yes
N1··Ir2··N4··91.68(12)····yes
N2··Ir2··N4··91.03(11)····yes
N3··Ir2··N4··171.32(11)····yes
N1··Ir2··C27··176.55(13)····yes
N2··Ir2··C27··104.13(12)····yes
N3··Ir2··C27··81.05(13)····yes
N4··Ir2··C27··91.77(13)····yes
N1··Ir2··C38··95.29(12)····yes
N2··Ir2··C38··167.59(12)····yes
N3··Ir2··C38··93.87(13)····yes
N4··Ir2··C38··80.62(14)····yes
C27··Ir2··C38··85.42(13)····yes
Ir2··N1··C1··125.7(2)····yes
Ir2··N1··C5··115.7(2)····yes
C1··N1··C5··118.6(3)····yes
Ir2··N2··C6··110.5(2)····yes
Ir2··N2··C10··126.8(2)····yes
C6··N2··C10··118.2(3)····yes
Ir2··N3··C17··126.4(3)····yes
Ir2··N3··C21··115.0(2)····yes
C17··N3··C21··118.4(3)····yes
Ir2··N4··C28··125.5(3)····yes
Ir2··N4··C32··115.8(2)····yes
C28··N4··C32··118.6(3)····yes
Ir1··N51··C51··126.4(2)····yes
Ir1··N51··C55··115.4(2)····yes
C51··N51··C55··118.2(3)····yes
Ir1··N52··C56··110.7(2)····yes
Ir1··N52··C60··126.3(2)····yes
C56··N52··C60··118.3(3)····yes
Ir1··N53··C67··125.1(3)····yes
Ir1··N53··C71··115.6(2)····yes
C67··N53··C71··119.3(3)····yes
Ir1··N54··C78··125.9(2)····yes
Ir1··N54··C82··114.8(2)····yes
C78··N54··C82··119.2(3)····yes
N1··C1··C2··122.8(4)····yes
N1··C1··H11··117.7····no
C2··C1··H11··119.5····no
C1··C2··C3··118.3(4)····yes
C1··C2··H21··120.7····no
C3··C2··H21··120.4····no
C2··C3··C4··119.5(4)····yes
C2··C3··H31··120.4····no
C4··C3··H31··121.0····no
C3··C4··C5··119.2(4)····yes

C3··C4··H41··121.3····no
C5··C4··H41··119.6····no
C4··C5··N1··121.7(4)····yes
C4··C5··C6··122.7(3)····yes
N1··C5··C6··115.6(3)····yes
C5··C6··N2··115.3(3)····yes
C5··C6··C7··122.7(3)····yes
N2··C6··C7··122.0(3)····yes
C6··C7··C8··119.1(4)····yes
C6··C7··H71··120.2····no
C8··C7··H71··120.7····no
C7··C8··C9··119.1(4)····yes
C7··C8··H81··120.1····no
C9··C8··H81··120.8····no
C8··C9··C10··119.6(4)····yes
C8··C9··H91··120.5····no
C10··C9··H91··119.9····no
C9··C10··N2··121.2(3)····yes
C9··C10··C11··119.9(3)····yes
N2··C10··C11··118.7(3)····yes
C10··C11··C12··121.8(4)····yes
C10··C11··C16··117.9(4)····yes
C12··C11··C16··120.3(4)····yes
C11··C12··C13··118.5(5)····yes
C11··C12··H121··120.6····no
C13··C12··H121··120.9····no
C12··C13··H131··119.5····no
C14··C13··H131··120.4····no
C13··C14··C15··121.0(5)····yes
C13··C14··H141··119.5····no
C15··C14··H141··119.5····no
C14··C15··C16··119.7(6)····yes
C14··C15··H151··119.9····no
C16··C15··H151··120.4····no
C11··C16··C15··120.5(5)····yes
C11··C16··H161··118.8····no
C15··C16··H161··120.6····no
N3··C17··C18··123.1(4)····yes
N3··C17··H171··117.8····no
C18··C17··H171··119.2····no
C17··C18··C19··119.0(4)····yes
C17··C18··H181··120.2····no
C19··C18··H181··120.9····no
C18··C19··C20··118.8(4)····yes
C18··C19··H191··120.1····no
C20··C19··H191··121.1····no
C19··C20··C21··120.7(4)····yes
C19··C20··H201··119.9····no
C21··C20··H201··119.4····no
C20··C21··N3··119.9(3)····yes
C20··C21··C22··125.6(3)····yes
N3··C21··C22··114.5(3)····yes
C21··C22··C23··123.3(3)····yes
C21··C22··C27··115.3(3)····yes
C23··C22··C27··121.4(3)····yes
C22··C23··C24··119.7(4)····yes
C22··C23··H231··119.3····no
C24··C23··H231··120.9····no
C23··C24··C25··120.1(4)····yes

C23··C24··H241··120.2····no
C25··C24··H241··119.7····no
C24··C25··C26··120.3(4)····yes
C24··C25··H251··120.0····no
C26··C25··H251··119.7····no
C25··C26··C27··120.9(4)····yes
C25··C26··H261··120.7····no
C27··C26··H261··118.4····no
C22··C27··C26··117.6(3)····yes
C22··C27··Ir2··113.8(2)····yes
C26··C27··Ir2··128.5(3)····yes
N4··C28··C29··122.5(4)····yes
N4··C28··H281··118.0····no
C29··C28··H281··119.4····no
C28··C29··C30··119.2(4)····yes
C28··C29··H291··120.3····no
C30··C29··H291··120.6····no
C29··C30··C31··119.0(4)····yes
C29··C30··H301··120.2····no
C31··C30··H301··120.8····no
C30··C31··C32··119.9(4)····yes
C30··C31··H311··120.4····no
C32··C31··H311··119.7····no
C31··C32··N4··120.8(4)····yes
C31··C32··C33··125.3(4)····yes
N4··C32··C33··113.9(3)····yes
C32··C33··C34··123.0(4)····yes
C32··C33··C38··115.2(3)····yes
C34··C33··C38··121.9(4)····yes
C33··C34··C35··118.9(4)····yes
C33··C34··H341··119.5····no
C35··C34··H341··121.1····no
C34··C35··C36··120.7(4)····yes
C34··C35··H351··119.4····no
C36··C35··H351··119.9····no
C35··C36··C37··120.5(4)····yes
C35··C36··H361··119.4····no
C37··C36··H361··120.1····no
C36··C37··C38··120.7(4)····yes
C36··C37··H371··120.4····no
C38··C37··H371··118.9····no
C33··C38··C37··117.3(3)····yes
C33··C38··Ir2··114.5(3)····yes
C37··C38··Ir2··128.1(3)····yes
C11··C39··C12··106.4(3)····yes
C11··C39··C13··108.9(4)····yes
C12··C39··C13··114.3(4)····yes
C11··C39··H391··107.8····no
C12··C39··H391··110.0····no
C13··C39··H391··109.2····no
N51··C51··C52··122.6(4)····yes
N51··C51··H511··117.8····no
C52··C51··H511··119.6····no
C51··C52··C53··118.0(3)····yes
C51··C52··H521··119.9····no
C53··C52··H521··121.1····no
C52··C53··C54··119.5(4)····yes
C52··C53··H531··120.6····no
C54··C53··H531··119.9····no
C53··C54··C55··118.8(4)····yes

C53··C54··H541··121.3····no
C55··C54··H541··119.8····no
C54··C55··N51··121.3(4)····yes
C54··C55··C56··122.8(3)····yes
N51··C55··C56··115.2(3)····yes
N52··C56··C55··115.5(3)····yes
C55··C56··C57··122.2(3)····yes
N52··C56··C57··122.3(3)····yes
C56··C57··C58··118.8(3)····yes
C56··C57··H571··120.5····no
C58··C57··H571··120.3····no
C57··C58··C59··119.0(3)····yes
C57··C58··H581··120.1····no
C59··C58··H581··120.9····no
C58··C59··C60··119.9(4)····yes
C58··C59··H591··120.5····no
C60··C59··H591··119.5····no
C59··C60··N52··120.7(3)····yes
C59··C60··C61··119.4(3)····yes
N52··C60··C61··119.7(3)····yes
C60··C61··C62··122.0(4)····yes
C60··C61··C66··118.6(3)····yes
C62··C61··C66··119.3(4)····yes
C61··C62··C63··119.8(4)····yes
C61··C62··H621··119.3····no
C63··C62··H621··120.9····no
C62··C63··C64··120.6(4)····yes
C62··C63··H631··119.4····no
C64··C63··H631··120.0····no
C63··C64··C65··120.4(4)····yes
C63··C64··H641··120.6····no
C65··C64··H641··119.0····no
C64··C65··C66··119.5(4)····yes
C64··C65··H651··120.4····no
C66··C65··H651··120.1····no
C65··C66··C61··120.4(4)····yes
C65··C66··H661··120.0····no
C61··C66··H661··119.6····no
N53··C67··C68··122.4(4)····yes
N53··C67··H671··118.1····no
C68··C67··H671··119.5····no
C67··C68··C69··118.8(4)····yes
C67··C68··H681··121.0····no
C69··C68··H681··120.3····no
C68··C69··C70··119.4(4)····yes
C68··C69··H691··120.5····no
C70··C69··H691··120.1····no
C69··C70··C71··120.3(4)····yes
C69··C70··H701··120.7····no
C71··C70··H701··119.0····no
C70··C71··N53··119.7(4)····yes
C70··C71··C72··126.4(3)····yes
N53··C71··C72··113.9(3)····yes
C71··C72··C73··123.4(3)····yes
C71··C72··C77··115.7(3)····yes
C73··C72··C77··120.9(4)····yes
C72··C73··C74··119.5(4)····yes
C72··C73··H731··119.8····no
C74··C73··H731··120.7····no
C73··C74··C75··120.4(4)····yes

C73··C74··H741··119.5····no
C75··C74··H741··120.1····no
C74··C75··C76··120.1(4)····yes
C74··C75··H751··119.8····no
C76··C75··H751··119.6····no
C75··C76··C77··121.1(4)····yes
C75··C76··H761··119.5····no
C77··C76··H761··119.0····no
C72··C77··C76··118.0(3)····yes
C72··C77··Ir1··114.0(3)····yes
C76··C77··Ir1··128.0(3)····yes
N54··C78··C79··122.6(3)····yes
N54··C78··H781··118.7····no
C79··C78··H781··118.7····no
C78··C79··C80··119.0(4)····yes
C78··C79··H791··119.5····no
C80··C79··H791··121.6····no
C79··C80··C81··119.0(4)····yes
C79··C80··H801··120.9····no
C81··C80··H801··120.1····no
C80··C81··C82··120.9(4)····yes
C80··C81··H811··120.0····no
C82··C81··H811··119.0····no
C81··C82··N54··119.3(3)····yes
C81··C82··C83··126.2(3)····yes
N54··C82··C83··114.4(3)····yes
C82··C83··C84··123.6(3)····yes
C82··C83··C88··115.4(3)····yes
C84··C83··C88··121.0(4)····yes
C83··C84··C85··119.3(4)····yes
C83··C84··H841··119.2····no
C85··C84··H841··120.7····no
C84··C85··C86··119.8(4)····yes
C84··C85··H851··119.9····no
C86··C85··H851··120.3····no
C85··C86··C87··120.2(4)····yes
C85··C86··H861··119.6····no
C87··C86··H861··120.0····no
C86··C87··C88··121.4(4)····yes
C86··C87··H871··119.4····no
C88··C87··H871··119.2····no
C83··C88··C87··117.4(3)····yes
C83··C88··Ir2··114.3(3)····yes
C87··C88··Ir1··127.5(3)····yes
F1··P1··F2··178.36(16)····yes
F1··P1··F3··90.16(15)····yes
F2··P1··F3··90.95(16)····yes
F1··P1··F4··89.20(13)····yes
F2··P1··F4··89.67(14)····yes
F3··P1··F4··178.81(17)····yes
F1··P1··F5··89.93(14)····yes
F2··P1··F5··88.87(14)····yes
F3··P1··F5··89.57(15)····yes
F4··P1··F5··89.43(13)····yes
F1··P1··F6··89.85(16)····yes
F2··P1··F6··91.34(16)····yes
F3··P1··F6··90.87(17)····yes
F4··P1··F6··90.13(15)····yes
F5··P1··F6··179.51(15)····yes
F11··P2··F12··178.8(2)····yes
```

```
F11··F2···F13···88.1(2)····yes
F12··F2···F13···90.7(2)····yes
F11··F2···F14···88.1(2)····yes
F12··F2···F14···93.0(3)····yes
F13··F2···F14···173.7(3)····yes
F11··F2···F15···87.7(2)····yes
F12··F2···F15···91.8(2)····yes
F13··F2···F15···86.5(3)····yes
F14··F2···F15···88.4(3)····yes
F11··F2···F16···87.8(2)····yes
F12··F2···F16···92.6(2)····yes
F13··F2···F16···90.9(3)····yes
F14··F2···F16···93.9(3)····yes
F15··F2···F16···174.9(3)····yes
```

bis(2-phenylpyridine-*C*,*N*)(6,6'-diphenyl-2,2'-bipyridine-*N*,*N*')iridium(III) hexafluorophosphate (**51**)

```
data_sg075_1_123k
_audit_creation_date·····07-09-30
_audit_creation_method·CRYSTALS_ver_12.84

_oxford_structure_analysis_title··'sg075_1_123k_0m·in·P2(1)/c'
_chemical_name_systematic·····?
_chemical_melting_point··?

_cell_length_a·····13.6575(6)
_cell_length_b·····8.8865(4)
_cell_length_c·····29.8329(12)
_cell_angle_alpha·····90
_cell_angle_beta···95.286(2)
_cell_angle_gamma·····90
_cell_volume·····3605.3(3)

_symmetry_cell_setting·····'Monoclinic'·
_symmetry_space_group_name_H-M···'P·21/c'·
_symmetry_space_group_name_Hall···'-P·2ybc'·
loop_
·_symmetry_equiv_pos_as_xyz
·'x,y,z'
·'-x,-y,-z'
·'-x,y+1/2,-z+1/2'
·'x,-y+1/2,z+1/2'

loop_
·_atom_type_symbol
·_atom_type_scat_dispersion_real
·_atom_type_scat_dispersion_imag
·_atom_type_scat_Cromer_Mann_a1
·_atom_type_scat_Cromer_Mann_b1
·_atom_type_scat_Cromer_Mann_a2
·_atom_type_scat_Cromer_Mann_b2
·_atom_type_scat_Cromer_Mann_a3
·_atom_type_scat_Cromer_Mann_b3
·_atom_type_scat_Cromer_Mann_a4
·_atom_type_scat_Cromer_Mann_b4
·_atom_type_scat_Cromer_Mann_c
·_atom_type_scat_source··
·C·····0.0033···0.0016···2.3100···20.8439···1.0200···10.2075···1.5886···0.5687
···0.8650···51.6512···0.2156·'International·Tables·Vol·C·4.2.6.8·and·6.1.1.4'
·H·····0.0000···0.0000···0.4930···10.5109···0.3229···26.1257···0.1402···3.1424
···0.0408···57.7998···0.0030·'International·Tables·Vol·C·4.2.6.8·and·6.1.1.4'
·N·····0.0061···0.0033···12.2126···0.0057···3.1322···9.8933···2.0125···28.9975
···1.1663···0.5826··11.5290·'International·Tables·Vol·C·4.2.6.8·and·6.1.1.4'
·F·····0.0171···0.0103···3.5392···10.2825···2.6412···4.2944···1.5170···0.2615
···1.0243···26.1676···0.2778·'International·Tables·Vol·C·4.2.6.8·and·6.1.1.4'
·P·····0.1023···0.0942···6.4345···1.9067···4.1791···27.1570···1.7800···0.5260
···1.4908···68.1645···1.1149·'International·Tables·Vol·C·4.2.6.8·and·6.1.1.4'
·Ir····-1.4442···7.9887···27.1049···16.7296···8.8655···15.6115···0.4179
···5.8338···45.0011···11.4722·'International·Tables·Vol·C·4.2.6.8·and·6.1.1.4'

_cell_formula_units_Z·····4

#·Given·Formula·=·C44·H32·F6·Ir1·N4·P1·
#·Dc·=·····1.76·Fooo·=···1880.00·Mu·=·····38.19·M·=····953.95
#·Found·Formula·=·C44·H32·F6·Ir1·N4·P1·
#·Dc·=·····1.76·FOOO·=···1880.00·Mu·=·····38.19·M·=····953.95


_chemical_formula_sum·····'C44·H32·F6·Ir1·N4·P1'
_chemical_formula_moiety·····'C44·H32·Ir·N4,·F6·P'
_chemical_compound_source·····?
_chemical_formula_weight·····953.95

_cell_measurement_reflns_used·····0
_cell_measurement_theta_min·····0
_cell_measurement_theta_max·····0
_cell_measurement_temperature·····123

_exptl_crystal_description·····'block'·
_exptl_crystal_colour·····'orange'·
_exptl_crystal_size_min·····0.20·
_exptl_crystal_size_mid·····0.24·
_exptl_crystal_size_max·····0.44·

_exptl_crystal_density_diffrn····1.757·
_exptl_crystal_density_meas·····?·
#·Non-dispersive·F(000)::
_exptl_crystal_F_000·····1880·
_exptl_absorpt_coefficient_mu····3.819·

#·Sheldrick·geometric·approximatio·0.40·0.47·
#·No·experimental·values·of·Tmin/max·available·
·_exptl_absorpt_correction_type··'multi-scan'·
_exptl_absorpt_process_details···'DENZO/SCALEPACK·(Otwinowski·&·Minor,·1997)'·
_exptl_absorpt_correction_T_min··0.40·
_exptl_absorpt_correction_T_max··0.47·
#·For·a·Kappa·CCD,·set·Tmin·to·1.0·and·
#·Tmax·to·the·ratio·of·max:min·frame·scales·in·scale_all.log·
_diffrn_measurement_device_type··'Nonius·KappaCCD'·
_diffrn_radiation_monochromator···'graphite'·
_diffrn_radiation_type·····'Mo·K\a'·
_diffrn_radiation_wavelength·····0.71073
_diffrn_measurement_method·····'\f·&·\w·scans'·

#·If·a·reference·occurs·more·than·once,·delete·the·author·
#·and·date·from·subsequent·references.·
_computing_data_collection·····'COLLECT·(Nonius,·1997-2001).'·
_computing_cell_refinement·····'DENZO/SCALEPACK·(Otwinowski·&·Minor,·1997)'·
_computing_data_reduction·····'DENZO/SCALEPACK·(Otwinowski·&·Minor,·1997)'·
_computing_structure_solution····'SIR92·(Altomare·et·al.,·1994)'·
_computing_structure_refinement···'CRYSTALS·(Betteridge·et·al.,·2003)'·
_computing_publication_material···'CRYSTALS·(Betteridge·et·al.,·2003)'·
_computing_molecular_graphics····'CAMERON·(Watkin·et·al.,·1996)'·

_diffrn_standards_interval_time··?·
_diffrn_standards_interval_count·?·
_diffrn_standards_number·····0·
_diffrn_standards_decay_%·····?·

_diffrn_ambient_temperature·····123
_diffrn_reflns_number·····207215·
_reflns_number_total·····20603·
_diffrn_reflns_av_R_equivalents···0.044·
#·Number·of·reflections·with·Friedels·Law·is·20603·
#·Number·of·reflections·without·Friedels·Law·is·0·
#·Theoretical·number·of·reflections·is·about·20672·

_diffrn_reflns_theta_min·····2.122·
_diffrn_reflns_theta_max·····38.790·
_diffrn_measured_fraction_theta_max·0.996·

_diffrn_reflns_theta_full·····38.790·
_diffrn_measured_fraction_theta_full·0.996·

_diffrn_reflns_limit_h_min·····-24·
_diffrn_reflns_limit_h_max·····24·
_diffrn_reflns_limit_k_min·····-15·
_diffrn_reflns_limit_k_max·····15·
_diffrn_reflns_limit_l_min·····-52·
_diffrn_reflns_limit_l_max·····52·
_reflns_limit_h_min·····-24·
_reflns_limit_h_max·····23·
_reflns_limit_k_min·····0·
_reflns_limit_k_max·····15·
_reflns_limit_l_min·····0·
_reflns_limit_l_max·····52·

_oxford_diffrn_Wilson_B_factor···0.00·
_oxford_diffrn_Wilson_scale·····0.00·

_atom_sites_solution_primary·····direct·#heavy,direct,difmap,geom
#·_atom_sites_solution_secondary··difmap
_atom_sites_solution_hydrogens···geom

_refine_diff_density_min·····-1.90·
_refine_diff_density_max·····2.13·

_refine_ls_number_reflns·····12996·
_refine_ls_number_restraints·····836·
_refine_ls_number_parameters····559·

#_refine_ls_R_factor_ref·0.0263·
_refine_ls_wR_factor_ref·····0.0254·
_refine_ls_goodness_of_fit_ref···1.0818·

#_refine_ls_number_all·20589·
_refine_ls_R_factor_all·····0.0543·
_refine_ls_wR_factor_all·····0.0293·

#·The·I/u(I)·cutoff·below·was·used·for·refinement·as·
#·well·as·the··gt·R-factors:
_refine_threshold_expression·····I>3.0\s(I)
_reflns_number_gt·····12996·
_refine_ls_R_factor_gt·····0.0263·
_refine_ls_wR_factor_gt·····0.0254·

_refine_ls_shift/su_max·····0.002583·

#·choose·from:·rm·(reference·molecule·of·known·chirality),·
#·ad·(anomalous·dispersion···Flack),·rmad·(rm·and·ad),·
#·syn·(from·synthesis),·unk·(unknown)·or··(not·applicable)·
_chemical_absolute_configuration·'.'·

_refine_ls_structure_factor_coef·F·
_refine_ls_matrix_type·····full
_refine_ls_hydrogen_treatment·····constr·····#·none,·undef,·noref,·refall,
·····refxyz,·refU,·constr·or·mixed
_refine_ls_weighting_scheme·····calc·
_refine_ls_weighting_details·
;
·Method,·part·1,·Chebychev·polynomial,·(Watkin,·1994,·Prince,·1982)·
·[weight]·=·1.0/[A·0·*T·0·(x)+A·1·*T·1·(x)·...·A·n·1·]*T·n·1·(x)]·
·where·A·1··are·the·Chebychev·coefficients·listed·below,and·x=·Fcalc/Fmax·
·Method·=·Robust·Weighting·(Prince,·1982)·
·W·=·[weight]·*·[1-(deltaF/6*sigmaF)^2^]^2^·
·A·1··are:·
·0.510·-0.721·0.279·-0.330·
;

#·Check·this·file·using·the·IUCr·facility·at:·
#·http://checkcif.iucr.org/·

#·The·content·below·is·held·in·the·file·'script/refcif.dat'.·This·is·a·text·
#·file·which·you·may·edit·to·reflect·local·conditions.·
#·Items·which·need·looking·at·are·represented·by·a·'?'.·
#·Items·for·which·there·are·choices·are·prefixed·with·'choose·from'.·

_publ_contact_letter·
;·
·Please·consider·this·CIF·submission·for·
·publication·as·a·Short·Format·Paper·in·Acta·
·Crystallographica·E.·The·figures·will·be·
·sent·by·e-mail.·
;
_publ_contact_author_name·····'Anthony·Other'·
_publ_contact_author_address·
;·
·Chemical·Crystallography·Laboratory,·
·Department·of·Chemistry,·
·University·of·Nowhere,·
·Nowhere,·NO1·4T,·UK.·
;·
_publ_contact_author_phone·····'+44·1865·000000'·
_publ_contact_author_fax·····'+44·1865·000000'·
_publ_contact_author_email·····'a.n.other@chem.no.ac.uk'·
_publ_requested_journal·····'Section·E'·
_publ_requested_category·····EO·#·choose·from:·FI·FM·FO·CI·CM·CO·AD·
_publ_requested_coeditor_name····'Prof·William·Clegg'·

_publ_section_title·
#·Title·of·paper···generally·just·the·systematic·or·trivial·name·
;·?·
;·
#·The·loop·structure·below·should·contain·the·names·and·addresses·of·all·
#·authors,·in·the·required·order·of·publication.··Repeat·as·necessary.·
loop_·
·_publ_author_name·
·_publ_author_address·

·_publ_author_footnote·
·'Other,·Anthony·N.'·#·Author·1·
;·
·?·#·Address·for·author·1·
;·
·?·#·Footnote·for·author·1·
;·
·'Else,·S.·O.'·#·Author·2·
;·
·?·#·Address·2·
;·
·?·#·Footnote·2·
;·

_publ_section_abstract·
#·Text·of·the·abstract·
#·(a)·The·Abstract·must·be·self-contained·and·comprehensible·
#·without·the·rest·of·the·paper.··This·means·no·references·
#·to·atom·names·or·to·compound·numbers;·compounds·must·be·
#·identified·as·the·title·compound,·or·by·name·or·by·some·other·
#·means·such·as·derivatives·of·each·other·(e.g.·"the·
#·corresponding·ketone").·
#·(b)·The·chemical·formula·of·"the·title·compound"·must·be·given.·
#·(c)·Any·crystallographic·molecular·symmetry·should·be·
#·mentioned,·and·also·the·presence·of·more·than·one·molecule·
#·in·the·asymmetric·unit·(i.e.·anything·other·than·Z'=1).·
;·
·?·
;·
_publ_section_comment·
#·Text·of·the·paper·
#·Note·that·atoms·are·referenced·as·N2,·not·N(2)·or·N·2·.·
#·If·text·containing·()·occur·within·(),·the·outer·ones·should·be·[]·
#·Figures·should·be·referenced·as·Fih.·
;·
·?·
;·
_publ_section_acknowledgements····#·Acknowledgments·
;·
·?·
;·
_publ_section_figure_captions·
#·Captions·to·figures·--·Start·each·caption·on·a·new·line·after·a·blank·line·
;·
Fig.·1·.·
The·title·compound·with·displacement·ellipsoids·drawn·at·the·50%·
probability·level.·H·atoms·are·shown·as·spheres·of·
arbitrary·radius.·
;·
·?·
;·
_publ_section_exptl_refinement·
#·Some·potentially·useful·phrases·are·donated·by·Bill·Clegg:·
;·
In·the·absence·of·significant·anomalous·scattering,·Friedel·pairs·were·
merged.·

The·absolute·configuration·was·arbitrarily·assigned.·
·
The·relatively·large·ratio·of·minimum·to·maximum·corrections·applied·
in·the·multiscan·process·(1:nnn)·reflect·changes·in·the·illuminated·
volume·of·the·crystal.·

Changes·in·illuminated·volume·were·kept·to·a·minimum,·and·were·
taken·into·account·(G\"orbitz,·1999)·by·the·multi-scan·inter-frame·
scaling·(DENZO/SCALEPACK,·Otwinowski·&·Minor,·1997)..
·
·
G\"orbitz,·C.·H.·(1999).·Acta·Cryst.·B55,·1090-1098.·
·
·
·
·
The·H·atoms·were·all·located·in·a·difference·map,·but·those·
attached·to·carbon·atoms·were·repositioned·geometrically.·
The·H·atoms·were·initially·refined·with·soft·restraints·on·the·
bond·lengths·and·angles·to·regularise·their·geometry.·
(C---H·in·the·range·0.93--0.98,·
N---H·in·the·range·0.86--0.89·
N---H·to·0.86·
O---H·=·0.82·
\%A).·
and·
U-iso·(H)·(in·the·range·1.2-1.5·times·U-eq·of·the·parent·atom),·
after·which·the·positions·were·refined·with·riding·constraints..
·
;·
·
_publ_section_exptl_prep·
#·Brief·details·or·a·reference.··Include·solvent·if·known·
;·
·?·
;·
·

#·PROCESSING·SUMMARY·(IUCr·Office·Use·Only):·
_journal_date_recd_electronic·····?·
_journal_date_to_coeditor·····?·
_journal_date_from_coeditor·····?·
_journal_date_accepted·····?·
_journal_date_printers_first·····?·
_journal_date_printers_final·····?·
_journal_date_proofs_out·····?·
_journal_date_proofs_in·····?·
_journal_coeditor_name·····?·
_journal_coeditor_code·····?·
_journal_coeditor_notes·····?·
_journal_techeditor_code·····?·
_journal_techeditor_notes·····?·
_journal_coden_ASTM·····?·
_journal_name_full·····?·
_journal_year·····?·
_journal_volume·····?·
_journal_issue·····?·
_journal_page_first·····?·
_journal_page_last·····?·
_journal_suppl_publ_number·····?·

_journal_suppl_publ_pages·····?·
·
#·End·of·'script/refcif.dat'·
·
·
#·Insert·your·own·references·if·required···in·alphabetical·order·
_publ_section_references·
;·
Altomare,·A.,·Cascarano,·G.,·Giacovazzo,·G.,·Guagliardi,·A.,·Burla,·M.C.,·
Polidori,·G.·&·Camalli,·M.·(1994).·J.·Appl.·Cryst.·27,·435.·
·
Betteridge,·P.W.,·Carruthers,·J.R.,·Cooper,·R.I.,·
Prout,·K.·&·Watkin,·D.J.·(2003).·J.·Appl.·Cryst.·36,·1487.·
·
Larson,·A.C.·(1970).·Crystallographic·Computing,·Ed·Ahmed,·F.R.,·
Munksgaard,·Copenhagen,·291-294.·
·
Nonius·(1997-2001).·COLLECT.·Nonius·BV,·Delft,·The·Netherlands.·
·
Otwinowski,·Z.·&·Minor,·W.·(1997).·Methods·in·Enzymology,·Vol.·276,·
edited·by·C.·W.·Carter·Jr·&·R.·M.·Sweet,·pp.·307--326.·
New·York:·Academic·Press.·
·
Prince,·E.·
Mathematical·Techniques·in·Crystallography·
and·Materials·Science.·
Springer-Verlag,·New·York,·1982.·
·
Watkin·D.J.·(1994).·
Acta·Cryst.·A50,·411-437.·
·
Watkin,·D.J.,·Prout,·C.K.·&·Pearce,·L.J.·(1996).·CAMERON,·Chemical·
Crystallography·Laboratory,·Oxford,·UK.·
;·

#·Unequiv·=·arithmetic·mean·of·Ui·i.e.·Ueqiv·=·(U1+U2+U3)/3·

#·Replace·last···with·number·of·unfound·hydrogen·atomsattached·to·an·atom.

#·___refinement_flags_...·
#·no·refinement·constraints·····S·special·position·constraint·on·site·
#·G·rigid·group·refinement·of·site·····R·riding·atom·
#·D·distance·or·angle·restraint·on·site·T·thermal·displacement·constraints·
#·U·Uiso·or·Uij·restraint·(rigid·bond)···P·partial·occupancy·constraint·

loop_·
·_atom_site_label·
·_atom_site_type_symbol·
·_atom_site_fract_x·
·_atom_site_fract_y·
·_atom_site_fract_z·
·_atom_site_U_iso_or_equiv·
·_atom_site_occupancy·
·_atom_site_adp_type·
·_atom_site_refinement_flags_posn·
·_atom_site_refinement_flags_adp·
·_atom_site_refinement_flags_occupancy·
·_atom_site_disorder_assembly·

·_atom_site_disorder_group·
·_atom_site_attached_hydrogens·
·Ir1·Ir·0.164234(5)·0.462357(8)·0.387062(2)·0.0215·1.0000·Uani·.·.·.·.·.·.·
·N1·N·0.22255(13)·0.64288(19)·0.42307(6)·0.0263·1.0000·Uani·.·.·.·.·.·.·
·N2·N·0.09941(12)·0.2983(2)·0.34709(5)·0.0237·1.0000·Uani·.·.·.·.·.·.·
·N3·N·0.12312(17)·0.3323(2)·0.44529(6)·0.0329·1.0000·Uani·.·.·.·.·.·.·
·N4·N·0.30398(15)·0.3519(2)·0.41356(6)·0.0293·1.0000·Uani·.·.·.·.·.·.·
·C1·C·0.21926(13)·0.5786(2)·0.33723(7)·0.0250·1.0000·Uani·.·.·.·.·.·.·
·C2·C·0.21431(15)·0.5419(3)·0.29170(7)·0.0331·1.0000·Uani·.·.·.·.·.·.·
·C3·C·0.25700(18)·0.6342(4)·0.26109(9)·0.0451·1.0000·Uani·.·.·.·.·.·.·
·C4·C·0.30326(19)·0.7662(4)·0.27523(11)·0.0512·1.0000·Uani·.·.·.·.·.·.·
·C5·C·0.30945(17)·0.8065(3)·0.32014(11)·0.0436·1.0000·Uani·.·.·.·.·.·.·
·C6·C·0.26738(14)·0.7131(2)·0.35110(9)·0.0310·1.0000·Uani·.·.·.·.·.·.·
·C7·C·0.27001(15)·0.7457(2)·0.39920(9)·0.0314·1.0000·Uani·.·.·.·.·.·.·
·C8·C·0.31894(18)·0.8672(3)·0.42154(12)·0.0444·1.0000·Uani·.·.·.·.·.·.·
·C9·C·0.31578(19)·0.8844(3)·0.46731(13)·0.0520·1.0000·Uani·.·.·.·.·.·.·
·C10·C·0.2636(2)·0.7825(3)·0.49082(11)·0.0464·1.0000·Uani·.·.·.·.·.·.·
·C11·C·0.21855(19)·0.6636(3)·0.46768(9)·0.0358·1.0000·Uani·.·.·.·.·.·.·
·C12·C·0.04100(14)·0.5709(2)·0.36323(7)·0.0232·1.0000·Uani·.·.·.·.·.·.·
·C13·C·0.01024(16)·0.7154(3)·0.37401(8)·0.0308·1.0000·Uani·.·.·.·.·.·.·
·C14·C·-0.07502(18)·0.7778(3)·0.35226(10)·0.0379·1.0000·Uani·.·.·.·.·.·.·
·C15·C·-0.13067(18)·0.6998(3)·0.31881(10)·0.0401·1.0000·Uani·.·.·.·.·.·.·
·C16·C·-0.10158(16)·0.5571(3)·0.30703(8)·0.0338·1.0000·Uani·.·.·.·.·.·.·
·C17·C·-0.01608(15)·0.4933(2)·0.32895(7)·0.0264·1.0000·Uani·.·.·.·.·.·.·
·C18·C·0.01674(15)·0.3408(2)·0.32057(7)·0.0256·1.0000·Uani·.·.·.·.·.·.·
·C19·C·-0.03045(16)·0.2376(3)·0.29051(7)·0.0310·1.0000·Uani·.·.·.·.·.·.·
·C20·C·0.00326(18)·0.0906(3)·0.28923(8)·0.0355·1.0000·Uani·.·.·.·.·.·.·
·C21·C·0.08381(18)·0.0481(3)·0.31814(8)·0.0333·1.0000·Uani·.·.·.·.·.·.·
·C22·C·0.12952(16)·0.1540(2)·0.34636(7)·0.0275·1.0000·Uani·.·.·.·.·.·.·
·C23·C·0.0332(2)·0.2877(3)·0.45569(8)·0.0404·1.0000·Uani·.·.·.·.·.·.·
·C24·C·0.0225(3)·0.1987(3)·0.49355(10)·0.0584·1.0000·Uani·.·.·.·.·.·.·
·C25·C·0.1032(4)·0.1544(4)·0.52118(11)·0.0676·1.0000·Uani·.·.·.·.·.·.·
·C26·C·0.1943(3)·0.1971(3)·0.51043(9)·0.0552·1.0000·Uani·.·.·.·.·.·.·
·C27·C·0.2033(2)·0.2854(3)·0.47230(8)·0.0406·1.0000·Uani·.·.·.·.·.·.·
·C28·C·0.3005(2)·0.3206(3)·0.45807(8)·0.0393·1.0000·Uani·.·.·.·.·.·.·
·C29·C·0.2841(3)·0.3158(5)·0.48812(11)·0.0637·1.0000·Uani·.·.·.·.·.·.·
·C30·C·0.4737(3)·0.3382(6)·0.47205(14)·0.0788·1.0000·Uani·.·.·.·.·.·.·
·C31·C·0.4790(2)·0.3587(5)·0.42706(13)·0.0615·1.0000·Uani·.·.·.·.·.·.·
·C32·C·0.3931(18)·0.3627(3)·0.39777(9)·0.0369·1.0000·Uani·.·.·.·.·.·.·
·C33·C·-0.0584(2)·0.3296(3)·0.42750(8)·0.0424·1.0000·Uani·.·.·.·.·.·.·
·C34·C·-0.1047(3)·0.2218(4)·0.39934(10)·0.0611·1.0000·Uani·.·.·.·.·.·.·
·C35·C·-0.1945(3)·0.2506(6)·0.37606(12)·0.0763·1.0000·Uani·.·.·.·.·.·.·
·C36·C·-0.2292(3)·0.3869(7)·0.38131(12)·0.0786·1.0000·Uani·.·.·.·.·.·.·
·C37·C·-0.1934(2)·0.4968(5)·0.40937(11)·0.0623·1.0000·Uani·.·.·.·.·.·.·
·C38·C·-0.1032(2)·0.4666(4)·0.43242(9)·0.0457·1.0000·Uani·.·.·.·.·.·.·
·C39·C·0.40202(16)·0.3686(3)·0.34877(9)·0.0357·1.0000·Uani·.·.·.·.·.·.·
·C40·C·0.36025(19)·0.2548(3)·0.32131(9)·0.0372·1.0000·Uani·.·.·.·.·.·.·
·C41·C·0.3747(3)·0.2474(5)·0.27626(11)·0.0619·1.0000·Uani·.·.·.·.·.·.·
·C42·C·0.4318(3)·0.3560(7)·0.25817(15)·0.0918·1.0000·Uani·.·.·.·.·.·.·
·C43·C·0.4735(3)·0.4696(6)·0.2845(2)·0.0936·1.0000·Uani·.·.·.·.·.·.·
·C44·C·0.4602(2)·0.4766(4)·0.33041(16)·0.0623·1.0000·Uani·.·.·.·.·.·.·
·P1·P·0.39462(6)·0.05859(11)·0.61434(2)·0.0482·1.0000·Uani·D·U·.·.·.·.·
·F1·F·0.4830(2)·0.1209(6)·0.64426(15)·0.0828·0.6500·Uani·D·U·.·.·.·.·
·F2·F·0.2986(3)·0.0011(4)·0.58143(10)·0.0643·0.6500·Uani·D·U·.·.·.·.·
·F3·F·0.3605(3)·0.2302(4)·0.59893(12)·0.0798·0.6500·Uani·D·U·.·.·.·.·
·F4·F·0.4162(3)·-0.1060(4)·0.62732(15)·0.0879·0.6500·Uani·D·U·.·.·.·.·
·F5·F·0.3234(2)·0.0704(4)·0.65318(10)·0.0596·0.6500·Uani·D·U·.·.·.·.·
·F6·F·0.4519(3)·-0.0514(7)·0.57082(13)·0.1081·0.6500·Uani·D·U·.·.·.·.·
·F11·F·0.4355(5)·0.1658(8)·0.5786(2)·0.0810·0.3500·Uani·D·U·.·.·.·.·
·F12·F·0.3742(4)·-0.0537(7)·0.65395(17)·0.0652·0.3500·Uani·D·U·.·.·.·.·
```

```
F13·F·0.2957(4)·-0.1301(8)·0.6136(2)·0.0842·0.3500·Uani·D·U·.....·
F14·F·0.5058(3)·-0.0251(6)·0.6170(2)·0.0734·0.3500·Uani·D·U·.....·
F15·F·0.3613(4)·-0.0600(8)·0.57800(19)·0.0838·0.3500·Uani·D·U·.....·
F16·F·0.4440(6)·0.1711(9)·0.6529(2)·0.1056·0.3500·Uani·D·U·.....·
H21·H·0.1827·0.4537·0.2816·0.0412·1.0000·Uiso·R·.....·
H31·H·0.2540·0.6064·0.2309·0.0557·1.0000·Uiso·R·.....·
H41·H·0.3308·0.8314·0.2544·0.0614·1.0000·Uiso·R·.....·
H51·H·0.3409·0.8951·0.3296·0.0530·1.0000·Uiso·R·.....·
H81·H·0.3541·0.9355·0.4053·0.0549·1.0000·Uiso·R·.....·
H91·H·0.3491·0.9636·0.4819·0.0636·1.0000·Uiso·R·.....·
H101·H·0.2584·0.7923·0.5217·0.0559·1.0000·Uiso·R·.....·
H111·H·0.1844·0.5929·0.4828·0.0433·1.0000·Uiso·R·.....·
H131·H·0.0464·0.7700·0.3958·0.0386·1.0000·Uiso·R·.....·
H141·H·-0.0954·0.8733·0.3601·0.0473·1.0000·Uiso·R·.....·
H151·H·-0.1890·0.7425·0.3046·0.0499·1.0000·Uiso·R·.....·
H161·H·-0.1386·0.5031·0.2848·0.0434·1.0000·Uiso·R·.....·
H191·H·-0.0832·0.2654·0.2715·0.0394·1.0000·Uiso·R·.....·
H201·H·-0.0290·0.0208·0.2694·0.0438·1.0000·Uiso·R·.....·
H211·H·0.1069·-0.0484·0.3187·0.0406·1.0000·Uiso·R·.....·
H221·H·0.1815·0.1241·0.3663·0.0334·1.0000·Uiso·R·.....·
H241·H·-0.0398·0.1672·0.5006·0.0708·1.0000·Uiso·R·.....·
H251·H·0.0962·-0.0971·0.5465·0.0868·1.0000·Uiso·R·.....·
H261·H·0.2502·0.1677·0.5282·0.0648·1.0000·Uiso·R·.....·
H291·H·0.3788·0.2987·0.5188·0.0759·1.0000·Uiso·R·.....·
H301·H·0.5311·0.3375·0.4916·0.0928·1.0000·Uiso·R·.....·
H311·H·0.5372·0.3693·0.4151·0.0712·1.0000·Uiso·R·.....·
H341·H·-0.0746·0.1296·0.3963·0.0786·1.0000·Uiso·R·.....·
H351·H·-0.2263·0.1765·0.3572·0.0957·1.0000·Uiso·R·.....·
H361·H·-0.2995·0.4043·0.3658·0.0946·1.0000·Uiso·R·.....·
H371·H·-0.2220·0.5905·0.4128·0.0781·1.0000·Uiso·R·.....·
H381·H·-0.0724·0.5391·0.4508·0.0573·1.0000·Uiso·R·.....·
H401·H·0.3228·0.1812·0.3333·0.0457·1.0000·Uiso·R·.....·
H411·H·0.3473·0.1691·0.2579·0.0742·1.0000·Uiso·R·.....·
H421·H·0.4416·0.3520·0.2282·0.1198·1.0000·Uiso·R·.....·
H431·H·0.5119·0.5433·0.2722·0.1114·1.0000·Uiso·R·.....·
H441·H·0.4878·0.5510·0.3488·0.0769·1.0000·Uiso·R·.....·
loop_
 _atom_site_aniso_label
 _atom_site_aniso_U_11
 _atom_site_aniso_U_22
 _atom_site_aniso_U_33
 _atom_site_aniso_U_23
 _atom_site_aniso_U_13
 _atom_site_aniso_U_12
Ir1·0.02353(3)·0.02071(2)·0.02064(2)·0.00140(3)·0.00413(17)·-0.00112(3)·
N1·0.0231(7)·0.0219(7)·0.0341(8)·-0.0037(6)·0.0029(6)·-0.0013(5)·
N2·0.0257(7)·0.0254(7)·0.0206(6)·-0.0020(5)·0.0056(5)·-0.0011(6)·
N3·0.0538(12)·0.0226(7)·0.0236(7)·-0.0020(6)·0.0099(7)·-0.0068(8)·
N4·0.0362(9)·0.0223(7)·0.0279(8)·-0.0004(6)·-0.0041(7)·0.0043(6)·
C1·0.0184(7)·0.0265(8)·0.0310(8)·0.0104(7)·0.0073(6)·0.0051(6)·
C2·0.0243(8)·0.0469(12)·0.0291(8)·0.0151(9)·0.0075(6)·0.0100(9)·
C3·0.0293(10)·0.0681(18)·0.0399(12)·0.0304(13)·0.0136(9)·0.0156(11)·
C4·0.0282(10)·0.0619(18)·0.0662(18)·0.0428(15)·0.0189(11)·0.0122(11)·
C5·0.0240(9)·0.0359(12)·0.0721(18)·0.0266(12)·0.0100(10)·0.0030(8)·
C6·0.0184(7)·0.0255(8)·0.0500(12)·0.0135(8)·0.0077(7)·0.0040(6)·
C7·0.0188(7)·0.0226(8)·0.0531(13)·0.0019(8)·0.0044(8)·0.0025(6)·
C8·0.0235(9)·-0.0256(10)·0.084(2)·-0.0069(12)·0.0050(11)·-0.0027(8)·
C9·0.0283(10)·0.0390(13)·0.088(2)·-0.0310(15)·0.0018(12)·-0.0038(10)·
C10·0.0358(12)·0.0445(14)·0.0582(16)·-0.0280(13)·0.0004(11)·0.0005(10)·
C11·0.0365(11)·0.0333(11)·0.0375(11)·-0.0111(9)·0.0041(9)·-0.0008(9)·

C12·0.0218(7)·0.0230(7)·0.0261(7)·0.0001(6)·0.0089(6)·-0.0004(6)·
C13·0.0260(9)·0.0272(9)·0.0402(11)·-0.0029(8)·0.0088(8)·0.0015(7)·
C14·0.0284(10)·0.0351(11)·0.0512(14)·-0.0030(10)·0.0088(9)·0.0065(9)·
C15·0.0274(10)·0.0449(13)·0.0481(13)·0.0002(11)·0.0042(9)·0.0098(10)·
C16·0.0244(8)·0.0454(13)·0.0318(9)·-0.0014(9)·0.0033(7)·0.0036(8)·
C17·0.0241(8)·0.0323(9)·0.0237(7)·0.0002(6)·0.0066(6)·0.0018(6)·
C18·0.0241(8)·0.0318(9)·0.0218(7)·-0.0011(7)·0.0057(6)·-0.0013(7)·
C19·0.0282(9)·0.0405(11)·0.0242(8)·-0.0070(8)·0.0019(7)·-0.0022(8)·
C20·0.0357(10)·0.0395(12)·0.0317(10)·-0.0140(9)·0.0052(8)·-0.0047(9)·
C21·0.0358(10)·0.0305(10)·0.0340(9)·-0.0094(8)·0.0054(8)·-0.0008(9)·
C22·0.0306(9)·0.0260(8)·0.0261(8)·-0.0026(7)·0.0036(7)·0.0009(7)·
C23·0.0694(17)·0.0269(9)·0.0285(9)·-0.0060(8)·0.0233(10)·-0.0167(10)·
C24·0.106(3)·0.0332(12)·0.0415(14)·-0.0005(11)·0.0386(16)·-0.0194(15)·
C25·0.138(3)·0.0339(13)·0.0360(13)·0.0096(11)·0.0346(18)·-0.0010(18)·
C26·0.106(3)·0.0343(12)·0.0257(10)·0.0051(9)·0.0102(13)·0.0134(15)·
C27·0.0737(18)·0.0265(10)·0.0227(8)·0.0011(7)·0.0047(10)·0.0039(11)·
C28·0.0575(15)·0.0327(11)·0.0255(9)·-0.0017(8)·-0.0081(9)·0.0111(11)·
C29·0.078(2)·0.071(2)·0.0371(14)·-0.0083(14)·-0.0237(15)·0.0284(19)·
C30·0.060(2)·0.108(3)·0.062(2)·-0.028(2)·-0.0337(17)·0.035(2)·
C31·0.0357(13)·0.080(2)·0.065(2)·-0.0203(18)·-0.0139(13)·0.0211(15)·
C32·0.0307(10)·0.0317(11)·0.0466(13)·-0.0043(9)·-0.0054(9)·0.0077(8)·
C33·0.0563(15)·0.0430(13)·0.0314(10)·-0.0122(9)·-0.0229(10)·-0.0264(12)·
C34·0.088(2)·0.0574(18)·0.0421(14)·-0.0212(13)·-0.0302(15)·-0.0477(18)·
C35·0.083(2)·0.104(3)·0.0460(16)·-0.0271(19)·0.0253(17)·-0.065(2)·
C36·0.0492(17)·0.146(4)·0.0437(16)·-0.021(2)·0.0198(13)·-0.046(2)·
C37·0.0464(15)·0.098(3)·0.0458(15)·-0.0168(17)·0.0220(12)·-0.0143(17)·
C38·0.0461(13)·0.0565(16)·0.0371(11)·-0.0153(12)·0.0171(10)·-0.0174(13)·
C39·0.0236(8)·0.0321(10)·0.0519(13)·0.0101(10)·0.0074(8)·0.0107(8)·
C40·0.0341(11)·0.0433(12)·0.0352(11)·0.0022(9)·0.0092(8)·0.0134(10)·
C41·0.0508(16)·0.097(3)·0.0401(14)·0.0023(16)·0.0149(12)·0.0386(18)·
C42·0.071(2)·0.143(4)·0.070(2)·0.056(3)·0.047(2)·0.062(3)·
C43·0.0538(19)·0.097(3)·0.140(4)·0.077(3)·0.061(2)·0.038(2)·
C44·0.0273(11)·0.0450(16)·0.117(3)·0.0300(18)·0.0202(15)·0.0109(11)·
P1·0.0435(4)·0.0679(5)·0.0327(3)·0.0023(3)·0.0007(3)·-0.0168(4)·
F1·0.0360(15)·-0.131(4)·0.079(3)·-0.020(3)·-0.0069(16)·-0.024(2)·
F2·0.082(2)·0.0601(18)·0.0453(15)·0.0113(14)·-0.0262(15)·-0.0254(17)·
F3·0.114(3)·0.058(2)·0.064(2)·0.0025(17)·-0.012(2)·-0.027(2)·
F4·0.076(2)·0.087(3)·0.097(3)·-0.001(2)·-0.015(2)·0.035(2)·
F5·0.0484(15)·0.085(2)·0.0476(15)·-0.0055(15)·0.0143(12)·-0.0003(15)·
F6·0.098(3)·0.171(5)·0.062(2)·-0.034(3)·0.042(2)·-0.038(3)·
F11·0.064(4)·0.094(5)·0.081(4)·0.058(4)·-0.011(3)·-0.007(4)·
F12·0.059(3)·0.085(4)·0.048(3)·0.031(3)·-0.012(2)·-0.028(3)·
F13·0.073(4)·0.090(5)·0.093(5)·0.012(4)·0.024(4)·0.033(4)·
F14·0.041(2)·0.061(3)·0.114(5)·0.041(3)·-0.013(3)·-0.009(3)·
F15·0.042(3)·0.145(6)·0.064(3)·-0.051(4)·-0.001(3)·-0.006(4)·
F16·0.116(5)·0.097(6)·0.095(5)·-0.005(5)·-0.040(5)·-0.057(5)·

_refine_ls_extinction_method·
····'None'
_oxford_refine_ls_scale·0.19815(8)·
loop_
 _geom_bond_atom_site_label_1
 _geom_bond_site_symmetry_1
 _geom_bond_atom_site_label_2
 _geom_bond_site_symmetry_2
 _geom_bond_distance
 _geom_bond_publ_flag
Ir1·-N1·.·2.0504(17)····yes
Ir1·-N2·.·2.0341(17)····yes
Ir1·-N3·.·2.0017(18)····yes

Ir1·-N4·.·2.2254(19)····yes
Ir1·-C1·.·2.0120(18)····yes
Ir1·-C12·.·2.012(2)·····yes
N1·-C7·.·1.366(3)·····yes
N1·-C11·.·1.350(3)·····yes
N2·-C18·.·1.371(3)·····yes
N2·-C22·.·1.347(3)·····yes
N3·-C23·.·1.354(3)·····yes
N3·-C27·.·1.364(4)·····yes
N4·-C28·.·1.362(3)·····yes
N4·-C32·.·1.350(3)·····yes
C1·-C2·.·1.393(3)·····yes
C1·-C6·.·1.408(3)·····yes
C2·-C3·.·1.395(3)·····yes
C2·-H21·.·0.931····no
C3·-C4·.·1.379(5)·····yes
C3·-H31·.·0.931····no
C4·-C5·.·1.382(5)·····yes
C4·-H41·.·0.952····no
C5·-C6·.·1.403(3)·····yes
C5·-H51·.·0.929····no
C6·-C7·.·1.460(4)·····yes
C7·-C8·.·1.400(3)·····yes
C8·-C9·.·1.378(5)·····yes
C8·-H81·.·0.936····no
C9·-C10·.·1.383(5)·····yes
C9·-H91·.·0.925····no
C10·-C11·.·1.376(3)·····yes
C10·-H101·.·0.936····no
C11·-H111·.·0.925····no
C12·-C13·.·1.398(3)·····yes
C12·-C17·.·1.408(3)·····yes
C13·-C14·.·1.395(3)·····yes
C13·-H131·.·0.918····no
C14·-C15·.·1.384(4)·····yes
C14·-H141·.·0.930····no
C15·-C16·.·1.384(4)·····yes
C15·-H151·.·0.947····no
C16·-C17·.·1.404(3)·····yes
C16·-H161·.·0.930····no
C17·-C18·.·1.456(3)·····yes
C18·-C19·.·1.398(3)·····yes
C19·-C20·.·1.387(4)·····yes
C19·-H191·.·0.908····no
C20·-C21·.·1.386(4)·····yes
C20·-H201·.·0.938····no
C21·-C22·.·1.374(3)·····yes
C21·-H211·.·0.913····no
C22·-H221·.·0.923····no
C23·-C24·.·1.398(4)·····yes
C23·-C33·.·1.488(5)·····yes
C24·-C25·.·1.372(6)·····yes
C24·-H241·.·0.937····no
C25·-C26·.·1.366(6)·····yes
C25·-H251·.·0.924····no
C26·-C27·.·1.397(3)·····yes
C26·-H261·.·0.925····no
C27·-C28·.·1.464(5)·····yes
C28·-C29·.·1.386(4)·····yes
C29·-C30·.·1.369(6)·····yes

C29·-H291·.·0.938····no
C30·-C31·.·1.363(6)·····yes
C30·-H301·.·0.933····no
C31·-C32·.·1.397(4)·····yes
C31·-H311·.·0.907····no
C32·-C39·.·1.478(4)·····yes
C33·-C34·.·1.387(4)·····yes
C33·-C38·.·1.376(5)·····yes
C34·-C35·.·1.377(6)·····yes
C34·-H341·.·0.925····no
C35·-C36·.·1.372(7)·····yes
C35·-H351·.·0.945····no
C36·-C37·.·1.396(5)·····yes
C36·-H361·.·0.921····no
C37·-C38·.·1.381(5)·····yes
C37·-H371·.·0.929····no
C38·-H381·.·0.923····no
C39·-C40·.·1.390(4)·····yes
C39·-C44·.·1.390(4)·····yes
C40·-C41·.·1.378(4)·····yes
C40·-H401·.·0.922····no
C41·-H411·.·0.942····no
C42·-C43·.·1.371(8)·····yes
C42·-H421·.·0.916····no
C43·-C44·.·1.398(7)·····yes
C43·-H431·.·0.935····no
C44·-H441·.·0.918····no
P1·-F1·.·1.537(3)·····yes
P1·-F2·.·1.645(3)·····yes
P1·-F3·.·1.647(4)·····yes
P1·-F4·.·1.534(4)·····yes
P1·-F5·.·1.583(3)·····yes
P1·-F6·.·1.578(3)·····yes
P1·-F11·.·1.570(5)·····yes
P1·-F12·.·1.591(4)·····yes
P1·-F13·.·1.492(5)·····yes
P1·-F14·.·1.686(17)····yes
P1·-F15·.·1.550(5)·····yes
P1·-F16·.·1.624(5)·····yes
loop_
 _geom_angle_atom_site_label_1
 _geom_angle_site_symmetry_1
 _geom_angle_atom_site_label_2
 _geom_angle_site_symmetry_2
 _geom_angle_atom_site_label_3
 _geom_angle_site_symmetry_3
 _geom_angle
 _geom_angle_publ_flag
N1·-Ir1·-N2··174.32(7)····yes
N1·-Ir1·-N3··78.44(7)·····yes
N2·-Ir1·-N3··87.56(7)·····yes
N1·-Ir1·-N4··83.10(7)·····yes
N2·-Ir1·-N4··101.82(7)····yes
N3·-Ir1·-N4··76.18(8)·····yes
N1·-Ir1·-C1··80.32(8)·····yes
N2·-Ir1·-C1··96.15(8)·····yes
N3·-Ir1·-C1··172.84(8)····yes
N4·-Ir1·-C1··97.03(7)·····yes
N1·-Ir1·-C12··94.71(7)····yes

N2·-Ir1·-C12··80.31(7)····yes
N3·-Ir1·-C12··105.34(8)···yes
N4·-Ir1·-C12··177.49(7)···yes
C1·-Ir1·-C12··81.37(7)····yes
Ir1·-N1·-C7··115.69(16)···yes
Ir1·-N1·-C11··125.06(16)··yes
C7·-N1·-C11··119.2(2)·····yes
Ir1·-N2·-C18··115.56(14)···yes
Ir1·-N2·-C22··125.08(14)···yes
C18·-N2·-C22··119.31(18)···yes
Ir1·-N3·-C23··129.58(19)···yes
Ir1·-N3·-C27··112.16(17)···yes
C23·-N3·-C27··118.1(2)·····yes
Ir1·-N4·-C28··109.30(17)···yes
Ir1·-N4·-C32··127.85(16)···yes
C28·-N4·-C32··118.0(2)·····yes
Ir1·-C1·-C2··127.75(17)····yes
Ir1·-C1·-C6··114.52(16)····yes
C2·-C1·-C6··117.72(19)·····yes
C1·-C2·-C3··121.0(3)·····yes
C1·-C2·-H21··119.6····no
C3·-C2·-H21··119.6····no
C2·-C3·-C4·-120.5(3)·····yes
C2·-C3·-H31··119.5····no
C4·-C3·-H31··120.0····no
C3·-C4·-C5·-120.1(2)·····yes
C3·-C4·-H41··121.1····no
C5·-C4·-H41··118.8····no
C4·-C5·-C6·-121.9(3)·····yes
C4·-C5·-H51··120.1····no
C6·-C5·-H51··120.4····no
C1·-C6·-C5·-121.1(3)·····yes
C1·-C6·-C7·-115.44(18)····yes
C5·-C6·-C7·-123.4(2)·····yes
N1·-C7·-C6·-113.93(19)····yes
C6·-C7·-C8·-126.4(2)·····yes
N1·-C7·-C8·-119.7(2)·····yes
C7·-C8·-C9·-120.1(3)·····yes
C7·-C8·-H81··119.9····no
C9·-C8·-H81··120.4····no
C8·-C9·-C10·-119.7(2)····yes
C8·-C9·-H91··119.9····no
C10·-C9·-H91·-121.0····no
C9·-C10·-C11·-118.4(3)····yes
C9·-C10·-H101·-121.9····no
C11·-C10·-H101·-119.7····no
C10·-C11·-N1·-122.9(3)····yes
C10·-C11·-H111·-119.5····no
N1·-C11·-H111·-117.2····no
Ir1·-C12·-C13·-128.20(16)····yes
Ir1·-C12·-C17·-114.29(14)····yes
C13·-C12·-C17·-117.31(19)····yes
C12·-C13·-C14·-120.9(2)·····yes
C12·-C13·-H131·-119.7·····no
C14·-C13·-H131·-119.4·····no
C13·-C14·-C15·-121.1(2)·····yes
C13·-C14·-H141·-120.1·····no
C15·-C14·-H141·-118.8·····no
C14·-C15·-C16·-119.4(2)·····yes
C14·-C15·-H151·-120.4·····no

C16·-C15·-H151·-120.2·····no
C15·-C16·-C17·-119.8(2)····yes
C15·-C16·-H161·-120.3·····no
C17·-C16·-H161·-119.9·····no
C12·-C17·-C16·-121.5(2)····yes
C12·-C17·-C18·-114.94(18)····yes
C16·-C17·-C18·-123.52(2)····yes
C17·-C18·-N2·-114.06(18)····yes
C17·-C18·-C19·-126.1(2)·····yes
N2·-C18·-C19·-119.7(2)·····yes
C18·-C19·-C20·-120.1(2)·····yes
C18·-C19·-H191·-120.9·····no
C20·-C19·-H191·-119.0·····no
C19·-C20·-C21·-119.1(2)·····yes
C19·-C20·-H201·-120.2·····no
C21·-C20·-H201·-120.7·····no
C20·-C21·-C22·-119.0(2)·····yes
C20·-C21·-H211·-121.3·····no
C22·-C21·-H211·-119.7·····no
C21·-C22·-N2·-122.0(2)·····yes
C21·-C22·-H221·-118.5·····no
N2·-C22·-H221·-118.8·····no
N3·-C23·-C24·-121.03(3)····yes
N3·-C23·-C33·-122.0(2)·····yes
C24·-C23·-C33·-116.9(3)····yes
C23·-C24·-C25·-120.7(3)····yes
C23·-C24·-H241·-120.9·····no
C25·-C24·-H241·-118.4·····no
C24·-C25·-C26·-118.5(3)····yes
C24·-C25·-H251·-120.8·····no
C26·-C25·-H251·-120.7·····no
C25·-C26·-C27·-119.9(3)····yes
C25·-C26·-H261·-120.6·····no
C27·-C26·-H261·-119.6·····no
C26·-C27·-N3·-121.8(3)····yes
C26·-C27·-C28·-130.5(3)····yes
N3·-C27·-C28·-117.6(2)····yes
C27·-C28·-N4·-116.1(2)····yes
C27·-C28·-C29·-121.4(3)····yes
N4·-C28·-C29·-122.4(3)····yes
C28·-C29·-C30·-118.6(3)····yes
C28·-C29·-H291·-120.2·····no
C30·-C29·-H291·-121.2·····no
C29·-C30·-C31·-119.6(3)····yes
C29·-C30·-H301·-120.4·····no
C31·-C30·-H301·-120.0·····no
C30·-C31·-C32·-120.2(3)····yes
C30·-C31·-H311·-122.0·····no
C32·-C31·-H311·-117.8·····no
C31·-C32·-N4·-120.7(3)····yes
C31·-C32·-C39·-118.6(3)····yes
N4·-C32·-C39·-120.4(2)····yes
C23·-C33·-C34·-118.8(3)····yes
C23·-C33·-C38·-121.3(2)····yes
C34·-C33·-C38·-119.5(3)····yes
C33·-C34·-C35·-120.8(4)····yes
C33·-C34·-H341·-119.2·····no
C35·-C34·-H341·-119.9·····no
C34·-C35·-C36·-119.5(3)····yes
C34·-C35·-H351·-120.6·····no

C36·-C35·-H351·-119.9·····no
C35·-C36·-C37·-120.4(4)····yes
C35·-C36·-H361·-118.6·····no
C37·-C36·-H361·-121.0·····no
C36·-C37·-C38·-119.5(4)····yes
C36·-C37·-H371·-121.6·····no
C38·-C37·-H371·-118.9·····no
C37·-C38·-C33·-120.3(3)····yes
C37·-C38·-H381·-119.8·····no
C33·-C38·-H381·-119.9·····no
C32·-C39·-C40·-119.7(2)····yes
C32·-C39·-C44·-120.8(3)····yes
C40·-C39·-C44·-119.2(3)····yes
C39·-C40·-C41·-121.5(3)····yes
C39·-C40·-H401·-120.0·····no
C41·-C40·-H401·-118.5·····no
C40·-C41·-C42·-119.0(4)····yes
C40·-C41·-H411·-121.2·····no
C42·-C41·-H411·-119.8·····no
C41·-C42·-C43·-120.7(4)····yes
C41·-C42·-H421·-119.5·····no
C43·-C42·-H421·-119.9·····no
C42·-C43·-C44·-120.6(4)····yes
C42·-C43·-H431·-120.6·····no
C44·-C43·-H431·-118.8·····no
C43·-C44·-C39·-119.1(4)····yes
C43·-C44·-H441·-122.3·····no
C39·-C44·-H441·-118.6·····no
F1·-P1·-F2·-177.0(2)····yes
F1·-P1·-F3·-90.9(2)·····yes
F2·-P1·-F3·-86.07(17)····yes
F1·-P1·-F4·-94.3(2)·····yes
F2·-P1·-F4·-88.79(19)····yes
F3·-P1·-F4·-174.5(2)····yes
F1·-P1·-F5·-93.08(19)····yes
F2·-P1·-F5·-87.01(18)····yes
F3·-P1·-F5·-88.0(2)·····yes
F4·-P1·-F5·-89.72(2)····yes
F1·-P1·-F6·-94.0(2)·····yes
F2·-P1·-F6·-85.7(2)·····yes
F3·-P1·-F6·-87.5(2)·····yes
F4·-P1·-F6·-94.1(3)·····yes
F5·-P1·-F6·-171.7(2)····yes
F11·-P1·-F12·-169.3(3)····yes
F11·-P1·-F13·-96.3(3)·····yes
F12·-P1·-F13·-93.3(3)·····yes
F11·-P1·-F14·-85.7(3)·····yes
F12·-P1·-F14·-84.7(3)·····yes
F13·-P1·-F14·-177.9(3)····yes
F11·-P1·-F15·-92.2(3)·····yes
F12·-P1·-F15·-87.9(3)·····yes
F13·-P1·-F15·-94.1(3)·····yes
F14·-P1·-F15·-86.5(3)·····yes
F11·-P1·-F16·-87.5(3)·····yes
F12·-P1·-F16·-87.1(3)·····yes
F13·-P1·-F16·-93.7(4)·····yes
F14·-P1·-F16·-85.7(3)·····yes
F15·-P1·-F16·-172.1(4)····yes
```

bis(2-(2,4-difluorophenyl) pyridine-*C*,*N*)(6-phenyl-2,2'-bipyridine-*N*,*N'*)iridium(III) hexafluorophosphate (**57**)

```
data_sg079_1_123k
_audit_creation_date·····08-10-13
_audit_creation_method·CRYSTALS_ver_12.84

_oxford_structure_analysis_title··'sg079_1_123k_0ma·in·P2(1)/c'
_chemical_name_systematic·····?
_chemical_melting_point·····?

_cell_length_a·····19.3540(9)
_cell_length_b·····10.2932(5)
_cell_length_c·····18.1712(8)
_cell_angle_alpha·····90
_cell_angle_beta·····114.558(2)
_cell_angle_gamma·····90
_cell_volume·····3292.5(3)

_symmetry_cell_setting·····'Monoclinic'·
_symmetry_space_group_name_H-M···'P·21/c'·
_symmetry_space_group_name_Hall··'-P·2ybc'·
loop_
 _symmetry_equiv_pos_as_xyz
 'x,y,z'
 '-x,-y,-z'
 '-x,-y+1/2,-z+1/2'
 'x,-y+1/2,z+1/2'

loop_
 _atom_type_symbol
 _atom_type_scat_dispersion_real
 _atom_type_scat_dispersion_imag
 _atom_type_scat_Cromer_Mann_a1
 _atom_type_scat_Cromer_Mann_b1
 _atom_type_scat_Cromer_Mann_a2
 _atom_type_scat_Cromer_Mann_b2
 _atom_type_scat_Cromer_Mann_a3
 _atom_type_scat_Cromer_Mann_b3
 _atom_type_scat_Cromer_Mann_a4
 _atom_type_scat_Cromer_Mann_b4
 _atom_type_scat_Cromer_Mann_c
 _atom_type_scat_source·
·C···0.0033···0.0016···2.3100··20.8439···1.0200··10.2075···1.5886···0.5687
···0.8650··51.6512···0.2156·'International·Tables·Vol·C·4.2.6.8·and·6.1.1.4'
·H·····0.0000···0.0000···0.4930··10.5109···0.3229··26.1257···0.1402···3.1424
···0.0408··57.7998···0.0030·'International·Tables·Vol·C·4.2.6.8·and·6.1.1.4'
·N·····0.0061···0.0033··12.2126···0.0057···3.1322···9.8933···2.0125··28.9975
···11.6623···0.5826···11.5290·'International·Tables·Vol·C·4.2.6.8·and·6.1.1.4'
·P·····0.0171···0.0103···3.5392··10.2825···2.6412···4.2944···1.5170···0.2615
···1.0243··26.1476···0.2776·'International·Tables·Vol·C·4.2.6.8·and·6.1.1.4'
·F·····0.0170···0.0106···3.5392··10.2825···2.6412···4.2944···1.5170···0.2615
···1.0243··26.1476···0.2776·'International·Tables·Vol·C·4.2.6.8·and·6.1.1.4'
·Ir····-1.4442···7.9887···27.3049···1.5928··16.7296···8.8655··15.6115···0.4179
···5.8338··45.0011···11.4722·'International·Tables·Vol·C·4.2.6.8·and·6.1.1.4'
·
·
_cell_formula_units_Z·····4

#·Given·Formula·=·C34·H28·F10·Ir1·N4·P1·
#·Dc·=·····1.83·Foo·=···1848.00·Mu·=·····41.93·M·=····905.80
#·Found·Formula·=·C38·H24·F10·Ir1·N4·P1·
#·Dc·=·····1.92·FOOO·=···1848.00·Mu·=·····41.98·M·=····949.81
```

```
_chemical_formula_sum·····'C38·H24·F10·Ir1·N4·P1'
_chemical_formula_moiety·····'C38·H24·F4·Ir·N4,·F6·P'
_chemical_compound_source·····?
_chemical_formula_weight·····949.81
·
·
_cell_measurement_reflns_used·····0
_cell_measurement_theta_min·····0
_cell_measurement_theta_max·····0
_cell_measurement_temperature·····123
·
_exptl_crystal_description·····'needle'·
_exptl_crystal_colour·····'yellow'·
_exptl_crystal_size_min·····0.07·
_exptl_crystal_size_mid·····0.09·
_exptl_crystal_size_max·····0.34·
·
_exptl_crystal_density_diffrn····1.916·
_exptl_crystal_density_meas·····?·
#·Non-dispersive·F(000)··
··exptl_crystal_F_000····1848·
_exptl_absorpt_coefficient_mu····4.198·
·
#·Sheldrick·geometric·approximatio·0.69·0.75·
·_exptl_absorpt_correction_type····multi-scan·
·_exptl_absorpt_process_details····'DENZO/SCALEPACK·(Otwinowski·&·Minor,·1997)''
·_exptl_absorpt_correction_T_min··0.69·
·_exptl_absorpt_correction_T_max··0.75·
#·For·a·Kappa·CCD,·set·Tmin·to·1.0·and·
#·Tmax·to·the·ratio·of·maximin·frame·scales·in·scale_all.log·
_diffrn_measurement_device_type····'Nonius·KappaCCD'·
_diffrn_radiation_monochromator···'graphite'·
_diffrn_radiation_type····'Mo·K\a'·
_diffrn_radiation_wavelength·····0.71073
_diffrn_measurement_method·····'\f·&·\w·scans'·
·
#·If·a·reference·occurs·more·than·once,·delete·the·author·
#·and·date·from·subsequent·references.·
_computing_data_collection·····'COLLECT·(Nonius,·1997-2001).''·
_computing_cell_refinement·····'DENZO/SCALEPACK·(Otwinowski·&·Minor,·1997)''
_computing_data_reduction·····'DENZO/SCALEPACK·(Otwinowski·&·Minor,·1997)''
_computing_structure_solution····'SIR92·(Altomare·et·al.,·1994)''
_computing_structure_refinement···'CRYSTALS·(Betteridge·et·al.,·2003)'·
_computing_publication_material···'CRYSTALS·(Betteridge·et·al.,·2003)'·
_computing_molecular_graphics····'CAMERON·(Watkin·et·al.,·1996)'·
·
_diffrn_standards_interval_time···?·
_diffrn_standards_interval_count···?·
_diffrn_standards_number·····0·
_diffrn_standards_decay_%·····?·
·
_diffrn_ambient_temperature·····123
_diffrn_reflns_number·····48711·
_reflns_number_total·····45640·
_diffrn_reflns_av_R_equivalents···0.051·
#·Number·of·reflections·with·Friedels·Law·is·45640·
#·Number·of·reflections·without·Friedels·Law·is·0·
#·Theoretical·number·of·reflections·is·about·46546·
·


·
_diffrn_reflns_theta_min·····2.292·
_diffrn_reflns_theta_max·····57.839·
_diffrn_measured_fraction_theta_max·0.979·
·
_diffrn_reflns_theta_full·····55.526·
_diffrn_measured_fraction_theta_full·0.995·
·
·
_diffrn_reflns_limit_h_min·····-45·
_diffrn_reflns_limit_h_max·····44·
_diffrn_reflns_limit_k_min·····-24·
_diffrn_reflns_limit_k_max·····24·
_diffrn_reflns_limit_l_min·····-43·
_diffrn_reflns_limit_l_max·····43·
_reflns_limit_h_min·····-45·
_reflns_limit_h_max·····40·
_reflns_limit_k_min·····0·
_reflns_limit_k_max·····24·
_reflns_limit_l_min·····0·
_reflns_limit_l_max·····43·
·
_oxford_diffrn_Wilson_B_factor···0.00·
_oxford_diffrn_Wilson_scale·····0.00·
·
_atom_sites_solution_primary·····direct·#heavy,direct,difmap,geom
#·_atom_sites_solution_secondary··difmap
_atom_sites_solution_hydrogens···geom
·
_refine_diff_density_min·····-0.81·
_refine_diff_density_max·····2.98·
·
·
_refine_ls_number_reflns·····27478·
_refine_ls_number_restraints····0·
_refine_ls_number_parameters·····487·
·
#·refine_ls_R_factor_ref·0.0172·
_refine_ls_wR_factor_ref·····0.0175·
_refine_ls_goodness_of_fit_ref···1.0654·
·
#·reflns_number_all·45624·
_refine_ls_R_factor_all·····0.0414·
_refine_ls_wR_factor_all·····0.0300·
·
#·The·I/u(I)·cutoff·below·was·used·for·refinement·as·
#·well·as·the··gt·R-factors:
_refine_threshold_expression····I>3.0\s(I)
_reflns_number_gt·····27478·
_refine_ls_R_factor_gt·····0.0172·
_refine_ls_wR_factor_gt·····0.0175·
·
_refine_ls_shift/su_max·····0.004331·
·
#·choose·from:·rm·(reference·molecule·of·known·chirality),·
#·ad·(anomolous·dispersion···Flack),·rmad·(rm·and·ad),·
#·syn·(from·synthesis),·unk·(unknown)·or··(not·applicable)··
·chemical_absolute_configuration·.'.'.·
·
·


_refine_ls_structure_factor_coef·F·
_refine_ls_matrix_type·····full
_refine_ls_hydrogen_treatment····constr·····#·none,·undef,·noref,·refall,
·····riding·····or·mixed·····constr·····#·refxyz,·refU,·constr·or·mixed
_refine_ls_weighting_scheme·····calc·
_refine_ls_weighting_details·
;
·Method,·part·1,·Chebychev·polynomial,·(Watkin,·1994,·Prince,·1982)·
·[weight]·=·1.0/[A~0~*T~0~(x)+A~1~*T~1~(x)·...·+A~n-1~*T~n-1~(x)]·
·where·A~i~·are·the·Chebychev·coefficients·listed·below·and·x=·Fcalc/Fmax·
·Method·-Robust·Weighting·(Prince,·1982)·
·W·=·[weight]·*·[1-(deltaF/6*sigmaF)^2^]^2^·
·A~i~·are:·
·0.596·0.578·0.564·0.192·0.949E-01·
;
·
·
·
#·Check·this·file·using·the·IUCr·facility·at:·
#·http://checkcif.iucr.org/·
·
#·The·content·below·is·held·in·the·file·'script/refclf.dat'.·This·is·a·text·
#·file·which·you·may·edit·to·reflect·local·conditions.·
#·Items·which·need·looking·at·are·represented·by·a·'?'.·
#·Items·for·which·there·are·choices·are·prefixed·with·'choose·from'.·
·
_publ_contact_letter·
;·
·Please·consider·this·CIF·submission·for·
·publication·as·a·Short·Format·Paper·in·Acta·
·Crystallographica·E.·The·figures·will·be·
·sent·by·e-mail..·
;·
_publ_contact_author_name·····'Anthony·Other'·
_publ_contact_author_address·
;·
·Chemical·Crystallography·Laboratory,·
·Department·of·Chemistry,·
·University·of·Nowhere,·
·Nowhere,·NO1·4T,·UK.·
;·
·
_publ_contact_author_phone·····'+44·1865·000000'·
_publ_contact_author_fax·····'+44·1865·000000'·
_publ_contact_author_email·····'a.n.other@chem.no.ac.uk'·
_publ_requested_journal·····'Section·E'·
_publ_requested_category·····EO·#·choose·from:·FI·FM·FO·CI·CM·CO·AD·
_publ_requested_coeditor_name····'Prof·William·Clegg'·
·
_publ_section_title·
#·Title·of·paper···generally·just·the·systematic·or·trivial·name·
;·?·
;·
·
#·The·loop·structure·below·should·contain·the·names·and·addresses·of·all·
#·authors,·in·the·required·order·of·publication.·Repeat·as·necessary.·
loop_·
··_publ_author_name·
··_publ_author_address·
··_publ_author_footnote·


··'Other,·Anthony·N.''·#·Author·1·
··;·
··?·#·Address·for·author·1·
··;·
··;·
··?·#·Footnote·for·author·1·
··;·
··'Else,·S.·O.''·#·Author·2·
··;·
··?·#·Address·2·
··;·
··;·
··?·#·Footnote·2·
··;·


··
··_publ_section_abstract·
··#·Text·of·the·abstract·
··#·(a)·The·Abstract·must·be·self-contained·and·comprehensible·
··#·without·the·rest·of·the·paper.·This·means·no·references·
··#·to·atom·names·or·to·compound·numbers;·compounds·must·be·
··#·identified·as·the·title·compound,·or·by·name·or·by·some·other·
··#·means·such·as·derivatives·of·each·other·(e.g.·"the·
··#·corresponding·ketone").··
··#·(b)·The·chemical·formula·of·"the·title·compound"·must·be·given.·
··#·(c)·Any·crystallographic·molecular·symmetry·should·be·
··#·mentioned,·and·also·the·presence·of·more·than·one·molecule.·
··#·in·the·asymmetric·unit·(i.e.·anything·other·than·Z'=1).··
··;·
··?·
··;·
_publ_section_comment·
··#·Text·of·the·paper·
··#·Note·that·atoms·are·referenced·as·N2,·not·N(2)·or·N·2···
··#·If·text·containing·()·occur·within·(),·the·outer·ones·should·be·[].·
··#·Figures·should·be·referenced·as·Fih.·
··;·
··?·
··;·
_publ_section_acknowledgements····#·Acknowledgments·
··;·
··?·
··;·
_publ_section_figure_captions·
··#·Captions·to·figures···Start·each·caption·on·a·new·line·after·a·blank·line·
··;·
··Fig.·1.·
··The·title·compound·with·displacement·ellipsoids·drawn·at·the·50%·
··probability·level.·H·atoms·are·shown·as·spheres·of·
··arbitary·radius.·
··;·
··;·
·
_publ_section_exptl_refinement·
#·Some·potentially·useful·phrases·are·donated·by·Bill·Clegg:·
;·
In·the·absence·of·significant·anomalous·scattering,·Friedel·pairs·were·
merged.·
·
The·absolute·configuration·was·arbitrarily·assigned.·


·
The·relatively·large·ratio·of·minimum·to·maximum·corrections·applied·
in·the·multiscan·process·(1rnnn)·reflect·changes·in·the·illuminated·
volume·of·the·crystal.·
·
Changes·in·illuminated·volume·were·kept·to·a·minimum,·and·were·
taken·into·account·(G\"orbitz,·1999)·by·the·multi-scan·inter-frame·
scaling·(DENZO/SCALEPACK,·Otwinowski·&·Minor,·1997).·
·
·
G\"orbitz,·C.·H.·(1999).·Acta·Cryst.·B55,·1090-1098.·
·
·
·
The·H·atoms·were·all·located·in·a·difference·map,·but·those·
attached·to·carbon·atoms·were·repositioned·geometrically.·
The·H·atoms·were·initially·refined·with·soft·restraints·on·the·
bond·lengths·and·angles·to·regularise·their·geometry·
(C---H·in·the·range·0.93·--·0.98,·
N---H·in·the·range·0.86·--·0.89·
N---H·to·0.86·
O---H·=·0.82·
\%A)·
and·
U~iso~(H)·(in·the·range·1.2·-1.5·times·U~eq~·of·the·parent·atom),·
after·which·the·positions·were·refined·with·riding·constraints..·
·
·
·
_publ_section_exptl_prep·
#·Brief·details·or·a·reference..·Include·solvent·if·known·
;·
?·
··
;·
·
#·PROCESSING·SUMMARY·(IUCr·Office·Use·Only):·
_journal_date_recd_electronic·····?·
_journal_date_to_coeditor·····?·
_journal_date_from_coeditor·····?·
_journal_date_accepted·····?·
_journal_date_printers_first·····?·
_journal_date_printers_final·····?·
_journal_date_proofs_out·····?·
_journal_date_proofs_in·····?·
_journal_coeditor_name·····?·
_journal_coeditor_code·····?·
_journal_coeditor_notes·····?·
_journal_techeditor_code·····?·
_journal_techeditor_notes·····?·
_journal_coden_ASTM·····?·
_journal_name_full·····?·
_journal_year·····?·
_journal_volume·····?·
_journal_issue·····?·
_journal_page_first·····?·
_journal_page_last·····?·
_journal_suppl_publ_number·····?·
_journal_suppl_publ_pages·····?·


#·End·of·'script/refclf.dat'.·
·
·
·
#·Insert·your·own·references·if·required···in·alphabetical·order·
_publ_section_references·
;·
Altomare,·A.,·Cascarano,·G.,·Giacovazzo,·G.,·Guagliardi,·A.,·Burla,·M.C.,·
Polidori,·G.·&·Camalli,·M.·(1994).·J.·Appl.·Cryst.·27,·435.·
·
Betteridge,·P.W.,·Carruthers,·J.R.,·Cooper,·R.I.,·
Prout,·K.·&·Watkin,·D.J.·(2003).·J.·Appl.·Cryst.·36,·1487.·
·
Larson,·A.C.·(1970).·Crystallographic·Computing,·Ed·Ahmed,·F.R.,·
Munksgaard,·Copenhagen,·291-294.·
·
Nonius·(1997-2001).·COLLECT.·Nonius·BV,·Delft,·The·Netherlands.·
·
Otwinowski,·Z.·&·Minor,·W.·(1997).·Methods·in·Enzymology,·Vol.·276,·
edited·by·C.·W.·Carter·Jr.·&·R.·M.·Sweet,·pp.·307·--·326.·
New·York:·Academic·Press.·
·
Prince,·E.·
Mathematical·Techniques·in·Crystallography·
and·Materials·Science·
Springer-Verlag,·New·York,·1982.·
·
Watkin·D.J.·(1994)..·
Acta·Cryst.·A50,·411-437.·
·
Watkin,·D.J.,·Prout,·C.K.·&·Pearce,·L.J..·(1996).·CAMERON,·Chemical·
Crystallography·Laboratory,·Oxford,·UK..·
;·
·
#·Uequiv·=·arithmetic·mean·of·Ui·i.e.·Ueqiv·=·(U1+U2+U3)/3·


#·Replace·last···with·number·of·unfound·hydrogen·atomsattached·to·an·atom.·


#·___·refinement_flags_···
#·..·no·refinement·constraints···········S·special·position·constraint·on·site·
#·O·rigid·group·refinement·of·site·····R·riding·atom·
#·D·distance·or·angle·restraint·on·site·T·thermal·displacement·constraints·
#·U·Uiso·or·Uij·restraint·(rigid·bond)···P·partial·occupancy·constraint·


loop_·
_atom_site_label·
_atom_site_type_symbol·
_atom_site_fract_x·
_atom_site_fract_y·
_atom_site_fract_z·
_atom_site_U_iso_or_equiv·
_atom_site_occupancy·
_atom_site_adp_type·
_atom_site_refinement_flags_posn·
_atom_site_refinement_flags_adp·
_atom_site_refinement_flags_occupancy·
_atom_site_disorder_assembly·
_atom_site_disorder_group·


··_atom_site_attached_hydrogens·
Ir1·Ir·0.2270546(14)·0.140262(2)·0.3500301(15)·0.0087·1.0000·Uani·.·.·.·.·.·
N1·N·0.12822(4)·0.21053(6)·0.35010(4)·0.0112·1.0000·Uani·.·.·.·.·.·
N2·N·0.31669(3)·0.04714(6)·0.34114(4)·0.0109·1.0000·Uani·.·.·.·.·.·
N3·N·0.27322(4)·0.32252(6)·0.33599(4)·0.0117·1.0000·Uani·.·.·.·.·.·
N4·N·0.29370(4)·0.20822(6)·0.47562(4)·0.0110·1.0000·Uani·.·.·.·.·.·
C1·C·0.17865(4)·-0.02819(7)·0.35911(4)·0.0113·1.0000·Uani·.·.·.·.·.·
C2·C·0.20708(5)·-0.15417(7)·0.36052(4)·0.0152·1.0000·Uani·.·.·.·.·.·
C3·C·0.16480(6)·-0.25951(8)·0.36493(6)·0.0180·1.0000·Uani·.·.·.·.·.·
C4·C·0.09472(6)·-0.24877(8)·0.36794(6)·0.0185·1.0000·Uani·.·.·.·.·.·
C5·C·0.06640(5)·-0.12468(8)·0.36380(6)·0.0153·1.0000·Uani·.·.·.·.·.·
C6·C·0.10511(4)·-0.01360(7)·0.35804(5)·0.0123·1.0000·Uani·.·.·.·.·.·
C7·C·0.07748(4)·0.11963(7)·0.35230(5)·0.0123·1.0000·Uani·.·.·.·.·.·
C8·C·0.00627(5)·0.15928(9)·0.34745(6)·0.0176·1.0000·Uani·.·.·.·.·.·
C9·C·-0.01261(5)·0.29001(10)·0.34009(6)·0.0196·1.0000·Uani·.·.·.·.·.·
C10·C·0.03984(5)·0.38059(9)·0.33811(6)·0.0186·1.0000·Uani·.·.·.·.·.·
C11·C·0.10950(5)·0.33755(8)·0.34364(5)·0.0148·1.0000·Uani·.·.·.·.·.·
C12·C·0.13795(4)·0.20517(8)·0.40535(5)·0.0135·1.0000·Uani·.·.·.·.·.·
C13·C·0.43485(5)·-0.06753(9)·0.39700(5)·0.0166·1.0000·Uani·.·.·.·.·.·
C14·C·0.42864(5)·-0.09445(10)·0.31959(6)·0.0187·1.0000·Uani·.·.·.·.·.·
C15·C·0.36487(5)·-0.05326(9)·0.25293(5)·0.0166·1.0000·Uani·.·.·.·.·.·
C16·C·0.30813(4)·-0.01553(7)·0.26480(4)·0.0118·1.0000·Uani·.·.·.·.·.·
C17·C·0.23340(4)·-0.05105(7)·0.20224(4)·0.0115·1.0000·Uani·.·.·.·.·.·
C18·C·0.20854(5)·-0.03244(8)·0.11887(4)·0.0136·1.0000·Uani·.·.·.·.·.·
C19·C·0.12475(5)·-0.05659(9)·0.06358(5)·0.0158·1.0000·Uani·.·.·.·.·.·
C20·C·0.08540(4)·-0.10471(8)·0.09443(5)·0.0149·1.0000·Uani·.·.·.·.·.·
C21·C·0.10675(4)·-0.12956(8)·0.17586(4)·0.0133·1.0000·Uani·.·.·.·.·.·
C22·C·0.18148(4)·-0.10294(7)·0.23121(4)·0.0107·1.0000·Uani·.·.·.·.·.·
C23·C·0.25428(5)·-0.38284(8)·0.26438(5)·0.0161·1.0000·Uani·.·.·.·.·.·
C24·C·0.28790(6)·-0.49780(9)·0.25698(6)·0.0194·1.0000·Uani·.·.·.·.·.·
C25·C·0.34365(6)·-0.55270(9)·0.32577(6)·0.0207·1.0000·Uani·.·.·.·.·.·
C26·C·0.36277(5)·-0.49247(9)·0.39993(6)·0.0180·1.0000·Uani·.·.·.·.·.·
C27·C·0.32644(4)·-0.37701(7)·0.40324(4)·0.0122·1.0000·Uani·.·.·.·.·.·
C28·C·0.34039(4)·-0.31030(7)·0.47998(4)·0.0119·1.0000·Uani·.·.·.·.·.·
C29·C·0.39565(5)·-0.35498(9)·0.55300(5)·0.0161·1.0000·Uani·.·.·.·.·.·
C30·C·0.40303(5)·-0.29687(10)·0.62486(5)·0.0182·1.0000·Uani·.·.·.·.·.·
C31·C·0.35398(5)·-0.19652(10)·0.62109(5)·0.0182·1.0000·Uani·.·.·.·.·.·
C32·C·0.30401(4)·-0.15491(7)·0.54611(4)·0.0131·1.0000·Uani·.·.·.·.·.·
C33·C·0.24395(5)·0.05470(8)·0.54597(5)·0.0135·1.0000·Uani·.·.·.·.·.·
C34·C·0.26231(6)·-0.07725(9)·0.55297(6)·0.0189·1.0000·Uani·.·.·.·.·.·
C35·C·0.32128(8)·-0.16764(10)·0.55989(7)·0.0250·1.0000·Uani·.·.·.·.·.·
C36·C·0.14351(8)·-0.12713(12)·0.56065(7)·0.0274·1.0000·Uani·.·.·.·.·.·
C37·C·0.12537(6)·0.00444(13)·0.55448(7)·0.0239·1.0000·Uani·.·.·.·.·.·
C38·C·0.17356(6)·0.09532(9)·0.54713(6)·0.0177·1.0000·Uani·.·.·.·.·.·
P1·P·0.530331(14)·0.27634(3)·0.377643(15)·0.0168·1.0000·Uani·.·.·.·.·.·
F1·F·0.19325(5)·-0.38076(6)·0.36848(7)·0.0304·1.0000·Uani·.·.·.·.·.·
F2·F·0.06221(4)·-0.11378(7)·0.36680(5)·0.0236·1.0000·Uani·.·.·.·.·.·
F3·F·0.01292(3)·0.13042(8)·0.04171(4)·0.0230·1.0000·Uani·.·.·.·.·.·
F4·F·0.25715(4)·-0.01017(7)·0.08831(4)·0.0202·1.0000·Uani·.·.·.·.·.·
F11·F·0.44415(4)·-0.22864(8)·0.33144(5)·0.0275·1.0000·Uani·.·.·.·.·.·
F12·F·0.51.61645(4)·0.32591(8)·0.42394(5)·0.0273·1.0000·Uani·.·.·.·.·.·
F13·F·0.50829(5)·0.41098(8)·0.32860(6)·0.0303·1.0000·Uani·.·.·.·.·.·
F14·F·0.55322(5)·0.14189(8)·0.42667(5)·0.0276·1.0000·Uani·.·.·.·.·.·
F15·F·0.51076(5)·0.33856(10)·0.44802(5)·0.0332·1.0000·Uani·.·.·.·.·.·
F16·F·0.55064(5)·0.21464(9)·0.30805(5)·0.0292·1.0000·Uani·.·.·.·.·.·
H21·H·0.2547·-0.1706·0.3604·0.0212·1.0000·Uiso·R·.·.·.·.·.·
H41·H·0.0681·-0.3203·0.3716·0.0246·1.0000·Uiso·R·.·.·.·.·.·
H81·H·-0.0264·0.0949·0.3489·0.0233·1.0000·Uiso·R·.·.·.·.·.·
H91·H·-0.0606·0.3189·0.3357·0.0265·1.0000·Uiso·R·.·.·.·.·.·
H101·H·0.0284·0.4673·0.3328·0.0234·1.0000·Uiso·R·.·.·.·.·.·


·
H111·H·0.1454·0.3966·0.3429·0.0190·1.0000·Uiso·R·.·.·.·.·.·
H121·H·0.3811·0.0267·0.4571·0.0169·1.0000·Uiso·R·.·.·.·.·.·
H131·H·0.4744·-0.0975·0.4427·0.0203·1.0000·Uiso·R·.·.·.·.·.·
H141·H·0.4658·-0.1399·0.3117·0.0233·1.0000·Uiso·R·.·.·.·.·.·
H151·H·0.3602·-0.0711·0.2010·0.0212·1.0000·Uiso·R·.·.·.·.·.·
H191·H·0.1215·0.0418·0.0098·0.0208·1.0000·Uiso·R·.·.·.·.·.·
H211·H·0.0699·0.1647·0.1927·0.0172·1.0000·Uiso·R·.·.·.·.·.·
H231·H·0.2178·0.3443·0.2198·0.0197·1.0000·Uiso·R·.·.·.·.·.·
H241·H·0.2719·0.5364·0.2049·0.0247·1.0000·Uiso·R·.·.·.·.·.·
H251·H·0.3684·0.6303·0.3220·0.0274·1.0000·Uiso·R·.·.·.·.·.·
H261·H·0.3994·0.5300·0.4479·0.0233·1.0000·Uiso·R·.·.·.·.·.·
H291·H·0.4284·0.4253·0.5549·0.0211·1.0000·Uiso·R·.·.·.·.·.·
H301·H·0.4405·0.3271·0.6745·0.0219·1.0000·Uiso·R·.·.·.·.·.·
H311·H·0.3559·0.1566·0.6667·0.0225·1.0000·Uiso·R·.·.·.·.·.·
H341·H·0.3094·-0.1049·0.5546·0.0258·1.0000·Uiso·R·.·.·.·.·.·
H351·H·0.2233·-0.2588·0.5639·0.0325·1.0000·Uiso·R·.·.·.·.·.·
H361·H·0.1093·-0.1906·0.5650·0.0367·1.0000·Uiso·R·.·.·.·.·.·
H371·H·0.0769·0.0330·0.5531·0.0313·1.0000·Uiso·R·.·.·.·.·.·
H381·H·0.1633·0.1874·0.5428·0.0237·1.0000·Uiso·R·.·.·.·.·.·
loop_·
··_atom_site_aniso_label·
··_atom_site_aniso_U_11·
··_atom_site_aniso_U_22·
··_atom_site_aniso_U_33·
··_atom_site_aniso_U_23·
··_atom_site_aniso_U_13·
··_atom_site_aniso_U_12·
Ir1·0.008917(7)·0.008589(6)·0.008769(6)·-0.000979(8)·0.003719(5)·-0.001052(8)·
N1·0.01181(18)·0.01035(18)·0.01226(18)·-0.00109(14)·0.00568(15)·-0.00037(15)·
N2·0.00980(17)·0.01217(18)·0.01047(17)·-0.00062(14)·0.00402(14)·-0.00050(14)·
N3·0.0135(2)·0.01130(19)·0.01060(18)·-0.00032(15)·0.00525(15)·-0.00224(16)·
N4·0.01201(18)·0.01106(18)·0.01002(17)·-0.00053(14)·0.00460(15)·-0.00101(15)·
C1·0.0117(2)·0.0101(2)·0.0128(2)·-0.00166(16)·0.00593(18)·-0.00154(16)·
C2·0.0161(3)·0.0101(2)·0.0218(3)·-0.00216(19)·0.0104(2)·-0.00096(18)·
C3·0.0204(3)·0.0096(2)·0.0263(4)·-0.0026(2)·0.0121(3)·-0.0021(2)·
C4·0.0196(3)·0.0121(3)·0.0262(4)·-0.0030(2)·0.0120(3)·-0.0051(2)·
C5·0.0140(2)·0.0135(3)·0.0203(3)·-0.0023(2)·0.0091(2)·-0.00338(19)·
C6·0.0124(2)·0.0108(2)·0.0149(2)·-0.00131(18)·0.00676(19)·-0.00194(17)·
C7·0.0119(2)·0.0127(2)·0.0139(2)·-0.00051(17)·0.00605(18)·-0.00031(16)·
C8·0.0138(2)·0.0178(3)·0.0236(3)·0.0008(2)·0.0102(2)·0.0013(2)·
C9·0.0166(3)·0.0186(3)·0.0257(4)·0.0006(3)·0.0110(3)·0.0047(2)·
C10·0.0128(3)·0.0138(3)·0.0237(3)·-0.0016(2)·0.0089(3)·0.0036(2)·
C11·0.0160(3)·0.0108(2)·0.0180(3)·-0.00148(19)·0.0074(2)·0.00057(18)·
C12·0.0115(2)·0.0159(3)·0.0120(2)·-0.00017(19)·0.00374(18)·0.00068(19)·
C13·0.0199(3)·0.0193(3)·0.0161(3)·-0.0001(2)·0.0035(2)·0.0031(2)·
C14·0.0135(3)·0.0229(4)·0.0186(3)·-0.0022(3)·0.0056(2)·0.0052(2)·
C15·0.0135(2)·0.0210(3)·0.0155(3)·-0.0030(2)·0.0063(2)·0.0028(2)·
C16·0.0164(3)·0.0128(2)·0.0114(2)·-0.00169(17)·0.00441(17)·-0.00030(17)·
C17·0.0113(2)·0.0126(2)·0.01003(19)·-0.00193(16)·0.00392(16)·-0.00054(17)·
C18·0.0151(2)·0.0148(2)·0.0110(2)·-0.00255(18)·0.00551(19)·-0.0004(2)·
C19·0.0164(3)·0.0181(3)·0.0103(2)·-0.0022(2)·0.00293(19)·-0.0001(2)·
C20·0.0125(2)·0.0162(3)·0.0121(2)·-0.0014(2)·0.00130(18)·0.0004(2)·
C21·0.01084(19)·0.0152(3)·0.0120(2)·-0.00129(19)·0.00293(16)·0.00048(18)·
C22·0.01038(19)·0.0108(2)·0.01053(19)·-0.00120(16)·0.00381(16)·-0.00084(16)·
C23·0.0196(3)·0.0147(3)·0.0112(2)·0.00049(18)·0.0065(2)·-0.0038(2)·
C24·0.0284(4)·0.0155(3)·0.0159(3)·0.0016(2)·0.0107(3)·-0.0047(3)·
C25·0.0265(4)·0.0160(3)·0.0204(3)·0.0007(2)·0.0106(3)·-0.0082(3)·
C26·0.0196(3)·0.0157(3)·0.0172(3)·-0.0007(2)·0.0062(2)·-0.0071(2)·
C27·0.0129(2)·0.0114(2)·0.0121(2)·-0.00074(16)·0.00489(17)·-0.00263(16)·
C28·0.0119(2)·0.0115(2)·0.0113(2)·-0.00074(17)·0.00385(17)·-0.00173(17)·


·
C29·0.0149(2)·0.0165(3)·0.0132(2)·-0.0018(2)·0.00220(18)·-0.0033(2)·
C30·0.0169(3)·0.0210(3)·0.0121(2)·-0.0011(2)·0.0015(2)·-0.0025(2)·
C31·0.0195(3)·0.0217(3)·0.0107(2)·0.0006(2)·0.0036(2)·-0.0023(3)·
C32·0.0141(2)·0.0142(3)·0.01047(19)·-0.00033(17)·0.00469(17)·-0.00051(18)·
C33·0.0172(3)·0.0129(2)·0.0120(2)·0.00054(18)·0.0075(2)·-0.00037(19)·
C34·0.0261(4)·0.0136(3)·0.0186(3)·0.0007(2)·0.0109(3)·0.0016(3)·
C35·0.0399(6)·0.0146(3)·0.0222(4)·0.0000(3)·0.0144(4)·-0.0049(3)·
C36·0.0362(5)·0.0274(5)·0.0232(4)·-0.0027(3)·0.0167(4)·-0.0146(4)·
C37·0.0231(4)·0.0315(5)·0.0220(4)·-0.0036(3)·0.0141(3)·-0.0072(4)·
C38·0.0185(3)·0.0190(3)·0.0181(3)·-0.0013(2)·0.0099(2)·-0.0033(2)·
P1·0.01648(8)·0.01799(9)·0.01445(8)·-0.00042(7)·0.00509(6)·-0.00444(7)·
F1·0.0314(3)·0.00898(18)·0.0582(5)·-0.0022(2)·0.0260(4)·0.00037(19)·
F2·0.0177(2)·0.0191(2)·0.0402(4)·-0.0015(2)·0.0182(3)·-0.00441(18)·
F3·0.0141(19)·0.0320(3)·0.0149(19)·-0.0032(2)·-0.00156(15)·0.0047(2)·
F4·0.0200(2)·0.0278(3)·0.0153(2)·-0.00451(19)·0.00974(18)·0.0020(2)·
F11·0.0192(3)·0.0286(3)·0.0261(3)·0.0014(3)·0.0008(2)·-0.0089(2)·
F12·0.0163(2)·0.0283(3)·0.0336(4)·-0.0046(3)·0.0068(2)·-0.0067(2)·
F13·0.0289(3)·0.0198(3)·0.0378(4)·0.0077(3)·0.0093(3)·-0.0007(2)·
F14·0.0265(3)·0.0277(3)·0.0246(3)·0.0112(3)·0.0067(2)·-0.0032(3)·
F15·0.0251(3)·0.0507(5)·0.0251(3)·-0.0123(3)·0.0116(3)·-0.0016(3)·
F16·0.0393(4)·0.0313(4)·0.0202(3)·-0.0015(3)·0.0154(3)·0.0006(3)·


·refine_ls_extinction_method·
····"None"·
··oxford_refine_ls_scale·0.17244(4)·
loop_·
··_geom_bond_atom_site_label_1·
··_geom_bond_site_symmetry_1·
··_geom_bond_atom_site_label_2·
··_geom_bond_site_symmetry_2·
··_geom_bond_distance·
··_geom_bond_publ_flag·
Ir1·-·N1··2.0455(6)····yes·
Ir1·-·N2··2.0463(6)····yes·
Ir1·-·N3··2.1382(6)····yes·
Ir1·-·N4··2.2169(6)····yes·
Ir1·-·C1··2.0099(7)····yes·
Ir1·-·C22··2.0011(7)····yes·
N1·-·C7··1.3691(10)····yes·
N1·-·C11··1.3487(10)····yes·
N2·-·C12··1.3476(10)····yes·
N2·-·C16··1.3663(9)····yes·
N3·-·C23··1.3479(11)····yes·
N3·-·C27··1.3500(9)····yes·
N4·-·C28··1.3666(9)····yes·
N4·-·C24··1.3550(9)····yes·
C1·-·C2··1.4047(10)····yes·
C1·-·C6··1.4232(10)····yes·
C2·-·C3··1.3807(11)····yes·
C2·-·H21··0.938···no·
C3·-·C4··1.3842(13)····yes·
C3·-·H31··0.9548(11)····yes·
C4·-·C5··1.3796(12)····yes·
C4·-·H41··0.917···no·
C5·-·C6··1.3945(10)····yes·
C5·-·F2··1.3561(10)····yes·
C6·-·C7··1.4598(11)····yes·
C7·-·C8··1.4045(11)····yes·
C8·-·C9··1.3862(13)····yes·
C8·-·H81··0.925···no·
```

bis(1-phenylisoquinoline-*C*,*N*)(6-phenyl-2,2'-bipyridine-*N*,*N*')iridium(III) hexafluorophosphate (**59**)

```
 _publ_author_footnote
 'Other, Anthony N.' # Author 1
;
 ? # Address for author 1
;
;
 ? # Footnote for author 1
;
 'Else, S. O.' # Author 2
;
 ? # Address 2
;
;
 ? # Footnote 2
;


_publ_section_abstract
# Text of the abstract
# (a) The Abstract must be self-contained and comprehensible
# without the rest of the paper. This means no references
# to atom names or to compound numbers; compounds must be
# identified as the title compound, or by name or by some other
# means such as derivatives of each other (e.g. "the
# corresponding ketone").
# (b) The chemical formula of "the title compound" must be given.
# (c) Any crystallographic molecular symmetry should be
# mentioned, and also the presence of more than one molecule
# in the asymmetric unit (i.e. anything other than Z'=1).
;
?
;
_publ_section_comment
# Text of the paper
# Note that atoms are referenced as N2, not N(2) or N~2~
# If text containing () occur within (), the outer ones should be []
# Figures should be referenced as Fih.
;
?
;
_publ_section_acknowledgements    # Acknowledgments
;
?
;
_publ_section_figure_captions
# Captions to figures - Start each caption on a new line after a blank line
;
Fig. 1.
The title compound with displacement ellipsoids drawn at the 50%
probability level. H atoms are shown as spheres of
arbitary radius.

;

_publ_section_exptl_refinement
# Some potentially useful phrases are donated by Bill Clegg:
;
In the absence of significant anomalous scattering, Friedel pairs were
merged.

The absolute configuration was arbitrarily assigned.

The relatively large ratio of minimum to maximum corrections applied
in the multiscan process (1:nnn) reflect changes in the illuminated
volume of the crystal.

Changes in illuminated volume were kept to a minimum, and were
taken into account (G\"orbitz, 1999) by the multi-scan inter-frame
scaling (DENZO/SCALEPACK, Otwinowski & Minor, 1997).


G\"orbitz, C. H. (1999). Acta Cryst. B55, 1090-1098.




The H atoms were all located in a difference map, but those
attached to carbon atoms were repositioned geometrically.
The H atoms were initially refined with soft restraints on the
bond lengths and angles to regularise their geometry
(C---H in the range 0.93--0.98,
N---H in the range 0.86--0.89
N---H to 0.86
O---H = 0.82
\%A)
and
U~iso~(H) (in the range 1.2-1.5 times U~eq~ of the parent atom),
after which the positions were refined with riding constraints.

;

_publ_section_exptl_prep
# Brief details or a reference. Include solvent if known
;
?
;


# PROCESSING SUMMARY (IUCr Office Use Only):
_journal_date_recd_electronic     ?
_journal_date_to_coeditor         ?
_journal_date_from_coeditor       ?
_journal_date_accepted            ?
_journal_date_printers_first      ?
_journal_date_printers_final      ?
_journal_date_proofs_out          ?
_journal_date_proofs_in           ?
_journal_coeditor_name            ?
_journal_coeditor_code            ?
_journal_coeditor_notes           ?
_journal_techeditor_code          ?
_journal_techeditor_notes         ?
_journal_coden_ASTM               ?
_journal_name_full                ?
_journal_year                     ?
_journal_volume                   ?
_journal_issue                    ?
_journal_page_first               ?
_journal_page_last                ?
_journal_suppl_publ_number        ?
_journal_suppl_publ_pages         ?

# End of 'script/refcif.dat'



# Insert your own references if required - in alphabetical order
_publ_section_references
;
User-defined structure solution reference

Betteridge, P.W., Carruthers, J.R., Cooper, R.I.,
Prout, K. & Watkin, D.J. (2003). J. Appl. Cryst. 36, 1487.

Larson, A.C. (1970) Crystallographic Computing, Ed Ahmed, F.R.,
Munksgaard, Copenhagen, 291-294.

Nonius (1997-2001). COLLECT. Nonius BV, Delft, The Netherlands.

Otwinowski, Z. & Minor, W. (1997). Methods in Enzymology, Vol. 276,
edited by C. W. Carter Jr & R. M. Sweet, pp. 307--326.
New York: Academic Press.

Prince, E.
Mathematical Techniques in Crystallography
and Materials Science
Springer-Verlag, New York, 1982.

Watkin D.J. (1994).
Acta Cryst, A50, 411-437.

Watkin, D.J., Prout, C.K. & Pearce, L.J. (1996). CAMERON, Chemical
Crystallography Laboratory, Oxford, UK.
;

# Uequiv = arithmetic mean of Ui i.e. Ueqiv = (U1+U2+U3)/3

# Replace last . with number of unfound hydrogen atomsattached to an atom.

# ..._refinement_flags_...
# . no refinement constraints           S special position constraint on site
# G rigid group refinement of site      R riding atom
# D distance or angle restraint on site T thermal displacement constraints
# U Uiso or Uij restraint (rigid bond)  P partial occupancy constraint


loop_
_atom_site_label
_atom_site_type_symbol
_atom_site_fract_x
_atom_site_fract_y
_atom_site_fract_z
_atom_site_U_iso_or_equiv
_atom_site_occupancy
_atom_site_adp_type
_atom_site_refinement_flags_posn
_atom_site_refinement_flags_adp
_atom_site_refinement_flags_occupancy
_atom_site_disorder_assembly
_atom_site_disorder_group
_atom_site_attached_hydrogens
Ir1 Ir 0.532440(5) 0.269373(4) 0.238809(3) 0.0136 1.0000 Uani . . . . . .
N1 N 0.44660(12) 0.34140(9) 0.33857(6) 0.0164 1.0000 Uani . . . . . .
N2 N 0.67283(12) 0.16618(9) 0.32859(6) 0.0163 1.0000 Uani . . . . . .
N3 N 0.42719(11) 0.13982(9) 0.25830(6) 0.0151 1.0000 Uani . . . . . .
N4 N 0.63214(11) 0.40134(9) 0.20667(6) 0.0153 1.0000 Uani . . . . . .
C1 C 0.34614(16) 0.43862(12) 0.33901(8) 0.0218 1.0000 Uani . . . . . .
C2 C 0.30613(17) 0.48752(13) 0.40382(9) 0.0245 1.0000 Uani . . . . . .
C3 C 0.37309(17) 0.43636(13) 0.47015(9) 0.0241 1.0000 Uani . . . . . .
C4 C 0.47376(16) 0.33535(13) 0.47058(8) 0.0224 1.0000 Uani . . . . . .
C5 C 0.50702(14) 0.28899(11) 0.40403(7) 0.0176 1.0000 Uani . . . . . .
C6 C 0.61285(15) 0.18162(11) 0.39938(7) 0.0193 1.0000 Uani . . . . . .
C7 C 0.6464(2) 0.10148(14) 0.46358(8) 0.0286 1.0000 Uani . . . . . .
C8 C 0.7450(2) 0.00163(14) 0.45551(10) 0.0341 1.0000 Uani . . . . . .
C9 C 0.8134(2) -0.01155(13) 0.38471(9) 0.0285 1.0000 Uani . . . . . .
C10 C 0.77847(15) 0.07289(11) 0.32230(8) 0.0190 1.0000 Uani . . . . . .
C11 C 0.86442(14) 0.06235(11) 0.24908(8) 0.0193 1.0000 Uani . . . . . .
C12 C 0.95054(16) 0.13893(13) 0.21974(9) 0.0236 1.0000 Uani . . . . . .
C13 C 1.03795(17) 0.12606(16) 0.15309(10) 0.0297 1.0000 Uani . . . . . .
C14 C 1.04009(19) 0.03617(17) 0.11609(11) 0.0333 1.0000 Uani . . . . . .
C15 C 0.9574(2) -0.04142(15) 0.14576(11) 0.0321 1.0000 Uani . . . . . .
C16 C 0.86992(17) -0.02934(13) 0.21235(9) 0.0252 1.0000 Uani . . . . . .
C17 C 0.32476(14) 0.12912(12) 0.31766(7) 0.0191 1.0000 Uani . . . . . .
C18 C 0.25816(15) 0.04085(12) 0.33220(8) 0.0207 1.0000 Uani . . . . . .
C19 C 0.30282(14) -0.04782(11) 0.28897(8) 0.0195 1.0000 Uani . . . . . .
C20 C 0.24563(18) -0.14595(13) 0.30638(10) 0.0272 1.0000 Uani . . . . . .
C21 C 0.2963(2) -0.23296(14) 0.26590(12) 0.0333 1.0000 Uani . . . . . .
C22 C 0.40719(19) -0.22688(14) 0.20865(12) 0.0311 1.0000 Uani . . . . . .
C23 C 0.46454(16) -0.13305(12) 0.19023(9) 0.0239 1.0000 Uani . . . . . .
C24 C 0.41014(13) -0.03847(11) 0.22804(7) 0.0172 1.0000 Uani . . . . . .
C25 C 0.46157(13) 0.06391(10) 0.21040(7) 0.0152 1.0000 Uani . . . . . .
C26 C 0.55243(13) 0.09888(11) 0.14328(7) 0.0156 1.0000 Uani . . . . . .
C27 C 0.57554(15) 0.05105(13) 0.07629(8) 0.0204 1.0000 Uani . . . . . .
C28 C 0.66468(15) 0.08981(14) 0.01608(8) 0.0225 1.0000 Uani . . . . . .
C29 C 0.73126(15) 0.17575(12) 0.02252(7) 0.0208 1.0000 Uani . . . . . .
C30 C 0.70130(14) 0.22861(11) 0.08654(7) 0.0181 1.0000 Uani . . . . . .
C31 C 0.61001(12) 0.19347(10) 0.14761(7) 0.0146 1.0000 Uani . . . . . .
C32 C 0.74895(14) 0.41070(11) 0.24137(7) 0.0177 1.0000 Uani . . . . . .
C33 C 0.81544(15) 0.49837(12) 0.21892(8) 0.0204 1.0000 Uani . . . . . .
C34 C 0.77032(14) 0.57814(11) 0.15409(7) 0.0185 1.0000 Uani . . . . . .
C35 C 0.84080(17) 0.66779(13) 0.12676(9) 0.0244 1.0000 Uani . . . . . .
C36 C 0.80070(18) 0.74035(13) 0.06106(9) 0.0267 1.0000 Uani . . . . . .
C37 C 0.69261(17) 0.72364(13) 0.01948(8) 0.0242 1.0000 Uani . . . . . .
C38 C 0.62119(15) 0.63868(12) 0.04511(8) 0.0212 1.0000 Uani . . . . . .
C39 C 0.65372(14) 0.56609(11) 0.11519(7) 0.0168 1.0000 Uani . . . . . .
C40 C 0.57673(13) 0.48027(10) 0.14859(7) 0.0158 1.0000 Uani . . . . . .
C41 C 0.43364(14) 0.47009(11) 0.13044(7) 0.0179 1.0000 Uani . . . . . .
C42 C 0.33588(16) 0.55422(13) 0.08693(9) 0.0238 1.0000 Uani . . . . . .
C43 C 0.19821(16) 0.53969(14) 0.07843(10) 0.0275 1.0000 Uani . . . . . .
C44 C 0.15594(15) 0.44229(14) 0.11487(9) 0.0252 1.0000 Uani . . . . . .
C45 C 0.25019(14) 0.36034(12) 0.16073(8) 0.0205 1.0000 Uani . . . . . .
C46 C 0.39007(13) 0.37163(11) 0.16961(7) 0.0168 1.0000 Uani . . . . . .
C47 C 0.1662(2) 0.34721(17) 0.62298(10) 0.0333 1.0000 Uani . . . . . .
Cl1 Cl 0.02034(5) 0.31453(4) 0.68498(3) 0.0350 1.0000 Uani . . . . . .
Cl2 Cl 0.33162(6) 0.28107(6) 0.66247(3) 0.0489 1.0000 Uani . . . . . .
P1 P 0.96734(4) 0.30041(3) 0.44058(2) 0.0194 1.0000 Uani . . . . . .
F1 F 0.79997(12) 0.35160(12) 0.42534(8) 0.0398 1.0000 Uani . . . . . .
F2 F 1.13601(11) 0.25040(9) 0.45515(6) 0.0311 1.0000 Uani . . . . . .
F3 F 0.97016(14) 0.40506(10) 0.47965(9) 0.0450 1.0000 Uani . . . . . .
F4 F 0.96408(16) 0.19669(13) 0.40066(10) 0.0554 1.0000 Uani . . . . . .
F5 F 1.01304(15) 0.36664(15) 0.36036(8) 0.0527 1.0000 Uani . . . . . .
F6 F 0.92379(18) 0.23460(15) 0.52063(8) 0.0576 1.0000 Uani . . . . . .
H11 H 0.3025 0.4745 0.2936 0.0259 1.0000 Uiso R . . . . .
H21 H 0.2367 0.5532 0.4024 0.0303 1.0000 Uiso R . . . . .
H31 H 0.3479 0.4688 0.5149 0.0305 1.0000 Uiso R . . . . .
H41 H 0.5209 0.2977 0.5142 0.0280 1.0000 Uiso R . . . . .
H71 H 0.5996 0.1149 0.5121 0.0333 1.0000 Uiso R . . . . .
H81 H 0.7666 -0.0580 0.4973 0.0393 1.0000 Uiso R . . . . .
H91 H 0.8854 -0.0769 0.3783 0.0331 1.0000 Uiso R . . . . .
H121 H 0.9484 0.1984 0.2442 0.0288 1.0000 Uiso R . . . . .
H131 H 1.0967 0.1764 0.1336 0.0369 1.0000 Uiso R . . . . .
H141 H 1.0998 0.0265 0.0698 0.0393 1.0000 Uiso R . . . . .
H151 H 0.9621 -0.1023 0.1212 0.0383 1.0000 Uiso R . . . . .
H161 H 0.8135 -0.0811 0.2321 0.0321 1.0000 Uiso R . . . . .
H171 H 0.2987 0.1863 0.3470 0.0232 1.0000 Uiso R . . . . .
H181 H 0.1831 0.0390 0.3688 0.0245 1.0000 Uiso R . . . . .
H201 H 0.1727 -0.1496 0.3461 0.0332 1.0000 Uiso R . . . . .
H211 H 0.2561 -0.2992 0.2763 0.0412 1.0000 Uiso R . . . . .
H221 H 0.4454 -0.2884 0.1831 0.0385 1.0000 Uiso R . . . . .
H231 H 0.5440 -0.1352 0.1527 0.0286 1.0000 Uiso R . . . . .
H271 H 0.5309 -0.0062 0.0723 0.0258 1.0000 Uiso R . . . . .
H281 H 0.6804 0.0576 -0.0290 0.0275 1.0000 Uiso R . . . . .
H291 H 0.7971 0.1974 -0.0179 0.0250 1.0000 Uiso R . . . . .
H301 H 0.7473 0.2898 0.0896 0.0208 1.0000 Uiso R . . . . .
H321 H 0.7818 0.3552 0.2815 0.0220 1.0000 Uiso R . . . . .
H331 H 0.8903 0.5056 0.2474 0.0248 1.0000 Uiso R . . . . .
H351 H 0.9160 0.6783 0.1544 0.0298 1.0000 Uiso R . . . . .
H361 H 0.8466 0.8025 0.0445 0.0322 1.0000 Uiso R . . . . .
H371 H 0.6682 0.7702 -0.0269 0.0295 1.0000 Uiso R . . . . .
H381 H 0.5515 0.6284 0.0167 0.0233 1.0000 Uiso R . . . . .
H421 H 0.3631 0.6194 0.0637 0.0261 1.0000 Uiso R . . . . .
H431 H 0.1328 0.5947 0.0479 0.0323 1.0000 Uiso R . . . . .
H441 H 0.0620 0.4315 0.1084 0.0304 1.0000 Uiso R . . . . .
H451 H 0.2201 0.2953 0.1866 0.0246 1.0000 Uiso R . . . . .
H471 H 0.1568 0.4284 0.6166 0.0409 1.0000 Uiso R . . . . .
H472 H 0.1617 0.3195 0.5757 0.0408 1.0000 Uiso R . . . . .
loop_
_atom_site_aniso_label
_atom_site_aniso_U_11
_atom_site_aniso_U_22
_atom_site_aniso_U_33
_atom_site_aniso_U_23
_atom_site_aniso_U_13
_atom_site_aniso_U_12
Ir1 0.01552(2) 0.01324(2) 0.01151(2) -0.00261(1) -0.00153(1) -0.00124(1)
N1 0.0186(4) 0.0156(4) 0.0150(4) -0.0042(3) -0.0007(3) -0.0026(3)
N2 0.0180(4) 0.0145(4) 0.0157(4) -0.0024(3) -0.0033(3) -0.0014(3)
N3 0.0159(4) 0.0163(4) 0.0135(4) -0.0041(3) 0.0002(3) -0.0036(3)
N4 0.0160(4) 0.0149(4) 0.0145(4) -0.0033(3) -0.0019(3) -0.0014(3)
C1 0.0232(6) 0.0193(5) 0.0212(5) -0.0061(4) -0.0013(4) 0.0011(4)
C2 0.0255(6) 0.0225(6) 0.0247(6) -0.0102(5) 0.0020(5) -0.0004(5)
C3 0.0255(6) 0.0271(6) 0.0216(6) -0.0118(5) 0.0027(5) -0.0054(5)
C4 0.0251(6) 0.0271(6) 0.0157(5) -0.0076(4) 0.0000(4) -0.0047(5)
C5 0.0196(5) 0.0184(5) 0.0150(5) -0.0043(4) -0.0003(4) -0.0037(4)
C6 0.0233(5) 0.0186(5) 0.0150(5) -0.0027(4) -0.0030(4) -0.0020(4)
C7 0.0412(8) 0.0240(6) 0.0156(5) 0.0003(5) -0.0038(5) 0.0008(6)
C8 0.0518(10) 0.0229(6) 0.0205(6) 0.0026(5) -0.0072(6) 0.0031(6)
C9 0.0382(8) 0.0183(5) 0.0236(6) -0.0008(5) -0.0076(6) 0.0050(5)
C10 0.0215(5) 0.0154(5) 0.0195(5) -0.0036(4) -0.0051(4) -0.0003(4)
C11 0.0178(5) 0.0182(5) 0.0208(5) -0.0052(4) -0.0043(4) 0.0009(4)
C12 0.0208(5) 0.0250(6) 0.0259(6) -0.0083(5) -0.0025(5) -0.0032(5)
C13 0.0210(6) 0.0369(8) 0.0316(7) -0.0092(6) 0.0005(5) -0.0056(5)
C14 0.0246(7) 0.0419(9) 0.0303(7) -0.0132(7) 0.0023(6) 0.0025(6)
C15 0.0335(8) 0.0290(7) 0.0329(8) -0.0159(6) -0.0020(6) 0.0028(6)
C16 0.0275(6) 0.0204(6) 0.0278(6) -0.0089(5) -0.0037(5) -0.0006(5)
C17 0.0201(5) 0.0219(5) 0.0155(5) -0.0063(4) 0.0035(4) -0.0047(4)
C18 0.0210(5) 0.0231(6) 0.0181(5) -0.0042(4) 0.0039(4) -0.0066(4)
C19 0.0176(5) 0.0183(5) 0.0220(5) -0.0022(4) 0.0003(4) -0.0045(4)
C20 0.0263(6) 0.0211(6) 0.0345(7) -0.0036(5) 0.0046(5) -0.0092(5)
C21 0.0328(8) 0.0201(6) 0.0480(10) -0.0074(6) 0.0044(7) -0.0094(5)
C22 0.0299(7) 0.0200(6) 0.0446(9) -0.0124(6) 0.0027(6) -0.0049(5)
C23 0.0212(6) 0.0201(5) 0.0304(7) -0.0091(5) 0.0016(5) -0.0024(4)
C24 0.0155(4) 0.0166(5) 0.0193(5) -0.0042(4) -0.0014(4) -0.0021(4)
C25 0.0135(4) 0.0170(5) 0.0150(4) -0.0043(4) -0.0010(3) -0.0020(3)
C26 0.0151(4) 0.0185(5) 0.0132(4) -0.0044(4) -0.0005(3) -0.0023(4)
C27 0.0189(5) 0.0279(6) 0.0168(5) -0.0098(4) 0.0001(4) -0.0055(4)
C28 0.0200(5) 0.0318(7) 0.0156(5) -0.0089(5) 0.0001(4) -0.0022(5)
C29 0.0190(5) 0.0255(6) 0.0148(5) -0.0021(4) 0.0024(4) -0.0009(4)
C30 0.0183(5) 0.0185(5) 0.0159(5) -0.0018(4) 0.0014(4) -0.0028(4)
C31 0.0139(4) 0.0171(4) 0.0124(4) -0.0029(4) -0.0008(3) -0.0019(3)
C32 0.0198(5) 0.0169(5) 0.0164(5) -0.0020(4) -0.0048(4) -0.0030(4)
C33 0.0230(5) 0.0197(5) 0.0192(5) -0.0012(4) -0.0060(4) -0.0056(4)
C34 0.0194(5) 0.0184(5) 0.0174(5) -0.0022(4) -0.0015(4) -0.0037(4)
C35 0.0269(6) 0.0228(6) 0.0244(6) -0.0002(5) -0.0041(5) -0.0091(5)
C36 0.0292(7) 0.0229(6) 0.0267(6) 0.0020(5) -0.0001(5) -0.0086(5)
C37 0.0269(6) 0.0230(6) 0.0192(5) 0.0030(5) -0.0001(5) -0.0038(5)
C38 0.0227(5) 0.0221(5) 0.0163(5) 0.0006(4) -0.0022(4) -0.0021(4)
C39 0.0187(5) 0.0161(5) 0.0143(4) -0.0018(4) -0.0015(4) -0.0019(4)
C40 0.0170(5) 0.0150(4) 0.0144(4) -0.0026(4) -0.0025(3) -0.0009(4)
C41 0.0165(5) 0.0183(5) 0.0174(5) -0.0012(4) -0.0033(4) -0.0014(4)
C42 0.0200(5) 0.0219(6) 0.0261(6) 0.0029(5) -0.0073(5) -0.0005(4)
C43 0.0190(6) 0.0286(7) 0.0307(7) 0.0033(6) -0.0083(5) 0.0000(5)
C44 0.0167(5) 0.0298(7) 0.0269(6) -0.0008(5) -0.0056(4) -0.0017(5)
C45 0.0175(5) 0.0227(5) 0.0209(5) -0.0027(4) -0.0036(4) -0.0037(4)
C46 0.0168(5) 0.0178(5) 0.0149(4) -0.0032(4) -0.0027(4) -0.0011(4)
C47 0.0313(8) 0.0389(9) 0.0264(7) 0.0037(6) -0.0074(6) -0.0055(6)
Cl1 0.03248(19) 0.0399(2) 0.03368(19) 0.00092(16) -0.00600(15) -0.01318(16)
Cl2 0.0314(2) 0.0736(4) 0.0318(2) 0.0025(2) -0.00755(16) 0.0024(2)
P1 0.02126(14) 0.01957(14) 0.01758(13) -0.00604(11) -0.00303(11) -0.00203(11)
F1 0.0211(4) 0.0567(7) 0.0442(6) -0.0230(6) -0.0074(4) -0.0003(4)
F2 0.0252(4) 0.0308(5) 0.0339(5) -0.0066(4) -0.0093(4) 0.0052(4)
F3 0.0384(6) 0.0314(5) 0.0712(9) -0.0306(6) -0.0197(6) 0.0041(4)
F4 0.0463(7) 0.0514(8) 0.0820(11) -0.0494(8) -0.0041(7) -0.0084(6)
F5 0.0407(7) 0.0750(10) 0.0303(6) 0.0208(6) -0.0044(5) -0.0098(6)
F6 0.0589(9) 0.0691(10) 0.0342(6) 0.0153(7) 0.0087(6) -0.0162(8)

_refine_ls_extinction_method
    'None'
_oxford_refine_ls_scale 0.35326(12)
loop_
 _geom_bond_atom_site_label_1
 _geom_bond_site_symmetry_1
 _geom_bond_atom_site_label_2
 _geom_bond_site_symmetry_2
 _geom_bond_distance
 _geom_bond_publ_flag
Ir1 . N1 . 2.1379(11)    yes
Ir1 . N2 . 2.2158(11)    yes
Ir1 . N3 . 2.0440(11)    yes
Ir1 . N4 . 2.0441(11)    yes
Ir1 . C31 . 2.0152(12)    yes
Ir1 . C46 . 1.9888(12)    yes
N1 . C1 . 1.3509(17)    yes
N1 . C5 . 1.3478(17)    yes
N2 . C6 . 1.3604(17)    yes
N2 . C10 . 1.3549(16)    yes
N3 . C17 . 1.3751(16)    yes
N3 . C25 . 1.3452(16)    yes
N4 . C32 . 1.3652(16)    yes
N4 . C40 . 1.3498(16)    yes
C1 . C2 . 1.381(2)    yes
C1 . H11 . 0.941    no
C2 . C3 . 1.384(2)    yes
C2 . H21 . 0.918    no
C3 . C4 . 1.385(2)    yes
C3 . H31 . 0.943    no
C4 . C5 . 1.3882(18)    yes
C4 . H41 . 0.934    no
C5 . C6 . 1.4773(19)    yes
C6 . C7 . 1.3878(19)    yes
C7 . C8 . 1.386(2)    yes
C7 . H71 . 0.957    no
C8 . C9 . 1.381(2)    yes
C8 . H81 . 0.953    no
C9 . C10 . 1.395(2)    yes
C9 . H91 . 0.945    no
C10 . C11 . 1.480(2)    yes
C11 . C12 . 1.394(2)    yes
C11 . C16 . 1.398(2)    yes
C12 . C13 . 1.392(2)    yes
C12 . H121 . 0.917    no
C13 . C14 . 1.388(3)    yes
C13 . H131 . 0.932    no
C14 . C15 . 1.382(3)    yes
C14 . H141 . 0.963    no
C15 . C16 . 1.390(2)    yes
C15 . H151 . 0.929    no
C16 . H161 . 0.931    no
C17 . C18 . 1.3611(19)    yes
C17 . H171 . 0.928    no
C18 . C19 . 1.4141(19)    yes
C18 . H181 . 0.919    no
C19 . C20 . 1.417(2)    yes
C19 . C24 . 1.4225(19)    yes
C20 . C21 . 1.371(2)    yes
C20 . H201 . 0.943    no
C21 . C22 . 1.398(3)    yes
C21 . H211 . 0.965    no
C22 . C23 . 1.371(2)    yes
C22 . H221 . 0.938    no
C23 . C24 . 1.4221(19)    yes
C23 . H231 . 0.957    no
C24 . C25 . 1.4357(18)    yes
C25 . C26 . 1.4667(17)    yes
C26 . C27 . 1.4045(17)    yes
C26 . C31 . 1.4211(18)    yes
C27 . C28 . 1.388(2)    yes
C27 . H271 . 0.923    no
C28 . C29 . 1.386(2)    yes
C28 . H281 . 0.945    no
C29 . C30 . 1.3904(19)    yes
C29 . H291 . 0.950    no
C30 . C31 . 1.3957(17)    yes
C30 . H301 . 0.971    no
C32 . C33 . 1.3613(19)    yes
C32 . H321 . 0.925    no
C33 . C34 . 1.4143(19)    yes
C33 . H331 . 0.947    no
C34 . C35 . 1.417(2)    yes
C34 . C39 . 1.4188(18)    yes
C35 . C36 . 1.374(2)    yes
C35 . H351 . 0.956    no
C36 . C37 . 1.403(2)    yes
C36 . H361 . 0.959    no
C37 . C38 . 1.370(2)    yes
C37 . H371 . 0.939    no
C38 . C39 . 1.4223(18)    yes
C38 . H381 . 0.920    no
C39 . C40 . 1.4388(18)    yes
C40 . C41 . 1.4707(18)    yes
C41 . C42 . 1.4009(18)    yes
C41 . C46 . 1.4215(19)    yes
C42 . C43 . 1.391(2)    yes
C42 . H421 . 0.920    no
C43 . C44 . 1.390(2)    yes
C43 . H431 . 0.943    no
C44 . C45 . 1.391(2)    yes
C44 . H441 . 0.956    no
C45 . C46 . 1.3986(18)    yes
C45 . H451 . 0.945    no
C47 . Cl1 . 1.7615(19)    yes
C47 . Cl2 . 1.7519(18)    yes
C47 . H471 . 0.975    no
C47 . H472 . 0.976    no
P1 . F1 . 1.6026(11)    yes
P1 . F2 . 1.6099(10)    yes
P1 . F3 . 1.5845(11)    yes
P1 . F4 . 1.5843(12)    yes
P1 . F5 . 1.5932(13)    yes
P1 . F6 . 1.5827(13)    yes
loop_
 _geom_angle_atom_site_label_1
 _geom_angle_site_symmetry_1
 _geom_angle_atom_site_label_2
 _geom_angle_site_symmetry_2
 _geom_angle_atom_site_label_3
 _geom_angle_site_symmetry_3
 _geom_angle
 _geom_angle_publ_flag
N1 . Ir1 . N2 . 76.33(4)    yes
N1 . Ir1 . N3 . 97.39(4)    yes
N2 . Ir1 . N3 . 84.80(4)    yes
N1 . Ir1 . N4 . 87.45(4)    yes
N2 . Ir1 . N4 . 100.65(4)    yes
N3 . Ir1 . N4 . 173.47(4)    yes
N1 . Ir1 . C31 . 176.79(5)    yes
N2 . Ir1 . C31 . 102.28(4)    yes
N3 . Ir1 . C31 . 79.56(5)    yes
N4 . Ir1 . C31 . 95.67(5)    yes
N1 . Ir1 . C46 . 95.92(5)    yes
N2 . Ir1 . C46 . 172.19(4)    yes
N3 . Ir1 . C46 . 95.36(5)    yes
N4 . Ir1 . C46 . 79.73(5)    yes
C31 . Ir1 . C46 . 85.41(5)    yes
Ir1 . N1 . C1 . 124.71(9)    yes
Ir1 . N1 . C5 . 116.21(8)    yes
C1 . N1 . C5 . 118.87(11)    yes
Ir1 . N2 . C6 . 111.49(8)    yes
Ir1 . N2 . C10 . 127.35(9)    yes
C6 . N2 . C10 . 117.94(11)    yes
Ir1 . N3 . C17 . 122.23(8)    yes
Ir1 . N3 . C25 . 117.42(8)    yes
C17 . N3 . C25 . 120.35(11)    yes
Ir1 . N4 . C32 . 122.58(9)    yes
Ir1 . N4 . C40 . 116.58(8)    yes
C32 . N4 . C40 . 120.84(11)    yes
N1 . C1 . C2 . 122.17(13)    yes
N1 . C1 . H11 . 118.9    no
C2 . C1 . H11 . 118.9    no
C1 . C2 . C3 . 118.91(13)    yes
C1 . C2 . H21 . 120.1    no
C3 . C2 . H21 . 121.0    no
C2 . C3 . C4 . 119.21(13)    yes
C2 . C3 . H31 . 120.2    no
C4 . C3 . H31 . 120.6    no
C3 . C4 . C5 . 119.16(13)    yes
C3 . C4 . H41 . 122.0    no
C5 . C4 . H41 . 118.8    no
C4 . C5 . N1 . 121.58(12)    yes
C4 . C5 . C6 . 122.77(12)    yes
N1 . C5 . C6 . 115.63(11)    yes
C5 . C6 . N2 . 115.88(11)    yes
C5 . C6 . C7 . 121.47(12)    yes
N2 . C6 . C7 . 122.65(13)    yes
C6 . C7 . C8 . 118.86(14)    yes
C6 . C7 . H71 . 119.9    no
C8 . C7 . H71 . 121.2    no
C7 . C8 . C9 . 118.77(14)    yes
C7 . C8 . H81 . 122.0    no
C9 . C8 . H81 . 119.3    no
C8 . C9 . C10 . 120.00(14)    yes
C8 . C9 . H91 . 120.4    no
C10 . C9 . H91 . 119.6    no
C9 . C10 . N2 . 121.33(13)    yes
C9 . C10 . C11 . 118.85(12)    yes
N2 . C10 . C11 . 119.74(12)    yes
C10 . C11 . C12 . 119.81(12)    yes
C10 . C11 . C16 . 120.49(13)    yes
C12 . C11 . C16 . 119.46(14)    yes
C11 . C12 . C13 . 120.23(14)    yes
C11 . C12 . H121 . 119.6    no
C13 . C12 . H121 . 120.1    no
C12 . C13 . C14 . 119.83(16)    yes
C12 . C13 . H131 . 120.6    no
C14 . C13 . H131 . 119.5    no
C13 . C14 . C15 . 120.23(16)    yes
C13 . C14 . H141 . 120.6    no
C15 . C14 . H141 . 119.1    no
C14 . C15 . C16 . 120.33(15)    yes
C14 . C15 . H151 . 119.3    no
```

bis(1-phenylpyrazole-*C*,*N*)(6-phenyl-2,2'-bipyridine-*N*,*N*')iridium(III) hexafluorophosphate (**60**)

```
C16···C15···H151···120.4····no
C11···C16···C15···119.87(16)···yes
C11···C16···H161···119.8····no
C15···C16···H161···120.3····no
N3···C17···C18···122.26(12)····yes
N3···C17···H171···117.6····no
C18···C17···H171···120.1····no
C17···C18···C19···119.42(12)···yes
C17···C18···H181···121.0····no
C19···C18···H181···119.6····no
C18···C19···C20···121.40(13)···yes
C18···C19···C24···118.70(12)···yes
C20···C19···C24···119.88(13)···yes
C19···C20···C21···120.09(15)···yes
C19···C20···H201···118.6····no
C21···C20···H201···121.3····no
C20···C21···C22···120.34(15)···yes
C20···C21···H211···120.8····no
C22···C21···H211···118.9····no
C21···C22···C23···121.01(15)···yes
C21···C22···H221···120.1····no
C23···C22···H221···118.9····no
C22···C23···C24···120.55(14)···yes
C22···C23···H231···117.5····no
C24···C23···H231···121.9····no
C19···C24···C23···117.93(12)···yes
C19···C24···C25···118.21(11)···yes
C23···C24···C25···123.80(12)···yes
C24···C25···N3···120.02(11)···yes
C24···C25···C26···127.17(11)···yes
N3···C25···C26···112.81(11)···yes
C25···C26···C27···124.75(12)···yes
C25···C26···C31···114.81(10)···yes
C27···C26···C31···120.27(11)···yes
C26···C27···C28···120.22(13)···yes
C26···C27···H271···119.8····no
C28···C27···H271···120.0····no
C27···C28···C29···119.65(12)···yes
C27···C28···H281···120.3····no
C29···C28···H281···120.1····no
C28···C29···C30···120.43(12)···yes
C28···C29···H291···118.3····no
C30···C29···H291···121.3····no
C29···C30···C31···121.47(12)···yes
C29···C30···H301···119.3····no
C31···C30···H301···119.2····no
C26···C31···C30···117.57(11)···yes
C26···C31···Ir1···114.35(8)···yes
C30···C31···Ir1···127.81(9)···yes
N4···C32···C32···122.05(12)····yes
N4···C32···H321···117.6····no
C33···C32···H321···120.4····no
C32···C33···C34···119.54(12)···yes
C32···C33···H331···119.5····no
C34···C33···H331···121.0····no
C33···C34···C35···121.39(12)···yes
C33···C34···C39···118.82(12)···yes
C35···C34···C39···119.78(12)···yes
C34···C35···C36···120.34(14)···yes
C34···C35···H351···119.8····no

C36···C35···H351···119.8····no
C35···C36···C37···119.93(14)···yes
C35···C36···H361···119.3····no
C37···C36···H361···120.7····no
C36···C37···C38···120.95(13)···yes
C36···C37···H371···120.6····no
C38···C37···H371···118.5····no
C37···C38···C39···120.66(13)···yes
C37···C38···H381···119.7····no
C39···C38···H381···119.6····no
C38···C39···C34···118.01(12)···yes
C38···C39···C40···124.00(12)···yes
C34···C39···C40···117.98(11)···yes
C39···C40···N4···119.67(11)····yes
C39···C40···C41···127.46(11)···yes
N4···C40···C41···112.74(11)····yes
C40···C41···C42···125.01(12)···yes
C40···C41···C46···114.35(11)···yes
C42···C41···C46···120.31(12)···yes
C41···C42···C43···120.43(14)···yes
C41···C42···H421···119.7····no
C43···C42···H421···119.9····no
C42···C43···C44···119.83(13)···yes
C42···C43···H431···121.1····no
C44···C43···H431···119.1····no
C43···C44···C45···120.14(13)···yes
C43···C44···H441···120.0····no
C45···C44···H441···119.9····no
C44···C45···C46···121.45(13)···yes
C44···C45···H451···119.9····no
C46···C45···H451···118.6····no
C41···C46···C45···117.96(12)···yes
C41···C46···Ir1···115.16(9)····yes
C45···C46···Ir1···126.68(10)···yes
C11···C47···C12···110.63(10)····yes
C11···C47···H471···107.4····no
C12···C47···H471···108.3····no
C11···C47···H472···107.4····no
C12···C47···H472···107.8····no
H471···C47···H472···113.8····no
F1···P1···F2···179.25(7)····yes
F1···P1···F3···89.83(7)····yes
F2···P1···F3···89.84(6)····yes
F1···P1···F4···89.87(7)····yes
F2···P1···F4···90.46(7)····yes
F3···P1···F4···179.36(9)····yes
F1···P1···F5···90.02(7)····yes
F2···P1···F5···89.30(7)····yes
F3···P1···F5···89.86(9)····yes
F4···P1···F5···89.58(10)····yes
F1···P1···F6···90.61(8)····yes
F2···P1···F6···90.06(8)····yes
F3···P1···F6···89.85(10)····yes
F4···P1···F6···90.72(10)····yes
F5···P1···F6···179.30(9)····yes
```

```
data_sg089_1_f18
_audit_creation_date·····08-09-04
_audit_creation_method·CRYSTALS_ver_12.84
·
_oxford_structure_analysis_title··'sg089_1_f18_123k_0m·in·Pbcm'
_chemical_name_systematic·····?
_chemical_melting_point·····?
·
_cell_length_a·····10.6947(3)
_cell_length_b·····16.7197(5)
_cell_length_c·····37.9704(11)
_cell_angle_alpha·····90
_cell_angle_beta·····90
_cell_angle_gamma·····90
_cell_volume·····6789.6(3)
·
_symmetry_cell_setting·····'Orthorhombic'·
_symmetry_space_group_name_H-M···'P·b·c·m·'·
_symmetry_space_group_name_Hall···'-P·2c·2b'·
loop_
·_symmetry_equiv_pos_as_xyz
·'x,y,z'
·'-x,-y,-z'
·'-x,y+1/2,z'
·'x,-y+1/2,-z'
·'x,-y+1/2,z+1/2'
·'-x,y+1/2,-z+1/2'
·'-x,-y,z+1/2'
·'x,y,-z+1/2'
·
loop_
·_atom_type_symbol
·_atom_type_scat_dispersion_real
·_atom_type_scat_dispersion_imag
·_atom_type_scat_Cromer_Mann_a1
·_atom_type_scat_Cromer_Mann_b1
·_atom_type_scat_Cromer_Mann_a2
·_atom_type_scat_Cromer_Mann_b2
·_atom_type_scat_Cromer_Mann_a3
·_atom_type_scat_Cromer_Mann_b3
·_atom_type_scat_Cromer_Mann_a4
·_atom_type_scat_Cromer_Mann_b4
·_atom_type_scat_Cromer_Mann_c
·_atom_type_scat_source··
·'C'·····0.0033···0.0016···2.3100···20.8439···1.0200···10.2075···1.5886···0.5687
···0.8650···51.6512···0.2156·'International·Tables·Vol·C·4.2.6.8·and·6.1.1.4'
·'H'·····0.0000···0.0000···0.0000···0.4930···10.5109···0.3229···26.1257···0.1402···3.1424
···0.0408···57.7998···0.0030·'International·Tables·Vol·C·4.2.6.8·and·6.1.1.4'
·'N'·····0.0061···0.0033···12.2126···0.0057···3.1322···9.8933···2.0125···28.9975
···1.1663···0.5826···11.5290·'International·Tables·Vol·C·4.2.6.8·and·6.1.1.4'
·'Ir'····-1.4442···7.9887···27.3049···1.5928···16.7296···8.8655···15.6115···0.4179
···5.8338···45.0011···11.4722·'International·Tables·Vol·C·4.2.6.8·and·6.1.1.4'
·'O'·····0.0106···0.0060···3.0485···13.2771···2.2868···5.7011···1.5463···0.3239
···0.8670···32.9089···0.2508·'International·Tables·Vol·C·4.2.6.8·and·6.1.1.4'

·
·
_cell_formula_units_Z·····4
·
#·Given·Formula:·=C70·H56·C12·F12·Ir2·N12·O0.25·P2·
#·Do:·=·····1.78·Fooo=···3512.00·Mu=·····41.29·M=····907.28
#·Found·Formula:·=C69·H54·C12·F12·Ir2·N12·P2·
#·Do:·=·····1.76·FOOO=···3512.00·Mu=·····41.27·M=····898.27

_chemical_formula_sum·····'C69·H54·C12·F12·Ir2·N12·P2'
_chemical_formula_moiety·····'2(C34·H26·Ir·N6),·C·H2·Cl2,·2(F6·P)'
_chemical_compound_source·····?
_chemical_formula_weight·····1796.54
·
·
_cell_measurement_reflns_used·····0
_cell_measurement_theta_min·····0
_cell_measurement_theta_max·····0
_cell_measurement_temperature·····123
·
_exptl_crystal_description·····'needle'·
_exptl_crystal_colour·····'yellow'·
_exptl_crystal_size_min·····0.08·
_exptl_crystal_size_mid·····0.16·
_exptl_crystal_size_max·····0.48·
·
_exptl_crystal_density_diffrn····1.757·
_exptl_crystal_density_meas·····?·
#·Non-dispersive·F(000)::·
_exptl_crystal_F_000·····3512·
_exptl_absorpt_coefficient_mu····4.127·
·
#·Sheldrick·geometric·approximatio·0.52·0.72·
_exptl_absorpt_correction_type····multi-scan·
_exptl_absorpt_process_details····'DENZO/SCALEPACK·(Otwinowski·&·Minor,·1997)'·
_exptl_absorpt_correction_T_min···0.52·
_exptl_absorpt_correction_T_max···0.72·
#·For·a·Kappa·CCD,·set·Tmin·to·1.0·and·
#·Tmax·to·the·ratio·of·maxmin·frame·scales·in·scale_all.log·
_diffrn_measurement_device_type····'Nonius·KappaCCD'·
_diffrn_radiation_monochromator····'graphite'·
_diffrn_radiation_type·····'Mo·Ka'·
_diffrn_radiation_wavelength·····0.71073
_diffrn_measurement_method·····'\f-s·\w·scans'·
·
#·If·a·reference·occurs·more·than·once,·delete·the·author·
#·and·date·from·subsequent·references.·
_computing_data_collection·····'COLLECT·(Nonius,·1997-2001).'·
_computing_cell_refinement·····'DENZO/SCALEPACK·(Otwinowski·&·Minor,·1997)'·
_computing_data_reduction·····'DENZO/SCALEPACK·(Otwinowski·&·Minor,·1997)'·
_computing_structure_solution····'SIR92·(Altomare·et·al.,·1994)'·
_computing_structure_refinement····'CRYSTALS·(Betteridge·et·al.,·2003)'·
_computing_publication_material····'CRYSTALS·(Betteridge·et·al.,·2003)'·
_computing_molecular_graphics·····'CAMERON·(Watkin·et·al.,·1996)'·
·
_diffrn_standards_interval_time···?·
_diffrn_standards_interval_count··?·
_diffrn_standards_number·····0·
_diffrn_standards_decay_%·····?·
·
```

```
_diffrn_ambient_temperature·····123
_diffrn_reflns_number·····121701·
_reflns_number_total·····15334·
_diffrn_reflns_av_R_equivalents···0.041·
#·Number·of·reflections·with·Friedels·Law·is·15334·
#·Number·of·reflections·without·Friedels·Law·is·0·
#·Theoretical·number·of·reflections·is·about·15655·
·
·
_diffrn_reflns_theta_min·····2.145·
_diffrn_reflns_theta_max·····35.625·
_diffrn_measured_fraction_theta_max·0.967·
·
_diffrn_reflns_theta_full·····30.281·
_diffrn_measured_fraction_theta_full·0.995·
·
·
_diffrn_reflns_limit_h_min·····-16·
_diffrn_reflns_limit_h_max·····17·
_diffrn_reflns_limit_k_min·····-27·
_diffrn_reflns_limit_k_max·····25·
_diffrn_reflns_limit_l_min·····-60·
_diffrn_reflns_limit_l_max·····48·
_refine_limit_h_min·····-9·
_refine_limit_h_max·····17·
_refine_limit_k_min·····0·
_refine_limit_k_max·····27·
_refine_limit_l_min·····-0·
_refine_limit_l_max·····60·
·
_oxford_diffrn_Wilson_B_factor···0.00·
_oxford_diffrn_Wilson_scale·····0.00·
·
_atom_sites_solution_primary·····direct·#heavy,direct,difmap,geom
#·_atom_sites_solution_secondary···difmap
_atom_sites_solution_hydrogens···geom
·
_refine_diff_density_min·····-3.16·
_refine_diff_density_max·····1.95·
·
·
_refine_ls_number_reflns·····8630·
_refine_ls_number_restraints·····26·
_refine_ls_number_parameters·····474·
·
#_refine_ls_R_factor_ref·0.0285·
_refine_ls_wR_factor_ref·····0.0278·
_refine_ls_goodness_of_fit_ref···1.0662·
·
#_reflns_number_all·15315·
_refine_ls_R_factor_all·····0.0660·
_refine_ls_wR_factor_all·····0.0365·
·
#·The·I/u(I)·cutoff·below·was·used·for·refinement.·as·
#·well·as·the·_gt·R-factors:·
_refins_threshold_expression·····I>3.0\s(I)
_reflns_number_gt·····8630·
_refine_ls_R_factor_gt·····0.0285·
_refine_ls_wR_factor_gt·····0.0278·
·

_refine_ls_shift/su_max·····0.007378·
·
_choose·from:·rm·(reference·molecule·of·known·chirality),·
#·ad·(anomolous·dispersion···Flack),·rmad·(rm·and·ad),·
#·syn·(from·synthesis),·unk·(unknown)·or··(not·applicable)·
_chemical_absolute_configuration·'·'·
·
·
_refine_ls_structure_factor_coef·'F'·
_refine_ls_matrix_type·····full
_refine_ls_hydrogen_treatment·····constr·····#·none,·undef,·noref,·refall,
·····#·refxyz,·refU,·constr·or·mixed
_refine_ls_weighting_scheme·····calc·
_refine_ls_weighting_details·
;
·Method,·part·1,·Chebychev·polynomial,·(Watkin,·1994,·Prince,·1982)·
·[weight]·=·1.0/[A~0~*T~0~(x)+A~1~*T~1~(x)·····+A~n-1~*T~n-1~(x)]·
·where·A~i~·are·the·Chebychev·coefficients·listed·below·and·x=·Fcalc/Fmax·
·Method·=·Robust·Weighting·(Prince,·1982)·
·W·=·[weight]·*·[1-(deltaF/6*sigmaF)^2^]^2^·
·A~i~·are:·
·1.41·-0.662·1.40·-0.214·0.345·
;
·
·
·
·
#·Check·this·file·using·the·IUCr·facility·at:·
#·http://checkcif.iucr.org/·
·
#·The·content·below·is·held·in·the·file·'script/refcif.dat'.·This·is·a·text·
#·file·which·you·may·edit·to·reflect·local·conditions.·
#·Items·which·need·looking·at·are·represented·by·a·'?'.·
#·Items·for·which·there·are·choices·are·prefixed·with·'choose·from'.·
·
_publ_contact_letter·
;·
·Please·consider·this·CIF·submission·for·
·publication·as·a·Short·Format·Paper·in·Acta·
·Crystallographica·E.·The·figures·will·be·
·sent·by·e-mail.·
;·
_publ_contact_author_name·····'Anthony·Other'·
_publ_contact_author_address·
;·
·Chemical·Crystallography·Laboratory,·
·Department·of·Chemistry,·
·University·of·Nowhere,·
·Nowhere,·NO1·4T,·UK.·
;·
·
_publ_contact_author_phone·····'+44·1865·000000'·
_publ_contact_author_fax·····'+44·1865·000000'·
_publ_contact_author_email·····'a.n.other@chem.no.ac.uk'·
_publ_requested_journal·····'Section·E'·
_publ_requested_category·····EO·#·choose·from:·FI·FM·FO·CI·CM·CO·AD·
_publ_requested_coeditor_name····'Prof·William·Clegg'·
·
_publ_section_title·
#·Title·of·paper···generally·just·the·systematic·or·trivial·name·
;·?·

;·
·
#·The·loop·structure·below·should·contain·the·names·and·addresses·of·all·
#·authors,·in·the·required·order·of·publication.·Repeat·as·necessary.·
loop_·
·_publ_author_name·
·_publ_author_address·
·_publ_author_footnote·
'Other,·Anthony·N.'·#·Author·1·
;·
·?·#·Address·for·author·1·
;·
;·
·?·#·Footnote·for·author·1·
;·
'Else,·S.·O.'·#·Author·2·
;·
·?·#·Address·2·
;·
·
;·?·#·Footnote·2·
;·
·
·
_publ_section_abstract·
#·Text·of·the·abstract·
#·(a)·The·Abstract·must·be·self-contained·and·comprehensible·
#·without·the·rest·of·the·paper.·This·means·no·references·
#·to·atom·names·or·to·compound·numbers;·compounds·must·be·
#·identified·as·the·title·compound,·or·by·name·or·by·some·other·
#·means·such·as·derivatives·of·each·other·(e.g.·"the·
#·corresponding·ketone").·
#·(b)·The·chemical·formula·of·"the·title·compound"·must·be·given.·
#·(c)·Any·crystallographic·molecular·symmetry·should·be·
#·mentioned,·and·also·the·presence·of·more·than·one·molecule·
#·in·the·asymmetric·unit·(i.e.·anything·other·than·Z'=1).·
;·
·?·
;·
_publ_section_comment·
#·Text·of·the·paper·
#·Note·that·atoms·are·referenced·as·N2,·not·N(2)·or·N·2·
#·Text·containing·()·occur·within·(),·the·outer·ones·should·be·[].·
#·Figures·should·be·referenced·as·Fih.·
;·
·?·
;·
·
_publ_section_acknowledgements····#·Acknowledgments·
;·
·?·
;·
_publ_section_figure_captions·
#·Captions·to·figures···Start·each·caption·on·a·new·line·after·a·blank·line·
;·
Fig.·1.·
The·title·compound·with·displacement·ellipsoids·drawn·at·the·50%·
probability·level.·H·atoms·are·shown·as·spheres·of·
arbitary·radius.·
·
;·
```

```
·
_publ_section_exptl_refinement·
#·Some·potentially·useful·phrases·are·donated·by·Bill·Clegg:·
·
In·the·absence·of·significant·anomalous·scattering,·Friedel·pairs·were·
merged.·
·
The·absolute·configuration·was·arbitrarily·assigned.·
·
The·relatively·large·ratio·of·minimum·to·maximum·corrections·applied·
in·the·multiscan·process·(1:nnn)·reflect·changes·in·the·illuminated·
volume·of·the·crystal.·
·
Changes·in·illuminated·volume·were·kept·to·a·minimum,·and·were·
taken·into·account·(G\"orbitz,·1999)·by·the·multi-scan·inter-frame·
scaling·(DENZO/SCALEPACK,·Otwinowski·&·Minor,·1997).·
·
·
·
The·H·atoms·were·all·located·in·a·difference·map,·but·those·
attached·to·carbon·atoms·were·repositioned·geometrically.·
The·H·atoms·were·initially·refined·with·soft·restraints·on·the·
bond·lengths·and·angles·to·regularise·their·geometry·
(C---H·in·the·range·0.93--0.98,·
N---H·in·the·range·0.86--0.89,·
N---H·to·0.86·
O---H·=·0.82·
\%A)·
and·
U-iso·(H)·(in·the·range·1.2-1.5·times·U-eq·of·the·parent·atom),·
after·which·the·positions·were·refined·with·riding·constraints.·
·
·
·
_publ_section_exptl_prep·
#·Brief·details·or·a·reference.·Include·solvent·if·known.·
·
·
·
·
·
·
#·PROCESSING·SUMMARY·(IUCr·Office·Use·Only):·
_journal_date_recd_electronic·····?·
_journal_date_to_coeditor·····?·
_journal_date_from_coeditor·····?·
_journal_date_accepted·····?·
_journal_date_printers_first·····?·
_journal_date_printers_final·····?·
_journal_date_proofs_out·····?·
_journal_date_proofs_in·····?·
_journal_coeditor_name·····?·
_journal_coeditor_code·····?·
_journal_coeditor_notes·····?·
_journal_techeditor_code·····?·
_journal_techeditor_notes·····?·
_journal_coden_ASTM·····?·
·
·
·
_journal_name_full·····?·
_journal_year·····?·
_journal_volume·····?·
_journal_issue·····?·
_journal_page_first·····?·
_journal_page_last·····?·
_journal_suppl_publ_number·····?·
_journal_suppl_publ_pages·····?·
·
#·End·of·'script/refcif.dat'·
·
·
·
#·Insert·your·own·references·if·required·-·in·alphabetical·order·
_publ_section_references·
;·
Altomare,·A.,·Cascarano,·G.,·Giacovazzo,·C.,·Guagliardi,·A.,·Burla,·M.C.,·
Polidori,·G.·&·Camalli,·M.·(1994).·J.·Appl.·Cryst.·27,·435.·
·
Betteridge,·P.W.,·Carruthers,·J.R.,·Cooper,·R.I.,·
Prout,·K.·&·Watkin,·D.J.·(2003).·J.·Appl.·Cryst.·36,·1487.·
·
Larson,·A.C.·(1970).·Crystallographic·Computing,·Ed·Ahmed,·F.R.,·
Munksgaard,·Copenhagen,·291-294.·
·
Nonius·(1997-2001).·COLLECT.·Nonius·BV,·Delft,·The·Netherlands.·
·
Otwinowski,·Z.·&·Minor,·W.·(1997).·Methods·in·Enzymology,·Vol.·276,·
edited·by·C.·W.·Carter·Jr·&·R.·M.·Sweet,·pp.·307--326.·
New·York:·Academic·Press.·
·
Prince,·E.·
Mathematical·Techniques·in·Crystallography·
and·Materials·Science·
Springer-Verlag,·New·York,·1982.·
·
Watkin·D.J.·(1994).·
Acta·Cryst.·A50,·411-437.·
·
Watkin,·D.J.,·Prout,·C.K.·&·Pearce,·L.J.·(1996).·CAMERON,·Chemical·
Crystallography·Laboratory,·Oxford,·UK.·
·
·

#·Uequiv·=·arithmetic·mean·of·Ui·i.e.·Ueqiv·=·(U1+U2+U3)/3·
·
·
#·Replace·last·'.'·with·number·of·unfound·hydrogen·atomsattached·to·an·atom.·
·
#·___·refinement_flags_···.·
#·.·no·refinement·constraints·····S·special·position·constraint·on·site·
#·G·rigid·group·refinement·of·site·····R·riding·atom·
#·D·distance·or·angle·restraint·on·site·T·thermal·displacement·constraints·
#·U·Uiso·or·Uij·restraint·(rigid·bond)···P·partial·occupancy·constraint·
·
·
loop_·
_atom_site_label·
_atom_site_type_symbol·
_atom_site_fract_x·
_atom_site_fract_y·
_atom_site_fract_z·
·
·
_atom_site_U_iso_or_equiv·
_atom_site_occupancy·
_atom_site_adp_type·
_atom_site_refinement_flags_posn·
_atom_site_refinement_flags_adp·
_atom_site_refinement_flags_occupancy·
_atom_site_disorder_assembly·
_atom_site_disorder_group·
_atom_site_attached_hydrogens·
Ir1·Ir·0.578630(10)·0.523984(6)·0.605031(3)·0.0146·1.0000·Uani·.·.·.·.·.·.·.·.·.·
N1·N·0.4437(2)·0.60524(15)·0.58517(7)·0.0172·1.0000·Uani·.·.·.·.·.·.·.·.·.·.·.·
N2·N·0.6242(2)·0.63766(15)·0.63119(7)·0.0177·1.0000·Uani·.·.·.·.·.·.·.·.·.·.·.·
N3·N·0.4619(3)·0.50111(16)·0.64575(7)·0.0193·1.0000·Uani·.·.·.·.·.·.·.·.·.·.·.·
N4·N·0.3811(3)·0.43953(17)·0.64015(8)·0.0234·1.0000·Uani·.·.·.·.·.·.·.·.·.·.·.·
N5·N·0.6969(2)·0.52827(17)·0.56386(7)·0.0196·1.0000·Uani·.·.·.·.·.·.·.·.·.·.·.·
N6·N·0.7928(2)·0.47478(19)·0.56535(7)·0.0209·1.0000·Uani·.·.·.·.·.·.·.·.·.·.·.·
C1·C·0.3709(3)·0.59318(19)·0.55694(9)·0.0215·1.0000·Uani·.·.·.·.·.·.·.·.·.·.·.·
C2·C·0.2804(3)·0.6478(2)·0.54684(10)·0.0253·1.0000·Uani·.·.·.·.·.·.·.·.·.·.·.·
C3·C·0.2628(3)·0.7160(2)·0.56664(10)·0.0262·1.0000·Uani·.·.·.·.·.·.·.·.·.·.·.·
C4·C·0.3381(3)·0.72915(19)·0.59599(10)·0.0225·1.0000·Uani·.·.·.·.·.·.·.·.·.·.·.·
C5·C·0.4285(3)·0.67266(15)·0.60442(9)·0.0178·1.0000·Uani·.·.·.·.·.·.·.·.·.·.·.·
C6·C·0.5204(3)·0.68362(18)·0.63322(9)·0.0190·1.0000·Uani·.·.·.·.·.·.·.·.·.·.·.·
C7·C·0.5005(4)·0.73812(19)·0.66044(10)·0.0252·1.0000·Uani·.·.·.·.·.·.·.·.·.·.·.·
C8·C·0.5916(4)·0.7452(2)·0.68619(10)·0.0298·1.0000·Uani·.·.·.·.·.·.·.·.·.·.·.·
C9·C·0.7024(4)·0.7038(2)·0.68247(11)·0.0293·1.0000·Uani·.·.·.·.·.·.·.·.·.·.·.·
C10·C·0.7187(3)·0.6522(2)·0.65391(9)·0.0224·1.0000·Uani·.·.·.·.·.·.·.·.·.·.·.·
C11·C·0.8425(3)·0.6168(2)·0.64649(10)·0.0245·1.0000·Uani·.·.·.·.·.·.·.·.·.·.·.·
C12·C·0.9137(4)·0.5814(3)·0.67330(11)·0.0375·1.0000·Uani·.·.·.·.·.·.·.·.·.·.·.·
C13·C·1.0318(4)·0.5527(4)·0.66599(14)·0.0485·1.0000·Uani·.·.·.·.·.·.·.·.·.·.·.·
C14·C·1.0807(4)·0.5606(3)·0.63269(14)·0.0448·1.0000·Uani·.·.·.·.·.·.·.·.·.·.·.·
C15·C·1.0124(3)·0.5966(3)·0.60610(13)·0.0350·1.0000·Uani·.·.·.·.·.·.·.·.·.·.·.·
C16·C·0.8921(3)·0.6239(2)·0.61309(10)·0.0261·1.0000·Uani·.·.·.·.·.·.·.·.·.·.·.·
C17·C·0.4399(3)·0.5264(2)·0.67829(9)·0.0259·1.0000·Uani·.·.·.·.·.·.·.·.·.·.·.·
C18·C·0.3454(4)·0.4823(3)·0.69388(11)·0.0342·1.0000·Uani·.·.·.·.·.·.·.·.·.·.·.·
C19·C·0.3097(3)·0.4278(2)·0.66914(11)·0.0304·1.0000·Uani·.·.·.·.·.·.·.·.·.·.·.·
C20·C·0.3930(3)·0.39901(18)·0.60755(10)·0.0234·1.0000·Uani·.·.·.·.·.·.·.·.·.·.·.·
C21·C·0.3138(4)·0.3366(2)·0.59856(12)·0.0364·1.0000·Uani·.·.·.·.·.·.·.·.·.·.·.·
C22·C·0.3320(5)·0.2989(2)·0.56671(12)·0.0422·1.0000·Uani·.·.·.·.·.·.·.·.·.·.·.·
C23·C·0.4275(5)·0.3238(2)·0.54473(11)·0.0393·1.0000·Uani·.·.·.·.·.·.·.·.·.·.·.·
C24·C·0.5061(4)·0.3867(2)·0.55418(10)·0.0278·1.0000·Uani·.·.·.·.·.·.·.·.·.·.·.·
C25·C·0.4906(3)·0.42712(18)·0.58610(8)·0.0197·1.0000·Uani·.·.·.·.·.·.·.·.·.·.·.·
C26·C·0.7010(4)·0.5616(2)·0.53195(9)·0.0259·1.0000·Uani·.·.·.·.·.·.·.·.·.·.·.·
C27·C·0.8000(4)·0.5295(3)·0.51281(9)·0.0314·1.0000·Uani·.·.·.·.·.·.·.·.·.·.·.·
C28·C·0.8560(3)·0.4747(3)·0.53451(10)·0.0274·1.0000·Uani·.·.·.·.·.·.·.·.·.·.·.·
C29·C·0.8067(3)·0.43224(19)·0.59744(8)·0.0189·1.0000·Uani·.·.·.·.·.·.·.·.·.·.·.·
C30·C·0.9066(3)·0.3807(2)·0.60349(11)·0.0263·1.0000·Uani·.·.·.·.·.·.·.·.·.·.·.·
C31·C·0.9137(4)·0.3427(2)·0.63593(10)·0.0278·1.0000·Uani·.·.·.·.·.·.·.·.·.·.·.·
C32·C·0.8242(4)·0.3576(2)·0.66138(10)·0.0268·1.0000·Uani·.·.·.·.·.·.·.·.·.·.·.·
C33·C·0.7245(3)·0.40974(19)·0.65470(9)·0.0207·1.0000·Uani·.·.·.·.·.·.·.·.·.·.·.·
C34·C·0.7132(3)·0.44932(18)·0.62240(8)·0.0177·1.0000·Uani·.·.·.·.·.·.·.·.·.·.·.·
C35·C·0.7401(10)·0.4523(6)·0.750000(10)·0.0500·0.8000·Uani·D·TU·.·.·.·.·.·.·.·.·
P1·P·0.09125(12)·0.34020(8)·0.7500·0.0227·1.0000·Uani·S·T·.·.·.·.·.·.·.·.·.·.·.·
P2·P·0.04257(12)·0.2500·0.5000·0.0253·1.0000·Uani·S·T·.·.·.·.·.·.·.·.·.·.·.·.·
F1·F·-0.0576(3)·0.3398(3)·0.7500·0.0445·1.0000·Uani·S·T·.·.·.·.·.·.·.·.·.·.·.·
F2·F·0.2407(3)·0.3396(2)·0.7500·0.0361·1.0000·Uani·S·T·.·.·.·.·.·.·.·.·.·.·.·
F3·F·0.0918(5)·0.4355(2)·0.7500·0.0500·1.0000·Uani·S·T·.·.·.·.·.·.·.·.·.·.·.·
F4·F·0.0925(4)·0.2447(2)·0.7500·0.0394·1.0000·Uani·S·T·.·.·.·.·.·.·.·.·.·.·.·
F5·F·0.0914(2)·0.33996(17)·0.70794(6)·0.0365·1.0000·Uani·.·.·.·.·.·.·.·.·.·.·.·
F6·F·-0.1053(4)·0.2500·0.5000·0.0925·1.0000·Uani·S·T·.·.·.·.·.·.·.·.·.·.·.·.·
F7·F·0.0450(4)·0.3234(2)·0.52658(10)·0.0768·1.0000·Uani·.·.·.·.·.·.·.·.·.·.·.·
F8·F·0.1892(3)·0.2500·0.5000·0.0574·1.0000·Uani·S·T·.·.·.·.·.·.·.·.·.·.·.·.·
F9·F·0.0430(3)·0.1919(2)·0.53288(9)·0.0572·1.0000·Uani·.·.·.·.·.·.·.·.·.·.·.·
C13·C1·0.6223(17)·0.1731(8)·0.7500·0.0952·0.2000·Uani·DS·TU·.·.·.·.·.·.·.·.·.·
C11·C1·0.6288(3)·0.37643(19)·0.7500·0.0834·1.0000·Uani·DS·TU·.·.·.·.·.·.·.·.·.·
C12·C1·0.6734(3)·0.54885(17)·0.7500·0.0592·0.8000·Uani·DS·TU·.·.·.·.·.·.·.·.·.·
H11·H·0.3823·0.5463·0.5437·0.0267·1.0000·Uiso·R·.·.·.·.·.·.·.·.·.·.·.·.·.·.·.·
H21·H·0.2312·0.6391·0.5269·0.0311·1.0000·Uiso·R·.·.·.·.·.·.·.·.·.·.·.·.·.·.·.·
H31·H·0.2017·0.7524·0.5602·0.0331·1.0000·Uiso·R·.·.·.·.·.·.·.·.·.·.·.·.·.·.·.·
H41·H·0.3286·0.7751·0.6099·0.0280·1.0000·Uiso·R·.·.·.·.·.·.·.·.·.·.·.·.·.·.·.·
H71·H·0.4279·0.7693·0.6608·0.0320·1.0000·Uiso·R·.·.·.·.·.·.·.·.·.·.·.·.·.·.·.·
H81·H·0.5786·0.7778·0.7058·0.0372·1.0000·Uiso·R·.·.·.·.·.·.·.·.·.·.·.·.·.·.·.·
H91·H·0.7665·0.7098·0.6988·0.0361·1.0000·Uiso·R·.·.·.·.·.·.·.·.·.·.·.·.·.·.·.·
H121·H·0.8807·0.5772·0.6961·0.0461·1.0000·Uiso·R·.·.·.·.·.·.·.·.·.·.·.·.·.·.·.·
H131·H·1.0786·0.5280·0.6836·0.0582·1.0000·Uiso·R·.·.·.·.·.·.·.·.·.·.·.·.·.·.·.·
H141·H·1.1608·0.5415·0.6282·0.0552·1.0000·Uiso·R·.·.·.·.·.·.·.·.·.·.·.·.·.·.·.·
H151·H·1.0459·0.6021·0.5835·0.0439·1.0000·Uiso·R·.·.·.·.·.·.·.·.·.·.·.·.·.·.·.·
H161·H·0.8448·0.6474·0.5952·0.0320·1.0000·Uiso·R·.·.·.·.·.·.·.·.·.·.·.·.·.·.·.·
H181·H·0.4832·0.5683·0.6888·0.0321·1.0000·Uiso·R·.·.·.·.·.·.·.·.·.·.·.·.·.·.·.·
H181·H·0.3130·0.4883·0.7163·0.0430·1.0000·Uiso·R·.·.·.·.·.·.·.·.·.·.·.·.·.·.·.·
H191·H·0.2472·0.3890·0.6713·0.0373·1.0000·Uiso·R·.·.·.·.·.·.·.·.·.·.·.·.·.·.·.·
H211·H·0.2496·0.3207·0.6136·0.0442·1.0000·Uiso·R·.·.·.·.·.·.·.·.·.·.·.·.·.·.·.·
H221·H·0.2801·0.2563·0.5601·0.0520·1.0000·Uiso·R·.·.·.·.·.·.·.·.·.·.·.·.·.·.·.·
H231·H·0.4399·0.2984·0.5229·0.0473·1.0000·Uiso·R·.·.·.·.·.·.·.·.·.·.·.·.·.·.·.·
H241·H·0.5703·0.4017·0.5388·0.0349·1.0000·Uiso·R·.·.·.·.·.·.·.·.·.·.·.·.·.·.·.·
H261·H·0.6450·0.6002·0.5238·0.0321·1.0000·Uiso·R·.·.·.·.·.·.·.·.·.·.·.·.·.·.·.·
H271·H·0.8238·0.5429·0.4900·0.0380·1.0000·Uiso·R·.·.·.·.·.·.·.·.·.·.·.·.·.·.·.·
H281·H·0.9245·0.4428·0.5294·0.0342·1.0000·Uiso·R·.·.·.·.·.·.·.·.·.·.·.·.·.·.·.·
H301·H·0.9662·0.3726·0.5861·0.0330·1.0000·Uiso·R·.·.·.·.·.·.·.·.·.·.·.·.·.·.·.·
H311·H·0.9787·0.3067·0.6407·0.0351·1.0000·Uiso·R·.·.·.·.·.·.·.·.·.·.·.·.·.·.·.·
H321·H·0.8301·0.3326·0.6832·0.0329·1.0000·Uiso·R·.·.·.·.·.·.·.·.·.·.·.·.·.·.·.·
H331·H·0.6644·0.4192·0.6723·0.0248·1.0000·Uiso·R·.·.·.·.·.·.·.·.·.·.·.·.·.·.·.·
H351·H·0.7912·0.4468·0.7706·0.0782·0.8000·Uiso·R·.·.·.·.·.·.·.·.·.·.·.·.·.·.·.·
C36·C·0.689(2)·0.2739(7)·0.750000(10)·0.1025·0.2000·Uani·DS·TU·.·.·.·.·.·.·.·.·.·
H361·H·0.7412·0.2731·0.7706·0.1212·0.2000·Uiso·R·.·.·.·.·.·.·.·.·.·.·.·.·.·.·.·
loop_·
_atom_site_aniso_label·
_atom_site_aniso_U_11·
_atom_site_aniso_U_22·
_atom_site_aniso_U_33·
_atom_site_aniso_U_23·
_atom_site_aniso_U_13·
_atom_site_aniso_U_12·
Ir1·0.01470(4)·0.01285(4)·0.01618(4)·-0.00100(4)·-0.00238(4)·0.00046(4)·
N1·0.0174(12)·0.0139(10)·0.0203(11)·-0.0012(8)·-0.0040(9)·0.0010(8)·
N2·0.0162(11)·0.0149(10)·0.0220(12)·-0.0009(9)·-0.0041(9)·-0.0019(9)·
N3·0.0188(10)·0.0166(9)·0.0226(12)·0.0013(9)·-0.0007(10)·-0.0015(9)·
N4·0.0195(11)·0.0221(11)·0.0291(14)·0.0032(11)·0.0011(11)·-0.0027(10)·
N5·0.0220(11)·0.0180(11)·0.0188(10)·0.0005(10)·-0.0005(9)·0.0012(11)·
N6·0.0198(11)·0.0217(11)·0.0213(11)·-0.0020(11)·0.0017(9)·0.0002(12)·
C1·0.0230(14)·0.0176(13)·0.0240(14)·0.0008(11)·-0.0072(12)·0.0022(11)·
C2·0.0223(14)·0.0207(15)·0.0283(15)·0.0013(13)·-0.0087(13)·0.0055(13)·
C3·0.0233(15)·0.0211(14)·0.0341(17)·0.0011(12)·-0.0071(14)·0.0072(12)·
C4·0.0198(14)·0.0169(13)·0.0309(16)·-0.0002(11)·-0.0021(11)·0.0048(11)·
C5·0.0153(12)·0.0152(12)·0.0229(12)·-0.0006(10)·0.0004(14)·-0.0006(10)·
C6·0.0192(14)·0.0138(11)·0.0240(14)·-0.0005(10)·-0.0023(11)·-0.0021(10)·
C7·0.0287(15)·0.0163(15)·0.0306(16)·-0.0054(11)·-0.0011(14)·0.0003(13)·
C8·0.0268(19)·0.0232(14)·0.0294(15)·-0.0094(12)·-0.0063(16)·-0.0026(15)·
C9·0.0312(18)·0.0248(15)·0.0319(17)·-0.0057(14)·-0.0111(15)·-0.0053(13)·
C10·0.0212(14)·0.0179(13)·0.0281(15)·-0.0004(11)·-0.0076(12)·-0.0039(11)·
C11·0.0195(14)·0.0208(14)·0.0331(17)·0.0005(12)·-0.0074(13)·-0.0066(12)·
·
·
·
_journal_name_full·····?·
_journal_year·····?·
_journal_volume·····?·
_journal_issue·····?·
_journal_page_first·····?·
_journal_page_last·····?·
_journal_suppl_publ_number·····?·
_journal_suppl_publ_pages·····?·
·
#·End·of·'script/refcif.dat'·
·
·
·
#·Insert·your·own·references·if·required·-·in·alphabetical·order·
_publ_section_references·
;·
Altomare,·A.,·Cascarano,·G.,·Giacovazzo,·C.,·Guagliardi,·A.,·Burla,·M.C.,·
Polidori,·G.·&·Camalli,·M.·(1994).·J.·Appl.·Cryst.·27,·435.·
·
Betteridge,·P.W.,·Carruthers,·J.R.,·Cooper,·R.I.,·
Prout,·K.·&·Watkin,·D.J.·(2003).·J.·Appl.·Cryst.·36,·1487.·
·
Larson,·A.C.·(1970).·Crystallographic·Computing,·Ed·Ahmed,·F.R.,·
Munksgaard,·Copenhagen,·291-294.·
·
Nonius·(1997-2001).·COLLECT.·Nonius·BV,·Delft,·The·Netherlands.·
·
Otwinowski,·Z.·&·Minor,·W.·(1997).·Methods·in·Enzymology,·Vol.·276,·
edited·by·C.·W.·Carter·Jr·&·R.·M.·Sweet,·pp.·307--326.·
New·York:·Academic·Press.·
·
Prince,·E.·
Mathematical·Techniques·in·Crystallography·
and·Materials·Science·
Springer-Verlag,·New·York,·1982.·
·
Watkin·D.J.·(1994).·
Acta·Cryst.·A50,·411-437.·
·
Watkin,·D.J.,·Prout,·C.K.·&·Pearce,·L.J.·(1996).·CAMERON,·Chemical·
Crystallography·Laboratory,·Oxford,·UK.·
·
·

#·Uequiv·=·arithmetic·mean·of·Ui·i.e.·Ueqiv·=·(U1+U2+U3)/3·
·
·
#·Replace·last·'.'·with·number·of·unfound·hydrogen·atomsattached·to·an·atom.·
·
#·___·refinement_flags_···.·
#·.·no·refinement·constraints·····S·special·position·constraint·on·site·
#·G·rigid·group·refinement·of·site·····R·riding·atom·
#·D·distance·or·angle·restraint·on·site·T·thermal·displacement·constraints·
#·U·Uiso·or·Uij·restraint·(rigid·bond)···P·partial·occupancy·constraint·
·
·
loop_·
_atom_site_label·
_atom_site_type_symbol·
_atom_site_fract_x·
_atom_site_fract_y·
_atom_site_fract_z·
·
·
_atom_site_U_iso_or_equiv·
_atom_site_occupancy·
_atom_site_adp_type·
_atom_site_refinement_flags_posn·
_atom_site_refinement_flags_adp·
_atom_site_refinement_flags_occupancy·
_atom_site_disorder_assembly·
_atom_site_disorder_group·
_atom_site_attached_hydrogens·
C12·C·0.0272(17)·0.051(2)·0.0341(18)·0.0098(17)·-0.0076(17)·-0.0004(19)·
C13·C·0.0250(19)·0.071(3)·0.050(3)·0.021(2)·-0.0103(18)·0.008(2)·
C14·C·0.0209(16)·0.059(2)·0.058(3)·0.014(2)·-0.006(2)·0.006(2)·
C15·C·0.0210(14)·0.0401(19)·0.044(2)·0.008(2)·0.0034(17)·-0.0021(14)·
C16·C·0.0185(13)·0.0218(14)·0.0379(19)·0.0052(13)·-0.0050(12)·-0.0037(11)·
C17·C·0.0238(15)·0.0304(15)·0.0236(13)·-0.0004(13)·0.0046(11)·-0.0037(15)·
C18·C·0.040(2)·0.0321(18)·0.0301(17)·0.0056(16)·0.0103(15)·0.0042(18)·
C19·C·0.0222(15)·0.0296(17)·0.039(2)·0.0105(15)·0.0101(14)·0.0014(14)·
C20·C·0.0223(13)·0.0166(11)·0.0313(16)·0.0010(12)·-0.0110(13)·-0.0018(10)·
C21·C·0.035(2)·0.0282(18)·0.046(2)·-0.0085(16)·-0.0145(18)·-0.0123(15)·
C22·C·0.060(3)·0.0231(17)·0.044(2)·0.0061(16)·-0.031(2)·-0.0149(18)·
C23·C·0.067(3)·0.0196(14)·0.0314(17)·-0.0049(13)·-0.026(2)·0.001(2)·
C24·C·0.0379(19)·0.0209(14)·0.0246(15)·-0.0047(12)·-0.0116(15)·0.0041(14)·
C25·C·0.0239(14)·0.0140(11)·0.0212(13)·0.0001(10)·-0.0104(11)·0.0016(11)·
C26·C·0.0312(17)·0.0252(16)·0.0212(14)·0.0046(12)·0.0009(13)·-0.0022(13)·
C27·C·0.0381(19)·0.0346(18)·0.0216(14)·0.0025(15)·0.0080(13)·-0.0042(17)·
C28·C·0.0270(15)·0.0281(15)·0.0273(14)·-0.0041(15)·0.0076(12)·-0.0020(16)·
C29·C·0.0178(12)·0.0196(12)·0.0193(13)·-0.0025(10)·-0.0021(9)·0.0009(11)·
C30·C·0.0193(14)·0.0267(14)·0.0328(15)·-0.0053(14)·-0.0009(14)·0.0053(11)·
C31·C·0.0230(15)·0.0260(14)·0.0344(17)·-0.0007(13)·-0.0078(15)·0.0076(14)·
C32·C·0.0312(17)·0.0243(15)·0.0250(15)·0.0024(12)·-0.0100(14)·0.0043(13)·
C33·C·0.0221(14)·0.0196(13)·0.0203(13)·-0.0011(10)·-0.0056(11)·0.0015(11)·
C34·C·0.0197(13)·0.0153(11)·0.0181(12)·-0.0033(9)·-0.0045(10)·0.0005(10)·
C35·C·0.061(5)·0.056(4)·0.032(4)·0.0000·0.0000·0.013(4)·
P1·P·0.0198(5)·0.0318(6)·0.0164(4)·0.0000·0.0000·0.0044(5)·
F1·F·0.0223(17)·0.079(3)·0.0327(18)·0.0000·0.0000·0.0099(17)·
F2·F·0.0209(15)·0.056(2)·0.0316(16)·0.0000·0.0000·0.0007(15)·
F3·F·0.068(3)·0.0300(17)·0.052(2)·0.0000·0.0000·0.009(2)·
F4·F·0.051(2)·0.0324(16)·0.0345(17)·0.0000·0.0000·-0.0029(17)·
F5·F·0.0341(12)·0.0586(15)·0.0169(9)·0.0039(9)·-0.0008(9)·0.0046(12)·
F6·F·0.073(18)·0.182(7)·0.078(3)·0.086(4)·0.0000·0.0000·
F7·F·0.120(3)·0.0532(19)·0.057(2)·-0.0140(16)·0.030(2)·0.036(2)·
F8·F·0.0203(16)·0.118(4)·0.0341(19)·-0.030(2)·0.0000·0.0000·
F9·F·0.0563(19)·0.063(2)·0.0521(17)·0.0359(15)·-0.0093(15)·0.0065(15)·
C13·C·0.133(12)·0.117(10)·0.036(5)·0.0000·0.0000·0.050(9)·
C11·C·0.102(2)·0.0915(19)·0.0568(13)·0.0000·0.0000·-0.0246(16)·
C12·C·0.0708(17)·0.0590(14)·0.0476(12)·0.0000·0.0000·0.0144(12)·
C36·C·0.127(15)·0.125(10)·0.056(13)·0.0000·0.0000·0.026(11)·
·
·
·
_refine_ls_extinction_method·
·····'None'·
_oxford_refine_ls_scale·0.12570(8)·
loop_·
·_geom_bond_atom_site_label_1·
·_geom_bond_site_symmetry_1·
·_geom_bond_atom_site_label_2·
·_geom_bond_site_symmetry_2·
·_geom_bond_distance·
·_geom_bond_publ_flag·
Ir1·-·N1·-·2.121(2)·····yes·
Ir1·-·N2·-·2.199(3)·····yes·
Ir1·-·N3·-·2.024(3)·····yes·
Ir1·-·N5·-·2.012(3)·····yes·
N1·-·C5·-·1.007(3)·····yes·
Ir1·-·C34·-·2.016(3)·····yes·
N1·-·C1·-·1.340(4)·····yes·
N2·-·C6·-·1.353(4)·····yes·
N2·-·C6·-·1.352(4)·····yes·
N2·-·C10·-·1.351(4)·····yes·
·
·
·
N3·-·N4·-·1.361(4)·····yes·
N3·-·C17·-·1.327(4)·····yes·
N4·-·C19·-·1.354(5)·····yes·
N4·-·C20·-·1.417(5)·····yes·
N5·-·N6·-·1.362(4)·····yes·
N5·-·C26·-·1.334(4)·····yes·
N6·-·C28·-·1.352(4)·····yes·
N6·-·C29·-·1.419(4)·····yes·
C1·-·C2·-·1.385(5)·····yes·
C1·-·H11·-·0.940·····no·
C2·-·C3·-·1.379(5)·····yes·
C2·-·H21·-·0.933·····no·
C3·-·C4·-·1.392(5)·····yes·
C3·-·H31·-·0.926·····no·
C4·-·C5·-·1.389(4)·····yes·
C4·-·H41·-·0.938·····no·
C5·-·C6·-·1.482(4)·····yes·
C6·-·C7·-·1.394(5)·····yes·
C7·-·C8·-·1.386(5)·····yes·
C7·-·H71·-·0.936·····no·
C8·-·C9·-·1.380(6)·····yes·
C8·-·H81·-·0.934·····no·
C9·-·C10·-·1.396(5)·····yes·
C9·-·H91·-·0.931·····no·
C10·-·C11·-·1.477(5)·····yes·
C11·-·C16·-·1.402(5)·····yes·
C11·-·C12·-·1.380(5)·····yes·
C12·-·C13·-·1.379(7)·····yes·
C12·-·H121·-·0.936·····no·
C13·-·C14·-·1.375(7)·····yes·
C13·-·H131·-·0.930·····no·
C14·-·C15·-·1.384(6)·····yes·
C14·-·H141·-·0.931·····no·
C15·-·C16·-·1.390(5)·····yes·
C15·-·H151·-·0.933·····no·
C16·-·H161·-·0.934·····no·
C17·-·C18·-·1.385(5)·····yes·
C17·-·H171·-·0.929·····no·
C18·-·C19·-·1.363(6)·····yes·
C18·-·H181·-·0.926·····no·
C19·-·H191·-·0.935·····no·
C20·-·C21·-·1.387(5)·····yes·
C20·-·C25·-·1.404(5)·····yes·
C21·-·C22·-·1.377(7)·····yes·
C21·-·H211·-·0.931·····no·
C22·-·C23·-·1.383(6)·····yes·
C22·-·H221·-·0.937·····no·
C23·-·C24·-·1.394(6)·····yes·
C23·-·H231·-·0.941·····no·
C24·-·C25·-·1.398(5)·····yes·
C24·-·H241·-·0.935·····no·
C26·-·C27·-·1.391(5)·····yes·
C26·-·H261·-·0.933·····no·
C27·-·C28·-·1.370(6)·····yes·
C27·-·H271·-·0.930·····no·
C28·-·H281·-·0.927·····no·
C29·-·C30·-·1.392(4)·····yes·
C29·-·C34·-·1.407(4)·····yes·
C30·-·C31·-·1.387(5)·····yes·
C30·-·H301·-·0.929·····no·
·
·
·
C17·-·C18·-·H181·-·127.5·····no·
C19·-·C18·-·H181·-·127.0·····no·
C18·-·C19·-·N4·-·107.7(3)·····yes·
C18·-·C19·-·H191·-·127.0·····no·
N4·-·C19·-·H191·-·125.2·····no·
N4·-·C20·-·C21·-·121.3(4)·····yes·
N4·-·C20·-·C25·-·114.4(3)·····yes·
C21·-·C20·-·C25·-·124.3(4)·····yes·
C20·-·C21·-·C22·-·118.3(4)·····yes·
C20·-·C21·-·H211·-·120.9·····no·
C22·-·C21·-·H211·-·120.8·····no·
C21·-·C22·-·C23·-·119.8(4)·····yes·
C21·-·C22·-·H221·-·119.9·····no·
C23·-·C22·-·H221·-·120.4·····no·
C22·-·C23·-·C24·-·121.1(4)·····yes·
C22·-·C23·-·H231·-·120.0·····no·
C24·-·C23·-·H231·-·118.9·····no·
C23·-·C24·-·C25·-·121.1(4)·····yes·
C23·-·C24·-·H241·-·118.9·····no·
C25·-·C24·-·H241·-·120.0·····no·
C20·-·C25·-·C24·-·115.4(3)·····yes·
C20·-·C25·-·Ir1·-·114.3(2)·····yes·
C24·-·C25·-·Ir1·-·130.2(2)·····yes·
N5·-·C26·-·C27·-·109.8(3)·····yes·
N5·-·C26·-·H261·-·124.5·····no·
C27·-·C26·-·H261·-·125.7·····no·
C26·-·C27·-·C28·-·106.0(3)·····yes·
C26·-·C27·-·H271·-·127.0·····no·
C28·-·C27·-·H271·-·126.9·····no·
C27·-·C28·-·N6·-·107.6(3)·····yes·
C27·-·C28·-·H281·-·127.2·····no·
N6·-·C28·-·H281·-·125.3·····no·
N6·-·C29·-·C30·-·122.2(3)·····yes·
N6·-·C29·-·C34·-·113.7(3)·····yes·
C30·-·C29·-·C34·-·124.1(3)·····yes·
C29·-·C30·-·C31·-·118.2(3)·····yes·
C29·-·C30·-·H301·-·120.4·····no·
C31·-·C30·-·H301·-·121.4·····no·
C30·-·C31·-·C32·-·120.0(3)·····yes·
C30·-·C31·-·H311·-·120.4·····no·
C32·-·C31·-·H311·-·119.6·····no·
C31·-·C32·-·C33·-·120.8(3)·····yes·
C31·-·C32·-·H321·-·119.6·····no·
C33·-·C32·-·H321·-·119.6·····no·
C32·-·C33·-·C34·-·121.3(3)·····yes·
C32·-·C33·-·H331·-·119.8·····no·
C34·-·C33·-·H331·-·118.9·····no·
C29·-·C34·-·C33·-·115.7(3)·····yes·
C29·-·C34·-·Ir1·-·114.4(2)·····yes·
C33·-·C34·-·Ir1·-·129.9(3)·····yes·
H351·8·556·C35·-·C11·-·108.6·····no·
H351·8·556·C35·-·C12·-·108.5·····no·
C11·-·C35·-·C12·-·113.0(6)·····yes·
H351·8·556·C35·-·H351·-·109.5·····no·
C11·-·C35·-·H351·-·108.6·····no·
C12·-·C35·-·H351·-·108.5·····no·
F5·8·556·P1·-·F1·-·90.05(10)·····yes·
F5·8·556·P1·-·F2·-·89.95(10)·····yes·
F1·-·P1·-·F2·-·179.4(3)·····yes·
F5·8·556·P1·-·F3·-·90.14(11)·····yes·
```

```
F1·..P1·..F3·..90.5(3)···yes
F2·..P1·..F3·..90.1(2)···yes
F5^8_556:P1·..P4·..89.86(11)···yes
F1·..P1·..F4·..90.3(2)···yes
F2·..P1·..F4·..89.2(2)···yes
F3·..P1·..F4·..179.3(2)···yes
F5^8_556:P1·..P5·..179.7(2)···yes
F1·..P1·..P5·..90.05(10)···yes
F2·..P1·..P5·..89.95(10)···yes
F3·..P1·..P5·..90.14(11)···yes
P4·..P1·..P5·..89.86(11)···yes
F7^4_556:P2·..F9^4_556:H8A(2)···yes
F7^4_556:P2·..P6·..90.93(17)···yes
F9^4_556:P2·..P6·..90.16(13)···yes
F7^4_556:P2·..F7·..178.1(3)···yes
F9^4_556:P2·..F7·..91.6(2)···yes
F6·..P2·..F7·..90.93(17)···yes
F7^4_556:P2·..F9·..89.07(13)···yes
F9^4_556:P2·..F8·..89.84(13)···yes
F6·..P2·..F8·..179.993···yes
F7·..P2·..F8·..89.07(17)···yes
F7^4_556:P2·..F9·..91.6(2)···yes
F9^4_556:P2·..F9·..179.7(3)···yes
F6·..P2·..F9·..90.16(13)···yes
F7·..P2·..F9·..88.4(2)···yes
F8·..P2·..F9·..89.84(13)···yes
C35·..C11·..C36·..116.2(8)···yes
C11·..C36·..C13·..136.3(12)···yes
C11·..C36·..H36A^8_556:102.5···no
C13·..C36·..H36A^8_556:102.4···no
C11·..C36·..H36I·..102.5···no
C13·..C36·..H36I·..102.4···no
H36A^8_556·C36·..H36I·..109.5···no
```

bis(3,5-dimethyl-1-phenylpyrazole-*C*,*N*)(6-phenyl-2,2'-bipyridine-*N*,*N*')iridium(III) hexafluorophosphate (**61**)

```
data_sg094_l_123k
_audit_creation_date·····08-10-09
_audit_creation_method·CRYSTALS_ver_12.84
·
_oxford_structure_analysis_title··'sg094_l_123k_0m·in·P2(1)/n'
_chemical_name_systematic·····?
_chemical_melting_point·····?
·
_cell_length_a·····21.5994(6)
_cell_length_b·····21.9541(10)
_cell_length_c·····12.8280(6)
_cell_angle_alpha·····90
_cell_angle_beta·····95.825(2)
_cell_angle_gamma·····90
_cell_volume·····3530.0(3)
·
_symmetry_cell_setting·····'Monoclinic'
_symmetry_space_group_name_H-M···'P·21/n.'.
_symmetry_space_group_name_Hall···'-P·2yn'
loop_
·_symmetry_equiv_pos_as_xyz
·'x,y,z'
·'-x,-y,-z'
·'-x+1/2,y+1/2,-z+1/2'
·'x+1/2,-y+1/2,z+1/2'
·
loop_
·_atom_type_symbol
·_atom_type_scat_dispersion_real
·_atom_type_scat_dispersion_imag
·_atom_type_scat_Cromer_Mann_a1
·_atom_type_scat_Cromer_Mann_b1
·_atom_type_scat_Cromer_Mann_a2
·_atom_type_scat_Cromer_Mann_b2
·_atom_type_scat_Cromer_Mann_a3
·_atom_type_scat_Cromer_Mann_b3
·_atom_type_scat_Cromer_Mann_a4
·_atom_type_scat_Cromer_Mann_b4
·_atom_type_scat_Cromer_Mann_c
·_atom_type_scat_source·
·'C'·····0.0033···0.0016···2.3100···20.8439····1.0200···10.2075····1.5886···0.5687
····0.8650··51.6512···0.2156·'International·Tables·Vol·C·4.2.6.8·and·6.1.1.4'
·'H'·····0.0000···0.0000···0.4930··10.5109····0.3229··26.1257····0.1402···3.1424
····0.0408··57.7998···0.0030·'International·Tables·Vol·C·4.2.6.8·and·6.1.1.4'
·'N'·····0.0061···0.0033···12.2126···0.0057····3.1322····9.8933····2.0125··28.9975
····1.1663···0.5826·-11.5290·'International·Tables·Vol·C·4.2.6.8·and·6.1.1.4'
·'F'·····0.0171···0.0103···3.5392··10.2825····2.6412····4.2944····1.5170····0.2615
····1.0243··26.1476···0.2776·'International·Tables·Vol·C·4.2.6.8·and·6.1.1.4'
·'P'·····0.1023···0.0942···6.4345···1.9067····4.1791··27.1570····1.7800···0.5260
····1.4908··68.1645···1.1149·'International·Tables·Vol·C·4.2.6.8·and·6.1.1.4'
·'Ir'····-1.4442···7.9887··27.3049····1.5928··16.7296····8.8655··15.6118····0.4179
····5.8338··45.0011··11.4722·'International·Tables·Vol·C·4.2.6.8·and·6.1.1.4'
·
_cell_formula_units_Z·····4
·
#·Given·Formula·=·C38·H34·P6·Ir1·N6·P1·
#·Dc·=·····1.72·Foo·=····1800.00·Mu·=·····38.97·M·=····911.91
#·Found·Formula·=·C38·H34·P6·Ir1·N6·P1·
#·Dc·=·····1.72·FOOO·=···1800.00·Mu·=·····38.97·M·=····911.91


_chemical_formula_sum·····C38·H34·F6·Ir1·N6·P1'
_chemical_formula_moiety·····'C38·H34·Ir·N6,·F6·P'
_chemical_compound_source·····?
_chemical_formula_weight·····911.91
·
_cell_measurement_reflns_used·····0
_cell_measurement_theta_min·····0
_cell_measurement_theta_max·····0
_cell_measurement_temperature·····123
·
_exptl_crystal_description·····'plate'·
_exptl_crystal_colour·····'yellow'·
_exptl_crystal_size_min·····0.04·
_exptl_crystal_size_mid·····0.17·
_exptl_crystal_size_max·····0.33
·
_exptl_crystal_density_diffrn····1.716·
_exptl_crystal_density_meas·····?·
#·Non-dispersive·F(000)·:
_exptl_crystal_F_000·····1800·
_exptl_absorpt_coefficient_mu····3.897·
·
#·Sheldrick·geometric·approximatio·0.52·0.86·
#·No·experimental·values·of·Tmin/max·available·
·_exptl_absorpt_correction_type···'multi-scan'·
_exptl_absorpt_process_details····'DENZO/SCALEPACK·(Otwinowski·&·Minor,·1997)'·
_exptl_absorpt_correction_T_min···0.52·
_exptl_absorpt_correction_T_max···0.86·
#·For·a·Kappa·CCD,·set·Tmin·to·1.0·and·
#·Tmax·to·the·ratio·of·max·min·frame·scales·in·scale_all.log·
_diffrn_measurement_device_type··'Nonius·KappaCCD'·
_diffrn_radiation_monochromator···'graphite'·
_diffrn_radiation_type·····'Mo·K\a'·
_diffrn_radiation_wavelength·····0.71073
_diffrn_measurement_method·····'\f·&·\w·scans'·
·
#·If·a·reference·occurs·more·than·once,·delete·the·author·
#·and·date·from·subsequent·references.·
_computing_data_collection·····'COLLECT·(Nonius,·1997-2001)'.·
_computing_cell_refinement·····'DENZO/SCALEPACK·(Otwinowski·&·Minor,·1997)'·
_computing_data_reduction·····'DENZO/SCALEPACK·(Otwinowski·&·Minor,·1997)'·
_computing_structure_solution····'SIR92·(Altomare·et·al.,·1994)'·
_computing_structure_refinement···'CRYSTALS·(Betteridge·et·al.,·2003)'·
_computing_publication_material···'CRYSTALS·(Betteridge·et·al.,·2003)'·
_computing_molecular_graphics·····'CAMERON·(Watkin·et·al.,·1996)'·
·
_diffrn_standards_interval_time···?·
_diffrn_standards_interval_count··?·
_diffrn_standards_number·····0·
_diffrn_standards_decay_%·····?·
·
_diffrn_ambient_temperature·····123
_diffrn_reflns_number·····175137·
_reflns_number_total·····38767·
_diffrn_reflns_av_R_equivalents···0.051·
#·Number·of·reflections·with·Friedels·Law·is·38767·
#·Number·of·reflections·without·Friedels·Law·is·0·
#·Theoretical·number·of·reflections·is·about·40163·
·
_diffrn_reflns_theta_min·····1.846·
_diffrn_reflns_theta_max·····51.913·
_diffrn_measured_fraction_theta_max·0.965·
·
_diffrn_reflns_theta_full·····44.645·
_diffrn_measured_fraction_theta_full·0.995·
·
·
_diffrn_reflns_limit_h_min·····-27·
_diffrn_reflns_limit_h_max·····27·
_diffrn_reflns_limit_k_min·····-48·
_diffrn_reflns_limit_k_max·····48·
_diffrn_reflns_limit_l_min·····-28·
_diffrn_reflns_limit_l_max·····28·
_reflns_limit_h_min·····-27·
_reflns_limit_h_max·····27·
_reflns_limit_k_min·····0·
_reflns_limit_k_max·····48·
_reflns_limit_l_min·····0·
_reflns_limit_l_max·····28·
·
_oxford_diffrn_Wilson_B_factor····0.00·
_oxford_diffrn_Wilson_scale·····0.00·
·
_atom_sites_solution_primary·····direct·#heavy,direct,difmap,geom
#·_atom_sites_solution_secondary···difmap
_atom_sites_solution_hydrogens····geom
·
_refine_diff_density_min·····-0.69·
_refine_diff_density_max·····1.91·
·
·
_refine_ls_number_reflns·····21034·
_refine_ls_number_restraints·····0·
_refine_ls_number_parameters·····469·
·
#·refine_ls_R_factor_ref·0.0222·
_refine_ls_wR_factor_ref·····0.0201·
_refine_ls_goodness_of_fit_ref···1.0936·
·
#_refins_number_all·38745·
·_refine_ls_R_factor_all·····0.0628·
_refine_ls_wR_factor_all·····0.0417·
·
#·The·I/u(I)·cutoff·below·was·used·for·refinement·as·
#·well·as·the·gt·R-factors:
_refins_threshold_expression····I>3.0\s(I)
_refins_number_gt·····21034·
·_refine_ls_R_factor_gt·····0.0222·
_refine_ls_wR_factor_gt·····0.0201·
·
_refine_ls_shift/su_max·····0.008279·
·
#·choose·from:·rm·(reference·molecule·of·known·chirality),·
#·ad·(anomolous·dispersion···Flack),·rmad·(rm·and·ad),·
#·syn·(from·synthesis),·unk·(unknown)·or·.·(not·applicable)..
_chemical_absolute_configuration·'.'·
·

·
_refine_ls_structure_factor_coef·F·
_refine_ls_matrix_type·····full
_refine_ls_hydrogen_treatment·····constr·····#·none,·undef,·noref,·refall,
·····refxyz,·refU,·constr·or·mixed
_refine_ls_weighting_scheme·····calc·
_refine_ls_weighting_details·
;
·Method,·part·1,·Chebychev·polynomial,·(Watkin,·1994,·Prince,·1982)·
·[weight]·=·1.0/[A~0~*T~0~(x)+A~1~*T~1~(x)·...·+A~n-1~*T~n-1~(x)]·
·where·A~i~·are·the·Chebychev·coefficients·listed·below·and·x=·Fcalc/Fmax·
·Method···Robust·Weighting·(Prince,·1982)·
·W·=·[weight]·*·[1-(deltaF/6*sigmaF)^2^]^2^·
·A~i~·are:·
·0.440···0.161·0.176·
;
·
·
#·Check·this·file·using·the·IUCr·facility·at:·
#·http://checkcif.iucr.org/·
·
#·The·content·below·is·held·in·the·file·'script/refcif.dat'.·This·is·a·text·
#·file·which·you·may·edit·to·reflect·local·conditions.·
#·Items·which·need·looking·at·are·represented·by·a·'?'..
#·Items·for·which·there·are·choices·are·prefixed·with·'choose·from'.·
·
_publ_contact_letter.
;
·Please·consider·this·CIF·submission·for·
·publication·as·a·Short·Format·Paper·in·Acta·
·Crystallographica·E.··Thx·figures·will·be·
·sent·by·e-mail.·
;·
_publ_contact_author_name·····'Anthony·Other'·
_publ_contact_author_address·
;·
·Chemical·Crystallography·Laboratory,·
·Department·of·Chemistry,·
·University·of·Nowhere,·
·Nowhere,·NO1·4T,·UK.·
;·
·
_publ_contact_author_phone·····'+44·1865·000000'·
_publ_contact_author_fax·····'+44·1865·000000'·
_publ_contact_author_email·····'a.n.other@chem.no.ac.uk'·
_publ_requested_journal·····'Section·E'·
_publ_requested_category·····ED·#·choose·from:·FI·FM·FO·CI·CM·CO·AD·
_publ_requested_coeditor_name·····'Prof·William·Clegg'·
·
_publ_section_title·
#·Title·of·paper···generally·just·the·systematic·or·trivial·name·
;·?·
·
#·The·loop·structure·below·should·contain·the·names·and·addresses·of·all·
#·authors,·in·the·required·order·of·publication.··Repeat·as·necessary.·
loop_·
·_publ_author_name·
·_publ_author_address·


·_publ_author_footnote·
·'Other,·Anthony·N.'·#·Author·1·
;·
·?·#·Address·for·author·1·
;·
;·
·?·#·Footnote·for·author·1·
;·
·
·'Else,·S.·O.'·#·Author·2·
;·
·?·#·Address·2·
;·
;·
·?·#·Footnote·2·
;·
·
·
_publ_section_abstract·
#·Text·of·the·abstract·
#·(e.g·The·Abstract·must·be·self-contained·and·comprehensible·
#·without·the·rest·of·the·paper.·This·means·no·references·
#·to·atom·names·or·to·compound·numbers;·compounds·must·be·
#·identified·as·the·title·compound,·or·by·name·or·by·some·other·
#·means·such·as·derivatives·of·each·other·(e.g.·"the·
#·corresponding·ketone").·
#·(b)·The·chemical·formula·of·"the·title·compound"·must·be·given.·
#·(c)·Any·crystallographic·molecular·symmetry·should·be·
#·mentioned,·and·also·the·presence·of·more·than·one·molecule·
#·in·the·asymmetric·unit·(i.e.·anything·other·than·2'=1)·.
;·
?·
;·
·_publ_section_comment·
#·Text·of·the·paper·
#·Note·that·atoms·are·referenced·as·N2,·not·N(2)·or·N~2~.·
#·If·text·containing·()·occur·within·(),·the·outer·ones·should·be·[].·
#·Figures·should·be·referenced·as·Fih.·
;·
·
;·
·_publ_section_acknowledgements···#·Acknowledgments·
;·
·
;·
·_publ_section_figure_captions·
#·Captions·to·figures·--·Start·each·caption·on·a·new·line·after·a·blank·line.·
;·
Fig.·1.·
The·title·compound·with·displacement·ellipsoids·drawn·at·the·50%·
probability·level.·H·atoms·are·shown·as·spheres·of·
arbitrary·radius.·
;·
·
;·
·_publ_section_exptl_refinement·
#·Some·potentially·useful·phrases·are·donated·by·Bill·Clegg·
;·
In·the·absence·of·significant·anomalous·scattering,·Friedel·pairs·were·
merged.·
·

·
The·absolute·configuration·was·arbitrarily·assigned.·
·
The·relatively·large·ratio·of·minimum·to·maximum·corrections·applied·
in·the·multiscan·process·(1:nnn)·reflect·changes·in·the·illuminated·
volume·of·the·crystal.·
·
Changes·in·illuminated·volume·were·kept·to·a·minimum,·and·were·
taken·into·account·(G\"orbitz,·1999)·by·the·multi-scan·inter-frame·
scaling·(DENZO/SCALEPACK,·Otwinowski·&·Minor,·1997).·
·
·
G\"orbitz,·C.·H.·(1999).·Acta·Cryst.·B55,·1090-1098.·
·
·
·
The·H·atoms·were·all·located·in·a·difference·map,·but·those·
attached·to·carbon·atoms·were·repositioned·geometrically.·
The·H·atoms·were·initially·refined·with·soft·restraints·on·the·
bond·lengths·and·angles·to·regularise·their·geometry·
(C---H·in·the·range·0.93--0.98,·
N---H·in·the·range·0.86--0.89·
N---H·to·0.86·
O---H·=·0.82·
\tAU·
and·
U-iso·(H)·(in·the·range·1.2-1.5·times·U-eq·of·the·parent·atom),·
after·which·the·positions·were·refined·with·riding·constraints.·
·
·
·
_publ_section_exptl_prep.·
#·Brief·details·or·a·reference.··Include·solvent·if·known·
;·
?·
;·
·
·
#·PROCESSING·SUMMARY·(IUCr·Office·Use·Only):·
_journal_date_recd_electronic·····?·
_journal_date_to_coeditor·····?·
_journal_date_from_coeditor·····?·
_journal_date_accepted·····?·
_journal_date_printers_first·····?·
_journal_date_printers_final·····?·
_journal_date_proofs_out·····?·
_journal_date_proofs_in·····?·
_journal_coeditor_name·····?·
_journal_coeditor_code·····?·
_journal_coeditor_notes·····?·
_journal_techeditor_code·····?·
_journal_techeditor_notes·····?·
_journal_coden_ASTM·····?·
_journal_name_full·····?·
_journal_year·····?·
_journal_volume·····?·
_journal_issue·····?·
_journal_page_first·····?·
_journal_page_last·····?·
_journal_suppl_publ_number·····?·
·
_journal_suppl_publ_pages·····?·
·
·End·of·'script/refcif.dat'.·
·
·
#·Insert·your·own·references·if·required·--·in·alphabetical·order·
_publ_section_references·
;·
·Altomare,·A.,·Cascarano,·G.,·Giacovazzo,·C.,·Guagliardi,·A.,·Burla,·M.C.,·
·Polidori,·G.·&·Camalli,·M.·(1994).·J.·Appl.·Cryst.·27,·435.·
;·
·
·Betteridge,·P.W.,·Carruthers,·J.R.,·Cooper,·R.I.,·
·Prout,·K.·&·Watkin,·D.J.·(2003).·J.·Appl.·Cryst.·36,·1487.·
·
·Larson,·A.C.·(1970).·Crystallographic·Computing,·Ed·Ahmed,·F.R.,·
·Munksgaard,·Copenhagen,·291-294.·
·
·Nonius·(1997-2001).·COLLECT.·Nonius·BV,·Delft,·The·Netherlands.·
·
·Otwinowski,·Z.·&·Minor,·W.·(1997).·Methods·in·Enzymology,·Vol.·276,·
·edited·by·C.·W.·Carter·Jr·&·R.·M.·Sweet,·pp.·307--326.·
·New·York:·Academic·Press.·
·
·Prince,·E.·
·Mathematical·Techniques·in·Crystallography·
·and·Materials·Science·
·Springer-Verlag,·New·York,·1982.·
·
·Watkin·D.J.·(1994).·
·Acta·Cryst.,·A50,·411-437.·
·
·Watkin,·D.J.,·Prout,·C.K.·&·Pearce,·L.J.·(1996).·CAMERON,·Chemical·
·Crystallography·Laboratory,·Oxford,·UK.·
;·
·
#·Uequiv·=·arithmetic·mean·of·Ui·i.e.·Ueqiv·=·(U1+U2+U3)/3·
·
#·Replace·last·..·with·number·of·unfound·hydrogen·atomsattached·to·an·atom.·
·
#·...·refinement_flags_...·
#·_refine_ls_refinement·constraints·····S·special·position·constraint·on·site·
#·G·rigid·group·refinement·of·site·····R·riding·atom·
#·D·distance·or·angle·restraint·on·site·T·thermal·displacement·constraints·
#·U·Uiso·or·Uij·restraint·(rigid·bond)·P·partial·occupancy·constraint·
·
·
loop_·
·_atom_site_label·
·_atom_site_type_symbol·
·_atom_site_fract_x·
·_atom_site_fract_y·
·_atom_site_fract_z·
·_atom_site_U_iso_or_equiv·
·_atom_site_occupancy·
·_atom_site_adp_type·
·_atom_site_refinement_flags_posn·
·_atom_site_refinement_flags_adp·
·_atom_site_refinement_flags_occupancy·
·_atom_site_disorder_assembly·
·
·
·_atom_site_disorder_group·
_atom_site_attached_hydrogens·
Ir1·Ir·0.76140(1)·0.718088(2)·0.33066(1)·0.0128·1.0000·Uani·.·.·.·.·.·
H1^0_556:N2·0.76210(9)·0.58982(5)·0.38817(9)·0.0191·1.0000·Uani·.·.·.·.·.·
N2·N·0.83023(8)·0.63554(5)·0.36339(9)·0.0175·1.0000·Uani·.·.·.·.·.·
N3·N·0.67249(10)·0.83049(5)·0.40557(9)·0.0205·1.0000·Uani·.·.·.·.·.·
C4·N·0.67902(9)·0.79850(5)·0.31365(8)·0.0175·1.0000·Uani·.·.·.·.·.·
N5·N·0.89633(8)·0.77503(5)·0.30783(8)·0.0166·1.0000·Uani·.·.·.·.·.·
N6·N·0.79480(8)·0.69808(5)·0.16570(8)·0.0160·1.0000·Uani·.·.·.·.·.·
C1·C·0.63812(9)·0.66794(6)·0.35662(9)·0.0154·1.0000·Uani·.·.·.·.·.·
C2·C·0.52604(10)·0.68779(7)·0.35584(10)·0.0195·1.0000·Uani·.·.·.·.·.·
C3·C·0.44564(11)·0.64879(8)·0.38421(12)·0.0257·1.0000·Uani·.·.·.·.·.·
C4·C·0.46983(12)·0.58947(9)·0.41524(14)·0.0298·1.0000·Uani·.·.·.·.·.·
C5·C·0.58437(13)·0.56824(7)·0.41903(13)·0.0272·1.0000·Uani·.·.·.·.·.·
C6·C·0.65333(10)·0.60740(6)·0.38925(10)·0.0187·1.0000·Uani·.·.·.·.·.·
C7·C·0.81650(13)·0.53615(6)·0.40246(12)·0.0250·1.0000·Uani·.·.·.·.·.·
C8·C·0.76904(12)·0.47616(7)·0.42773(16)·0.0346·1.0000·Uani·.·.·.·.·.·
C9·C·0.92171(13)·0.54836(7)·0.38748(13)·0.0281·1.0000·Uani·.·.·.·.·.·
C10·C·0.92769(11)·0.61055(7)·0.36325(11)·0.0223·1.0000·Uani·.·.·.·.·.·
C11·C·1.02314(12)·0.64624(8)·0.33908(14)·0.0295·1.0000·Uani·.·.·.·.·.·
C12·C·0.75688(10)·0.74149(6)·0.48153(9)·0.0178·1.0000·Uani·.·.·.·.·.·
C13·C·0.79291(12)·0.70730(8)·0.57085(10)·0.0255·1.0000·Uani·.·.·.·.·.·
C14·C·0.78500(14)·0.72987(10)·0.67139(11)·0.0341·1.0000·Uani·.·.·.·.·.·
C15·C·0.74059(14)·0.78708(11)·0.68600(11)·0.0365·1.0000·Uani·.·.·.·.·.·
C16·C·0.70375(13)·0.82244(9)·0.59983(12)·0.0302·1.0000·Uani·.·.·.·.·.·
C17·C·0.71148(11)·0.79896(6)·0.49927(10)·0.0202·1.0000·Uani·.·.·.·.·.·
C18·C·0.62100(13)·0.88492(7)·0.38524(13)·0.0266·1.0000·Uani·.·.·.·.·.·
C19·C·0.60146(18)·0.93230(8)·0.46485(17)·0.0381·1.0000·Uani·.·.·.·.·.·
C20·C·0.59382(14)·0.88687(7)·0.27816(14)·0.0285·1.0000·Uani·.·.·.·.·.·
C21·C·0.63082(12)·0.83260(6)·0.23635(11)·0.0221·1.0000·Uani·.·.·.·.·.·
C22·C·0.62029(16)·0.81274(8)·0.12434(12)·0.0308·1.0000·Uani·.·.·.·.·.·
C23·C·0.94244(11)·0.81335(6)·0.38137(10)·0.0205·1.0000·Uani·.·.·.·.·.·
C24·C·1.01783(13)·0.85643(7)·0.35977(12)·0.0260·1.0000·Uani·.·.·.·.·.·
C25·C·1.04638(15)·0.86064(8)·0.25797(14)·0.0318·1.0000·Uani·.·.·.·.·.·
C26·C·0.99932(13)·0.82149(8)·0.18179(12)·0.0278·1.0000·Uani·.·.·.·.·.·
C27^0_556:C·0.92496(10)·0.77842(6)·0.20898(9)·0.0186·1.0000·Uani·.·.·.·.·.·
C28·C·0.87739(10)·0.73208(6)·0.13469(9)·0.0180·1.0000·Uani·.·.·.·.·.·
C29·C·0.92195(11)·0.72123(8)·0.04121(10)·0.0235·1.0000·Uani·.·.·.·.·.·
C30·C·0.88185(13)·0.67470(8)·-0.02468(11)·0.0260·1.0000·Uani·.·.·.·.·.·
C31·C·0.80028(12)·0.63909(7)·0.00685(11)·0.0250·1.0000·Uani·.·.·.·.·.·
C32·C·0.75815(10)·0.65136(6)·0.10228(9)·0.0186·1.0000·Uani·.·.·.·.·.·
C33·C·0.67262(10)·0.60916(6)·0.12971(10)·0.0200·1.0000·Uani·.·.·.·.·.·
C34·C·0.69770(13)·0.54696(7)·0.13820(15)·0.0295·1.0000·Uani·.·.·.·.·.·
C35·C·0.61788(16)·0.50431(8)·0.15106(18)·0.0374·1.0000·Uani·.·.·.·.·.·
C36·C·0.51258(15)·0.52337(9)·0.15439(17)·0.0361·1.0000·Uani·.·.·.·.·.·
C37·C·0.48737(12)·0.58515(9)·0.14630(13)·0.0288·1.0000·Uani·.·.·.·.·.·
C38·C·0.56737(11)·0.62809(7)·0.13438(11)·0.0225·1.0000·Uani·.·.·.·.·.·
P1·P·0.80305(3)·0.51749(2)·0.74422(4)·0.0303·1.0000·Uani·.·.·.·.·.·
F1·F·0.87053(9)·0.53055(8)·0.64724(10)·0.0474·1.0000·Uani·.·.·.·.·.·
F2·F·0.73578(11)·0.50746(9)·0.84291(12)·0.0611·1.0000·Uani·.·.·.·.·.·
F3·F·0.69573(9)·0.53520(6)·0.67352(10)·0.0387·1.0000·Uani·.·.·.·.·.·
F4·F·0.91066(11)·0.49870(10)·0.81295(13)·0.0731·1.0000·Uani·.·.·.·.·.·
F5·F·0.81920(13)·0.58748(8)·0.77875(12)·0.0556·1.0000·Uani·.·.·.·.·.·
F6·F·0.78478(14)·0.44818(7)·0.70890(19)·0.0742·1.0000·Uani·.·.·.·.·.·
H21·H·0.5102·0.7269·0.3330·0.0248·1.0000·Uiso·R·.·.·.·.·.·
H31·H·0.3759·0.6637·0.3828·0.0325·1.0000·Uiso·R·.·.·.·.·.·
H41·H·0.4139·0.5634·0.4352·0.0375·1.0000·Uiso·R·.·.·.·.·.·
H51·H·0.5950·0.5273·0.4387·0.0349·1.0000·Uiso·R·.·.·.·.·.·
H81·H·0.7092·0.4651·0.3768·0.0540·1.0000·Uiso·R·.·.·.·.·.·
H82·H·0.7422·0.4777·0.4965·0.0547·1.0000·Uiso·R·.·.·.·.·.·
```

```
H83·H·0.8200·0.4447·0.4315·0.0553·1.0000·Uiso·R·.·.·.·.·
H91·H·0.9807·0.5211·0.3897·0.0352·1.0000·Uiso·R·.·.·.·.·
H111·H·1.0177·0.6547·0.2644·0.0465·1.0000·Uiso·R·.·.·.·.·
H112·H·1.0295·0.6850·0.3778·0.0472·1.0000·Uiso·R·.·.·.·.·
H113·H·1.0868·0.6229·0.3585·0.0468·1.0000·Uiso·R·.·.·.·.·
H131·H·0.8224·0.6680·0.5637·0.0314·1.0000·Uiso·R·.·.·.·.·
H141·H·0.8110·0.7065·0.7282·0.0424·1.0000·Uiso·R·.·.·.·.·
H151·H·0.7357·0.8028·0.7525·0.0457·1.0000·Uiso·R·.·.·.·.·
H161·H·0.6746·0.8611·0.6084·0.0384·1.0000·Uiso·R·.·.·.·.·
H191·H·0.5567·0.9161·0.5135·0.0605·1.0000·Uiso·R·.·.·.·.·
H192·H·0.5695·0.9657·0.4233·0.0612·1.0000·Uiso·R·.·.·.·.·
H193·H·0.6711·0.9439·0.4995·0.0603·1.0000·Uiso·R·.·.·.·.·
H201·H·0.5559·0.9181·0.2441·0.0368·1.0000·Uiso·R·.·.·.·.·
H221·H·0.5661·0.8340·0.0840·0.0483·1.0000·Uiso·R·.·.·.·.·
H222·H·0.6123·0.7707·0.1142·0.0481·1.0000·Uiso·R·.·.·.·.·
H223·H·0.6869·0.8225·0.0939·0.0472·1.0000·Uiso·R·.·.·.·.·
H231·H·0.9192·0.8104·0.4499·0.0263·1.0000·Uiso·R·.·.·.·.·
H241·H·1.0512·0.8821·0.4140·0.0315·1.0000·Uiso·R·.·.·.·.·
H251·H·1.0962·0.8897·0.2418·0.0399·1.0000·Uiso·R·.·.·.·.·
H261·H·1.0173·0.8239·0.1131·0.0349·1.0000·Uiso·R·.·.·.·.·
H291·H·0.9783·0.7451·0.0260·0.0303·1.0000·Uiso·R·.·.·.·.·
H301·H·0.9099·0.6674·-0.0893·0.0333·1.0000·Uiso·R·.·.·.·.·
H311·H·0.7698·0.6059·-0.0348·0.0320·1.0000·Uiso·R·.·.·.·.·
H341·H·0.7702·0.5340·0.1335·0.0370·1.0000·Uiso·R·.·.·.·.·
H351·H·0.6349·0.4623·0.1579·0.0477·1.0000·Uiso·R·.·.·.·.·
H361·H·0.4556·0.4939·0.1640·0.0447·1.0000·Uiso·R·.·.·.·.·
H371·H·0.4163·0.5982·0.1497·0.0360·1.0000·Uiso·R·.·.·.·.·
H381·H·0.5491·0.6698·0.1313·0.0283·1.0000·Uiso·R·.·.·.·.·
loop_
 _atom_site_aniso_label
 _atom_site_aniso_U_11
 _atom_site_aniso_U_22
 _atom_site_aniso_U_33
 _atom_site_aniso_U_23
 _atom_site_aniso_U_13
 _atom_site_aniso_U_12
Ir1·0.013260(12)·0.014173(12)·0.011496(11)·-0.000050(16)·0.003717(8)·
0.000052(17)·
N1·0.0200(4)·0.0162(4)·0.0221(4)·0.0039(3)·0.0063(3)·0.0015(3)·
N2·0.0160(4)·0.0174(4)·0.0198(4)·0.0032(3)·0.0060(3)·0.0016(3)·
N3·0.0235(5)·0.0186(4)·0.0205(4)·-0.0041(3)·0.0074(4)·0.0021(4)·
N4·0.0206(4)·0.0160(3)·0.0165(4)·-0.0011(3)·0.0046(3)·0.0022(3)·
N5·0.0170(3)·0.0178(4)·0.0154(3)·0.0001(3)·0.0033(3)·-0.0026(3)·
N6·0.0168(4)·0.0180(4)·0.0139(3)·-0.0013(3)·0.0046(3)·-0.0014(3)·
C1·0.0141(4)·0.0187(4)·0.0141(4)·-0.0004(3)·0.0046(3)·-0.0004(3)·
C2·0.0157(4)·0.0253(5)·0.0181(4)·-0.0005(4)·0.0051(3)·0.0004(4)·
C3·0.0156(4)·0.0375(8)·0.0249(5)·0.0011(5)·0.0065(4)·-0.0027(5)·
C4·0.0221(6)·0.0366(8)·0.0318(7)·0.0064(6)·0.0088(5)·-0.0095(5)·
C5·0.0254(6)·0.0253(6)·0.0323(7)·0.0079(5)·0.0086(5)·-0.0055(5)·
C6·0.0187(4)·0.0187(5)·0.0197(4)·0.0018(4)·0.0065(4)·-0.0016(4)·
C7·0.0317(7)·0.0179(5)·0.0268(6)·-0.0044(4)·0.0098(5)·0.0060(5)·
C8·0.0472(10)·0.0187(6)·0.0401(9)·0.0053(6)·0.0150(8)·0.0033(6)·
C9·0.0298(7)·0.0243(6)·0.0322(7)·0.0074(5)·0.0124(5)·0.0117(5)·
C10·0.0200(5)·0.0251(6)·0.0230(5)·0.0044(4)·0.0079(4)·0.0065(4)·
C11·0.0183(5)·0.0357(8)·0.0359(7)·0.0097(6)·0.0098(5)·0.0066(5)·
C12·0.0171(4)·0.0240(5)·0.0128(4)·-0.0012(3)·0.0032(3)·-0.0019(4)·
C13·0.0239(5)·0.0379(8)·0.0147(4)·0.0027(4)·0.0016(4)·-0.0001(5)·
C14·0.0290(7)·0.0586(12)·0.0142(4)·0.0017(6)·-0.0004(4)·-0.0014(7)·
C15·0.0327(7)·0.0619(12)·0.0154(5)·-0.0113(6)·0.0043(5)·-0.0013(8)·
C16·0.0282(6)·0.0418(9)·0.0216(5)·-0.0139(6)·0.0072(5)·-0.0012(6)·

C17·0.0198(5)·0.0251(5)·0.0165(4)·-0.0054(4)·0.0057(4)·-0.0018(4)·
C18·0.0290(6)·0.0192(5)·0.0337(7)·-0.0041(5)·0.0126(5)·0.0037(5)·
C19·0.0456(10)·0.0253(7)·0.0463(10)·-0.0116(7)·0.0185(8)·0.0059(7)·
C20·0.0329(7)·0.0197(5)·0.0344(7)·0.0036(5)·0.0109(6)·0.0090(5)·
C21·0.0258(5)·0.0191(5)·0.0221(5)·0.0032(4)·0.0056(4)·0.0049(4)·
C22·0.0421(9)·0.0284(7)·0.0214(6)·0.0053(5)·0.0007(6)·0.0083(6)·
C23·0.0209(5)·0.0219(5)·0.0189(5)·-0.0018(4)·0.0027(4)·-0.0058(4)·
C24·0.0269(6)·0.0259(6)·0.0253(6)·-0.0029(5)·0.0031(5)·-0.0104(5)·
C25·0.0342(8)·0.0329(8)·0.0292(7)·-0.0017(6)·0.0080(6)·-0.0173(6)·
C26·0.0327(7)·0.0297(7)·0.0226(5)·-0.0002(5)·0.0101(5)·-0.0144(6)·
C27·0.0198(4)·0.0203(5)·0.0163(4)·0.0011(4)·0.0056(3)·-0.0037(4)·
C28·0.0190(4)·0.0213(5)·0.0146(4)·0.0003(3)·0.0059(3)·-0.0031(4)·
C29·0.0258(5)·0.0296(6)·0.0167(4)·-0.0004(5)·0.0101(4)·-0.0057(5)·
C30·0.0282(6)·0.0338(7)·0.0178(5)·-0.0039(5)·0.0111(4)·-0.0039(5)·
C31·0.0277(6)·0.0302(6)·0.0184(5)·-0.0077(4)·0.0088(4)·-0.0048(5)·
C32·0.0190(4)·0.0214(5)·0.0163(4)·-0.0044(4)·0.0062(3)·-0.0023(4)·
C33·0.0200(5)·0.0223(5)·0.0187(4)·-0.0059(4)·0.0064(4)·-0.0048(4)·
C34·0.0272(6)·0.0237(6)·0.0398(8)·-0.0081(6)·0.0137(6)·-0.0043(5)·
C35·0.0360(8)·0.0242(7)·0.0548(11)·-0.0094(7)·0.0178(8)·-0.0088(6)·
C36·0.0310(8)·0.0347(8)·0.0444(10)·-0.0108(7)·0.0129(7)·-0.0146(6)·
C37·0.0206(5)·0.0392(8)·0.0274(6)·-0.0068(6)·0.0061(5)·-0.0075(5)·
C38·0.0198(5)·0.0289(6)·0.0192(5)·-0.0039(4)·0.0036(4)·-0.0029(4)·
P1·0.01941(15)·0.0424(2)·0.02938(19)·0.00072(17)·0.00333(13)·0.00410(15)·
F1·0.0352(6)·0.0773(10)·0.0318(5)·-0.0001(6)·0.0132(4)·0.0162(6)·
F2·0.0339(6)·0.1066(14)·0.0448(7)·0.0155(8)·0.0135(5)·-0.0140(8)·
F3·0.0267(5)·0.0459(6)·0.0418(6)·-0.0129(5)·-0.0045(4)·0.0136(4)·
F4·0.0243(5)·0.1328(17)·0.0601(9)·0.0502(11)·-0.0058(6)·-0.0012(8)·
F5·0.0607(9)·0.0615(9)·0.0466(7)·-0.0285(7)·0.0149(6)·-0.0224(7)·
F6·0.0561(10)·0.0342(7)·0.1312(18)·-0.0076(9)·0.0048(10)·0.0167(7)·

_refine_ls_extinction_method·
····'None'
_oxford_refine_ls_scale·0.25919(7)·
loop_
 ·geom_bond_atom_site_label_1
 ·geom_bond_site_symmetry_1
 ·geom_bond_atom_site_label_2
 ·geom_bond_site_symmetry_2
 ·geom_bond_distance
 ·geom_bond_publ_flag
Ir1··N2··2.0344(11)···yes
Ir1··N4··2.0483(11)···yes
Ir1··N5··2.1539(10)···yes
Ir1··N6··2.2421(10)···yes
Ir1··C1··2.0217(11)···yes
Ir1··C12··2.0091(11)···yes
N1··N2··1.3788(15)···yes
N1··C6··1.4251(17)···yes
N1··C7··1.3661(17)···yes
N2··C10··1.3450(16)···yes
N3··N4··1.3820(15)···yes
N3··C17··1.4302(19)···yes
N3··C18··1.3721(19)···yes
N4··C21··1.3380(17)···yes
N5··C23··1.3504(16)···yes
N5··C27··1.3552(14)···yes
N6··C28··1.3720(15)···yes
N6··C32··1.3604(16)···yes
C1··C2··1.4049(17)···yes
C1··C6··1.4108(18)···yes

C2··C3··1.4023(19)···yes
C2··H21··0.923···no
C3··C4··1.387(3)···yes
C3··H31··0.935···no
C4··C5··1.393(2)···yes
C4··H41··0.962···no
C5··C6··1.3971(18)···yes
C5··H51··0.962···no
C7··C8··1.495(2)···yes
C7··C9··1.385(2)···yes
C8··H81··0.977···no
C8··H82··0.977···no
C8··H83··0.940···no
C9··C10··1.404(2)···yes
C9··H91··0.953···no
C10··C11··1.494(2)···yes
C11·H111··0.972···no
C11··H112··0.984···no
C11··H113··0.963···no
C12··C13··1.4060(18)···yes
C12··C17··1.4132(19)···yes
C13··C14··1.401(2)···yes
C13··H131··0.947···no
C14··C15··1.394(3)···yes
C14··H141··0.918···no
C15··C16··1.391(3)···yes
C15··H151··0.928···no
C16··C17··1.4017(18)···yes
C16··H161··0.936···no
C18··C19··1.495(2)···yes
C18··C20··1.382(2)···yes
C19··H191··0.951···no
C19··H192··0.971···no
C19··H193··0.976···no
C20··C21··1.406(2)···yes
C20··H201··0.920···no
C21··C22··1.494(2)···yes
C22··H221··0.938···no
C22··H222··0.937···no
C22··H223··0.984···no
C23··C24··1.3883(19)···yes
C23··H231··0.957···no
C24··C25··1.392(2)···yes
C24··H241··0.958···no
C25··C26··1.388(2)···yes
C25··H251··0.933···no
C26··C27··1.3998(18)···yes
C26··H261··0.934···no
C27··C28··1.4788(18)···yes
C28··C29··1.3953(16)···yes
C29··C30··1.388(2)···yes
C29··H291··0.920···no
C30··C31··1.384(2)···yes
C30··H301··0.948···no
C31··C32··1.4088(17)···yes
C31··H311··0.961···no
C32··C33··1.4901(18)···yes
C33··C34··1.404(2)···yes
C33··C38··1.3967(19)···yes
C34··C35··1.396(2)···yes

C34··H341··0.964···no
C35··C36··1.396(3)···yes
C35··H351··0.949···no
C36··C37··1.395(3)···yes
C36··H361··0.983···no
C37··C38··1.400(2)···yes
C37··H371··0.945···no
C38··H381··0.944···no
P1··F1··1.6024(13)···yes
P1··F2··1.6085(14)···yes
P1··F3··1.5978(12)···yes
P1··F4··1.5947(14)···yes
P1··F5··1.6062(16)···yes
P1··F6··1.5977(17)···yes
loop_
 ·_geom_angle_atom_site_label_1
 ·_geom_angle_site_symmetry_1
 ·_geom_angle_atom_site_label_2
 ·_geom_angle_site_symmetry_2
 ·_geom_angle_atom_site_label_3
 ·_geom_angle_site_symmetry_3
 ·_geom_angle
 ·_geom_angle_publ_flag
N2··Ir1··N4··172.10(4)····yes
N2··Ir1··N5··102.67(4)····yes
N4··Ir1··N5··83.33(4)····yes
N2··Ir1··N6··84.46(4)····yes
N4··Ir1··N6··102.13(4)····yes
N5··Ir1··N6··76.07(4)····yes
N2··Ir1··C1··79.31(4)····yes
N4··Ir1··C1··94.52(5)····yes
N5··Ir1··C1··177.14(4)····yes
N6··Ir1··C1··106.28(4)····yes
N2··Ir1··C12··94.70(5)····yes
N4··Ir1··C12··79.54(5)····yes
N5··Ir1··C12··94.73(4)····yes
N6··Ir1··C12··170.28(4)····yes
C1··Ir1··C12··83.01(5)····yes
N2··N1··C6··115.27(10)····yes
N2··N1··C7··110.07(11)····yes
C6··N1··C7··134.60(12)····yes
Ir1··N2··N1··115.71(8)····yes
Ir1··N2··C10··137.15(9)····yes
N1··N2··C10··107.05(11)····yes
N4··N3··C17··115.21(10)····yes
N4··N3··C18··110.39(12)····yes
C17··N3··C18··134.17(12)····yes
Ir1··N4··N3··114.87(8)····yes
Ir1··N4··C21··138.42(9)····yes
N3··N4··C21··106.63(11)····yes
Ir1··N5··C23··123.79(8)····yes
Ir1··N5··C27··116.59(8)····yes
C23··N5··C27··118.87(11)····yes
Ir1··N6··C28··112.80(8)····yes
Ir1··N6··C32··128.85(8)····yes
C28··N6··C32··117.27(10)····yes
Ir1··C1··C2··127.71(10)····yes
Ir1··C1··C6··115.49(8)····yes
C2··C1··C6··116.48(11)····yes
C1··C2··C3··121.36(13)····yes

C1··C2··H21··117.8···no
C3··C2··H21··120.8···no
C2··C3··C4··120.30(13)····yes
C2··C3··H31··118.9···no
C4··C3··H31··120.8···no
C3··C4··C5··120.24(13)····yes
C3··C4··H41··119.2···no
C5··C4··H41··120.5···no
C4··C5··C6··118.78(14)····yes
C4··C5··H51··123.4···no
C6··C5··H51··117.8···no
N1··C6··C1··113.94(10)····yes
N1··C6··C5··123.24(13)····yes
C1··C6··C5··122.83(12)····yes
N1··C7··C8··125.62(14)····yes
N1··C7··C9··106.78(13)····yes
C8··C7··C9··127.59(14)····yes
C7··C8··H81··111.8···no
C7··C8··H82··110.4···no
H81··C8··H82··107.4···no
C7··C8··H83··111.8···no
H81··C8··H83··109.2···no
H82··C8··H83··106.8···no
C7··C9··C10··107.01(12)····yes
C7··C9··H91··129.0···no
C10··C9··H91··123.9···no
C9··C10··N2··109.07(13)····yes
C9··C10··C11··128.20(13)····yes
N2··C10··C11··122.72(13)····yes
C10··C11··H111··109.1···no
C10··C11··H112··112.0···no
H111··C11··H112··109.1···no
C10··C11··H113··109.5···no
H111··C11··H113··109.3···no
H112··C11··H113··107.9···no
Ir1··C12··C13··127.61(11)····yes
Ir1··C12··C17··115.78(9)····yes
C13··C12··C17··116.61(12)····yes
C12··C13··C14··121.20(16)····yes
C12··C13··H131··120.3···no
C14··C13··H131··118.5···no
C13··C14··C15··120.38(15)····yes
C13··C14··H141··118.5···no
C15··C14··H141··121.1···no
C14··C15··C16··120.37(13)····yes
C14··C15··H151··121.2···no
C16··C15··H151··118.4···no
C15··C16··C17··118.51(16)····yes
C15··C16··H161··121.1···no
C17··C16··H161··120.4···no
N3··C17··C12··114.01(10)····yes
N3··C17··C16··123.06(14)····yes
C12··C17··C16··122.93(14)····yes
N3··C18··C19··125.69(16)····yes
N3··C18··C20··106.29(12)····yes
C19··C18··C20··128.01(16)····yes
C18··C19··H191··109.7···no
C18··C19··H192··103.8···no
H191··C19··H192··113.7···no
C18··C19··H193··106.8···no

H191··C19··H193··111.3···no
H192··C19··H193··110.9···no
C18··C20··C21··107.14(13)····yes
C18··C20··H201··124.0···no
C21··C20··H201··128.8···no
C20··C21··N4··109.55(13)····yes
C20··C21··C22··127.86(14)····yes
N4··C21··C22··122.59(12)····yes
C21··C22··H221··112.0···no
C21··C22··H222··114.7···no
H221··C22··H222··110.6···no
C21··C22··H223··108.7···no
H221··C22··H223··106.0···no
H222··C22··H223··104.1···no
N5··C23··C24··122.65(12)····yes
N5··C23··H231··116.8···no
C24··C23··H231··120.6···no
C23··C24··C25··118.66(13)····yes
C23··C24··H241··120.9···no
C25··C24··H241··120.4···no
C24··C25··C26··119.10(13)····yes
C24··C25··H251··119.8···no
C26··C25··H251··121.1···no
C25··C26··C27··119.45(13)····yes
C25··C26··H261··120.1···no
C27··C26··H261··120.5···no
C26··C27··N5··121.25(12)····yes
C26··C27··C28··122.81(11)····yes
N5··C27··C28··115.86(10)····yes
C27··C28··N6··117.21(10)····yes
C27··C28··C29··119.95(11)····yes
N6··C28··C29··122.65(12)····yes
C28··C29··C30··119.71(12)····yes
C28··C29··H291··118.2···no
C30··C29··H291··122.1···no
C29··C30··C31··118.23(12)····yes
C29··C30··H301··120.8···no
C31··C30··H301··120.9···no
C30··C31··C32··120.16(13)····yes
C30··C31··H311··122.2···no
C32··C31··H311··117.7···no
C31··C32··N6··121.93(12)····yes
C31··C32··C33··115.57(11)····yes
N6··C32··C33··122.49(10)····yes
C32··C33··C34··117.44(12)····yes
C32··C33··C38··122.52(13)····yes
C34··C33··C38··119.57(13)····yes
C33··C34··C35··120.17(15)····yes
C33··C34··H341··119.3···no
C35··C34··H341··120.5···no
C34··C35··C36··120.05(17)····yes
C34··C35··H351··120.3···no
C36··C35··H351··119.7···no
C35··C36··C37··119.95(15)····yes
C35··C36··H361··121.0···no
C37··C36··H361··119.0···no
C36··C37··C38··120.13(15)····yes
C36··C37··H371··120.1···no
C38··C37··H371··119.8···no
C37··C38··C33··120.11(15)····yes

C37··C38··H381··118.8···no
C33··C38··H381··121.1···no
F1··P1··F2··177.51(10)····yes
F1··P1··F3··90.05(7)····yes
F2··P1··F3··89.83(8)····yes
F1··P1··F4··89.26(8)····yes
F2··P1··F4··90.90(8)····yes
F3··P1··F4··178.74(10)····yes
F1··P1··F5··88.89(8)····yes
F2··P1··F5··88.63(9)····yes
F3··P1··F5··90.00(8)····yes
F4··P1··F5··91.04(11)····yes
F1··P1··F6··91.30(10)····yes
F2··P1··F6··91.18(11)····yes
F3··P1··F6··88.94(8)····yes
F4··P1··F6··90.02(11)····yes
F5··P1··F6··178.92(9)····yes
```

Curriculum Vitae

Stefan Graber, PhD

Personal Details

Kienbergstrasse 9
4058 Basel
Switzerland
stefan.graber@unibas.ch

Marital Status: Married
Place of Birth: Basel, Switzerland
Date of Birth: 04/11/1980
Citizenship: Swiss

Skills

Languages: German, English, French (all fluent, spoken and written)

Education

06/2009 – present **Postdoctoral studies**, *Synthesis of Ir(III) complexes for solid state lighting applications*, and *Oxidation of primary alcohols using MnO_2 nanoparticles*, Supervisor: Prof. Dr. E. C. Constable, University of Basel, Switzerland.

01/2005 – 05/2009 **PhD studies**, *From STM to LEECs: Syntheses and Applications of Multifunctional Bipyridine Ligands and their Iridium(III) Complexes*, Supervisor: Prof. Dr. E. C. Constable, University of Basel, Switzerland.

01/2004 – 04/2004 **Diploma work (equivalent to a MSc)**, *Synthesis and STM Imaging of Novel Chiral Bipyridine Ligands*, Supervisor: Prof. Dr. E. C. Constable, University of Basel, Switzerland.

10/1999 – 10/2003 **Diploma studies**, University of Basel, Switzerland.

06/1999 **Matura (Typus C, Science)**, Gymnasium Kirschgarten, Basel, Switzerland.

Employment

06/2004 – 01/2005 **Informatics Engineer**, *InnoTix GmbH*, Zürich, Switzerland.
Programming engineer with direct customer contact for customisation. Developed skills in: computer programming (PHP, ColdFusion, JavaScript, SQL); database technologies (database design, maintenance and data manipulation); mobile technologies (push/pull phone ‹› web gateways).

08/2002 – 09/2002 **Research and Development Laboratory Technician**, Organic Chemistry, *Solvias AG*, Basel, Switzerland.

05/2001 – 12/2001 & 03/2002 – 07/2002 **Quality Assurance Technician**, *Solvias AG*, Basel, Switzerland.
Worked under GMP quality standards in the field of medical analysis.

02/2001 – 06/2003 **Logistics Technician**, *Swiss Post*, Basel, Switzerland.

Teaching

02/2009 – 05/2009 **Lecturer**, Anorganische Chemie II (2nd year) with Prof. Dr. E. C. Constable.

05/2005 – 07/2005 & 10/2008 – 12/2008 **Supervising two 4th year undergraduate students**, University of Basel, Switzerland.

01/2005 – 12/2008	**Laboratory Demonstrator**, General Chemistry (1st year), University of Basel, Switzerland.

Presentations

06/2008	International Krutyn Summer School 2008, Krutyn, Poland.
08/2006	1st European Chemistry Congress, Budapest, Hungary.
07/2006	International Conference on Nanoscience and Technology (ICN+T) 2006, Basel, Switzerland.
05/2006	DENSOM, Obernai, France.
03/2005	Leopoldina-Symposium zur Dendrimer-Forschung, Heidelberg, Germany.

Publications

R. D. Costa, E. Ortí, H. J. Bolink, S. Graber, M. Neuburger, S. Schaffner, C. E. Housecroft, and E. C. Constable, Archetype Cationic Iridium Complexes and Their Use in Solid-State Light-Emitting Electrochemical Cells, *Advanced Functional Materials*, **2009**, DOI: 10.1002/adfm.200900911.

R. D. Costa, E. Ortí, H. J. Bolink, S. Graber, C. E. Housecroft, M. Neuburger, S. Schaffner, and E. C. Constable, Two are not always better than one: ligand optimisation for long-living light-emitting electrochemical cells, *Chemical Communications*, **2009**, 2029–2031.

S. Graber, K. Doyle, M. Neuburger, C. E. Housecroft, E. C. Constable, R. D. Costa, E. Ortí, D. Repetto, and H. J. Bolink, A Supramolecularly-Caged Ionic Iridium(III) Complex Yielding Bright and Very Stable Solid-State Light-Emitting Electrochemical Cells, *Journal of the American Chemical Society*, **2008**, *130*, 14944–14945.

H. J. Bolink, E. Coronado, R. D. Costa, E. Ortí, M. Sessolo, S. Graber, K. Doyle, M. Neuburger, C. E. Housecroft, and E. C. Constable, Long-Living Light-Emitting Electrochemical Cells – Control through Supramolecular Interactions, *Advanced Materials*, **2008**, *20*, 3910–3913.

E. C. Constable, S. Graber, B. A. Hermann, C. E. Housecroft, M. S. Malarek, and L. J. Scherer, The Introduction of Asymmetry into Alkyl-Decorated Fréchet-Type Dendrons, *European Journal of Organic Chemistry*, **2008**, 2644–2651.

Awards and Memberships

- Awarded a Reisefonds scholarship in support of conference attendance and presentation at the 1st European Chemistry Congress.
- Awarded a European scholarship in support of conference attendance and presentation at the DENSOM conference.
- Attended a leadership course at the University of Basel (2006).
- Member of the Swiss Chemical Society.

Extracurricular Activities

- Enjoy outdoor activities (cycling, hiking, running, inline skating), scuba diving (PADI certification), photography, cooking, travelling.
- Programming websites (PHP+MySQL), computer and network support for friends.
- Performing semi-professional saxophone concerts in the “4SX Quartet”.

During my studies, I attended courses of the following lecturers:

H. Burkhart
E. C. Constable
G. Gescheidt
B. Giese
H.-J. Güntherodt
P. Hauser
H.-C. Im Hof
U. Jenal
J. Jourdan
T. A. Kaden
J. P. Maier
A. Mezzetti
J. Müller
W. Nau
M. Neuburger-Zehnder
M. Oehme
A. Pfaltz
C. Schönenberger
U. Séquin
D. Sick
H. Sigel
P. Strazewski
D. Trautmann
A. Vedani
H. Wennemers
H.-J. Wirz
W.-D. Woggon
A. D. Zuberbühler